PATTERNING THE RETINA OF
DROSOPHILA MELANOGASTER FOR COLOR
AND POLARIZED LIGHT VISION

Inaugural-Dissertation

Zur Erlangung des Doktorgrades

Der Mathematisch-Naturwissenschaftlichen Fakultät

Der Universität zu Köln

vorgelegt von

Mathias F. Wernet

Aus Strasbourg

Köln

2004

Berichterstatter: Prof. Dr. Diethard Tautz

                                    Prof. Dr. Siegfried Roth

Tag der mündlichen Prüfung: 5. 1. 2005

TEILPUBLIKATIONEN

Wernet, MF, Mazzoni, EO, Duncan, DM, Celik, A, Duncan, I, and Desplan, C. Stochastic expression of the *Drosophila* Dioxin receptor Spineless creates the retinal mosaic required for color vision, in preparation.

Wernet, MF and Desplan, C. Building a retinal mosaic: cell-fate decision in the fly eye. Trends Cell Biol. 2004 Oct; 14(10):576-84.

Wernet MF, Labhart T, Baumann F, Mazzoni EO, Pichaud F, Desplan C. Homothorax switches function of *Drosophila* photoreceptors from color to polarized light sensors. Cell. 2003 Oct 31;115(3):267-79.

Tahayato A, Sonneville R, Pichaud F, Wernet MF, Papatsenko D, Beaufils P, Cook T, Desplan C. Otd/Crx, a dual regulator for the specification of ommatidia subtypes in the *Drosophila* retina. Dev Cell. 2003 Sep;5(3):391-402.

Mollereau B, Wernet MF, Beaufils P, Killian D, Pichaud F, Kühnlein R, Desplan C. A green fluorescent protein enhancer trap screen in *Drosophila* photoreceptor cells. Mech Dev. 2000 May;93(1-2):151-60.

TABLE OF CONTENTS

IV. DISCUSSION

V. MATERIAL & METHODS

VI. REFERENCES

VII. ACKNOWLEDGEMENTS

VIII. APPENDIX

LIST OF FIGURES

LIST OF TABLES

I. ABSTRACT

Across the animal kingdom, specialized sensory epithelia are used for photoreception, allowing individuals to interact with their environment based on visual cues. Generally, neuronal photoreceptor cells (PRs) are organized in the retina, a specialized part of body tissue exposed to the outside world, and transform the energy of incoming electromagnetic radiation into neuronal excitation. This process depends on the large family of opsin proteins which are required in PRs of all animal species. This lead to the theory, that the very divergent eye structures may share a common ancestor, although they most likely arose several times independently during evolution. PRs transmit their electrical excitation to higher order neurons, which are organized in the brain of the animal. How the brain then integrates the incoming signals from a multitude of PRs to reproduce a reliable representation of the world remains one of the central questions of neurobiology.

Most animals can extract different kinds of visual information from their environment. Besides detecting the shape and movement of objects, additional qualities like color or degree of polarization can also be distinguished. In most cases, different classes of PRs are used for each of these visual tasks. For instance, color discrimination is achieved by comparing the outputs of PRs having different spectral sensitivity, as they express different opsin molecules. In humans, three different subclasses of so-called cone PRs, are specialized to absorb light of either short, medium or long wavelengths, corresponding to blue, green or red colors, respectively. Loss of any one of these PR classes leads to a dramatic impairment in the ability to discriminate between colors. Cones are most highly concentrated in the center of the retina (fovea), where the three subclasses form a random mosaic. Much remains to be understood about how different PR subtypes choose expression of their opsin and how they distribute in the retina.

The developing eye of the fruitfly *Drosophila melanogaster* was used here as a model system to investigate both nature and regulation of the different strategies involved in retinal patterning. The adult *Drosophila* eye consists of ~800 stereotypical unit eyes (ommatidia), each containing exactly 8 PRs (R1-R8). The six 'outer PRs' (R1-R6) are molecularly identical in all ommtidia as they always express the same opsin. They form a separate visual system contributing to the detection of shapes and motion. The morphological and molecular differences between inner PRs (R7 and R8) from different ommatidia leads to the formation of a retinal mosaic in *Drosophila*. Three ommatidial subtypes can be distinguished: while the ommatidia of the 'dorsal rim area' (DRA) are always found precisely localized in the dorsal periphery, the remaining 'pale' and yellow' ommatidia are distributed stochastically through the rest of the retina. Only DRA ommatidia can be identified based on morphologic criteria, as these ommatidia form a polarizing filter which the fly uses to measure e-vector orientation of polarized sunlight for navigational purposes. The remaining two ommatidial subtypes are believed to serve color discrimination. They can only be identified based on the combination of opsins their inner PRs express. In order to identify genes and pathways involved in generating the retinal mosaic in *Drosophila*, a GAL4 enhancer trap screen was performed. Genes exhibiting expression patterns similar to inner PR opsins were analyzed genetically.

The homeodomain transcription factor Homothorax (Hth) was identified as the key regulator of DRA specification. Hth is both necessary and sufficient for the formation of the polarization sensors. During pupal development, positional information provided by the diffusible morphogen Wingless (Wg), as well as the dorsal selector genes of the *Iroquois* complex (*IRO-C*) and the gene *optomotorblind* (*omb*) get integrated, leading to the specific induction of Hth expression in inner PRs of prospective DRA ommatidia. In contrast to this localized specification approach, stochastic expression of the *Drosophila* arylhydrocarbon receptor Spineless (Ss) in a large subset of pupal R7 cells is responsible for the specification of color ommtidia. Ss is both necessary and sufficient to induce the 'yellow' R7 fate (yR7). Ss was therefore identified as the

key effector of a stochastic specification approach. How stochastic expression of Ss is regulated, remains obscure. However, an activating effect of the Notch (N) pathway on yR7 specification indicates that retinal patterning in *Drosophila* might combine the inductive effects of both *wg* and *N* signaling once again during pupal development.

Further investigation of the regulatory relationship between Hth and Ss (or Wg and N) will provide a better understanding how retinal patterning contributes to the integration of different kinds of visual information.

I. ZUSAMMENFASSUNG

Das Tierreich bietet eine Vielzahl von Beispielen, wie es spezialisiserte Sinnesepithelien einem Individuum erlauben, aufgrund optischer Eindrücke mit seiner Umgebung zu interagieren. Neuronale Photorezeptorzellen (PRs) sind grundsätzlich in der Retina organisiert - einem spezialisierten Teil der Körperoberfläche, welcher der Aussenwelt ausgesetzt ist - und wandeln die Energie der einfallenden elektromagnetischen Strahlung in neuronale Erregung um. Dieser Prozess involviert die grosse Familie der Opsinproteine, welche in den PRs aller Lebewesen benötigt werden. Dies begründete die Theorie, dass sich die sehr vielgestaltigen Augenstrukturen auf einen gemeinsamen Vorfahren zurück führen lassen, obwohl sie im Laufe der Evolution aller Wahrscheinlichkeit nach mehrfach unabhängig voneinander entstanden. PRs übertragen ihre elektrische Erregung auf Neuronen höherer Ordnung, welche im Gehirn des Tieres organisiert sind. Wie das Gehirn dann die eintreffenden Signale einer Vielzahl von PRs integriert, um eine zuverlässige Reproduktion der Welt zu erzeugen, bleibt eine der zentralen Fragen der Neurobiologie.

Die meisten Tiere können verschiedene Arten visueller Information von ihrer Umgebung ableiten. Neben der Detektion von Form und Bewegung von Objekten, können auch zusätzliche Qualitäten wie Farbe und Polarisierungsgrad unterschieden werden. In den meisten Fällen werden unterschiedliche Klassen von PRs für jede visuelle Augabe eingesetzt. Das Unterscheiden von Farben, zum Beispiel, wird durch Vergleich der Ausgangssignale von PRs verschiedener spektraler Sensitvität erreicht, da diese unterschiedliche Opsinmoleküle exprimieren. Beim Menschen sind drei unterschiedliche Subklassen der sogenannten Zapfen darauf spezialisiert, entweder Licht kurzer, mittlerer oder langer Wellenlänge zu absorbieren, was blauer, grüner oder roter Farbe entspricht. Verlust einer dieser PR Subklassen führt zu einer dramatischen

Einschränkung der Fähigkeit, Farben unterscheiden zu können. Zapfen treten in höchster Konzentration in der Fovea (dem 'gelben Fleck') auf, wo die drei Subklassen ein zufälliges Mosaik bilden. Bisher ist nicht klar, wie unterschiedliche PR Unterarten die Expression ihres Opsins wählen, oder wie sie sich in der Retina verteilen.

Das sich entwickelnde Auge der Fruchtfliege *Drosophila melanogaster* wurde hier benutzt, um die Art, sowie die Regulation der unterschiedlichen Strategien zu untersuchen, welche in der retinalen Musterbildung involviert sind. Das adulte Auge von *Drosophila* besteht aus ca. 800 Komplexaugen (Ommatidien), von welchen jedes genau acht PRs enthält (R1 bis R8). Die sechs 'äusseren PRs' (R1 bis R6) sind molekular identisch in allen Ommatidien, da sie immer das selbe Opsin exprimieren. Sie bilden ein abgesondertes visuelles System, welches zur Wahrnehmung von Formen und Bewegung beiträgt. Die morphologischen, sowie molekularen Unterschiede zwischen den 'inneren PRs' (R7 und R8) unterschiedlicher Ommatidien führen zur Bildung eines retinalen Mosaiks in *Drosophila*. Drei Subtypen von Ommatidien können unterschieden werden: Während die Ommatidien der 'dorsal rim area' (DRA, dorsale Randregion) immer präzise lokalisiert, in der dorsalen Peripherie angetroffen werden, sind die verbleibenden 'pale' ('blass') und 'yellow' ('gelb') Ommatidien stochastisch über den Rest der Retina verteilt. Lediglich DRA Ommatidien können aufgrund morphologischer Kriterien identifiziert werden, da diese Ommatidien einen Polarisationsfilter bilden, welchen die Fliege zu Navigationszwecken zur Bestimmung der Orientierung des e-Vektors polarisierten Sonnenlichts benutzt. Es wird angenommen, dass die beiden verbleibenden Ommatidien-Subtypen der Unterscheidung von Farben dienen. Sie können nur aufgrund der Opsine, welche ihre inneren PRs exprimieren, identifiziert werden. Um Gene und Signalwege zu identifizieren, welche bei der Bildung des retinalen Mosaiks in *Drosophila* eine Rolle spielen, wurde ein GAL4 'enhancer trap screen' durchgeführt. Gene, welche Expressionsmuster vorweisen die denen der inner PR Opsinen ähneln, wurden weiter genetisch untersucht.

5

Der Homeodomänen-Transkriptionsfaktor Homothorax (Hth) wurde identifiziert als der zentrale Regulator der Spezifikation von DRA Ommatidien. Hth is sowohl notwendig als auch hinreichend für die Bildung der Polarisations-Sensoren. Während des Puppenstadiums werden verschiedene Aspekte räumlicher Information, welche vom diffundierenden Morphogen Wingless (Wg), den dorsalen Selektor-Genen des *Iroquois* Komplexes (*IRO-C*) und dem Gen *optomotorblind* (*omb*) bereit gestellt werden, in einer Weise integriert so dass Hth spezifisch in den inneren PRs der sich entwickelnden DRA Ommatidien exprimiert wird. Im Gegensatz zu diesem lokalisierten Spezifikationsansatz ist die stochastische Expression des *Drosophila* Arylhydrocarbonrezeptors Spineless (Ss) in einer grossen Subpopulation pupaler R7 Zellen zuständig für die Spezifikation jener Ommatidien, welche dem Farbensehen dienen. Ss ist sowohl notwendig als auch hinreichend für die Spezifikation von 'yellow' R7 Zellen (yR7). Ss wurde somit als zentraler Effektor eines stochastischen Spezifikationsansatzes identifiziert. Wie die stochastische Expression von Ss reguliert wird, bleibt ein Rätsel. Die aktivierende Wirkung des Signaltransduktionsweges um den Notch Rezeptor (N) auf die Spezifikation von yR7 Zellen birgt nichtsdestotrotz den Hinweis, dass retinale Musterbildung in *Drosophila* die induktiven Effekte der wg und N Signalwege während des Puppenstadiums aufs Neue kombiniert.

Eine weitere Untersuchung der regulativen Zusammenhänge zwischen Hth und Ss (oder Wg und N) wird ein besseres Verständnis davon ermöglichen, wie retinale Musterbildung zur Integration verschiedener Arten von visueller Information beiträgt.

II. INTRODUCTION

Despite the broad range of eye structures across the animal kingdom, all visual systems use similar cellular mechanisms to respond to environmental cues. For instance, all animals use related opsin proteins in their photoreceptor cells (PRs) to capture photons (for review: Arendt and Wittbrodt, 2001). In addition, the eyes of most animals can be used to perform two distinct visual tasks: They not only form images of the surrounding environment, but they can also detect the 'quality' of the visual stimulus, *e.g.* color or skylight polarization, through the use of specialized PR subclasses. These PR subclasses exhibit important morphological and molecular differences as well as characteristic distribution patterns through the retina in order to maximize the amount of information extracted from the environment. Emerging data indicate that retinal patterning includes a series of highly coordinated and organized processes. Several recent works in the fly eye have begun to identify many of the factors involved, and interestingly, similar patterning events occur in the vertebrate retina that are sometimes regulated by orthologous factors. These data further imply that the vertebrate single lens eye and the insect compound eye use similar strategies to achieve their function and to control the development of the retina. Rather than reflecting common ancestry of the visual systems, this might represent convergent mechanisms used to control opsin expression in different PR subtypes and may provide insight into understanding how the complexity of the retina is created and maintained.

1. Retinal mosaics in humans and flies

Humans use rod PRs ('rods') for detecting objects under low-light conditions, while the cone PRs ('cones') participate in color discrimination as well as high resolution vision. To serve these purposes most efficiently, the different subclasses of cones (called S, M and L, indicating their maximal sensitivity to <u>s</u>hort, <u>m</u>edium or <u>l</u>ong wavelengths) are highly concentrated in the center of the retina, the fovea. Interestingly, their distribution there appears to be stochastic,

resulting in a cone mosaic that can be visualized *in vivo* (**Fig 1A**). This allows the fovea to serve as the color and high acuity center for the eye. Rods, on the other hand, are concentrated towards the periphery of the eye which specializes in shape and motion vision under low light conditions.
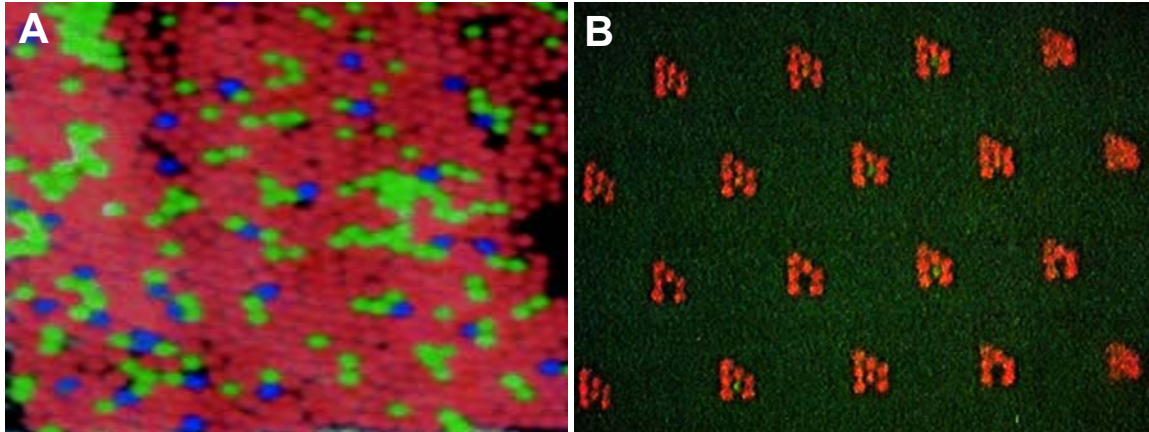
Fig II.1 Retinal mosaics in humans and flies
(A) Pseudocolor image of the trichromatic cone mosaic from a living human retina. Blue, green and red colors represent the S, M, and L cones, respectively.
(B) Visualization of the ommatidial mosaic in the housefly, *Musca domestica*, using epifluorescence and water immersion microscopy.

Even species as distantly related to humans as flies share important similarities in the organization of their retina. For instance, specialized groups of PRs are used to discriminate between colors (in analogy to cones), whereas other PRs have been optimized for the detection of shapes and for motion detection (in analogy to rods). As in the human retina, the different fly PRs also exhibit specific distribution (**Fig 1B**). For instance, despite the dramatic differences in retinal organization, both fly and human color PR subtypes show a similar random distribution through the retina or the fovea, repectively. Additionally, another group of fly PRs is highly concentrated in a certain part of the retina, thereby forming a specialized eye region similar to the human fovea. The retinal mosaic of the fruitfly therefore represents an attractive model system for the study of both stochastic and localized specification events occurring during retinal patterning (for review: Wernet and Desplan, 2004).

2. The *Drosophila* compound eye

The *Drosophila* eye consists of ~800 stereotypical unit eyes (ommatidia), each containing 8 light-sensing PRs (called R1-8) as well as accessory cells involved in forming the lens or in shielding PRs from light coming from other ommatidia (**Fig 2A**, **B** and **C**; for review: Hardie, 1985). The light gathering membranes (rhabdomeres) of the six outer PRs (R1-R6) are organized in a chiral trapezoid. The center of each ommatidial trapezoid is occupied by the two inner PRs, R7 and R8. The rhabdomere diameter of these two inner PRs is significantly reduced as compared to outer PRs and they span only half of the
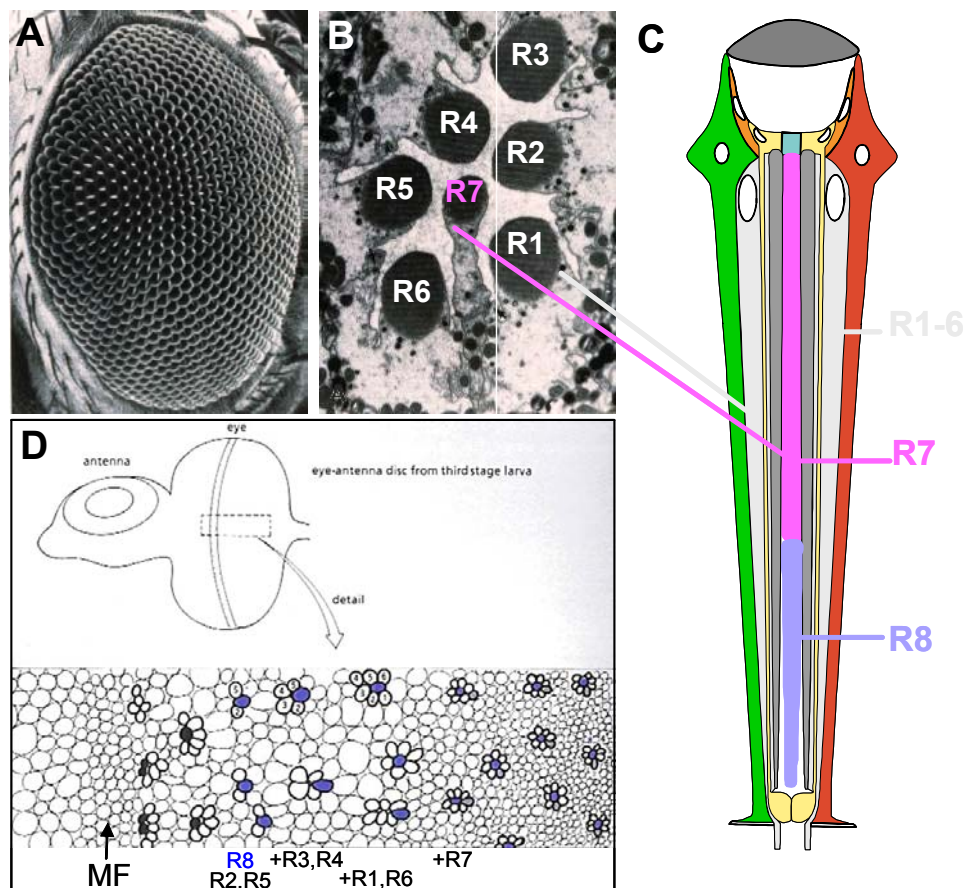
Fig II.2 The *Drosophila* compound eye

(A) Scanning electron micrograph of an adult Drosophila eye, composed of ~800 unit eyes (ommatidia).

(B) Cross section through an adult *Drosophila* ommatidium. The light gathering structures (rhabdomeres) of seven photoreceptors are visible (R8 is below focal plane). The Rhabdomere diameter is larger for outer PRs (R1-R6) which are aligned as a chiral trapezoid. R7 has a smaller rhabdomere diameter and is located in the center of the trapezoid.

(C) Schematic representation of an adult ommatidium. In the center of the ommatidium, R7 (pink) is located distally on top of R8 (blue) in the same path of light. Outer PRs (grey) span the entire retina from the apical to the basal side. Pigment cells Green and red) shield the ommatidium from light received by neighboring ommatidia, while cone cells (yellow) secrete the lens.

(D) PRs get specified during third instar larval stages from a pool of undifferentiated cells. Top: third instar larval eye-antennal disc (anterior to the left). Bottom: posterior to the morphogenetic furrow (MF), neuronal PR cells get recruited sequentially. First R8 (blue), then R2+R5, then R3+R4, then R1+R6 and finally R7.

retina, with the R7 rhabdomere located distally on top of that of R8: they are therefore in the same path of light, providing the ideal configuration to compare their outputs. This is absolutely required for the two functions of inner PRs, color vision and detection of the vector of polarized light. During third instar larval life, the eight *Drosophila* PRs of each ommatidium (R1-R8) are selected from an undifferentiated pool of cells (**Fig 2D**; for review: Brennan and Moses, 2000). Through a process that is now fairly well understood, the interplay of the Notch, EGFR and Sevenless signaling pathways at the 'morphogenetic furrow' (MF) leads to a sequential recruitment of PRs into evenly spaced clusters. R8 is the first PR to be determined. This 'founder cell' then recruits all six outer PRs in a pair-wise fashion (first R2 and R5, then R3 and R4, finally R1 and R6). R7 is the last PR to be recruited (Freeman, 1996; Wolff, 1993).

3. The *Drosophila* ommatidium: outer photoreceptors

According to their morphology, axonal projections and opsin expression, the fly PRs of every adult ommatidium can be grouped into two functional categories: The outer PRs are the fly equivalent of the vertebrate rods and are involved in motion detection and image formation (**Fig 3A**). Computation of their outputs begins in the first optic lobe of the fly, the lamina (L), where the outer PRs project their axons. Inner PRs project to the second optic lobe, the medulla (M), where the neuronal processing both color and polarized light vision begins (for review: Meinertzhagen and Hanson, 1993; Morante and Desplan, 2004). The outer PRs have been shown to be both molecularly and morphologically identical in all ommatidia. They capture photons with high efficiency, due to the expression of their broad spectrum rhodopsin Rh1, as well as the large diameter of their rhabdomeres which extend from the basal to the apical side of the retina (Zuker et al., 1985); **Fig 3B)**. Different techniques have been used to characterize the adult *Drosophila* visual system and the first PR subclass to be studied molecularly in detail was the outer PR system. Cloning of the *rh1/ninaE* gene allowed the visualization of Rh1 expression using antibodies against the Rh1 protein (**Fig 3C**, top). Furthermore, axon projections of the outer
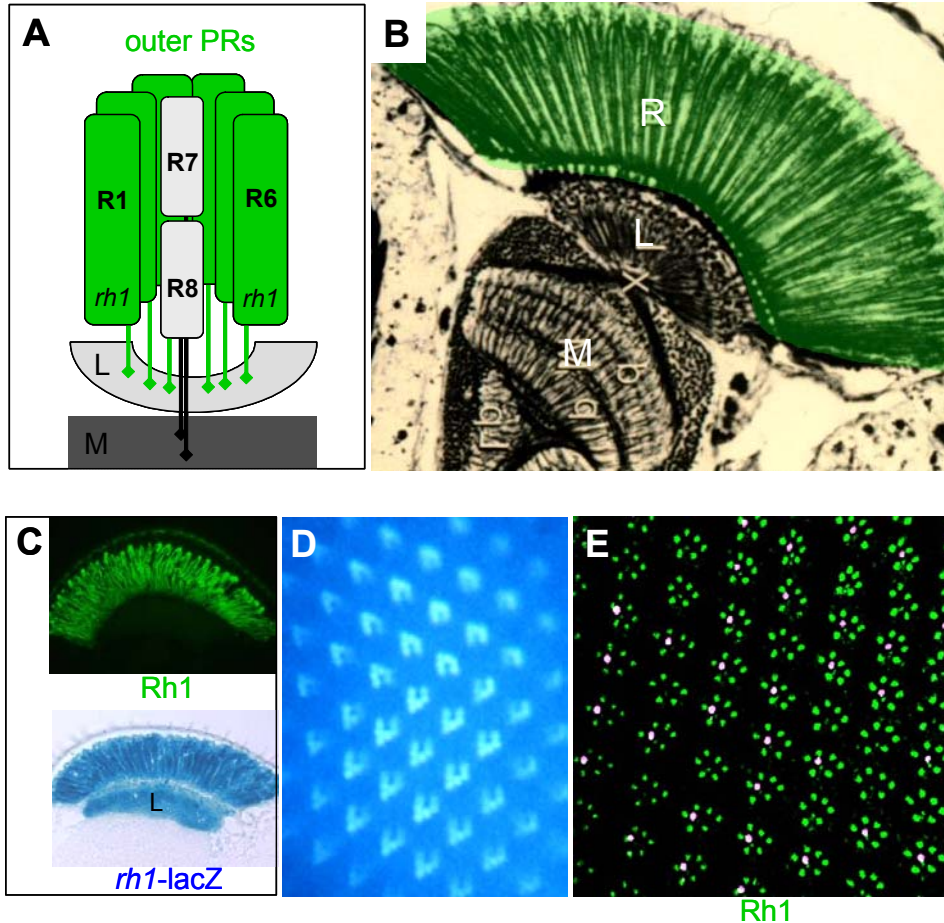
Fig II.3 The *Drosophila* ommatidium: outer photoreceptors
(A) Schematic representation of an adult ommatidium. The outer PRs R1-R6 are identical in all ommatidia.. They express the broad band opsin Rh1 (ninaE) and project to the first layer of the optic lobe, the lamina (L).
(B) Silver-stained section through the Drosophila visual system. Outer PRs are highlightened in green. Their rhabdomeres span the entire retina. L=lamina; M=medulla.
(C)-(E) Expression of *rh1* in outer PRs. Top: Frozen sections (10 μm) through adult heads from wildtype flies stained with an antibody against Rh1 (green). Bottom: Expression of *rh1*-lacZ visualized on frozen sections, using X-Gal. βGal activity is detectable in the entire retina as well as in axonal projections to the lamina (L). (D) Visualization of Rh1 using autofluorescence under UV illumination. (E) Thin section (1 μm) through through an adult wildtype eye double labeled with Anti-Rh1 (green) and an antibody labeling a subset of inner PRs (pink).

PR axons to the lamina could be visualized by fusing the *ninaE* promoter to reporter genes like lacZ (Sheng et al., 1997; **Fig 3C**, bottom). These new histological techniques proved to be significantly more reliable than the previously developed water immersion microscopy, under which auto-fluorescence of Rh1 could be observed in outer PRs (**Fig 3D**). The use of this technique was limited due to the rapid bleaching of the visual pigment (Pichaud and Desplan, 2001). Finally, visualization of the ommatidal mosaic was revolutionized by the development of multi-colored fluorescent antibodies as well as whole mount and thin section techniques (**Fig 3E**).

4. The *Drosophila* retinal mosaic: inner photoreceptors

Although the general external morphology of the fly eye does not indicate heterogeneity among ommatidia, three ommatidial subtypes have been described in *Drosophila* (**Fig 4A**). In all three cases, molecular and sometimes morphological features of the inner PRs have been used to categorize the ommatidial subtypes. Detailed morphological analysis of adult eyes from different fly species has revealed a first subset of ommatidia always found in one or two rows at the dorsal rim of the fly eye, called the 'dorsal rim area' (DRA**,** shown in pink in **Fig 4A**; (Hardie, 1984; Wada, 1971; Wada, 1974). These ommatidia exhibit an enlarged rhabdomere diameter as well as specialized rhabdomeric microvilli, making them strongly polarization sensitive (**Fig 4B** and **C**). It is believed that DRA ommatidia are used to improve navigation by measuring the oscillation plane of polarized skylight (Wolf et al., 1980)for review: Labhart and Meyer, 1999; Labhart and Meyer, 2002). The remaining two ommatidial subtypes have first been characterized in elegant studies by Franceschini and Kirschfeld (Franceschini et al., 1981). Fluoroscopy revealed the existence of two separate classes of ommatidia interspersed randomly within the fly retina: inner PRs appeared either **pale** (**p**) or **yellow** (**y**), with 30% being **p** and the remaining 70% being **y**. Based on their different spectral sensitivities, **p** and **y** ommatidia were proposed to contribute to the discrimination between different colors.

Approximately 25 years later, the cloning of the *rhodopsin* genes (*rh*) from *Drosophila* has provided a molecular basis for all three ommatidial subtypes. Inner PRs in DRA ommatidia were found to be monochromatic as they express the UV opsin Rh3 in both R7 and R8 (**Fig 4D** left; (Fortini and Rubin, 1990; Fortini and Rubin, 1991; Fryxell and Meyerowitz, 1987; Fryxell and Meyerowitz, 1991). Outside of the DRA, ommatidia with monochromatic inner PRs have never been reported, suggesting that this situation developed to specifically avoid confusion between color and polarization. The **p** ommatidia were found to always contain the UV-sensitive Rh3 in R7 and the blue-sensitive Rh5 in R8 (middle). A different UV-sensitive Rh4, was found in the R7 of **y** ommatidia, which always express the green-sensitive Rh6 in R8 (Chou et al., 1996; Huber et al., 1997;
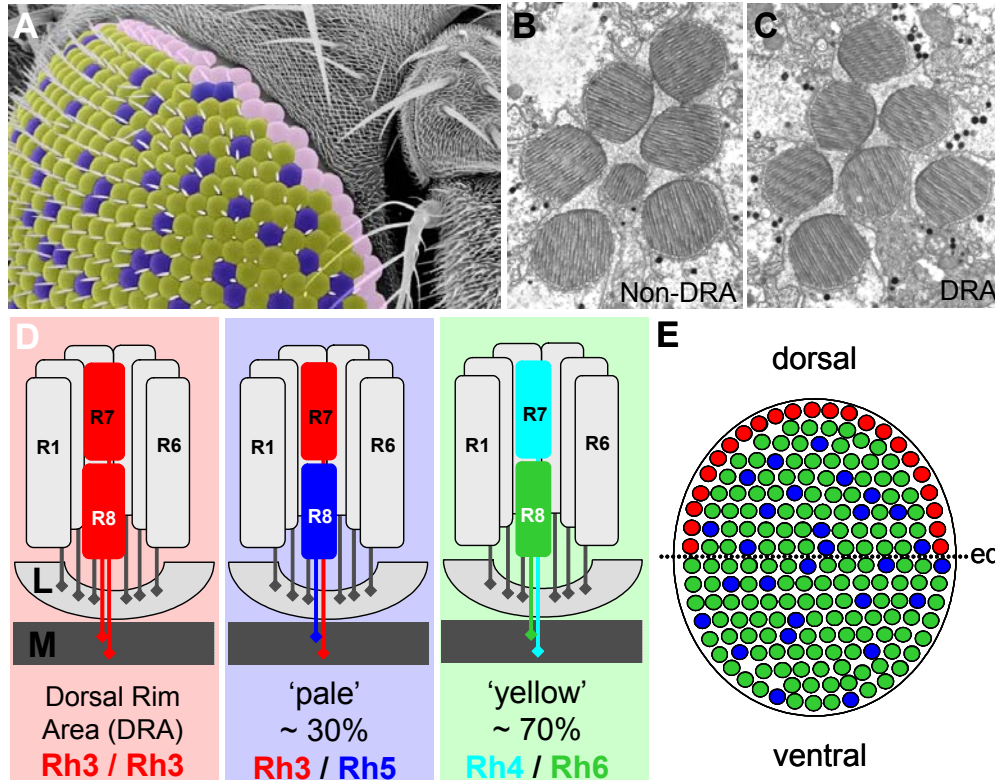
Fig 4. The *Drosophila* retinal mosaic: inner photoreceptors
(A) Three ommatidial subtypes are distributed throughout the *Drosophila* retina. Scanning electron micrograph illustrating the fact that, although they look identical from this point of view, ommatidia fall into three categories.
(B)+(C) DRA ommatidia were identified morphologically. The vast majority of ommatidia manifests a small inner PR rhabdomere diameter. (C) In the one or two dorsal-most rows of ommatidia, the 'dorsal rim area' (DRA), however, inner PRs R7 and R8 have a dramatically enlarged rhabdomere diameter.
(D) Based on opsin expression and rhabdomere morphology, three ommatidial subtypes can be distinguished. Inner PRs of ommatidia located in the DRA always both express the UV-specific opsin Rh3 (left). So-called 'pale' (**p**) ommatidia always express Rh3 in R7 and Rh5 in R8 cells (middle) whereas 'yellow' (**y**) ommatidia express Rh4 in R7 and Rh6 in R8 cells (right).
(E) DRA ommatidia are always found in 1-2 rows at the dorsal periphery of the adult retina, whereas **p** (~30%) and **y** (~70%) ommatidia are distributed randomly through the retina (eq = equator).

specialized in the perception of longer wavelengths, reaching into the green part of the spectrum. Interestingly, the human cones, which express blue-, red- or green-specific opsins are also distributed stochastically in the fovea, but there is no tight coupling of the opsin expression between different cells (for review: Nathans, 1999). Taken together, the retinal mosaic of the fruitfly is composed of three ommatidial subtypes, which are found either localized (DRA) or randomly distributed (**p** and **y**) throughout the retina (**Fig 4E**).

5. Visualization of the p and y ommatidial subtypes

Cloning of the genes encoding the 4 *Drosophila* inner PR Rhodopsins (*rh3-rh6*) allowed a more precise characterization of **p** and **y** ommatidia (Chou et

al., 1996; Chou et al., 1999; Fryxell and Meyerowitz, 1987; Huber et al., 1997; Montell et al., 1987; Papatsenko et al., 1997). Fusion of the *rh3* and *rh4* promoters with lacZ allowed the visualization of the **p** and **y** subtypes in R7 cells (**Fig 5A**). Expression of these reporter transgenes was shown to faithfully re-produce the expression pattern of the endogenous opsin proteins: expression of *rh3*-lacZ was restricted to the DRA inner PRs (arrow) as well as to the **p**R7 cells, whereas *rh4*-lacZ expression is specific to the **y**R7 cells. Due to the cytoplasmic localization of the βGal protein, these transgenes have also been used to
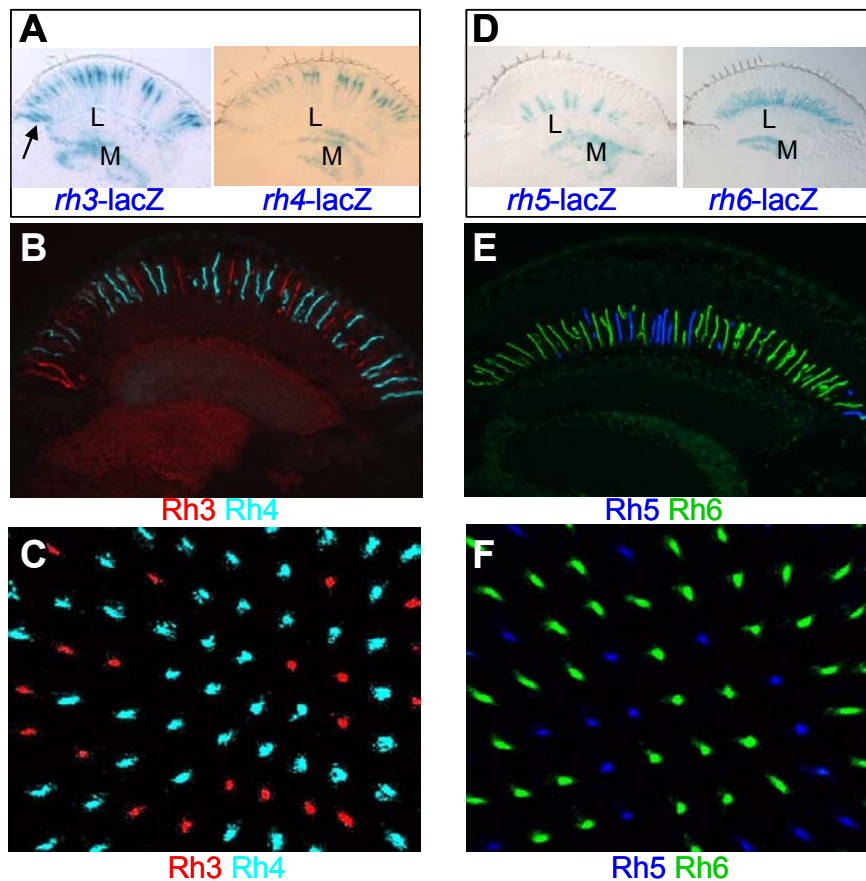
Fig II.5 Visualization of the p and y ommatidial subtypes
(A)-(C) Visualization o **p** and **y** subtypes in R7 cells. Frozen sections through an adult head from wildtype flies carrying the opsin reporter constructs *rh3*-lacZ (left) and *rh4*-lacZ (right). βGal activity is detectable in the DRA (rh3, arrow) and in subsets of R7 cells with cell bodies in the distal half of the retina and projections to the medulla (M). (B) Frozen section double labeled with antibodies against Rh3 (red) and Rh4 (cyan) allows simultaneous visualization of both R7 subtypes. pR7 and yR7 are non-overlapping. (C) Whole mounted retina double labeled with Anti-Rh3 and Anti-Rh4 reveales ~70 of yR7 and ~30% of pR7.
(D)-(F) Visualization o **p** and **y** subtypes in R7 cells. Opsin reporter constructs *rh5*-lacZ (left) and *rh6*-lacZ (right)are expressed in subsets of R8 cells with cell bodies in the proximal half of the retina and projections to the medulla (M). (E) Double labeled with antibodies against Rh5 (blue) and Rh6 (green) allows simultaneous visualization of both R8 subtypes. (F) Whole mounted retina double labeled with Anti-Rh5 and Anti-Rh6 reveales ~70 of yR8 and ~30% of pR8.

visualize the axonal projections of inner PRs to the medulla (M). Furthermore, antibodies raised against the Rh3 and Rh4 proteins have been used on frozen sections to simultaneously visualize exclusive expression of these opsins in **p**R7 and **y**R7 cells, respectively (**Fig 5B**). Recently, this technique has been applied to whole mounted retinas from adult flies (Cook et al., 2003), thereby specifically visualizing the ommatidial mosaic in R7 cells (**Fig 5C**).

Similar techniques have recently been applied to visualize **p** and **y** subtypes in the R8 cells. Fusions of the *rh5* and *rh6* promoters with lacZ were used to specifically visualize **p**R8 and **y**R8 cells and their axonal projections to the medulla (**Fig 5D**). Antibodies against Rh5 and Rh6 were used on frozen sections to visualize exclusion between both subsets in R8 cells (**Fig 5E**). Finally, the ommatidial mosaic in R8 cells has only recently been visualized by applying these antibodies on whole mounted adult retinas (**Fig 5F**).

6. Maturation and re-organization of pupal ommatidia

During third instar larval life, the eight *Drosophila* PRs of each ommatidium (R1-R8) are selected from an undifferentiated pool of cells (**Fig 6A**+**B**; for review: Brennan and Moses, 2000). Based on their order of recruitment and the combination of transcription factors that they express, the eight larval PRs represent at least 5 different cells types (R8, R2+R5, R3+R4, R1+R6, and R7). It should be noted that the larval R3 and R4 cells can also be viewed as individual cell types as they respond differently to the positional information that establishes the chirality of the ommatidium in a process called planar polarity (see below; for review: Tree et al., 2002). During the next four days of pupal development, the PRs undergo dramatic morphological changes, with the formation of the rhabdomeres as well as the onset of opsin expression (**Fig 6C**+**D**). At the end, only three functional classes of PRs can be distinguished in the adult ommatidium: the outer PRs R1-R6 and the two inner PRs R7 and R8 (**Fig E**+**F**; for review: Wolff, 1993). The outer PRs have now become virtually identical. They all express the same opsin gene (*rh1/ninaE*) and their rhabdomere morphology as well as axon projection pattern allows the fly to use
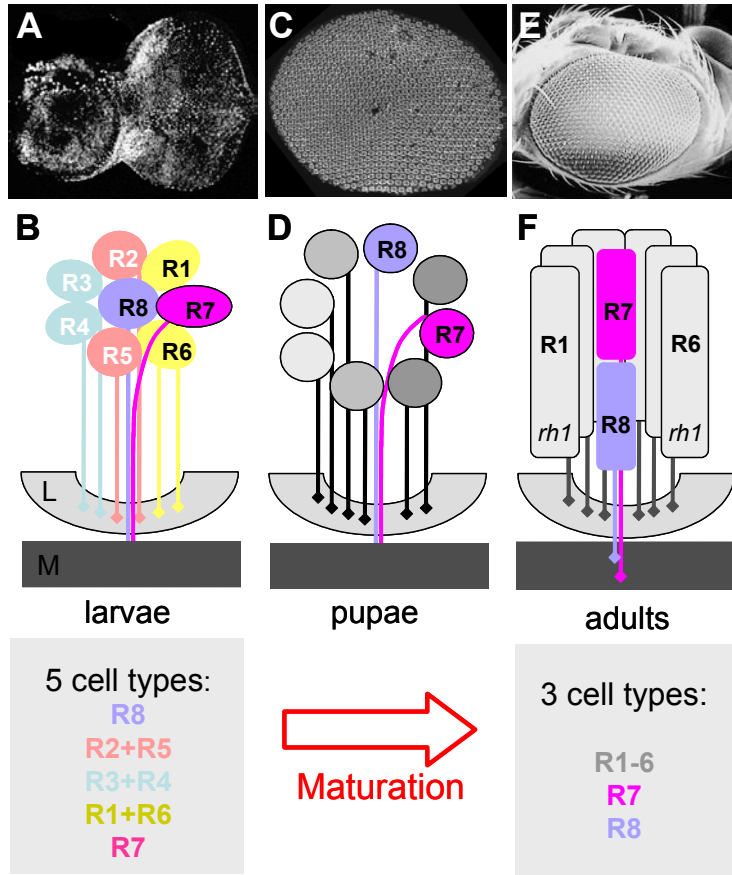
Fig II.6 Maturation and re-organization of pupal ommatidia
(A)+(B) Third instar larval PRs develop in the eye imaginal disc, posterior to the morphogenetic furrow. They can be grouped into at least 5 categories, based on the order of their recruitment and the combination of transcription factors they express. R7 and R8 are already distinguishable based on their axon projection to the same layer of the brain, the medulla (M)..
(C)+(D) The pupal retina starts to re-organize. Approximately 48 hrs later, the disc has everted and a flat retina is visible. PRs start to move apart. Opsin expression and rhabdomere formation are about to begin.
(D)+(E) The adult retina: another 2-3 days later, the re-organization is complete. The eye and the head capsule are fused. PRs have developed elongated rhabdomeres and R7 has moved on top of R8. Outer PRs express rh1, whereas inner PR opsin expression and rhabdomere morphology dictate the subtype of the ommatidium.

this group of PRs as a separate visual system for shape and motion vision (Lee et al., 2001). The two inner PRs, which, interestingly were the first (R8) and the last (R7) PR to be recruited into the ommatidium, are now grouped together to form the second visual system. They have become morphologically similar, with both rhabdomeres spanning opposite halves of the retina (R8 proximally and R7 distally). Both inner PRs from a given ommatidium always project to the same position in the medulla. However, terminations of R7 and R8 are found at slightly different layers (with R8 terminating before R7; for review: Clandinin and Zipursky, 2002). Adult R7 and R8 cells therefore provide the optimal configuration for comparing stimuli, both by working together in the same optical

path and by allowing further processing in the brain. Taken together, all pupal ommatidia have to re-organize their PRs by grouping them into the two functional categories represented in the adult eye.

7. Specification of inner PRs: the role of *spalt*

An important first step towards understanding ommatidial maturation came with the description of the role of the *spalt* gene complex, which encodes two homologous zinc finger transcription factors (Kuhnlein et al., 1994). The *spalt* genes are specifically expressed in R7 and R8 (**Fig 7A**) and loss of *spalt* leads
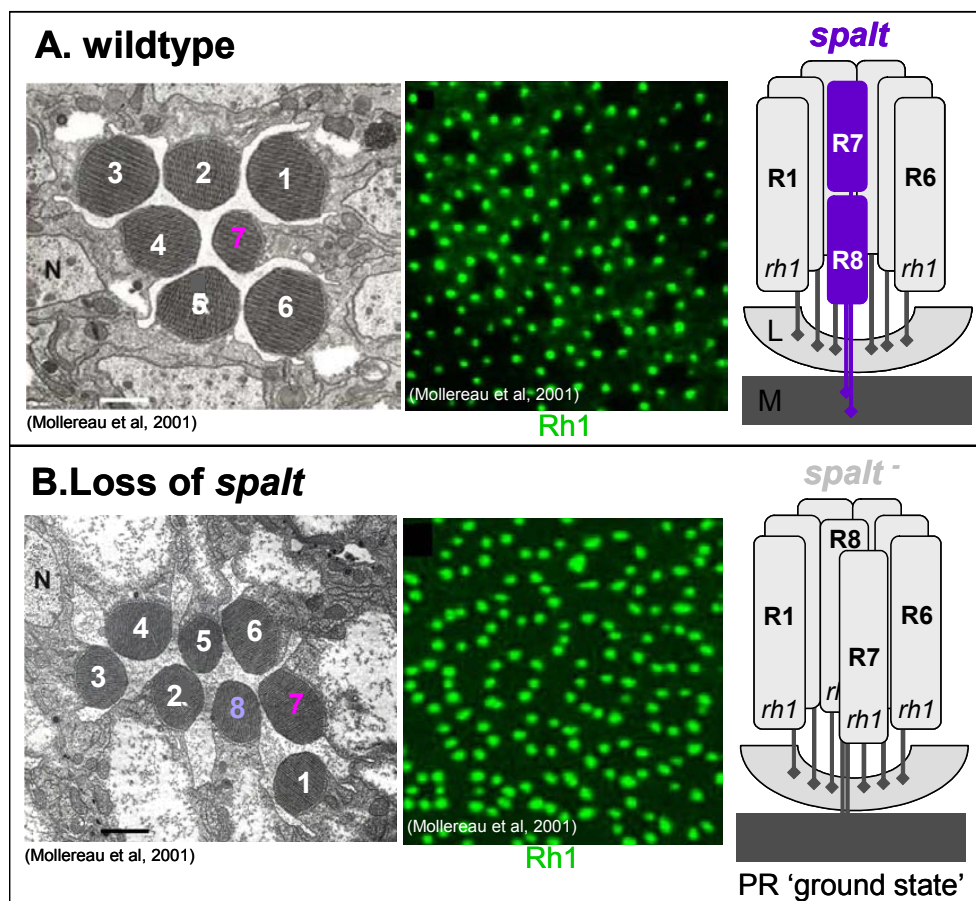
Fig II.7 Specification of inner PRs: the role of *spalt*
(A) Spalt is expressed specifically in inner PRs R7 and R8, in the wildtype (purple).
(B) In *spalt* mutants, inner PRs get mis-specified. Electron microscopy revealed loss of the typical inner PR rhabdomeres with small diameter, in *sal* (-/-) eyes. (compare to A,left). (B) Antibody staining on thin sections revealed that all 8 PRs express Rh1 (green) in the absence of Sal (compare to A, center: Only six outer PRs per ommatidium express Rh1, in the wildtype). Right: schematic representation of the spalt (-/-) phenotype: Both molecular as well as morphological features of inner PRs are lost. Instead, these PRs gain all characteristica of outer PRs, except their axon projection pattern: R7 and R8 still project to the medulla (m), whereas R1-R6 terminate in the lamina (L). This indicates that, in the absence of Spalt, inner PRs got originally specified correctly, but then failed to mature into adult inner PRs. Instead, they seem to be stuck in an outer-PR-like PR 'ground state'.

to a loss of inner PR characteristics, both morphologically and molecularly, *i.e.* loss of Rh3, Rh4, Rh5 and Rh6. Instead, R7 and R8 gain outer PR markers, like rhabdomere morphology and *rh1* expression (**Fig 7B**). However, the axonal projections of these transformed inner PRs to the medulla are maintained (Domingos et al., 2004; Mollereau et al., 2001). It was therefore concluded that, in s*palt* mutants, inner PRs are initially properly specified but then lose their identity and instead terminally differentiate into outer PRs. Spalt*,* is therefore necessary to distinguish differentiating inner PRs from an otherwise outer PR-like 'ground state' toward which all PRs tend to develop (right). This provided a molecular basis to the existence of two overlapping visual systems in the adult. This is also particularly interesting as it might provide a simple explanation of how the originally very divergent outer PRs R1-R6 adopt their uniform cell fate simply by being denied further differentiation signals like *spalt* expression. The presence of the two distinct genetic programs of specification, followed by differentiation, might illustrate the dual function of *Drosophila* PRs: They are first specified as neurons that must find their appropriate target in the optic lobes. They subsequently differentiate as light sensing cells. In contrast, the vertebrate retina has two cell types to perform these roles: rods and cones to detect light, and retinal ganglion cells to project out of the retina into the brain.

8. Distinguishing between R7 and R8 cell fates

Both inner PRs require *spalt* to adopt their appropriate cell fate (Domingos et al., 2004). Nevertheless, R7 or R8 represent different PRs, both morphologically (position within the retina) and molecularly (different *rhodopsins*), and other factors are therefore necessary to further distinguish between the two inner PR cell fates. By screening for factors that bind to conserved sequences in the *Drosophila* opsin promoters, the gene *prospero* was recently shown to be necessary for distinguishing R7 from the R8 cell fate (Cook et al., 2003). Prospero is a homeodomain transcription factor that is known to be important for peripheral nervous system development as well as asymmetric cell division (Kauffmann et al., 1996). In the adult eye, Prosper*o* is expressed specifically in

the R7 cell in response to the signaling pathways responsible for R7 specification, Notch, EGFR and Sevenless (**Fig 8A**, left and center). It has been shown that Prospero binds to conserved sequences in the R8 opsin promoters (*rh5* and *rh6*), thereby leading to their repression in R7. Loss of *prospero* indeed leads to a de-repression of *rh5* and *rh6* in adult R7 cells, creating a second R8-like cell per ommatidium (R8*, right). Interestingly, loss of *prospero* also results in repression of the proper R7 *rhodopsins*, most likely to avoid co-expression of opsin genes, a situation that is generally not observed in sensory receptors (for review: Celik et al., in press). These observations suggested that *prospero* is able to act on the generic inner PR fate and to push cells toward and R7 fate and away from an R8 fate. However, although R7 cells mis-express R8 rhodopsins in *prospero* mutants, they do not gain all R8 markers and their rhabdomeres are still positioned correctly in the distal part of the retina. This observation can be interpreted as a reversion of R7 back to a generic inner PR fate, which favors expression of R8 *rhodopsins*. This suggests that other genes are necessary to fully push the generic inner PR fate toward the R8 cell type.

One gene necessary for both specification and maturation of R8 cells encodes the Zn finger transcription factor Sensless (*sens*; (Nolo et al., 2000). Sens had been shown to be specifically expressed in R8 cells, throughout eye development (**Fig 8B**): PRs get mis-specified in *sens* mutants: Although R8 cells are originally specified correctly, they then develop into outer PRs and loose their inner PR identity (Frankfort et al., 2001). Consequently, R7 cells are not recruited in sens (-/-) mutants, due to the loss of the R8-specific Boss signal required for Sevenless receptor activation in potential R7 cell precursors (Cooper and Bray, 2000; Reinke and Zipursky, 1988; Tomlinson and Struhl, 2001). Fewer PRs are therefore counted in ommatidia lacking Sens function (right). Sens has recently been shown to be sufficient for activation of *rh6* expression when ectopically expressed in developing PRs, further suggesting that Sens is both necessary and sufficient to induce R8 cell maturation (Domingos et al., 2004). Finally, expression of both Pros and Sens has been shown to be lost in *sal*
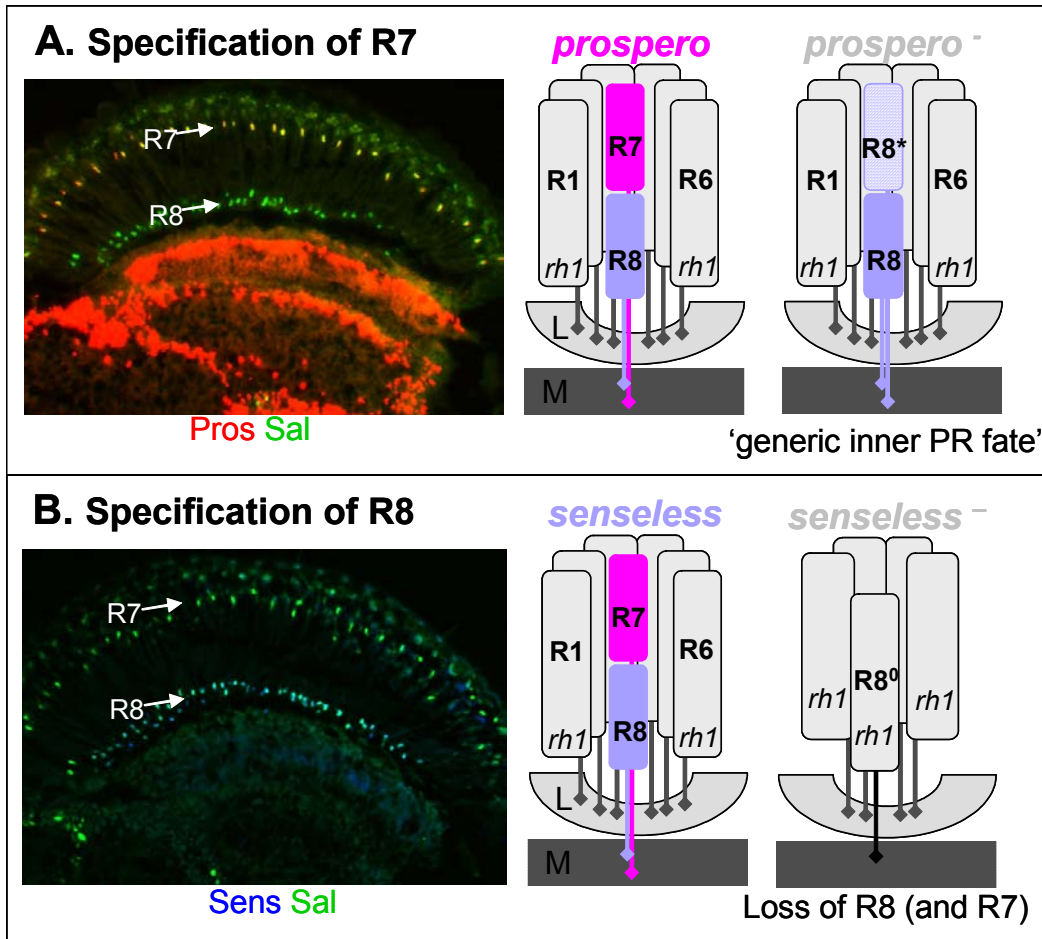
Fig II.8 Distinguishing between R7 and R8 cell fates
(A) The transcription factor Prospero (Pros) is expressed specifically in R7 cells, as seen on frozen sections double labeled for Pros (red) and Sal (green). Only R7 cells co-stain for Pros and Sal (top arrow). Loss of Pros results in R7 cells losing their typical adult characteristica (opsin expression, nuclear position - not shown); instead, these cells now resemble R8 cells (R8*; bottom, right). This suggests that Pros is necessary to distinguish the fate of R7 cells from an R8-like 'generic inner PR fate', in particular by repressing R8 opsin expression.
(B) The transcription factor Senseless (Sens) is expressed specifically in R8 cells, as seen on frozen sections double labeled for Sens (blue) and Sal(green). Only R8 cells co-stain for Sens and Sal (bottom arrow). Loss of Sens results in the R8 cell developing into an outer PR (R^0); consequently, R7 cells never get specified due to the lack of the Boss signal.

(-/-) PRs (Domingos et al., 2004). This suggested that inner PRs undergo a series of consecutive determination steps, by gaining expression of different combinations of transcription factors. It appears therefore that R7 cells (Sal + Pros) and R8 cells (Sal + Sens) are the products of such a combinatorial code.

9. Dorso-ventral development of the *Drosophila* eye

All developing *Drosophila* ommatidia rotate by 90 degrees. Interestingly, the clusters rotate into opposite directions in the ventral and dorsal half of the eye

(**Fig 9A**; (Cooper and Bray, 1999); for review: Strutt and Strutt, 2003). In the adult eye, two compartments can therefore be distinguished within which all chiral ommatidia point towards the nearest pole (**Fig 9B**; (Tomlinson and Struhl, 1999). Ommatidia of the dorsal and ventral compartments meet at a sharp
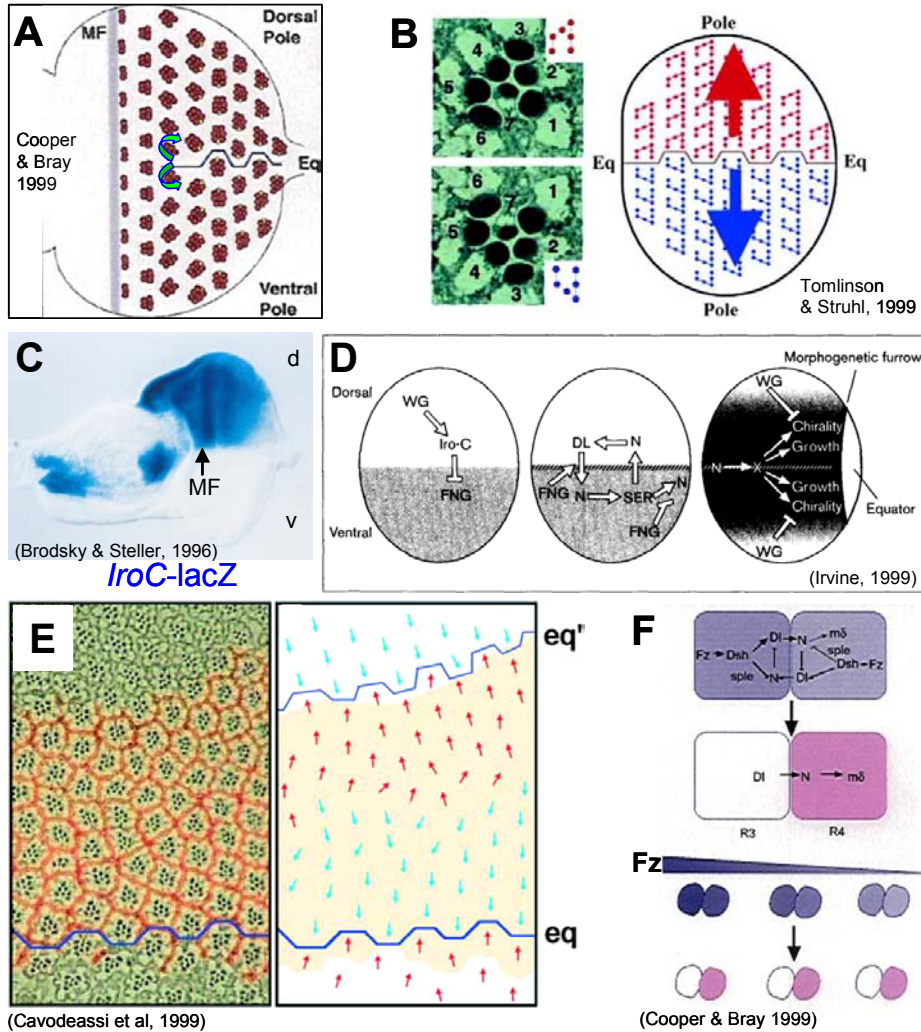
Fig II.9 Dorso-ventral development of the *Drosophila* eye

(A)+(B) Larval ommtidia rotate by 90 degrees. Dorsal and ventral ommatidia rotate in opposite directions (blue arrows). The two ommatidial forms meet at the ventral midline, the equator (Eq). (B) Left: Dorsal ommatidia point with R3 towards the dorsal pole (up), while ventral ommatidia point with R3 towrds the ventral pole (bottom). Dorsal ommatidia (red) and ventral ommatidia (blue) have opposite chirality. Right: In the wildtype, all ommmtidia on either side of the equat have the same chirality.

(C) Expression of the *IRO-C* complex is specific to the dorsal compartment. Thord instar larval eye disc from flies carrying a lacZ enhancer trap in IRO-C. βGal activity is specific to the dorsal half of the developing eye (d=dorsal, v=ventral, MF=morphogenetic furrow).

(D)+(E) The *IRO-C* complex is essential for generating the equator. *IRO-C* contributes to generating Notch (N) pathway activity a the equator, by restricting *fringe* (*fng*) expression to the ventral eye. N activity is crucial for establishment of ommatidial polarity as well as eye growth. The *wingless* (*wg*) pathway represses growth from the poles (DL=Delta, SER=Serrate). (E) Ectopic equators form at the boundary of IRO-C (-/-) clones.

(F) The N pathway serves as an amplification system in R4, to read small local differences in the Wg morphogen gradient (= Frizzled/Fz receptor activity gradient). N responsive genes (mδ) get specifically activated in R4 (dsh=disheveled).

boundary at the midline of the adult eye, called the equator (Eq). Very early during eye development, the undifferentiated cells of the *Drosophila* eye imaginal disc anterior to the morphogenetic furrow are subdivided into dorsal and ventral compartments. The dorsal selector genes *araucan (ara)*, *caupolican (caup),* and *mirror (mirr)* encode homologous homeodomain transcription factors and form the *Iroquois* complex (*IRO-C;* for review, see (Cavodeassi et al., 2001). During early larval stages these genes become specifically expressed in the territory that will give rise to the dorsal eye and head capsule (**Fig 9C**; (Brodsky and Steller, 1996). The *IRO-C* complex is activated very early during eye development by the diffusible morphogen Wingless *(wg*; (Lee and Treisman, 2001)*.* At this stage, the most important function of *IRO-C* is the repression of the gene *fringe*, whose expression is thereby limited to the ventral eye tissue (**Fig 9D** left; for review: Irvine, 1999). This was shown to be crucial for the generation of localized Notch (N) pathway activation at the developing equator, through a complicated interplay of the proteins Fringe, Serrate and Delta (center). N activity at the equator is essential for both growth of the eye as well as for the establishment of ommatidial polarity (right; (Cho and Choi, 1998). At later stages, *wg* expression becomes restricted to the peripodial membrane at the dorsal and ventral poles of the imaginal disc, from where the Wg morphogen is believed to form two gradients towards the equator (Heberlein et al., 1998; Treisman and Rubin, 1995). The *IRO-C* complex is therefore particularly important for dorsoventral development and ectopic equators form at the border of clones of eye tissue lacking *IRO-C* function (**Fig 9E**; (Cavodeassi et al., 1999; McNeill et al., 1997). The interplay of the *N* and *wg* pathways during the establishment of ommatidial polarity has been studied in great detail. In this context, the two outer PRs R3 and R4 proved to be a particularly interesting model system, as their position within the ommatidium determines its chirality. Using sophisticated *Drosophila* genetics, the *N* pathway was shown to serve as an amplification system in R4 that allows the decoding of tiny local differences in the Wg gradient over the distance of only one cell diameter (**Fig 9F**). Important *wg* pathway components like the receptor Frizzled and the effectors Armadillo, Disheveled and TCF were

shown to be required in this process, as well as the N pathway components mδ and suppressor of Hairless / su(H) (Cooper and Bray, 1999); for review: Irvine, 1999). Mutations in these genes will be used in this report, to test a possible role of the *N* and *wg* pathways during ommatidial subtype specification.

10. The current model for ommatidial subtype specification

Outside of the DRA, **p** and **y** ommatidia are found in a ratio of 30:70, distributed randomly through the fly retina (Chou et al., 1996; Fortini and Rubin, 1990; Franceschini et al., 1981). Although an elegant model has been proposed to explain the distribution of M and L cones in humans (Nathans, 1999), it is still not clear how stochastic choices are made between different PR cell fates in humans, or in flies. Nevertheless, two simple mutant backgrounds were used in *Drosophila* to build a mechanistic model describing the instructive signals specifying **p** and **y** ommatidia. In the absence of R7 cells (*sevenless*), R8 cells always express the **y**R8 opsin *rh6* (Banerjee et al., 1987; Hafen et al., 1987; Tomlinson et al., 1987). It was therefore proposed that *rh6* represents the 'ground state opsin' expressed in R8 cells (**Fig 10A;** (Chou et al., 1999). Furthermore, a signal from those R7 cells that have chosen to express the **p** opsin *rh3* (**p**R7) is necessary for R8 to acquire the **p** fate (*rh5*). Chou and colleagues (1999) have further elaborated on this model; they generated adult ommatidia lacking R8 cells and found that both *rh3* and *rh4* were expressed randomly in the R7 cells of these retinas, suggesting that R8 is not necessary for the stochastic choice to occur in R7 cells. Similarly, when several R7 cells were induced within one ommatidium (*seven-up*), these extra R7 were found to choose randomly between the **p** and **y** fates (Chou et al., 1999; Mlodzik et al., 1990); **Fig 10B**). The model for stochastic specification of **p** and **y** ommatidia that was drawn from these experiments can therefore be divided into two steps (**Fig 10C**). First, the stochastic, but biased choice between **p** and **y** fates appears to be made in R7 cells (left), which then impose the corresponding fate onto the underlying R8 cells (right; (Chou et al., 1999). The result is the fly color vision system: a mosaic of two ommatidial subsets with the R8 cells exhibiting highest

spectral sensitivity in the blue (**p**) or green (**y**) part of the spectrum, comparing their inputs with UV-sensitive R7 cells.

A. no R7 cells

B. extra R7 cells

C. Model: specification of color ommatidia
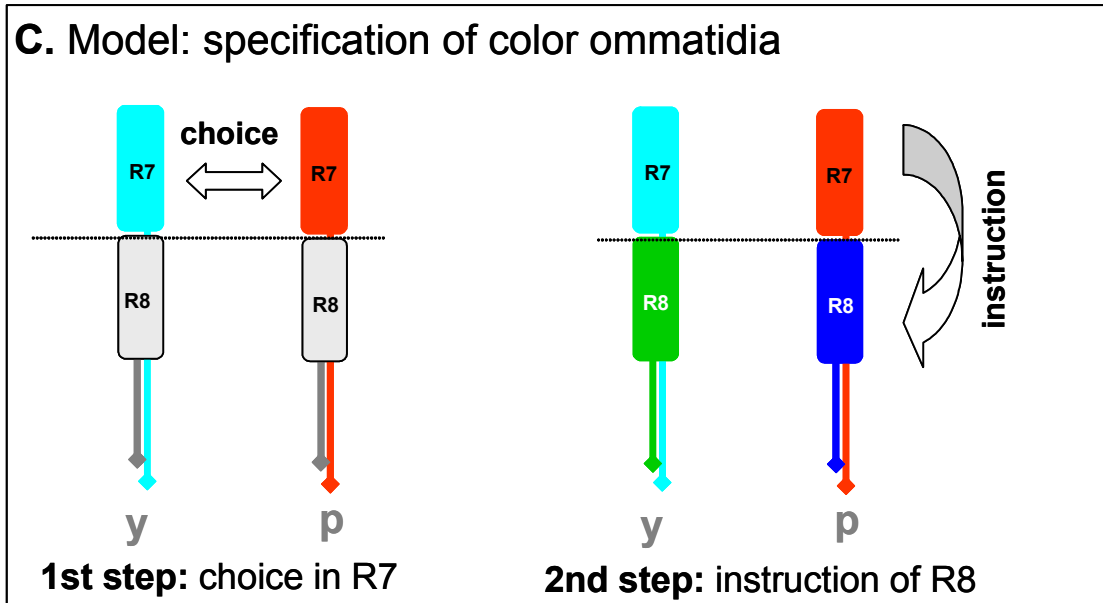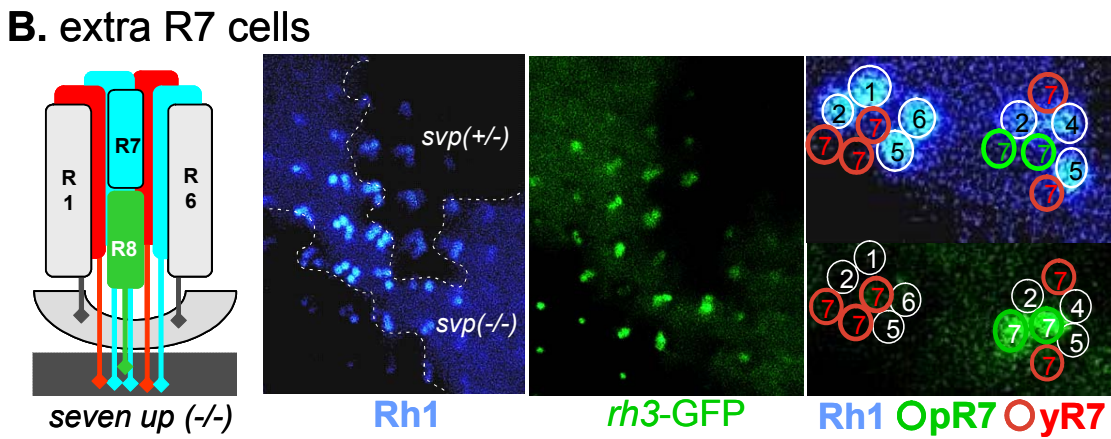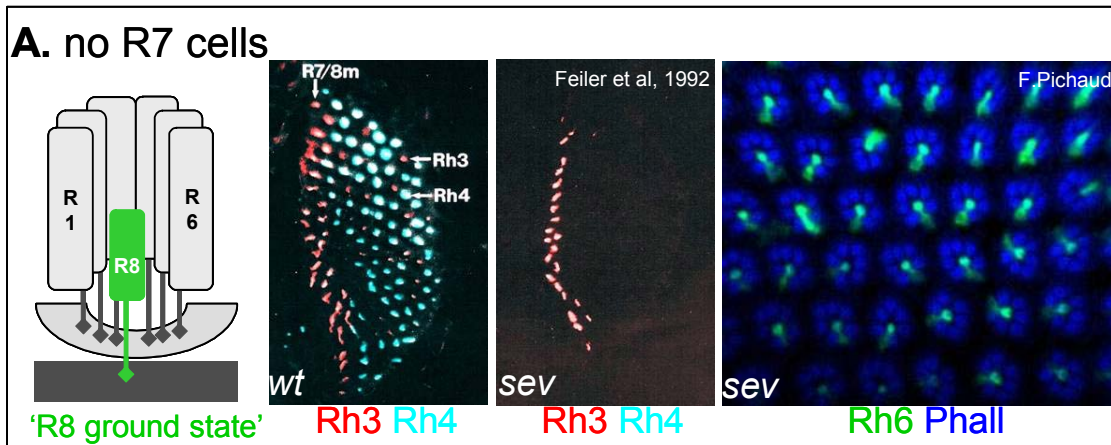
Fig II.10 The current model for ommatidial subtype specification
(A) R8 cells express *rh6* in *sevenless* mutants. Left: schematic representation of the sev mutant situation. R7 cells are not specified due to the inability to receive the boss signal from R8. Center: In the wildtype, Rh3 (red) and Rh4 expression (cyan) are found distributed stochastically through the retina, while DRA inner PRs (R7/R8m) always express Rh3. In sev mutants, however, Rh4 expression is completely gone and only R8m expression of Rh3 persists (Feiler et al., 1992). Right: Double labeling of whoile mounted adult sev retinas with Ph6 (green) and the rhabdomere marker Phalloidin (blue) reveals expression of Rh6 in all R8 cells. Due to the lack of instruction by R7 cells in *sev* mutants, *rh6* has therefore been called the 'R8 ground state' opsin.
(B) Extra R7 cells choose stochastically between **p** and **y** fates. Left: schematic representation of the seven up (svp) loss-of-fuction phenotype. Loss of svp leads to the specification of extra R7 cells. Center: Mitotic *svp* (-/-) clones induced using the ey-flip/FRT technique. Outer PRs were marked by Rh1 autofluorescence. Co-staining with *rh3*-GFP (green) allows assessing the cell fate decisions within svp(-/-) clones under water immersion. Right: Both pR7 (green circles) as well as yR7 (redcircles) were induced within the same mutant ommatidia, indicating that extra R7 cells choose autonomously.
(C) The current model for specification of color-esensitive ommatidia. The available data on opsin regulation has previously been integrated into a two-step model for **p/y** specification. In a first step, **p** and **y** subtypes get specified in R7 cells (choice). In a second step, this choice gets transmitted to the underlying R8 cell via an unknown signal transduction pathway (instruction).

11. GFP in living flies: the GAL4 enhancer traps screen

A multitude of enhancer trap screens has been performed in *Drosophila*. In most cases, transgenic P-elements carrying the cDNA of a reporter gene (lacZ, GFP, GAL4) under the control of a weak enhancer were remobilized to new, unknown genomic locations (Brand and Perrimon, 1993; O'Kane and Gehring, 1987). The expression pattern of nearby genes was then reproduced by the reporter gene. Recently, we reported a GAL4/UAS-GFP enhancer trap screen to identify new genes expressed in subsets of PRs of the living fly (Mollereau et al., 2000). In this context, the phenomenon of the "deep pseudopupil" was used as a natural amplification system for GFP-expression in PRs. The pseudopupil is a virtual image in the center of the fly eye, which is created by the superimposition of 20-30 ommatidia, due to the curvature of the cornea (**Fig 11A+B**; (Franceschini and Kirschfeld, 1971). By remobilizing a GAL4 P-element, we have shown that living flies could be analyzed in F1 for PR-specific GFP expression in the pseudopupil (**Fig 11C**). By this technique, genes expressed in different photoreceptor cell subsets (inner PR, outer PR or all PR) have been identified in F1 after P-element remobilization, by quickly screening the eyes of anesthetized adult flies under blue illumination (**Fig 11D**). However, as the "deep pseudopupil" is the product of the superimposition of signals emanating from different ommatidia, isolation of genes specifically expressed in **y** or **p** subsets of inner PRs required an additional step in the screening procedure. By neutralizing the refraction of the cornea using water immersion microscopy on
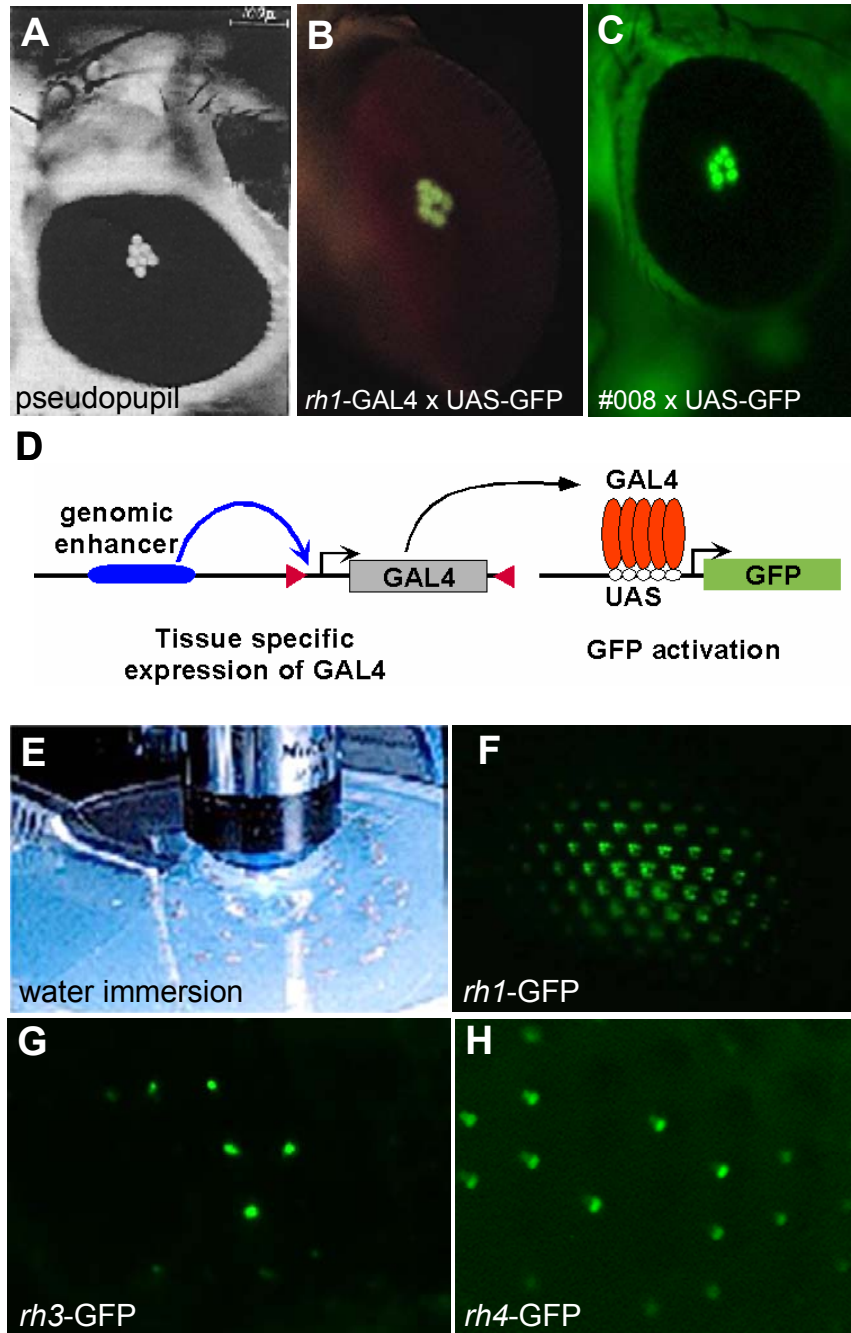
Fig II.11 Expression of GFP in living flies: enhancer traps screen and corneal neutralization
(A)-(C) Deep pseudopupil in the living fly. A virtual image is created in the center of the curved eye, due to the superposition of several neighboring ommatidia. Deep pseudopupil of a fly expressing GFP in outer PRs under the control of rh1-GAL4, visualized by blue illumination. Note that inner PRs – in the center of the trapezoid – are negative. (C) Deep pseudopupil of a GAL4 enhancer trap (#008, see appendix) visualized with GFP under blue illumination. Expression is also specific to outer PRs.
(D) Schematic representation of the GAL4 / UAS-GFP enhancer trap technique. A transgenic P-element GAL4 (red triangles) carrying a GAL4 cDNA (grey box) comes under the influence of a tissue specific genomic enhancer (blue). GAL4 expression (orange) activates GFP (green) *in cis* via binding to pentamerized GAL UAS sites (white circles).
(E)-(H) Cornea neutralization using water immersion microscopy. Anesthetized flies are immobilized in agarose, covered with water and a water immersion objective (20x) is placed onto their eye. Using this technique, signals emanating from single ommatidia can be visualized. Examples are *rh1*-GFP (F), with expression of GFP in R1-R6 in every ommatidium, *rh3*-GFP (G) with GFP being retricted to a small subset of inner PRs and finally *rh4*-GFP (H) with GFP expression in a clearly larger subset of ommatidia.

26

the eyes of living, immobilized flies, the signals emanating from individual ommatidia could be visualized (**Fig 11E**; (Pichaud and Desplan, 2001). In this context, opsin reporter constructs driving the expression of GFP under the control of different opsin promoters (*rh1*-GFP, *rh3*-GFP, *rh4*-GFP) proved to be valuable tools for the investigation of ommatidial subtype specification (**Fig 11F-H**).

III. RESULTS

1. The GAL4 enhancer trap screen

The GAL4 enhancer trap technique was used to identify genes involved in opsin gene regulation and late retinal patterning. Genomic enhancers directing the expression of nearby transcripts in subsets of photoreceptors (PR) were targeted using the GAL4 enhancer trap P-element pGawB (Brand and Perrimon, 1993) and special UAS-GFP reporter constructs (see below). To improve the efficiency of a previously performed GAL4/GFP enhancer trap screen in adult PRs (Mollereau et al., 2000), both the jump start insertion as well as the reporter system were changed. For the jump start, we chose a molecularly mapped, as well as homozygous lethal insertion of pGawB in the gene *apterous* (Bourgouin et al., 1992; Calleja et al., 1996; Cohen et al., 1992). The jump frequency of this line was calculated as being ~12% (M.F. Wernet, Diplomarbeit). To improve the efficiency of the UAS-GFP reporter flies, the „green fluorescent protein" cDNA was fused „in frame" to the last 26 amino acids of the PR-specific kinase NINAC (Montell and Rubin, 1988); M.F. Wernet, Diplomarbeit). Such NINAC fusion proteins have previoulsly been shown to be localized into the PR rhabdomeres, thereby concentrating them in the path of light (Porter et al., 1992). When driven under UAS-control, these reporters were significantly (~2-fold) more effective as the original UAS-GFP system (M.F. Wernet, Diplomarbeit).

Large numbers of flies (> 500'000) were generated (for the crossing scheme, see materials and methods), about ~3% of which carried new, stable insertions of pGawB at unknown genomic locations. Due to the nature of this phenotypic F1 enhancer trap screen, only a subset of new insertions was detectable: ~20% of all 13 000 genes are believed to be expressed in the eye (Mollereau et al., 2000). Furthermore, only those lines showing striking expression of GAL4/GFP:NinaC in PRs were retained. This allow us to keep the number of retained stocks extremely low, but it also made a more detailed statistical analysis of the enhancer trap screen impossible.

line#	*inserted near gene…*	nature of trapped gene	expression pattern	chr.	map pos.
002	*CG14408*	SH3 domain binding protein	inner PR specific	**X**	**12F7**
008	*19F-20A*	Unknown, inserted in repetitive sequences	beautiful outer PRs	**X**	**19F**
010	*Elbow*	transcription factor (Zn-finger)	subsets of inner PRs	**2**	**35A1**
012	*α-Man-IIb*	mannosyl-oligosaccharide 1,3-1,6-α-mannosidase	all PRs	**3**	**89A**
013	*CG9602*	ubiquitin conjugating enzyme	lamina and ocellar lobe	**3**	**87F**
015	*CG2991*	EGF-domain containing protein	very weak all PRs	**2**	**23B**
016	*rh1*	outer PR opsin	outer PRs + ocelli	**3**	**92B**
021	*Kekkon-1*	TM molecule, negative regulator of DER signaling	all PRs	**2**	**34A**
022	*slamdance*	alanyl (membrane) aminopeptidase	outer PRs	**3**	**97D6**
030	*Dlats*	Ser-/Thr-kinase involved in cell-cycle regulation	subsets of inner&outer PRs	**3**	**100A**
033	*no ocelli*	transcription factor (Zn-finger)	subsets of inner PRs	**2**	**35A4**
040	*dachsous*	Cadherin-family TM cell-adhesion molecule	ocelli	**2**	**21CD**
041	*rdgB*	Ca-transporting ATPase	all PRs	**X**	**12B8**
043	*CG30159*	No homolgies	inner PRs and cone cells	**2**	**42D**
046	*CG4449*	Ubiquitin-like	very weak inner PRs	**3**	**94E**
053	*homothorax*	homeodomain transcription factor	DM inner PRs	**3**	**86BC**
056	*CG32767*	DNA binding	very weak inner PRs	**X**	**4D5**
058	*PRK2*	*CG2049, a* novel PKC family kinase	all PRs	**2**	**45C**
062	*Tsp42Ec*	cell-surface molecule of the tetraspan family	very weak all PRs	**2**	**42E**
063	*CG10600*	predicted nuclear protein	outer PRs	**2**	**37B**
069	*bunched*	transcription factor, TSC22-homologue	weak PRs, strong dorsally	**2**	**33E**
072	*Slit*	Robo ligand, inner PR specific	inner PRs	**2**	**52D**
073	*combgap*	transcription factor with 10 Zn fingers	all PRs	**2**	**50E**
075	*hybrid male rescue*	transcription factor	subset of antenna cells	**X**	**9D2**
077	*CG6424*	nuclear; homologue of human KIAA0914	very weak PRs	**2**	**54E3**
078	*CG30428*	No homologies	weak PRs	**2**	**60F3**
092	CG6241	Metalloendopeptidase	lamina and ocellar lobe	**3**	**85F**
098	CG6499	predicted (methyl) ammonium transporter	subset of antennal cells	**3**	**88E**
100	*l(3)06951*	no gene near GAL4 promoter, but lethal P l(3)06951	second antennal segment	**3**	**88C5**
103	CG5735	RRM domain RNA binding protein	all PRs	**3**	**66E4**
112	CG14045	Cdc42 RhoGEF, PDZ domain, C2 domain	R7 cells	**X**	**2F6**
114	CG14186	No homologies	PRs,inners very strong	**3**	**76F2**
116	*Lama*	"lamina ancestor"; no homologies	Ocelli, optic lobes	**3**	**64D2**
123	*no ocelli*	transcription factor (Zn-finger)	subsets of inner PRs	**2**	**35A4**
128	*CG11732*	odorant binding protein 85b	Inner PRs and CCs	**3**	**85A1**
129	*unknown*	Repetitive sequences; copia element	Weak PRs	**?**	**?**
134	CG7145	δ-1-Pyrrolidine-5-Carboxylate Dehydrogenase)	weak PRs	**3**	**79A5**
137	CG2264	EF-hand cell adhesion molecule	ocelli	**2**	**46D8**
139	*CG3130*	Immunoglobulin protein	**All PRs**	**3**	**99C7**
141	*methuselah-like 8*	G-protein coupled receptor	PRs, strong DRA	**3**	**61A1**
142	*no ocelli*	transcription factor (Zn-finger)	subsets of inner PRs	**2**	**35A4**
145	*Coronin*	Actin binding	Inner PRs + PCs	**2**	**42D4**
147	*Lola*	"longitudinals missing"; Zn-finger TF	All PRs, weak	**2**	**47A9**
148	*polyhomeotic*	"polyhomeotic distal"	Weak PRs	**X**	**2D1-5**
149	*Unknown*	inserted in repetitive sequences	inner PRs and retina	**1,2,3**	**?**
154	*CG6024*	LDL-receptor ligand binding domain protein	All PRs	**3**	**68D1**
155	*Gilgamesh*	*drosophila* casein kinase I	All PRs	**3**	**89B17**
156	*RhoGAP18b*	no homologies	outer PRs	**X**	**18B2**
158	CG1847	Tetraspan TM protein	Inner PRs?	**2**	**42D5**
163	CG8005	Deoxyhyposine synthase	All PRs?	**3**	**66C1**
173	*Doa*	"darkener of abricot", LAMMER kinase	R7 cells	**3**	**98F1**
175	CG14408	SH3 domain binding protein	inner PRs	**X**	**12F7**
181	*no ocelli*	Zn finger transcription factor	Inner PRs	**2**	**35A4**
184	*Mindmelt*	nuclear Cys3His-type zinc-finger protein	inner PRs and cone cells	**2**	**54B8**
185	CG3927	RNA-binding; p62 tumor suppr. homologue	All PRs	**2**	**58E10**
186	*Stich1*	RNA polymerase II transcription factor	Inner PRs and CCs	**3**	**86B1**
190	*Syndecan*	Cytoskeletal anchor protein	All PRs	**2**	**57D11**
193	CG31038	Immunoglobulin protein	strong all PRs	**3**	**99C7**
194	*RhoGAP18b*	Predicted GTPase activating protein	All PRs?	**X**	**18B2**
196	*methuselah-like 8*	G-protein coupled receptor	Inner PRs	**3**	**61A1**
197	*Mindmelt*	nuclear Cys3His-type zinc-finger protein	Inner PRs and cone cells	**2**	**54B8**

Table III.1: enhancer trap lines retained from the pGawB/UAS-GFP screen.

61 lines were molecularly mapped based on their expression pattern in photoreceptors or the optic lobes.

About ~200 individual insertion lines showing interesting GAL4/GFP expression in adult PRs were retained for further characterization (for a short summary, see **Appendix**). Out of these lines, 61 P-elements were localized molecularly by „inverse PCR" (see **Table III.1**; materials and methods).

The targeted genes fell into different functional categories (**Table III.2**). Very large fractions were nuclearly localized genes / transcription factors (27%) and cell surface proteins (receptors, transporters; 24%). Howeverer, cytoplasmatic proteins (signal transduction molecules, cytoskelletal proteins), kinases and other enzymes represented an even larger fraction (30%), when grouped together. Only three genes were identified that encoded secreted / extracellular proteins (5%). Finally, 14% of the genes (N=8) either did not map near a known (or predicted) gene, were inserted in repetitive genomic sequences or their transcript manifested no homologies to previously characterized genes.

Gene product	N (genes)	%	Enhancer traps
Nuclear / TF	15	27	10, 33 (123, 142, 182), 53, 56, 63, 69, 73, 75, 77, 103, 147, 148, 184 (197), 185, 186
Kinase	4	7	30, 58, 155, 173
cytoplasmic	7	13	02 (175), 46, 056 (194),112, 145, 190
Enzyme	5	9	12, 13, 92, 134, 163
cell surface / receptors	13	24	16, 21, 22, 40, 41, 62, 98, 137, 139, 141 (196), 154, 193
Extrcellular	3	5	15, 72, 128
no homologies / annotation	4	7	43, 78, 114, 116
Unknown gene product	4	7	08, 100, 129, 149

Table III.2: Screen results: targeted genes grouped into functional categories.
The total number of genes listed is lower than the number of enhancer traps retained, as several genes were targeted multiple times independently. More than half of the identified genes (51%) were either nuclear proteins (transcription factors) or cell surface molecules (cell surface receptors).

It was therefore concluded that the GAL4/GFP screen in living flies represented a powerful tool to identify genes specifically expressed in adult PRs. The identified genes fall into all major protein classes, none of which was significantly under-represented (for review: Celniker and Rubin, 2003). The sensitivity of the gene identification system was therefore not limited to a subgroup of potential targets, like strongly expressed structural proteins.

2. Specification of the polarization sensitive ommatidia in the 'dorsal rim area'

2.1. A GAL4 enhancer trap insertion in *homothorax*

One of the insertions of the P-element pGawB (line #053, see appendix) was studied in greater detail due to its particularly interesting expression pattern. When crossed to UAS-GFP reporter flies, strong expression was visible in the antennae as well as in the proboscis and the body of the fly (**Fig 1A** and **1B**). When viewed from the side, no GFP expression was detectable in the eye, especially not in PRs as there was no GFP-signal in the pseudopupil (see material and methods). However, when viewed from the top, strong GFP expression was detected in the pseudopupil of both eyes, when looking close to the head tissue (white arrows in **Fig 1C**). GFP staining disappeared when the fly was moved so that the pseudopupil formed further away from the dorsal margin of the eye. No GFP pseudopupil was detectable at the ventral rim. As the pseudopupil is an optical phenomenon based on the superposition of the individual signals coming from a population of ~20 neighboring ommatidia it was concluded that only ommatidia in the dorsal periphery of the adult eye expressed GAL4 (Franceschini and Kirschfeld, 1971b; Pichaud and Desplan, 2001).

Genomic sequences flanking the P-element #053 were identified by nested inverse PCR (**Fig 1D**, see material and methods). A BLAST search, using 224 bp of genomic sequence (shown in black letters), was performed at the Berkeley Drosophila Genome Project (BDGP). The BLAST search resulted in an unambiguous molecular localization of the P-element insertion site (**Fig 1E**). Insertion #053 was found to be inserted in intron 3 of the gene *homothorax* (*hth*) which encodes a TALE-class homeodomain transcription factor (Pai et al., 1998; Rieckhof et al., 1997); Pai et al., 1998).

Neutralization of the cornea by using water immersion microscopy in living flies (Franceschini and Kirschfeld, 1971a); (Pichaud and Desplan, 2001) revealed that *hth*-GAL4 was expressed in a single row of ommatidia along the dorsal head
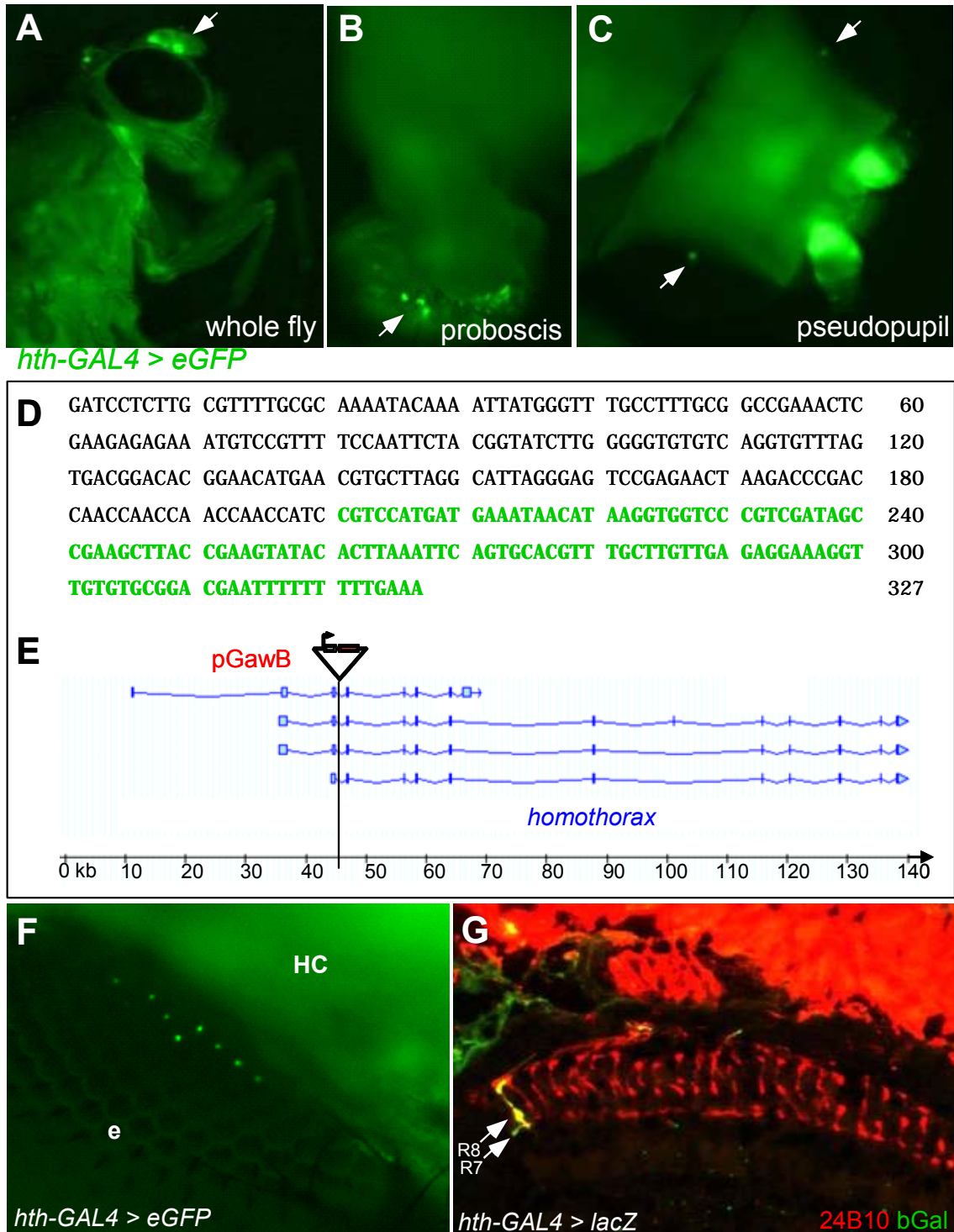
FigIII.2.1 A GAL4 enhancer trap insertion in *homothorax*
(A)-(C) Expression of *#53*-GAL4 in a living anesthetized fly: #53-GAL4 expression visualized with UAS-GFP constructs. Strong expression was observed in the antenna (A) and the proboscis (B). (C) A pseudopupil signal was only detectable when flies were observed from above (white arrows), suggesting that only PRs at the dorsal rim of the eye expressee GAL4. (D) Genomic DNA sequence flanking #53-GAL4 at the 3' end, obtained by inverse nested PCR. P-element sequences are shown in green. (E) Schematic diagram of the pGawB insertion #53 localized in the *homothorax* (*hth*) gene, encoding a homeomdomain transcription factor. (F) Expression of *hth*-GAL4 (*#53*-GAL4) in living flies: Individual ommatidia in the DRA of a living fly were visualized using cornea neutralization by water immersion microscopy. Combining *hth*-GAL4 and UAS-GFP transgenes allowed detection

cuticle in the adult eye (**Fig 1F**). At most dorsal locations, two (but never more) positive rows of ommatidia were observed (data not shown). Changing the reporter to UAS-lacZ (Brand and Perrimon, 1993) allowed the visualization of the projections of GAL4-positive cells to the optic lobe (**Fig 1G**). Frozen sections (10 µm) through adult heads (*hth*-GAL4 > UAS-lacZ) were double labeled with antibodies against βGal and the PR-specific cell-surface antigen 24B10 (Chaoptin; (Van Vactor et al., 1988). All βGal-expressing axons (shown in green) terminated at the dorsal-most edge of the medulla (marked in red) with projections to both R7 and R8 layers (white arrows). Projections to the lamina, where outer PRs project their axons, were never observed. It was concluded that *hth*-GAL4 was expressed exclusively in inner PRs located at the dorsal rim of the adult eye.

2.2. Inner photoreceptors in the DRA express Homothorax

To verify that the observed GAL4 expression pattern in developing DRA inner PRs was indeed that of endogenous Hth protein, pupal retinas (~48 hours after puparium formation, APF) were dissected. These were then double stained with antibodies against Hth and the the neuronal marker ElaV (**Fig 2A**). A band of Hth-positive ommatidia (shown in green) was visualized in the dorsal half of the developing eye. Hth expression was always detected in one, at most two rows of ommatidia and only at the dorsal rim of the pupal retina. This observed expression pattern was highly reminiscent of the well-described ommatidia of the 'dorsal rim area' (DRA, **Fig 2B**; for review:(Labhart and Meyer, 1999; Labhart and Meyer, 2002). A *lacZ* enhancer trap insertion in the gene *seven-up* (*svp*-lacZ is strongly expressed in the photoreceptors R3 and R4 and only faintly in R1 and R6 at these later stages; (Mlodzik et al., 1990b) was introduced as a reference to allow identification of the Hth-positive PRs (**Fig 2C**). Triple labeling using antibodies against Hth, βGal and ElaV was performed on pupal retinas (48 hrs APF). The majority of ommatidia located in the two dorsal-most rows expressed Hth in two cells per cluster, which were identified as R7 and R8 because of their stereotypical positioning as compared to the landmark *svp*-lacZ (for review:
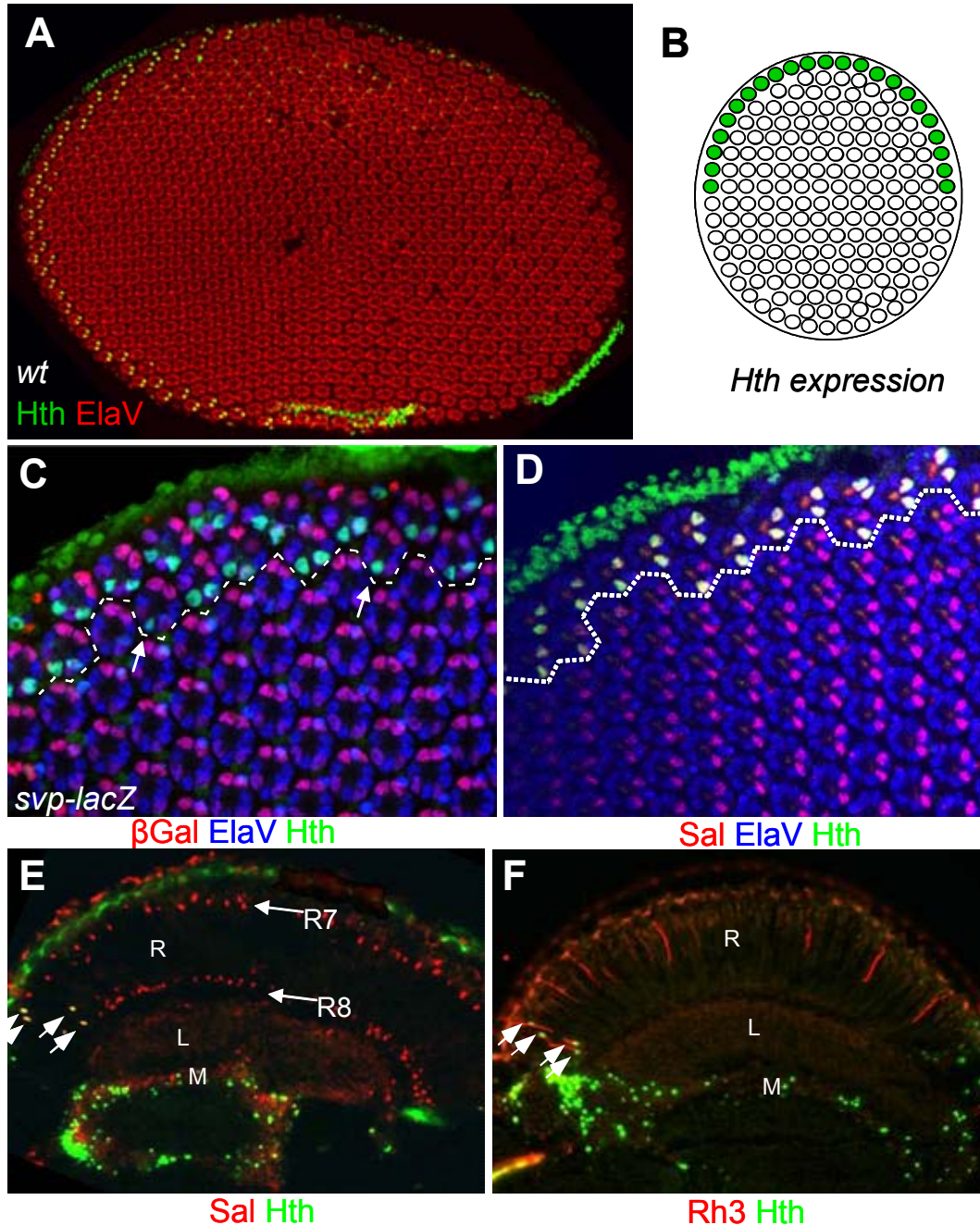
Fig III.2.2 Inner photoreceptors in the DRA express Homothorax

(A) Expression of Hth in pupal PRs: Flat mounted pupal retinas (~48 hrs after puparium formation, APF) dissected from wildtype flies. Double-labeling of ElaV (blue) and Hth (green) showed specific expression of Hth in one row of ommatidia at the dorsal rim. A sharp boundary between DRA and non-DRA ommatidia was always observed. (B) Schematic representation of Hth expression in the pupal retina (dorsal is up). This expression pattern was highly reminiscent of the DRA ommatidia.

(C)+(D) Hth is specifically expressed in R7 and R8 at the dorsal rim: Flat mounted pupal retinas (~48 hrs APF). Using the *svp*-lacZ landmark (weak expression in R1 and R6; strong expression in R3 and R4), triple-labeling of ElaV (blue), Hth (green) and βGal (red) revealed Hth expression to be specific to R7 and R8 cells in DRA ommatidia (dashed line). (D) Specific expression of Hth in inner PRs of the DRA (dashed line) was confirmed by triple-labeling ElaV (blue), Hth (green) and the inner PR marker Spalt (red), expressed in all R7 and R8.

(E)+(F) Expression of Hth in the adult DRA: Frozen sections Frozen sections (10 μm) along the D/V axis (D to the left) through adult heads of *yw* flies (R= retina, L= lamina, M=medulla). Hth (green) was always found co-expressed with the inner PR marker Sal (red), expressed in R7 and R8 (white arrows). (F) Frozen sections through adult *yw* heads (R= retina, L= lamina, M=medulla). Double labeling of the DRA rhodopsin Rh3 (red) and Hth (green) revealed specific co-expression in DRA inner PRs (arrows).

35

(Wolff, 1993). Ommatidia with only one Hth expressing cell per ommatidium could also rarely be observed (white arrows) without showing any obvious preference towards R7 or R8. To confirm this result, pupal retinas were also triple stained using antibodies against the inner PR marker Spalt (Sal), Hth and ElaV (**Fig 2D**). Hth-positive PRs (shown in green) always co-stained with Sal (shown in red) which was also expressed in Hth-negative ommatidia throughout the rest of the retina. It was concluded from these experiments, that Hth is specifically expressed in both inner PRs R7 and R8 in one or two rows of ommatidia located at the dorsal margin of the developing retina.

Characterization of Hth expression in PRs was concluded by staining of frozen sections (10 µm) through adult heads of wildtype flies. First, a double labeling with Anti-Sal and Anti-Hth was performed (**Fig 2E**). This staining revealed that in the adult, Hth (shown in green) also co-localized with the inner PR marker Sal (shown in red). Hth expression was therefore maintained in dorsal-most inner PRs throughout adulthood. Finally, another staining of Anti-Hth was performed, double labeling with an antibody against the R7 opsin Rh3, which is the only rhodopsin expressed by both inner PRs of the DRA (Fortini and Rubin, 1990); **Fig 2F**). It was observed that inner PRs of the DRA (marked by Rh3 in red) always co-expressed Hth (shown in green), whereas Rh3-expressing pale R7 cells outside of the DRA were always negative for Hth (white arrows).

It was concluded from these experiments, that Hth is a highly specific marker for the developing inner PRs in the DRA, as well as for the terminally differentiated polarization-sensitive inner PRs of the adult DRA.

2.3. Molecular characterization of the DRA

In order to better understand the possible signaling pathways involved in DRA development, the time-course of Hth expression in PRs was characterized. The role of *hth* in early eye development has been studied in detail. However, *hth* expression has never been detected in developing PRs of third instar eye imaginal discs (Pichaud and Casares, 2000); (Bessa et al., 2002). Instead, Hth expression has been shown in un-differentiated cells anterior to the MF as well

36

as in non-neuronal 'posterior progenitor cells', which give rise to pigment cells (Pichaud and Casares, 2000).

The absence of Hth expression in larval PRs was confirmed by dissecting third instar larval eye imaginal discs and double labeling them with antibodies against Hth and ElaV (**Fig 3A**). No co-staining between Hth (shown in green) and ElaV (shown in blue) was detectable. Early pupal retinas (~ 24 hrs APF) were also dissected and stained for Hth and ElaV (**Fig 3B**). This staining revealed strong expression of Hth in both inner PRs of the the DRA ommatidia (white arrows) at this early pupal stage (rarely, only one positive cell was observed), where it remained expressed until adulthood. Additionally, weaker expression of Hth was detectable in pigment cells. This pigment cell expression of Hth was transient, following a wave-like pattern, with no detectable Hth expression remaining in these cells after 50% pupation. As previously described for Hth and Rh3 expression in the adult DRA, a sharp boundary between Hth-positive ommatidia and those in the rest of the eye was always observed throughout DRA development. Finally, mid-pupal retinas (48 hrs APF) were dissected. Using the asymmetric expression pattern of *svp*-lacZ as well as the symmetric distribution of ommatidia on either side of the equator, we assessed the extent of the DRA these retinas (**Fig 3C**). Triple labeling of Hth, *svp*-lacZ and ElaV revealed that Hth expression (shown in green) extended from the posterior end of the equator (marked with a straight line) all the way to the dorsal pole of the eye and continued to the anterior limit of the equator, therefore spanning the entire rim of the dorsal compartment. This contrasts with the more restricted DRAs that have been described for most insect species (for review: Labhart and Meyer, 1999). It was found that, in most of the cases, Hth expression was excluded from the most equatorial ommatidia (anterior and posterior) of the dorsal compartment (white arrow), indicating that equatorial ommatidia bear information which excludes DRA formation. In fact, these ommatidia at the equator are made of cells that come from both dorsal and ventral compartments. It was concluded that Hth expression could be used to characterize the extent of the DRA, which appears rather large in *Drosophila*. Expression of Hth in DRA inner PRs had its onset very
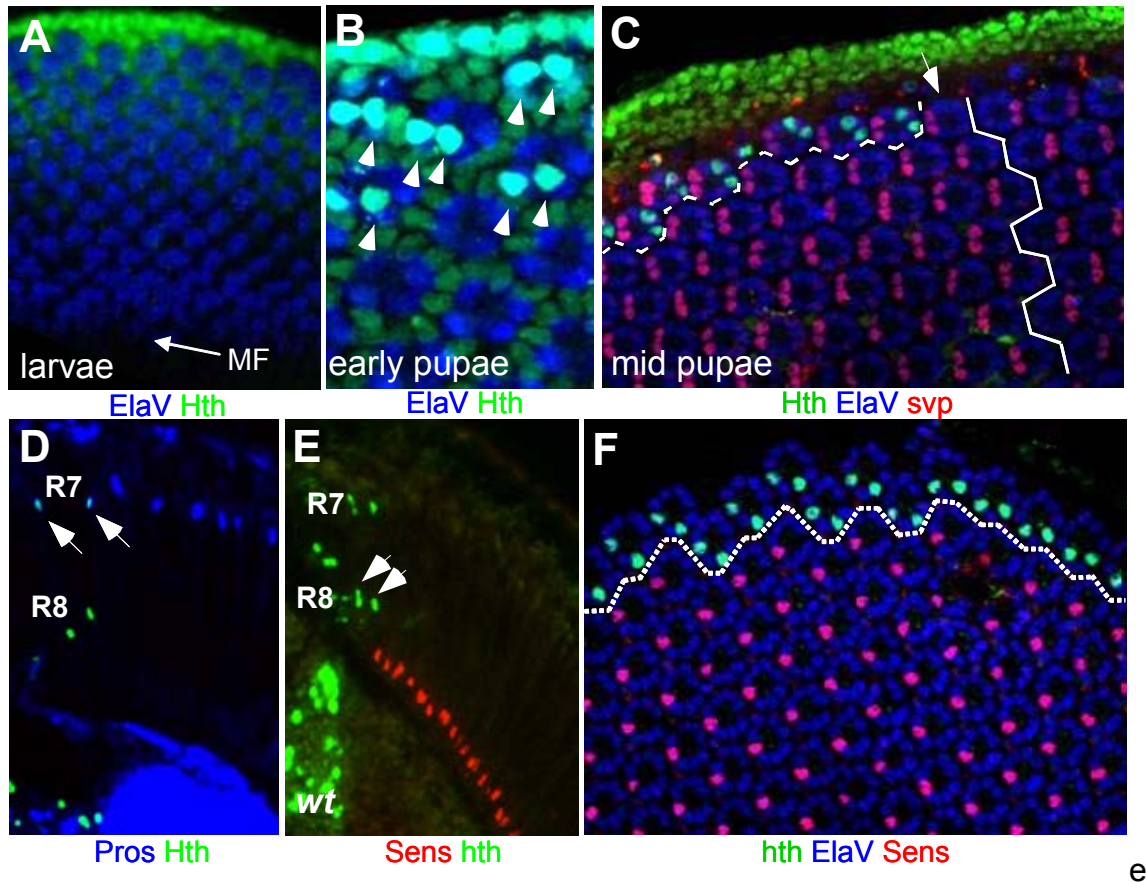
Fig III.2.3 Molecular characterization of the DRA

 (A)-(C) Characterization of DRA development using Hth: Whole mounted larval third instar eye disc (anterior to the left) stained with antibodies against Hth (green) and ElaV (blue). Hth is not detectable in PRs at this stage, but in non-neuronal posterior cells. (B) Early pupal Hth expression in the DRA and in pigment cells: Flat mounted pupal retina dissected from *yw* flies. Double-labeling of ElaV (blue) and Hth (green) revealed two rows of developing DRA ommatidia with inner PRs co-expressing Hth and ElaV (arrow heads) and additional Hth staining in pigment cells surrounding all PR clusters (DRA and non-DRA). (C) The DRA does not cross the equator of the eye: Flat mounted pupal retina (~48 hrs APF). Triple-labeling of ElaV (blue), Hth (green) and *svp*-lacZ (red) revealed one row of developing DRA ommatidia (dashed line) in the dorsal half of the eye, stopping one cluster before the equator (white line).

(D) R7 cells in the DRA co-express Pros and Hth: Frozen sections (10 µm) along the D/V axis (dorsal to the left) through adult *yw* heads. Double labeling of the R7 marker Prospero (blue) and Hth (green) revealed co-expression only in DRA R7 cells.

(E)-(F) Exclusion of the R8 marker Senseless from the DRA: Frozen sections (10 µm) through adult heads. Double labeling of the R8 marker Senseless (red) and *hth*-lacZ (green) revealed specific exclusion of Sens expression from DRA R8 cells as well as an elevated position of the DRA R8 nuclei (arrows). (F) Flat mounted pupal retina (~48 hrs APF). Triple-labeling of ElaV (blue), Hth (green) and Sens (red) revealed specific exclusion of Sens from R8 cells located within the DRA (dashed line).

arly during pupation and remained expressed there, whereas pigment cell expression vanished during late pupation.

The molecular Characterization of the DRA was extended by focusing on the individual cell fates of R7 and R8 cells in the DRA. First, frozen sections through adult heads from wildtype flies were stained for the R7 marker Prospero (Pros) and Hth (**Fig 3D**). It was found that only R7 cells in the DRA co-stained for both Hth (shown in green) and Pros (shown in blue), whereas R8 cells only

stained for Hth. It was therefore concluded that R7 cells in the DRA are true R7 cells based on the combination of transcription factors they express. Frozen section were also stained with antibodies against the R8-marker Senseless (*sens* or *Lyra*) and co-labeled with a *hth*-lacZ transgene (**Fig 3E**). It was found that R8 cells in the DRA represent a special cell type as *hth*-lacZ positive R8 cells (shown in green) specifically lacked expression of Sens (shown in red) which is expressed by all other R8 cells outside the DRA. To confirm this result, pupal retinas (48 hrs APF) were dissected and triple-labeled with antibodies against *hth-lacZ*, Sens and ElaV (**Fig 3F**). While Sens (shown in red) was expressed in all R8 cells outside of the DRA (marked by a dashed line), it was specifically excluded from the inner PRs of the DRA (marked in green). Taking into account that DRA R8 cells also express an otherwise R7-specific opsin (Rh3) and manifest morphological features not found in non-DRA R8 cells, like the enlarged rhabdomere diameter or the distal position of their nucleus (white arrows), it appears that R8 cells in the DRA are highly atypical. In contrast, DRA R7 cells resemble much more regular R7 cells: Although these cells exhibit special enlarged rhabdomeres, their nuclei are located in the same layer as those of other R7 cells outside of the DRA they express an R7 rhodopsin (Rh3) as well as R7-specific markers like Prospero (Kauffmann et al., 1996; Cook et al., 2003).

It was therefore concluded, that the R8 cell of the DRA can be classified as a new inner PR cell fate, marked by expression of the inner PR marker Spalt, lacking expression of both R7 (Pros) and R8 markers (Sens) and expressing an R7 rhodopsin.

2.4. Development of the DRA

Coordinated inner PR rhodopsin expression in the main part of the fly retina results from a two-step process involving pale versus yellow subtype choice in R7 followed by an instructive signal from R7 to R8 (Chou et al., 1996), 1999; (Papatsenko et al., 1997). It was therefore assessed whether a signal from R7 cells was needed in the DRA for the underlying R8 cells to differentiate properly, by analyzing the development of the DRA in *sevenless* (*sev*) mutants

both molecularly and morphologically (Banerjee et al., 1987; Hafen et al., 1987; Tomlinson et al., 1987).

First, pupal retinas (48 hrs APF) were dissected from *sev* mutants, which lack all R7 cells, and triple stained using antibodies against Hth, the inner PR marker Sal and ElaV (**Fig 4A**). Throughout the retina, only one PR per ommatidium stained for Sal (shown in red) and this cell always co-stained for Hth (shown in green) in the DRA. This suggested that in pupae, the DRA develops normally, although being limited to R8 cells. To test whether the DRA maturated correctly, frozen sections through adult heads of *sev* mutants were double labeled using antibodies against Rh3 and Hth (**Fig 4B**). At the dorsal rim of these eyes, Rh3 (shown in red) and Hth (shown in green) were found co-staining one or two rows of R8 cells, suggesting that the DRA developed normally in these flies. Inner PR rhabdomere morphology was also assessed by performing Epon thin sections on adult heads of *sev* mutants (**Fig 4C**). Light microscopic analysis of these sections revealed that *sev* mutants manifested a sharp boundary (marked by a red line) between DRA ommatidia in which R8 had an enlarged rhabdomere diameter (marked by yellow arrows), and non-DRA ommatidia with narrow R8 rhabdomeres.

It was therefore concluded, that unlike in the main part of the retina, no inductive signal from R7 cells was needed for the DRA R8 cells to correctly differentiate into the DRA fate, as the DRA is present in *sev* mutants based on both molecular, as well as morphlogical criteria.

It has previously been reported that ommatidia at the edge of the eye, which often lack the full complement of photoreceptors and support cells, undergo apoptosis during early pupation (Lin et al., 2004). This cell death was shown to be triggered by the morphogen Wingless and the pro-apoptotic factors *head involution defective* (*hid;(Grether et al., 1995)*. Apoptosis might therefore play a role in defining the correct number of DRA ommatidial rows.

To show that the morphogen Wingless is expressed in the developing head tissue surrounding the developing eye, pupal retinas (48 hrs APF) were dissected and triple stained for a *wg*-lacZ transgene as well as Hth and ElaV (**Fig**
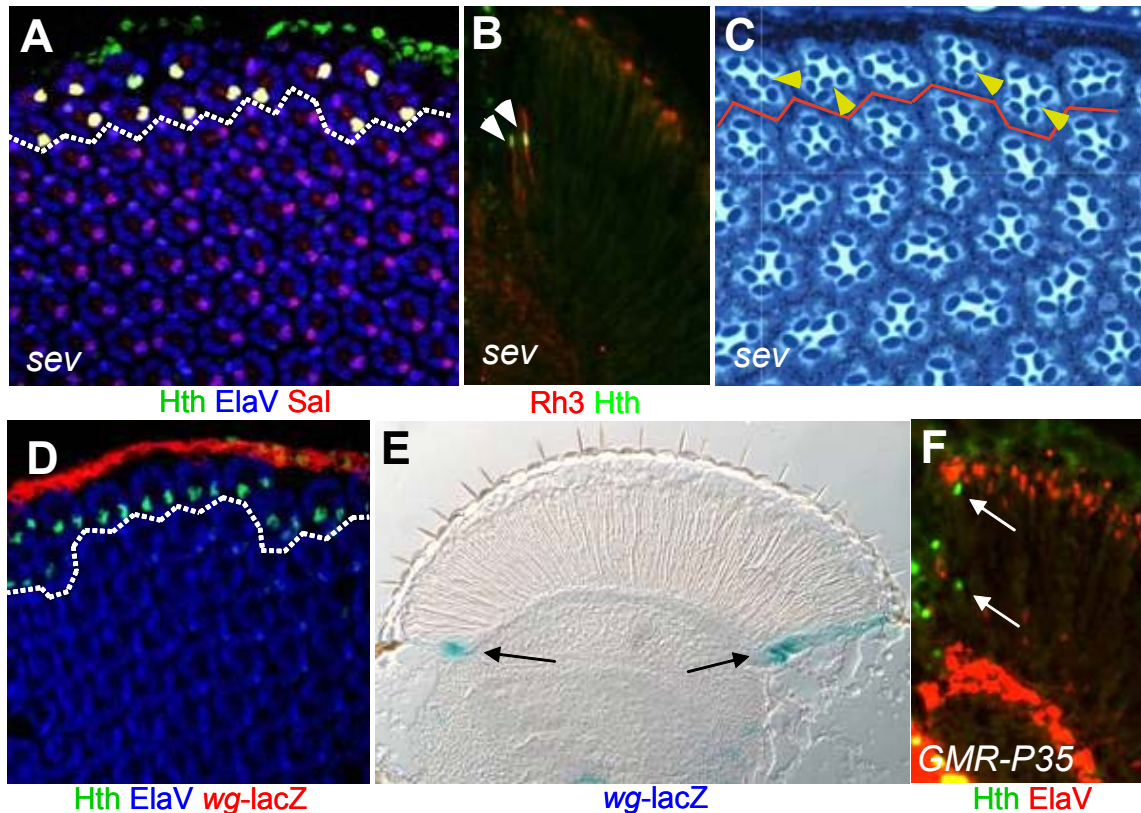
Fig III.2.4 Development of the DRA

(A)-(C) The DRA develops normally in *sevenless* mutants: Flat mounted pupal retina (~48 hrs APF) dissected from *sev* mutants and triple-labeled for ElaV (blue), Hth (green) and the inner PR marker Sal (red). One Sal-positive cell (R8) per omatidium was observed, always co-expressing Hth in the developing DRA ommatidia (dashed line). (B) Frozen section (10 μm) along the D/V axis (D to the left, equator runs horizontally) through an adult head of a *sev* mutant. Double labeling of Rh3 (red) and Hth (green) identified the DRA in the two dorsal-most rows of R8 cells (arrows). (C) Rhabdomere morphology of *sevenless* mutants: Epon thin section through the dorsal-most part of an adult *sev* eye at a level where the rhabdomeres of R8 first appear. The presence of only one inner PR rhabdomere per ommatidium was verified by serial sections. The R8 cells of the DRA exhibit enlarged rhabdomere diameters (arrows) and a sharp boundary between DRA and non-DRA ommatidia can be observed (red line). Mis-positioning of R8 cells was observed as peviously reported (Campos-Ortega et al., 1979).

(D)-(F) Extent of the DRA is not regulated by Wg-induced apoptosis: Flat mounted pupal retina (~48 hrs APF) triple-labeled for ElaV (blue), Hth (green) and *wg*-lacZ (red). βGal expression was detectable in the developing head cuticle all around the eye. Expression of *wg* was never observed in the DRA (dashed line). (E) Expression of *wg*-lacZ in the adult fly visualized by X-Gal staining on frozen sections. βGal expression was restricted to the head cuticle adjacent to the eye (arrows). (F) Blocking apoptosis in PRs using a GMR-P35 transgene had no effect on PRs. Expression of Hth (green) and ElaV (red) on frozen sections revealed one (sometimes two) rows of DRA ommatidia at the dorsal rim of the adult eye.

4D). Strong *wg*-lacZ staining (shown in red) was obtained all around the eye, including dorsally, adjacent to the DRA (marked by Hth in green). Frozen sections through adult fly heads carrying the *wg*-lacZ transgene were also stained for βGal activity (**Fig 4E**). Strong X-Gal staining was detectable in cells adjacent to peripheral PRs (black arrows), demonstrating that Wg remains expressed in the head tissue until adulthood. Wg could therefore play a role in limiting the number of ommatidial rows contributing to the DRA. To test this, a transgene over-expressing the anti-apoptotic viral protein P35 under the control

of the GMR promoter was used to rescue the eliminated ommatidia. Frozen sections of GMR-P35 flies were then double labeled for Hth and ElaV (**Fig 4F**). Based on co-expression of Hth (shown in green) and ElaV (red), no change in the number of ommatidial rows of the DRA fate could be detected (white arrows).

It was therefore concluded that Wg-induced apoptosis occurring at the eye margins does not drastically influence the appearance of the DRA.

2.5. Genetic manipulation of the DRA: cell fate decisions at the dorsal rim

The R8 cell, founder of the ommatidial cluster, cannot be removed experimentally from ommatidia without destroying the eye (Mlodzik et al., 1990a). Therefore, a different strategy had to be used to differentiate between two possible scenarios to explain how inner PRs develop into into the DRA fate. The possibility remained that an inductive signal from R8 to R7 existed, unless the mere location of both cells within the dorsal-most clusters of the retina provided the necessary positional information. To differentiate between these two models, three different mutant backgrounds were used to induce extra inner PRs throughout the retina and cell fate decisions of inner PRs located within the DRA were then assessed.

In the wildtype, the two inner PRs R7 and R8 represent very distinct cell types whereas the remaining six outer PRs develop into virtually identical PRs (**Fig 5A**). In flat pupal retinas (48 hrs APF), R7 cells were visualized using an antibody against the R7 marker Prospero (Pros) and the DRA was marked with Ant-Hth (**Fig 5B**). By triple-labeling with Elav (shown in red) it was possible to specifically mark both R7 and R8 in the DRA, as only one Hth-positive cell (shown in green) co-stained with Pros (shown in blue). As a second control, the DRA was also visualized in the adult by double-labeling frozen sections (10 μm) with antibodies against Hth and ElaV (**Fig 5C**). Usually between 2 and 4 nuclei expressing both Hth (shown in green) and ElaV (shown in red) were observed.

The three mutant backgrounds used to induce extra inner PRs throughout the retina were a constitutively activated form of Ras driven by the *sevenless* promoter (*sev*>RasVal12; (Gaul et al., 1992), as well as mutants in the genes

A wt

one **R7** cell
one **R8** cell

B wt — Pros ElaV Hth

C wt — ElaV Hth

D sev > RasVal12 — svp (-) — ro (-)

E sev>RasVal12 — Pros ElaV Hth

F sev>RasVal12 — ElaV Hth

G svp (-/-) — Arm-lacZ ElaV Hth

H svp (-/-) — Pros ElaV Hth

J svp (-/-) — ElaV Hth

K roX63 (-/-) — Arm-lacZ ElaV Hth

L roX63 (-/-) — Pros ElaV Hth

M roX63 (-/-) — ElaV Hth
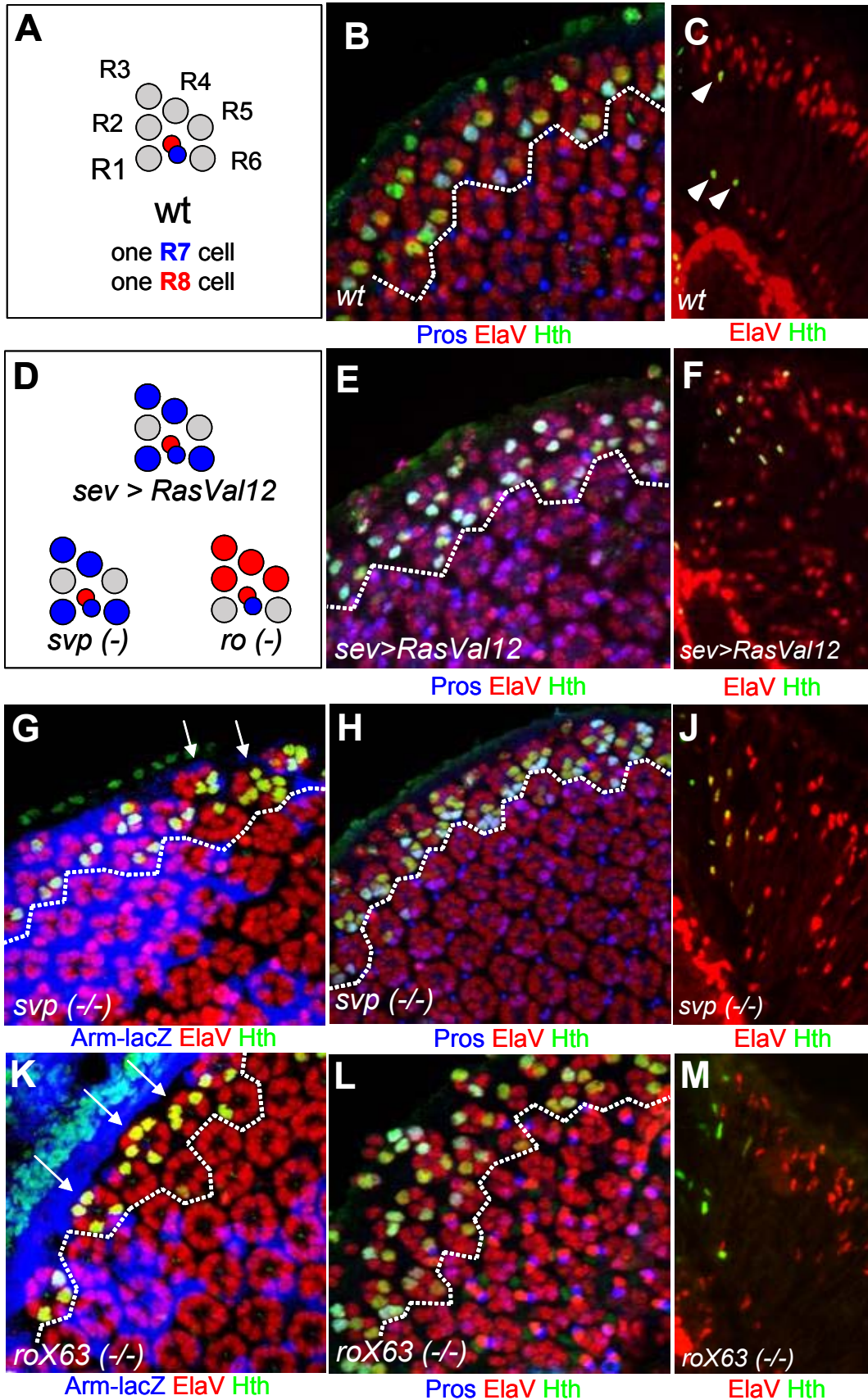
Fig III.2.5 Genetic manipulation of the DRA: cell fate decisions at the dorsal rim
(A)-(C) Expression of Hth, Pros and ElaV in wildtype flies: schematic diagram of the three cell types in a wildtype ommatidium: outer PRs R1-R6 (grey), R7 (blue) and R8 (red). (B) Flat mounted pupal retinas (~48 hrs APF) dissected from *yw* flies labeled for ElaV (red), Hth (green) and Pros (blue). Within the DRA (dashed line) both inner PRs (R7 and R8) stained for Hth. One of these cells (R7) co-expressed Pros (white cells) whereas R8 did not express this R7 marker (yellow cells). (C) Frozen sections (10 μm) along the D/V axis (dorsal to the left, equator runs horizontally) through adult heads of *yw* flies: double labeling of ElaV (red) and Hth (green) revealed 2-4 Hth-positive inner PR nuclei per section co-expressing ElaV.
(D) Schematic diagrams of the different mutation used to induce extra inner PRs. In *sev>RasVal12* mutants, R1, R3, R4 and R6 get transformed in R7 cells (blue), by over-activation of the Ras pathway. In *seven up* (*svp*) mutants, the same cells R1, R3, R4 and R6 choose the R7 fate (blue). In *rough* (*ro*) mutants, R2, R3, R4 and R5 get specified as R8 cells (red).
(E)-(F) Cell fate decisions in a DRA with extra R7 cells induced by activated Ras: in pupal retinas (48 hrs APF) dissected from *sev>RasVal12* flies, multiple Pros-positive cells (blue) are obtained per cluster (marked with ElaV, in red) throughout the retina. Within the DRA (dashed line), multiple cells (3-4) expressed Hth (green), all except one (R8, yellow cell) co-expressing Pros (white cells). Therefore, extra R7 cells born within the DRA always chose the DRA R7 cell fate. (F) This situation was maintained until adulthood: an increased number (7-9) of Hth positive cells (green) were observed in the DRA, by double labeling Hth and ElaV (red) on frozen sections.
(G)-(J) Cell fate decisions of extra R7 cells in the DRA of *svp* mutants: Pupal retinas with mitotic *svpE22 (-/-)* clones triple labeled for Hth (green) Arm-lacZ (blue) and ElaV (red). Clones were marked by the absence of βGal and the number of Hth positive cells was always specifically increased within clones touching the DRA (dashed line). (H) In whole mutant *svpE22 (-/-)* pupal retinas, multiple Pros-positive cells (blue) are obtained per cluster (red) throughout the retina. Within the DRA (dashed line), multiple cells (3-4) expressed Hth (green), some of which co-expressing Pros (white cells). Therefore, extra R7 cells born within the DRA always chose the DRA inner PR fate. However, not all extra inner PRs chose the R7 fate, suggesting that the remaining cells developed into R8 cells. (F) DRA of *svp* mutants in the adult: an increased number (7-9) of Hth positive cells (green) was observed in the DRA, by double labeling Hth and ElaV (red) on frozen sections.
(K)-(M) Cell fate decisions of extra R8 cells in the DRA of *ro* mutants: Pupal retinas with mitotic *roX63 (-/-)* clones triple labeled for Hth (green) Arm-lacZ (blue) and ElaV (red). The number of Hth positive cells was always specifically increased within clones (lacking βGal expression) touching the DRA (dashed line). (L) In whole mutant *roX63 (-/-)* pupal retinas, multiple cells (3-4) expressed Hth (green) within the DRA (dashed line), most of which excluded expression of the R7 marker Pros (white cells). Therefore, extra R7 cells born within the DRA always chose the DRA inner PR fate. However, not all extra inner PRs seemed to choose the R8 fate, suggesting that some cells developed into R7-like cells. (M) Adult DRA of *ro* mutants: a slightly increased number (5-6) of Hth positive cells (green) was observed in the DRA, by double labeling Hth and ElaV (red) on frozen sections.

seven-up (*svp*) and *rough* (*ro*) (**Fig 5D**; (Tomlinson et al., 1988). Over-expression of RasVal12 by the *sev* promoter leads to the transformation of outer PRs R1, R3, R4, and R6 into R7 cells. Pupal retinas from these *sev>*RasVal12 flies were dissected and triple labeled for Hth, Pros and ElaV (**Fig 5E**). Multiple Hth-positive cells per ommatidium were observed in the DRA of these flies (shown in green). As expected, all Hth-positive cells, except for one (the R8 cell), also co-expressed the R7 marker Pros (shown in blue). Multiple Pros-positive cells per cluster were also observed outside of the DRA, but those always lacked Hth expression. As in the wild type, only one or two rows of DRA ommatidia were found (marked by a dashed line). An increased number of Hth-positive PRs was also detected in the adult as seen on frozen sections (**Fig 5F**), suggesting that these extra inner PRs are not sorted out and later eliminated by apoptosis. Between 8-10 Hth-positive nuclei (shown in green) co-staining for ElaV (shown in red) were observed per section in the adult. It was concluded that extra inner PRs induced by over-expression of activated Ras always chose the DRA fate when located within one or two rows distance to the dorsal head tissue.

44

The development of extra R7 cells was also induced by following an alternative strategy. In *seven-up* mutants, outer PRs R1, R3, R4, and R6 also wrongly adopt the R7 fate (Mlodzik et al., 1990b). First, mitotic clones of eye tissue homozygous for the *svp* null allele *svpE22* were created using the ey-flip/FRT system (see material and methods). Pupal retinas (48 hrs APF) were dissected and triple labeled with antibodies against Hth, ElaV and Gal, as the clones were marked by the absence of *Armadillo*-lacZ (**Fig 5G**). Within *svpE22* (-/-) clones (marked by the absence of blue) that touched the dorsal rim, more than two Hth-positive cells (shown in green) were observed, while the DRA developed normally outside of the clones. This suggested that extra inner PRs always expressed Hth when located in the DRA. In a similar experiment, whole mutant eyes lacking *svp* function were generated by introducing the GMR-*hid* system (Stowers and Schwarz, 1999)see material and methods). Pupal retinas (48hrs APF) were then triple labeld with Anti-Hth, Anti-Pros and Anti-ElaV (**Fig 5H**). These retinas looked virtually identical to the *sev>RasVal12* mutants, with multiple Hth-positive cells at the dorsal rim (green), most of which expressed Pros (blue). However, sometimes more than one R8 cell (Hth$^+$, Pros$^-$) per ommatidium was observed, indicating that both R7- and R8-like cells might get induced in *svp* mutants (also: T. Cook, in preparation. Extra Hth-positive cells were also detected in the adult DRA of whole mutant *svpE22* eyes (**Fig 5J**) with 8-10 cells per section positive for both Hth (green) and ElaV (red). This data supported the hypothesis, that extra inner PRs always chose the DRA fate when located closse to the developing dorsal head tissue.

In a third approach, *rough* mutants were used to create several extra R8 cells per ommatidium (Tomlinson et al., 1988). Mitotic clones homozygous for the null allele *roX63* were induced using the ey-flip/FRT system. Pupal retinas (48 hrs APF) were then labeled for Arm-lacZ, Hth and ElaV (**Fig 5K**). Like in *svpE22* clones, several Hth positive cells per ommatidium (shown in green) were obtained in *roX63* clones touching the dorsal rim (marked by absence of blue). Similar results were obtained by triple-labeling pupal retinas of homozygous *roX63* flies with Anti-Hth, Anti-Pros and Anti-ElaV (**Fig 5L)**. Due to the strong

disorganization of ommatidia in *roX63* (-/-) mutants, the ratio of Hth-positive cells per ommatidium was difficult to count. It was clear, however, that more than two cells expressing Hth (shown in green) were obtained in the DRA of these flies. Interestingly, a high ratio of Pros-positive cells (shown in blue) indicated that, like in *svp* mutants, the extra inner PRs induced in *ro* mutants, seemed to fall into both R7-like and R8-like categories (T. Cook, in preparation). Finally, a slightly elevated number of Hth-positive cells was also detected in the adult DRA of *roX63* (-/-) mutants (**Fig 5M**). Again, the strong eye phenotype made it difficult to count nuclei co-staining for Hth (green) and ElaV (red).

It was concluded from these experiments that, when extra inner PRs are induced ectopically, R7 or R8 always choose the DRA fate independently from each other as long as they are located in close proximity to the dorsal head capsule. This fits well with previous observations of wildtype omkmatidia expressing Hth in only on inner PR. Furthermore, it suggests the existence of a factor emanating from this tissue that induces DRA cell fate in inner PRs over a range of a few cell diameters.

2.6. Extradenticle co-localizes with Homothorax during DRA development

Homothorax was shown to be specifically expressed in DRA inner PRs and provides a reliable marker for DRA development in various mutant situations. Homothorax acts as a co-factore for *Drosophila* HOX proteins together with another homeodomain protein, Extradenticle (Exd). Exd transcription is pleiotropic but its nuclear localization depends on the presence of Hth (Pai et al., 1998; Rieckhof et al., 1997). According to the current model, Hth and Exd depend on each other for nuclear translocation and form a sequence-specific transcriptional complex on genomic DNA (Rossel and Wehner, 1986) . It was therefore tested whether Exd was expressed in the DRA and whether Exd is necessary and eventually its nuclear localization sufficient for DRA development. Pupal retinas (48 hrs APF) were dissected and triple labeled using antibodies against Hth, Exd and ElaV (**Fig 6A**). It was found that every cell expressing Hth (shown in green) also showed nuclear Anti-Exd staining (shown in red), which
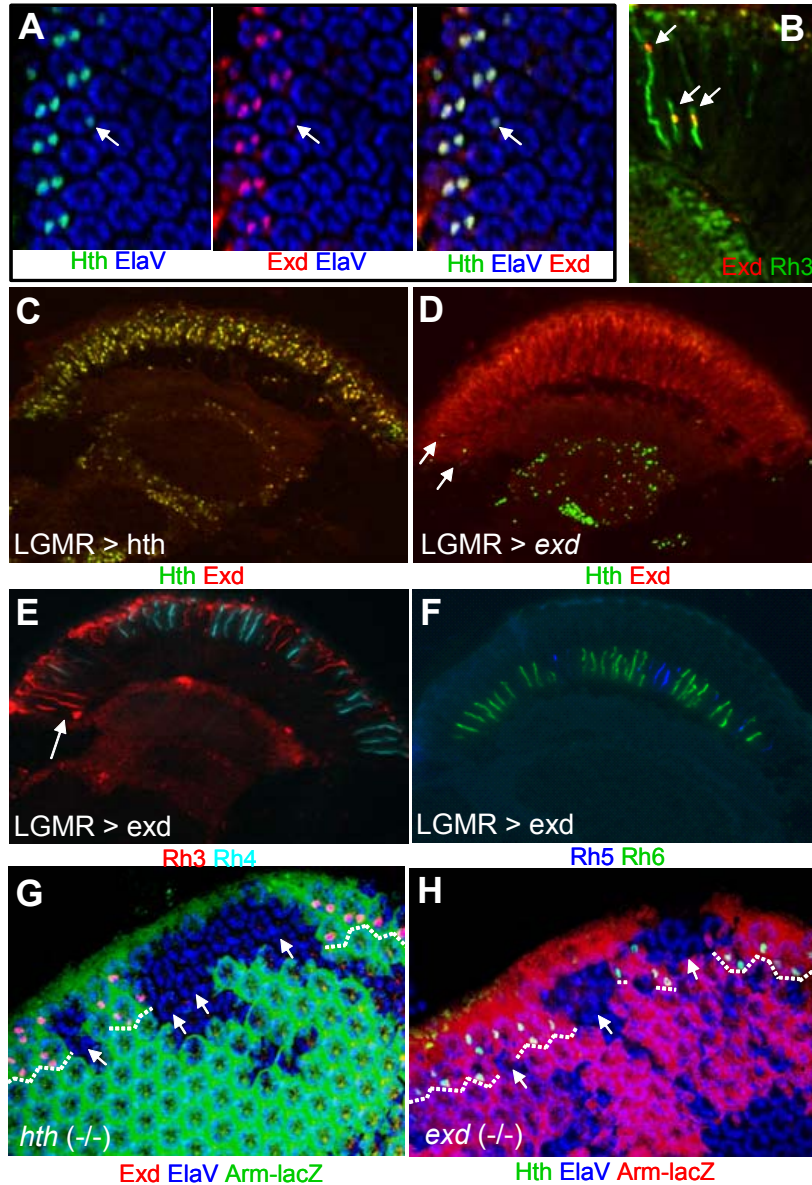
Fig III.2.6 Extradenticle co-localizes with Homothorax during DRA development
(A)-(B) DRA inner PRs express Exd: Pupal retinas (48 hrs APF) triple labeled for Hth (green), Exd (red) and ElaV (blue). DRA inner PRs always co-expressed Hth and Exd, although sometimes very faintly (arrow). (B) Expression of Exd in the adult DRA, visualized by double labeling Exd (red) and DRA-rhodopsin Rh3 (green) on frozen sections through wildtype eyes (dorsal left, equztor runs horizontally). Exd always co-localized with Rh3 in DRA R7 cells (upper arrow) as well as DRA R8 cells (bottom arrows).
(C) Over-expression of Hth leads to nuclear localization of Exd: Frozen sections through adult eyes from flies expressing Hth under GMR-GAL4 control (GMR > hth) double labeled against Hth (green) and Exd (red). Hth was sufficient to localize Exd into the nucleus, when ectopically expressed.
(D) Ectopic Exd does not affect Hth expression: Frozen sections through adult eyes from flies expressing Exd under GMR-GAL4 control (GMR > Exd) double labeled against Hth (green) and Exd (red). Hth edxpression remained restricted to DRA iner PRs (arrows).
(E)+(F) Over-expression of Exd has no effect on ommatidial subtype specification: (F) Opsin expression in R7 cells of GMR > Exd flies was normal as expression of Rh3 (red) and Rh4 (cyan) was unaffected on frozen sections. (F) Frozen sections through GMR > Exd eyes: Expression of R8 opsins Rh5 (blue) and Rh6 (green) was also unaffected.
(G) Nuclear localization of Exd is lost in absence of Hth: Pupal retinas with hth^{P2} (-/-) clones marked by the absence of Arm-lacZ (green). Nuclear Exd (red) was specifically lost in clones lacking Hth, touching the DRA (dashed line).
(H) Hth expression is lost in Exd clones: Pupal retinas with exd^1 (-/-) clones, triple labeled for Hth (green), Arm-lacZ (red) and ElaV (blue). Hth expression was specifically lost ion clones touching the DRA (dashed line).

was sometimes rather faint (white arrow). Outside of the DRA, cytoplasmatic Exd was not observed, although this is generally attributed to the dilution of Exd protein when distributed throughout the cytoplasm.

Nuclear localization of Exd was also visualized in the adult DRA by performing frozen sections through adult eyes and using antibodies against Exd and Rh3 (**Fig 6B**). Strong nuclear staining for Exd (shown in red) was always detectable in the DRA inner PRs R7 and R8 (white arrows), both expressing Rh3 (shown in green). Outside of the DRA, Exd was again not detectable in the cytoplasm.

It was therefore concluded that Exd is co-expressed with Hth in the nuclei of DRA inner PRs. As no cytsoplasmic staining outside of the DRA was detectable and as no reporter constructs or in-situ hybridizations were performed, it could not be excluded that *exd* shows the same expression pattern than *hth*.

Over-expression of Hth in all larval PRs is sufficient to translocate Exd to the larval PR nuclei (Jaw et al., 2000). This result was reproduced in the adult retina, by over-expressing Hth using the GAL4/UAS-system (see material and methods). Hth was ectopically expressed in all PRs posterior to the morphogenetic furrow, using GMR-GAL4 (LGMR > *hth*). Frozen sections through adult eyes from LGMR > *hth* flies were then performed and were double labeled with Anti-Hth and Anti-Exd (**Fig 6C**). Every PR expressing Hth (shown in green) was also positive for nuclear Exd (shown in red). Hth is therefore sufficient to translocate Exd into the nucleus of adult PRs. However, the possibility remains, that ectopic Hth transcriptionally activates Exd expression. In a similar experiment, Exd was over-expressed using GMR-GAL4 to test whether it would induce Hth expression. Frozen sections through adult eyes from LGMR > *exd* flies were then double labeled for Hth and Exd (**Fig 6D**). Ectopic Exd (shown in red) had no effect on Hth expression (shown in green), as it remained specifically expressed in DRA inner PR nuclei (white arrows). Furthermore, GAL4-induced Exd expression outside of the DRA was largely cytoplasmic, again confirming that Exd requires the presence of Hth to be nuclearly localized in adult PRs.

As Exd and Hth are both required for transcriptional activation of their target genes, ectopic Exd alone should not be able to induce any phenotype outside of the DRA in LGMR > *exd* flies. This was tested by assessing opsin gene epression in these flies. Frozen sections through adult eyes from LGMR > *exd* flies were first labeled with antibodies against Rh3 and Rh4 (**Fig 6E**). It was found that expression of Rh3 (shown in red) and Rh4 (shown in cyan) were indistinguishable from the wildtype, confirming that ectopic Exd has no effect on R7 opsin expression or DRA development. Analysis of the LGMR > exd flies was completed by assessing R8 opsin gene expression using antibodies against Rh5 and Rh6 on frozen sections (**Fig 6F**). No phenotype was observed as Rh5 expression (shown in blue) and Rh6 expression (shown in green) were normal. It was therefore concluded that over-expression of Exd in developing PRs has no effect on their development in the absence of Hth.

To investigate nuclear localization of both Exd and Hth in developing inner PRs of the DRA, their localization was analyzed in clones of tissue lacking the dimerization partner. First, Exd localization in clones of homozygous eye tissue lacking Hth protein was investigated. Mitotic clones were induced using the *ey*-flip/FRT technique (see material and methods) and the *hth* null allele *hth*[P2]. Pupal retinas exhibiting *hth*[P2] (-/-) clones, marked by the absence of Armadillo-lacZ (Arm-lacZ) were then dissected and triple labeled for Exd, βGal and ElaV (**Fig 6G**). Nuclear staining of Exd (shown in red) was lost in *hth*[P2] (-/-) clones touching the dorsal rim of the eye (shown by the absence of green βGal staining). In the absence of Hth, Exd could therefore not translocate to the nucleus of DRA inner PRs. It could therefore be excluded that *exd* showed the same expression pattern than Hth. However, transcriptional activation of *exd* by Hth still remains a possibility. Finally, Hth localization was assessed in clones of eye tissue lacking Exd function, by using the *exd* null allele *exd*[1] recombined onto an FRT19 chromosome. Pupal retinas (48 hrs APF) with *exd*[1] (-/-) clones marked by the absence of Arm-lacZ were then dissected and triple stained for Hth, βGal and ElaV (**Fig 6H**). Nuclear Hth staining (shown in green) was also lost in *exd*[1] (-/-) clones (marked by the absence of red staining) touching the dorsal rim of the

eye. Therefore, the presence of Exd is necessary for Hth to translocate to the nucleaus, as had been suggested before in other model systems.

It was concluded from these experiments that Hth and Exd are both expressed in DRA inner PRs, where they co-localize in the nucleus. Exd is not sufficient to induce Hth expression or to influence PR development. Finally, both Hth and Exd rely on each other's presence to correctly translocate into the nucleus of developing PRs. While Hth is specifically expressed in the DRA inner PRs, Exd expression seems to be at low levels and to be pleiotropic.

2.7. Expression of Hth/Exd is conserved between *Musca* and *Drosophila*

The homeodomain transcription factors Homothorax (Hth) and Extradenticle (Exd) specifically co-localize in inner PRs of the DRA. Dorsal rim areas, specialized in the detection of polarized light, have been described in many insect species (Labhart and Meyer, 1999). However, after morphologic analysis of these very polymorphic DRAs, the hypothesis was presented that different polarization sensors have arisen independently during insect evolution. Strikingly, a very similar group of PRs specialized in the detection of e-vector orientation have even been described at the ventral rim of the principal eyes of Wolf spiders (Lycosidae; (Dacke et al., 2001). Although the principal eyes of spiders and flies are clearly not homologous structures, they appear to use similar molecular programs (PAX6) in different animal species to create analogous structures (for review: Gehring, 2002). A similar model has been proposed for the eyes of vertrebrates and flies. Antibodies against Hth were therefore used to begin an investigation of evolutionary conservation of transcription factor expression in the DRA of other insect species, beginning with the housefly, *Musca domestica*.

The ommatidial mosaic of the housefly (*Musca domestica*) has been investigated in much detail, by using water immersion microscopy (Franceschini et al., 1981; Kirschfeld and Franceschini, 1968). Eye morphology of this species is very similar to *Drosophila*, which is also a higher dipteran. The pale and yellow ommatidial subtypes were in fact first characterized in *Musca*, based on
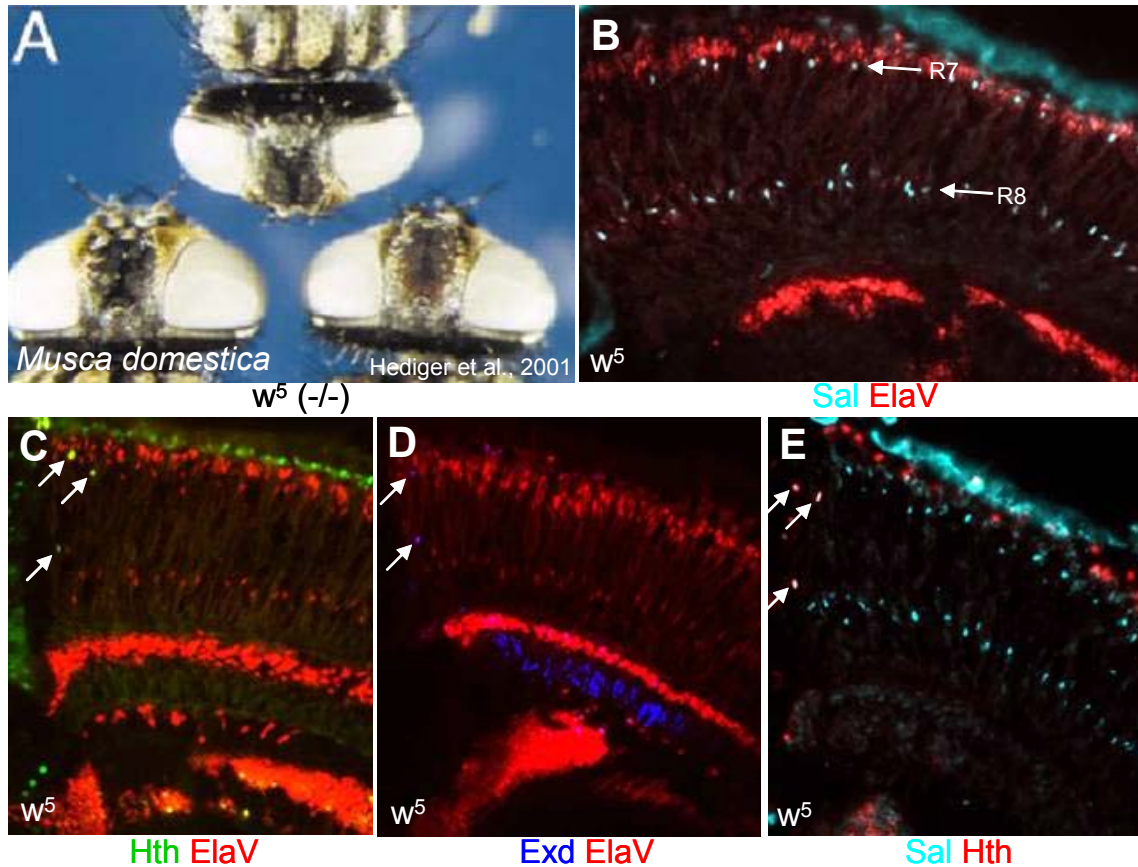
Fig III.2.7 Expression of Hth/Exd is conserved between *Musca* and *Drosophila*
(A) *Musca domestica white* mutants (w^5) used for antibody stainings on frozen sections.
(B) Frozen section (16-18 μm) through adult w^5 Musca eyes, double labeled with antibodies against *Drosophila* inner PR marker Sal (cyan) and ElaV (red). R7 and R8 cells were also specifically marked in Musca.
(C) Frozen section through adult w^5 Musca eyes, double labeled with antibodies against *Drosophila* DRA marker Hth (green) and ElaV (red). Between 3-4 Hth-positive PR nuclei were detected at the dorsal rim, very similar to *Drososphila*.
(D) Frozen section through adult w^5 Musca eyes, double labeled with antibodies against *Drosophila* Exd (blue) and ElaV (red). As for Hth, specific nuclear expression of Exd was detected in 2-4 nuclei at the dorsal rim of *Musca*.
(E) Double labeling of Hth (red) and Sal (cyan) on frozen sections revealed specific co-expression in the DRA inner PRs. Like in Drosophila, only inner PRs at the DRA therefore express Hth and Exd in *Musca domestica*.

autofluorescence of their visual pigments (Franceschini et al., 1981). To date, PR cell fate decisions and ommatidial subtype specification have not been analyzed molecularly in *Musca*. Testing eventual cross-reaction of antibodies generated against *Drosophila* proteins was technically difficult due to very dark pigmentation of *Musca* adult eyes. All *Musca* experiments were therefore performed in *white* mutants (w^5), lacking eye pigmentation (**Fig 7A**; (Hediger et al., 2001). Specification of inner PRs R7 and R8 was investigated   first by double labeling frozen sections through adult *Musca* w^5 mutant eyes with antibodies raised against *Drosophila* Spalt (Sal) and ElaV proteins (**Fig 7B**). Sal expression in *Musca* (shown in cyan) was found to be indistinguishable from *Drosophila*, as all

R7 and R8 cells were found to express Sal. Specification of inner PRs in the DRA was assessed next by double labeling frozen sections through adult *Musca* heads with antibodies against the *Drosophila* proteins Hth and ElaV (**Fig 7C**). Hth expressing nuclei (shown in green) were detected exclusively at the dorsal rim of the adult eye. As in *Drosophila*, DRA R8 nuclei could be identified due to their more apical location as compared to non-DRA R8 nuclei (bottom white arrow). R7 nuclei also stained for Hth (top white arrows), however, they could not be specifically marked, as the *Drosophila* antibodies against the R7 marker Prospero did not cross-react in *Musca* (data not shown). It was striking that, although the adult eye of *Musca* is significantly larger than the one of *Drosophila,* and contains a much higher number of ommatidia, only one or two rows of ommatidia were found to be Hth-positive in *Musca*, like in *Drosophila*. Nuclear localization of the Hth dimerization partner Extradenticle (Exd) was also visualized on frozen sections through adult Musca eyes, using the antibodies against *Drosophia* Exd and ElaV (**Fig 7D**). Nuclear localization of Exd (shown in blue) was detected specifically in DRA inner PRs, suggesting that the role of Hth and Exd in the DRA is conserved between *Musca* and *Drosophila*. Finally, the identity of DRA inner PRs was confirmed in *Musca*, by double labeling frozen sections through adult w^5 eyes with antibodies against *Drosophila* Sal and Hth (**Fig 7E**). Hth-expressing cells in the DRA (shown in red) were always Sal-positive (shown in cyan), clearly demonstrating that Hth expression in the adult DRA of *Musca* is specific to inner PRs R7 (top arrows) and R8 (bottom arrow).

It was concluded from these experiments, that Hth/Exd expression in DRA inner PRs is conserved between *Musca* and *Drosophila*. The DRAs of more distantly related species could in the future be analyzed using these antibodies, if they cross-react and this might allow a further investigation of the evolutionary relationship between the DRA structures in these species.

4.2.8. Homothorax is sufficient to induce DRA ommatidia

Homothorax is specifically expressed in the inner PRs of the DRA. A potential role of *hth* in inducing the DRA-specific inner PR cell fate was tested by
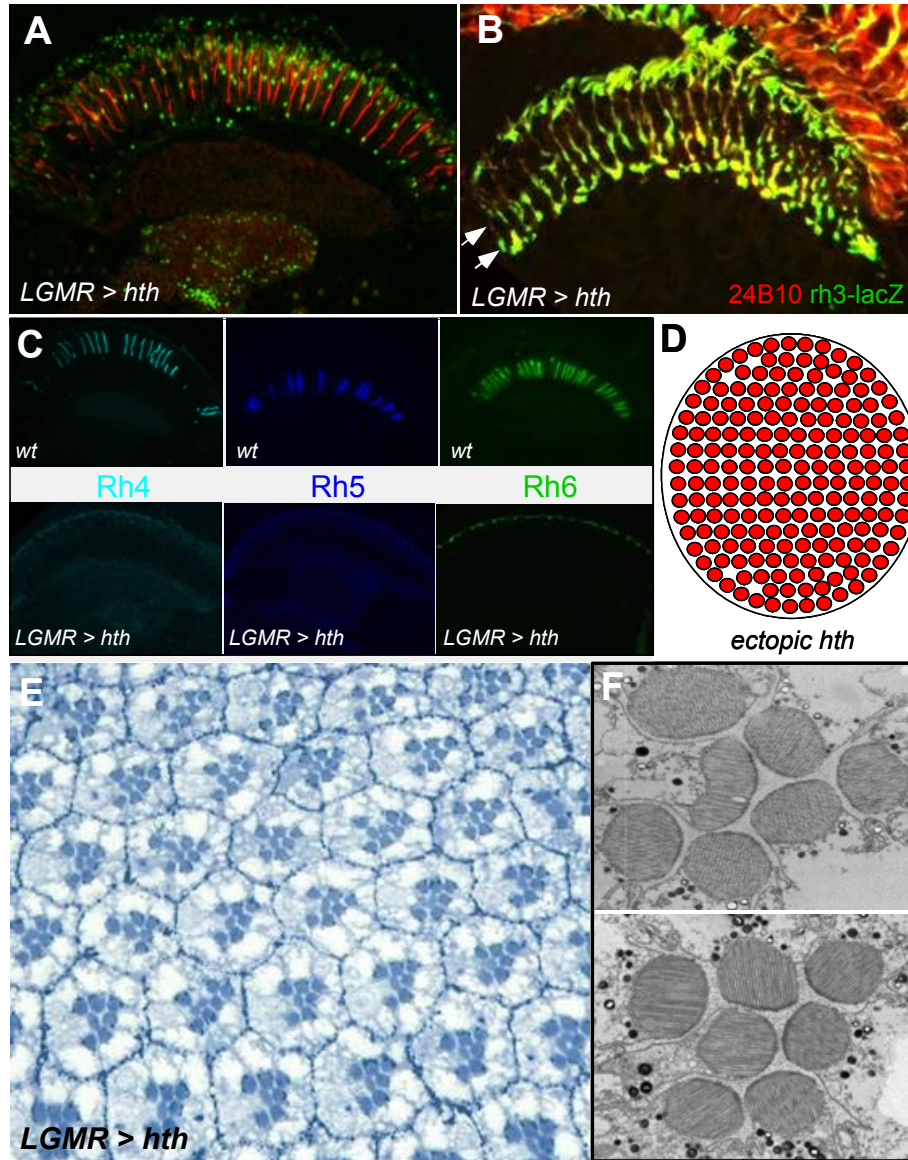
Fig III.2.8 Homothorax is sufficient to induce the DRA fate in inner PRs
(A) Over-expression of *hth* expands Rh3 expression: Frozen section (10 μm) along the D/V axis (D to the left) through an adult head of flies over-expressing *hth* under the control of 'Long'GMR-GAL4 (GMR>*hth*; see Experimental Procedures). Double labeling of Rh3 (red) and Hth (green) revealed co-expression of Hth and Rh3 in all inner PRs (R= retina, L= lamina, M=medulla).
(B) Axonal projections of *rh3* expressing fibers to the optic lobes: Frozen sections along the D/V axis (dorsal to the left) through adult heads of GMR>*hth* flies carrying *rh3*-lacZ transgenes. All inner PRs projecting to the medulla express the DRA opsin *rh3* as seen by double labeling of the PR marker 24B10 (red) and Anti-βGal (green). Projections to both R7 and R8 layers (white arrows), but not to the Lamina were observed, suggesting that all inner PRs were driven into the DRA fate (R=Retina, L=Lamina, M=Medulla).
(D) Homothorax gain-of-function: schematic diagram of ectopic induction of DRA ommatidia (red) by Hth.
(E) Over-expression of Hth results in loss of *rh4*, *rh5* and *rh6* expression: Frozen sections through adult heads of wildtype flies immuno stained for Rh4 (top left), Rh5 (top center) and Rh6 (right). All expression of these non-DRA inner PR rhodopsins is lost in flies over-expressing Hth (GMR>hth): Rh4 (bottom left), Rh5 (bottom center) and Rh6 (bottom right) are not detectable, further suggesting that all ommatidia were transformed into DRA.
(E) Expression of Hth is sufficient to ectopically induce DRA morphology: In Epon thin sections through non-DRA ommatidia located dorsally from the equator in GMR>*hth* flies, all ommatidia exhibit DRA morphology (compare Fig 1F) showing the enlarged diameter of their inner PR rhabdomeres.
(F) Rhabdomere morphology in ectopic DRA ommatidia: Further analysis of rhabdomere morphology in GMR>*hth* flies using electron microscopy revealed occasional malformations, like kidney-shaped inner PR rhabdomeres (top). Nevertheless, the ommatidia are virtually identical to DRA ommatidia of wildtype flies (bottom, compare Fig 1E).

53

assessing whether its over-expression was sufficient to induce ectopic DRA development. Hth was mis-expressed in all developing PRs posterior to the morphogenetic furrow using UAS-*hth* (Ryoo et al., 1999) under the control of LGMR-GAL4 (LGMR>*hth*; (Moses and Rubin, 1991). This resulted in slightly rough adult eyes, but without severely disrupting the retina. Frozen sections (10 µm) through adult eyes of LGMR > *hth* flies were double labeled using antibodies against Hth and Rh3 (**Fig 8A**). Unlike in the wildtype, Rh3 expression (shown in red) was now dramatically expanded throughout the whole retina. To test whether *rh3* transcription was also induced by over-expression of *hth*, expression of *rh3*-lacZ was analyzed on frozen sections (**Fig 8B**). This transgene is normally expressed in 30% of R7 cells as well as in all DRA inner PRs and was visualized using Anti-βGal antibodies (shown in green). Additionally, all axonal projections to the optic lobes were visualized using antibodies against the PR-specific cell-surface antigen 24B10 (Zipursky et al., 1984). Double labeling revealed that in GMR>*hth* flies, all inner PRs project to the medulla and express *rh3*-lacZ. Although the morphology of the medulla was somewhat disturbed, both R7 and R8 termination layers could be distinguished (white arrows). No overshooting of fibers or dramatic mis-projections were observed. The outer PRs projected correctly to the lamina and never expressed *rh3*. Alternatively, *rh3* expression was visualized in living LGMR > hth flies using a *rh3*-GFP transgene and corneal neutralization by water immersion microscopy (Franceschini and Kirschfeld, 1971a). While *rh3*-GFP was correctly expressed in ~30% of non-DRA ommatidia in wild type flies (Pichaud and Desplan, 2001), its expression was expanded to all ommatidia in flies expressing *hth* under GMR control (data not shown). Ectopic *hth* therefore lead to the expression of *rh3* in all inner PRs.

Expression of all other inner PR rhodopsins (Rh4, Rh5 and Rh6) in LGMR > *hth* flies was also tested (**Fig 8C**). While these opsins showed correct subtype-specific expression in wildtype R7 and R8 (top row), expression of all three opsins was completely lost in LGMR > hth flies (bottom row). Expression of the outer PR opsin Rh1, however, remained normal since expression of a *rh1*-GFP transgene (Pichaud and Desplan, 2001) was not affected (not shown). It was

concluded that Rh3 is the only opsin expressed in inner PRs in these *hth* gain-of-function flies. As Rh3 is the only rhodopsin expressed in the *Drosophila* DRA, it is thus likely that *hth* was sufficient to induce the DRA fate in all ommatidia (**Fig 8D**).

To test this hypothesis, PR morphology was evaluated in LGMR > *hth* flies by performing Epon thin sections (1 µm) through the adult retina (**Fig 8E**). Light microscopic analysis revealed that the rhabdomere diameter of all inner PRs was considerably enlarged in GMR>*hth* flies compared to the wildtype. As a significant number of inner PR rhabdomeres over-expressing Hth were found to have severely deformed, their morphology was analyzed in more detail by electron microscopy (**Fig 8F**, see material and methods). Cross-sections of some inner PR rhabdomeres exhibited a kidney-like shape and some were split in two (data not shown). However, the area of inner PR rhabdomere cross sections was always significantly enlarged.

Therefore, expression of Hth is sufficient to force any inner PR, independent of its location within the retina, into choosing the fate of a polarization-sensitive DRA cell. Outer PRs do not get transformed morphologically or molecularly.

2.9. Mutual exclusion between Sens expression and DRA development

Homothorax is specifically expressed in the inner PRs of the DRA and it is sufficient to induce the DRA fate in all ommatidia when ectopically expressed. Expression of the R8 marker Senseless (Sens) is specifically excluded from the dorsal rim, suggesting that absence of Sens is important for these cells to acquire their specialized function. It was therefore tested whether Hth and Exd are sufficient to repress Sens in R8, when ectopically expressed.

As Sens is one of the first markers expressed in R8 cells, it was first tested whether Hth was able to efficiently repress Sens expression early in third instar larvae. Eye imaginal discs from flies over-expressing a GFP:hth fusion protein under GMR-GAL4 control (LGMR > GFP:*hth*) were dissected and triple stained with antibodies against GFP, Sens and ElaV (**Fig 9A**). Strong expression

of Sens (shown in red) was detected in R8 cells starting right posterior to the morphogenetic furrow (MF, white arrow). Hth expression, induced in all developing PRs by GMR-GAL4 (shown in green) started ~3-5 rows posterior to the furrow. Clear co-staining of Sens and Hth was found all the way to the posterior edge of the eye imaginal disc, suggesting that Hth is not sufficient to repress larval Sens expression. However, it was tested whether late Sens expression, which has been proposed to be required for the terminal differentiation of color-sensitive R8 cells, was affected by ectopic Hth. Pupal retinas (48 hrs APF) were dissected from LGMR > GFP:*hth* and triple stained for GFP, Sens and ElaV (**Fig 9B**). At this developmental stage, strong GFP:Hth expression (shown in green) was detectable in all PRs (shown in blue), as well as in non-PR cells. No Sens expression was detectable in these flies, suggesting that ectopic over-expression of Hth is sufficient to repress Sens at this developmental stage. Frozen sections through adult heads from LGMR > *hth* flies were also double stained for Sens and ElaV (**Fig 9C**). Sens expression (shown in green) was not detectable in PRs (shown in red). It was therefore concluded that, similar to the DRA of wildtype flies, induction of ectopic DRA ommatidia in LGMR > *hth* flies results in the total loss of Sens expression.

As the DRA fate and Sens expression seemed to efficiently exclude each other, it was tested whether over-expression of Sens was sufficient to repress DRA development. Sens was therefore over-expressed in all developing PRs using GMR-GAL4, and pupal retinas were triple stained using antibodies against Sens, Exd and ElaV (**Fig 9D**). In the DRA of sGMR > *sens* flies (shown as a dashed line), Sens (shown in red) was found to be co-expressed with Exd (shown in green). This suggested that Sens was not able to repress nuclear localization of Exd. Sens and Exd were also double labeled in frozen sections through adult sGMR > sens eyes (**Fig 9E**). As in pupae, strong co-expression of Sens (shown in red) and Exd (shown in green) was observed. Nuclear localization of Exd in sGMR > *sens* flies suggested that Hth expression was unaffected. Hth expression was visualized in frozen sections using antibodies against Hth and ElaV (**Fig 9F**). As expected, Hth expression (shown in green)
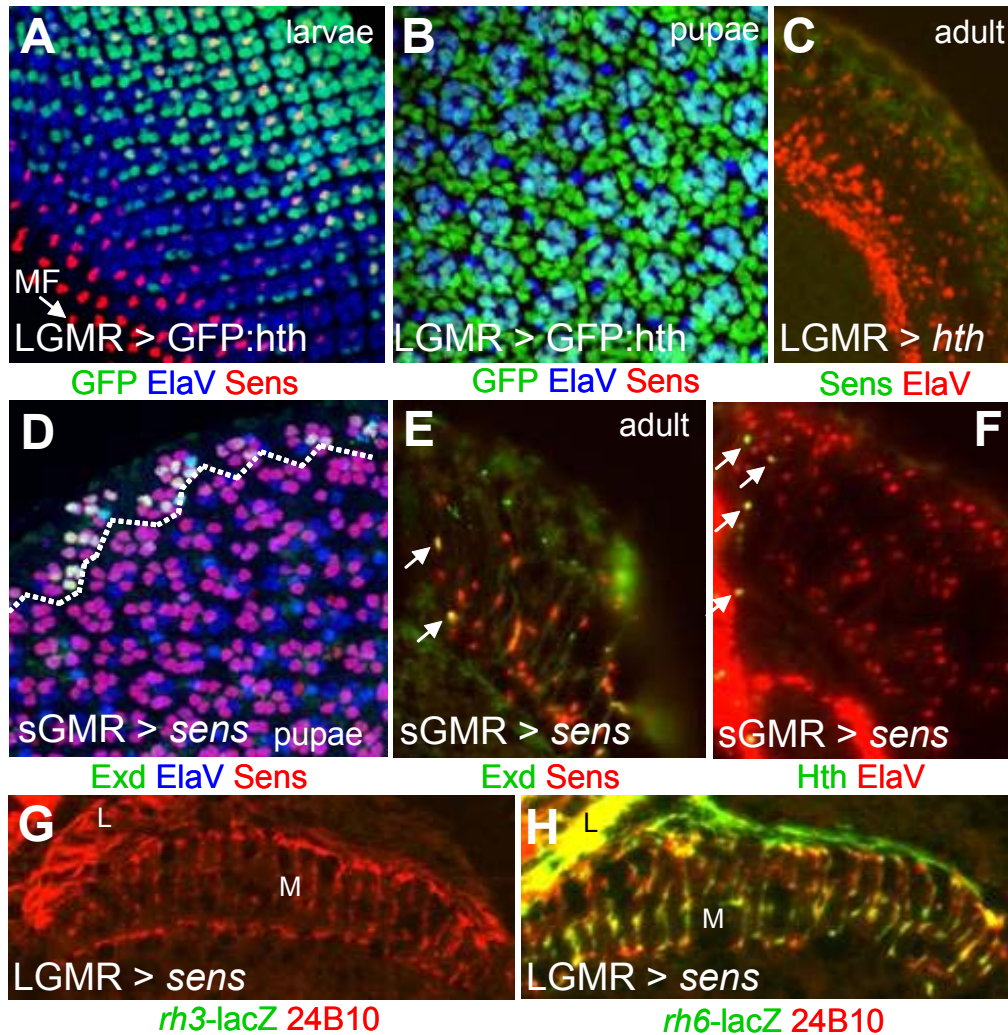
Fig III.2.9 Mutual exclusion between Sens expression and DRA development
(A)-(C) Repression of Sens by ectopic Hth: Third instar eye imaginal discs fro flies over-expressing Hth under GMR-GAL4 control (LGMR > hth) triple labeled for Hth (green), Sens (red) and ElaV (blue). Hth did not reperess Sens expression in larvae (white nuclei). (B) Pupal retinas (48 hrs APF) dissected from LGMR > *hth* flies and triple labeled for Hth (green), Sens (red) and ElaV (blue). At this developmental stage, no SEns expression was detectable, suggesting that ectopic Hth was sufficient to repress the R8 marker. (C) Frozen sections through adult eyes from LGMR > *hth* flies, double stained for Sens (green) and ElaV (red). No Sens expression was detectable at this stage.
(D)-(F) Over-expression of Sens does not repress Hth or Exd: Pupal retinas from flies over-expressing Sens under GMR-GAL4 control (sGMR > *sens*) triple labeled for Exd (green), Sens (red) and ElaV (blue). Exd expression in the DRA (dashed line) persisted and co-expression with Sens was observed. (E) Co-expression of Exd (green) and Sens (red) on frozen sections through adult sGMR > *sens* eyes. (F) Expresion of Hth (green) was unaffected on frozen sections through adult sGMR > *sens* eyes (ElaV in red).
(G)-(H) Over-expression leads to a loss of the DRA: Frozen sections through adult eyes from LGMR > *sens* flies carrying a *rh3*-lacZ transgene. βGal expression (green) in PR axon fibers was completely lost (L, lamina; M, medulla). (H) Frozen sections through adult eyes from LGMR > *sens* flies carrying a *rh6*-lacZ transgene. βGal expression (green) in PR axon fibers was dramatically expanded into all PRs, with rh6-lacZ expr4essing fibers terminating in the lamina (L) as well as the medulla (M).

was found to be unaffected in adult sGMR > *sens* flies. Therefore, nuclear localization of both Hth and Exd is not affected by ectopic over-expression of

Sens. Based on these markers, DRA development appears to proceed normally under these conditions.

To complete the analysis of Sens gain-of-function flies, it was tested whether the forced co-expression of Hth/Exd and Sens leads to an interruption of DRA maturation by blocking the transcriptional network downstream of Hth. As GMR > Sens flies have dramatic adult eye phenotypes, it was impossible to assess inner PR rhabdomere diameter. However, *rh3* expression was tested by introducing *rh3*-lacZ transgenes into a LGMR > *sens* background and double labeling with Anti-βGal and the PR-specific cell-surface-antigen 24B10 (**Fig 9F**). Expression of *rh3*-lacZ (shown in green) was completely lost in adult LGMR > *sens* eyes, as no βGal-expressing axonal fibers were detectable in the optic lobe (labeled in red). This result suggested that DRA development was indeed perturbed in these flies as Rh3 is always found in DRA inner PRs. Finally, introduction of *rh6*-lacZ into the LGMR > *sens* background allowed to determine the fate of the DRA, by double labeling frozen sections with antibodies against βGal and 24B10 (**Fig 9G**). Expression of *rh6*-lacZ (shown in green) was expanded into all PRS, staining axonal projections to both the lamina (L) as well as the medulla (M) layers of the optic lobe (labeled in red). Ectopic expression of Sens therefore has a strong activating effect on *rh6* expression whereas *rh3* expression is completely repressed. Interestingly, expression of *rh1*-lacZ was not affected by ectopic Sens (data not shown), suggesting that Sens is not sufficient to fully transform outer PRs into **y**R8 cells.

It was concluded from these experiments that Sens expression and DRA development exclude each other. Over-expression of Hth leads to the loss of Sens expression, thereby providing the first pupal marker for DRA induction. Futhermore, over-expression of Sens leads to a mis-specification of DRA ommatidia: although Hth and Exd remain properly expressed, forced co-expression of Exd leads to a loss of the DRA-type *rh3* expression while inducing **y**R8-like expression of *rh6* in all PRs. It appears therefore that in the wildtype, Sens has to be excluded from DRA R8 cells, due to its strong ability to induce the **y**R8 fate.

2.10. Transcriptional activity of Hth is required for DRA development

Tissue-specific expression of Hth is required for nuclear localization of pleiotropic Exd (Pai et al., 1998; Rieckhof et al., 1997). One model proposes that Hth's unique function is to translocate the transcription factor Exd into the nucleus (Kurant et al., 2001). However, it has been suggested, that DNA binding of Hth via its homeodomain is required for most of Hth's functions. It had therefore been proposed that a ternary complex consisting of Hth, Exd and a Hox factor is activating the transcription of target genes (Ryoo et al., 1999). To date, no Hox factor has been shown to be required for eye development. In developing DRA R8 cells, however, the R8 marker Senseless (Sens) was shown to be repressed by Hth/Exd. Using the exclusion of Sens from the DRA as a marker, it was therefore tested whether Hth and Exd behave during DRA development as has previously been described in other model systems.

To test whether nuclear localization of Exd is sufficient to induce the DRA ommatidial subtype, the Exd protein fused to an additional 'nuclear localization sequence' (NLS) was ectopically expressed in developing PRs using the GAL4/UAS-system (Ryoo et al., 1999; see material and methods). Frozen sections through adult eyes of flies over-expressing UAS-*exd*:NLS under the control of GMR-GAL4 (LGMR > exd:NLS) were then double labeled with antibodies against Sens and Exd (**Fig 10A**). Sens expression (shown in green) was not lost in these retinas, unlike when wildtype Hth is over-expressed. However, Exd was found to be nucler in all PRs. Therefore, nuclear localization of Exd is not sufficient for the repression of Sens. To confirm this result, DRA development was assessed in the adult eye by double labeling frozen sections with antibodies against Rh3 and Rh4 (**Fig 10B**). Rh3 expression (shown in red) and Rh4 (shown in green) were unaffected in LGMR > *exd*:NLS, again suggesting that the DRA was indistinguishable from the wildtype (white arrow). Finally, it was confirmed that ectopic nuclear Exd did not affect Hth expression in LGMR > *exd*:NLS flies by double labeling frozen sections with Anti-Exd and Anti-Hth (**Fig 10C**). Hth expression (shown in green) remained specific to the DRA inner PR nuclei (white arrows), whereas Exd was expressed in all PR nuclei
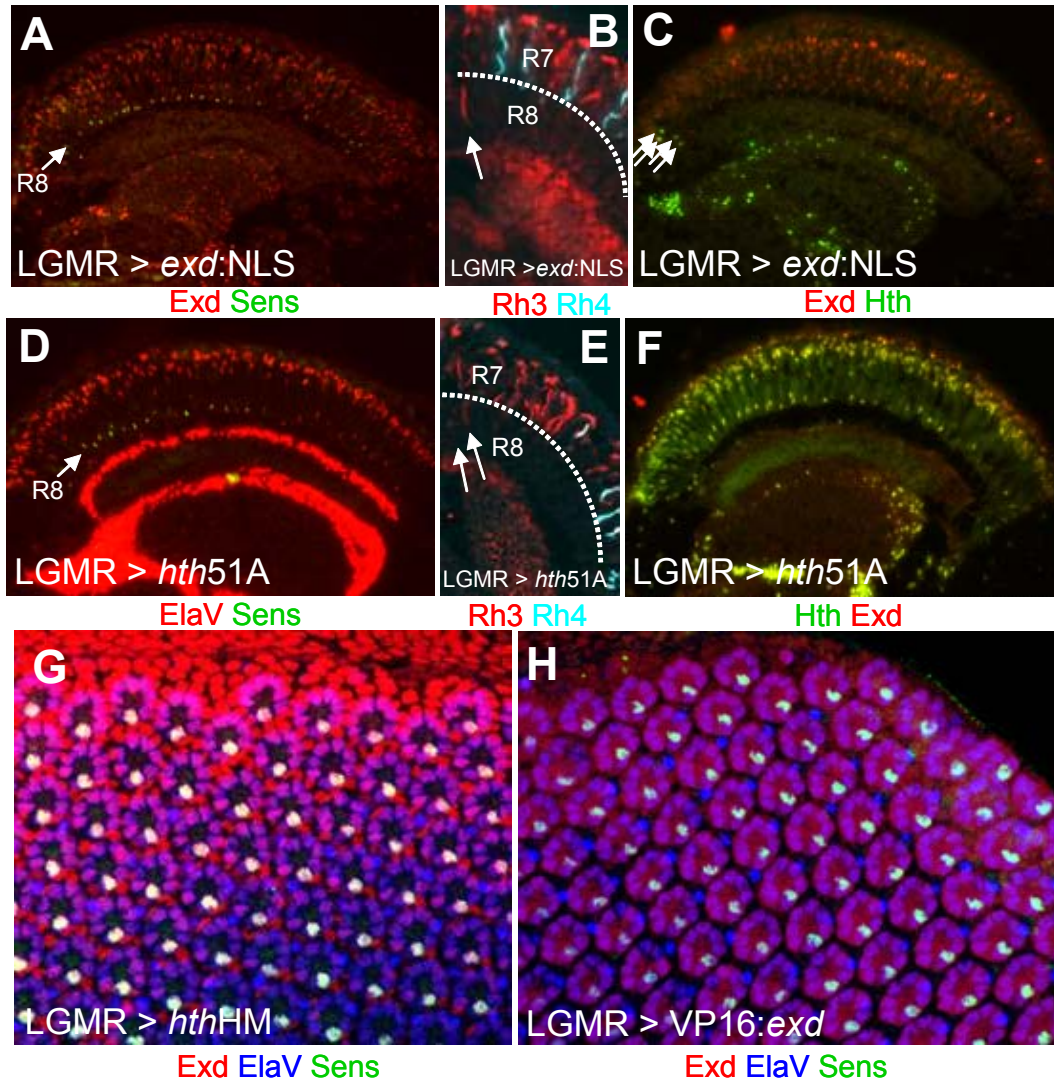
Fig III.2.10 Transcriptional activity of Hth is required for DRA development

(A)-(C) Nuclear localization of Exd is not sufficient to induce DRA development: Frozen sections through adult eyes from flies over-expressing nuclearly localized Exd (exd:NLS) under GMR-GAL4 control (LGMR > exd:NLS). Co-expression of Exd (red) and Sens (green) suggested that nuclear Exd was not sufficient to induce DRA development. (B) Frozen sections through LGMR > exd:NLS eyes double labeled for Rh3 red) and Rh4 (cyan). DRA-type Rh3 expression in R8 cells (white arrow) was not expanded outside of the DRA. (C) Expression of Hth (green) remained specific to inner PR nuclei in the DRA and was therefore not affected by ectopic expression of exd:NLS, as seen on frozen sections (white arrows).

(D)-(F) Mutation of the Homeodomain abolishes Hth function: Frozen sections through adult eyes from flies over-expressing Hth with a point-mutated Homeodomain (Hth51A) under GMR-GAL4 control (LGMR > hth51A). Sens expression (green) was not repressed by Hth51A (ElaV in red), probably due to its impaired ability to bind DNA. (E) DRA-type Rh3 expression (red) in R8 cells (white arrows) is not expanded in LGMR > hth51A flies. However, some ventral R8 cells were found to express Rh3 (not shown), suggesting some residual transforming potential for Hth51A. (F) Double labeling of frozen sections through LGMR > hth51A eyes with antibodies against Hth (green) and Exd (red) revealed that Hth51A was sufficient to localize Exd the nucleus.

(G) Deletion of the Hth homeodomain has a dominant negative effect: Pupal retinas (48 hrs APF) dissected from flies aver-expressing a from of Hth lacking the entire homeodomain (Hth^{HM}) under the control of GMR-GAL (LGMR > hth^{HM}). Triple labeling of Exd (red), Sens (green) and ElaV (blue) revealed, that Sens was no longer excluded from the dorsal-most ommatidia.

(H) Constitutively active Exd acts as a dominant negative: Pupal retinas dissected from flies aver-expressing a Exd fused to the transcriptional activator VP16 from yeast (Exd:VP16) under GMR-GAL control (LGMR > exd:VP16). Triple labeling of Exd (red), Sens (green) and ElaV (blue) revealed that Sens was no longer excluded from the dorsal-most ommatidia, very similar to LGMR > hth^{HM} flies.

(shown in red). Nuclear translocation of Exd without Hth is therefore not sufficient to induce DRA development.

In similar experiments, it was tested whether binding of Hth to target DNA was required for its function in DRA development. A mutant form of Hth that was impaired in its ability to bind DNA due to the mutation of amino acid Asn51 to Ala (Hth51A; (Ryoo et al., 1999), was ectopically expressed. Frozen sections through adult eyes from LGMR > *hth*51A flies were then double labeled with antibodies against Sens and ElaV (**Fig 10D**). Sens expression (shown in green) was not lost in these flies, suggesting that DNA-binding of Hth is required for Sens repression. However, some R8 cells in the ventral half of the eye (labeled by ElaV, shown in red) were found to lack Sens expression, suggesting that Hth51A has a very weak DRA-inducing potential. To confirm this result, Rh3 and Rh4 expression were visualized in adult LGMR > *hth*51A flies (**Fig 10E**). Rh3 expression (shown in red) was not induced in R8 cells and Rh4 expression remained unchanged in R7, suggesting that Hth51A has no significant DRA-inducing potential. Some ventral R8 cells were found to express Rh3 (data not shown), again suggesting that mutation of Asn51 does not abolish all of Hth's function. Finally it was tested whether Hth51 had lost its ability to localize Exd into the nucleus, by double labeling adult LGMR > *hth*51A eyes for Hth and Exd (**Fig 10F**). Strong co-staining for both Hth (shown in green) and Exd (shown in red) was detected in all adult PRs. It was therefore concluded that although Hth51A has lost most of its potential to repress Sens, it is still able to correctly translocate Exd to the nucleus.

The repression of Sens by Hth/Exd was further studied by over-expressing another mutant form of Hth which lacks the whole homeodomain. However, this truncated protein still contains the Exd-interacting HM domain and is therefore called *hth*HM (Ryoo et al., 1999). Over-expression of HthHM acts as a dominant negative in some cases, by translocating Exd in the nucleus and keeping it bound into an inactive complex. Pupal retinas were dissected from LGMR > *hth*HM flies and triple labeled for Sens, Exd and ElaV (**Fig 10G**). Sens expression (shown in green) was not excluded from the dorsal-most row of

ommatidia and instead, all PRs co-expressed nuclear Exd (shown in red) and Sens. Therefore, HthHM acts as a dominant negative in the developing DRA, as ectopic over-expression leads to the expansion of Sens expression into all R8 cells although it is still able to localize Exd to the nucleus. Due to the phenotype described above for Exd/Sens co-expression in *sens* gain-of-function flies (sGMR > *sens*), DRA development should be impaired in LGMR > *hth*HM flies and their R8 cells should express Rh6.

To complete the analysis of Sens repression by Hth/Exd, another mutant form of Exd was over expressed, in which the activation domain from the yeast transcription factor VP16 was fused to the ORF (VP16:Exd; Culi and Mann, unpublished). In different model systems, such VP16-fusion proteins transform transcription factors into constitutive activators. Pupal retinal from LGMR > VP16:*exd* were dissected and triple labeled using antibodies against Sens, Exd and ElaV (**Fig 10H**). Surprisingly, the phenotype observed was identical to the over-expression of HthHM: Sens expression (shown in green) was expanded into the R8 cells of the dorsal-most ommatidia. Sens was always found to be co-expressed with Exd:VP16 (shown in red) which was detected in the cytoplasm as well as in the nucleus. Therefore, ectopic expression of constitutively active Exd results in a dominant negative loss of DRA development, potentially due to the direct activation of Sens expression in DRA R8 cells.

It was concluded from these experiments that nuclear localization of both Hth and Exd is required for inducing the DRA ommatidial subtype. Furthermore, DNA-binding of Hth was required, suggesting that needs to be transcriptionally active. Finally, the transformation of Exd into a constitutively active form leads to a dominant negative effect on DRA development, raising the possibility that Hth/Exd directly repress *sens* expression in DRA R8 cells. Exd and Hth therefore behave very similarly to what has been described in other model systems. However, it remains to be shown whether a Hox factor is required for Exd/Hth function in DRA development.

2.11. Only inner PRs are competent to become DRA: the role of Spalt

Homothorax is sufficient to induce the DRA subtype throughout the eye when extopically expressed. However, outer PRs are not transformed into Rh3-expressing cells by Hth, suggesting that only inner PRs are competent to respond to Hth over-expression. Furthermore, generation of extra inner PRs at the dorsal rim results in induction of Hth only in the inner PRs R7 and R8, but never in outer PRs. Therefore, it appears that only PRs that have previously commited to the inner PR fate are competent to both induce Hth expression as well as provide the genetic environment for Hth to unfold its transforming potential. The *spalt* complex encodes the two homologous transcription factors Spalt major (*salm*) and Spalt related (*salr*) that are indispensable for inner PR maturation (Kuhnlein et al., 1994; Mollereau et al., 2001). It was therefore tested whether *sal* is required for Hth's role in DRA development.

To confirm that all Spalt-positive cells located at the dorsal rim induce Hth expression, when extra R7 cells were induced throughout the retina, pupal retinas from flies over-expressing activated Ras under the control of the *sevenless* promoter (*sev* > RasVal12; (Gaul et al., 1992) were dissected and triple labeled using antibodies against Sal, Hth and ElaV (**Fig 11A**). In this mutant background, many extra Spalt-positive cells (shown in red) were counted per ommatidium throughout the retina, suggesting that extra R7 cells induced by RasVal12 were real inner PRs. Furthermore, Sal-positive cells in the DRA (marked by a dashed line) were always found to co-express Hth (shown in green). It was therefore concluded that only cells marked with Spalt are competent to respond to the DRA-inducing signal emanating from the dorsal head cuticle.

It was tested whether Sal expression in a given PR was sufficient to induce the DRA fate at the DRA, by over-expressing Salm in all PRs, using the GAL4/UAS-system (see material and methods). Over-expression of Salm using GMR-GAL4 drivers (LGMR > *salm*) resulted in a very rough eye phenotype. However, pupal retinas were dissected and triple labeled for Sal, Hth and ElaV (**Fig 11B**). Retinal organization was rather perturbed and Salm expression levels
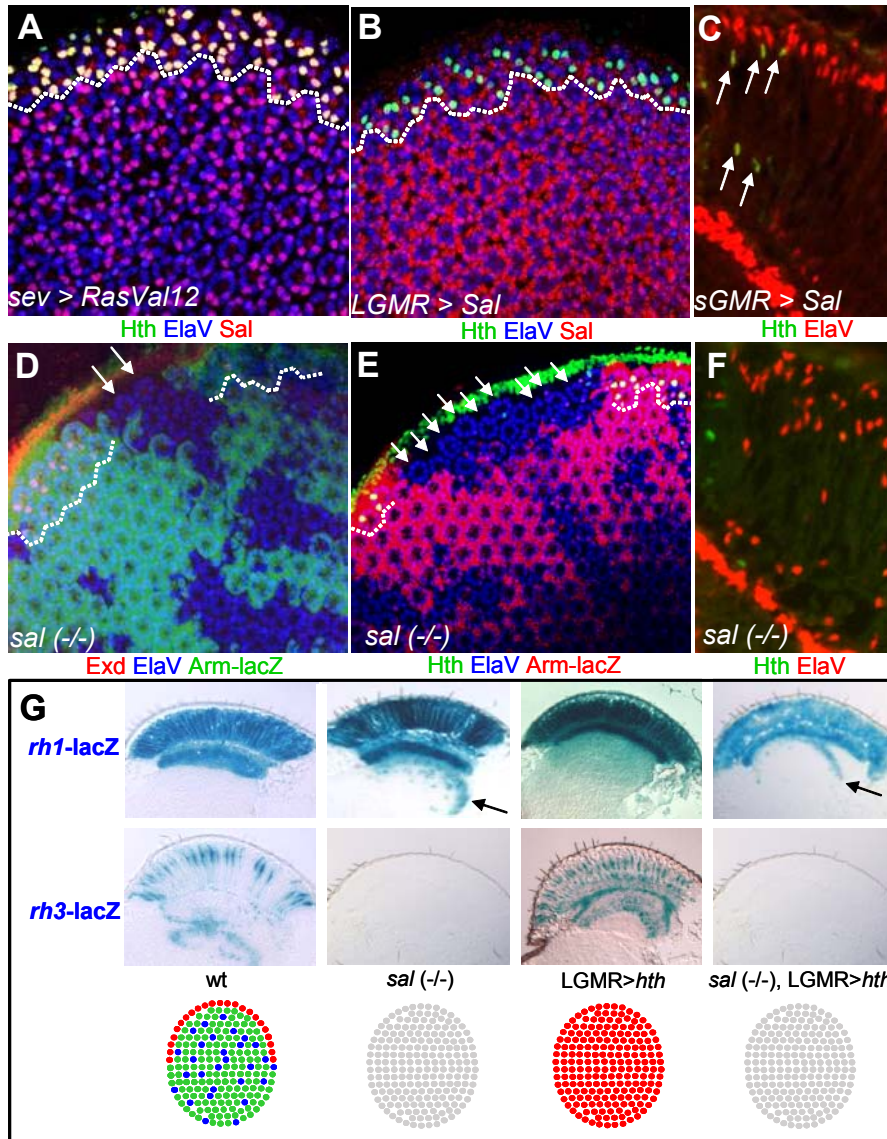
Fig III.2.11 Only inner PRs are competent to become DRA: the role of Spalt

(A) PRs choosing the DRA fate are always Spalt positive: Pupal retinas dissected from flies over-expressing activated Ras (RasVal12) under control of the sev promoter (sev > RasVal12). Triple labeling with antibodies against Hth (green), inner PR marker Sal (red) and ElaV (blue) revealed that all the induced inner PRs at the DRA (dashed line) co-expressed Hth and Sal.

(B)-(C) Ectopic Spalt is not sufficient to induce the DRA fate at the dorsal rim: Pupal retina dissected from flies over-expressing Sal under GMR-GAL4 control (LGMR > Sal). Triple labeling with antibodies against Hth (green), Sal (red) and ElaV (blue) revealed that no extra Hth-positive cells were induced at the DRA (dashed line) as compared to the wildtype.

(D) Nuclear Exd is lost in *sal* clones: Pupal retinas from flies inducing mitotic clones lacking *sal* function were triple labeled for Exd (red), Arm-lacZ (green) and ElaV (blue). Nuclear Exd was specifically lost in sal (-/-) clones (marked by the absence of Arm-lacZ) touching the DRA (dashed line).

(E)-(F): Hth expression is lost in *sal* clones: Pupal retinas from flies inducing mitotic clones lacking *sal* function were triple labeled for Hth (green), Arm-lacZ (red) and ElaV (blue). Hth expression was specifically lost in sal (-/-) clones (marked by the absence of Arm-lacZ) touching the DRA (dashed line).

(G) Specification of inner PRs is required for Hth function: Expression of the opsin reporter constructs *rh1*-lacZ and *rh3*-lacZ visualized by X-Gal staining on frozen sections in the wildtype (first column), *sal* mutants (second column), *hth* gain-of-function flies (LGMR > *hth*) and flies ectopically expressing hth in a *sal* (-/-) mutant background (last column). It was found that the opsin phenotype of sal(-/-) + LGMR > hth flies was identical to *sal* mutants: expression of *rh1*-lacZ was expanded into all PRs, while *rh3*-lacZ expression was completely lost. Hth was therefore not able to ectopically induce the *rh3*-expressing DRA fate in inner PRs, in the absence of *sal* function.

(shown in red) seemed to be variable. However, Hth expression (shown in green) was not expanded into all the Sal-expressing nuclei located within the DRA (marked by a dashed line), suggesting that Salm over-expression is not sufficient to induce Hth expression there. This result was confirmed by double labeling frozen sections through adult LGMR > *salm* eyes with antibodies against Hth and ElaV (**Fig 11C**). As in pupae, it was observed that the number of Hth-expressing nuclei (shown in green) was not significantly increased compared to the wildtype (white arrows). It was therefore concluded that ectopic Salm over-expression in developing PRs is not sufficient to induce Hth expression and therefore DRA development in outer PRs at the dorsal margin of the eye.

It was tested next whether Sal was necessary for DRA development by assessing Hth expression in mitotic clones of eye tissue homozygous for a null mutation in the *sal* locus. Clones were induced using the ey-flip/FRT technique (Xu and Rubin, 1993) see material and methods) and pupal retinas with sal (-/-) clones (marked by the absence of Arm-lacZ) were triple labeled using antibodies against Exd, βGal and ElaV (**Fig 11D**). Nuclear Exd expression (shown in red) was absent from sal (-/-) clones (marked by the absence of green staining) touching the DRA (marked by a dashed line). Nuclear localization of Exd was therefore lost in the absence of *sal* function, probably due to the loss of Hth expression. This was tested by triple labeling pupal retinas with sal (-/-) clones with antibodies against Hth, βGal and ElaV (**Fig 11E**). Hth expression (shown in green) was absent from sal (-/-) clones (marked by the absence of red staining) touching the DRA (marked by a dashed line). Both Hth and Exd expression are therefore lost in the absence of *sal*. To test whether this situation persists throughout PR maturation, frozen sections through whole mutant adult eyes lacking *sal* function were created using the ey-flip/FRT/GMR-hid technique (see material and methods) and double labeled for Hth and ElaV (**Fig 11F**). No Hth expression (shown in green) was detectable in adult PRs (marked in red) in the absence of *sal*. It was concluded that Hth/Exd expression, and therefore DRA development, depend on *sal* function. Ommatidia cannot develop into the DRA subtype without prior commitment of their inner PRs to the correct fate.

65

Finally, it was tested whether Hth was still able to induce DRA ommmatidia when ectopically over-expressed in sal (-/-) omatidia. Flies with whole mutant eyes lacking *sal* function, simultaneously over-expressing *hth* under the control of GMR-GAL4, were created using a combination of the ey-flip/FRT/GMR-hid and GAL4/UAS systems (see material and methods). The two different opsin-lacZ reporter constructs *rh1*-lacZ and *rh3*-lacZ were then introduced to assess ommatidial specification (**Fig 11G**). βGal activity was visualized on frozen sections through four different genotypes: wt, *sal* (-/-), LGMR > *hth* and *sal* (-/-) + LGMR > *hth*, using X-Gal staining (see material and methods). In the wildtype, expression of *rh3*-lacZ was detected in pale R7 cells as well as DRA R7 and R8 (top left), whereas expression of *rh1*-lacZ was specific to the outer PRs (bottom left). Due to the loss of inner PR identity, *rh3*-lacZ expression was totally lost in *sal* (-/-) mutants, whereas *rh1*-lacZ expression was expanded into all PRs, as seen by staining of axonal projections to both layers of the optic lobe (black arrow). As previously described, *rh3*-lacZ expression was expanded into all inner PRs in LGMR > *hth* flies, due to ectopic DRA formation. Expression of *rh1*-lacZ, however, was unaffected, as only inner PRs were transformed. Finally, flies lacking *sal* function as well as over-expressing *hth* in all PRs phenocopied *sal* (-/-) mutants: *rh3*-lacZ expression was completely lost (top right) and *rh1*-lacZ was expanded into all PRs (bottom right) as judged by their axonal projections (black arrow). It was therefore concluded that DRA ommatidia cannot be induced by Hth in the absence of *sal*.

Therefore, in order for DRA development to proceed, specification of inner PRs by Sal must have occurred in ommatidia at the dorsal rim. Sal expression in inner PRs is necessary but ectopic over-expression is not sufficient to induce Hth expression in outer PRs in the DRA. Establishment of the Sal-induced cell fate is furthermore crucial for the ability of Hth to develop its transforming potential.

2.12. Loss of Homothorax results in loss of the Dorsal Rim Area

Homothorax is expressed specifically in the inner PRs of the DRA and ectopically expressed Hth is able to induce DRA ommatidia in the entire retina.

To test whether *hth* is also necessary for DRA development, the Flip/FRT system (Golic, 1991; Xu and Rubin, 1993) was used to induce mitotic clones of homozygous eye tissue carrying the hypomorphic mutation *hth*[B2]. Epon thin sections (1µm) were performed and the iner PR rhabdomere diameter was analyzed under the light microscope (**Fig 12A**). Ommatidia located in such *hth*[B2](-/-) clones touching the dorsal eye margin lost their typical enlarged inner PR rhabdomere morphology (black arrows) while the DRA ommatidia outside of the clones retained their morphology (yellow arrows). It was therefore proposed that hth was necessary for DRA ommatidia to form (**Fig 12B**). According to this model, loss of *hth* would lead to the loss of typical DRA-type omatidia (white circles). However, Hth is could be recovered (Bessa et al., 2002). These clones were difficult to analyze in the adult eye, and the observed rhabdomere phenotype could therefore be explained by 'morphological stress' within the clone. To further test the hypothesis, the dominant negative Hth transgene hth[HM], containing the Exd-interacting 'HM domain' but lacking the entire homeodomain (*hth*[HM]; (Ryoo et al., 1999), was over-expressed. Adult flies expressing Hth[HM] under GMR control (GMR>*hth*[HM]) exhibited no obvious external eye phenotype (data not shown). As expected, this Hth[HM] could not transform inner PRs into DRA: Frozen sections through adult heads revealed that expression of the inner PR rhodopsins Rh3 and Rh4 was normal outside of the DRA (**Fig 12C**). In the DRA however, Rh3 was no longer expressed in R8 cells (white arrows), suggesting a loss of DRA fate, at least in the R8 cell layer. A *lacZ* enhancer trap insertion in *hth* was introduced to specifically mark the DRA in frozen sections through GMR>*hth*[HM] eyes (**Fig 12D**). R8 cells in the DRA of wildtype flies are a specialized cell type because they express neither the R8 marker Senseless (Sens) nor the R7 marker Prospero (Pros). However, *hth*-lacZ (shown in green) and Senseless (shown in pink) were co-expressed in the presence of GMR>*hth*[HM] (both arrows). Additionally, the nuclei of DRA R8 cells were now located significantly more basal (white arrow) as is typical for regular R8 cells. This further suggested that R8 cells had lost DRA identity and chosen the regular R8 cell fate. Axonal projections of *rh3*-lacZ expressing fibers were also visualized

in GMR> *hth^{HM}* flies (**Fig 12E**). Double labeling of βGal (shown in green) and the PR-specific cell-surface antigen 24B10 (shown in red) on frozen sections revealed that projections of *rh3*-lacZ expressing fibers to the R8 cell layer of the medulla were lost (top arrow), whereas *rh3*-lacZ expressing R7 terminations remained (bottom arrow): over-expession of dominant negative *hth^{HM}* leads to a

*hth*B2 (-/-)

Loss of hth

LGMR > *hthHM*   24B10 rh3-lacZ

LGMR > *hthHM*
Rh3 Rh4

LGMR > *hthHM*
Sens hth-lacZ

LGMR > *hthHM*
Rh3 hth-lacZ

LGMR > *hthHM*
Rh6 hth-lacZ

LGMR > *hthHM*
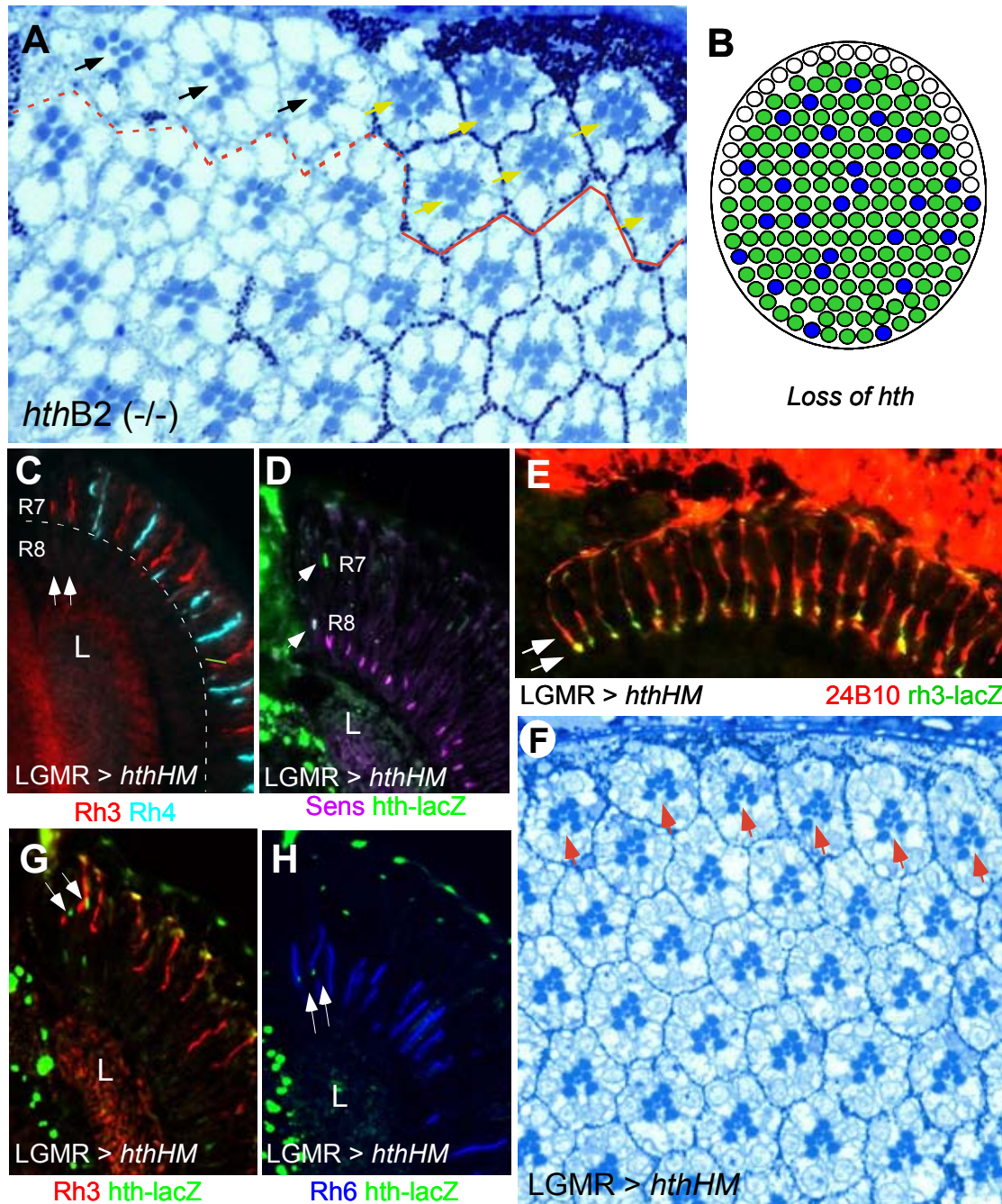
Fig III.2.12 Loss of Homothorax results in loss of the Dorsal Rim Area
(A) Loss of *hth* leads to a loss of DRA morphology: Epon thin section through adult eyes of flies with clones of eye tissue homozygous for the *hth* hypomorph B2, labeled by absence of *white* pigment (left). Analysis of inner PR rhabdomere morphology in clones touching the DRA revealed that mutant ommatidia (black arrows) located at the dorsal eye rim lose the enlarged inner PR rhabdomere phenotype (yellow arrows) and resemble non-DRA ommatidia instead.
(B) Schematic diagram depicting the specific loss of DRA ommatidia (shown in white) in retinas lacking hth function.
(C)-(E) Dominant negative Hth leads to loss of DRA fate in R8 cells: Frozen section (10 μm) along the D/V axis (dorsal to the left, equator runs horizontally, L=Lamina) through adult heads of flies over-expressing dominant negative Hth under the control of 'Long'GMR-GAL4 (GMR>hthHM). Double labeling of Rh3 (red) and Rh4 (cyan) revealed a loss of Rh3 expression in R8 cells of the DRA (white arrows).
(D) Double-labeling of *hth*-lacZ (green, both arrows) and Sens (red) in GMR>hthHM flies revealed that R8 cells in the DRA maintain Sens expression (white arrow) and that the position of their nuclei is almost at the same level as those of non-DRA R8 (compare Fig 3F). In some instances the nuclear position was even identical to non-DRA R8 cells (data not shown). This suggests they have lost their DRA identity, as Sens is usually strictly excluded from DRA R8 cells (compare Fig 3F).
(E) Projections of *rh3*-lacZ expressing cells to the R8 layer in the medulla is lost in GMR>*hth*^{HM} flies. Double labeling of lacZ (green) and the PR marker 24B10 (red) reveals no projections of the dorsal-most fibers to the R8 layer (top arrow) whereas rh3-lacZ expressing fibers still are seen to project to the corresponding R7 layer (bottom arrow) indicating that R8 cells clearly lost the DRA fate.
(F)+(G) Loss of Hth transforms the DRA into 'atypical' color-sensitive ommatidia: Double labeling of the DRA (*hth*-lacZ) and inner PR opsins in frozen sections through adult heads of GMR>*hth*^{HM} flies (dorsal to the left, equator runs horizontally). DRA R7 cells marked by lacZ expression (E, arrows) still expressed Rh3 (red), but the underlying R8 cells marked by lacZ (F, arrows) always expressed Rh6 (blue) suggesting that loss of *hth* function leads to transformation of the DRA into a color-sensitive eye region containing atypical Rh3/Rh6 ommatidia.
(H) Dominant negative *hth* leads to loss of DRA morphology in R7 and R8: Epon thin sections through adult eyes of flies over-expressing dominant negative Hth in all PRs (GMR>*hth*^{HM}) revealed a loss of DRA morphology in both R7 and R8. The typical increase of the rhabdomere diameter in central PRs observed in the wildtype DRA is lost in GMR>*hth*^{HM} flies, resulting in otherwise normal eyes, completely lacking a specialized DRA (black arrows).

clear loss of DRA identity only in R8 cells, as R7 cells in the DRA maintain *rh3*-expression.

To assess whether *rh3*-expressing R7 cells in the DRA of GMR>*hth*^{HM} flies had lost their DRA identity, their inner PR rhabdomere morphology was analyzed (**Fig 12F**). Epon thin sections (1μm) were performed on these retinas and analyzed under the light microscope. All central PR cells (R7 and R8) at the dorsal rim of adult GMR>*hth*^{HM} retinas had lost their typical large rhabdomere diameter (red arrows). Morphologically, these flies had therefore completely lost their DRA.

Finally, analysis of opsin expression of dorsal-most ommatidia in GMR>*hth*^{HM} flies was completed by double labeling all four inner PR opsins and *hth*-lacZ. First, frozen sections were double labeled for Anti-Rh3 and *hth*-lacZ (**Fig 12G**). It was clear that all *hth*-lacZ expressing R7 cells (shown in green) had retained Rh3 expression (shown in red) as suggested by previous stainings (white arrows). In a similar experiment, *hth*-lacZ was co-labeled with Anti-Rh6 on frozen sections (**Fig 12H**). All Hth-positive R8 cells (green) always expressed Rh6 (shown in blue), resulting in DRA ommatidia with an 'odd-coupled' Rh3/Rh6 expression (white arrows). Rh4 or Rh5 were never found to be expressed in hth-lacZ positive DRA inner PRs of these flies (data not shown). In wildtype flies, a

low ratio (~6%) of 'atypical' odd-coupled Rh3/Rh6 ommatidia exists outside of the DRA, whereas R4/Rh5 ommatidia never occur (Chou et al., 1996). Therefore, over-expression of dominant-negative Hth appears to prevent DRA development and atypical color-sensitive ommatidia are always formed instead.

It was concluded from these experiments that *hth* is necessary for inner PRs in the DRA to induce development into polarization detectors. Interestingly, loss of Hth function always results in the formation of atypical color-sensitive (Rh3/Rh6) ommatidia rather than in a stochastic choice between correctly specified **p** and **y** subtypes. As this effect was independent of Hth, the high levels of *wg* pathway activity at the dorsal rim might be directly repressing stochastic choice of color sensitive ommatidial fates.

2.13. The DRA forms normally in *orthodenticle* and *prospero* mutants

It was shown that Homothorax is part of the regulatory network specifying PR cell fate decisions during ommatidial substype specification. Hth is both necessary and sufficient for inducing the DRA ommatidial subtype. Furthermore, definition of inner PRs by the *spalt* (*sal*) complex is necessary for Hth expression in DRA inner PRs. The genes *propspero* (*pros*) and *orthodenticle* (*otd*) play important roles in inner PR maturation downstream of *sal*. DRA development was therefore assessed in these mutants.

Both, loss of Hth and Sal, lead to a loss of DRA ommatidia. Genetic experiments have further shown that *hth* is most likely required downstream of *sal*, as *hth* expression is lost in *sal* (-/-) mutant clones and *hth* is no longer able to induce DRA ommatidia in the absence of *sal* function. According to this model, specification of inner PRs should proceed normally in hth (-/-) mutant clones. To test this, mitotic clones of mutant eye tissue lacking *hth* function were induced, using the ey-flip/FRT-system (see material and methods). Pupal retinas with clones homozygous for the *hth* null allele *hth*P2 were dissected and triple labeled with antibodies against the inner PR marker Spalt (Sal), βGal and ElaV (**Fig 13A**). Sal expression (shown in red) was unaffected by the loss of Hth (marked by the absence of βGal, shown in green) in clones touching the DRA. This

suggested that inner PR sepecification is normal in the absence of *hth*, supporting a role of *hth* downstream of *sal*.

The gene *pros* had previously been shown to play a crucial role for R7 maturation, by directly repressing *rh5* and *rh6* expression in R7 cells, where Pros was found to be specifically expressed (Cook and Desplan, 2001). Recently, *pros* function has been shown to be required downstream of *sal*, as *pros* expression was found to be lost in *sal* clones (Domingos et al., 2004). As R7 cells in the DRA co-expressed Hth and Pros, it was tested whether pros was required for DRA development. Whole mutant eyes lacking *pros* function were created using the *ey*-flip/FRT/GMR-*hid* technique (Stowers and Schwarz, 1999; Xu and Rubin, 1993) Stowers and Schwarz, 1999) and the *pros* null allele *pros*[17.17]. Frozen sections through pros (-/-) mutant eyes were then double labeled with antibodies against Rh3 and Rh4 (**Fig 13B**). It was found that Rh3 expression (shown in red) was lost in most R7 cells, whereas Rh4 expression (shown in cyan) appeared to be unaffected by the loss of pros. However, Rh3 expression was always detectable in the DRA inner PRs (white arrow), suggesting that the DRA develops normally in *pros* (-/-) mutant eyes. This was tested by double labeling frozen sections through *pros*[17.17] mutant eyes with antibodies against Hth and ElaV (**Fig 13C**). Hth expression (shown in green) was found to be indistinguishable from wildtype in R7 cells (top arrows) as well as R8 cells (bottom arrow). It was therefore concluded that, although loss of *pros* affects *rh3*-expressing pale-type R7 cells, it has no effect on Hth expression and DRA development.

Ommmatidial specification had been shown to be severely affected in flies lacking the homeodomain transcription factor Orthodenticle (Finkelstein et al., 1990; Vandendries et al., 1996). Otd had been shown to regulate inner PR opsin expression by directly binding to the *rh3*, *rh5* and *rh6* promoters (Tahayato et al., 2003). As DRA inner PRs always expressed Rh3, it was tested whether DRA development was affected in the absence of Otd. Whole mutant eyes lacking *otd* function were generated by usig the *ey*-flip/FRT/GMR-*hid* technique (Stowers and Schwarz, 1999; Xu and Rubin, 1993) and the *otd* null allele *otd*[2].

A Sal ElaV Arm-lacZ

B Rh3 Rh4

C Hth ElaV

D *otd (-/-)* Rh3 Rh4

E *otd (-/-)* Rh5 Rh6

F *otd2(-/-)* Hth ElaV Arm-lacZ
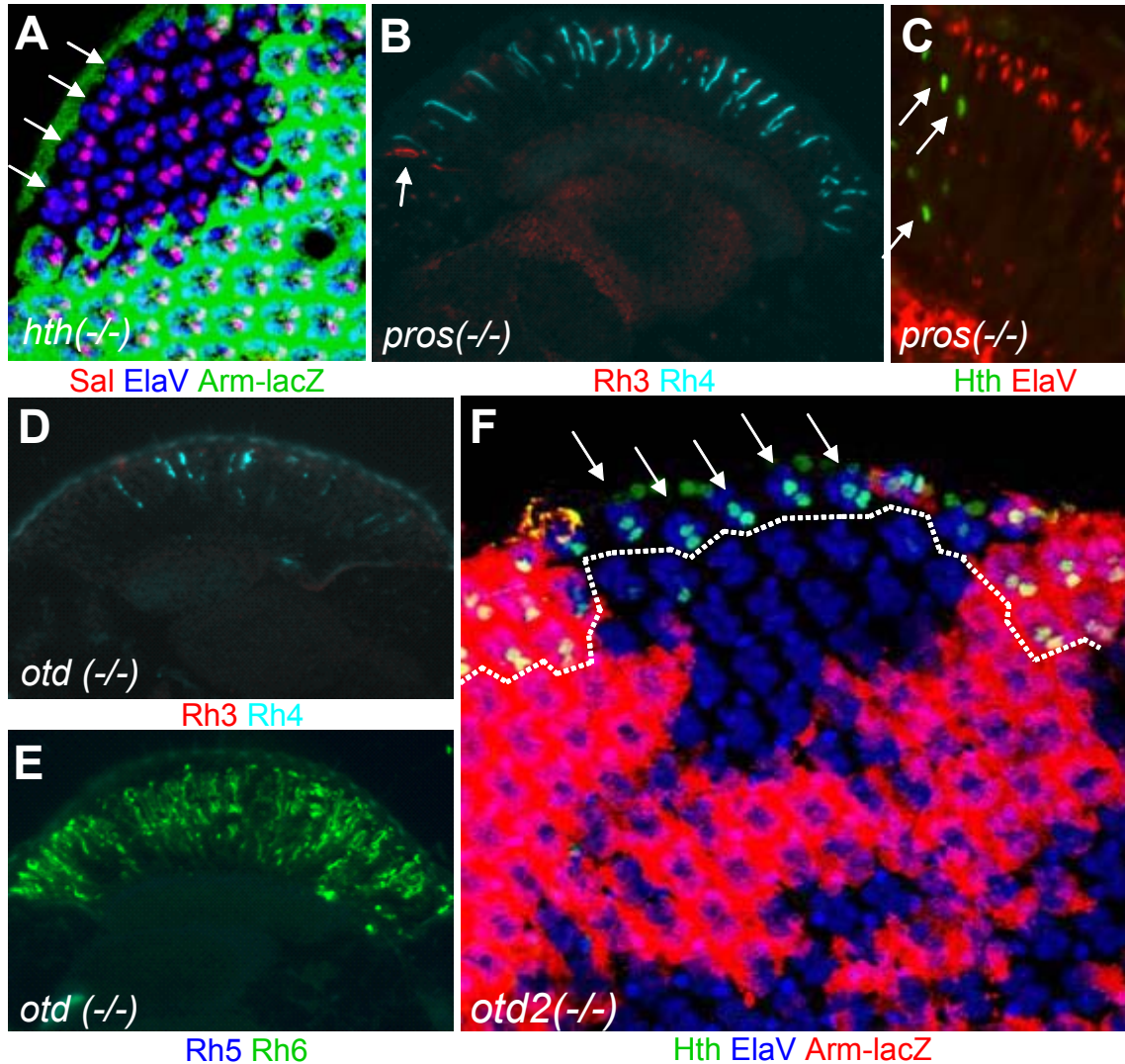
Fig III.2.13 The DRA forms normally in *orthodenticle* and *prospero* mutants
(A) Inner PRs get specified correctly in *hth^P2* (-/-) clones: Pupal retina (48 hrs APF) dissected from flies inducing mitotic clones lacking hth function triple labeled for the inner PR marker Sal (red), Arm-lacZ(green) and ElaV (blue). No change in Sal expression was detected within or outside of hthP2 (-/-) clones (marked by the absence of Arm-lacZ) touching the DRA.
(B)-(C) The DRA develops normally in *pros* mutants: Frozen sections through whole mutants eyes lacking *pros* function, double labeled for Rh3 (red) and Rh4 (cyan). While Rh3 expression was lost in **p**R7 cells, expression persisted in the DRA (arrow). Expression of Rh4 was not affected by the loss of *pros*. (C) Hth expression is unaffected in *pros^17.17* (-/-) mutant eyes, as visualized on frozen sections double labeled with antibodies against Hth (green) and ElaV (red).
(D)-(E) *otd* mutants have a dramatic opsin phenotype: Frozen sections through whole mutants eyes lacking *otd* function were double labeled for Rh3 (red) and Rh4 (cyan). Rh3 expression was completely lost, while some expression of Rh4 persisted in *otd^2* (-/-) eyes. (E) Expression of R8 opsins Rh5 (blue) and Rh6 (green) was severely affected on frozen sections through *otd^2* (-/-) eyes. While Rh5 was completely lost, Rh6 expression was dramatically expanded throughout the retina.
(F) The DRA develops normally in *otd* mutants: Pupal retina dissected from flies inducing mitotic clones lacking *otd* function were triple labeled for Hth (green), Arm-lacZ(red) and ElaV (blue). Hth expression persisted within *otd^2* (-/-) clones (marked by the absence of Arm-lacZ) touching the DRA. However, the extent of the DRA (dashed line) seemed reduced to one row as compared to two rows in the surrounding wildtype tissue.

Frozen sections through otd (-/-) eyes were then double labeled with antibodies against Rh3 and Rh4 (**Fig 13D**). Rh3 expression (shown in red) was completely lost in the absence of *otd,* whereas Rh4 expression (shown in cyan) was still

detectable. However, only few Rh4-positive cells were detectable. This had previously been explained by the strong rhabdomere degeneration phenotype observed in otd^2 (-/-) eyes. It was therefore concluded that Rh3 expression is specifically lost in the absence of Otd. Frozen sections through otd^2 (-/-) eyes were also labeled with antibodies against the R8 opsins Rh5 and Rh6 (**Fig 13E**). As in R7 cells, the pale opsin Rh5 (shown in blue) seemed to be specifically lost in R8 cells. Expression of the yellow R8 opsin Rh6 (shown in green), however, was dramatically expanded throughout the retina. This was consistent with the model that Otd acts as an activator for *rh3* and *rh5* transcription in pale ommatidia and as a repressor of *rh6* experrsion in outer PRs (Tahayato et al., 2003). Differentiatin of the DRA was therefore severely affected in otd^2 (-/-) eyes, as Rh3 expression was lost. However, secific binding of Otd to the opsin promoters suggested a role for Otd as a terminal effector downstream of hth in DRA development. This was tested by inducing mitotic clones of otd^2 (-/-) eye tissue, negatively marked by the absence of Arm-lacZ (see material and methods). Pupal retinas (48 hrs APF) were then dissected and triple labeled with antibodies against Hth, βGal and ElaV (**Fig 13F**). Hth expression (shown in green) clearly persisted in otd^2 (-/-) clones (marked by the absence of βGal, in red) touching the DRA (marked by a dashed line). Interestingly, the number of ommatidial rows seemed to be reduced from two to one inside the clone, suggesting that there might be some role for *otd* in regulating *hth* expression. However, as Hth expression was not lost in these clones, it was concluded that the DRA was still developing in the absence of *otd*, supporting a late role for this gene during the terminal differentiation of DRA ommatidia.

Therefore, DRA development is not affected by the loss of *prospero*, whereas loss of *orthodenticle* results in loss of Rh3 expression, but not in loss of Hth, thereby affecting terminal differentiation of DRA ommatidia.

2.14. Orthodenticle is required downstream of *hth* in DRA development

It has been shown that Rh3 expression is lost in otd^2 mutants. However, Hth expression persisted in these null mutants, suggesting that *otd* might play an

important role in DRA development downstream of *hth*. A homozygous viable, eye-specific *otd* mutant had previously been reported, called *otd*^{UVI} (Vandendries et al., 1996). This mutant was used to further investigate the relationship between *hth* and *otd* in DRA development.

Frozen sections through adult heads from homozygous *otd*^{UVI} mutants were double labeled using antibodies against Rh3 and Rh4 (**Fig 14A**). The R7 opsin phenotype obtained was virtually identical to the one observed for *otd*^{2} flies: Rh3 expression (shown in red) was completely lost, including in the DRA, and Rh4 expression (shown in cyan) was persistent, but weak, due to a rhabdomere degeneration phenotype. It was therefore concluded that *otd*^{UVI} mutants were lacking all otd function in the eye. Development of the DRA was then characterized in more detail in *otd*^{UVI} mutants, by dissecting pupal retinas (48 hrs APF) and triple labeling with antibodies against Exd, Sens and ElaV (**Fig 14B**). In wildtype flies, expression of the R8 marker Sens (shown in green) was always found to be excluded from the DRA (marked by Exd, shown in red), at this developmental stage. In *otd*^{UVI} mutants, most Exd-expressing DRA ommatidia were also found to exclude Sens expression. However, some ommatidia co-expressing Exd and Sens in R8 cells were observed in these mutants (white arrows). This suggested that DRA development might be slightly affected in the absence of *otd*. Interestingly, a reduced number of ommatidial rows of the DRA subtype has been observed in *otd*^{2} mutants. Due to the relatively strong dis-organization of the *otd*^{UVI} retina, detection of Hth expression in the adult DRA was rather difficult. Frozen section were performed and double labeled for Hth and ElaV (**Fig 14C**). Hth expression (shown in green) was detectable in the DRA of *otd*^{UVI} mutants, suggesting that DRA was initially specified in these mutants.

As *rh3* expression was completely lost and *rh4* expression did not seem to expand in the different *otd* mutants, it was asked which opsin genes the inner PRs were expressing in *otd*^{UVI} mutants, within or outside the DRA. First, *rh1*-lacZ reporter constructs were introduced and frozen sections through adult heads were stained with antibodies against βGal and the PR-specific cell-surface

74

antigen 24B10 (**Fig 14D**). In wildtype flies, expression of this reporter was always found to be restricted to outer PRS, with axonal projections exclusively terminating in the lamina part of the optic lobe. In otd^{UVI} mutants, however, some axon fibers expressing βGal (shown in green) were found to terminate in the medulla (M), where inner PRs usually terminate. It was concluded that some inner PRs lacking otd could therefore be expressing Rh1. However, the small numer of $rh1$-expressing R7 cells did not account for all the cells having lost $rh3$ expression. Strong expansion of $rh6$ expression into outer had been shown before for otd^2 mutants. It was therefore tested whether $rh6$ expression had also expanded into R7 cells, by introducing $rh6$-lacZ reporter constructs and double labeling frozen sections through adult otd^{UVI} heads with antibodies against βGal and 24B10 (**Fig 14E**). Strong expansion of βGal expression (shown in green) was observed in outer PRs (terminating in the lamina, L) and R8 cells (terminating in the upper layer of the medulla, M). However, several R7 cells were found to express $rh6$, based on βGal expression (white arrows). It was therefore concluded that R7 cells in otd^{UVI} mutants expressed either $rh1$, $rh4$ or $rh6$. The inner PRs projecting to the dorsal-most edge of the medulla did not seem to show any preference among the three opsins suggesting that they behave like regular inner PRs.

The ability of Hth to induce DRA ommatidia in an otd^{UVI} mutant background was finally tested. The opsin drivers $rh1$-lacZ, $rh3$-lacZ and $rh6$-lacZ were introduced and βGal activity was visualized on frozen sections, using X-Gal (**Fig F**). Four different genotypes were compared: wt, otd^{UVI}, LGMR>hth and otd^{UVI} + LGMR>hth. In the wildtype (first column), $rh1$-lacZ was restricted to the outer PRs, projecting to the Lamina (L). The two inner PR-specific transgenes $rh3$-lacZ and $rh6$-lacZ were specifically expressed in medulla-projecting subsets of R7 cells or R8 cell, repectively. In otd^{UVI} mutants (second clumn), opsin-lacZ constructs behaved as previously described: $rh1$-lacZ expression was expanded to the medulla (black arrow), $rh3$-lacZ was lost and $rh6$-lacZ expression expanded with βGal-expressing axons terminating in both lamina and medulla. Opsin-lacZ expression in LGMR > hth (third column) had previously been

described: while *rh1*-lacZ expression was unaffected, *rh3*-lacZ was expanded to all inner PRs projecting to the medulla and *rh6*-lacZ was completely lost. Opsin expression in flies over-expressing *hth* in a *otd*^UVI mutant background (*otd*^UVI, (**Fig** (**Fig 14F**). Four different genotypes were compared: wt, *otd*^UVI, LGMR>*hth* and *otd*^UVI + LGMR>*hth*. In the wildtype (first column), *rh1*-lacZ was restricted to
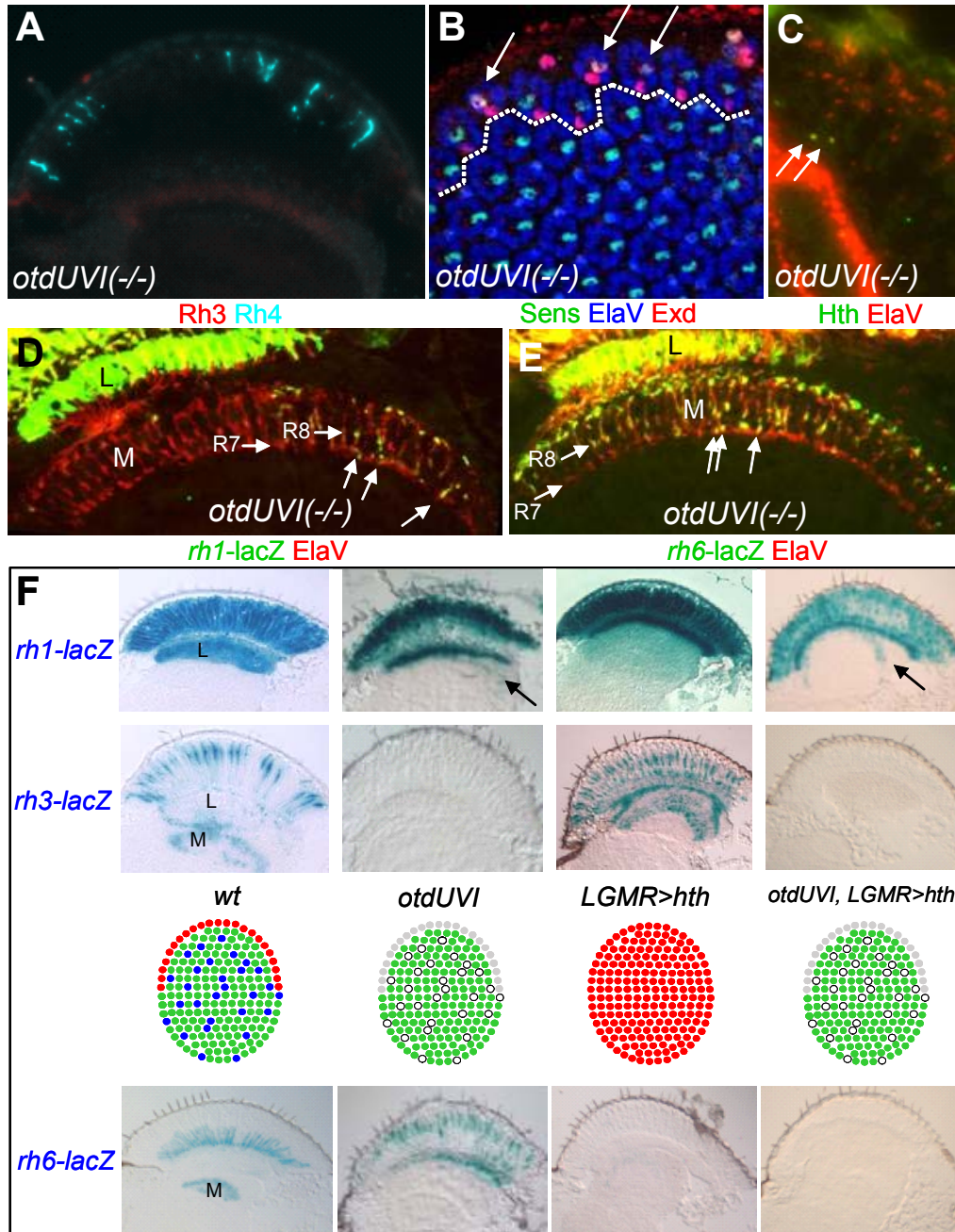
Fig III.2.14 Orthodenticle is required downstream of *hth* in DRA development

(A) Expression of Rh3 is lost in *otdUVI* mutants: Frozen sections through adult eyes from *otdUVI* mutants double labeled with antibodies against Rh3 (red) and Rh4 (cyan). Rh3 expression was completely lost, including in the DRA; some Rh4 expression persisted.

(B)-(C) The DRA gets specified in *otdUVI* mutants: Triple labeling of pupal retinas (48 hrs APF) from *otdUVI* mutants for Exd (red), Sens (green) and ElaV (blue). Nuclear Exd was detected in the DRA (dashed line). In some cases, co-expression between Exdand Sens was detected (arrows) suggesting that DRA development is perturbed in *otdUVI* mutants. (C) Double labeling of frozen sections through *otdUVI* mutant eyes with antibodies against Hth (green) and ElaV (red): Hth expression in the DRA persisted in these mutants (white arrows).

(D) Some Inner PRs express *rh1* in *otdUVI* mutants: Frozen sections through adult eyes from *otdUVI* mutants carrying a rh1-lacZ reporter transgene. Double labeling with antibodies against βGal (green) and the PR-specific cell-surface marker 24B10 (red) revealed that some inner PRs, projecting axon projections into the medulla (M) expressed *rh1*-lacZ (white arrows). Most of the βGal–positive axons were found to terminate in the deeper level of the medulla, suggesting that *rh1*-lacZ was expressed in R7 cells.

(E) Some R7 cells express *rh6* in *otdUVI* mutants: Frozen sections through adult eyes from *otdUVI* mutants carrying a *rh6*-lacZ reporter transgene. Double labeling with antibodies against βGal (green) and 24B10 (red) revealed that βGal expression was dramatically expanded into outer PRs, projecting axons into the lamina (L). Furthermore, some R7 cells, projecting axon projections into the lower level of the medulla (M) had also gained expression of *rh6*-lacZ (white arrows).

(F) Otd is required for DRA induction by *hth*: expression of the opsin reporter constructs *rh1*-lacZ, *rh3*-lacZ and *rh6*-lacZ was visualized by X-Gal staining on frozen sections in the wildtype (first column), *otdUVI* mutants (second column), *hth* gain-of-function flies (LGMR > *hth*) and flies ectopically expressing *hth* in a *otdUVI* mutant background (last column). It was found that the opsin phenotype of *otdUVI* + LGMR > hth flies was largely identical to *otdUVI* mutants: expression of *rh1*-lacZ was expanded into inner PRs (black arroe), while *rh3*-lacZ expression was completely lost. Hth was therefore not able to ectopically induce the *rh3*-expressing DRA fate in inner PRs, in the absence of *otd* function. However, *rh6*-lacZ expression was lost in *otdUVI* + LGMR > hth flies, suggesting that *hth* was still able to repress *rh6* expression in these flies.

the outer PRs, projecting to the Lamina (L). The two inner PR-specific transgenes *rh3*-lacZ and *rh6*-lacZ were specifically expressed in medulla-projecting subsets of R7 cells or R8 cell, repectively. In *otd*^UVI mutants (second clumn), opsin-lacZ constructs behaved as previously described: *rh1*-lacZ expression was expanded to the medulla (black arrow), *rh3*-lacZ was lost and *rh6*-lacZ expression expanded with βGal-expressing axons terminating in both lamina and medulla. Opsin-lacZ expression in LGMR > *hth* (third column) had previously been described: while *rh1*-lacZ expression was unaffected, *rh3*-lacZ was expanded to all inner PRs projecting to the medulla and *rh6*-lacZ was completely lost. Opsin expression in flies over-expressing *hth* in a *otd*^UVI mutant background (*otd*^UVI, LGMR>*hth*) was examined last (fourth column). *Rh1*-lacZ expression was found to be expanded into all PRs, judging by projections to both lamina and medulla (black arrow) and *rh3*-lacZ expression was completely lost despite ectopic hth. Based on these results, it was therefore concluded that *otd*^UVI, LGMR>*hth* flies phenocopied *otd*^UVI mutants, demonstrating that otd acted downstream of hth. However, *rh6*-lacZ expression (bottom right) was lost in these flies, demonstrating that ectopic *hth* was able to induce repression of *rh6* in all PRs.

It was concluded from these experiments that otd is required downstream of hth for activation of rh3 expression in the DRA ommatidia.

2.15. The dorsal selector genes are not necessary for DRA formation

Homothorax is necessary as well as sufficient to induce formation of the DRA ommatidia which are always found in a band of maximally two rows along the head cuticle throughout the dorsal eye compartment. Regulatory mechanisms therefore seem to exist, limiting the extent of the DRA to the dorsal eye. One group of genes representing ideal candidates for providing such positional information are the members of the *IRO-C* complex (Gomez-Skarmeta et al., 1996; McNeill et al., 1997). These genes are required to specify the dorsal region of the eye imaginal disc and to define the D/V pattern organizer, the equatorial region of the disc that is critical for growth and patterning of the eye (for review: Cavodeassi et al., 2000). The *IRO-C* genes *mirror (mirr)*, *araucan (ara)* and *caupolican (caup)* have been shown to be expressed dorsally anterior to the morphogenetic furrow from where their their expression faded away after late 3rd instar stages (Dominguez and de Celis, 1998); (Kehl et al., 1998);(Cavodeassi et al., 1999). Therefore, no role had yet been assigned to these genes in developing PRs posterior to the MF. Since the DRA is restricted to the dorsal retina, it was tested whether the *IRO-C* complex played a role in its development.

Several enhancer traps inserted in the *IRO-C* complex have been reported. In some of them, the reporter gene *white* (*w*) comes under the influence of adjacent genomic enhancers, leading to an expression of *w* which was limited to the dorsal eye (**Fig 15A**; (Brodsky and Steller, 1996). Although this dorsal-specific *w* expression could have been reminiscent of an early expression in PRs, it was tested whether *IRO-C* genes were expressed in PRs during late phases of eye development. As there were no reliable antibodies available, *IRO-C* expression was assessed at time points when *hth* expression had been observed before, by using several available *IRO-C lacZ* enhancer trap lines. First, expression of the the nuclear lacZ enhancer trap *caup-lacZ* (rF209) was

visualized in the adult. Frozen sections (10 µm) through adult heads form rF209 flies were double labeled for βGal as well as the DRA opsin Rh3 (**Fig 15B**). It was found that βGal (shown in cyan) was strongly expressed in all cells in the dorsal retina, including the DRA (white arrow). Expression of several enhancer trap insertions in *mirr* were also tested but showed no expression at this stage. Although Mirr protein might behave differently, differences in the expression of *ara* and *caup* versus *mirr* had previously been reported (Pichaud and Casares, 2000). It was concluded that at least one of the *IRO-C* genes shows dorsal-specific expression in the adult eye.

The onset of Homothorax expression in DRA inner PRs was found to be in early pupation. We therefore assessed expression of rF209 (*caup*) in pupal retinas (48 hrs APF) by triple labeling Hth, rF209 and ElaV (**Fig 15C**). Consistent with previously reported down-regulation of *IRO-C* genes posterior to the morphogenetic furrow in larvae, rF209 (*caup*) expression (shown in blue) was much weaker but still present in dorsal PRs at in pupae, resulting in co-expression with Hth (shown in green). Expression was strongest in the most dorsal ommatidia and faded away few rows away from the dorsal cuticle rather than manifesting uniform expression levels in the dorsal compartment. The observed expression pattern therefore remained specific to the dorsal retina but manifested important changes in its expression level over time, since we found these genes to be strongly expressed in all dorsal PRs of the dorsal eye in the adult. It was concluded that *caup* (and maybe *ara* and *mirr*), was transiently down-regulated during pupation as it showed only weak co-expression with Hth in DRA inner PRs at that time.

Co-expression of *caup* (rF209) and Hth was then assessed in the adult eye, by double labeling frozen sections with antibodies against βGal and Hth (**Fig 15D**). As before, strong *caup* expression was detected in all dorsal PRs (shown in cyan), however, expression in DRA inner PRs was significantly down-regulated as only weak co-expression with Hth (shown in red) was observed. This suggested that low levels of *IRO-C* might specifically be required in DRA inner PRs, or that Hth was able to repress *IRO-C* expression. To test the
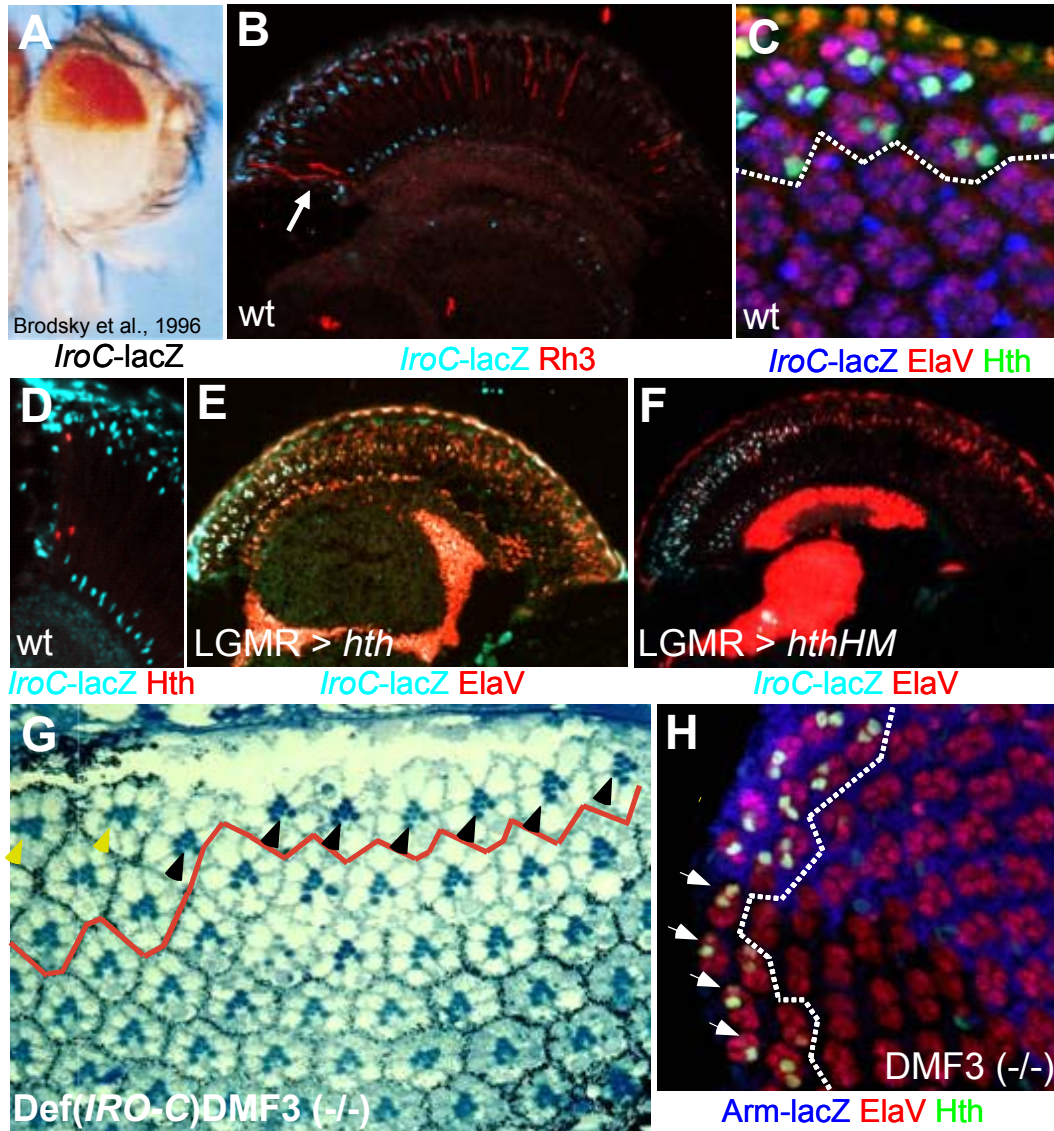
Fig III.2.15 The dorsal selector genes are not necessary for DRA formation

(A)-(D) The *IRO-C* complex is specifically expressed in the dorsal eye: In several enhancer traps, the selection marker *white* (*w*) has come under the influence of genomic enhancers belonging to the *IRO-C* comlex. Eye pigmentation had been reported to be specific to the dorsal compartment of the adult eye. (B) Adult expression of *caup*-lacZ: Frozen section (10 μm) along the D/V axis (dorsal to the left) through adult heads of flies carrying the *caup* (rF209) enhancer trap. Double-labeling using antibodies against Rh3 (red) and βGal (cyan) revealed strong lacZ expression throughout the adult dorsal eye. (C) Weak pupal expression of *IRO-C* genes in dorsal PRs: Flat mounted pupal retina (~48 hrs APF) dissected from flies carrying the caup (rF209) insertion. Triple-labeling against ElaV (red), Hth (green) and βGal (blue) revealed weak rF209 expression in all PRs of dorsal ommatidia, fading towards the equator but clearly co-expressed with Hth in the developing DRA ommatidia (dashed line). (D) *IRO-C* expression is low in inner PRs of the adult DRA, as visualized on frozen sections double labeled with Anti-Hth (red) and rF209 (cyan).

(E) Over-expression of Hth has no effect on *IRO-C* expression: Frozen sections through adult eyes from flies ectopically expressing Hth (LGMR > *hth*) were double labeled for rF209 (cyan) and ElaV (red).

(F) Over-expression of dominant negative Hth^{HM} has no effect on *IRO-C* expression: Frozen sections through adult eyes from flies ectopically expressing dominant negative Hth^{HM} (LGMR > *hth^{HM}*) were double labeled for rF209 (cyan) and ElaV (red).

(G)+(H) Loss of *IRO-C* complex does not lead to loss of the DRA: Epon thin section through adult eyes of flies with clones of eye tissue homozygous for the IRO-C deficiency DMF3 were labeled by absence of *white* pigment (left). Analysis of inner PR rhabdomere morphology in clones touching the DRA revealed that mutant ommatidia (black arrows) located at the dorsal rim did not lose the enlarged inner PR rhabdomere phenotype of adjacent wildtype ommatidia (yellow arrows). (H) Flat mounted pupal retina (~48 hrs APF) dissected from flies where clones of tissue homozygous for DMF3 were labeled by absence of Arm-lacZ expression (shown in blue). Triple-labeling of ElaV (red), Hth (green) and βGal (blue) revealed that Hth expression (arrows) persisted in DMF3(-/-) clones located in the DRA (dashed line).

latter possibily, *caup* (rF209) expression was visualized in adult flies over-expressing Hth in all developing PRs under control of the GMR promoter (**Fig 15E**). Strong expression of *caup*-lacZ (shown in cyan) was observed in dorsal PRs (labeled by ElaV in red), suggesting that Hth was not able to repress *IRO-C* expression. Alternatively, *caup* expression was visualized in flies over-expressing dominant negative Hth[HM] (**Fig 15F**). No change in *caup*-lacZ expression (shown in cyan) within or outside the DRA was observed in these flies, suggesting that hth had no influence on adult *IRO-C* expression.

As *IRO-C* expression remained specific to the dorsal eye throughout eye development, it was tested whether the *IRO-C* complex was necessary for DRA formation. Mitotic clones of eye tissue lacking *IRO-C* function were induced using the ey-flip/FRT system (Stowers and Schwarz, 1999; Xu and Rubin, 1993). The deletion DMF3 was used, which had been reported to cover all three *IRO-C* genes (Cavodeassi et al. 1999). First, inner PR rhabdomere morphology was assessed in clones touching the dorsal rim, by performing Epon thin sections (**Fig 15G**). Ommatidia located in DMF3 (-/-) mutant tissue (marked by the absence of *w* pigment) and located within the DRA (marked by a red line) always retained the typical enlarged inner PR rhabdomere morphology similar to those outside the clone (yellow arrows). This suggested that the *IRO-C* complex was not necessary for DRA development. To confirm this, DMF3 (-/-) clones were investigated in pupal retinas (**Fig 15H**). Triple labeling of Hth (shown in green), Arm-lacZ (blue) and Elav (red) revealed that Hth expression persisted (white arrows) within DMF (-/-) clones (marked by the absence of Arm-lacZ). It was therefore concluded that the *IRO-C* complex is not necessary for DRA development to proceed.

The *IRO-C* complex provides an attractive model system for studying how dorsal-specific positional information gets transduced during late eye development. However, the loss-of-function data suggest that the available *IRO-C* deficiencies do not remove all activity of the dorsal selector genes (Tomlinson, 2003). It can therefore not be excluded that the *IRO-C* complex is still necessary for DRA development.

2.16. The *IRO-C* complex is sufficient to induce DRA formation ventrally

As it had been reported that the only available *IRO-C* deletions (DMF3) might not fully remove all *IRO-C* function (Diez del Corral et al., 1999), it still remained a possibility that *IRO-C* genes play a role in DRA development. It was therefore tested whether *IRO-C* was sufficient to induce DRA development.

IRO-C genes were ectopically mis-expressed in developing PRs posterior to the morphogenetic furrow using a weaker insertion of GMR-GAL4 (sGMR-GAL4, see material and methods) as high levels of expression led to strong disruptions in PR development (not shown).

First, pupal retinas (48 hrs APF) were dissected from flies expressing the *IRO-C* complex member *araucan* (*ara*) under sGMR-GAL4 control (GMR>*ara)* and double labeled with antibodies against Hth and ElaV (**Fig 16A**). Unlike in the wildtype, DRA-type expression of Hth (shown in green) in two cells per cluster was detected in a band of ommatidia all around the pupal eye. This suggested that ectopic Ara induces DRA development in the ventral eye, leading to the hypothesis that *IRO-C* is sufficient for DRA development at the eye margins (**Fig 16B**). To confirm expansion of Hth expression into the ventral domain in sGMR > *ara* flies, an enhancer trap indsertion in seven-up (*svp*-lacZ) was introduced as a landmark to visualize the equator (**Fig 16C**). Using the asymmetric expression of *svp*-lacZ (shown in blue), the equator could be localized (shown as a white line). Hth expression (shown in green) was clearly detectable in marginal R7 and R8 on both sides of the equator (white arrows), a situation that is never observed in the wildtype. Interestingly, Hth expression was also induced in the equatorial ommatidia themselves.

Development of the 'ventral rim area' induced in sGMR > *ara* was then analyzed in the adult eye by introducing *rh3*-lacZ transgenes and visualizing βGal activity on frozen sections (**Fig 16D**). In the wildtype, *rh3*-lacZ is expressed in **p**R7 cells as well as the R7 and R8 cells in the DRA. However, in sGMR > *ara* flies, βGal-activity was clearly detectable in both inner PRs at the dorsal as well as the ventral margins (black arrows). This suggested that the whole genetic program of DRA development proceeds all around the eye in IRO-C gain-of-

function flies. To further test the fate of ventrally induced DRA ommatidia, inner PR rhabdomere morpohology was investigated in sGMR > *ara* flies by performing
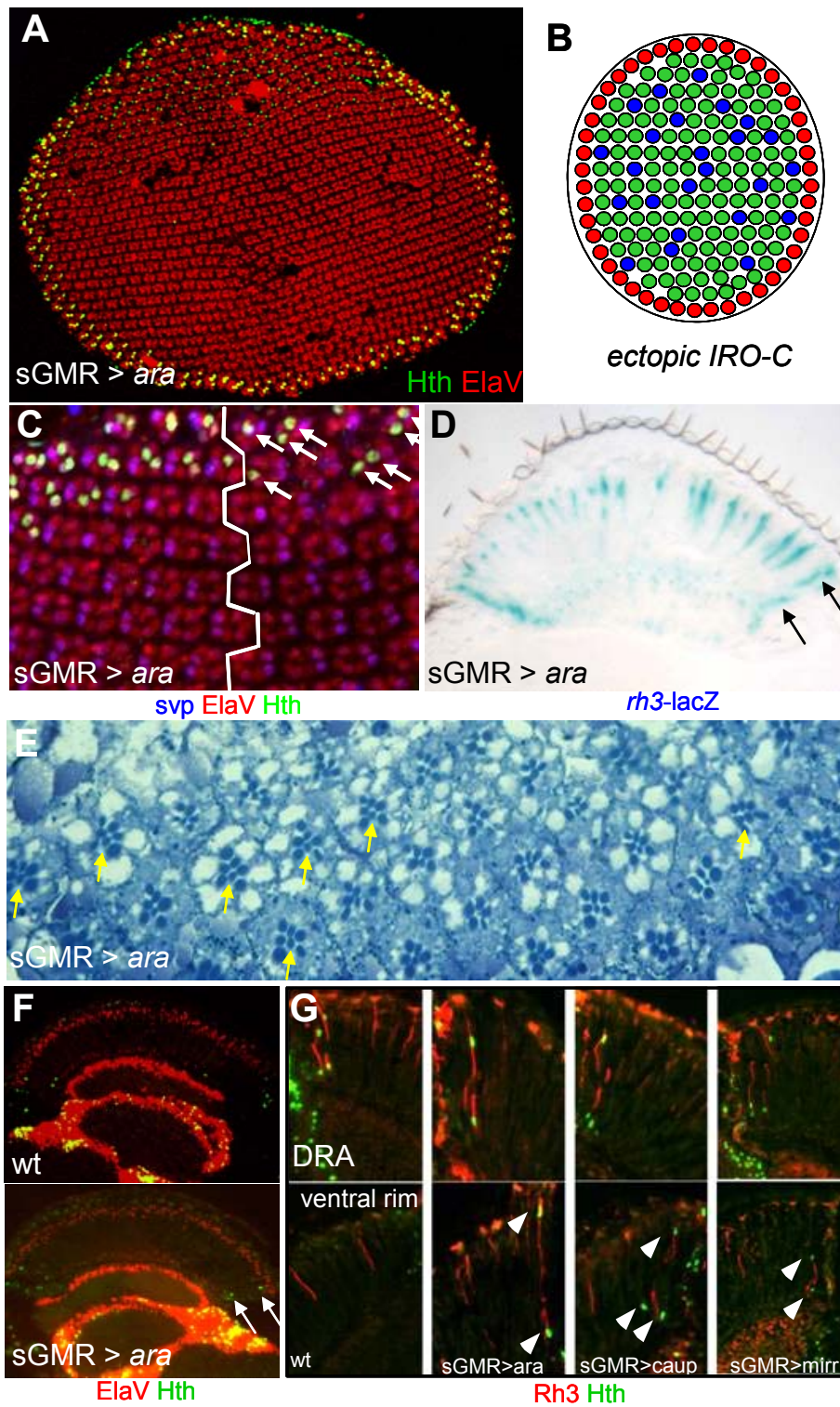
Fig III.2.16 The *IRO-C* complex is sufficient to induce DRA formation ventrally
(A)-(C) Ectopic *IRO-C* is sufficient to induce DRA all around the eye: Flat mounted pupal retina (~48 hrs APF) dissected from flies over-expressing *araucan* using GMR-GAL4 (sGMR>*ara*). Double-labeling of ElaV (red) and Hth (green) revealed DRA formation all around the developing eye. (B) Schematic representation of the *IRO-C* gain-of-function phenotype: DRA ommatidia (red) are found all around the developing eye. (C) Introduction of *svp*-lacZ (blue) into the sGMR > *ara* background allowed marking the equator (white line). Triple labeling of pupal retinas (48 hrs APF) further showed that DRA-specific Hth expression (green) clearly crosses the equator into the ventral compartment, including the equatorial ommatidia (arrows).
(D)-(G) Mis-expression of *IRO-C* genes induces 'Ventral Rim Areas' in the adult: Using X-Gal stainings, *rh3*-lacZ expression was visualized on frozen sections through adult eyes from flies over-expressing the *IRO-C* member *araucan* (*ara*) under GMR-GAL4 control (sGMR > *ara*). At the ventral rim, unusual βGal expression was detected in R7 and R8 cells (black arrows). (E) Epon thin section through the ventral rim of adult eyes from sGMR > *ara* flies. Analysis of inner PR rhabdomere morphology was very difficult due to strong rhabdomere degeneration. However, inner PRs in several ommatidia at the ventral rim manifested the typical DRA-like enlarged rhabdomere phenotype (yellow arrows). (F) Frozen section (dorsal to the left) through adult heads of wildtype flies (top) and sGMR > *ara* flies (bottom) were double-labeled with antibodies against Hth (green) and ElaV (red). Additionally, to the expression in DRA inner PRs, Hth-positive nuclei were detectable at the ventral rim, in sGMR > *ara* flies white arrows). (G) Frozen sections through wildtype eyes (first column), sGMR > *ara* eyes (second column), sGMR > *caup* eyes (third column) and sGMR > *mirr* eyes (fourth column) were double-labeled for Rh3 (red) and Hth (green). In addition to the DRA (top row), an unusual 'ventral rim area' (VRA) was induced in all three cases were IRO-C members were over-expressed (bottom row). Both R7 and R8 in these VRAs co-expressed Hth and Rh3 (white arrow heads), a situation never observed in wildtype flies (bottom left).

1 µm Epon thin sectins (**Fig 16E**). Rhabdomere morphology was generally very perturbed in all PRs in this genetic background, which made analysis of 'vetral rim area' development extremely difficult. However, sections from the ventral rim were obtained, clearly showing the existence of a hight ratio of DRA-like ommatidia with inner PRs exhibiting large rhabdomere diameters (yellow arrows). It was therefore concluded that over-expression of the *IRO-C* gene Ara is sufficient to induce an unusual 'ventral rim area' morphology.

Analysis of adult 'ventral rim areas' was completed by assessing Hth expression in frozen sections through adult sGMR > *ara* eyes (**Fig 16F**). While Hth expression (shown in green) was restricted to few inner PRs at the doral rim in the wildtype (top row), inner PRs co-staining for Hth and ElaV (shown in red) were obtained both at the dorsal and ventral margins in sGMR > *ara* eyes (bottom row). Hth expression of Hth in the 'ventral rim area' therefore persisted until adulthood. Finally, it was investigated whether Rh3 was correctly expressed in inner PRs of the unsusual 'ventral rim areas' (**Fig G**). First, it was confirmed that Rh3 (shown in red) and Hth expression (shown in green) were indistinguishable in the DRA of wildtype, sGMR > *ara*, sGMR > *caup* and sGMR > *mirr* flies (top row). Furthermore, co-expression of Hth and Rh3 was observed at the ventral rim in all three cases when *IRO-C* members were ectopically expressed (white arrows), whereas Rh3 and Hth were never detected in the ventral rim of the wildtype control (bottom left).

It was concluded from these experiments that, when ectopically expressed, each of the three *IRO-C* members is sufficient to induce an unusual 'ventral rim area' with enlarged inner PR rhabdomeres as well as expression of Rh3 and Hth. The lack of a DRA pnenotype in *IRO-C* mutant clones has been explained by residual *IRO-C* activity in the DMF3 deficiency used. These results therefore indicate for the first time that the *IRO-C* complex plays an important role in developing PRs posterior to the morphogenetic furrow.

2.17. Expansion of the DRA in *optomotorblind* Quadroon mutants

The DRA forms as one or two rows of specialized ommmatidia all along the dorsal head cuticle. The *IRO-C* complex is important for providing crucial positional information that limits the DRA to the dorsal side of the eye. Little was known, however, how the DRA is limited to one or two ommatidial rows in the wildtype, as well as in GMR > *IRO-C* flies. Recently, a gain-of-function mutant in the *optomotorblind* (*omb*) locus has been published, that shows a dramatic expansion of the DRA (Pflugfelder et al., 1992; Tomlinson, 2003). This mutant, called *omb*QUADROON, was analyzed in more detail using Hth as a marker for DRA development.

Pupal retinas (48 hrs APF) were dissected from *omb*QUADROON mutants (*omb*Qd[For]) were stained with antibodies against Hth and ElaV (**Fig 17A**). The number of ommatidial rows expressing Hth (shown in green) was dramatically increased throughout the dorsal eye. Hth-positive ommatidia were not detected at the ventral margin, however, and Hth expression was never observed in more than 2 cells per cluster. Therefore, the DRA is expanded through most of the dorsal half of the eye, in *omb*QUADROON mutants (**Fig 17B**). It was tested whether the DRA ommatidia reached all the way to the equator by introducing a lacZ enhancer trap insertion in the gene *seven up* (*svp*-lacZ) to visualize the equator. Pupal retinas were then dissected and triple labeled for Hth, *svp* and ElaV (**Fig 17C**). Hth-expressing ommatidia (shown in green) did not reach the equator (shown as a white line). Instead, the expanded DRA terminated ~4-6 ommatidia before reaching the equator. Interestingly, most of the extra DRA

ommatidia closest to the equator exhibited expression of Hth only in one cell per ommatidium. Using *svp*-lacZ as a landmark, this cell was identified as R7. It was concluded from these experiments that the DRA is dramatically expanded in *omb*QUADROON mutants throughout most of, but not the entire, dorsal half of the eye.

Hth expression was further analysized in the DRA ommatidia of adult *omb*QUADROON flies. First, frozen sections were double stained for Hth and the inner PR marker Spalt (**Fig 17D**). Like in the wildtype, all Hth-positive cells (shown in green) co-stained with Spalt (shown in red). However, the DRA was dramatically expanded through the dorsal eye as had been observed in pupae. Expansion of nuclear Exd expression in *omb*QUADROON flies was also visualized by double labeling frozen sections through adult eyes with antibodies against Exd and Hth (**Fig 17E**). As expected, Exd (shown in red) co-localized with Hth (shown in green) in all inner PR nuclei of the expanded DRA of QUADROON mutants. Exclusion of Sens expression by Hth/Exd is important for the proper specification of DRA ommatidia. Exclusion of Sens from the expanded DRA in *omb*QUADROON mutants was therefore assessed next by were triple staining pupal retinas with antibodies against Exd, Sens and ElaV (**Fig 17F**). Exd expression (shown in red) was clearly expanded throughout the dorsal compartment of the pupal eye and very effectively excluded the expression of the R8 marker Sens (shown in green), as was observed in the much more restricted DRA of wildtype flies. Based on these molecular markers, the extra DRA ommatidia in these flies were therefore indistinguishable from the wildtype. Terminal differentiation of DRA ommatidia in *omb*QUADROON flies was assessed in the adult, by visualizing Sens exclusion by Exd on frozen sections (**Fig 17G**). Exclusion of Sens (shown in green) clearly persisted until adulthood. R8 cells in the expanded DRA expressed Exd (shown in red) and manifested the typical elevated position of their nuclei also observed in the wildtype DRA. Interestingly, expression of Hth/Exd in R7 cells expanded further towards the center of the eye as it did in R8 cells, as previously observed in pupae. Finally, analysis of *omb*QUADROON was completed by assessing Rh3 expression in the
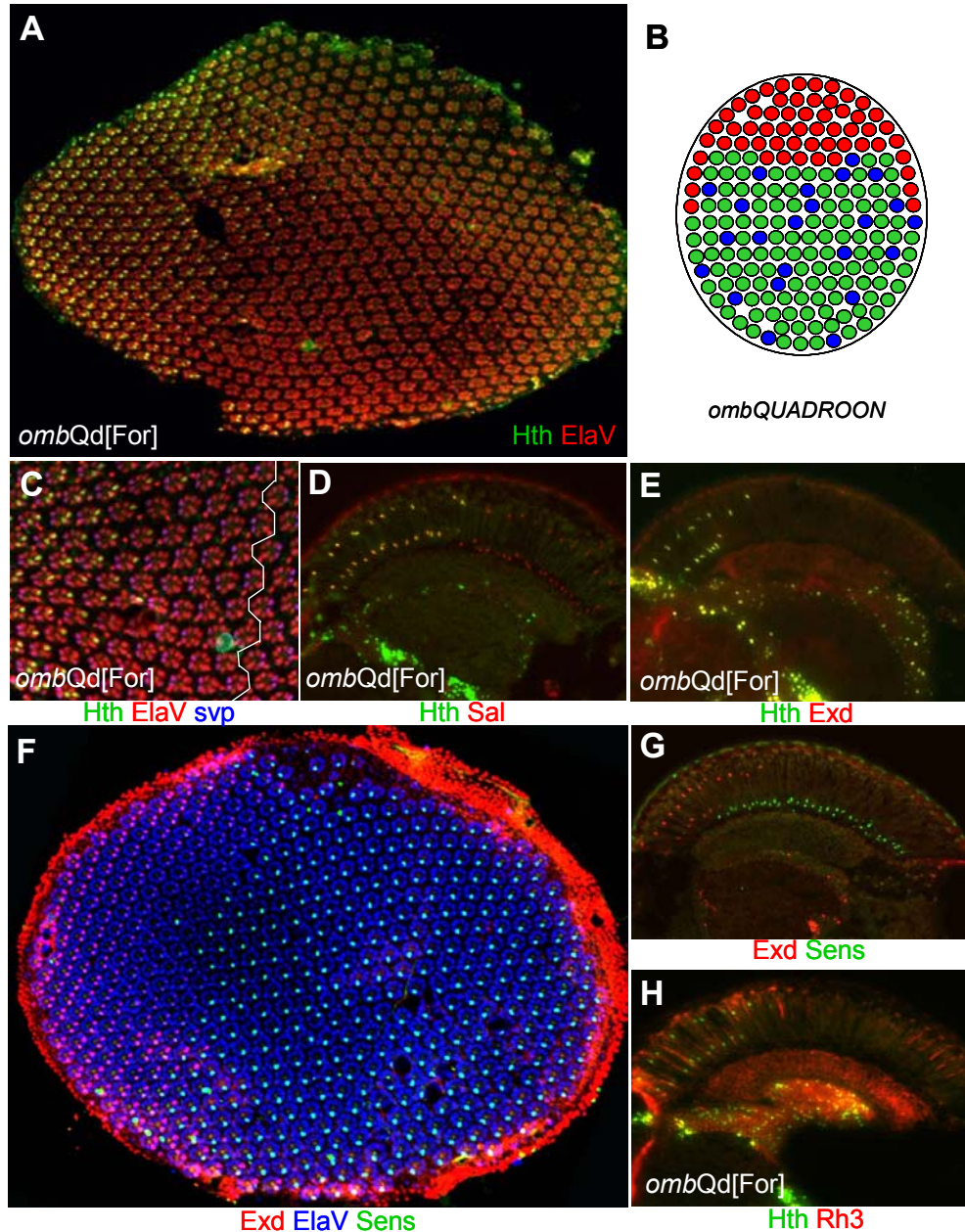
Fig III.2.17 Expansion of the DRA in *optomotorblind* Quadroon mutants
(A)-(C) Expansion of the DRA in pupae: Flat mounted pupal retina (~48 hrs APF) dissected from *omb*QUADROON mutants (ombQd[For]). Double-labeling of ElaV (red) and Hth (green) revealed that DRA ommatidia were dramatically expanded through most of the dorsal eye.
(B) Schematic representation of the *omb*QUADROON phenotype: multitple DRA ommatidia (red) are found in the dorsal eye.
(C) Introduction of *svp*-lacZ (blue) into the *omb*QUADROON background allowed marking the equator (white line). Triple labeling of pupal retinas (48 hrs APF) further showed that DRA-specific Hth expression (green) was daramtically expanded throughout the dorsal compartment. However, DRA ommatidia did not reach the equator.
(D)+(E) Expansion of the adult DRA: Frozen sections through adult *omb*QUADROON eyes double labeled with antibodies against Hth (green) and the inner PR marker Sal (red). Expansion of Hth expression was specific to inner PRs, as Hth always co-localized with Sal. (E) Frozen sections double labeled with antibodies against Hth (green) and Exd (red). Exd was localized to the nucleus of all Hth-expressing inner PRs throughout the expanded DRA of ombQUADROON mutants.
(F)+(G) Exclusion of Sens from the epanded DRA. Flat mounted *omb*QUADROON pupal retina triple labeled for Exd (red), Sens (green) and ElaV (blue). Exd expression is dramatically expanded through most of the dorsal eye, while Sens is excluded. (G) Frozen section double labeled for Exd (red) and Sens (green). Co-exprression of Exd and Sens was never observed.
(H) Frozen sections through adult *omb*QUADROON eyes double labeled for Hth (green) and the DRA opsin Rh3 (red). Extra DRA ommatidia in these mutants expressed both DRA markers Hth and Rh3 in R7 and R8.

87

expanded DRA. Rh3 is the only opsin found in the *Drosophila* DRA and this marker was therefore used to confirm that extra DRA ommatidia maturated correctly in this mutant situation. Frozen sections were double labeled using antibodies against Hth and Rh3 (**Fig 17H**). Expansion of Rh3 expression (shown in red) in R7 and R8 cells throughout the dorsal eye suggested that extra DRA ommatidia in *omb*QUADROON mutants did correctly mature into polarization sensors. This result was confirmed by double labeling with antibodies against all other Drosophila opsin genes which are not expressed in this domain (data not shown). Rhabdomere morphology of the extra DRA ommatidia in *omb*QUADROON was not tested. However, an enlarged rhabdomere diameter had recently been reported for most dorsal ommatidia in these mutants (Tomlinson, 2003).

Taken together, *omb*QUADROON mutants exhibit a dramatically enlarged DRA throughout eye development. This phenomenon could be visualized using antibodies against Hth and is most likely due to the gain-of-function in the *optomorblind* (*omb*) locus. These results suggest that *hth* and *omb* might interact and that *hth* might be required downstream of *omb* for DRA development to occur.

2.18. *optomotorblind* is not required for DRA develpoment

The DRA is dramatically expanded in *omb*QUADROON mutants. It was therefore tested whether Omb is expressed in PRs during eye development. The *omb* locus encodes a T-box transcription factor which had previously been shown to be required for correct development of *Drosophila* appendages as well as for the establishment of planar polarity in the abdomen (Grimm and Pflugfelder, 1996; Kopp and Duncan, 1997; Pflugfelder et al., 1992). Using genetic techniques it was further tested whether Omb was necessary and sufficient for DRA development.

Several enhancer trap elements inserted into the *omb* locus have been reported, in which the transformation marker *white* (*w*) comes under the influence of adjacent genomic sequences (**Fig 18A**; (Tsai et al., 1997). In these flies (*omb-*

lacZ), eye pigmentation is found exclusively at the dorsal and ventral poles of the eye (white and black arrows), suggesting that Omb is specifically expressed at the dorsal and ventral eye margins. Expression of *omb* was first visualized in developing PRs of wandering third instar larvae, using the lacZ reporter construct *pomb19*-lacZ (Sivasankaran et al., 2000). Eye imaginal discs were dissected and triple labeled with antibodies against βGal, the inner PR marker Spalt (Sal) and ElaV (**Fig 18B**). Very weak *omb* expression (shown in blue) was observed in a narrow band of 1-2 omatidial rows at the disc margins. Co-staining with Sal (shown in green) suggested that *omb* expression was not restricted to inner PRs. Expression was detected in all PRs and quickly faded away with increasing distance to the rim. Expression of *omb* was next visualized in the DRA of pupal retinas (48 hrs APF) by using antibodies against Hth, βGal and ElaV (**Fig 18C**). Strong expression of *omb* (shown in blue) was detectable in pigment cells. In the DRA (marked by a dashed line), however, expression in Hth-positive PRs (shown in green) was extremely faint and thus hardly detectable. Analysis of *omb* expression was completed by staining frozen sections through adult heads from flies expressing nuclearly localized lacZ under the control of *omb*-GAL4 (**Fig 18D**). Double labeling of Hth (shown in green) and βGal (shown in blue) revealed clear co-expression in dorsal rim inner PRs (white arrows). As observed in larvae, expression of *omb* was not restricted to inner PRs. Interestingly, the expression domain of *omb* was always larger in the ventral eye, suggesting that the number of ommatidial rows expressing Omb is higher at the ventral rim. Therefore, *omb* seems to be weakly expressed in few rows of marginal ommatidia, starting at pupal stages. Co-staining with Hth suggested that *omb* might indeed play an important role in DRA development together with Hth. However, additional positional information must be required to restrict the DRA to the dorsal half of the eye rim, as *omb* expression was detected to be even stronger at the ventral margin. It has been shown before that dorsal-specific expression of the of the *IRO-C* complex genes is most likely used to provide this additional information.

It was tested next whether *omb* was necessary for the DRA to develop. Mitotic clones of homozygous eye tissue lacking *omb* function were created using the ey-flip/FRT technique (see material and methods). Pupal retinas exhibiting homozygous clones for the *omb* null alleles *omb*3198 and *bi*D4 were dissected and triple stained using antibodies against Hth, βGal and ElaV (**Fig 18E**). Hth expression (shown in green) inside these omb (-/-) clones (marked by the absence of Arm-lacZ, shown in blue) was unchanged as compared to the adjacent heterozygous tissue (white arrows). As the DRA (marked by a dashed line) developed normally in these clones, *omb* is apparently not necessary for DRA development.

It had been reported that the phenotype of ombQUADROON flies was due to a gain-of-function mutation in the *omb* promoter. Unfortunately, there are no Anti-Omb antibody available to test an expansin of Omb expression in these mutants. Investigation of the role of *omb* in DRA development was therefore completed by testing whether it was sufficient to induce DRA development when over-expressed in developing PRs (**Fig 18F**). Over-expression of Omb in all developing PRs using strong GAL4 drivers resulted in partial lethality and deleterious eye phenotypes in the few survivers obtained. Omb was therefore mis-expressed with a weak GMR-GAL4 driver (sGMR > *omb*) and a *rh3*-lacZ transgene was introduced to assess the development of the DRA. Frozen sections through adult heads were stained for βGal activity using X-GAL (see material and methods). As controls, *rh3*-lacZ expression was compared to wildtype flies as well as to the 'positive controls' GMR > *hth* and *omb*QUADROON, two mutant situation in which *rh3*-lacZ expression has been shown to be expanded due to a gain of DRA ommatidia. No visible DRA phenotype was detected in sGMR > *omb* flies (picture far right), as *rh3*-lacZ expression looked similar to the wildtype (picture far left). Therefore, the DRA does not seem to be expanded by over-expression of Omb.

Although *omb* seems to be expressed in marginal ommatidia at the dorsal and ventral rim throughout eye development, it is neither necessary nor sufficient for DRA development. However, discovery of homologous T-box genes resulting
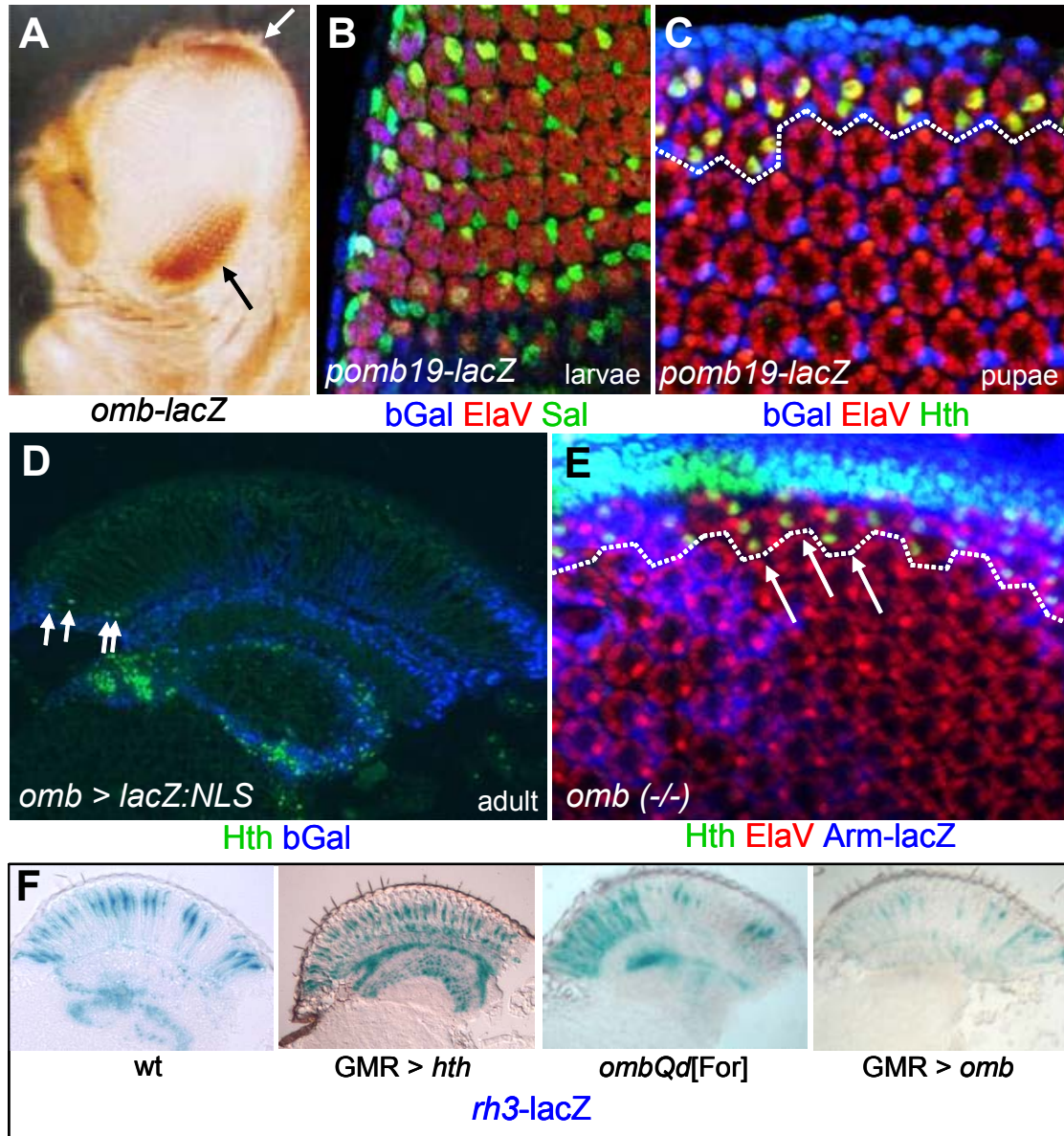
Fig III.2.18 *optomotorblind* **is not required for DRA develpoment**

(A)-(D) Omb is expressed in PRs at the eye margins: In several enhancer traps, the selection marker *white* (*w*) has come under the influence of genomic enhancers belonging to the *omb* locus. Eye pigmentation had been reported to be specific to the dorsal and ventral poles of the adult eye. (B) Expression of omb visualized in eye imaginal discs of wandering third instar larvae, using the reporter construct pomb19-lacZ. Triple labeling with antibodies against βGal (blue), the inner PR marker Sal (green) and ElaV (red) revealed weak omb expression at few larval PRs at the eye margins. (C) Expression of omb was visualized in pupal retinas (48 hrs) dissected from pomb19-lacZ flies and triple labeling for βGal (blue), Hth (green) and ElaV (red). Expression in marginal ommatidia was extremely faint at this developmental stage. (D) Expression of omb-GAL4 was visualized on frozen sections through adult eyes, using UAS-lacZ:NLS reporter constructs and double labeling with Anti-βGal (blue) and Anti-Hth (green). Omb expression was detected in PR nuclei at the dorsal and ventral rim. More ommatidia were found to express *omb*-GAL4 on the ventral side.

(E) Hth expression persist in omb (-/-) clones: Pupal retina (48 hrs APF) from flies inducing mitotic clones for the omb null allele *biD4* (marked by the absence of Arm-lacZ) were triple labeled with antibodies against βGal (blue), Hth (green) and ElaV (red). Hth expression in DRA inner PRs (dashed line) clearly persisted in *biD4* (-/-) clones (white arrows).

(F) Omb is not sufficient to induce DRA evelopment. Using X-Gal stainings, *rh3-lacZ* expression was visualized on frozen sections through adult eyes from flies over-expressing the Omb under GMR-GAL4 control (sGMR > *omb*). DRA-type expression of *rh3-lacZ* had been shown to be expanded in *omb*QUADROON mutants, as well as in flies over-expressing Hth (LGMR > *hth*), while *rh3* expression was restricted to **p**R7 cells and DRA inner PRs in the wildtype (left). In sGMR > *omb* flies, however, rh3-lacZ expression was not expanded.

in very similar abdominal phenotypes than ombQUADROON (*Scruffy*) raises the possibility of several redundant factors. Similarly, mis-expression of *omb* might be required earlier, right posteriour (or even anterior) to the morphogenetic furrow, before the onset of GMR-GAL4 expression, to be sufficient. The possibility remains therefore, that the *omb*QUADROON phenotype is due to an expansion of early Omb expression.

2.19. Interaction of *IRO-C* and *optomotorblind* Quadroon mutants

The number of ommatidial rows belonging to the DRA subtype is dramatically increased in *omb*QUADROON mutants. Moreover, the *IRO-C* complex is sufficient to induce the formation of an unusual 'ventral rim area'. It was therefore tested what effect the ectopic expression of *IRO-C* would have in an *omb*QUADROON background. As *omb* was shown to be expressed at both eye margins, an expansion of induced 'ventral rim area' was expected.

Using the lacZ enhancer trap rF209 (*caup*-lacZ), co-expression of IRO-C and Hth was visualized in frozen sections through adult *omb*QUADROON eyes, using antibodies against Hth and βGal (**Fig 19A**). Hth expression (shown in green) seemed to be expanded through the whole *IRO-C* expression domain, which, in the adult, spans ~a third of the eye (shown in cyan), starting from the dorsal rim (see introduction). It was therefore concluded that DRA ommatidia expand throughout the adult expression domain of *IRO-C* in this mutant situation. This result was confirmed by double labeling Rh3 and rF209 expression in frozen sections through adult *omb*QUADROON eyes (**Fig 19B**). DRA-type expression of Rh3 in R8 cells (shown in red) was only detectable within the *IRO-C* expression domain (white arrow). However, some gaps seemed to remain, that did not express Rh3. As it had previously been shown that the dorsal third of the adult *omb*QUADROON eye has a rough eye phenotype and that *rh3*-lacZ is expanded throughout this expression domain, it was concluded that the observed gaps in Rh3 expression were due to rhabdomere degeneration. This could be confirmed by the fact that no other rhodopsin was found to be expressed within the expanded DRA in *omb*QUADROON mutants (data not shown). Therefore, the

DRA is expanded throughout the dorsal third of the eye in adult *omb*QUADROON flies, which seems to corresponded to the adult expression domain of *IRO-C*.

The *IRO-C* gene *araucan* (*ara*) was over-expressed in an *omb*QUADROON mutant background using the Gal4/UAS-system (see material and methods). Pupal retinas from these *omb*Qd[For] + sGMR > *ara* flies were then double labeled with antibodies against Hth and ElaV (**Fig 19C**). The phenotype obtained at the ventral eye margin was dramatically different from the simple *IRO-C* gain-of-function (sGMR > *ara*). Instead of inducing Hth expression (shown in green) in merely one or two ommatidial rows, Hth expression was now detectable in many additional ommatidial rows. This suggested that *omb*QUADROON has an enhancing effect on the *IRO-C* gain-of-function phenotype. The 'ventral rim area' is therefore expanded in *omb*Qd[For] + sGMR > *ara* flies, similar to the DRA in *omb*QUADROON mutants, creating a mirror-image duplication of its DRA expansion phenotype (**Fig 19D**). Frozen sections through adult eyes from *omb*Qd[For] + sGMR > *ara* were also double labeled with antibodies against Hth and ElaV to confirm that this phenotype persisted until adulthood (**Fig 19E**). Indeed, expanded Hth expression (shown in green) was detectable in both the dorsal and ventral compartments. Hth expression always seemed to be excluded from the center of the eye. Expression of Exd was also expanded in these flies, as visualized by double labeling frozen sections with antibodies against Hth and Exd (**Fig 19F**). As expected, every Hth-positive nucleus (shown in green) in both the expanded DRA as well as the 'ventral rim area' also co-expressed Exd (shown in red). Finally, Maturation of the expanded 'ventral rim' ommatidia induced by ectopic Ara was assessed by double labeling Rh3 and Hth (**Fig 19G**). Strong Rh3 expression (shown in red) and Hth expression (shown in green) were detected throughout the dorsal and ventral thirds of the eye (white arrows), suggesting that the extra DRA ommatidia formed at both eye margins in *omb*Qd[For] + sGMR > *ara* flies indeed maturate correctly into polarization sensors.
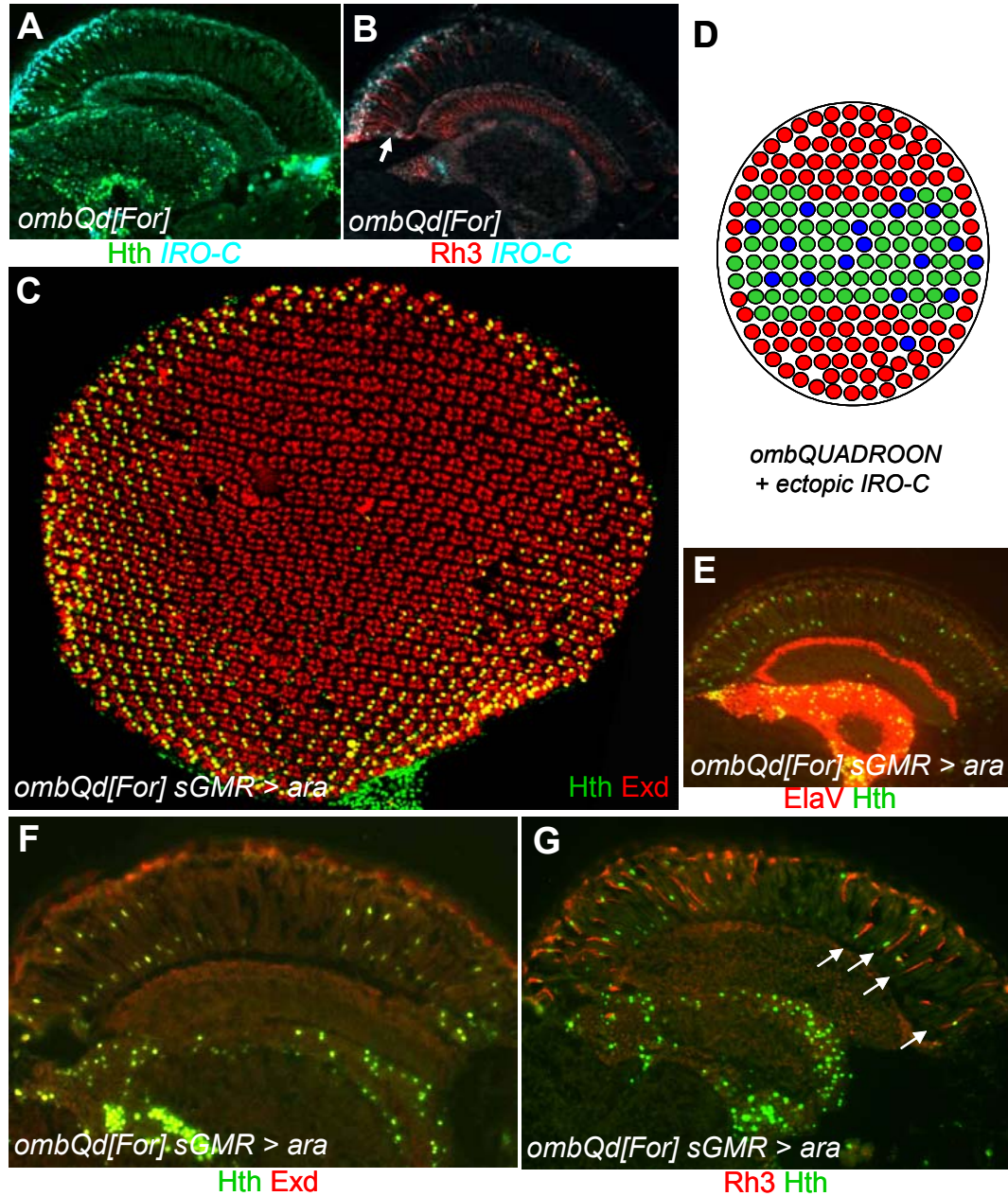
Fig III.2.19 Interaction of *IRO-C* and *optomotorblind* Quadroon mutants

(A)+(B) *IRO-C* expression is normal in *omb*QUADROON mutants: Frozen section through adult eyes from *omb*QUADROON mutants double labeled with antibodies against Hth (green) and the *IRO-C* enhancer trap rF209 (cyan). DRA-type Hth expression was found expanded throughout the adult *IRO-C* expression domain. (B) Co-labeling of Rh3 (red) and rf209 (cyan) on frozen sections through *omb*QUADROON eyes revealed the expansion of Rh3 expression of Rh3 in R8 cells in the domain of expression of *IRO-C*.

(C)-(G) Ectopic *IRO-C* induces an expanded VRA in *omb*QUADROON mutants: Pupal retina from flies over-expressing the *IRO-C* member Araucan (*ara*) under GMR-GAL4 control in a *omb*QUADROON mutant background (*omb*Qd[For] + sGMR > *ara*), double labeled with antibodies against Hth (green) and ElaV (red). The 'ventral rim area' (VRA) induced by *ara* is dramatically expanded in this mutant background (equator runs vertically), creating a mirror image of the ombQUADROON phenotype ventrally. (D) Schematic representation of the *omb*Qd[For] + sGMR > *ara* phenotype: a multitude of DRA-type ommatidia (red) are found in the dorsal eye as well as ventrally. (E) Frozen section through adult eyes from (*omb*Qd[For] + sGMR > *ara* flies double labeled for Hth (green) and ElaV (red). The dramatically expanded 'ventral rim area' (VRA) induced by *ara* in this mutant background persists until adulthood. (F) Frozen section double lebeled with antibodies against Exd (red) and Hth (green). Nuclear Exd co-localizes with Hth throughout both the expanded DRA and VRA. (G) Double labeling of frozen sections through adult *omb*Qd[For] + sGMR > *ara* eyes with antibodies against Rh3 (red) and Hth (green) confirmed the correct maturation of the expanded VRA, expressing both DRA-type Hth and Rh3 in inner PRs.

It was concluded from these experiments that the *optomotorblind* gain-of-function mutation *omb*QUADROON has a strong inducing effect on DRA development at both the dorsal as well as ventral margin, as revealed by over-expression of *IRO-C*. Based on these findings, an expansion of Omb expression at both margins would be expected in *omb*QUADROON mutants.

2.20. The DRA develops in response to *wingless* signaling

DRA ommatidia form as one or two rows right adjacent to the dorsal head cuticle. The gene encoding the morphogen Wingless (Wg) is strongly expressed in the developing head cuticle all around the eye (Treisman and Rubin, 1995). It was therefore tested whether activation of the *wingless* pathway in developing PRs had an activating effect on DRA development.

The *wg* pathway was activated in PRs by ectopically expressing a constitutively active form of the *wg* effector protein Armadillo (ArmS10) under the control of GMR-GAL4 drivers (van de Wetering et al., 1997). These GMR>ArmS10 flies had rough eyes, with some ommatidia losing PRs when strong drivers were used. However, pupal retinas (~48 hrs APF) were dissected and double labeled for Hth and ElaV (**Fig 20A**). Hth expression (shown in green) was dramatically expanded through the entire dorsal half of the eye. This DRA expansion phenotype was highly reminiscent of the *omb*QUADROON phenotype. However, DRA ommatidia seemed to populate a slightly larger portion of the pupal eye. This result suggested that activation of the *wg* pathway in all PRs leads to a specific transformation of all dorsal ommatidia into the DRA subtype (**Fig 20B**).

This hypothesis was tested by dissecting GMR>ArmS10 pupal retinas carrying *svp*-lacZ to visualize the equator (**Fig 20C**). Triple labeling of Hth, βGal and ElaV revealed that DRA ommatidia, marked by Hth (shown in green) extended all the way to the equator (marked with a white line). Ventral ommatidia were never found expressing Hth in GMR>ArmS10 flies. Interestingly, one row of dorsal ommatidia often remained unmarked (white arrow), a situation similar to what we observed for the much more restricted DRA of wild type flies. Therefore, the DRA

expansion phenotype caused by *wg* pathway activation in all developing PRs is significantly different from the one observed for *omb*QUADROON mutants.

DRA Expansion was next assessed in adult GMR>ArmS10 flies by double labeling frozen section with antibodies against Hth and the inner PR marker Spalt (**Fig 20D**). Spalt (shown in red) was expressed in inner PRs throughout the whole eye, and Hth-expressing dorsal PRs (shown in green) always costained for both Hth and Spalt. This suggested that although ArmS10 was expressed in all PRs, only inner PRs located dorsally showed a molecular response by turning on Hth expression. As expression of Hth is sufficient to localize its dimerization partner Exd to the nucleus, the expansion of Exd expression throughout the dorsal eye was assessed by double labeling frozen sections with antibodies against Exd and Hth (**Fig 20 E**). As expected, Exd (shown in red) was found co-expressed with Hth (shown in green) in the nuclei of all dorsal inner PRs. In wildtype flies, as well as *omb*QUADROON mutants, expression of Hth/Exd in the DRA excludes the expression of the R8 marker Sens. Pupal retinas from LGMR > ArmS10 flies were dissected to test the exclusion of Sens from the expanded DRA and triple labeled with antibodies against Exd, Sens and ElaV (**Fig F**). Expression of Exd (shown in red) was specific to all dorsal inner PRs (R7 and R8), while Sens expression (shown in green) was specifically detected in ventral R8 cells. The expression domains of Exd/Hth and Sens were therefore separated by the equator, as the DRA had expanded throughout the dorsal eye in these flies. The exclusion of Sens from the dorsal eye persisted until adulthood, as revealed by double labeling frozen sections through LGMR > ArmS10 eyes for Exd and Sens (**Fig G**). As observed in pupae, dorsal expression of Exd/Hth and ventral expression of Sens excluded each other.

Finally, terminal differentiation of the ectopic DRA ommatidia in the dorsal eye was tested by double labeling frozen sections through GMR>ArmS10 eyes with antibodies against Hth and Rh3 (**Fig 20E**). Although rhabdomere morphology was severely affected by *wg* pathway activation, it was found that Rh3 (shown in red) was the only inner PR Rhodopsin expressed in the dorsal half of the eye labeled by Hth (shown in green).
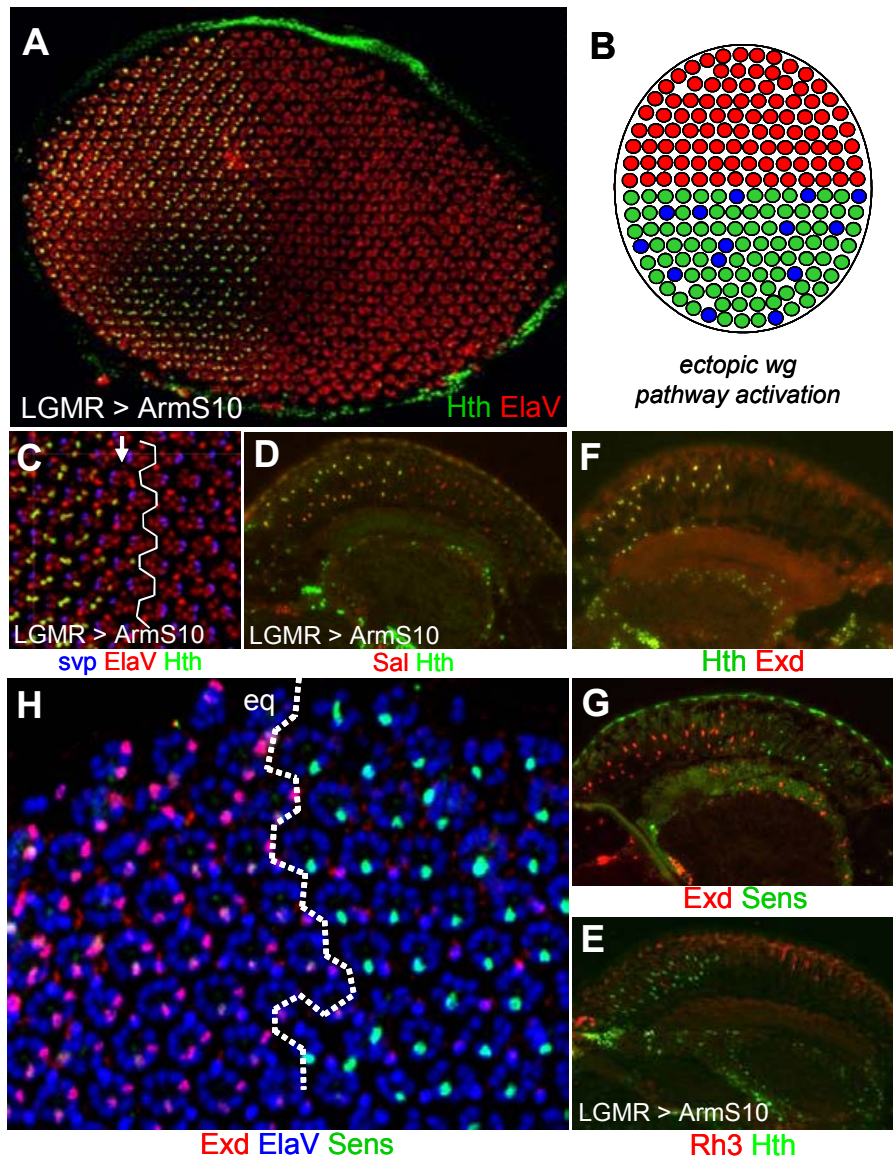
Fig III.2.20 The DRA develops in response to *wingless* signaling

 (A)-(C) Activating the *wingless* pathway transforms all dorsal PRs into DRA: Flat mounted pupal retinas (~48 hrs APF) dissected from flies over expressing an activated form of the *wg* pathway effector Armadillo (ArmS10) under GMR-GAL4 control (LGMR > ArmS10) flies were double-labeled against ElaV (red) and Hth (green). DRA-specific Hth expression spanned the entire dorsal half of the developing eye. (B) Schematic representation of the LGMR > ArmS10 phenotype: DRA ommatidia (red) are found in the entire dorsal eye (C) Introduction of *svp*-lacZ (blue) into the LGMR > ArmS10 background further showed that DRA-specific Hth expression almost reached the equator (white line) in pupal retinas, most of the times Hth expression was only excluded from the equatorial ommatidia.

(D)+(E) The expanded DRA in adult flies: Frozen section (10 μm) along the D/V axis (D to the left) through adult heads of LGMR > ArmS10 flies. Double labeling using antibodies against Hth (green) and the inner PR marker Sal (red) clearly showed that only inner PRs gained Hth expression throughout the dorsal eye. (E) Frozen section through adult LGMR > ArmS10 heads double labeled with antibodies against Exd (red) and Hth (green). Nuclear localization of Exd was detected in all dorsal, Hth-positive inner PR nuclei of the extended DRA.

(G)+(H) Exclusion of Sens expression from the expanded DRA. Frozen section double labeled with antibodies against Exd (red) and Sens (green). Expression of the R8 marker Sens was restricted to the ventral half of the eye, whereas Exd was expressed in all dorsal R7 and R8 nuclei. Co-expression was never observed. (H) Pupal retina from LGMR > ArmS10 flies triple labeled for Exd (red) Sens (green) and ElaV (blue). Exd-expressing inner PRs in dorsal half of the eye were separated by the equator (eq) from Sens-expressing R8 cells in the ventral eye.

(E) Maturation of DRA omatidia in the expanded DRA: Frozen section through adult heads of LGMR > ArmS10 flies double-labeled for Rh3 (red) and Hth (green) revealed that Rh3 was the only inner PR opsin expressed in the adult dorsal eye. The expaned DRA ommatidia of therefore maturated correctly into polarization sensors.

97

It was concluded from these experiments that only dorsal ommatidia are transformed into the DRA subtype when the *wg* pathway is ectopically activated, suggesting that these ommatidia rely on positional information provided by the *IRO-C* complex. Furthermore, only inner PRs are competent to respond to the DRA inducing signal, indicating that a prior commitment to the Spalt-induced inner PR-fate is necessary for a response.

2.21. *Optomotorblind* and *IRO-C* expression in the expanded DRA

Gain-of-function situations for both the *optomotorblind* and *IRO-C* loci have dramatic effects on DRA development. Interestingly, both genes have previously been shown in the eye to be under the control of the *wg* pathway, which also had a strong DRA-inducing effect (Maurel-Zaffran and Treisman, 2000; Zecca et al., 1996). It was therefore tested whether *omb* and *IRO-C* expression were affected by ectopic over-activation of the *wg* pathay in developing PRs.

First, *IRO-C* expression (rF209) was visualized in frozen sections through adult LGMR > ArmS10 eyes using antibodies against βGal and Hth (**Fig 21A**). *IRO-C* expression (shown in cyan) was not affected as it was still specific to the same dorsal portion of the eye. It was also obvious that expanded Hth expression (shown in green) co-localized with *IRO-C* expression in LGMR > ArmS10 flies, again suggesting that only ommatidia located within the *IRO-C* compartment could become transformed into the DRA fate. *IRO-C* expression was also shown to be unaffected by double labeling adult LGMR > ArmS10 eyes with antibodies against Rh3 and βGal (**Fig 21B**). DRA-type expression of Rh3 in R8 cells (shown in red) was always restricted to ommatidia located within the IRO-C expression domain (shown in cyan), suggesting that IRO-C expression had not expanded into ventral PRs due to over-activation of the *wg* pathway. Finally, *IRO-C* expression was assessed in pupal retinas (48 hrs APF) as only weak expression had been detectable under wildtype condition, at this developmental stage. Pupal retinas from LGMR > ArmS10 flies were therefore triple labeled with antibodies against Hth, βGal and ElaV (**Fig 21C**). As in the

adult, no change in IRO-C expression was observed, as βGal expression (shown in blue) was still weak and only detectable in a few rows of ommatidia, quickly fading away with growing distance to the dorsal rim. Most Hth-positive ommatidia (shown in green) located in the expanded DRA did therefore not seem to express *IRO-C* at this stage. *IRO-C* expression is therefore not affected by the late over-activation of the *wg* pathway in developing PRs posterior to the morphogenetic furrow. It appears therefore that some important aspects of the positional information provided by *IRO-C* are executed very early during eye development.

Similar experiments were performed to assess *omb* expression in LGMR > ArmS10 flies. First, pupal retinas (48 hrs APF) carrying the *omb* reporter construct pomb19-lacZ (LGMR > ArmS10, pomb19-lacZ) were dissected and triple-stained with antibodies against βGal, Hth and ElaV (**Fig 21D**). It was found that *omb* expression (shown in blue) was not expanded in PRs (shown in red), within or outside of the expanded DRA (visualized by Hth, shown in green). Furthermore, *omb* expression in marginal PRs remained extremely faint (**Fig 21E**). Pupal expression of *omb* in PRs was strikingly similar to that of *IRO-C* as it was only expressed in very few PRs, fading away quickly. Furthermore, it did not seem to be affected by *wg* pathway activation at this develoipmental stage, leaving the vast majority of Hth-positive DRA ommatidia negative for *omb* expression. It has previously been reported, however, that clones of eye tissue expressing an activated from of Armadillo induce the expression of *omb* in third instar larvae. It must be noted that these clones had been induced much earlier, anterior to the morphogenetic furrow and could therefore influence PRs as early as at their time of birth. *omb* expression was visualized in the eye imaginal discs of LGMR > ArmS10 wandering third instar larvae by triple labeling for βGal, Spalt and ElaV (**Fig 21F**). As for the wildtype, *omb* expression (shown in blue) was only detectable in few marginal PRs of the eye disc, including inner PRs (marked by Spalt, shown in green). Therefore, larval as well as pupal expression of *omb* is not influenced by the late ectopic activation of *wg* signaling in developing PRs.

It was concluded from these experiments, that neither the expression pattern of *IRO-C* nor that of *omb* are affected by the late ectopic activation of the
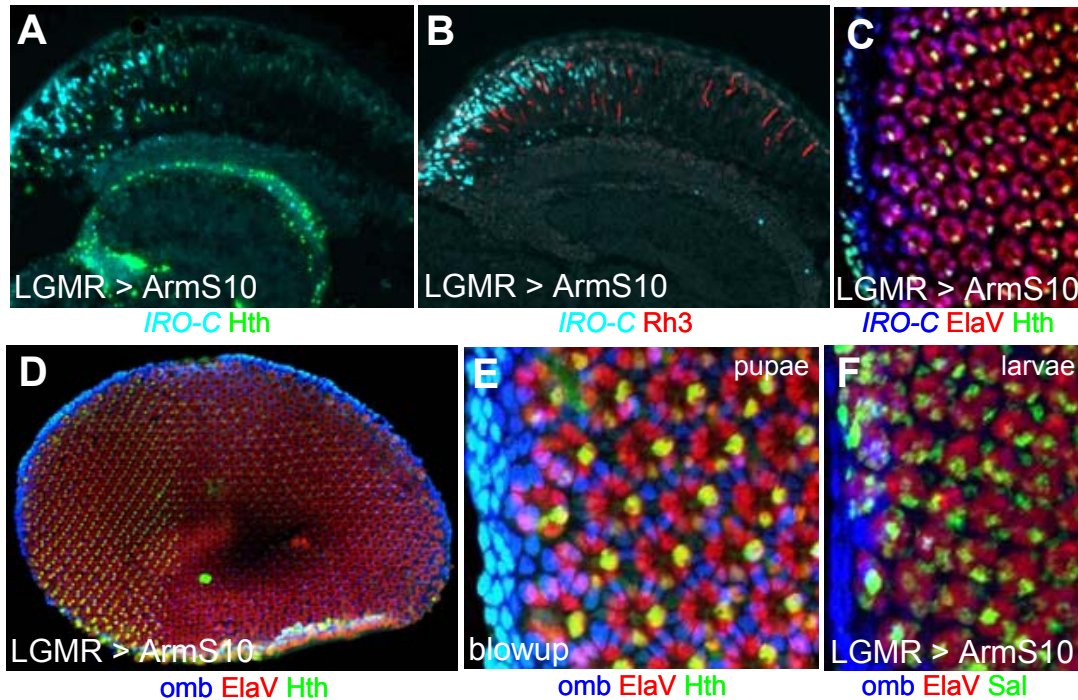
Fig III.2.21 *IRO-C* and *optomotorblind* expression in the expanded DRA
(A)-(C) Expression of *IRO-C* is not affected by late ectopic *wg* pathway activation: IRO-C expression was visualized on frozen sections through adult eyes from flies over-expressing activated Armadillo (ArmS10), using the enhancer trap rF209. Double labeling with antibodies against βGal (cyan) and Hth (green) revealed the expansion of DRA-type Hth expression in inner PRs to span the entire *IRO-C* expression domain. IRO-C expression appeared not to be affected by ectopic wg pathway activation. (B) Frozen sections through adult eyes from LGMR > ArmS10 + rF209 were double labeled with antibodies against βGal (cyan) and Rh3 (red). Expression of rF209 remained specific to the dorsal comp[artment as visualized by DRA-type Rh3 expression in R8 cells, expanded in this mutant background. (C) IRO-C expression in pupal retinas (48 hrs APF) dissected from LGMR > ArmS10 + rF209 flies and triple labeled with antibodies against Hth (green), βGal (blue) and ElaV (red). Ectopic wg pathway activation in developing PRs had no effect on pupal rF209 expression, which was weak and faded away few rows from the dorsal rim; a situation also observed for the wildtype.
(D)-(F) Expression of *omb* is not affected by ectopic *wg* pathway activation: Pupal retinas dissected from LGMR > ArmS10 flies also carrying the pomb19-lacZ reporter transgene. Triple labeling using antibodies against Hth (green), βGal (blue) and ElaV (red) revealed no change in pupal *omb* expression. (E) As seen in the blowup, βGal expression in marginal ommatidia was still faint and not expanded into a higher number of dorsal ommatidia. (F) Eye imaginal discs dissected from wandering third instar larvae carrying the pomb19-lacZ transgene. Triple staining using antibodies against Sal (green), βGal (blue) and ElaV (red) revealed no change in larval *omb* expression. As in the wildtype, only very few marginal ommatidia expressed βGal.

wg pathway in developing PRs. This was particularly interesting for *IRO-C*, as reporters seemed to become re-expressed at later stages of PR development and late over-expression of *IRO-C* genes is sufficient to induce DRA ommatidia ventrally. Regulation of late *IRO-C* function therefore remains to be understood. An inducing effect of *wg* on the *omb* complex, however, seems to be required very early during eye development.

2.22. DRA development requires unusual *wg* signal transduction

Over-activation of the *wg* pathway in all developing PRs has a strong DRA-inducing effect in all dorsal ommatidia. Wingless can act through different

receptors as well as different signal transduction cascades. It was therefore tested whether DRA cells respond directly to Wg through either of the two well characterized pathways ('canonical' and 'non-canonical' signaling; for review: Veeman et al., 2003) by following three different approaches.

First, mitotic clones of eye tissue lacking both well-characterized Wingless receptors, Fz and DFz2 (Chen and Struhl, 1999) were induced using the ey-flip/FRT technique. Pupal retinas (48 hrs APF were dissected and triple labeled with antibodies against Hth, GFP and ElaV (**Fig 22A**). Only very few and very small clones (labeled by the absence of *ubi*-GFP (shown in blue) were obtained touching the DRA. However, Hth expression (shown in green) persisted in such clones (white arrow heads), suggesting that Wg receptors Fz and DFz2 are not required in PRs for DRA development.

To confirm this result, mitotic clones of eye tissue lacking the signal transduction molecule Disheveled (*dsh*) were induced using the ey-flip/FRT technique. Dsh is absolutely required most cellular responses to Wg (Klingensmith et al., 1994; Noordermeer et al., 1994). Pupal retinas (48 hrs APF) were dissected and triple labeled with antibodies against Hth, βGal and ElaV (**Fig 22B**). Very large clones were obtained and eye morphology was visibly affected resulting in large clonal outgrowths due to the loss of Dsh-mediated inhibition of the morpgogenetic furrow. Similarly to Fz + DFz2 (-/-) clones, no loss of Hth expression (shown in green) was observed in dsh^{V26} (-/-) clones (marked by the absence of Arm-lacZ, shown in blue). Hth expression was sometimes partially lost in small clones that did not extend into the head cuticle. However, it clearly persisted in the large clones and in several cases more than two additional DRA rows were detected in the adjacent wildtype tissue. Although eye development is somewhat disturbed, DRA development proceeds normally in the absence of Dsh.

A final strategy was used to make DRA ommatidia un-responsive to Wg, by over-expressing a dominant negative form of TCF/Pangolin in all developing PRs. TCF, the main transcriptional effector of the *wingless* pathway, was over-expressed using GMR-GAL4 (TCFΔN; (van de Wetering et al., 1997). Depending
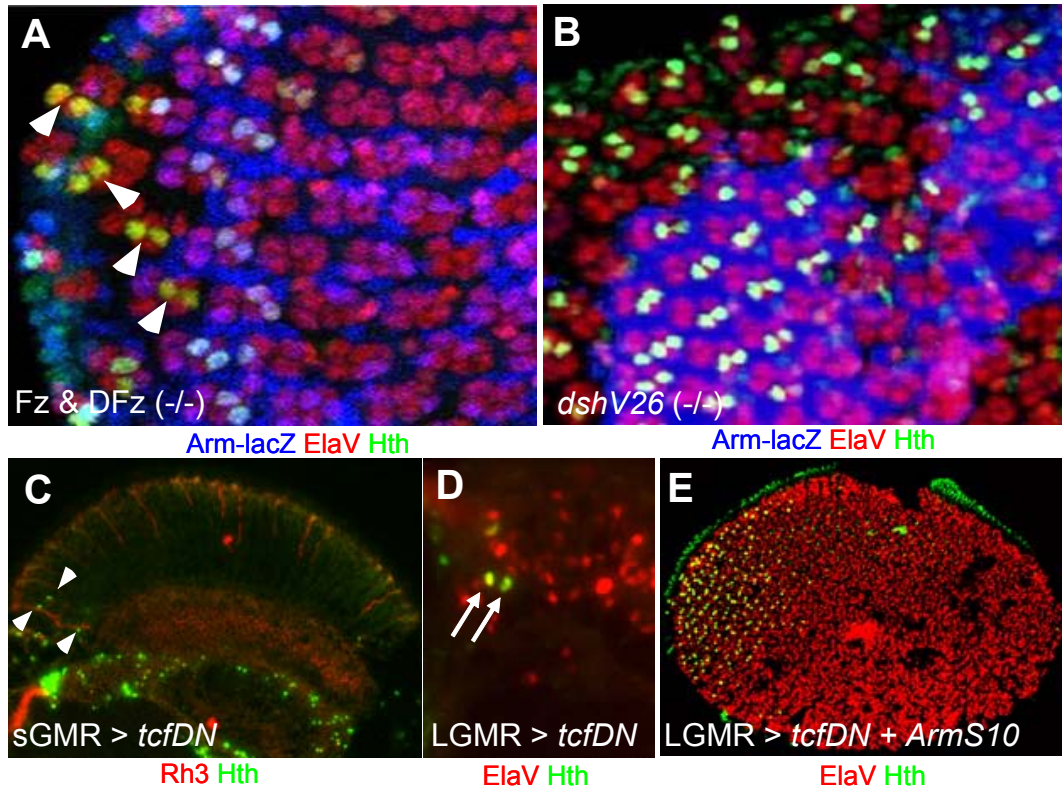
Fig III.2.22 DRA development requires unusual *wg* signal transduction
(A)+(B) DRA ommatidia do not directly respond to *wingless*: (A) Flat mounted pupal retinas (~48 hrs APF) dissected from flies with small *ey*-Flip induced clones of eye tissue homozygous mutant for both *wg* receptors Fz and Fz2 (fz^{H51} $fz2^{C1}$ -/-): triple labeling of Hth (green) and ElaV (red) in clones marked by loss of fluorescence from a ubiquitin-GFP transgene (shown in blue) and located in the DRA revealed Hth expression was not lost in fz^{H51} $fz2^{C1}$ double mutant tissue (white arrows). (B) Larger homozygous mutant clones of a null allele of *disheveled* (*dsh*), marked by the absence of Arm-lacZ (shown in blue) were analyzed in pupal retinas (~48 hrs APF). Triple labeling with Hth (green) and ElaV (red) revealed DRA-specific Hth expression to persist in *dshV26⁻/⁻* mutant tissue (top). Additional DRA rows were obtained in wildtype tissue adjacent to *dshV26* clones (center) probably due to over-proliferation.
(C)-(E) Dominant negative TCF does not block DRA development: Frozen section (10 µm) along the D/V axis (D to the left) of adult heads of flies over-expressing a dominant negative form of Dtcf (*pangolin*) using GMR-GAL4 (sGMR > *dTCFΔ*N). Double labeling of Rh3 (red) and Hth (green) revealed that the DRA remains unaffected in these flies (arrows). (D) Frozen sections through adult eyes from flies over-expressing DtcfΔN under control of a stronger GMR-GAL4 driver (LGMR > *dTCFΔ*N). Double labeling using antibodies against Hth (green) and ElaV (red) revealed normal DRA development in these flies, although eye morphology was severely affected. (E) Pupal retinas (48 hrs APF dissected from flies co-over-expressing both 'activated Armadillo' (ArmS10) and *dTCFΔ*N using GMR-GAL4 (LGMR > ArmS10 + *dTCFΔ*N). Double labeling with antibodies against Hth (green) and ElaV (red) revealed that *dTCFΔ*N did not neutralize DRA-inducing activity of ArmS10.

on the strength of the GMR driver used, adult GMR> TCFΔN flies had eye phenotypes ranging from wild type to very rough. First, a weaker driver (sGMR-GAL4) was used and frozen sections from sGMR > TCFΔN flies were double labeled for Rh3 and Hth (**Fig 22C**). Hth-positive inner PR nuclei (shown in green) co-staining for Rh3 (shown in red) were datectable at the DRA, indicating the DRA development was not affected by expression of dominant negative TCF. A strong GAL4 driver (LGMR-GAL4) was used next, to rule out the possibility that TCFΔN expression levels ghad been too low. Double labeling of frozen sections

through LGMR> TCFΔN eyes with antibodies against Hth and ElaV were performed (**Fig 22D**). Although eye development was severely affected, Hth-positive PR nuclei (labeled by co-staining of Hth in green and Elav in red) were detected in the DRA in LGMR> TCFΔN retina (white arrows), confirming that dominant negative TCF does not abolish DRA development.

A factor downstream of activated Armadillo might be non-cell-autonomously required for DRA induction. It remained therefore possible that Wg expression was primarily restricted to the head cuticle, inducing the expression of a second diffusible protein there, in an autocrine way. According to this model, diffusion of such unknown factor over a short range into the eye would then be responsible for induction of Hth and therefore DRA development. This factor has not been identified yet. However, it has been reported that *wg* induced its own expression in those marginal ommatidia that are to be eliminated by apoptosis. It was therefore tested whether the unknown factor was Wg itself by over-expressing both UAS-ArmS10 and UAS-TCFΔN under the control of LGMR-GAL4. Pupal retinas (48 hrs APF) from LGMR> ArmS10 + TCFΔN flies were double labeled with antibodies against Hth and ElaV (**Fig 22E**). Eye morphology of these flies was dramatically affected. However, dominant negative TCF was not able to efficiently prevent expansion of Hth expression (shown in green) caused by activated Armadillo. It was concluded that the DRA does not develop in direct response to Wg via TCF.

Together, these data indicate that ectopic activation of the *wingless* pathway is sufficient to induce DRA development dorsally, but reception of the Wg signal through the *Fz/DFz2, dsh, TCF* pathway is not absolutely necessary in PRs for DRA development to proceed, suggesting the involvement of a redundant DRA inducing factor and/or additional Wnt receptor pathway(s).

2.23. Removing Hth function in the expanded DRA: odd coupled ommatidia

The DRA is dramatically expanded in gain-of-function mutants affectiung wg signaling in the developing eye, like *omb*QUADROON and LGMR > ArmS10. Over-expression of dominant negative Homothorax (*hth*HM) in these mutant

backgrounds was used to confirm that removing Hth function in the DRA always leads to formation of odd-coupled Rh3/Rh6 ommatidia. First, Hth^{HM} was over-expressed in all developing PRs in an *omb*QUADROON background. Frozen sections from adult *omb*QUADROON + LGMR > *hth*^{HM} eyes were double labeled with antibodies against Rh3 and Rh6 (**Fig 23A**). Indeed, all ommatidia located in the dorsal third of the eye expressed Rh3 (shown in red) in R7 and Rh6 (shown in green) in R8. Expression of Rh4 and Rh5 was specifically excluded from the expandd DRA (not shown). Therefore, ectopic expression of dominant negative Hth had transformed the entire expanded DRA in *omb*QUADROON mutants into odd-coupled ommatidia, confirming previous observations in the more restricted DRA (**Fig 23B**).

The dominant negative form of Homothorax (*hth*^{HM}) was also over-expressed in all developing PRs, together with the constitutively active Form of Armadillo. In these LGMR > *hth*HM + ArmS10 flies, the dorsal half of the eye should be driven into the specification as DRA ommatidia. However, due to the co-expression of *hth*HM, terminal differentiation of these DRA ommatidia should be blocked. Therefore, differentiation of the whole dorsal eye into unusually coupled Rh3/Rh6 expressing ommatidia was predicted. To test this hypothesis, frozen sections through adult LGMR > ArmS10 + *hth*^{HM} eyes were dauble labeled with antibodies against Rh3 and Rh6 (**Fig 23C**). Although rhabdomere morphology was quite affected, Rh3 (shown in red) and Rh6 (shown in green) were clearly the only inner PR opsins expressed in the dorsal eye. Therefore, removing Hth function downstream of activated Armadillo indeed leads to the transformation of the whole dorsal eye into odd-coupled ommatidia (**Fig 23D**). To further confirm this result, opsin-lacZ reporter constructs were introduced and frozen sections through adult eyes were performed (**Fig 23A**). By visualizing βGal activity using X-Gal, *rh1*-lacZ expression was not affected in LGMR > *hth*HM + ArmS10 (top left). However, inner PR expression was severely affected: For instance, *rh4*-lacZ and *rh5*-lacZ were never expressed in the dorsal half of the eye (black arrows), a situation reminiscent of LGMR > ArmS10 flies. However, clear expression of *rh3*-lacZ in R7 cells throughout the dorsal eye was

A — *omb*Qd[For] + LGMR > *hthHM*
Rh3
Rh6

B — *ombQUADROON + hthHM*

C — LGMR > ArmS10 + *hthHM*
Rh3
Rh6

D — *ectopic wg and hthHM*

E — *rh1*-lacZ   *rh3*-lacZ   *rh4*-lacZ   *rh5*-lacZ   *rh6*-lacZ

F — Rh3 Hth-lacZ

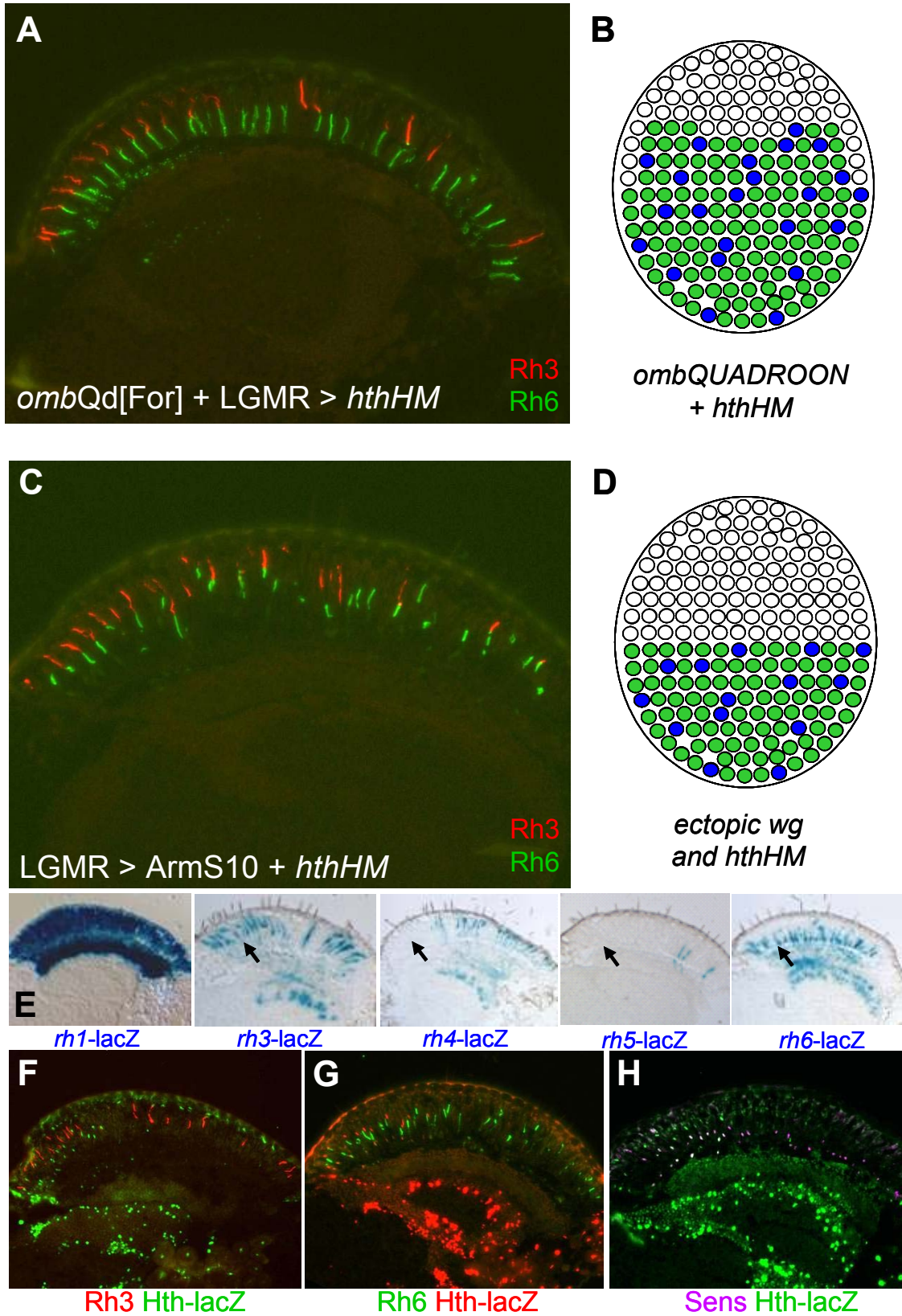**G** — Rh6 Hth-lacZ

H — Sens Hth-lacZ

Fig III.2.23 Removing Hth function in expanded DRAs: odd coupled ommatidia
(A)+(B) Transformation of the expanded DRA in *omb*QUADROON mutants in odd-coupled ommatidia: Frozen section through adult eyes from flies over-expressing dominant negative Hth (Hth[HM]) in an *omb*QUADROON mutant background. Double labeling with antibodies against Rh3 (red) and Rh6 (green) revealed odd-coupled ommatidia throughout the dorsal part of the eye. (B) Schematic representation of of the ombQdFor + LGMR > *hth*[HM] phenotype: The extra DRA ommatidia induced throughout the dorsal eye by the gain-of-function effect of Omb are transformed into odd-coupled ommatidia expressing the 'default' opsins Rh3 and Rh6, due to the inactivation of Hth function.
(C)-(G) Transformation of the whole dorsal eye into 'odd-coupled' Rh3/Rh6 ommatidia: Frozen section through adult eyes from flies co-over-expressing activated Armadillo and dominant negative Hth (Hth[HM]). Double labeling with antibodies against Rh3 (red) and Rh6 (green) revealed odd-coupled ommatidia throughout the dorsal half of the eye. (D) Schematic representation of the LGMR > Arms10 + *hth*[HM] phenotype: Due to the interaction of activated Armadillo and dominant negative Hth, odd coupled (Rh3/Rh6) ommatidia (white) are found covering the entire dorsal eye. (E) Expression of the opsin reporter constructs *rh1*-lacZ, *rh3*-lacZ, *rh4*-lacZ, *rh5*-lacZ and *rh6*-lacZ visualized by X-Gal staining on frozen sections through adult eyes from flies co-over-expressing both 'activated Armadillo' (ArmS10) and dominant negative Hth[HM] (LGMR > ArmS10 + *hth*[HM]). While *rh1*-lacZ expression was not affected, *rh4*-lacZ and *rh5*-lacZ were excluded from the expanded DRA, as in *omb*QUADROON mutants. However, *rh3*-lacZexpression was found expressed in all dorsal R7 cells, whereas all underlying R8 cells expressed *rh6*-lacZ. (F) All dorsal R7 cells express Rh3: Frozen section through adult LGMR > Arms10 + *hth*[HM] eyes double labeled for Rh3 (red) and Hth-lacZ (green). Rh3 was the only R7 opsin expressed in this domain. (G) All dorsal R8 cells express Rh6: Frozen section through adult LGMR > Arms10 + *hth*[HM] eyes double labeled for Rh6 (green) and Hth-lacZ (red). Rh6 was the only R8 opsin expressed in this domain. (H) Expansion of Sens expression into dorsal R8 cells: Frozen section through adult LGMR > Arms10 + *hth*[HM] eyes double labeled for Sens (pink) and Hth-lacZ (green). Co-expression of Hth-lacZ and Sens was detected throughout the dorsal eye.

observed (black arrow). Simultaneously, strong *rh6*-lacZ expression was observed in R8 cells throughout the dorsal half of the adult eye (black arrow), confirming the formation of *rh3*/*rh6* expressing ommatidia dorsally (**Fig 23F**). Finally, inner PRs in the dorsal half of the eye of LGMR > ArmS10 + *hth*[HM] flies were specifically marked with *hth*-lacZ, whose expressein was expanded in these flies. Frozen sections were then double labeled for βGal and Rh3 (**Fig 23F**). Hth-positive inner PRs (shown in green) always expressed Rh3 (shown in red), while Rh4 was never expressed in this domain (not shown). Frozen sections were also double labeled for βGal and Rh6 (**Fig 23G**). Similarly, dorsal inner PRs expressing hth (shown in red) always expressed Rh6 (shown in green), but never Rh5 (not shown), confirming that all dorsal ommatidia were transformed into odd-coupled ommtidia. Frozen sections were also double labeled for βGal and the R8 marker Sens (**Fig 23G**). In the wildtype, Sens is always specifically excluded from DRA R8 cells while over-expression of *hth*[HM] is sufficient to de-repress it in the DRA. Strong co-expression of Sens (shown in pink) and *hth*-lacZ (shown in green) was detected in all dorsal R8 cells, confirming that all dorsal ommatidia have lost their DRA identity.

Taken together, these results clearly show that removing Hth function from DRA ommatidia always leads to the formation of odd-coupled Rh3/Rh6 expressing ommatidia. Therefore, *hth* acts downstream of *wg* to specify the DRA.

2.24. Homothorax, *IRO-C* and Wingless interact to form the DRA

One concluding experiment was performed to demonstrate the power of the DRA model system. Combination of the DRA phenotypes obtained by ectopic expression of ArmS10, *IRO-C* and Hth allowed a better understanding of how these genes co-operate.

The *IRO-C* gene *araucan* (*ara*) was ectopically over-expressed together with ArmS10. It has been shown that activating the *wg* pathway is sufficient to transform the *IRO-C* expressing dorsal ommatidia into the DRA subtype. Furthermore, as providing ectopic *IRO-C* was sufficient to induce atypical 'ventral

ectopic wg and IRO-C
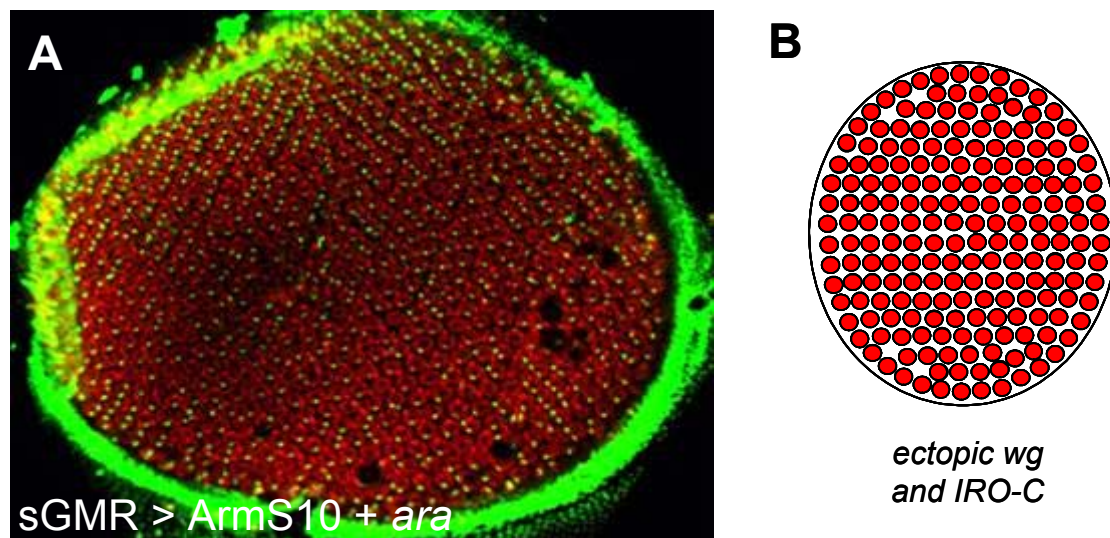
Fig III.2.24 Homothorax, *IRO-C* and Wingless interact to form the DRA
(a)+(B) Transformation of the whole retina into DRA ommatidia: Pupal retina dissected from flies co-over-expressing both ArmS10 and the *IRO-C* member Ara (sGMR > ArmS10 + *ara*). Double labeling with antibodies against Hth (green) and ElaV (red) revealed transformation of the whole retina into DRA-type ommatidia, expressing Hth.
(B) Schematic representation of the sGMR > ArmS10 + *ara* phenotype: DRA ommatidia (red) are found throughout the entire dorsal eye, a situation identical to the hth gain-of-funbction (LGMR > *hth*).

rim areas'. It was therefore expected that ectopic expression of both *ara* and ArmS10 should transform the whole retina into DRA omatidia, a situation that would be identical to Hth over-expression. Pupal retinas (sGMR > ara + ArmS10) were dissected and double labeled using antibodies against Hth and ElaV (**Fig 24A**). As predicted, Hth expression (shown in green) was detected in inner PRs of virtually all ommatidia throughout the retina. Sometimes, only one PR per ommatidia seemed to express Hth. This partial transformation was due to the relatively weak GMR-GAL4 driver that had to be used to avoid the excess cell

death observed in LGMR > *ara* flies (data not shown). It was concluded from this experiment that ectopic expression of activated Armadillo and *IRO-C* is sufficient to transform the whole retina into DRA ommatidia, thereby mimicking the effect of *hth* gain-of-functin (**Fig 24B**).

DRA ommatidia therefore provide a powerful model system to study the interaction of the dorsal selector genes with the *wg* pathway as well as its target genes.

3. Generating the ommatidial mosaic required for color vision: Specification of pale and yellow ommatidia

Following a candidate approach, the gene *spineless (ss) was* identified as essential for the establishment of the retinal mosaic of pale and yellow ommatidia. It was found that *ss* is specifically expressed in a large subset of R7 cells where it is necessary and sufficient to induce *rh4* expression and consequently, to impose the yellow fate onto the whole ommatidium. The most striking *ss* phenotype is the transformation of antenna into distal leg structures, leading to the *aristapedia* phenotype (Burgess and Duncan, 1990). *ss* is the homologue of the human arylhydrocarbon ('Dioxin') receptor and encodes a bHLH-PAS transcription factor (Duncan et al., 1998). Like other factors in this class (e.g. Sim or Sima/Hif), Ss usually acts by nuclearly localizing its obligatory hetero-dimerization partner, the pleiotropic protein Tango (Crews and Fan, 1999; Emmons et al., 1999).

3.1. *spineless* mutants show a dramatic opsin phenotype in R7 cells

Viable mutants in the gene *spineless*/*aristapedia* (*ss*) show a partial transformation of the antennae into distal leg structures, which is very similar to the loss of *homothorax* (Burgess and Duncan, 1990; Casares and Mann, 1998). However, the precise regulatory relationship between *hth* and *ss* in the antennae is not known. Following a candidate gene approach, *spineless* mutants were therefore tested for ommatidial specification and opsin expression. As *spineless* null mutants are homozygous lethal, whole mutant eyes in otherwise heterozygous animals had to be generated using the flip/FRT system. The *ss* null allele *ss*D115.7, recombined onto an FRT82B chromosome (gift from I. and D. Duncan, Washington University), the eye-specific flipase *ey*-flp and the FRT82B GMR-*hid* technique were used. The resulting flies showed the previously described antenna-to-leg transformation, due to the activity of ey-flip in the antennal part of the eye-antennal imaginal disc (**Fig 1A**). The eye morphology of

these flies, however, was indistinguishable from the wild type. It should be noted that the lack of bristles on the vertex of the fly's head (arrow in Fig) indicates a possible role of *ss* in the patterning of the head cuticle. However, a possible role of *ss* in this process was not pursued. Instead, the
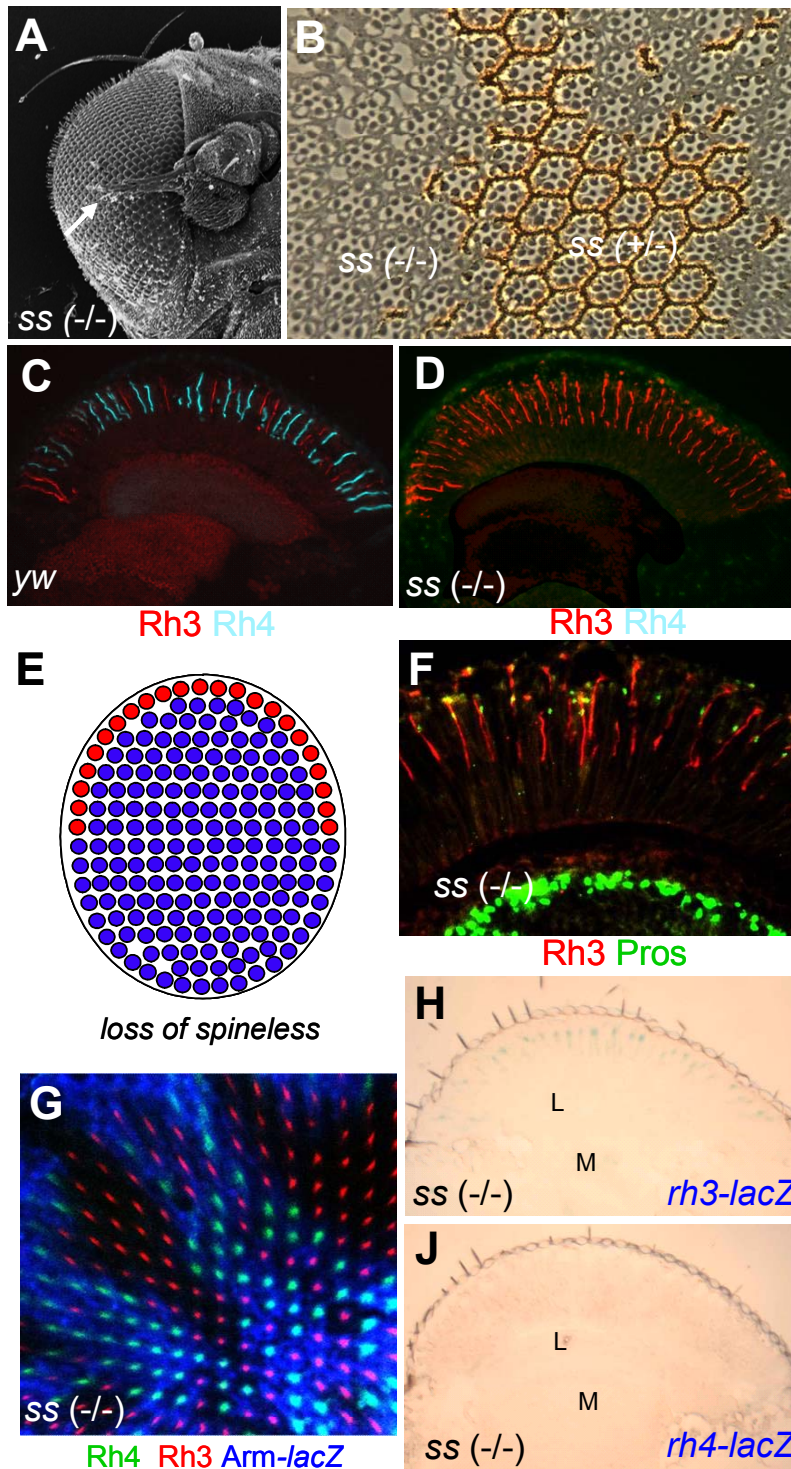
ss (-/-)

ss (-/-)   ss (+/-)

yw
Rh3 Rh4

ss (-/-)
Rh3 Rh4

loss of spineless

ss (-/-)
Rh3 Pros

ss (-/-)
Rh4 Rh3 Arm-*lacZ*

ss (-/-)   *rh3-lacZ*

ss (-/-)   *rh4-lacZ*

Fig III.3.1 *spineless* **mutants show a dramatic opsin phenotype in R7 cells**
(A)+(B) Eye morphology is unaffected by loss of *ss*: Scanning electron micrograph of an adult head from a fly with homozygous *ssD115.7* (-/-) eyes in an otherwise herterozygous animal. The distal part of the antenna was transformed into leg structures (arrow), as previously reported. (B) Plastic sections through the adult retina from a fly inducing mitotic *ssD115.7* (-/-) clones (marked by the absence of pigment) using the flip/FRT technique. Rhabdomere morphology and ommatidial polarity were identical within and outside the clones.
(C)+(D) Rh3 expresion is lost in *ss* whole mutant eyes: Frozen sections through adult eyes double labeled with antibodies against Rh3 (red) and Rh4 (cyan). In the wildtype, 30% of R7 cells as well as DRA R7 and R8 express Rh3, while the remaining R7 express Rh4. (D) R7 opsin expression was dramatically altered in flies with *ssD115.7* (-/-) whole mutant eyes. Rh4 expression was completely lost and expression of Rh3 was expanded into all R7 cells.
(E) Schematic representation of the *ss* (-/-) phenotype: *rh4* expressing **y** ommatidia (originally green) are lost and replaced by **p** ommatidia (blue).
(F) Rh4 expression is expanded into all R7 cells in *ss* mutants: Frozen sections through whole mutant *ssD115.7* (-/-) eyes double labeled with antibodies against Rh3 (red) and the R7 marker Pros (green). No Rh4-negative R7 cell was detected.
(G) Cell-autonomous loss of Rh4 expression in *ss* clones: Whole mounted adult retina from flies inducing mitotic clones of homozygous *ssD115.7* (-/-) tissue (marked by the absence of Arm-lacZ) were triple labeled with antibodies against βGal (blue), Rh3 (red) and Rh4 (green). Expression of Rh4 was completely lost within the mutant clones, whereas the p/y mosaic was intact in heterozygous wildtype tissue outside and right adjacent to the clones.
(H)+(J) Opsin gene transcription is altered in *ss* mutants: Expression of the opsin reporter transgenes *rh3*-lacZ and *rh4*-lacZ was visualized on frozen sections through *ssD115.7* (-/-) whole mutant eyes, using X-Gal staining. Expression of *rh3*-lacZ was dramatically expanded into all R7 cells. (J) Expression of *rh4*-lacZ was completely lost in *ssD115.7* mutant eyes.

homozygous mutant eyes were analyzed for more subtle morphological abnormalities by inducing mitotic clones of eye tissue homozygous for *ss*D115.7 using the Flip/FRT system (Xu and Rubin, 1993). Several eyes exhibiting such clones which were marked by the absence of red eye pigment were fixed and cut into 1 μm thin sections. Light microscopic analysis of these sections did not reveal any morphological abnormalities of the mutant (= unpigmented) tissue, like rhabdomere malformation or ommatidial misrotation and was instead indistinguishable from the adjacent pigmented (w^+) heterozygous tissue (**Fig 1B**). The phenotypic characterization of *ss* mutants was completed by assessing inner PR opsin expression in whole mutant eyes (*ey*-flip, FRT82-GMR-*hid*, FRT82B-*ss*D115.7). The pale and yellow ommatidia were visualized on frozen sections (10 μm) by using antibodies against the R7 opsins Rh3 and Rh4. In the wildtype, ~30% of R7 cells as well those R7 and R8 located in the DRA express Rh3 (shown in red in **Fig 1C**) while the remaining ~70% express Rh4 (shown in cyan). Eyes lacking *ss* function, however, manifested a dramatic change in opsin expression: They completely lacked Rh4 expression while Rh3 was expanded into apparently all R7 cells (**Fig 1D**). This result strongly suggested that all ommatidia had chosen the pale fate in *ss* mutants (shown schematically in **Fig 1E**). However, this could not be tested further, as there are no pale or yellow subset-specific markers besides the opsin genes themselves. Instead, it was teste whether indeed all R7 cells expressed Rh3 by co-staining frozen sections of

whole mutant eyes with antibodies against Rh3 and the R7 marker Prospero (**Fig 1F**). Every Pros-positive R7-nucleus (shown in green) was right adjacent to a rhabdomere expressing Rh3 (shown in red), demonstrating that indeed all R7 cells expressed Rh3 in the absence of *ss* function. Opsin expression in *Drosopphila* is regulated at the transcriptional level. It was therefore tested whether the strong R7 opsin phenotype observed in ss mutants was due to altered opsin transcription rather than to mis-localization or transport of the two R7 opsin proteins. The R7 opsin reporters *rh3-lacZ* and *rh4-lacZ* were introduced into flies with whole *ss* mutant eyes (*ey*-flip, FRT82-GMR-*hid*, FRT82B-*ss*D115.7) and frozen sections of their heads were stained for βGal activity using X-Gal (Stowers and Schwarz, 1999). It was observed that, in these mutants, *rh3*-lacZ expression was dramatically expanded to all R7 cells (**Fig 1G**), as had been observed for the corresponding opsin protein. Simultaneously, *rh4*-lacZ expression was completely lost in the same mutant background (**Fig 1H**). It was concluded from these observations that loss of ss activity in the eye leads to the loss of *rh4* transcription and to the transcription of *rh3* in all **y**R7 cells. Finally, the cell-autonomy of the *ss* phenotype was tested by inducing mitotic clones homozygous for *ss*D155.7 and marked by the absence of the reporter construct Armadillo-lacZ (Arm-lacZ). Triple labeling of whole mounted adult retinas (see material and methods) using antibodies against βGal, Rh3 and Rh4 confirmed the extreme opsin phenotype within the clones, whereas a normal Rh3/Rh4 ratio was observed in the heterozygous tissue marked by Arm-lacZ (shown in white in Fig). Furthermore, the R7 opsin ratio was not affected in the wildtype ommatidia right adjacent to mutant clones, indicating that ss is required cell-autonomously.

It was therefore concluded that *spineless* is necessary for the activation of *rh4* expression in ~70% of the R7 cells, as well as for the repression of *rh3* in these cells, possibly by cell-autonomously inducing the yellow fate in these ommatidia. Besides its role in ommatidial subtype specification, no other role was found for *ss* in eye development.

3.2. *spineless* mutants show a less dramatic opsin phenotype in R8 cells

R8 opsin expression in *ss* mutants was assessed next, by double labeling frozen sections with antibodies against the R8 opsins Rh5 and Rh6. In the wildtype, ~30 of the R8 cells express the pale opsin Rh5 (shown in blue) while the remaining R8 express the yellow opsin Rh6 (shown in green; **Fig 2A**). The pale R8 cells were visualized by labeling all R8 nuclei with the R8 marker Senseless (*sens; (Nolo et al., 2000); (Frankfort et al., 2001)* and the **y**R8 cells with Anti-Rh6 (**Fig 2B**). Pale ommatidia could therefore be identified due to the lack of co-staining of Sens and Rh6 expression (white arrows). Frozen sections (10 µm) through *spineless* whole mutant eyes (*ey*-flip, FRT82-GMR-*hid*, FRT82B-*ss*D115.7) were also double labeled for Rh5 and Rh6 (**Fig 2C**). The vast majority of R8 cells now expressed the pale opsin Rh5 and only very few cells expressed Rh6. However, the *ss* phenotype in R8 cells was variable: while in most cases ~80-90% of R8 expressed Rh5, rare cases were observed where both Rh5 and Rh6 were expressed in ~50% of the ommatidia. The R8 phenotype was therefore significantly different from the loss of Rh4 in R7 cells, which always occurred with 100% penetrance. The *ss* (-/-) opsin phenotype in R8 cells was further characterized by double labeling frozen sections for Sens and Rh6 (**Fig 2D**). In the vast majority of the cases, the number of Sens-positive cells (shown in pink) not co-expressing Rh6 (show in green) was dramatically increased. Therefore, the **p** ommatidial subtype (with paired expression of Rh3/Rh5) was dramatically expanded throughout the retina, but that a significant amount of mis-coupled ommatidia (with paired expression of Rh3/Rh6) were created in *ss* mutant eyes as well.

A low ratio of odd-coupled (Rh3/Rh6) ommatidia (~7%) can be observed in wildtype flies. However, in most of the cases, Rh3 expressing R7 cells are not located on top of Rh6 expressing R8 cells, in the same ommatidium. This situation was visualized on frozen sections through adult eyes from wildtype flies using antibodies against Rh3 and Rh6 (**Fig 2E**). The **p**R7 opsin Rh3 (shown in red) was always found in R7 cells located above a gap between **y**R8 cells expressing Rh6 (shown in green). Due to the different *ss* (-/-) opsin phenotypes

in R7 and R8 cells, increased mis-coupling in *ss* was tested by double labeling frozen sections through *spineless* whole mutant eyes (*ey*-flip,
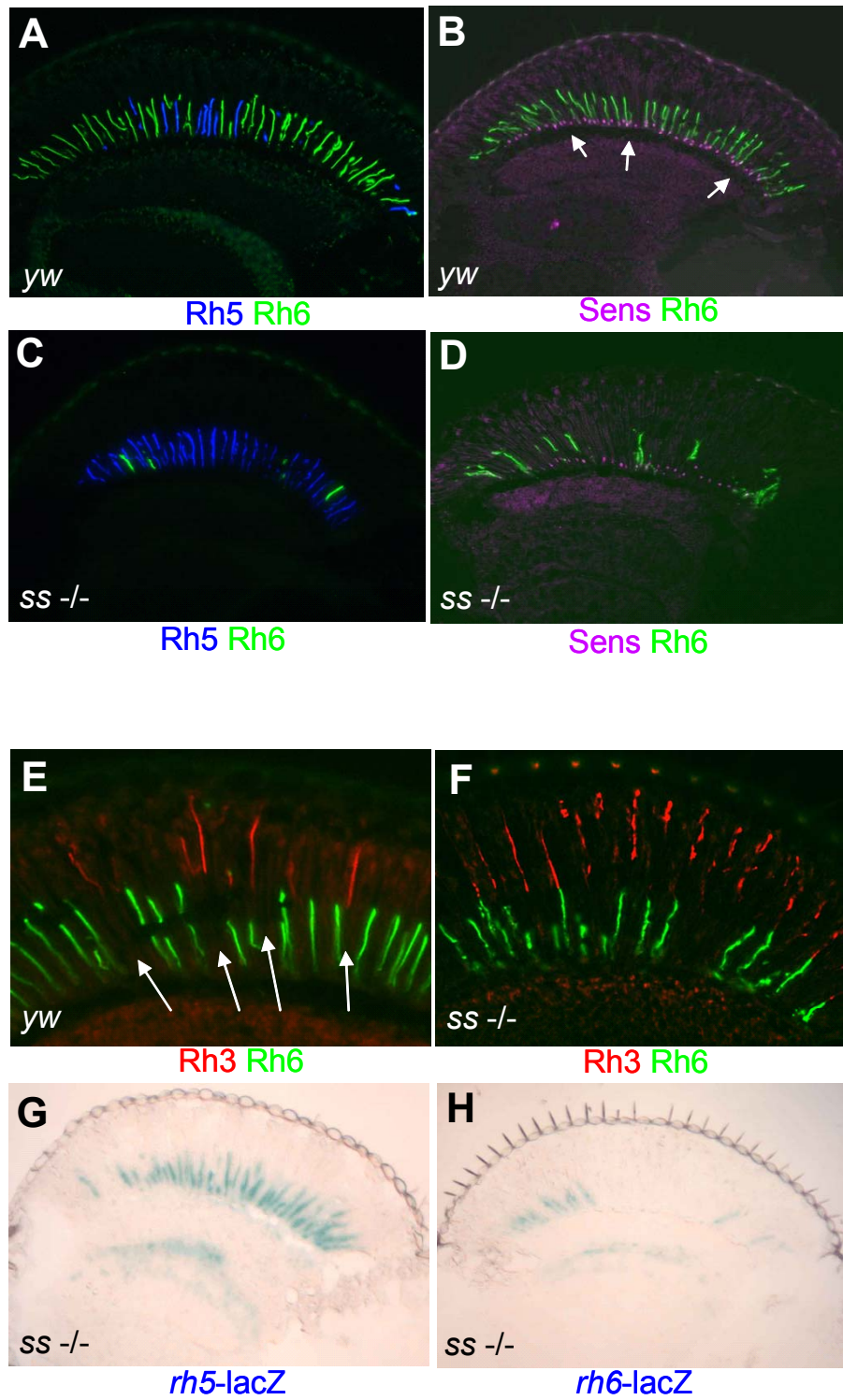
Fig III.3.2 s*pineless* mutants show a less dramatic opsin phenotype in R8 cells
(A)+(B) Pale and yellow subtypes in wildtype R8 cells: Frozen section through adult eyes from wildtype flies double labeled with antibodies against Rh5 (blue) and Rh6 (green). A large subset of R8 cells (~70) always expressed Rh6, the rest expressed Rh5. (B) Double labeling of wildtype eyes with antibodies against Rh6 (green) and the R8 marker Sens (pink). Pale ommatidia could be identified by the absence of Rh6 on top of Sens-positive nuclei (white arrows).
(C)+(D) Strong R8 opsin phenotype in *ss* mutants: Frozen section through *ssD115.7* (-/-) whole mutant eyes double labeled with antibodies against Rh5 (blue) and Rh6 (green). Rh6 expression was dramatically reduced and the number of Rh5 expressing R8 cells increased. (B) Double labeling of *ssD115.7* (-/-) whole mutant eyes with antibodies against Rh6 (green) and the R8 marker Sens (pink). The number of **p** ommatidia identified by the absence of Rh6 on top of Sens-positive nuclei was dramatically increased.
(E) Exclusion of Rh3 and Rh6 from the same wildtype ommatidium: Frozen sections through adult eyes from wildtype flies double labeled with antibodies against Rh3 (red) and Rh6 (green). **p**R7 cells (*rh3*) were always found above gaps between **y**R8 (*rh6*) cells (white arrows).
(F) Mis-coupling of Rh3 and Rh6 in *ss* mutants: Frozen sections through adult eyes from *ssD115.7* (-/-) flies double labeled for Rh3 (red) and Rh6 (green). As all R7 cells expressed *rh3*, mis-coupling of Rh3 and those R8 cells expressing Rh6 was found within several ommatidia.
(G)+(H) Transcriptional up-regulation of the **p**R8 subtype in *ss* mutants: Expression of the opsin reporter transgenes *rh5*-lacZ and *rh6*-lacZ was visualized on frozen sections through *ssD115.7* (-/-) whole mutant eyes, using X-Gal staining. Expression of *rh5*-lacZ was dramatically expanded into most R8 cells. (H) The number of *rh6*-lacZ expressing R8 cells was dramatically reduced in *ssD115.7* mutant eyes. However, *rh6* expression was not completely lost.

FRT82-GMR-*hid*, FRT82B-*ss*D115.7) with antibodies against Rh3 and Rh6 (**Fig 2F**). While Rh3 (shown in red) was detected in all R7 cells, Rh6 (shown in green) was always found in a subset of R8 cells. Depending on the Rh6 ratio of the individual fly, between 10-50% of mis-coupled ommatidia were observed. It was therefore concluded that, while the majority of ommatidia in *ss* mutant eyes were of the p subtype, a significant number of Rh3/Rh6 ommatidia were also created.

Finally, it was tested whether the ss (-/-) opsin phenotype in R8 cells was due to altered gene transcription. First, a *rh5*-lacZ transgene was introduced into the *ey*-flip, FRT82-GMR-*hid*, FRT82B-*ss*D115.7 background and βGal activity was visualized on frozen sections using X-Gal stainings (**Fig 2G**). The numer of *rh5*-lacZ expressing R8 cells was dramatically increased, as had previously been observed with Anti-Rh5 antibodies. Finally, expression of a *rh6*-lacZ transgene was visualized on frozen sections through adult *ss* (-/-) eyes (**Fig 2H**). The number of βGal expressing R8 cells was significantly reduced, supporting previous observations. It was therefore concluded that the dramatic re-organization of the R8 opsin mosaic in favor of the **p** subset was regulated at the transcriptional level.

Therefore, loss of *ss* leads to a dramatic gain of pR8 cells. However, the y subtype is not completely lost in R8 cells, resulting in a significant number of odd-coupled ommatidia expressing Rh3 in R7 and Rh6 in R8.

3.3. *spineless* is required in R7 cells

The current model of how opsin expression is co-ordinated in *Drosophila* in order to result in the two ommatidial classes (pale and yellow) includes two consecutive events: first, the choice between *rh3* and *rh4* expression in R7 and then the consecutive instruction of the underlying R8 cell by R7 to choose expression of the same class opsin (*rh5* or *rh6*; (Chou et al., 1999). *Spineless* mutants exhibited a strong opsin phenotype both in R7 cells as well in R8 cells, both cell types dramatically increasing their pale opsin ratio (see above). It was therefore tested whether the R8 opsin phenotype was due to the loss of *ss* in R8 cells rather than to the loss of *ss* in R7 cells (choice of *rh3* over *rh4*), followed by the instruction of underlying R8 cells to express *rh5* instead of *rh6*.

First, expression of Rh5 and the inner PR marker Spalt (Sal) was visualized on frozen sections through adult eyes from wildtype flies (**Fig 3A**). Sal expression (shown in red) was detected in all R7 and R8 cells throughout the retina and Rh5 (shown in blue) was expressed in a relatively small subset of the R8 cells. Homozygous viable *sevenless* (*sev*) mutants lacking all R7 cells were then characterized by performing the same double staining (**Fig 3B**). Sal expression (shown in red) remained in R8 cells, none of which expressed Rh5 (shown in blue). This loss of Rh5 expression in *sev* mutants has previously been reported. In a next step, double mutants for both *sev* and *ss* were generated (*sev*, *ey*-flip, FRT82-GMR-*hid*, FRT82B-*ss*D115.7) and further analized. First, the genotype of sev + ss (-/-) was confirmed by double labeling frozen sections with Anti-Rh3 and Anti-Rh4 (**Fig 3C**). While Rh4 expression (shown in cyan) was completely lost, expression of Rh3 (shown in red) only persisted in the R8 cells of the DRA (white arrows). These flies therefore clearly had no R7 cells. Next, frozen sections through adult eyes from *ss* + *sev* (-/-) flies were double stained for Sal and Rh5 (**Fig 3C**). The R8 cells were marked by Sal (shown in red) and Rh5 expression (shown in blue) was completely lost, as is observed in *sev* mutants. Double mutants (*ss* + *sev*) therefore phenocopied *sev* mutants (loss of Rh5) rather than *ss* mutants (dramatically increased
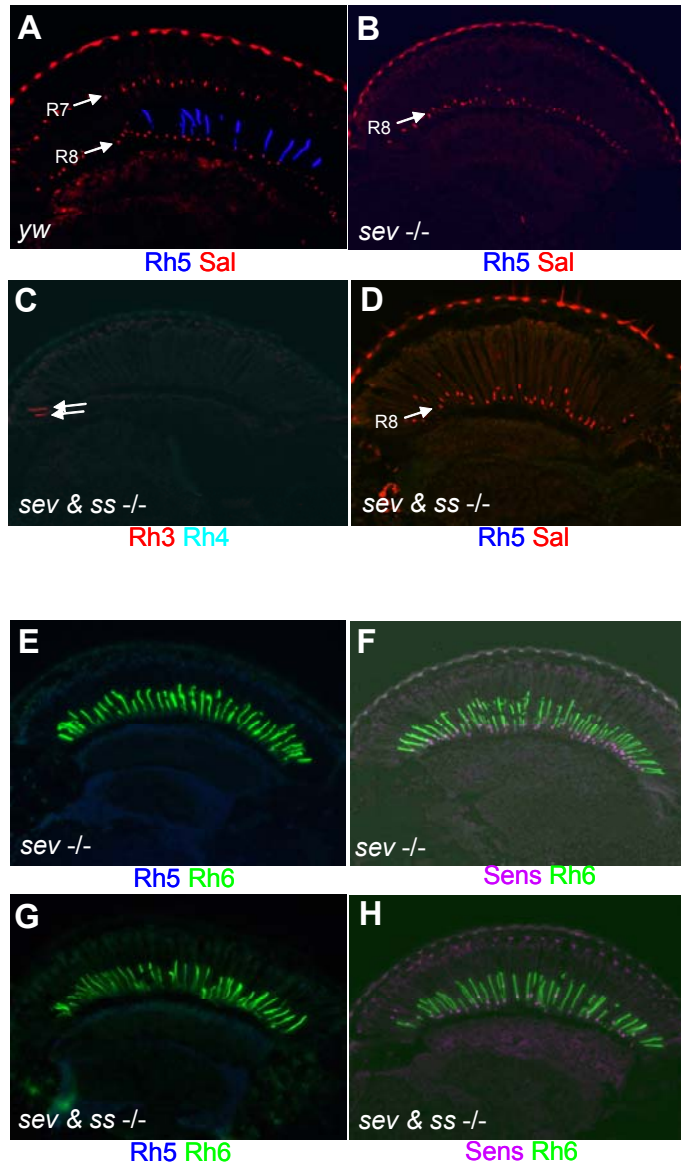
Fig III.3.3 *spineless* **is required in R7 cells**
(A) Expression of Spalt and Rh5 in wildtype flies: Frozen sections through adult eyes from wildtype flies were double labeled using antibodies against Rh5 and the inner PR marker Spalt (Sal). Sal expression (red) was detected in R7 and R8 cells. Rh5 expression (blue) was restricted to a small subset of R8 cells.
(B) Expression of Spalt and Rh5 in *sev* mutants: Frozen sections through adult eyes from *sev* mutants were double labeled for Rh5 and Sal. Due to the loss of R7 cells, Sal expression (red) was specific to the R8 cells (arrow). Rh5 expression (blue) was completely lost.
(C) Characterization of *ss + sev* double mutants: Flies were generated with whole mutant eyes lacking both *ss* and *sev* (*ss + sev*). First, the genotype was tested by double labeling frozen sections with antibodies against Rh3 and Rh4. Expression of Rh4 was completely lost, while Rh3 remained specific to the R8 cells in the DRA (white arrows).
(D) Expression of Spalt and Rh5 in *ss + sev* double mutants: Frozen sections through adult eyes from *ss + sev* mutants double labeled with Anti-Rh5 and Anti-Sal. Sal expression (red) was specific to the R8 cells (arrow) and Rh5 expression (blue) was completely lost. The *ss + sev* double mutants therefore phenocopied *sev* mutants.
(E)+(F) Loss of **p** ommatidia in *sev* mutants: Frozen section through adult eyes from *sev* mutants double labeled for Rh5 (blue) and Rh6 (green). Rh6 was detected in all R8 cells, whereas Rh5 was almost always lost. (B) Double labeling of *sev* eyes with antibodies against Rh6 (green) and the R8 marker Sens (pink). All Sens-positive nuclei could be associated with a Rh6-positive R8 rhabdomere, suggesting that the **p** subtype was lost.
(G)+(H) Loss of both *ss* and *sev* phenocopies *sev*: Frozen section through adult eyes from *sev + ss* double mutant eyes double labeled for Rh5 (blue) and Rh6 (green). As in sev mutants, Rh6 was detected in all R8 cells, whereas Rh5 was almost always lost. (B) Double labeling of *sev + ss* (-/-) eyes with antibodies against Rh6 (green) and the R8 marker Sens (pink). All Sens-positive R8 cells co-expressed Rh6. This phenotype was identical to *sev* mutants, suggesting that *ss* is required in R7 cells.

117

number of Rh5 expressing R8 cells).

Comparison of *sev* mutants and *sev* + *ss* double mutants was completed by double labeling frozen sections through adult heads from both genotypes with antibodies against Rh5 and Rh6 (**Fig 3E**). A strong opsin phenotype was observed in *sev* mutants: as previously described, virtually all R8 cells expressed Rh6 (shown in green), which was consistent with the loss of Rh5 expression already reported above. It had therefore been proposed that Rh6 represented the 'ground state' opsin in these cells, as they did not receive any instructive signal from R7 (see introduction). This phenotype was further confirmed by double labeling *sev* mutants for Sens and Rh6 (**Fig 3F**). The vast majority of R8 cells (marked by Sens in pink) expressed Rh6 (shown in green). Next, frozen sections through *ss* + *sev* double mutant eyes were double labeled with Anti-Rh5 and Anti-Rh6 (**Fig 3G**). All R8 cells in the double mutant co-expressed Rh6 (**Fig 3G**), which was consistent with the loss of Rh5 expression already reported above. Exclusive expression of Rh6 in the *ss* + *sev* double mutant was then confirmed by labeling of Rh6 and Sens (**Fig 3H**). No R8 cell (marked by Sens in pink) was found to lack Rh6 expression (shown in green). It was therefore concluded that *ss* + *sev* double mutants clearly phenocopied *sev* mutants, and not *ss (-/-)*.

It was concluded from these genetic experiments, that *spineless* activity is only required in R7 cells and that the dramatic up-regulation of **p**R8 is most likely a secondary effect following the instruction by **p**R7 cells. Interestingly, this instructive process does not seem to be 100% effective, as a significant amount of mis-coupled ommatidia (Rh3/Rh6) are observed.

3.4. Spineless is specifically expressed in a large subset of R7 cells

The *spineless* gene is a complex locus of >50kb that has been studied extensively (Duncan et al., 1998). Dissection of its enhancer regions has lead to the identification of short DNA fragments driving expression in different tissues (I. and D. Duncan, unpublished). In this context, a ~1.6 kb fragment of genomic DNA reported to drive expression of the reporter gene beta-galactosidase in the eye imaginal disc was discovered and therefore called 'eye enhancer'.

Expression of this 'eye enhancer' (E1.6) was studied in more detail. As all pre-existing enhancer-lacZ lines showed extremely weak expression in the eye, the 1.6 kb genomic DNA fragment was used to generate a new ss[E1.6]-GAL4 construct (ss_{eye}-GAL4). The promoter-less E1.6 fragment was combined with the TATA box sequence of the *Drosophila hsp70* gene, fused to the GAL4 cDNA from yeast and ligated into a *Drosophila* injection vector pCasper4 (see material and methods). Transgenic flies carrying insertions of this GAL4 construct were obtained and stable stocks were established.

Several different ss_{eye}-GAL4 transgenic lines were crossed to UAS-lacZ::NLS reporter flies expressing a βGal protein fused to a nuclear localization signal, under the control of GAL4 UAS-sites. GAL4 expression was first examined in the eye imaginal discs of wandering third instar larve (see material and methods). Triple labeling of these eye discs (ss_{eye}-GAL4 > UAS-lacZ::NLS) with antibodies against βGal, the R7 marker Prospero (Pros) as well as the neuronal marker ElaV revealed no expression of ss_{eye}-GAL4 in larval PRs (**Fig 4A**). However, at the posterior end of the eye imaginal disc, expression of βGal was observed in non-neuronal cells, most likely developing cone and pigment cells (**Fig 4B**). Expression of ss_{eye}-GAL was then examined in the adult eye by double labeling frozen sections (10 μm) through the eyes of ss_{eye}-GAL4 > UAS-lacZ::NLS flies with antibodies against βGal and Pros (**Fig 4C**). No co-staining of βGal (shown in green) with Pros (shown in red) or ElaV (not shown) was detectable. As in the larval visual system, strong of βGal staining was observed in non-neuronal cells. Therefore, the *ss* 'eye enhancer' does not drive significant expression of GAL4 in larval or adult PRs.

To complete the expression pattern analysis of ss_{eye}-GAL4, flat pupal retinas (48 hrs APF) were double labeled with Anti-βGal and Anti-ElaV (**Fig 4D**). At this developmental stage, robust expression of βGal (shown in red) was detectable in PRs (shown in blue). The expression pattern of ss_{eye}-GAL4 consisted of single PRs that appeared to be randomly 'sprinkled' through the retina. Only one positive PR per ommatidium was observed and many ommatidia did not stain for βGal at all. Expression levels appeared to be variable, which

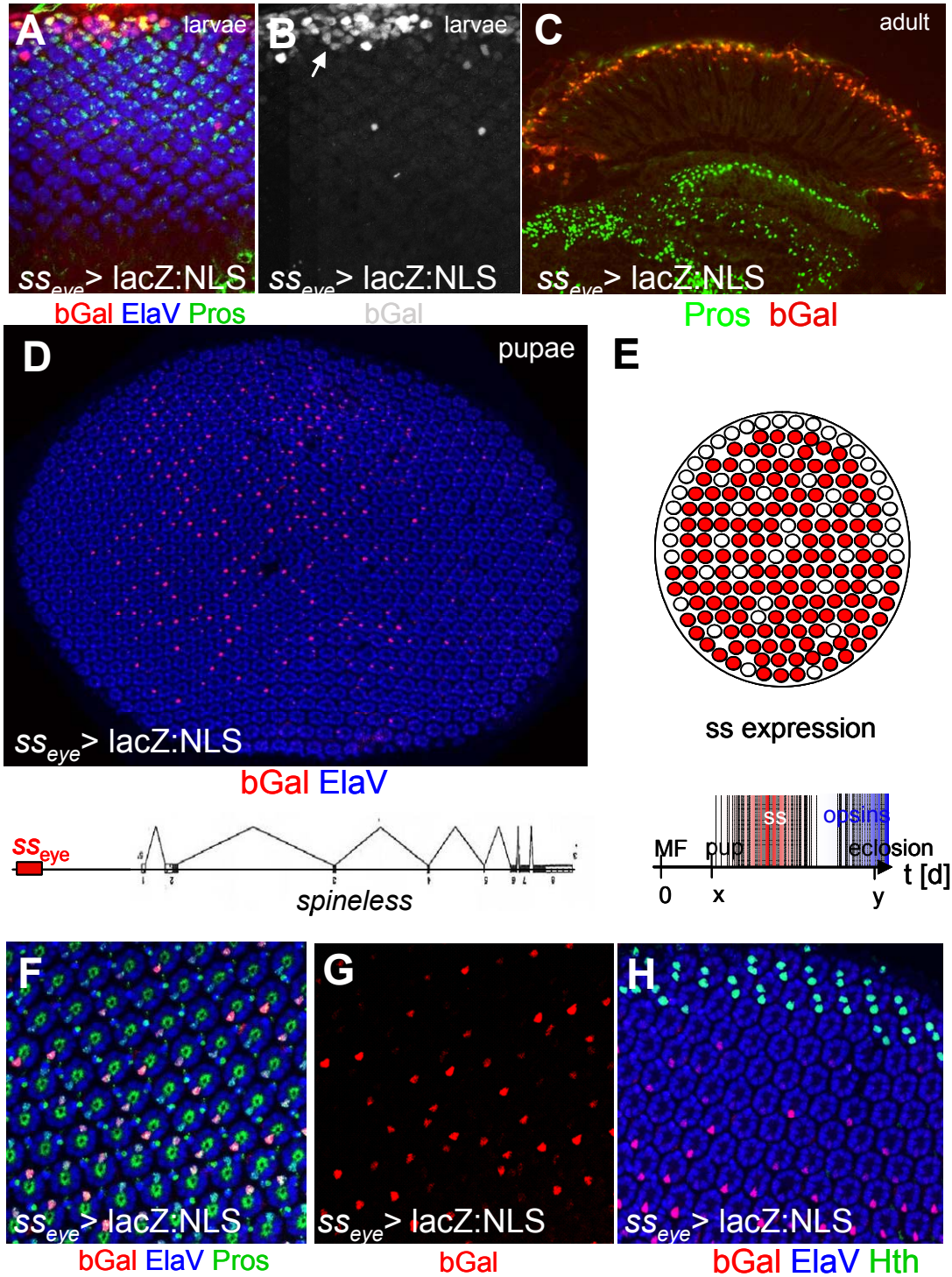made a statistical analysis (ratio of stained ommatidia vs. unstained,

Fig III.3.4 Spineless is specifically expressed in a large subset of R7 cells
(A)-(C) ss$_{eye}$-GAL4 is not expressed in larval or adult PRs: Eye imaginal discs dissected fom wandering third instar larvae driving lacZ:NLS under control of ss$_{eye}$-GAL4, triple labeled with antibodies against βGal (red), the R7 marker Pros (green) and ElaV (blue). Expression of βGal was detectable at the posterior end of the disc (top), but no co-localization with ElaV was detectable, suggesting that ss$_{eye}$-GAL4 is not expressed in PRS at this developmental stage. (B) Expression of ss$_{eye}$-GAL4 was detected in developing cone cells (arrow) in third instar eye imaginal discs. (C) Adult expression of ss$_{eye}$-GAL4 detected by double labeling frozen sections through the eyes from ss$_{eye}$-GAL4 > lacZ:NLS flies uisn g antibodies against βGal (red) and Pros (green). No βGal expression was detected in R7 cells or other ElaV-positive PRs (not shown).
(D) Pupal expression of ss$_{eye}$-GAL4 in PRs (top): Pupal retina (48 hrs APF) from flies driving lacZ:NLS under control of ss$_{eye}$-GAL4, double labeled with antibodies against βGal (red) and ElaV (blue). Strong expression of βGal was detectable in one cell per cluster in a subset of ommatidia. Overview over the location of the E1.6 ss eye enhancer within the ss gene (bottom): The E1.6 enhancer is a short ~1.6 kb stretch of genomic DNA in the 5' regulatory sequence of the ss gene.
(E) Schematic representation of the ss$_{eye}$-GAL4 expression pattern (top): GAL4 expression driven by the ss E1.6 eye enhancer (red) was specific to a large subset of R7 cells, highly reminiscent of the **y**R7 subtype. Proposed time course of ss$_{eye}$-GAL4 in developing PRs (bottom): Onset of GAL4 expression (red) was observed during pupation and no remaining expression was detectable at the onset of opsin expression (blue), shortly before eclosion.
(F)+(G) ss$_{eye}$-GAL4 expression in a large subset of pupal R7 cells: Pupal ss$_{eye}$-GAL4 > lacZ:NLS retina riple labeled with antibodies against βGal (red), Pros (green) and ElaV (blue). All cells expressing βGal were Pros-positive. (G) Ratio of R7 cells negative for βGal expression (white arrows) was ~21%. However, false positives may have been counted due to faint signals.
(H) Expression of ss$_{eye}$-GAL4 is excluded from the DRA: Pupal retina from ss$_{eye}$-GAL4 > lacZ:NLS flies triple labeled with antibodies against βGal (red), the DRA marker Hth (green) and ElaV (blue). Expression of βGal was never observed in Hth-posiitive inner PRs of the DRA.

see below) difficult. Interestingly, βGal-positive PRs seemed to be more abundant in the dorsal half of the pupal retina (left in Fig D). **Y** ommatidia also occur at a higher ratio (>70%) in the dorsal half of the eye, whereas **p** ommatidia preferentially populate the ventral part (>30%). The observed pupal expression pattern of ss$_{eye}$-GAL4 as well as the loss-of-function data presented above therefore lead to the hypothesis that ss might be transiently expressed in PRs, and specific to the **y** subset of ommatidia at this stage (**Fig 4E**).

As genetic experiments have shown that ss function is required in R7 cells, it was tested whether ss$_{eye}$-GAL4 was expressed specifically in R7 cells. Pupal retinas (48 hrs APF; ss$_{eye}$-GAL4 > UAS-lacZ::NLS) were triple labeled for βGal, Anti-Pros and ElaV (**Fig 4G**). It was observed that βGal-positive PRs always co-stained for Pros, demonstrating that ss$_{eye}$-GAL4 was indeed expressed in a subset of R7 cells during pupal development. Furthermore, a rough statistical analysis of ss$_{eye}$-GAL4 expression was performed on these retinas by calculating the ratio of βGal-positive R7 cells. As a representative example, a field of 84 ommatidia at an equatorial location is shown (**Fig 4H**). ~71% of the ommatidia (59/25) had βGal-expressing R7 cells (negative ommatidia are marked with white arrow heads), a ratio which is virtually identical to the ratio measured for **y** ommatidia (70%). Finally, it was tested whether ss$_{eye}$-GAL4 expression extended into the dorsal rim area. DRA ommatidia develop in response to high wg signaling emanating from the dorsal head cuticle and that **p**

or **y** ommatidia never occur in the dorsal-most row of ommatidia. Pupal retinas (48 hrs APF; ss$_{eye}$-GAL4 > UAS-lacZ::NLS) were therefore triple labeled for βGal, Anti-Hth and ElaV (**Fig 4J**). Hth (shown in green) never co-stained with βGal (shown in red), indicating that *ss* expression, just like **p** and **y** ommatidia, might be specifically excluded form the DRA.

It was concluded from these experiments, that GAL4 expression driven by the previously identified ss 'eye enhancer' shows a very specific expression pattern in PRs, both temporally as well as spatially. Expression is restricted to the pupal phase of eye development and is specific to a large subset of R7 cells very likely to be the **y** subset.

3.5. Photoreceptor cell fates are specified correctly in *spineless* mutants

The dramatic opsin phenotypes described above, as well as the ss$_{eye}$-GAL4 expression pattern, suggested that *ss* might play an important role in the specification of the color-sensitive **y** ommatidia. As it is not known when **p** and **y** ommatidia are first determined, it was tested whether all basic cell fate determination steps occur normally in *spineless* mutants: specification of outer versus inner PRs, of R7 versus R8, as well as specification of the DRA. Expression of ss$_{eye}$-GAL4 suggested that **p** and **y** could be specified relatively late, at mid-pupation. It was therefore hypothesized that *ss* would be epistatic to the genes required for proper ommatidial development, like *sal* and *pros* and that loss of *ss* would not affect expression of these genes. Furthermore, expression of genes necessary for DRA or R8 maturation (Hth, Sens) should also not be affected by the loss of *ss*.

To test whether R7 cells are properly specified in *ss* mutants, mitotic clones of mutant eye tissue homozygous for *ss*D115.7, marked by the absence of Arm-lacZ, were created using the ey-flip/FRT system. Flat pupal retinas (48 hours after puparium formation, APF) were collected, fixed and labeled with antibodies against the R7 marker Prospero (Pros), which is essential for correct specification of adult R7 cells, as well as the neuronal marker ElaV and βGal (**Fig
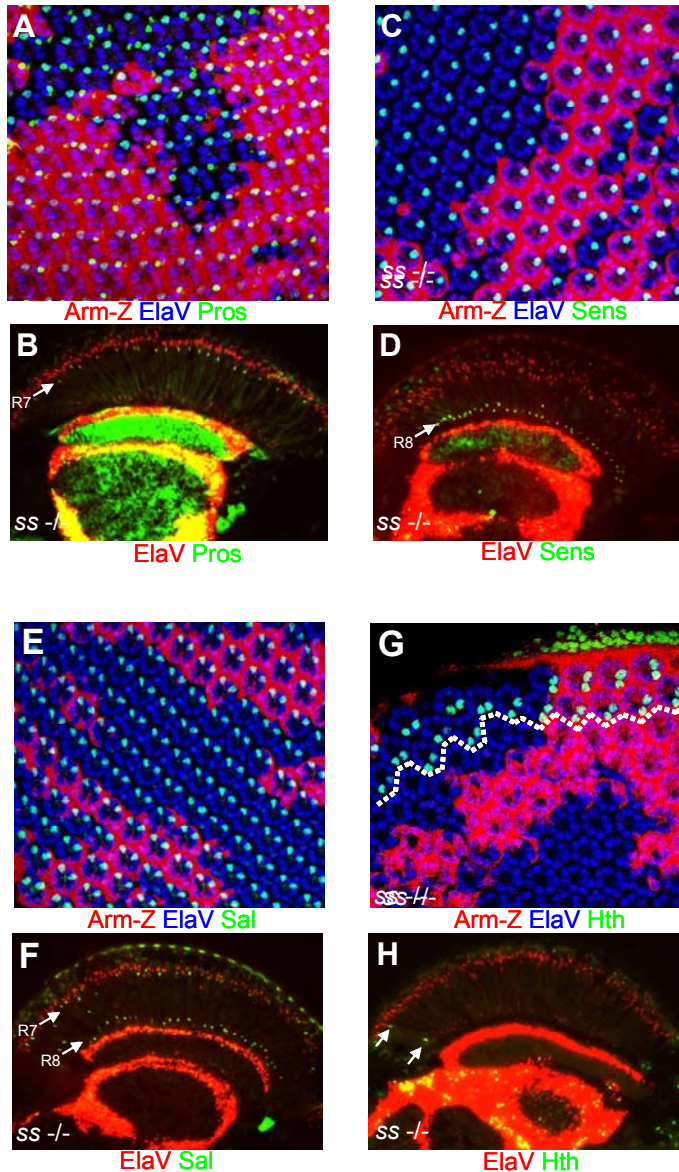
FigIII.3.5 Photoreceptor cell fates get specified correctly in *spineless* mutants
(A)+(B) R7 cells get correctly specified in *ss* mutants: Pupal retina from flies inducing mitotic clones of *ss*^D115.7 (-/-) tissue (marked by the absence of Arm-lacZ) triple labeled with antibodies against βGal (red), the R7 marker Pros (green) and ElaV (blue). Pros expression was indistinguishable in R7 cells inside and outside of *ss* (-/-) mutant clones. (B) Frozen sections through whole mutant *ss*^D115.7 (-/-) eyes double labeled with antibodies against Pros (green) and ElaV (red). Adult Pros expression was unaffected by the loss of *ss*.
(C)+(D) R8 cells get correctly specified in *ss* mutants: Pupal retina from flies inducing mitotic clones of *ss*^D115.7 (-/-) tissue (marked by the absence of Arm-lacZ) triple labeled with antibodies against βGal (red), the R8 marker Sens (green) and ElaV (blue). Sens expression was indistinguishable in R8 cells inside and outside of *ss* (-/-) mutant clones. (B) Frozen sections through whole mutant *ss*^D115.7 (-/-) eyes double labeled with antibodies against Sens (green) and ElaV (red). Adult Sens expression was unaffected by the loss of *ss*.
(E)+(F) Inner PRs get correctly specified in *ss* mutants: Pupal retina from flies inducing mitotic clones of *ss*^D115.7 (-/-) tissue (marked by the absence of Arm-lacZ) triple labeled with antibodies against βGal (red), the inner PR marker Sal (green) and ElaV (blue). Sal expression was indistinguishable in R7 and R8 cells inside and outside of *ss* (-/-) mutant clones. (B) Frozen sections through whole mutant *ss*^D115.7 (-/-) eyes double labeled with antibodies against Sal (green) and ElaV (red). Adult Sal expression in R7 and R8 cells was unaffected by the loss of *ss*.
(G)+(H) The DRA gets correctly specified in *ss* mutants: Pupal retina from flies inducing mitotic clones of *ss*^D115.7 (-/-) tissue (marked by the absence of Arm-lacZ) triple labeled with antibodies against βGal (red), the DRA marker Hth (green) and ElaV (blue). Hth expression was indistinguishable in inner PRs inside and outside of *ss* (-/-) mutant clones touching the DRA (dashed line). (B) Frozen sections through whole mutant *ss*^D115.7 (-/-) eyes double labeled with antibodies against Hth (green) and ElaV (red). Adult Hth expression was unaffected in the DRA of flies lacking *ss* expression (arrows).

5A). No difference in Pros expression (shown in green) was visible inside and outside the clone. Alternatively, Pros expression was visualized in eyes lacking ss function (*ey*-flip, FRT82-GMR-*hid*, FRT82B-*ss*D115.7): Frozen sections (10 µm) through these heads were labeled with AntiPros as well as ElaV (**Fig 5B**). As in pupae, Pros expression (shown in green) in R7 cells was unaffected in the adult. It was therefore concluded that *ss* most likely acts downstream or in parallel with Pros as loss of *ss* does not affect its expression.

Specification of R8 cells was studied in pupae (**Fig 5C**) as well as in the adult (**Fig 5D**) using an antibody against the R8 marker Senseless (Sens) which is indispensable for R8 cell maturation (Frankfort et al., 2001). No difference in Sens expression (shown in green) was observed inside the *ss* (-/-) pupal clones as well as in whole clonal adult eyes. The same studies were performed for the transcription factor Spalt (Salm), which is essential for the specification of both inner PRs R7 and R8: labelling of *ss* (-/-) homozygous clones in pupae (**Fig 5E**) as well as whole clonal eyes (**Fig 5F**) with Anti-Salm did not reveal any changes of Salm expression (shown in green) in the absence of *ss* function. Finally, the specification of the DRA was assessed in ss(-/-) clones (**Fig 5G**) as well as in the adult (**Fig 5H**), by staining pupal retinas as well as frozen sections with an antibody against Hth (shown in green). Again, no change in *hth* expression was observed in *ss* mutant tissue.

It was concluded from these experiments, that all basic PR cell fate determination steps occur normally in the absence of *ss*. The results described ndicate that *ss* acts downstream of, or in parallel with these genes (*sal*, *pros*) or that it is not required in the cells that depend on the determination events investigated (*sens*, *hth*).

3.6. *spineless* is sufficient to induce the yellow R7 fate

The *Drosophila* gene *spineless* is transiently expressed in a large subset of R7 cells and is necessary for the development of the yellow ommatidial subset, by leading to the activation *rh4* expression and repression of *rh3*. It was

therefore tested, whether ss also was sufficient to induce the yellow R7 fate when mis-expressed in other PRs.

Transgenic flies ectopically over-expressing Spineless in all developing PRs under the control of a strong GMR-GAL4 driver (LGMR > ss) had rough eyes and were analyzed for opsin expression. First, *rh4*-lacZ transgenes were introduced and frozen sections (10 µm) through adult heads were stained for βGal activity (see materials and methods). In the wildtype, *rh4*-lacZ is expressed in a large subset of R7 cells (**Fig 6A**). In flies over-expressing *ss* under the control of the LGMR promoter, expression of *rh4*-lacZ was dramatically expanded (**Fig 6B**). A multitude of projections from βGal-expressing PRs to the medulla, as well as to the lamina part of the optic lobe were observed (black arrows), whereas in the wildtype only a subtype of PRs projecting to the R7 layer of the medulla are stained. Over-expression of *ss* therefore leads to the expansion of *rh4*-lacZ expression into all PRs.

An antibody against Rh4 was used to test whether over-expression of *ss* also led to the expansion of Rh4 protein into outer PRs. Whole mounted retinas from adult *ss* gain-of-function flies (LGMR > *ss*) were double-labeled with antibodies against Rh3 and Rh4 (**Fig 6C**). These flies also showed a dramatic opsin phenotype, expressing Rh4 (shown in cyan) in every PR cell. Furthermore, expression of Rh3 was not detectable. It was therefore concluded that *ss* is sufficient to induce Rh4 expression as well as to repress Rh3 expression, when over-expressed in developing PRs. Therefore, *ss* is not only necessary for the **y** subtype to develop, but is also sufficient to induce this ommatidial subtype (**Fig 6D**). It must be noted that the ommatidia induced throughout the retina of LGMR > *ss* were not real **y** ommatidia (shown in green) as they expressed Rh4 in all PRs. However, as *ss* seemed to be specifically expressed in **y** R7 cells under wildtype conditions (see above), it was concluded that *ss* is necessary as well as sufficient to induce the **y** fate.

Due to the rough eye phenotype described for LGMR > *ss* flies, the possibility remained that some PRs escaped an analysis of Rh expression due to
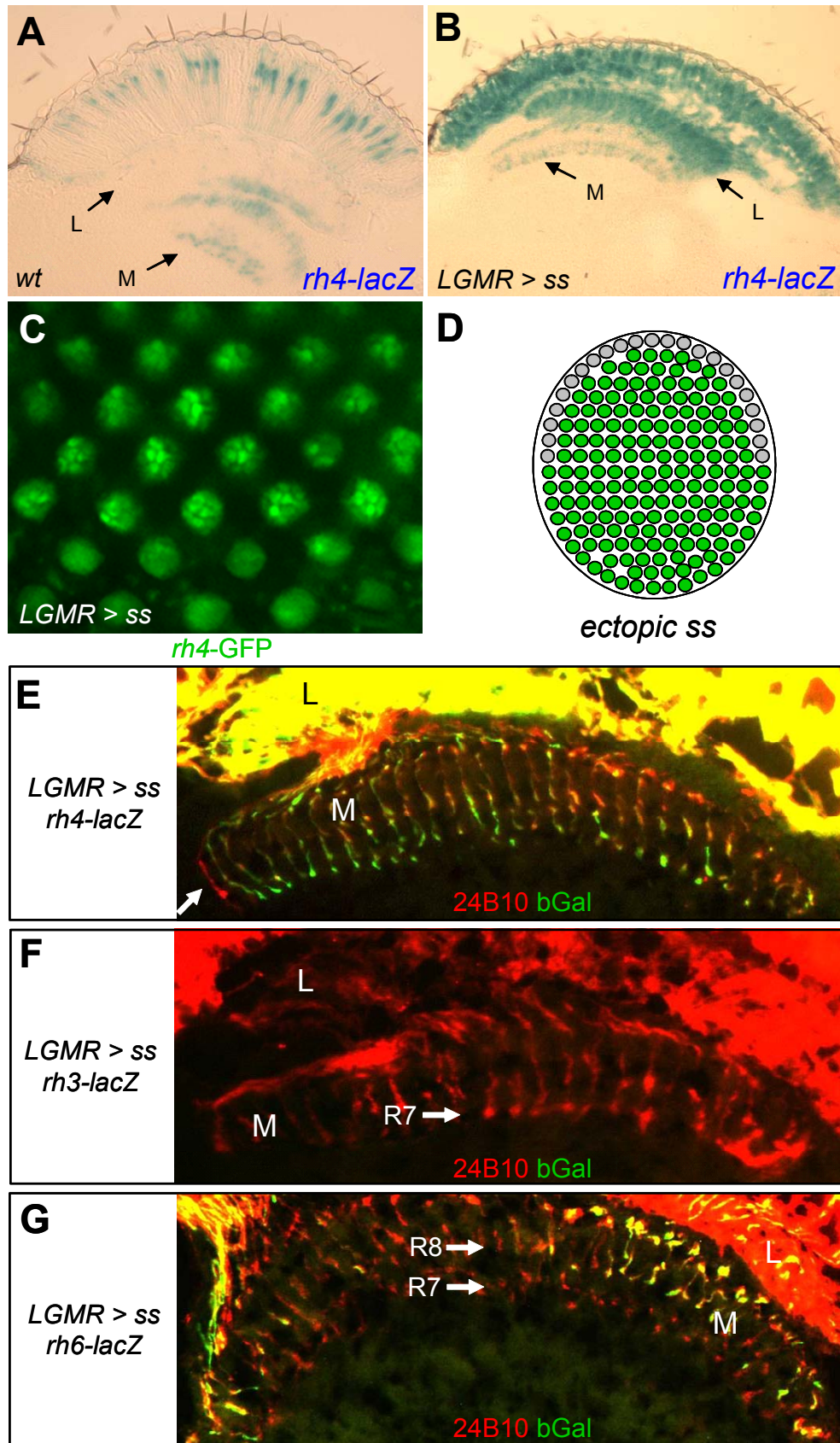
Fig III.3.6. *spineless* is sufficient to induce the yellow R7 fate

(A)+(B) Ectopic Ss induced *rh4* expression in all PRs: Expression of the reporter construct *rh4*-lacZ visualized by X-Gal stainaing on frozen sections through adult eyes from wildtype flies. βGal expression was detected exclusively in the **y** subtype of R7 cells, projecting axons to the medulla (M). (B) Frozen sections through adult eyes from flies over-expressing *ss* under GMR-GAL4 control (LGMR > *ss*) manifested a dramatic expansion of *rh4*-lacZ expression into all PRs, with rhabdomeres spanning the entire retina and axon projections to both the lamina (L) and medulla (M).

(C) All rhabdomeres express Rh4 in the ss gain-of-function: Corneal neutralization (water immersion microscopy) of living LGMR > *ss* flies carrying *rh4*-GFP reporter constructs. Expression of GFP was detected in all PRs, suggesting that rh4 ws expressed in all PRs in every ommatidium.

(D) Schematic representation of the *ss* gain-of-function phenotype: All ommatidia throughout the retina had chosen the **y**R7-like, Rh4-expressing fate (green). However, this situation was unusual as outer PRs also expressed *rh4*. Furthermore, the fate of DRA omatidia (grey) in this background had to be determined.

(E) ss induced *rh4* expression in all PRs, except in the DRA: Frozen sections through adult heads from LGMR > *ss* flies also carrying the opsin reporter *rh4*-lacZ double labeled with antibodies against βGal (green) and the PR-specific cell-surface marker 24B10 (red). Expression of *rh4*-lacZ was expanded into all PRs, with projections to both the lamina (L) and the medulla (M). However, inner PRs in the DRA, projecting axons to the dorsal-most medulla (white arrow) did not express *rh4*.

(F) Repression of *rh3* expression by *ss*: Frozen sections through adult heads from LGMR > *ss* flies also carrying the opsin reporter *rh3*-lacZ double labeled with antibodies against βGal (green) and 24B10 (red). Expression of *rh3*-lacZ was completely lost in flies ectopically expressing *ss*, including in the DRA.

(G) *ss* does not repress *rh6* expression: Frozen sections through adult heads from LGMR > *ss* flies also carrying the opsin reporter *rh6*-lacZ double labeled with antibodies against βGal (green) and 24B10 (red). Expression of *rh6*-lacZ was specifically detected in a subset of R8 cells, and was therefore unaffected by ectopic expression of *ss*.

the collapse of their opsin-baring rhabdomeres. An alternative stategy was therefore chosen to confirm the *ss* gain-of-function results. The *rh4*-lacZ reporter construct was introduced into the LGMR > *ss* background and frozen sections through adult heads were stained with antibodies against the PR-specific cell-surface antigen 24B10 (Chaoptin; (Van Vactor et al., 1988) as well as βGal (**Fig 6E**). All PR axons (labeled in red) were co-labeling with βGal (shown in green), indicating that indeed all PRs, outer PRs projecting to the lamina (L) as well as inner PRs projecting to the medulla (M), expressed *rh4* in this mutant situation. Interestingly, a very small population of inner PRs at the dorsal rim of the eye did not express *rh4*-lacZ (white arrow). *ss* is thus sufficient to induce *rh4* expression in all PRs, except in DRA inner PRs - possibly due to an antagonistic effect of high *wg* signaling levels and dorsal-specific *IRO-C* genes, in response to which the DRA inner PRs are specified (Tomlinson, 2003; Wernet and Desplan, 2004).

Using the same technique, *rh3*-lacZ expression was visualized in the optic lobes of adult *ss* gain-of-function flies (**Fig 6F**). Double-labeling of βGal (shown in green) and 24B10 (shown in red) confirmed the absolute loss of *rh3* expression in all R7 cells (white arrow) that had been observed before in whole mounted retinas. Finally, *rh5*-lacZ and *rh6*-lacZ expression (**Fig 6G**) were assessed using the same technique. While *rh5*-lacZ expression was lost in LGMR > *ss* retinas (not shown), *rh6*-lacZ expression was detectable. A subset of R8 axons (upper

arrow) co-expressed βGal (shown in green) and 24B10 (shown in red), indicating that these R8 cells had to be co-expressing *rh4* and *rh6*. Therefore, gain of *ss* (and *rh4*) does not simultaneously exclude all other inner PR opsins.

It was concluded from these experiments that expression of *ss* in developing PRs was sufficient to induce Rh4 expression as well as to repress Rh3. Interestingly, DRA ommatidia were immune to the activating effect of *ss* and the **y** R8 opsin *rh6* was not repressed by *ss*.

3.7. Spineless does not depend on *spalt*

The spalt gene complex is required for the specification of inner PRs. In the absence of *sal*, PRs are tranformed into outer PRs, both morphologically as well as molecularly (gain of *rh1* expression; (Mollereau et al., 2001). Furthermore, the crucial differentiation markers of R7 (Pros) and R8 (Sens) are also lost in the absence of *sal*. It was shown before that the DRA marker Hth is lost in *sal* (-/-) clones, and that only those PRs that have previously committed to the inner PR fate gain Hth expression at the dorsal rim. Furthermore, only the inner PRs are competent to execute the developmental program imposed by Hth when ectopically expressed. It was shown that Spineless is capable of inducing rh4 expression (and possibly the true **y**R7 cell fate) in any developing PR, when mis-expressed there. This suggested that prior commitment to the inner PR fate by *sal* was not necessary for *ss* function. This hypothesis was therefore tested in more detail.

First, pupal retinas (48 hrs APF) were dissected from flies driving expression of lacZ:NLS under the control of ss_{eye}-GAL4 (ss_{eye} > lacZ:NLS) and then triple labeled using antibodies against βGal, Sal and ElaV (**Fig 7A**). Strong ss expression (shown in red) was detected in a subset of R7 cells, as described before. More importantly, *ss*-positive cells always co-expressed Sal (shown in green). This situation was therefore similar to the DRA, where Hth always co-expressed Sal. To further demonstrate the close relationship between ss and sal, expression of ss_{eye}-GAL4 was visualized on pupal retinas from sev mutants (Fig B). Triple staining of these *sev* + ss_{eye} > lacZ:NLS pupal retinas with antibodies

against βGal, Sal and ElaV revealed a complete loss of ss expression (shown in red), while expression of Sal (shown in green) persisted in R8 cells. It was therefore concluded that *ss* always co-localizes with the inner PR marker Sal.
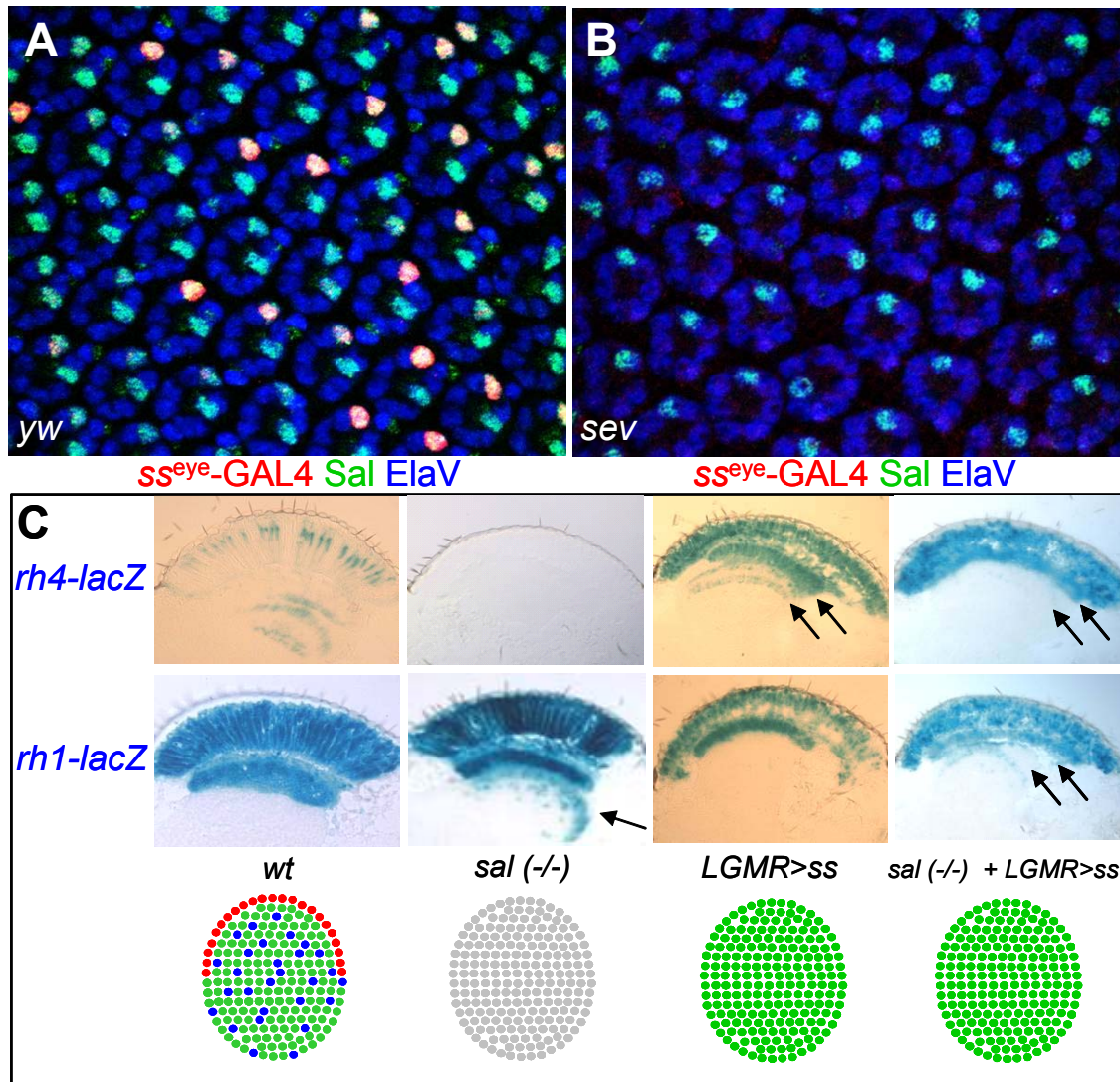

Fig III.3.7 Spineless does not depend on *spalt*
(A) A subset of Spalt-positive cells express ss: Pupal retina (48 hrs APF) dissected from flies driving lacZ:NLS under ss_{eye}-GAL control (ss_{eye} > lacZ:NLS) triple labeled using antibodies against βGal (red), the inner PR marker Spalt (green) and ElaV (blue). A subset of Sal-positive cells was found co-expressing ss.
(B) Co-expression of Sal and *ss* is lost in *sev* mutants: Pupal retina dissected from ss_{eye} > lacZ:NLS flies additionally carrying the *sev* mutation. Triple labeling with antibodies against βGal (red), Sal (green) and ElaV (blue) revealed a complete loss of *ss* expression.
(C) *ss* and *sal*: Expression of the opsin reporter constructs *rh1*-lacZ and *rh4*-lacZ visualized by X-Gal staining on frozen sections in the wildtype (first column), *sal* mutants (second column), *ss* gain-of-function flies (LGMR > *ss*) and flies ectopically expressing ss in a *sal* (-/-) mutant background (last column).

It was then tested whether Ss was still able to induce **y**R7-like cells when ectopically over-expressed in sal (-/-) omatidia. Flies with whole mutant eyes lacking *sal* function, simultaneously over-expressing *ss* under the control of

GMR-GAL4, were generated using a combination of the ey-flip/FRT/GMR-hid and GAL4/UAS systems (see material and methods). The two different opsin-lacZ reporter constructs *rh1*-lacZ and *rh4*-lacZ were then introduced to assess ommatidial specification (**Fig 7C**). βGal activity was visualized on frozen sections through four different genotypes: wt flies (first column), *sal* (-/-) flies (second column), LGMR > *ss* flies (third column) and *sal* (-/-) + LGMR > *ss flies* (last column*)*, using X-Gal staining (see material and methods). In the wildtype, expression of *rh4*-lacZ was detected exclusively in **y**R7 cells (top left), whereas expression of *rh1*-lacZ was specific to the outer PRs (bottom left). Due to the loss of inner PR identity, *rh4*-lacZ expression was totally lost in *sal* (-/-) mutants, whereas *rh1*-lacZ expression was expanded into all PRs, as seen by staining of axonal projections to both layers of the optic lobe (black arrow). As previously described, *rh4*-lacZ expression was expanded into all PRs in LGMR > *ss* flies. Expression of *rh1*-lacZ, however, was unaffected. Finally, flies lacking *sal* function over-expressing *ss* in all PRs phenocopied the *ss* gain-of-function phenotype: expression of *rh4*-lacZ was expanded into all PRs (projections of βGal-positive fibers are marked with black arrows) while *rh1*-lacZ expression was unaffected. It was therefore concluded that ss can induce *rh4* expression even in the absence of *sal*, which is consistent with the strong *rh4*-inducing of *ss* in wildtype outer PRs.

Therefore, specification of inner PRs by *sal* is not absolutely required for *ss* to unfold its transcriptional program, when over-expressed. Specification of color ommatidia therefore follows a strategy which is different from the specification of DRA ommatidia by Hth. It remains likely, however, that *ss* expression is lost in *sal* (-/-) tissue, as indicated by the total loss of *rh4* expression in *sal* mutant eyes. It appears that, in this case, *ss* activity would be regulated exclusively on a transcriptional level downstream of *sal*.

3.8. Spineless over-expression does not alter photoreceptor cell fates

The gene *spineless* is necessary as well as sufficient to induce the yellow R7 cell fate. Its expression pattern suggests that this cell fate decision occurs

rather late, during pupal development. Basic cell fate determination steps (specification of outer versus inner PRs, R7 vs R8 and DRA) occur normally in *ss* mutants, supporting this model. It was tested whether basic cell fate determination steps occur normally in flies over-expressing *ss*.

To test whether specification of outer and inner PRs proceeds normally in *ss* gain-of-function flies (LGMR > *ss*), the genes *spalt* and *seven-up* were chosen as markers (**Fig 8A**). The *spalt* complex (*sal*) is necessary for the maturation of inner PRs R7 and R8, where it is specifically expressed (shown in red). The gene *seven-up* (*svp*) is expressed in outer PRs R1, R3, R4, and R6 (shown in green) where it is indispensable for establishing the outer PR cell fate by repressing development into R7 cells. As a control, pupal retinas (48 hrs APF) were dissected from wildtype flies and triple labeled with antibodies against Sal, *svp*-lacZ and the neuronal marker ElaV (**Fig 8B**). As *svp* expression in R1 and R6 is very weak at this developmental stage (M. Mlodzik, personal communication), two *svp*-positive cells and two Sal-positive cells were counted per ommatidium. The same staining was performed on pupal retinas from LGMR > *ss* flies (**Fig 8C**). Although the retinal morphology was somewhat disturbed due to the over-expression of ss using such a strong driver, two *svp*-positive cells as well as two *sal*-positive cells per ommatidium could clearly be identified. It was therefore concluded that induction of rh4 expression by ss does not result from the induction of extra inner PRs.

Specification of R7 cells and R8 cells was tested using antibodies against the R7 marker Prospero (Pros) and against Senseless (Sens), which is specific to R8 cells (**Fig 8D;** (Frankfort et al., 2001; Kauffmann et al., 1996). Using Anti-Pros, Anti-Sal and Anti-ElaV on pupal retinas (48hrs APF) from wildtype flies, a stereotypical pattern was obtained, with one Sens-positive PR per ommatidium being separated from the Pros-positive cells by one outer PR, R1 (**Fig 8E**). The same pattern was observed in retinas dissected from LGMR > *ss* flies (**Fig 8F**), although a considerable number of ommatidia (white arrows) consisted of only seven cells, missing the R8 cell. This effect was due to the toxicity of GAL4 and has previously been described. It was
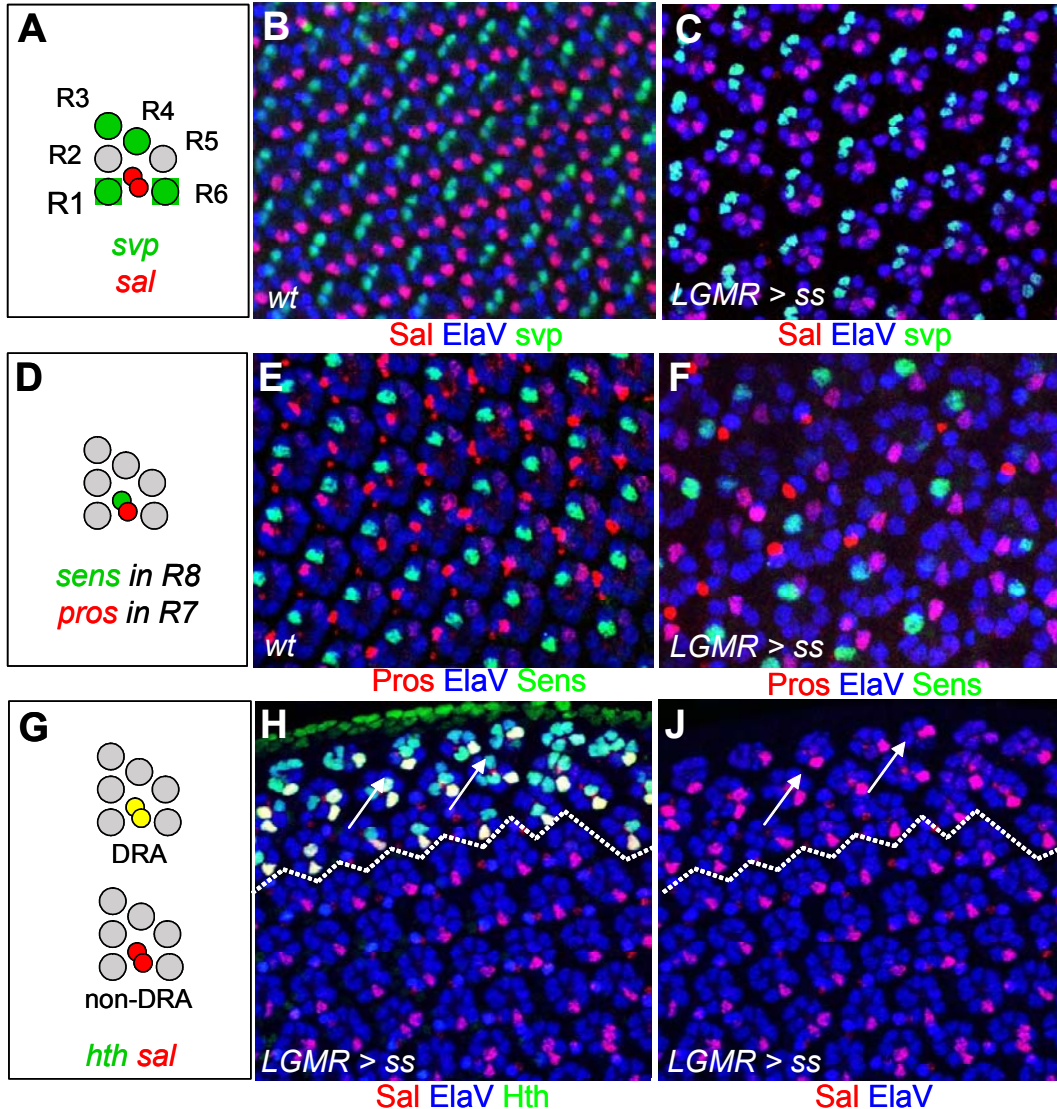
Fig III.3.8 Spineless over-expression does not alter photoreceptor cell fates

(A)-(C) Ectopic *ss* does not affect inner vs outer PR specification: Expression of the genes *spalt* (*sal*) and *seven up* (*svp*) was assed in wildtype flies as well as flies over-expressing *ss* under GMR-GAL4 control (LGMR > *ss*). While Sal was specifically expressed in inner PRs R7 and R8 (red), *svp* was specific to a subset of outer PRs (R1&R6 weak; R3&R4 strong, shown in green). (B) Pupal retina (48 hrs APF) dissected from wildtype flies carrying a lacZ enhancer trap In svp (svp-lacZ) and triple labeled using antibodies against βGal (green), Sal (red) and ElaV (blue). Two Sal-positive cells and two cells with strong *svp*-lacZ expression were detectable in each wildtype ommatidium. (C) Pupal retina dissected from LGMR > *ss* flies also carrying the svp-lacZ enhancer trap triple labeled using antibodies against βGal (green), Sal (red) and ElaV (blue). Although PR morphology was affected, expression of *Sal* and *svp* was not altered.

(D)-(F) Ectopic *ss* does not affect specification of R7 and R8: Expression of the genes *prospero* (*pros*) and *senseless* (*sens*) was assed in wildtype and LGMR > *ss* flies. While Pros was specifically expressed in R7 cells (red), Sens was specific to the R8 cells (green). (B) Pupal retina dissected from wildtype flies and triple labeled using antibodies against Sens (green), Pros (red) and ElaV (blue). One Sens-positive cells and one cell expressing Pros were detectable in each ommatidium in the wildtype. (C) Pupal retina dissected from LGMR > *ss* flies triple labeled using antibodies against Sens (green), Pros (red) and ElaV (blue). PR morphology was so affected that several ommatidia lost the R8 cell due to toxicity of GAL4 and/or *ss*. However, expression of Sens and Pros was not altered in most ommatidia.

(G)-(J) Ectopic *ss* does not disrupt specification of DRA ommatidia: Expression of the genes *homothorax* (*hth*) and *spalt* (*sal*) was assed in wildtype and LGMR > *ss* flies. Hth was specifically expressed in inner PRs of the DRA (yellow), while Sal was expressed in all inner PRs (red). (B) Pupal retina dissected from LGMR > *ss* flies triple labeled using antibodies against Hth (green), Sal (red) and ElaV (blue). Expression of Hth was detected in more than two cells per ommatidium in the DRA (dashed line). (C) This induction of Hth was not due to extra inner PRs, as Sal expression was not expanded in these ommatidia (white arrows). Ss therefore had the ability to induce Hth expression in outer PRs of the DRA.

concluded that R7 and R8 cells develop normally in flies over-expressing ss. The gain of *rh4* expression is therefore not due to the induction of extra R7 cells.

Finally, the specification of DRA ommatidia in LGMR > *ss* was assessed, using the gene *hth* as a DRA-specific marker marker (**Fig 8G**). Inner PRs (expressing *sal*, shown in red) also express *hth* in the DRA (shown in green). Interestingly, more than two cells expressing Hth were detected in the DRA of *ss* gain-of-function flies (**Fig 8H**). This was particularly interesting as previous experiments had suggested that *ss* was incapable of acting as an activator in the DRA (see above). The inner PR marker was therefore used to test whether the extra Hth-positive cells were true inner PRs. However, only two Sal-positive cells were always in the DRA of LGMR > *ss* flies (**Fig 8J**). It was therefore concluded that over-expression of *ss* in the DRA (where it is usually not expressed) most likely leads to the direct activation of *hth*, rather than leading to the creation of extra inner PRs in the DRA.

It was concluded from these experiments that induction of the **y**R7 fate by *ss* is a relatively late event during PR development that can be placed downstream of the basic PR specification events, like specification of outer PRs, inner PRs (R7 and R8) as well as DRA. Interestingly, *ss* is able to activate *hth* expression in outer PRs, under the influence of high *wg* signaling.

3.9. Genetic manipulation of pale and yellow ommatidia

Although rare exceptions exist, co-expression of different sensory receptor molecules (opsins, olfactory receptors) within the same cell is prevented by most animals, using special molecular mechanisms (for review: Celik et al., 2004). As ectopic *spineless* very potently activates *rh4* expression, it was tested in more detail, expression of which other opsins was excluded by Rh4. For this purpose, a weak GMR-Gal4 driver leading to variegated expression of GAL4 in subsets of PRs (sGMR-GAL4, see material and methods) was used to randomly over-express *ss.*

The eyes of adult flies over-expressing Ss under the control of sGMR-GAL4 (sGMR > *ss*) were cut into 10 µm frozen sections and double stained with

antibodies against Rh3 and Rh4 (**Fig 9A**). As observed with stronger drivers, expression of Rh4 (shown in cyan) was dramatically expanded. Some Rh3-expressing R7 cells (shown in red) remained, which, however, never seemed to co-express Rh4 (white arrows). To confirm this exclusion of Rh3 and Rh4, whole mounted retinas were dissected from adult flies of the same genotype (sGMR > ss) and stained with antibodies against Rh3 and Rh4 (**Fig 9B**). In these retinas, Rh4 expression was randomly expanded into variable numbers of outer PRs in all ommatidia. It was clearly visible in inner PRs, however, that those ommatidia that had retained Rh3, never co-expressed Rh4 in the same R7 cell (white arrows). It was therefore concluded that in R7 cells, activation of Rh4 expression by Ss always lead to the loss of Rh3 expression.

Over-expression of *ss* using sGMR-GAL4 driver is an efficient way to activate Rh4 in outer PRs. For instance, *sevenless* flies were generated expressing the **y**R7 opsin Rh4 (shown in cyan) in many outer PRs (**Fig 9C**). As these flies had no R7 cells, Rh3 expression remained completely lost, further demonstrating how Ss mis-expression could be used to generate transgenic flies expressing novel combinations of opsin genes. Outer PRs normally express *rh1/ninaE*. As specification of outer PRs is not affected in flies over-expressing *Ss*, it was tested whether gain of Rh4 expression excludes Rh1 expression. Whole mounted retinas from sGMR > ss flies were therefore double stained for Rh1 and Rh4 (**Fig 9D**). In contrast to the exclusion observed between Rh3 and Rh4, expansion of Rh4 expression by *ss* (shown in cyan) in these flies did not affect Rh1 expression (shown in red), leading to many PRs co-expressing the two opsins. Therefore, co-expression of Rh1 and Rh4 is tolerated by *Drosophila* outer PRs.

Another mutant background was used to assess previously described co-expression of *rh4* and *rh6*. In the eye-specific mutant of the gene encoding the transcription factor *orthodenticle* (*otdUVl*; (Vandendries et al., 1996)*,* expression of Rh3 and Rh5 is specifically lost, whereas expression of Rh6 expands into outer PRs (Tahayato et al., 2003). Ss was over-expressed in a otdUVl mutant background, using sGMR-GAL4 (*otdUVl, sGMR > ss).* Double labeling of frozen
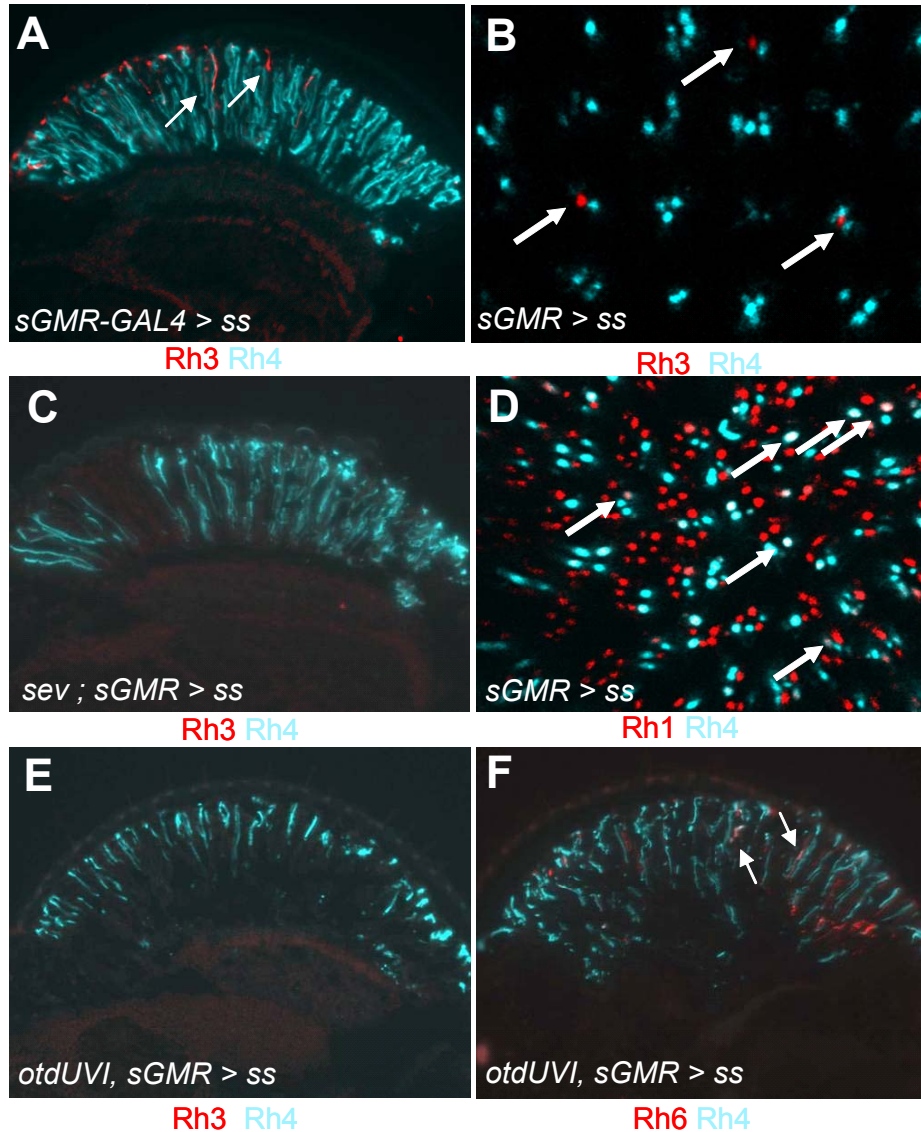
Fig III.3.9 Genetic manipulation of the pale and yellow ommatidia

(A)+(B) Gain of Rh4 expression by *ss* excludes Rh3: Frozen section through adult eyes from flies over-expressing *ss* under the control of a weak GMR-GAL4 transgene (sGMR > *ss*) double labeled with antibodies against Rh3 (red) and Rh4 (cyan). Expression of Rh4 was dramatically expanded through the whole retina while some expression of Rh3 persisted. (B) Whole mounted adult retina from sGMR > *ss* flies double labeled with antibodies against Rh3 (red) and Rh4 (cyan). Due to variegated expression of GMR-GAL4, Rh4 was expressed in a variable number of PRS in each ommatidium. However, co-expression of Rh3 and Rh4 was never observed, suggesting that gain of Rh4 was sufficient to exclude Rh3 expression.

(C) Ss is sufficient to activate Rh4 expression in *sev* mutants: Frozen section through adult eyes from flies over-expressing *ss* under sGMR-GAL4 control in a sev mutant background (sev + sGMR > *ss*). Double labeling with antibodies against Rh3 (red) and Rh4 (cyan) revealed strong expression of Rh4 throughout the retina. Due to the absence of R7 cells, Rh3 expression was limited to the R8 cells of the DRA (arrow).

(D) Gain of Rh4 expression by *ss* does not exclude Rh1: Whole mounted adult retina from sGMR > *ss* flies double labeled with antibodies against Rh1 (red) and Rh4 (cyan). Rh4 was expressed in a variable number of PRs in each ommatidium and co-expression of Rh1 and Rh4 was observed in many cases (arrows). This suggested that ectopic expression of *ss* did not affect *rh1* expression and that expression of Rh4 did not exclude expression of Rh3 within the same PR.

(E)+(F) Gain of Rh4 expression by *ss* does not exclude Rh6 in *otdUVI* mutants: Frozen section through adult eyes from flies over-expressing *ss* under sGMR-GAL4 control in a otdUVI mutant background (*otdUVI* + sGMR > *ss*). Double labeling with antibodies against Rh3 (red) and Rh4 (cyan) revealed a strong activation of Rh4 expression while Rh3 was completely lost. (F) Frozen sections through adult *otdUVI* + sGMR > *ss* eyes double labeled with antibodies against Rh4 (cyan) and Rh6 (red). Co-expression of Rh4 and Rh6 was observed in some cases (arrows) confirming that expression of Rh4 did not exclude Rh6 expression within the same PR.

sections through adult heads from these flies (**Fig 9E**) using Anti-Rh3 (shown in red) and Rh4 (shown in cyan) revealed that expansion of Rh4 into outer PRs appeared weaker that in a wildtype flies. It should be noted, however, that this could be due to the degeneration of PR rhabdomeres as observed in *otdUVI* flies, an effect which was possibly worsened by the morphological stress induced by the over-expression of *ss*. Nevertheless, eye morphology in *otdUVI, sGMR > ss* was good enough to assess co-expression of Rh4 and Rh6, by performing antibody stainings on frozen sections (**Fig 9F**). Clear co-expression of Rh4 (shown in cyan) and Rh1 (shown in red) was observed in these flies, confirming that gain of Rh4 did not exclude Rh1.

It was concluded from these experiments, that induction of the yellow R7 fate by *Ss* very efficiently represses **p**-type Rh3 expression, avoiding a situation where Rh3 and Rh4 are co-expressed. In contrast, over-expression of Ss, which was shown not to affect establishment of the outer PR fate, also does not repress its final marker Rh1, resulting in Rh1/Rh4 co-expression. Finally, it was confirmed that no exclusion mechanism seems to exist in *Drosophila* that avoid co-expression of both **y** opsins Rh4 and Rh6.

3.10. Spineless acts in a limited window of time

The expression pattern described for the *spineless* 'eye enhancer' (ss_{eye}-GAL4) suggests that *ss* acts during pupation to specify the yellow subset of R7 cells. Furthermore, the R8 opsin phenotype observed in *ss* mutants is the consequence of the lack of an instructive signal coming from mutant R7 cells. Specific GAL4 drivers with different opsin-based promoters driving GAL4 expression during late PR development were used to examine the time window in which *ss* was able to induce both the choice of **y** identity in R7 cells as well as well as the instruction of R8 cells.

First, *rh1*-GAL4 drivers were used to specifically mis-express *ss* at a later time point in outer PRs **(Fig 10A)**. Expression of this driver begins around 60% pupation and therefore significantly later than both GMR-GAL4 as well as ss_{eye}-GAL4. Frozen sections through adult *rh1 > ss* eyes (10 µm) were double-labeled

136

with antibodies against Rh3 (shown in red) and Rh4 (shown in cyan). Since the *rh1* promoter is specific to outer PRs, expression of both opsins was unaffected in R7 cells as well as in the DRA. However, expansion of Rh4 expression into the outer PRs was observed (white arrows). Therefore, Ss is sufficient to induce *rh4* expression when mis-expressed late in outer PRs. In a similar experiment, *rh3*-GAL4 drivers were used to mis-express *ss* in the pale R7 subtype (**Fig 10B**). Double labeling of Rh3 (red) and (Rh4) revealed co-expression of both R7 opsins in most R7 cells as well as the DRA (white arrows). This was particularly interesting as over-expression of Ss using GMR-GAL4 drivers (whose expression starts over 3 days earlier) always resultes in the choice of Rh4 over Rh3. Late over-expression of Ss in the **p**R7 subtype therefore leads to the co-expression of Rh3 and Rh4.

A different GAL4 driver that is expressed in all R7 cells was used to over-express *ss* late in all R7 cells ([*rh3*+*rh4*]-GAL4, see material and methods). The promoter of this GAL4 driver consists of a fusion of *rh3* and *rh4* promoters. Frozen sections through adult heads of [*rh3*+*rh4*] > *ss* flies were double stained with Anti-Rh3 and Anti-Rh4 (**Fig 10C**). Rh4 expression (shown in cyan) was found to be expanded into apparently all R7 cells as well as the DRA (white arrow), whereas Rh3-expressing R7 cells (shown in red) were not detectable. Co-stainings using antibodies against the R7 marker Prospero and Rh4 were used to assess whether all R7 cells expressed Rh4 (**Fig 10D**). Indeed, no R7 cell marked by the presence nuclear Pros staining (shown in red) was observed to be negative for Rh4 (shown in cyan), suggesting that *ss* had induced the **y** fate in all R7 cells. It was concluded from these experiments that R7 cells could be completely transformed by Ss, when over-expressed late.

The expression of Rh4 in the DRA of [*rh3*+*rh4*] > *ss* flies was particularly interesting as wildtype *Drosophila* always expresses the UV-opsin Rh3 in these cells. Other insect species, however, have been shown to express green- , blue-as well as UV-sensitive opsins in their DRAs (for review: Labhart and Meyer, 1999). Expression of Rh4 in the DRA of [*rh3*+*rh4*] > *ss* flies was confirmed by double-labeling frozen sections with an antibody against the DRA inner PR
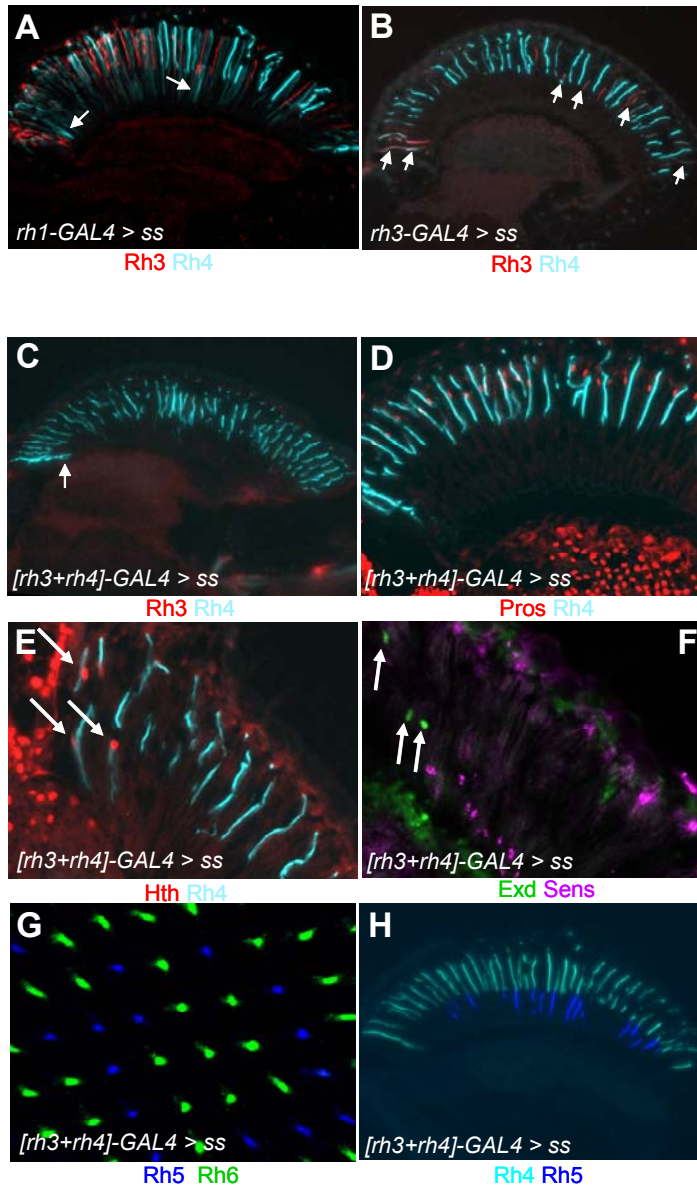
Fig III.3.10 Spineless acts in a limited window of time

(A) Late mis-expression of *ss* in outer PRs: Frozen section through adult eyes from flies over-expressing *ss* under the control of the outer PR-specific opsin driver *rh1*-GAL4 (*rh1 > ss*) double labeled with antibodies against Rh3 (red) and Rh4 (cyan). Expression of Rh4 was expanded into outer PRs spanning the entire retina (arrows), while Rh3 expression was unaffected.

(B) Late mis-expression of *ss* in **p**R7 cells: Frozen section through adult eyes from flies over-expressing *ss* under the control of the subset-specific R7 opsin driver *rh3*-GAL4 (*rh3 > ss*) double labeled with antibodies against Rh3 (red) and Rh4 (cyan). Strong expression of Rh4 was detected in **y**R7 cells. However, weak Rh4 expression was induced in most **p**R7, leading to co-expression with Rh3 (arrows).

(C)-(H) Late mis-expression of *ss* in all R7 cells: Frozen section through adult eyes from flies over-expressing *ss* under the control of the artificial opsin driver *[rh3+rh4]*-GAL4, expressed in all R7 cells (*[rh3+rh4] > ss*). Double labeling with antibodies against Rh3 (red) and Rh4 (cyan) revealed expansion of Rh4 expression into all R7 cells, while Rh3 expression was completely lost. (D) Double labeling of Rh4 (cyan) and the R7 marker Pros (red) on frozen sections through *[rh3+rh4] > ss* eyes revealed that Rh4 expression had indeed expanded into all R7 cells. (E) DRA inner PRs expressed Rh4 in *[rh3+rh4] > ss*) flies, as visualized by double labeling Rh4 (cyan) and Hth (red) on frozen sections. (F) Expression of *ss* in the DRA did not prevent repression of Sens by Hth/Exd: Double labeling of Exd (green) and Sens (pink) on frozen sections through *[rh3+rh4] > ss* eyes. DRA inner PRs (arrows) never co-expressed Exd and Sens. (G) R8 opsin expression was unaffected by late over-expression of ss in all R7 cells: Whole mounted adult retina from *[rh3+rh4] > s*s flies double labeled with antibodies against Rh5 (blue) and Rh6 (green) revealed no change in R8 opsin expression. Frozen section through adult eyes from *[rh3+rh4] > ss* flies double labeled with Anti-Rh4 (cyan) and Anti-Rh5 (blue) revealed that all Rh5-expressing ommatidia were mis-coupling expression of Rh4 in R7 and Rh5 in R8 (arrows).

marker Hth, whose expression was unaffected in these flies (**Fig 10E**). It was confirmed that, unlike in *rh3* > ss flies, all DRA inner PRs expressed exclusively Rh4 and that Rh3 had been lost due to *ss* over-expression (white arrows). To complete the analysis of inner PR cell fate decisions in the DRA of [*rh3+rh4*] > *ss* flies, frozen sections were stained for the R8 marker Senseless, which is usually excluded from DRA R8 cells, and the other DRA marker Extradenticle (**Fig 10F**). Like in wildtype flies, Sens (shown in pink) did not co-stain with Exd (shown in green) in this mutant situation. It was concluded that, despite induction of Rh4 and repression of Rh3 by *ss*, the presence of Hth/Exd still provides some crucial aspects of DRA identity.

Finally, R8 opsin expression in [*rh3+rh4*] > *ss* flies was visualized in whole mounted adult retinas, using antibodies against Rh5 and Rh6 (**Fig 10G**). Unlike in R7 cells, both pale and yellow subtypes seemed to be properly specified in R8 cells, as expression of both Rh5 (shown in blue) and Rh6 (shown in green) were indistinguishable from the wildtype. This result suggested that a large number of ommatidia had to manifest unusually coupled expression of Rh4 in R7 and Rh5 in R8 cells, a situation that never occurs in wildtype flies. Adult frozen sections from [*rh3+rh4*] > *ss* flies were therefore stained with antibodies against Rh4 and Rh5 (**Fig 10H**). As the previous result suggested, every R8 cell expressing Rh5 (shown in blue) was located underneath an R7 cell expressing Rh4 (shown in cyan), leading to Rh4/Rh5 expressing ommatidia. Therefore, late over-expression of ss in all R7 cells using [*rh3+rh4*]-GAL4 is sufficient to induce the **y**R7 fate in all GAL4-expressing cells, but although all R7 cells exclusively expressed Rh4, instruction of Rh6 expression in the underlying R8 cells was not successful. This indicates that the instruction of **p**R8 cells to express Rh5 had already occurred before the onset of [*rh3+rh4*]-GAL4 expression.

It was concluded from these mis-expression experiments using late opsin promoter-derived GAL4 drivers that R7 cells, as well as DRA inner PRs, could be transformed by Ss into cells exclusively expressing Rh4. However, this transformation was successful only when the *rh4* promoter-portion was present in the GAL4 driver. Interestingly, newly induced **y**-like R7 cells were not able to

instruct the formation of yellow R8 cells in the same ommatidium. This suggested that while the **p** / **y** choice in R7 is reversible, instruction of R8 cells could not be reverted by forcing Ss expression late in R7 cells.

3.11. The PAS HLH dimerization partner Tango is not required in the eye

All *Drosophila* PAS HLH proteins have been shown to require the hetero-dimerization partner Tango (Tgo) during a multitude of developmental processes (Sonnenfeld et al., 1997; Ward et al., 1998). Tgo expression is pleiotropic and the presence of another PAS domain protein like Ss was required for Tgo translocation into the nucleus. The Ss/Tgo system of transcriptional regulation is therefore strikingly similar to the one described for Exd and Hth, whose role in developing PRs was described above (Pai et al., 1998; Rieckhof et al., 1997). Hth depends on its co-factor Exd to correctly specify the ommatidial subtype located in the DRA (Wernet et al., 2003). It was therefore tested whether Tgo was required for the induction of the **y** R7 fate by Ss.

Strong hypomorphic alleles of *tgo* are homozygous lethal. Heterozygous flies with whole mutant eyes lacking *tgo* function were therefore created using the *ey*-flip/FRT/GMR-*hid* technique (Stowers and Schwarz, 1999) and the two hypomorphic mutations tgo^1 and tgo^5. These mutants manisfest very strong phenotypes in different model systems and are therefore classified as 'almost null' (S. Crews, personal communication). Flies with *tgo* (-/-) mutant eyes exhibited a strong aristapedia phenotype, due to the actificty of *ey*-flip in the antennal part of the eye imaginal disc. The eyes, however, developed normally in these mutants as described earlier for *ss* (-/-) flies. Frozen sections through adult heads from tgo^1 mutants were then double labeled with antibodies against Rh3 and Rh4 (**Fig 11A**). R7 opsin expression was indistinguishable from the wildtype, as Rh4 expression (shown in cyan) was found in a subset of R7 cells, whereas the remaining R7 and DRA R8 expressed Rh3 (shown in red). tgo^1 mutants did therefore not phenocopy $ss^{D115.7}$, suggesting that *tgo* is not required for *ss* function. This hypothesis was confirmed by double labeling frozen sections through adult eyes from tgo^5 (-/-) flies using antibodies against Rh3 and Rh4 (**Fig**
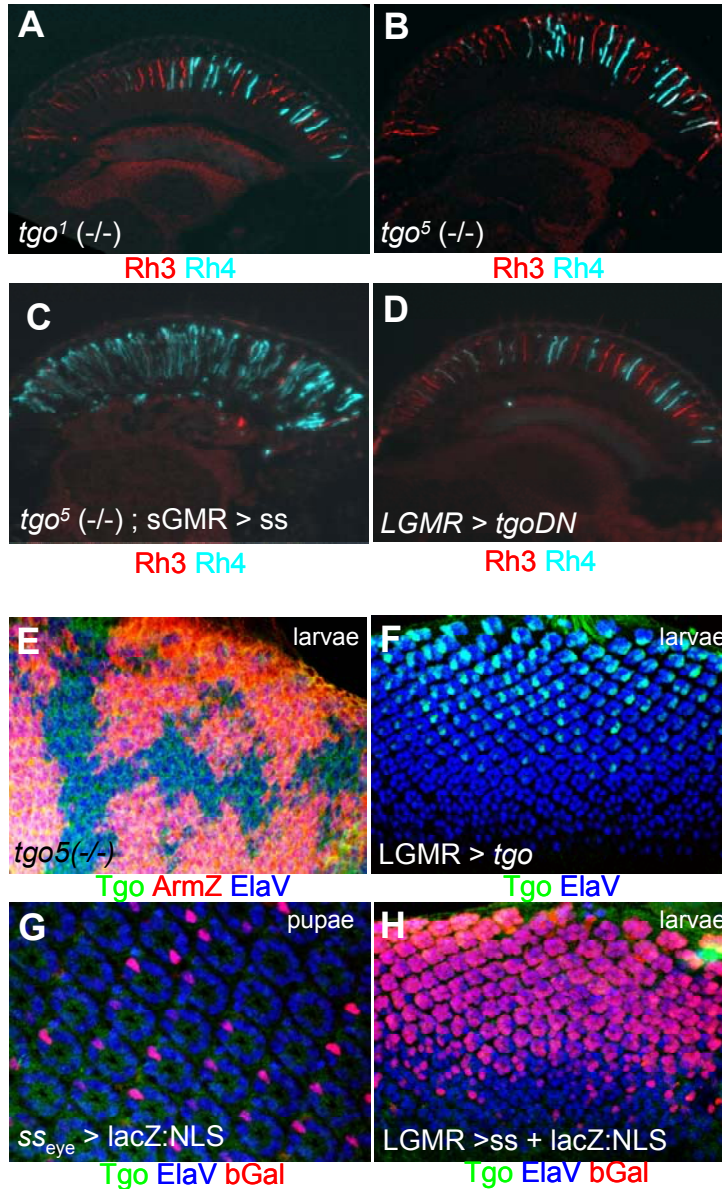
Fig III.3.11 The PAS HLH dimerization partner Tango is not required in the eye

(A)+(B) Opsin expression is normal in *tango* mutants: Frozen section through whole mutant adult eyes lacking the *ss* dimerization partner tango (*tgo¹*), double labeled with antibodies against Rh3 (red) and Rh4 (cyan). Expression of both R7 opsins was identical to wildtype flies. (B) Frozen section through *tgo⁵* (-/-) whole mutant eyes double labeled for Rh3 (red) and Rh4 (cyan) also revealed no change in opsin expression.

(C) *ss* induces *rh4* expression in *tango* mutants: Frozen section through adult eyes from flies over-expressing ss under GMR-GAL4 control in a *tgo⁵* (-/-) mutant background. Double labeling with antibodies against Rh3 (red) and Rh4 (cyan) revealed a dramatic expansion of Rh4 expression throughout the retina.

(D) Dominant negative *tango* has no effect on ommatidial subtype specification: Frozen section through adult eyes from flies over-expressing dominant negative tango (*tgoᴰᴺ*) under GMR-GAL4 control (LGMR > *tgoᴰᴺ*) double labeled with antibodies against Rh3 (red) and Rh4 (cyan). No change in Rh3 and Rh4 expression was detectable.

(E)+(F) Expression of Ss in PRs does not localize Tango into the nucleus: Pupal retina (48 hrs APF) dissected from flies expressing lacZ:NLS under *ss*$_{eye}$-GAL4 control (*ss*$_{eye}$ > lacZ:NLS) triple labeled with antibodies against βGal (red), Tango (green) and ElaV (blue). Nuclear localization of Tango was not detectable in **y**R7 cells expressing *ss*$_{eye}$-GAL4. (F) Similarly, Tgo (green) was not localized to the PR nuclei in eye imaginal discs of LGMR > *ss*) third instar larvae (ss was labeled by βGal in red.

(G)+(H) Characterization of *tango* mutants and Anti-Tango: Eye imaginal discs dissected from wandering third instar larvae inducing mitotic *tgo⁵* (-/-) clones marked by the absence of Arm-lacZ. Triple labeling with antibodies against βGal (red), Tango (green) and ElaV (blue) revealed no change in Tgo expression within the clone, suggesting that *tgo⁵* is not a null allele or that Anti-Tgo staining is unspecific. (H) Strong Anti-Tgo staining was detected in larval developing PRs in LGMR > *tgo* flies, suggest8ing that the Anti-Tgo antibody is specific.

11B). Rh4 expression (shown in cyan) as well as Rh3 (shown in red) also persisted in these mutant eyes. Based on this genetic data, it was therefore concluded that *tgo* function is not required for *ss* function in developing PRs.

To further test whether *tgo* was required for the development of **y** R7 cells, *ss* was over-expressed in a *tgo* mutant background. Frozen sections through adult eyes from flies with whole mutant *tgo⁵* (-/-) eyes over-expressing Ss under the control of GMR-GAL4 were then double labeled for Rh3 and Rh4 (**Fig 11C**). Rh4 expression (shown in cyan) was expanded throughout the whole retina in these *tgo⁵* (-/-) + GMR > *ss* flies, whereas few Rh3-expressing R7 cells remained. This phenotype was identical to the gain-of-function previously described for *ss* (sGMR > *ss*). It was therefore concluded that *tgo* function is not required for Ss to transform PRs into Rh4-expressing **y**R7 cells.

As the possibility remained that residual *tgo* activity persisted in *tgo¹* and *tgo⁵* (-/-) mutant eyes, a different approach was chosen to abolish Tgo function in the developing eye. A dominant negative form of Tgo, in which a 13 amino acid basic region (SRENHCEIERRRR) was replaced by the sequence GIL, was ectopically expressed using GMR-GAL4 (LGMR > *tgo*^DN; (Ohshiro and Saigo, 1997). This truncated from of Tgo has been shown to act as a dominant negative in the developing trachea of *Drosophila* larvae. Frozen sections though adult eyes from LGMR > *tgo*^DN flies were double labeled using antibodies against Rh3 and Rh4 (**Fig 11D**). Rh4 expression (shown in cyan), as well as Rh3 (shown in red) were unaffected, confirming previous observations.

So far, the activity of Ss and its other *Drosophila* homologues has been shown to be completely dependent on Tgo. Due to the absence of an opsin phenotype in *tgo⁵* mutant eyes, this strong hypomorphic allele was tested for persisting Tgo expression. Third instar eye imaginal discs from flies inducing clones of tgo⁵ (-/-) homozygous tissue, labeled by the absence of Arm-lacZ, were triple labeled for βGal, Tgo and ElaV (**Fig 11E**). Diffuse cytoplasmic Anti-Tgo staining was detectable throughout the eye disc, within as well as outside the mutant clones. This is consistent with previous reports that Tgo expression is pleiotropic. It appears therefore, *tgo⁵* is not a null-allele. However, the possibility

remained that Tgo is not expressed at all in the developing visual system and that the detected cytoplasmic staining is unspecific. Eye imaginal discs from flies over-expressing Tgo under the control of GMR-GAL4 (LGMR > *tgo*) were therefore double labeled with antibodies against Tgo and ElaV (**Fig 11F**). Specific Anti-Tgo staining (shown in green) was detectable in developing PRs, starting several rows posterior to the morphogenetic furrow (MF, runs horizontally at the bottom). An increasing number of PRs per ommatidial cluster expressed Tgo, with growing distance to the MF, as previously described for GMR-GAL4. Interestingly, Tgo seemed to be localized in the nucleus, possibly due to the high level of over-expression. Strong staining was also detected in PR axons, suggesting that Tgo was also expressed in the cytoplasm of developing PRs. Therefore, the Anti-Tgo antibody specifically recognizes its epitope and was used for a more detailed analysis of Tgo expression in the *Drosophila* visual system.

Expression of Ss is necessary for the nuclear translocation of Tgo in different model systems. It was therefore tested whether Tgo localization is nuclear in those pupal R7 cells specifically expressing ss_{eye}-GAL4. Pupal retinas from ss_{eye}-GAL4 > lacZ:NLS flies were triple labeled with antibodies against βGal, Tgo and ElaV (**Fig 11G**). No anti-Tgo signal (green) was detected, while strong *ss* expression (red) was visible in a large subset of R7 cells. It appears therefore that Tgo is not localized to the nucleus of pupal R7 cells. The ability of Ss to localize Tgo into the nucleus of developing PRs was further tested by labeling Tgo expression in eye imaginal discs from flies ectopically expressing Ss under the control of GMR-GAL4 (**Fig 11H**). Again, no Tgo expression (green) was detectable in PRs, while the expression domain of GAL4 was labeled by βGal (shown in red). Therefore, Tgo is not expressed developing *Drosophila* PRs, explaining the absence of an opsin phenotype in *tgo* mutants.

It was therefore concluded from these experiments, that the role of *spineless* in specifying **y** ommatidia does not require *tango*. Nuclear localization of Tango was not detectable in developing PRs. This is particularly surprising as all *Drosophila* PAS HLH proteins have previously been shown to depend on Tgo.

3.12. Antagonism between *spineless* and *homothorax*

The hoeodomain transcription factor Homothorax is sufficient to ectopically induce the DRA subtype when over-expressed in all ommatidia (Wernet et al., 2003). Furthermore, *homothorax* was shown to be specifically expressed in DRA inner PRs and was therefore never found to be co-expressed with **y**R7-specific *spineless*. Ommatidial subtype scecification was therefore assessed in flies co-over-expressing both *hth* and *ss*.

Co-over-expression using GMR-GAL4 drivers (LGMR > *hth* + *ss*) resulted in a relatively severe rough eye phenotype with considerable rhabdomere degeneration (not shown). Ommatidial subtype specification was therefore visualized by introducing inner PR opsin-lacZ reporter constructs and detecting βGal activity on frozen sections through adult eyes, using X-Gal (**Fig 12A**). Four different genotypes were compared: *wt*, LGMR > *ss*, LGMR > *hth* and LGMR > *hth* + *ss*. Both *ss* and *hth* gain-of-function phenotypes were described before: Compared to the wildtype (first column), *rh4*-lacZ expression was dramatically expanded in LGMR > *ss* flies (second column), as concluded from βGal–expressing fibers terminating in both the lamina and medulla (black arrows). *rh3*-lacZ and *rh5*-lacZ were completely lost and *rh6*-lacZ expression persisted. Over-expression of *hth* (LGMR > *hth*) resulted in a very different phenotype (third column), with *rh3*-lacZ expression specifically expanded into all inner PRs projecting to the medulla (black arrow), while expression of all other inner PR opsins (*rh4*-lacZ, *rh5*-lacZ and *rh6*-lacZ) was lost. It was found that the opsin phenotyope in LGMR > *hth* + *ss* flies (fourth column) phenocopied *ss* over-expression: *rh4*-lacZ was expanded into all PRs (black arrows), whereas *rh3*-lacZ and *rh5*-lacZ expression were lost and *rh6*-lacZ persisted. It was therefore concluded that the cell fate change induced by Ss dominated over *hth*-depended DRA-induction, when co-expression of these two proteins was forced in the same PR.

Although Homothorax was present in inner PRs, it was no longer able to repress *rh4* expression when Ss was present. First, frozen sections through adult heads from LGMR > *hth* flies were double labeled for Hth and Rh4 (**Fig 12B**). As
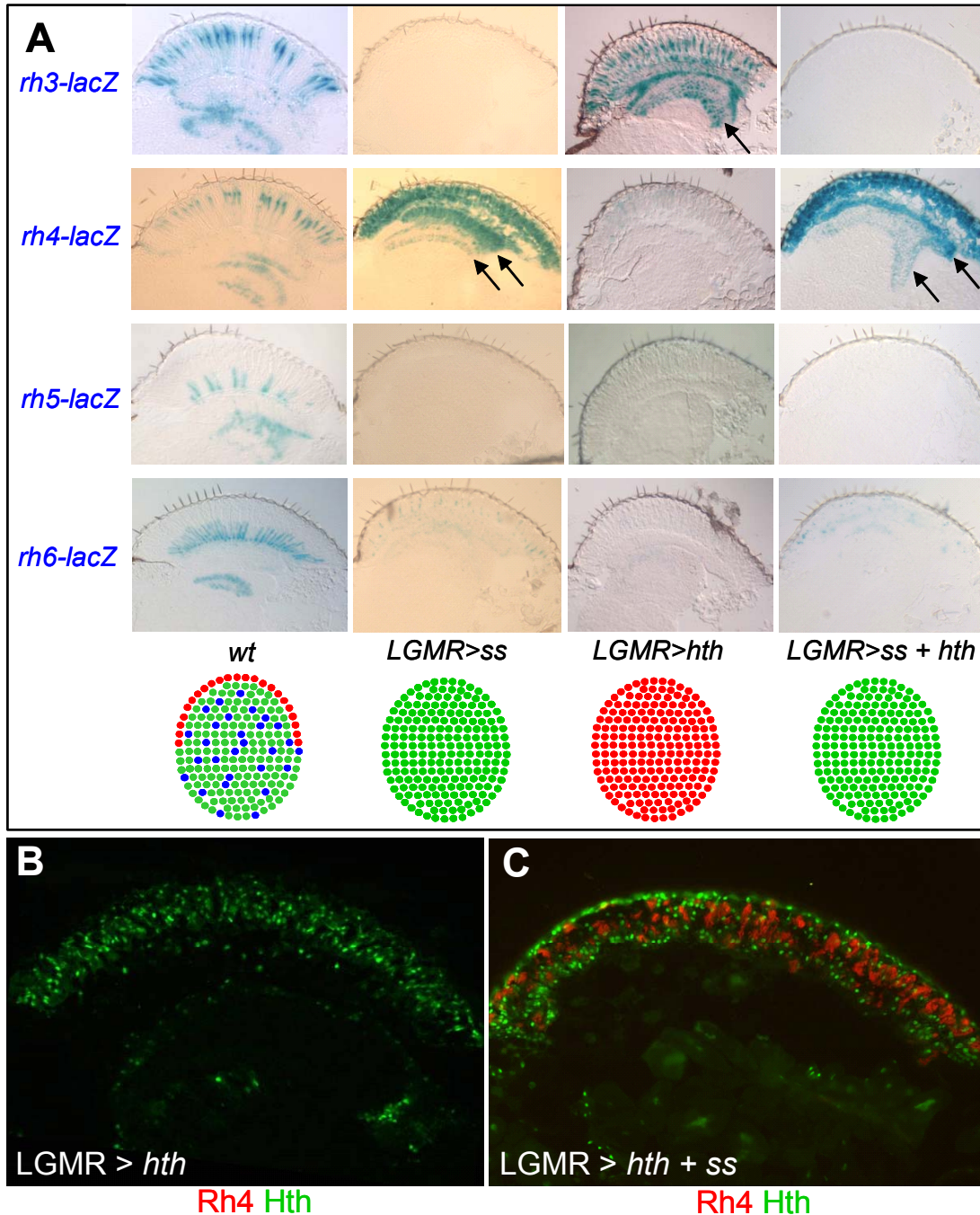
144

Fig III.3.12 Antagonism between *spineless* and *homothorax*

(A) Ectopic Ss neutralizes ectopic Hth: Expression of the opsin reporter constructs *rh3*-lacZ, *rh4*-lacZ, *rh5*-lacZ and *rh6*-lacZ visualized by X-Gal staining on frozen sections in the wildtype (first column), in *ss* gain-of-function flies (second column), in *hth* gain-of-function flies (third column) and flies ectopically expressing both *ss* and *hth* (last column). Over-expression of *ss* lead to the very characteristic expansion of *rh4* expression into all PRs (black arrows), whereas ectopic *hth* resulted in the expression of *rh3* in all inner PRs, as described above. The opsin phenotype of LGMR > *ss* + *hth* flies was identical to the *ss* gain-of-function: *rh4*-lacZ was expressed in all PRs (black arrows), while *rh3* and *rh5* were completely lost and *rh6*-lacZ persisted.

(B)+(C) Co-expression of Ss abolishes repression of Rh4 by Hth: Frozen section through adult heads from LGMR > *hth* flies double labeled with antibodies against Hth (green) and Rh4 (red). As previously described, Rh4 expression was completely repressed by ectopic Hth. (C) Double labeling of frozen sections through adult heads from LGMR > *ss*+ *hth* flies with Anti-Hth (green) and Anti-Rh4 (red) revealed strong co-expression of Hth and Rh4, suggesting that Ss overcame the repressive role of Hth.

145

was reported before, ectopic Hth (shown in green) led to a complete loss of Rh4 expression (shown in red). Co-over-expression of Ss, however, resulted in strong co-expression of these two proteins within the entire retina (**Fig 12C**). The possibility could therefore be excluded, that over-expression of Ss directs degradation of the Hth protein.

It was therefore concluded that cell fate changes induced by Hth and Ss excluded each other, as co-expressin of Rh3 and Rh4 was prevented. Instead Ss-mediated induction of the **y** R7 fate was found to be dominant over Hth function.

3.13. Analysis of the *spineless* 'eye enhancer' using Bioinformatics

Spineless is necessary and sufficient to induce the *rh4*-expressing yellow R7 fate. Furthermore, a 1.6 kb fragment of genomic DNA is sufficient to visualize specific reporter gene expression in a large subset of R7 cells and was therefore called '*spineless* eye enhancer'. The signaling pathways responsible for subset-specific expression of Spineless therefore seemed to converge onto the identified piece of regulatory DNA. The Matinspector software from Genomatix Inc was used for a preliminary bioinformatics analysis to locate potential transcription factor binding sites within the *ss* 'eye enhancer' (Quandt et al., 1995). A more precise analysis was impossible due to the high probability of unspecific hits in such a relatively long sequence. However, four different consensus sites were detected multiple times with high scores (see **table III.3.1**).

Binding sites for Pax6 were obtained twice, STAT (signal transcucers and activators of transcription) binding sites were detected four times, as were dTCF binding sites. Finally, three binding sites for the effector of the Notch (N) pathway, Suppressor of Hairless / *su(H)* were found. These sites were distributed within the *ss* 'eye enhancer' (**Fig 13**). Site-directed mutagenesis of these sites has not been performed yet and the ss eye anhencer sequences from other *Drosophila* species remain to be identified in order to perform a conservation analysis. However, they provide interesting clues for candidate genes approaches.

```
                        PAX6
gaattcttac atttttttaat aattctattg actattctga ctatatcgat gcaataaaac    60

cgaataccta aataactacg ttccacgcgc ttatcccagc ctccaactaa taagtggagc   120

acaaccattg gctaattagg aaaactgttg ggtaagattt gccagtcggg cgtcggctaa   180

ttgcaattaa ttattgctgt aatccatcat acatactcag agccgttttc gagtgtgagt   240

ttttcagttt gggccgactt gccatcatcg tagtcgtctg catggcgacg gcggcggctt   300

ctttttggca acgaaaataa tggaggcgga aaactttgga gggccaaaca cgcgaatgtc   360

gtataagcaa ttgttttttgt cccttaattt gttcttgggc tggttgcttt tataatgcaa   420
                                                          STAT
aatgcaaatt agagcagcca acgagcgaca gctgaaggag aataagcgcc ataaaattct   480

ggcaaagtca tatgggattt gggattgcat catgtaggaa acttggcatg gcaagataag   540
        STAT                  PAX6
aaatgaccgg gaaatgtaca caattcactt agagtacttg taaagtaatt ttaccattaa   600

gtaataaagt ttttaaagaa attcggctat tagtagatga ttcatttaag tacgcatacc   660
                        su(H)
atgattttta atagcaatcg atattcccac gcccgaaatg aaagtacata acgcagcacg   720
                                    TCF
ttaatttttga actatgcgtg tctttcccat agaagttcaa agtttttacg aacttgtgaa   780

aagtgcggac ccgaaatgaa atgttatttta atgttgtgac gtgtacttaa gtccgaaaga   840

gaagcaaaaa gcgaaaaacg caacgaacac cgtcgatgat gaagattaac aattgtgtgc   900

gacaattgtc aactttaatt atttactaat tgtgtctgaa ttatgaagaa ctgtggcggc   960
                                                          STAT
cgcttaattg tcgggtaatt aagcagcaac aacaaacggt tggcttcact tttttcggtt  1020
                        TCF
aaaaaagtga aaaagtcgta ctttacacga cctcaaaggg aaaaagctat gctccgccca  1080

caaagtcgtt gcttttacaa gtgtgagcga gtgagtgagt gagcgaatga aacaacatgg  1140
              su(H)
cgttgttcca gttcccactt tttccaagca ctggaagttg agtggaaccc atccactcac  1200

actcgcactc actcacactc atagaagttg agtggaccaa aacaatgcaa cttcaacgcc  1260
                            TCF
tcgcaaagtg cagacatcgc agaagaatgg aacaaaggta acaattgcaa ttgcacatca  1320
                su(H)
acagcaacaa cagagtgtga gtacctgtgt tccctgttcc ccagttatta attattctag  1380
                                                  TCF
tttggttccc ccacaaatgc tctccgagtg taaacacatt taaccacgtc aaaggtccg  1440
              STAT
gagaacttgg gctattacgg gaatagggga accgaaagct ctgcatcttg ataagaaaat  1500

gccactgcga aacattgggc tcttgctgct taatgcagcg caaattgctg gtgttacctg  1560

gacaaaaacg gggacaatgg gaggggtcac aggataagtg tccacataat aagggacaca  1620

agataccagg atccaaaaat gaatgctgcc aaattcactt taggtgtata ttcttaacaa  1680

ggtctgttga attc                                                    1694
```

Fig III.3.13 Analysis of the *spineless* 'eye enhancer' using Bioinformatics
Bioinformatic analysis of the ~1.6 kb genomic 'eye enhancer' identified of ss: several potential transcription factor binding sites were identified using Genomatic Matinspector software (see table).

site /pathway	number	position	core sim.	Matrix sim.	Sequence
PAX6	2	14-34	0.758	0.785	ttttaa**TAAttctATTG**a
		557-577	0.578	0.800	gtactc**TAAgtgaATTG**
STAT	4	472-490	0.769	0.872	taaaa**TTctgGCAA**agt
		540-558	1.000	0.765	tac**atTTCCcGGTCat**tt
		1011-1025	1.000	0.825	tt**tttaagcGAAA**aa
		1450-1468	1.000	0.986	ggcta**ttacgGGAA**tag
TCF / wg	4	753-763	0.750	0.807	**ACTTtgaactt**
		1049-1059	1.000	0.752	**CCTTtgaggtc**
		1288-1298	1.000	0.746	**CCTTtgttcca**
		1425-1435	1.000	0.752	**CCTTtgacgtg**
Su(H) / Notch	3	681-693	1.000	0.895	ggc**GTGGgaa**tat
		1149-1161	1.000	0.917	aaa**GTGGgaa**ctg
		1334-1346	0.891	0.825	agt**GTGAgta**cct

Table III.3 Putative transcription factor binding sites in the *ss* eye enhancer
The ~1.6 kb *ss* eye enhancer was analyzed using the Matinspector software fomr Genomatix. Four different binding sites were detetced multiple times: Binding sites for Drosophila PAX6 (*eyless/twin of eyless*) in blue, binding sites for 'signal transducers and activators of transcription' (STAT), effectors of the JAK/STAT pathway (in yellow), binding sites for dTCF (*pangolin*), the transcriptional effector of wg signaling and finally, three putative binding sites for suprressor of Hairless / su(H), a transcriptional effector of the N pathway (in green). Core sim = core similarity; Matrix sim. = Matrix similarity

All six *Drosophila* opsin genes have previously been shown to contain highly conserved PAX6 binding sites within their basic promoters (Papatsenko et al., 2001; for review: Cook and Desplan, 2001). These sequences were shown to be crucial for Rhodopsin expression in the adult eye and site-directed mutation of these sites always lead to a loss of reporter gene expression. Pax6 sites were therefore expected in the *ss* eye enhancer, as *ss* expressed late in PR development. However, functionality of these sites was proven in the following experiments.

It was concluded from these experiments that bioinformatics tools could be used to analyze the *ss* eye enhancer. However, the results obtained remain purely speculative for now. A possible role of JAK/STAT, Wingless and Notch signaling were therefore tested using fly genetics.

3.14. JAK/STAT signaling and ommatidial subtype specification

Bioinformatic analysis of the *ss* eye enhancer using Matinspector revealed four potential binding sites for STATs (signal transducers and activators of transcription; for review: Hou et al., 2002) within the ~1.6 kb sequence. This raised the possiblity that the JAK/STAT pathway could be regulating *ss* expression. STAT proteins have previously been shown to activate transcription in vertebrates as well as in invertebrates, after phosphorylation-induced nuclear translocation in response to cytokine receptor activation. In *Drosophila*, one such receptor exists (*domeless;* (Brown et al., 2001), and its ligand is Unpaired (*outsretched, os;* Harrison et al., 1998). Sequencing of the *Drosophila* genome further revealed the presence of only one STAT gene (*stat92E;* Yan et al., 1996), thereby dramatically reducing the problem of redundancy reported in vertebrate model systems. A possible role for JAK/STAT signaling in ommatidial subtype specification was tested by over-expressing Unpaired as well as analyzing Upd / *os* and *stat92E* mutants.

Expression of *Drosophila* STAT is negatively regulated by the JAK/STAT pathway (Zeidler et al., 1999). STAT-lacZ expression was reported to be absent from the equatorial region of the eye imaginal disc (**Fig 14A**), where JAK/STAT signaling is required for the establishment of ommatidial polarity. Expression of STAT-lacZ was visualized in the adult eye by double labeling frozen sections with antibodies against βGal and ElaV (**Fig 14B**). Weak expression of STAT-lacZ (shown in green) was detected in all PRs throughout the eye, but Anti-βGal staining was particularly strong in the inner PRs of the DRA (white arrows). This suggested a possible role for JAK/STAT signaling in DRA specification, possibly by repressing *ss* expression in the inner PRs. As *stat92E* mutants are homozygous lethal, whole mutant eyes were created in otherwise heterozygous animals, using the *ey*-flip/FRT/GMR-*hid* technique (Stowers and Schwarz, 1999) and the hypomorphic allele s*tat92E*[06346]. These stat92E (-/-) mutant flies manifested a rough eye phenotype and were further analyzed by double labeling frozen sections using antibodies against Rh3 and Rh4 (**Fig 14C**). Expression of Rh3 (shown in red) and Rh4 (shown in cyan) were found to be indistinguishable
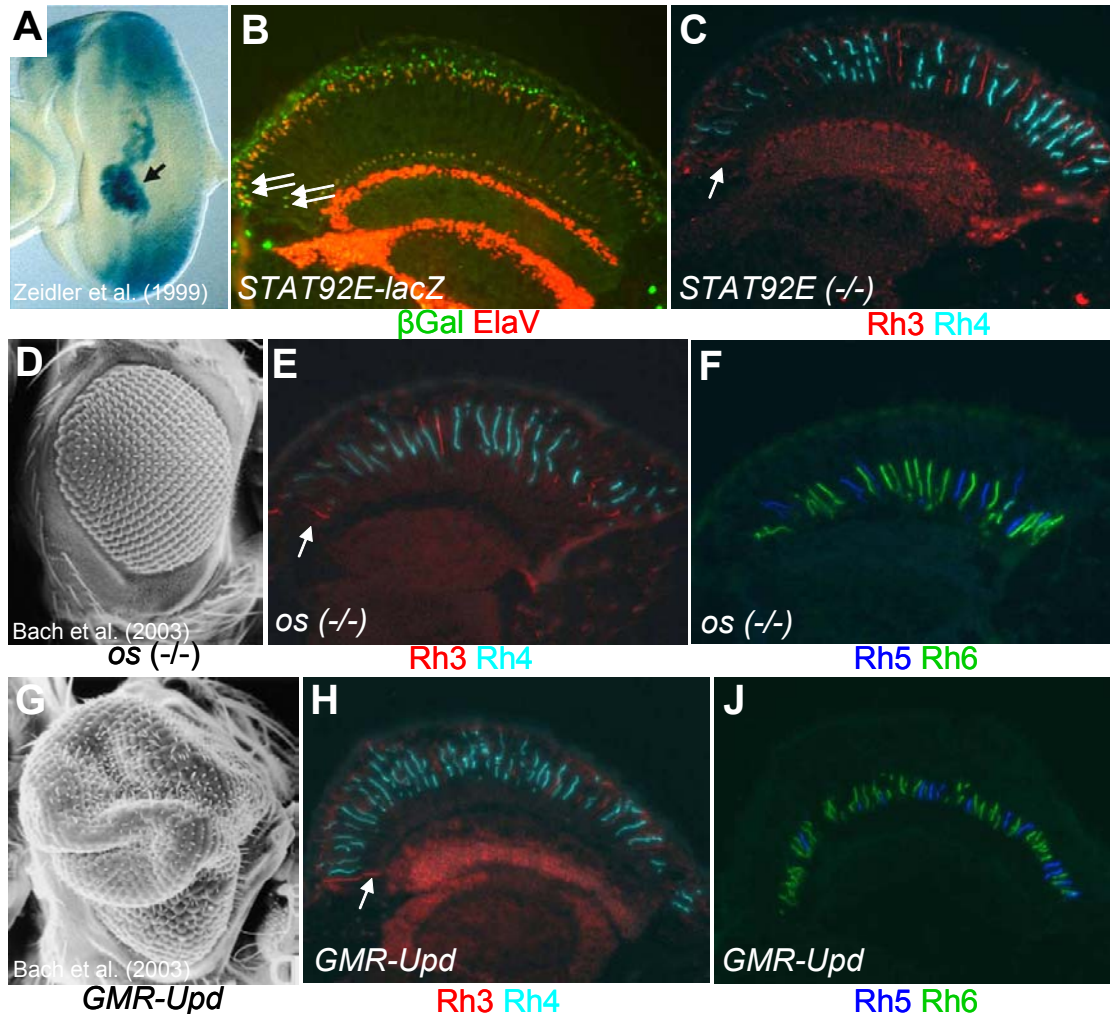
Fig III.3.14 JAK/STAT signaling and ommatidial subtype specification
(A)+(B) Expression of *STAT*-lacZ in developing PRs: Expression of STAT-lacZ visualized in developing PRs by X-Gal staining on of eye imaginal discs from wandering third instar larvae. βGal activity was detected at the dorsal and ventral poles of the eye disc, as well as in macrophages (arrow). (B) Adult expression of STAT-lacZ visualized by double labeling frozen sections with antibodies against βGal (green) and ElaV (red). Weak expression of STAT-lacZ was detected in all PRs. However, slightly stronger expression was observed in DRA inner PRs (arrows).
(C) Loss of *STAT92E* has no effect on ommatidial subtypes: Frozen section through a whole mutant eye lacking stat92E function double labeled with antibodies against Rh3 (red) and Rh4 (cyan). Expression of both R7 opsins was indistinguishable from the wildtype, in R7 cells as well as in the DRA (arrow).
(D)-(F) Loss of *Unpaired / outstretched* has no effect on ommatidial subtypes: Loss of Unp / os function had previously been shown to result in a small eye phenotype. (E) Frozen section through os1A (-/-) whole mutant eyes double labeled with antibodies against Rh3 (red) and Rh4 (cyan). No change in expression was detectable in R7 cells and the DRA (arrow). (F) Frozen section through os1A (-/-) whole mutant eyes double labeled with antibodies against Rh5 (blue) and Rh4 (green). No change in expression was detectable in R8 cells.
(G)-(J) Ectopic *Unpaired* does not alter ommatidial subtype specification: Flies over-expressing Unp under GMR-control (GMR-Unp) had previously been shown to manifest a dramatic eye overgrowth phenotype. (H) Frozen section through GMR-Upd eyes double labeled with antibodies against Rh3 (red) and Rh4 (cyan). No change in expression was detectable in R7 cells and the DRA (arrow). (F) Frozen section through GMR-Unp eyes doublelabeled with antibodies against Rh5 (blue) and Rh4 (green). No change in expression was detectable in R8 cells.

from the wildtype in the main part of the eye, as well as in the DRA (white arrow). It was therefore concluded that loss of *stat92E* does not result in misspecification of *Drosophila* ommatidia.

As the *stat92E* allele used was not a null allele, residual *stat* activity could have persisted in the whole mutant eyes. Mutants in the JAK/STAT ligand Unpaired (*os*) were therefore analyzed. Eye growth had previously been shown to be affected in *os* mutants (**Fig 14D**; (Bach et al., 2003), suggesting a role for the JAK/STAT pathway in regulating growth in the eye imaginal discs. However, no role has been reported for Unp in ommatidial subtype specification. Flies with homozygous whole mutant eyes for the strong *os* allele os^{1A} were therefore generated using the GMR-*hid* technique. Mutant eyes were rough and reduced in size and frozen sections were labeled using antibodies against Rh3 and Rh4 (**Fig 14E**). Rh3 expression (shown in red) and Rh4 expression (shown in cyan) were not affected in os^{1A} mutants, when compared to the wildtype. To complete the analysis of *os* mutants, R8 opsin expression was also tested by double labeling frozen sections with antibodies against Rh5 and Rh6 (**Fig 14F**). However, Rh5 expression (shown in blue) as well as Rh6 (shown in green) were indistinguishable from the wildtype), suggesting that loss of *os* function does not have an effect on ommatidial subtype specification.

Over-exppression of the JAK/STAT ligand Unpaired in all developing PRs using the GMR-promoter (GMR-Upd) has a dramatic growth-promoting effect, resulting in the massive bulging of eye tissue (**Fig 14G**; (Bach et al., 2003). This effect is thought to be the result of Unp diffusion from developing PRs posterior to the morphogenetic furrow into the anterior domain of the disc, where eye growth was taking place in a population of un-committed mitotic cells. Ommatidial specification was tested in the enlarged GMR-Upd eyes by double labeling frozen sections using antibodies against Rh3 and Rh4 (**Fig 14H**). It was found that Rh3 expression (shown in red) and Rh4 expression (shown in cyan) were not affected by ectopic exprerssion of Upd, suggesting that Upd was not sufficient to induce changes in the ommatidial pattern. Analysis of GMR-Upd retinas was completed by double labeling frozen sections with antibodies against the R8 opsins Rh5 and Rh6 (**Fig 14J**). However, the expression patterns of Rh5 (shown in blue) and Rh6 (shown in green) were found to be unaffected in flies ectopically over-expressing Upd.

It was therefore concluded from these experiments, that the JAK/STAT pathway does not play a role in specifying *Drosophila* ommatidia. It appears therefore, that the four STAT binding sites that have been found in the *ss* eye enhancer should not be required for **y**R7-specific expression of *ss* in response to this signal transduction pathway.

3.15. The *wingless* pathway antagonizes *spineless* function

The *wingless* pathway was shown to have a very strong inducing effect on the formation of DRA ommatidia throughout the dorsal half of the eye (Tomlinson, 2003; Wernet et al., 2003). Homothorax was found to be a key player, both necessary as well as sufficient to induce these DRA ommatidia downstream of Wg, whereas Spineless was shown to be crucial for the specification of **y**R7 cells. Hth and Ss were never found co-expressed in the wildtype and cell fate changes induced by Ss were dominant over Hth, when co-expression was induced. Furthermore, four binding sites for an important *wg* pathway effector, the transcription factor TCF were found within the ~1.6 kb eye enhancer of ss. It was therefore tested at whether the *wg* pathway was repressing *ss* function independently of Hth.

The DRA was shown to be expanded in two different mutant backgrounds, the *optomotorblind* gain-of-function allele *omb*QUADRRON and the *wg* gain-of-function induced by using over-expression of activated Armadillo (LGMR > ArmS10). Although both phenotypes were very similar, slight differences were detectable (**Fig 15A**). Expression of the opsin reporter *rh3*-lacZ, expressed specifically in pale R7 cells as well as DRA inner PRs in the wild type (top left) was expanded into a multitude of dorsal inner PRs, in both mutant situations (top row). It had been shown that this expansion was due to induction of the DRA fate in most dorsal ommatidia (*omb*QUADRRON) or the whole dorsal compartment (LGMR > ArmS10), respectively (bottom row). It was further shown that these transformation events were marked by an expansion of Hth, the DRA-inducing

A

rh3-lacZ

rh4-lacZ

rh3-lacZ

rh4-lacZ

green rh4-lacZ

rh3-lacZ

rh4-lacZ

wt   ombQd[For]   LGMR > ArmS10   LGMR > ss   LGMR > hth + ss

B LGMR > *hth + ss*

rh3-lacZ 24B10   *rh4*-lacZ 24B10

C LGMR > *hthHM + ss*

rh3-lacZ 24B10   *rh4*-lacZ 24B10

D LGMR > *ArmS10 + ss*

rh3-lacZ 24B10   *rh4*-lacZ 24B10

153
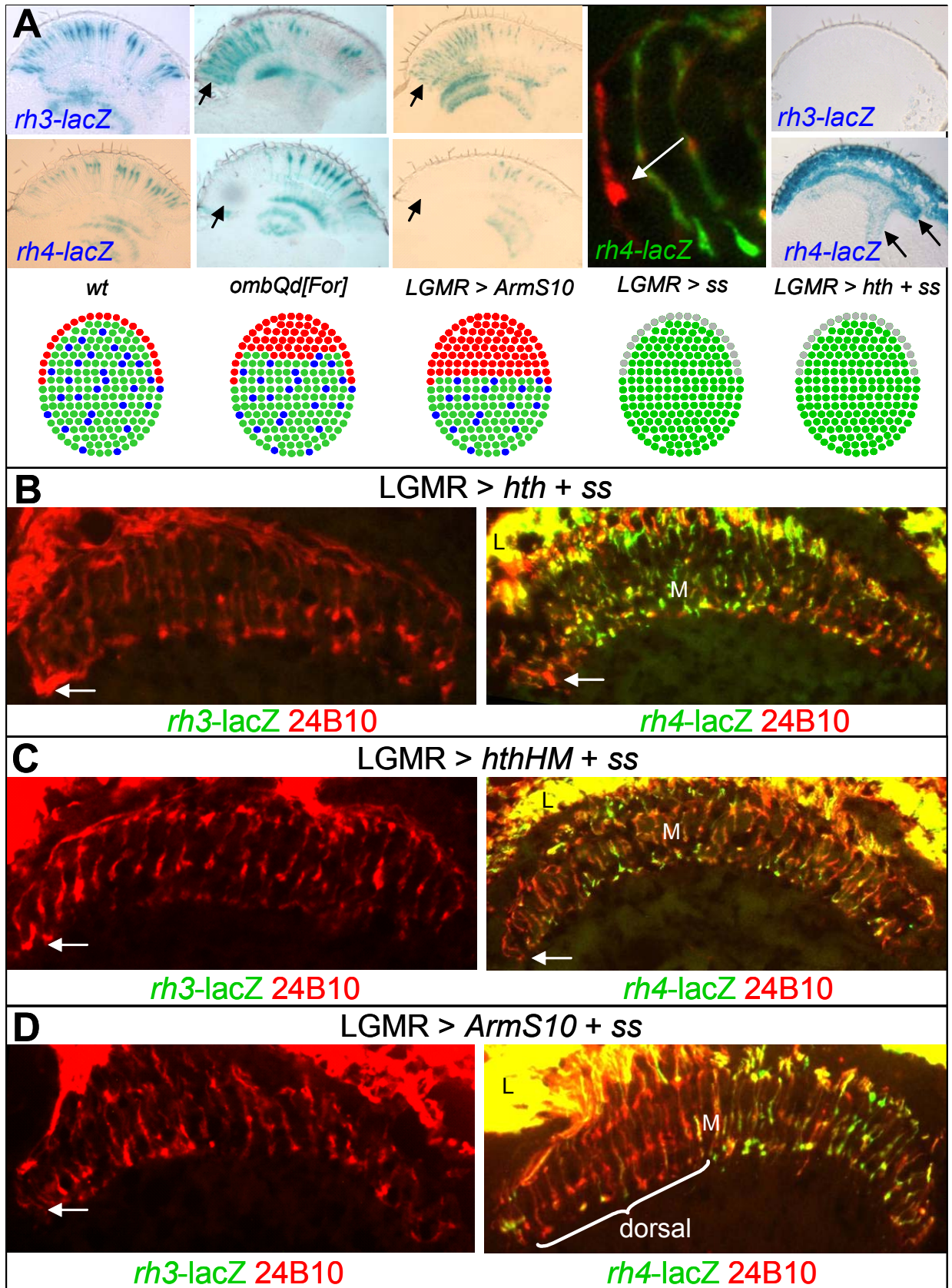
Fig III.3.15. The *wingless* pathway antagonizes *spineless* function

(A) The *wingless* pathway influences ommatidial specification events: Two mutant situations linked to the wg pathway had been reported to influence ommatidial subtype specification. Induction of extra DRA ommatidia by *omb*QUADROON (second column) as well as ectopically expressed activated Armadillo (third column) always resulted in suppression of **p** and **y** ommatidia formation. Furtjermore, ectopic ss was incapable of inducing *rh4* expression in DRA inner PRs, where high *wg* levels are present (fourth column). Finally, co-over-expresion of both *ss* and *hth* (LGMR > *ss* + *hth*) abolished DRA-induction by *hth* and *ss* dominated (last column).

(B) Co-over-expression of *ss* and *hth*. LEFT: Frozen sections through adult heads from LGMR > *ss* + *hth* flies also carrying the opsin reporter *rh3*-lacZ double labeled with antibodies against βGal (green) and the PR-specific cell-surface marker 24B10 (red). Expression of *rh3*-lacZ was completely lost in flies ectopically expressing both *ss and hth*, including in the DRA. RIGHT: Frozen sections through adult heads from LGMR > *ss* + *hth* flies also carrying the opsin reporter *rh4*-lacZ double labeled with antibodies against βGal (green) and 24B10 (red). Expression of *rh4*-lacZ was expanded into all PRs, with projections to both the lamina (L) and the medulla (M). However, inner PRs in the DRA, projecting axons to the dorsal-most medulla (white arrow) did not express *rh4* (arrow).

(C) Co-over-expression of *ss* and dominant negative *hth*: LEFT: Frozen sections through adult heads from LGMR > *ss* + *hth*[HM] flies also carrying the opsin reporter *rh3*-lacZ double labeled with antibodies against βGal (green) and 24B10 (red). Expression of *rh3*-lacZ was completely lost in flies ectopically expressing both *ss and hth*[HM], including in the DRA. RIGHT: Frozen sections through adult heads from LGMR > *ss* + *hth*[HM] flies also carrying the opsin reporter *rh4*-lacZ double labeled with antibodies against βGal (green) and 24B10 (red). Expression of *rh4*-lacZ was expanded into all PRs, with projections to both the lamina (L) and the medulla (M). However, inner PRs in the DRA, projecting axons to the dorsal-most medulla (white arrow) did not express *rh4* (arrow).

(D) Co-over-expression of *ss* and activated Armadillo: LEFT: Frozen sections through adult heads from LGMR > *ss* + *ArmS10* flies also carrying the opsin reporter *rh3*-lacZ double labeled with antibodies against βGal (green) and 24B10 (red). Expression of *rh3*-lacZ was completely lost in flies ectopically expressing both *ss and ArmS10,* including in the DRA. RIGHT: Frozen sections through adult heads from LGMR > *ss* + *ArmS10* flies also carrying the opsin reporter *rh4*-lacZ double labeled with antibodies against βGal (green) and 24B10 (red). Expression of *rh4*-lacZ was expanded into many PRs, with projections to both the lamina (L) and the medulla (M). However, most inner PRs of the expanded DRA, projecting axons into the entire dorsal half of the medulla (white bracket) did not express *rh4*.

factor in inner PRs. By introducing the *rh4*-lacZ transgene into the same mutant backgrounds, it was shown that the **y** R7 fate was always repressed in those dorsal ommatidia acquiring the DRA fate (middle row). As it had been shown that Hth efficiently represses Rh4 expression in inner PRs, this effect was attributed to Hth function. However, ss gain-of-function experiments (LGMR > *ss*) revealed that ss was not able to induce *rh4*-lacZ expression in DRA inner PRs, where Hth expression persisted (white arrow). However, the inability of Ss to activate *rh4* was not due to Hth, as rh4-lacZ expression was expanded to all PRs in flies ectopically expressing both proteins (LGMR > *hth* + *ss*). It seemed therefore likely that the *wg* pathway is repressing *ss* function independently of Hth.

This hyopothesis was tested by comparing the projection of their inner PR axon projections to the medulla in three different gain-of-function phenotypes. The three phenotypes were: expression of both Ss and Hth (LGMR > *ss* + *hth*), ectopic expression of both Ss and dominant negative Hth (LGMR > *ss* + *hth*[HM]) and ectopic expression of Ss and activated Armadillo (LGMR > *ss* + *ArmS10*).

First, opsin reporter constructs *rh3*-lacZ or *rh4*-lacZ were introduced into the LGMR > *ss* + *hth* background and frozen sections through adult eyes were double labeled using antibodies against βGal and the PR-specific cell-surface

antigen 24B10 (**Fig 15B**). As previously observed, *rh3*-lacZ expression (shown in green) was completely lost, including in DRA inner PRs (left). Instead, *rh4*-lacZ expression (shown in green) was expanded into all PRs with βGal-expressing fibers projecting to both the lamina (L) and the medulla (M). However, *rh4*-lacZ expression was still expluded from the DRA inner PRS (white arrow), as had been observed in LGMR > *ss* flies, suggesting that only the DRA inner PRs were able to neutralize *ss* function. These results therefore supported the hypothesis that high *wg* signaling levels antagonize Ss function.

Expression of *rh3*-lacZ or *rh4*-lacZ was also visualized in LGMR > *ss* + *hth*^{HM} flies by double labeling frozen sections using antibodies against βGal and 24B10 (**Fig 15C**). DRA development is blocked in flies ectopically expressing dominant negative Hth (LGMR > *hth*^{HM}), resulting in the formation of unusually Rh3/Rh6-coupled ommatidia at the dorsal rim. However, *rh3*-lacZ expression (shown in green) was completely lost in LGMR > *ss* + *hth*^{HM} retinas (left). Expression of *rh4*-lacZ (shown in green) was found to be expanded into all PRs except the DRA inner PRs (white arrow). The observed phenotype was therefore identical to the co-over-expression of Ss and wildtype Hth. It was therefore concluded that disruption of DRA development had no effect on the inability of Ss to repress *rh4* expression there, suggesting that high *wg* signaling levels upstreamn of *hth* were responsible for this neutralizing effect.

Finally, *rh3*-lacZ or *rh4*-lacZ expression was also visualized in LGMR > *ss* + ArmS10 flies by double labeling frozen sections using antibodies against βGal and 24B10 (**Fig 15D**). Ectopic expression of activated Armadillo results in the expansion of the DRA through the whole dorsal eye, with all dorsal ommatidia expressing Hth and Rh3 in their inner PRs. In LGMR > *ss* + ArmS10 retinas, however, *rh3*-lacZ expression (shown in green) was completely lost, as no βGal-expressing fibers were detectable (left). Expression of *rh4*-lacZ was found to be dramatically expoanded into outer PRs, based on the projection of βGal-expressing fibers to the Lamina (L). In inner PRs, however, expansion of *rh4*-lacZ seemed to be limited largely to the ventral half of the eye. It was found that most inner PRs projecting to the dorsal half of the medulla (white brackets) were

unable to activate *rh4*-lacZ expression in response to Ss over-expression. It was therefore concluded that high levels of wg signaling antagonized Ss function in developing PRs.

It was concluded from these experiments, that the ability of *ss* to induce the **y** R7 subset was antagonized by the *wg* pathway. As Ss and Hth were never seen co-expressed in the DRA, the neutralization off *ss* may be achieved by transcriptional repression of *ss* by Hth or TCF. However, it was shown that Ss function is even repressed, when co-expression of Hth and Ss is forced. It therefore appears likely that DRA inner PRs create a a transcriptional environment which is unfavorable to Ss, most likely by involving other *wg*-responsive genes,

3.16. Notch signaling might induce formation of y ommatidia

Spineless was shown to be necessary and sufficient for the *rh4*-expressing **y**R7 cell fate. Furthermore, using a reporter construct driven by the *ss* eye enhancer, specific expression was detected in a large subset of R7 cells. Bioinformatic analysis of the ~1.6 kb *ss* eye enhancer sequence revealed three putative binding sites for the crucial Notch pathway effector *suppressor of Hairless* [su(H)], encoding a transcriptional repressor (Fortini and Artavanis-Tsakonas, 1994; Schweisguth and Posakony, 1992). The Notch (N) pathway plays a crucial role in many developmental processes in flies as well as in vertebrates (for review: Lai, 2004). In *Drosophila*, the current model involves the membrane-bound protein Delta as the ligand for the transmembrane protein Notch, whose intracellular domain (N^{intra}) gets cleaved upon activation and translocates in the nucleus to induce transcriptional response (Kopczynski et al., 1988; Struhl and Adachi, 1998). In *Drosophila* PRs, Notch signaling is required to select the founder neuron of the ommatidial cluster, in a process called lateral inhibition (Baonza and Freeman, 2001). Additionally, the Notch pathway had recently been identified to provide an important additional signal required for R7 specification, co-operating with EGFR and *sev* signaling (Cooper and Bray, 2000; Tomlinson and Struhl, 2001). It was therefore tested whether Notch activity was

also required for a later step in R7 differentiation, the segregation of **p** and **y**R7 cells by differential expressin of ss.

Expression of the gene *mδ* was shown to be induced in R7 in response to N pathway activation (Cooper and Bray, 2000). It was therefore tested whether *mδ* expression in R7 cells persisted until the time point of *ss* expression and whether the Notch pathway was necessary and sufficient to induce the **y** ommatidial subtype. The enhancer fusion constructs *mδ0.5*–lacZ and *mδ0.5*–GAL4 had previously been used as reporters to visualize N pathway activation in the two developing PRs R4 and R7 (**Fig 16A**). Double labeling of larval eye imaginals discs with antibodies against βGal (shown in red) and the cell surface marker Coracle (shown in green) have been used to show expression of *mδ0.5*–lacZ in R4, starting in the very first rows posterior to the morphogenetic furrow, as well as a later onset of expression several ommatidial rows more posteriorly, in R7 cells (white arrows). The onset of *ss* expression was found to be later, during pupation. It was therefore tested whether *mδ0.5*–lacZ was expressed at that time by dissecting pupal retinas (48 hrs APF) and triple labeling them with antibodies against βGal, the R7 marker Prospero (Pros) and ElaV (**Fig 16B**). Strong βGal expression was detectable in one PR per ommatidium, which was not the R7 cell, marked by Pros (shown in green). Due to the stereotypical arrangement of ommatidial PRs, the βGal-expressing was identified as R4. It was therefore concluded that, during pupal development, the N pathway no longer activates *mδ*–lacZ expression in R7 cells. Characterization of *mδ* expression in PRs was completed by visualizing expression of *mδ0.5*–GAL4 driving the expression of nuclear lacZ. Frozen sections through adult eyes from these *mδ0.5* > lacZ:NLS flies were then double labeled using antibodies against βGal and Pros (**Fig 16C**). Strong GAL4 expression (shown in red) was detected in nuclei at the surface of the retina. However, no co-staining with Pros (shown in green) was observed, excluding the possibility that *mδ* becomes re-expressed in R7 cells at later stages, when opsin genes were turned on. Co-staining with ElaV revealed that the vast majority of βGal–positive nuclei were not neuronal PRs (data not shown), suggesting that *mδ* fades away in adult PRs. Therefore, reporter
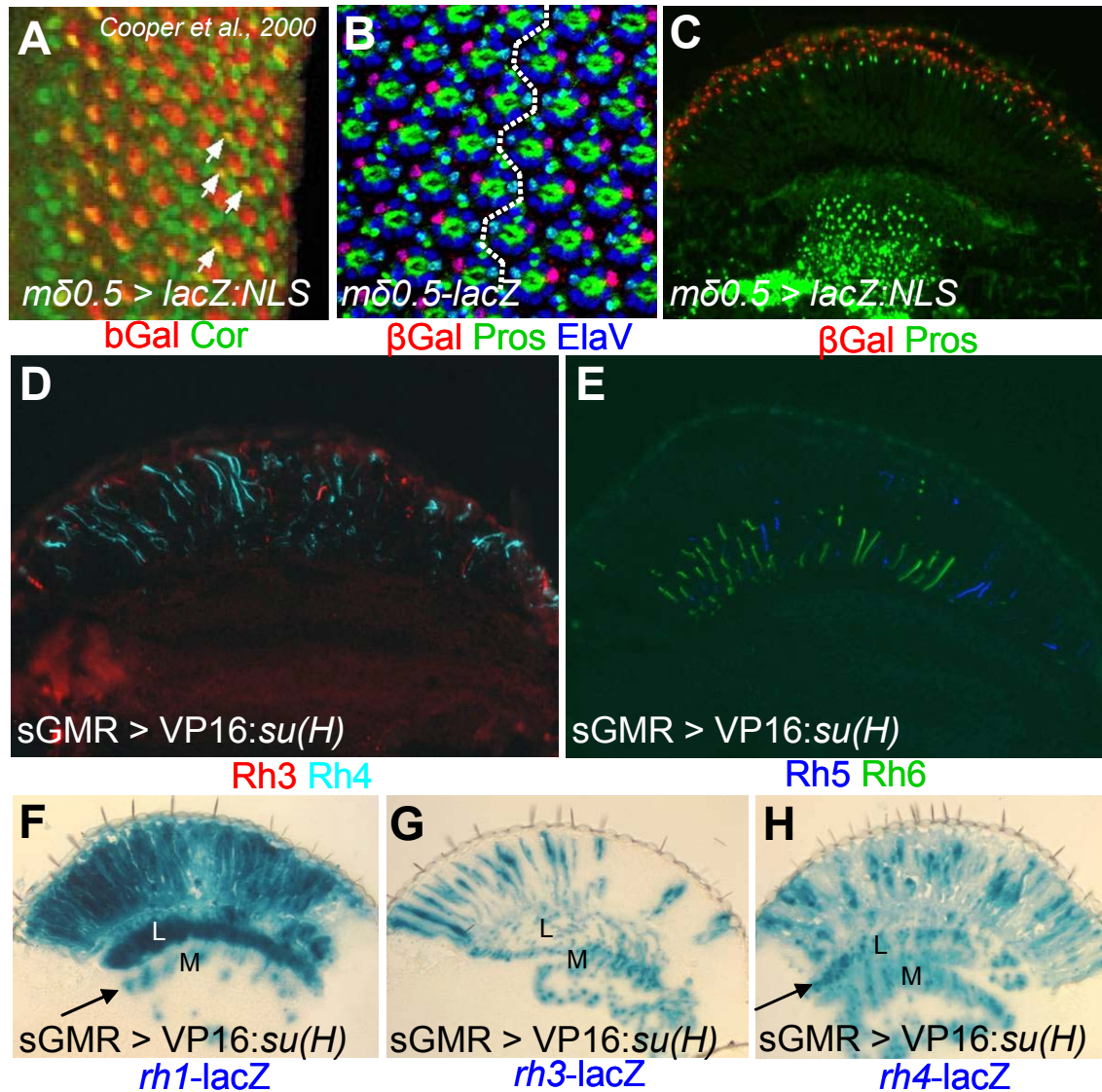
Fig III.3.16 Notch signaling might induce formation of y ommatidia
(A)-(C) Expression of the N pathway reporter mδ0.5 in PRs: Eye imaginal discs from third instar wandering larvae carrying the N pathway reporter mδ0.5-lacZ had previously been double labeled with antibodies against βGal (red) and the cell-surface marker Coaracle (green). Strong N pathway activity was detectable in R4, while weaker activity was detectable in R7 cells (arrows). (B) Pupal retinas (48 hrs APF) were dissected from wildtype flies carrying the mδ0.5-lacZ transgene and triple labeled with antibodies against βGal (red), the R7 marker Pros (green) and ElaV (blue). N pathway activity was only detectable in R4, at this developmental stage. (C) Frozen sections through adult heads from flies carrying the mδ0.5-lacZ transgene double labeled with antibodies against βGal (red) and the R7 marker Pros (green). No expression of βGal was detectable in R7 cells. mδ0.5-lacZ expression was specific to non-PR cells, as no co-expression with ElaV was observed in the adult (data not shown).

(D)+(E) Activated Su(H) induces Rh4 expression: Frozen sections through adult heads from flies over-expressing a fusion between the N effectors u(H) and the transcriptional activator domain from yeast VP16 (su(H):VP16) under GMR-GAL4 control (sGMR > su(H):VP16). Double labeling with antibodies against Rh3 (red) and Rh4 (cyan) revealed. (E) Frozen sections through adult heads from sGMR > su(H):VP16 flies double labeled with antibodies against Rh5 (blue) and Rh6 (green).

(F)-(H) Activated Su(H) induces *rh4* transcription: Frozen sections through adult eyes from sGMR > su(H):VP16 flies carrying different opsin-lacZ reporter constructs. Expansion of *rh1*-lacZ into inner PRs was observed, as βGal expressing fibers were found projecting to both layers of the optic lobe, the lamina (L) and the medulla (M). (G) Expression of *rh3*-lacZ was unaffected on frozen sections through sGMR > su(H):VP16 eyes: strong expression was detected in **p**R7 cells and DRA inner PRs. (H) Expression of *rh4*-lacZ was expanded throughout the retina on frozen sections through sGMR > su(H):VP16 eyes: strong expression was detected in rhabdomeres spanning the entire retina and projecting to both layers of the optic lobe, the lamina (L) and the medulla (M).

constructs visualizing N pathway activation via the gene *mδ* are expressed in both larval PRs R4 and R7 cells. Expression in R7 is vanishes quickly, whereas expression in R4 persists throughout pupal stages.

Three putative binding sites of the N pathway effector *suppressor of Hairless* had been identified in the eye enhancer of *spineles*s. It was therefore tested whether the N pathway activated **y**R7 development via Su(H). Over-expression of a fusion protein between the *suppressor of hairless* transcriptional repressor from *Drosophila* and the activation domain of the yeast transcritptional activator VP16 has previously been shown to effectively mimic N pathway activation (Furriols and Bray, 2000; Kidd et al., 1998). The fusion *su(H)*:VP16 was therefore ectopically expressed in developing PRs, using the GAL4/UAS-system (see material and methods). However, ectopic N pathway activation had a deleterious effect on PR development, as flies died at late pupal stages, when *su(H)*:VP16 was over-expressed at room temperature. However, attenuating GAL4-expression at lower temperatures (18°C) resulted in survival of few flies until adulthood. These sGMR > *su(H)*:VP16 flies had very disorganized eyes and were so severely paralyzed that they died after only a few days. Frozen sections through adult eyes from sGMR > *su(H)*:VP16 flies were labeled with antibodies against Rh3 and Rh4 (**Fig 16D**). While expression of Rh3 (shown in red) remained specific to very few cells, expression of Rh4 (shown in cyan) seemed unusually frequent. Expression of Rh4 in rhabdomeres spanning the entire retina was observed. This was particularly interesting, as it suggested that Rh4 expression was specifically expanded into outer PRs. To test such a possible specific effect of N pathway activation on rh4 expression, frozen sections were also double labeled with antibodies against Rh5 and Rh6 (**Fig 16E**). Expression of Rh5 (shown in blue) and Rh6 (shown in green) seemed normal in sGMR > *su(H)*:VP16 flies, confirming that only *rh4* expression might be expanded in these flies.

To confirm a possible activation of *rh4* expression by *su(H)*:VP16, the opsin-lacZ transgenes *rh1*-lacZ, *rh3*-lacZ and *rh4*-lacZ were introduced into the sGMR > *su(H)*:VP16 background and βGal activity was visualized on frozen

sections through adult eyes using X-Gal (see material and methods). Expression of *rh1*-lacZ was analyzed first (**Fig 16F**). βGal expression was expanded into all PRs as axon fibers expressing *rh1*-lacZ were found to terminate in both layers of the optic lobe, the lamina (L) as well as the medulla (M). It was therefore concluded that either development of outer PR was affected in these mutants, or that some inner PRs had gained expression of *rh1*. Development of R7 cells was therefore assessed by visualizing *rh3*-lacZ expression (**Fig 16G**). βGal expression was indistinguishable from wildtype flies. Over-expression of *su(H)*:VP16 therefore does not influence *rh3* expression or **p**R7 development. Finally, *rh4*-lacZ expression was investigated in sGMR > *su(H)*:VP16 flies (**Fig 16H**). βGal activity was expanded through the whole retina. Rhabdomeres spanning the whole retina were found to express *rh4*-lacZ and axon projections to the lamina (L) were observed (black arrow), suggesting that outer PRs had gained expression of the **y**R7 opsin.

It was concluded from these experiments that the N pathway is active in R7 cells clearly before *ss* expression becomes induced in the **y** subset. Ectopic activation of the N pathway using over-expression of VP16:*su(H)* is sufficient to induce **y**R7-like expression of *rh4* in outer PRs. However, inner PRs are also affected, as they seem to gain *rh1* expression.

3.17. The activated Notch receptor induces yR7 specification

The N pathway was shown to be active in developing R7 cells and over-activating it using a VP16:su(H) fusion protein resulted in the specific activation of *rh4* expression. Over-expression of the intracellular domain of Notch (N^{intra}) using the GAL4/UAS-system (see material and methods) had previously been shown to be sufficient for Notch pathway activation (Giraldez and Cohen, 2003; Struhl and Adachi, 1998; Struhl and Greenwald, 2001). To test a possible role for Notch in ommatidial subtype specification, N^{intra} was over-expressed using GMR-GAL4 drivers (GMR > N^{intra}). As for sGMR > *su(H)*:VP16 flies, over-expression had to be performed at low temperatures (18° C) using weak GMR-Gal4 insertions. Frozen sections through adult eyes from sGMR > N^{intra} flies were
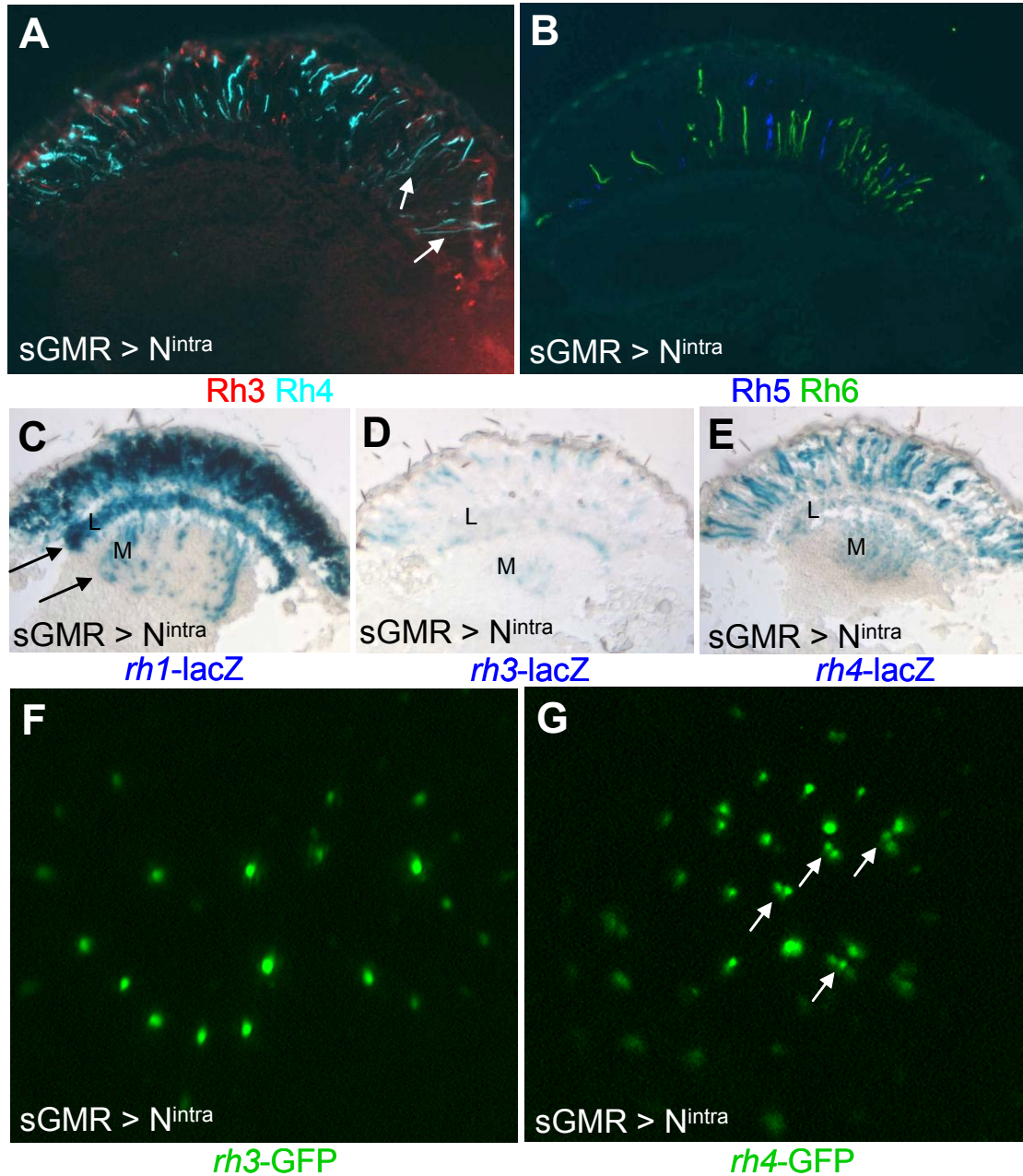
Fig III.3.17 The activated Notch receptor induces yR7 specification

(A)+(B) Activated Notch receptor induces Rh4 expression: Frozen sections through adult heads from flies over-expressing the intracellular domain of the N receptor (N^{intra}) under GMR-GAL4 control (sGMR > N^{intra}). Double labeling with antibodies against Rh3 (red) and Rh4 (cyan) revealed expansion of *rh4* expression into several rhabdomeres spoanning the entire retina (arrows). (B) Frozen sections through adult heads from sGMR > N^{intra} flies double labeled with antibodies against Rh5 (blue) and Rh6 (green). No obvious phenotype was detected in R8 cells.

(C)-(E) Activated Notch receptor induces *rh4* transcription: Frozen sections through adult eyes from sGMR > N^{intra} flies carrying different opsin-lacZ reporter constructs. Expansion of *rh1*-lacZ into inner PRs was observed, as βGal expressing fibers were found projecting to both layers of the optic lobe, the lamina (L) and the medulla (M). (D) Expression of *rh3*-lacZ appeared unaffected on frozen sections through sGMR > N^{intra} eyes as βGal expression was detected in a subset of R7 cells. (E) Expression of *rh4*-lacZ was expanded throughout the retina on frozen sections through sGMR > N^{intra} eyes: strong expression was detected in rhabdomeres spanning the entire retina and projecting to both layers of the optic lobe, the lamina (L) and the medulla (M).

(F)+(G) Ectopic N^{intra} specifically induces several *rh4* positive cells per ommatidium: Corneal neutralization (water immersion microscopy) of living sGMR > N^{intra} flies carrying opsin-GFP reporter constructs. No change in *rh3*-GFP expression was detectable as strong fluorescence was always observed in only PR in a subset of ommatidia. (G) Expression of *rh4*-GFP was expanded into more than one PR per ommatidium, confirming that outer PRs had gained expression of *rh4*.

161

generated and double labeled using antibodies against Rh3 and Rh4 (**Fig 17A**). Rh3 expression (shown in red) seemed unaffected, whereas Rh4 expression (shown in cyan) appeared to be expanded, when compared to the wildtype. Particularly interesting was Rh4 expression in rhabdomeres spanning the whole retina (white arrows), suggesting that Rh4 expression had expanded into outer PRs. R8 opsin expression was also assessed in sGMR > N^{intra} flies, by double labeling frozen sections through adult retinas for Rh5 and Rh6 (**Fig 17B**). However, taking in account the considerable retinal disorganization, it appeared that expression of Rh5 (shown in blue) and Rh6 (shown in green) was indistinguishable from the wildtype. It was therefore concluded that ectopic N pathway activation might have an activating effect on *rh4* expression.

This hypothesis was further tested by introducing the opsin-lacZ reporter constructs *rh1*-lacZ, *rh3*-lacZ and *rh4*-lacZ into the sGMR > N^{intra} background. Expression of these transgenes was then visualized on frozen sections through adult eyes, using X-GAL. First, *rh1*-lacZ expression was found to be severely affected in sGMR > N^{intra} flies (**Fig 17C**). In wildtype flies, *rh1*-lacZ is expressed exclusively in the outer PRs R1-R6, projecting to the lamina (L). In sGMR > N^{intra} flies, however, βGal activity was detectable in all PRs as *rh1*-lacZ expressing fibers were detected to terminate in both layers of the optic lobe (black arrows), a situation very similar to sGMR > su(H):VP16 flies. This suggested that either outer PRs mis-projected some axons to the medulla, or that inner PRs now expressed *rh1*. Expression of *rh3*-lacZ was tested next (**Fig 17D**). Despite the severe eye phenotype, a low ratio of R7 cells was found to express βGal, a situation comparable to the wildtype. Based on previous observations with Anti-Rh3 antibodies, it was therefore concluded that *rh3* expression is not affected by ectopic N pathway activation, as had previously been observed in sGMR > su(H):VP16 flies. Finally, *rh4*-lacZ expression was assessed in sGMR > N^{intra} flies (**Fig 17E**). βGal expression was significantly increased throughout the retina, confirming previous observations with Anti-Rh4 antibodies. Furthermore, βGal expression was detected in rhabdomeres spanning the whole retina, again suggesting that outer PRs had become *rh4*-lacZ expressing. This result was

again highly reminiscent of the opsin phenotype described for sGMR > su(H):VP16 flies. Expression of *rh4*-lacZ was weaker compared to *rh1*-lacZ expression levels, and strength of βGal staining in the lamina (top black arrow) was also fairly low. It was therefore concluded that only a subset of outer PRs have become *rh4* expressing in sGMR > N^{intra} flies.

To confirm expression of *rh4* in multiple PRs per ommatidium, opsin-GFP reporter transgenes were introduced into the sGMR > N^{intra} background and analyzed by water immersion microscopy (Pichaud and Desplan, 2001). This technique allows the visualization of GFP signals emanating from individual ommatidia by neutralizing the curvature of the retina (see material and methods). First, expression of *rh3*-GFP was analyzed in sGMR > N^{intra} flies (**Fig 17F**). Strong GFP signals were detected emanating from a subset of ommatidia. Only one PR per ommatidium was found to be expressing GFP. This expression pattern was virtually identical to the expression of *rh3*-GFP in wildtype flies. It was therefore concluded that N pathway activation does not lead to the expansion of *rh3* expression. However, expression of *rh4*-GFP in sGMR > N^{intra} flies was different (**Fig 17G**). Strong GFP signals were found emanating from a large subset of ommatidia. Interestingly, more than one GFP-expressing cell was observed in many ommatidia (white arrows). Such a phenotype had never been observed before. Therefore, ectopic over-expression of N^{intra} leads to a specific expansion of *rh4* expression into outer PRs.

It was concluded from these experiments, that ectopic activation of the Notch pathway in developing PRs appears to have an activating effect on *rh4* expression.This effect is specific, as *rh3* expression is not altered. If the observed phenotype was the product of N-induced late re-specification of outer PRs into extra R7 cells, these new R7 cells then always choose the **y** fate. However, sGMR > N^{intra} flies remained to be analyzed in more detail, as inner PR identity also seemed to be affected.

3.18. Activated Notch specifically induces *rh4* in *sevenless* mutants

Ectopic activation of the Notch pathway in all developing PRs was shown to have a specific activating effect on *rh4* expression. However, analysis of N-induced **y**R7 opsin expression in outer PRs was difficult as endogenous *rh3* and *rh4* expression persisted in R7. The effect of Notch pathway activation was therefore studied in *sevenless* (*sev*) mutants, lacking all R7 cells.

Opsin expression had previously is severely altered in *sev* mutants. As a control, expression of Rh3 and Rh4 was visualized on frozen sections through adult *sev* eyes (**Fig 18A**). It was obvious that Rh4 expression (shown in cyan) was totally lost, consistent with the fact that induction of R7 cells had failed in these mutants. Rh3 expression (shown in red), persisted in R8 cells of the DRA (white arrow), whereas Rh3 expression in DRA R7 cells and pale R7 cells was totally lost. This observation again confirmed the *sev* phenotype. Expression of R8 osins was visualized next by labeling frozen sections through adult sev eyes with antibodies against Rh5 and Rh6 (**Fig 18B**). It was found that Rh5 expression (shown in blue) was lost in most of the cases (rarely, very few Rh5-expressing ommatidia remained, data not shown), while Rh6 expression (shown in green) was expanded into all R8 cells. It was therefore concluded that R8 cells expressed the 'ground state' opsin Rh6, due to the lack of an instructive signal from pale R7 cells. Alternatively, opsin expression in *sev* mutants was visualized by introducing the opsin-lacZ reporter transgenes *rh1*-lacZ, *rh3*-lacZ and *rh4*-lacZ and detecting βGal activity on frozen sections using X-Gal (see material and methods). It was found that removing R7 cells did not affect expression of *rh1*-lacZ (**Fig 18C**). As in wildtype flies βGal activity was detected in rhabdomeres spanning the entire retina and projecting their axons to the lamina (L), exclusively. Expression of *rh3*-lacZ was only detectable in DRA R8 cells spanning the basal half of the dorsal-most retina (**Fig 18D**). Finally, *rh4*-lacZ was completely lost in *sev* mutants (**Fig 18E**). Occasionally, some unspecific βGal activity was detected in the head cuticle. It was therefore concluded that antibody staining as well as opsin-lacZ transgenes were a powerful way to visualize the sev background.

164
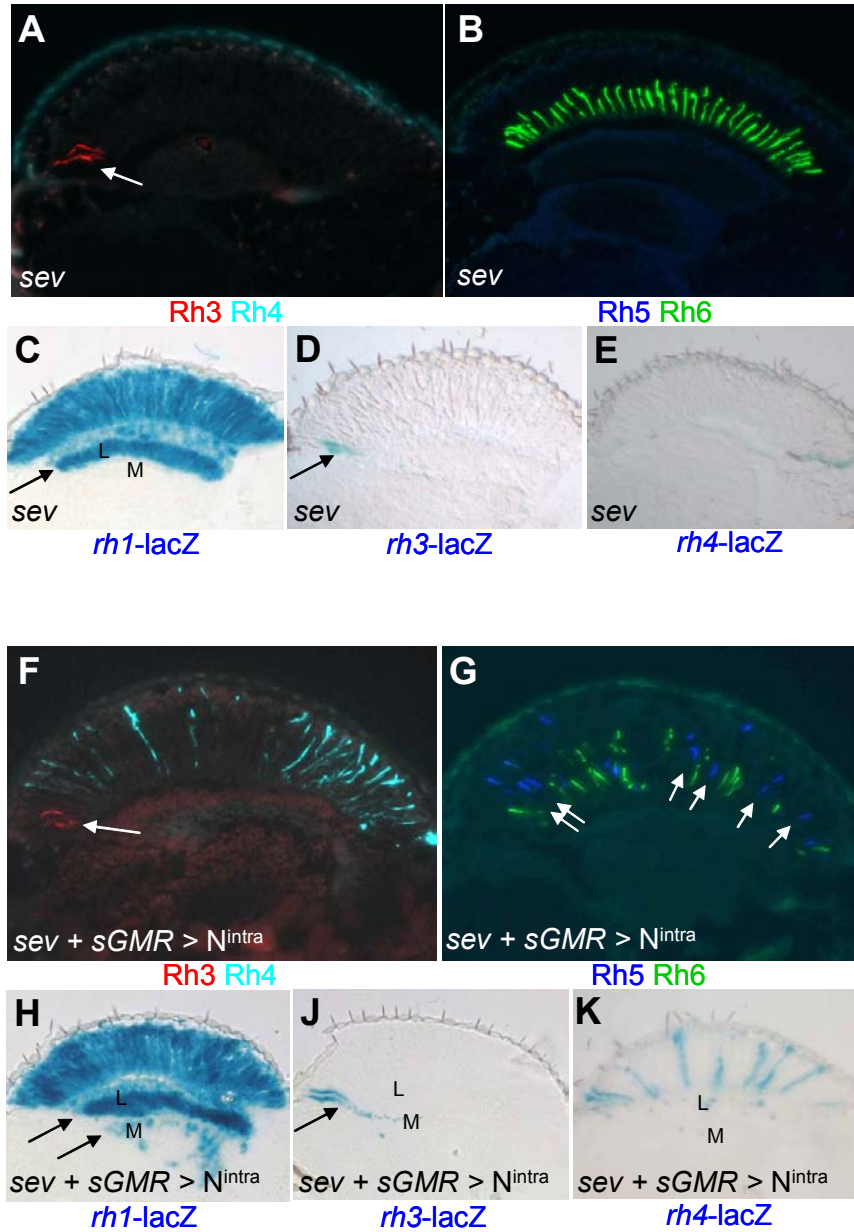
Fig III.3.18 Activated Notch specifically induces *rh4* in *sevenless* mutants
(A)-(E) Inner PR opsin expression in *sev* mutants: Frozen sections through adult heads from *sev* mutants. Double labeling with antibodies against Rh3 (red) and Rh4 (cyan) revealed a complete loss of Rh4 expression, while Rh3 persisted only in R8 cells in the DRA (arrows). (B) Frozen sections through adult heads from *sev* mutants double labeled with antibodies against Rh5 (blue) and Rh6 (green). Expression of Rh5 was completely lost in the majority of the cases, while Rh6 expression was expanded into all R8 cells. (C) Frozen sections through adult eyes from *sev* mutants also carrying different opsin-lacZ reporter constructs. No change in *rh1*-lacZ was observed. (D) In *sev* mutants, expression of *rh3*-lacZ was detectable only in DRA R8 cells. (E) Expression of *rh4*-lacZ was completely lost in *sev* mutants (background βGal activity can be seen in the head cuticle).
(F)-(K) Ectopic N^{intra} alters opsin expression in *sev* mutants: Frozen sections through adult heads from flies over-expressing N^{intra} under GMR-GAL4 control in a *sev* mutant background (*sev* + sGMR > N^{intra}). Double labeling with antibodies against Rh3 (red) and Rh4 (cyan) revealed expansion of Rh4 expression into several rhabdomeres spanning the entire retina, while Rh3 expression always remained restricted to the R8 of the DRA (arrow). (G) Frozen sections through adult heads from *sev* + sGMR > N^{intra} flies double labeled with antibodies against Rh5 (blue) and Rh6 (green). Several R8 cells were found to express Rh5 (arrows). (H) Frozen sections through adult eyes from *sev* + sGMR > N^{intra} flies carrying different opsin-lacZ reporter constructs. Expansion of *rh1*-lacZ into inner PRs was observed, as βGal expressing fibers were found projecting to both layers of the optic lobe, the lamina (L) and the medulla (M). (J) Expression of *rh3*-lacZ appeared unaffected on frozen sections through sev + sGMR > N^{intra} eyes as βGal expression was only detectable in DRA R8 cells. (K) Expression of *rh4*-lacZ was expanded into several ommatidia throughout the retina on frozen sections through *sev* + sGMR > N^{intra} eyes: strong expression was detected in rhabdomeres spanning the entire retina and projecting to both layers of the optic lobe, the lamina (L) and the medulla (M).

Mutant flies over-expressing activated Notch (N^{intra}) under the control of sGMR-GAL4 in a *sevenless* background (*sev* + sGMR > N^{intra}) were generated. Eye morphology was identical to sGMR > N^{intra} flies. Frozen sections through adult eyes were double labeled using antibodies against Rh3 and Rh4 (**Fig 18F**). Rh3 expression (shown in red) was completely lost, except in the DRA R8 cells (white arrow). However, expression of Rh4 (shown in cyan) was detectable in numerous rhabdomeres throughout the *sev* + sGMR > N^{intra} retinas. Interestingly, these Rh4-positive rhabdomeres appeared to span the whole retina, suggesting that outer PRs were expressing Rh4. Extra Rh3-expressing rhabdomeres outside the DRA were never observed in these flies. It was therefore concluded that ectopic activation of the N pathway leads to a specific activation of Rh4 expression in outer PRs, as visualized in *sev* mutants. R8 opsin expression was then assessed next in *sev* + sGMR > N^{intra} flies, by double labeling frozen sections through adult heads with antibodies against Rh5 and Rh6 (**Fig 18G**). Expression of Rh6 (shown in green) was detected in many short rhabdomeres in the basal half of the retina, suggesting that many R8 cells retained *rh6* expression in *sev* + sGMR > N^{intra} flies. An unusually high number of PRs with short rhabdomeres expressed Rh5 (shown in blue). As rhabdomere morphology was affected, a clear identification of the cell type that expressed Rh5 was difficult. However, the Rh5-expressing cells appeared to be R8 cells, altough many of their rhabdomeres had moved distally. This R8 rhabdomere phenotype typical for *sev* mutants and is most likely due to the extension of R8 rhabdomeres into the part of the retina that is usually occupied by R7 rhabdomeres, in the wildtype. As Rh5-positive rhabdomeres always appeared in gaps between Rh6-expressing R8 cells (white arrows), it appeared that an unusually high ratio of R8 cells chose expression of Rh5 in these flies. It was therefore concluded, that ectopic activation of the N pathway in *sev* mutants lead to the specification of more **p**R8 cells than normally observed in *sev* mutants. Expression of *rh5* was never observed in outer PRs. It appears therefore that the N pathway may influence both the induction of **y**R7 cells as well as the instruction of **p**R8 cells.

The opsin phenotypes observed in *sev* + sGMR > N^{intra} flies were reproduced by introducing the opsin-lacZ reporter transgenes *rh1*-lacZ, *rh3*-lacZ and *rh4*-lacZ and detecting βGal activity on frozen sections using X-Gal. First, expression of *rh1*-lacZ was visualized in *sev* + sGMR > N^{intra} flies (**Fig 18H**). The phenotype observed looked identical to sGMR > N^{intra} flies: *rh1*-lacZ expression was expanded into all PRs, as βGal expressing fibers were found to terminate in both the lamina (L) as well as the medulla (M). The partial mis-specification of inner PRs by N^{intra} was therefore reproduced in this background. Next, *rh3*-lacZ expression was assessed in *sev* + sGMR > N^{intra} flies (**Fig 18J**). The only βGal expressing cells detectable were the R8 cells of the DRA (black arrow), confirming the previous observation, that no extra *rh3*-expressing cells were induced in these mutants. Finally, *rh4*-lacZ expression was expanded into a considerable number of rhabdomeres spanning the entire retina, a situation never observed in *sev* mutants. Activation of the N pathway therefore leads to a specific gain of *rh4* expression in outer PRs.

It was concluded from these experiments that ectopic activation of the N pathway in *sev* mutants results in an opsin phenotype both in outer PRs and R8 cells. An unusually high number of **p**R8 cells is induced while expression of the **y**R7 opsin Rh4 is expanded into outer PRs. It appears therefore, that the N pathway might influence both the instruction of R8 cells as well as the choice of the **y** ommatidial subtype in R7, possibly by directly specifying **y**R7 cells. This effect could be mediated by regulating *ss* expression, as three putative *su(H)* binding sites had been identified in the *ss* eye enhancer.

3.19. Activated Ras induces both *rh3* and *rh4* in *sevenless* mutants

A consitutively active form of the small G-Protein Ras is sufficient to force developing PRs into the R7 cell fate by mimicking Sev- and EGF receptor activation (*sev* > RasVal12; (Gaul et al., 1992). It has been shown that both **p**R7 and **y**R7 cells get stochastically induced in *sev* > RasVal12 flies (Chou et al., 1996). In contrast, over-activation of the N pathway leads to the specific gain of *rh4* expression. To further demonstrate the specific activation of **y**R7-like *rh4*
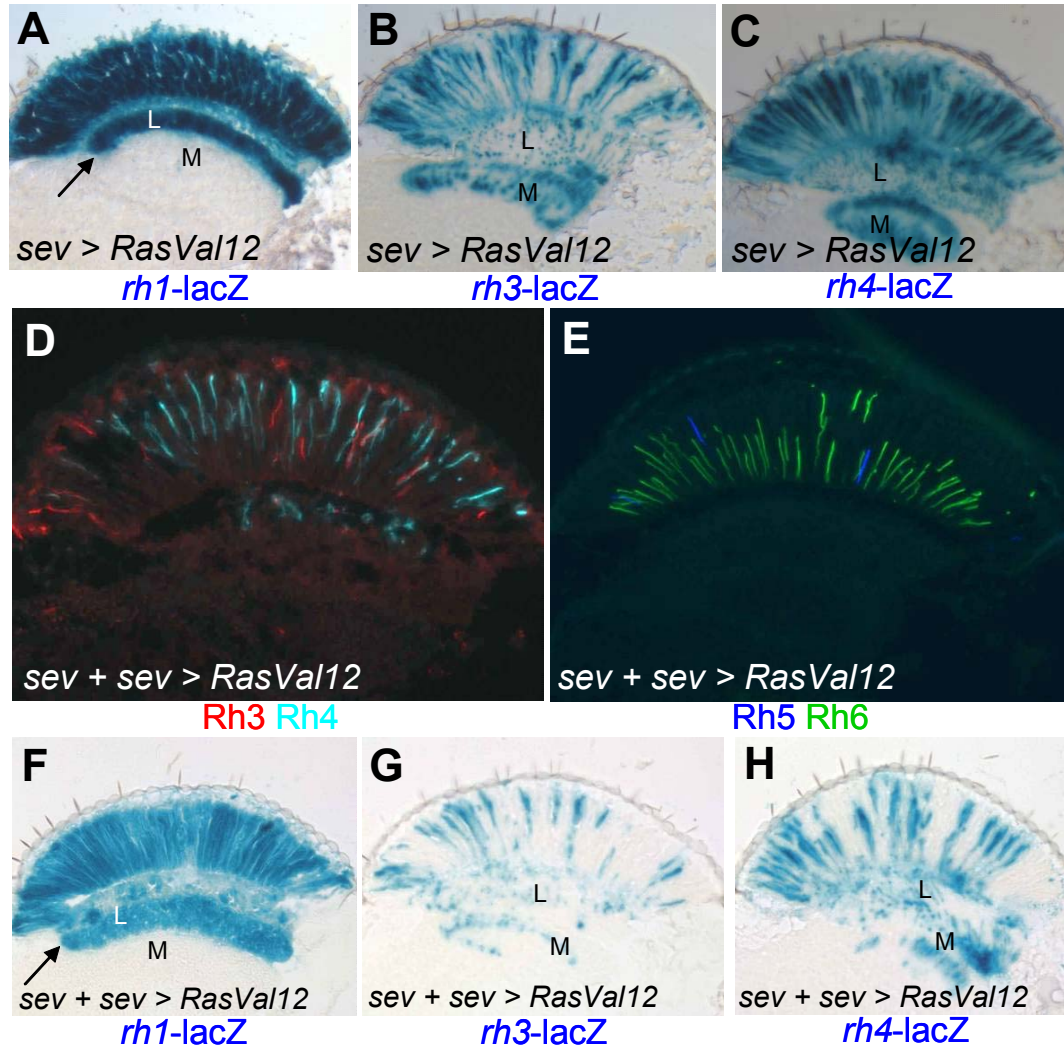
Fig III.3.19 Activated Ras induces both *rh3* and *rh4* in *sevenless* mutants
(A)-(C) Inner PR opsin expression is altered by activated Ras: Frozen sections through adult eyes from flies over-expressing activated Ras (RasVal12) under the control of the *sev* promoter (*sev* > RasVal12) also carrying different opsin-lacZ reporter constructs. Expression of *rh1*-lacZ was normal, as βGal positive rhabdomeres spanned the whole retina and their axon fibers were found projecting to the lamina (L). (B) Expression of *rh3*-lacZ appeared up-regulated in *sev* > RasVal12 eyes. However, βGal expression remained specific to R7 cells, with rhabdomeres in the distal half of the retina and axons projecting to the medulla (M). (C) Expression of *rh4*-lacZ was also expanded throughout the R7 layer of the adult retina on frozen sections through *sev* > RasVal12 eyes: strong expression was detected in rhabdomeres spanning the distal half of the retina and projecting to the medulla (M).
(D)-(H) Inner PR opsin expression is altered by activated Ras in *sev* mutants: Frozen sections through adult heads from flies over-expressing activated Ras in a *sev* mutant background (*sev* + *sev* > RasVal12). Double labeling with antibodies against Rh3 (red) and Rh4 (cyan) revealed expression of both Rh3 and Rh4 throughout the retina. A higher ratio of Rh4 expressing PRs was observed. (G) Frozen sections through adult heads from *sev* + *sev* > RasVal12 flies double labeled with antibodies against Rh5 (blue) and Rh6 (green). Few R8 cells expressing Rh5 were observed. (H) Frozen sections through adult eyes from *sev* + *sev* > RasVal12 flies carrying different opsin-lacZ reporter constructs. Expression of *rh1*-lacZ was unaffected, as βGal expression was detected in rhabdomeres spanning the whole retina with axons projecting to the lamina (L). (J) On frozen sections through sev + *sev* > RasVal12 eye, expression of *rh3*-lacZ was detected in R7-like cells, with βGal expressing rhabdomeres spanning the distal half of the retina and axons projecting to the medulla (M). (K) Expression of *rh4*-lacZ was also detected in R7-like cells on frozen sections through *sev* + *sev* > RasVal12 eyes. Interestingly, a higher number of extra R7 cells was found to express *rh4*, similar to the **p** / **y** distribution in wildtype R7 cells.

expression by N, cell fate decisions were assessed in outer PRs of flies over-expressing RasVal12 in a *sev* mutant background.

Opsin expression was visualized in flies over-expressing RasVal12 in a subset of PRs (R1, R3, R4, R6 and R7) under the control of the *sev* promoter (*sev* > RasVal12; (Gaul et al., 1992). The opsin-lacZ reporter constructs *rh1*-lacZ, *rh3*-lacZ and *rh4*-lacZ were introduced and βGal activity was visualized on frozen sections through adult heads using X-Gal (see material and methods). Expression of *rh1*-lacZ seemed to be unaffected in *sev* > RasVal12 flies (**Fig 19A**). The rhabdomeres of PRs expressing rh1-lacZ spanned the whole retina and axonal fibers were always found to terminate in the Lamina (L, black arrow) showing that most outer PRs retain their original cell in this mutant situation. Expression of *rh3*-lacZ was also visualized on frozen sections through *sev* > RasVal12 eyes (**Fig 19B**). The number of βGal-expressing PRs detected throughout the retina was significantly higher than in wildtype flies. Based on the distal location of their cell bodies and the termination of their axon fibers in the medulla (M), they could be identified as extra R7 cells. Extra **p**R7 cells were induced in these transgenic flies. Finally, expression of *rh4*-lacZ was visualized in *sev* > RasVal12 flies (**Fig 19C**). Again, the number of βGal-expressing PRs was significantly higher than in wildtype flies. Cell bodies were located distally and axons projected into the medulla (M), confirming that a large number of extra **y**R7 cells had also been created in these flies. Therefore, over-expression of activated Ras in outer PRs leads to the specification of extra R7 cells that belong to both subtypes, **p** as well as **y**.

To remove the regular R7 cells, activated Ras was over-expressed in *sev* mutants (*sev* + *sev* > RasVal12). Opsin expression in R7 cells was then visualized on frozen sections using antibodies against Rh3 and Rh4 (**Fig 19D**). In sev mutants, Rh3 expression had been shown to be restricted to the DRA R8 cells (see above). In *sev* + *sev* > RasVal12 retinas, however, Rh3 expression (shown in red) was detectable in several ommatidia outside of the DRA. Strong expression of Rh4 was also observed, while this opsin was always absent from *sev* retinas. Therefore, extra R7 cells induced by Ras pathway activation indeed fell into either of the two subtypes, **p** or **y**. Interestingly, more **y**R7 cells than **p**R7 cells were induced, suggesting that choice between these two fates might have

occurred stochastically in a 70:30 ratio, as in wildtype R7 cells. R8 opsin expression was also visualized in *sev* + *sev* > RasVal12 by double labeling frozen sections with antibodies against Rh5 and Rh6 (**Fig 19E**). Expression of both Rh5 (shown in blue) and Rh6 (shown in green) were detected in R8 cells in the basal half of the retina. Occasionally, rhabdomeres moved distally, as previously described for sev mutants. The vast majority of R8 cells expressed the 'ground state' opsin Rh6 found almost exclusively in *sev* mutants. However, a low ratio of R8 cells expressing Rh5 was detectable, suggesting that some of the **p**R7 cells induced by activated Ras are able to properly instruct R8 cells in these flies.

Finally, opsin expression in *sev* + *sev* > RasVal12 flies was confirmed by instroducing the opsin-lacZ reporter constructs *rh1*-lacZ, *rh3*-lacZ and *rh4*-lacZ visualizing βGal activity on frozen sections using X-Gal (see material and methods). Expression of *rh1*-lacZ seemed unaffected in *sev* + *sev* > RasVal12 flies (**Fig 19F**). This suggested that many outer PRs remained untransformed, which is consistent with the fact that the sev promoter is not expressed in the outer PRs R2 and R5. Expression of *rh3*-lacZ was also visualized in *sev* + *sev* > RasVal12 flies (**Fig 19G**). While expression of *rh3*-lacZ was only detectable in DRA R8 cells in *sev* mutants, several βGal expressing ommatidia were detectable in presence of *sev* > RasVal12. Positive cell bodies were always found distally and their axons projected to the medulla (M), clearly identifying these cells as R7 cells. This observation further confirms the previously described induction of **p**R7 cells by activated Ras. Finally, expression of *rh4*-lacZ was assessed in *sev* + *sev* > RasVal12 flies (**Fig 19H**). A large number of βGal expressing cells were detected, whose cell bodies were located distally and projected axons into the medulla (M). While expression of *rh4*-lacZ is totally lost in *sev* mutants, activation of the Ras pathway induces a large number of **y**R7 cells. As described before, the number of **y**R7 cells induced by RasVal12 always clearly exceeded the number of induced **p**R7 cells.

Therefore, it was concluded from these experiments that new R7 cells induced by Ras pathway activation in *sev* mutants fall into both categories

described for the wildtype: **p**R7 and **y**R7. These extra R7 cells seem to respect the 70:30 ratio and are, in some cases, able to instruct R8 cells to express Rh5. This phenotype is clearly different from the specific induction of **y**R7 cells observed when the Notch pathway is ectopically activated in *sev* retinas.

3.20. The Notch receptor might not necessary for retinal patterning

Notch signaling has been shown to be required at different stages during eye development (Cagan and Ready, 1989). Blocking N signaling results in dramatically impaired eye growth and phenotypes are usually too dramatic to reliably analyze ommatidial subtype specification (Baker et al., 1990). Two different approaches were therefore chosen to assess N loss-of-function. First a dominant negative form of Notch, lacking the intracellular domain, was ectopically expressed in developing PRs, using GMR-GAL4 (LGMR > N^{DN}). Notch loss-of-function phenotypes have been reported for this construct, when over-expressed early during wing or eye development (Kumar and Moses, 2001; Llimargas, 1999). However, LGMR > N^{DN} flies did not have a very strong eye phenotype. Nevertheless, frozen sections through adult eyes were double labeled using antibodies against Rh3 and Rh4 (**Fig 20A**. Expression of both Rh3 (shown in red) and Rh4 (shown in cyan) were found to be indistinguishable from wildtype flies, suggesting that over-expression of this version of dominant negative Notch has no effect on late R7 development. Expression of R8 opsins was also assessed by double labeling frozen sections through adult eyes using antibodies against Rh5 and Rh6 (**Fig 20B**). Expression of Rh5 (shown in blue) and Rh6 (shown in green) were also unaffected, suggesting that over-expression of N^{DN} has no effect on ommatidial subtype specification. These results were confirmed by introducing the opsin-lacZ reporter constructs *rh1*-lacZ, *rh3*-lacZ and *rh4*-lacZ into the LGMR > N^{DN} background and visualizing βGal activity on frozen sections using X-Gal (see material and methods). Expression of *rh1*-lacZ was unaltered, restricted to outer PRs projecting to the Lamina (**Fig 20C**). Expression of *rh3*-lacZ was specific to a subset of R7 cells projecting to the medulla (M) as well as DRA inner PRs (black arrows) and therefore
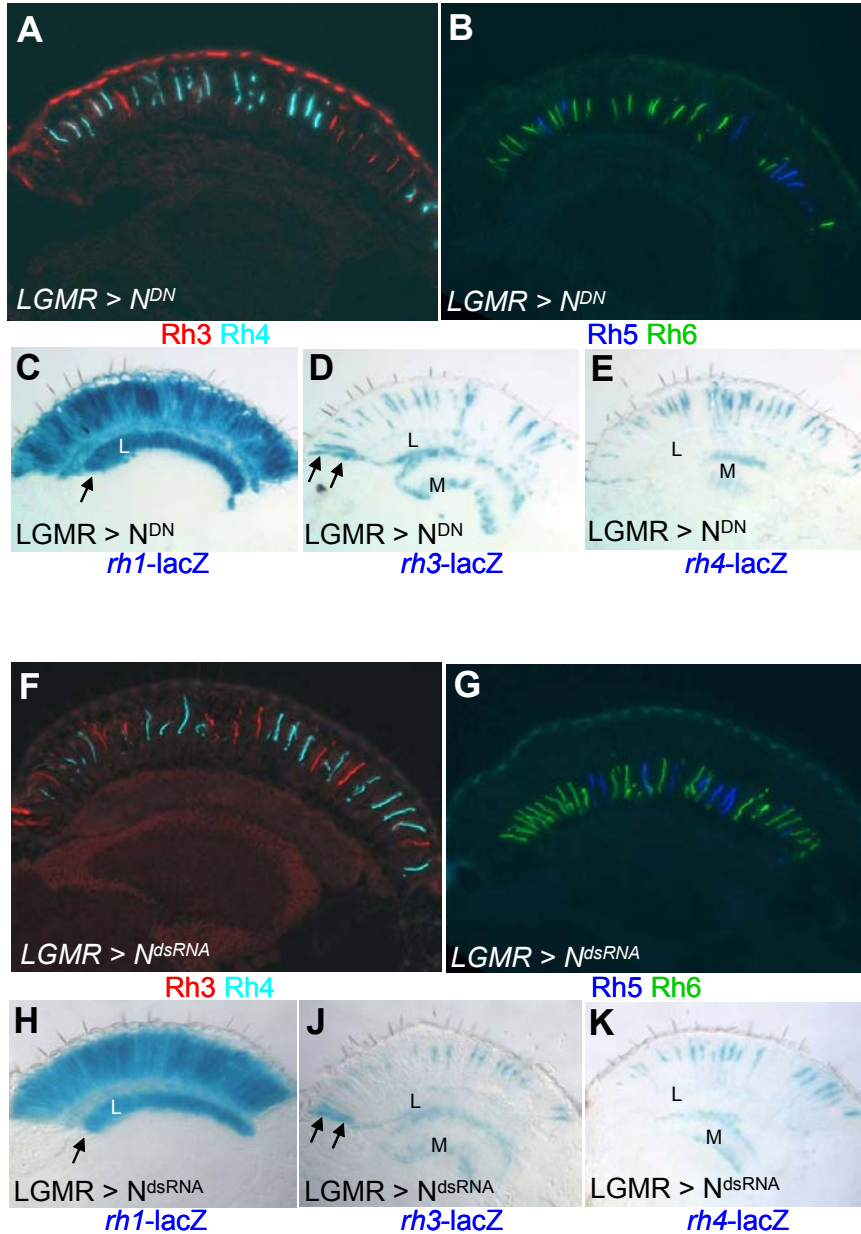
Fig III.3.20 The Notch rerceptor might not necessary for retinal patterning
(A)-(E) Inner PR opsin expression is not affected by dominant negative Notch: Frozen sections through adult heads from flies over-expressing dominant negative N under the control of GMR-GAL4 (LGMR > N^{DN}). Double labeling with antibodies against Rh3 (red) and Rh4 (cyan) revealed revealed no change in R7 opsin expression. (B) Frozen sections through adult heads from LGMR > N^{DN} flies double labeled with antibodies against Rh5 (blue) and Rh6 (green). Both R8 opsins were expressed normally. (C) Frozen sections through adult eyes from LGMR > N^{DN} flies also carrying different opsin-lacZ reporter constructs. No change in *rh1*-lacZ was observed. (D) Expression of *rh3*-lacZ was detectable in **p**R7 cells and in inner PRs of the DRA, as in the wildtype. (E) Expression of *rh4*-lacZ was not affected by dominant negative N.
(F)-(K) RNA interference against N has no effect on inner PR opsin expression: Frozen sections through adult heads from flies over-expressing N^{dsRNA} under GMR-GAL4 (LGMR > N^{dsRNA}). Double labeling with antibodies against Rh3 (red) and Rh4 (cyan) revealed noi change in R7 opsin expression. (G) Frozen sections through adult heads from LGMR > N^{dsRNA} flies double labeled with antibodies against Rh5 (blue) and Rh6 (green). R8 opsin expression was indistinguishable from the wildtype. (H) Frozen sections through adult eyes from LGMR > N^{dsRNA} flies carrying different opsin-lacZ reporter constructs. Expression of *rh1*-lacZ in outer PRs was normal, as βGal expressing fibers were found projecting to the lamina (L) and the medulla (M). (J) Expression of *rh3*-lacZ appeared unaffected on frozen sections through LGMR > N^{dsRNA} eyes as βGal expression was only detectable in **p**R7 cells as well as the DRA, both projecting to the medulla (M). (K) Expression of *rh4*-lacZ was unchanged in LGMR > N^{dsRNA} flies: βGal was detected in a large subset of R7 cells projecting axons to the medulla (M).

indistinguishable from wildtype flies. Finally, *rh4*-lacZ expression was found unaltered (**Fig 20D**). It was therefore concluded that ectopic expression of N^{DN} posterior to the morphogenetic furrow has no effect on opsin expression and therefore ommatidial subtype specification.

As these results suggested that N^{DN} might not be very efficient in developing PRs, another dominant negative construct was tested. In this case, double stranded *notch* RNA was produced under the control of GAL UAS sites (UAS-N^{dsRNA}), leading to the hydrolysis of *notch* mRNA by RNA interference (RNAi). Behavioral loss-of-function phenotypes have also been reported for this construct when mis-expressed (Presente et al., 2002). However, LGMR > N^{dsRNA} flies did not have a very strong eye phenotype. Nevertheless, frozen sections through adult eyes were double labeled using antibodies against Rh3 and Rh4 (**Fig 20F**). Expression of Rh3 (shown in red) and Rh4 (shown in cyan) was found to be unaffected by N^{dsRNA}. Similarly, no phenotype was observed for R8 opsion (Llimargas, 1999) expression (**Fig 20G**). Expression of Rh5 (shown in blue) and Rh6 (shown in green) was identical to the wildtype. These negative results were again confirmed by introducing the opsin-lacZ reporter constructs *rh1*-lacZ, *rh3*-lacZ and *rh4*-lacZ into the LGMR > N^{dsRNA} background and visualizing βGala activity on frozen sections using X-Gal. Outer PRs were unaffected by over-expression of N^{dsRNA}, as expression of *rh1*-lacZ was indistinguishable from the wildtype (**Fig 20H**). Similarly, expression of *rh3*-lacZ (**Fig 20J**) and *rh4*-lacZ (**Fig 20K**) was unaltered. Therefore, over-expression of different dominant negative Notch constructs in developing PRs does not result in any phenotype.

It was therefore concluded from these experiments that, while activating the N pathway is sufficient to induce expression of *rh4*, dominant-negative constructs fail to produce opsin phenotypes. Over-expression of dominant negative Notch might have been induced late enough for initial specification of R7 to occur. Later events, however, like ommatidial subtype specification might not depend on the Notch receptor itself. A clear role for N signaling in specifying **y** ommatidia therefore remains to be shown.

IV. DISCUSSION

Homothorax provides new insights into PR development

It was shown here that the transcription factor Homothorax specifies those PRs that provide input to the polarization compass by distinguishing them from prospective color-sensitive PRs. With the onset of pupation, the inner PRs R7 and R8 along the dorsal rim specifically turn on expression of Hth and maintain it through adult life (**Fig 1A**). This late onset of Hth expression in DRA ommatidia is particularly interesting since a gradient of PR maturation still exists at these early pupal stages: ommatidial clusters have continuously been recruited in the MF progressing along the A/P axis and therefore, differ in age by several days (for review: (Wolff, 1993). It is unclear why specification of DRA ommatidia by Hth does not occur immediately posterior to the MF, especially as the morphogen Wg that is able to induce it is already expressed in the peripodial membrane at the dorsal and ventral poles of the imaginal disc (Treisman and Rubin, 1995). Additional temporal triggers such as the pulses of ecdysone occurring at the onset of metamorphosis might therefore be necessary to induce Hth expression and consequently the important morphological and physiological changes in DRA inner PR cells. The ecdysone receptor (EcR) of *Drosophila* is a member of the large superfamily of ligand-activated nuclear receptors (for review: (Thummel, 1996). The role of both EcR and its hetero-dimerization partner RXR (*ultraspiracle*) in early eye development has been studied in some detail (Koelle et al., 1991; Oro et al., 1990). However, a possible riole in later events like DRA specification remains to be tested. Although *wg* pathway activation was shown to have a strong DRA inducing effect throughout the dorsal eye, all attempts to demonstrate specification of DRA inner PRs in direct response to the Wg morphogen failed (Wernet and Desplan, 2004). The DRA developed normally in mutants lacking Wg receptors (Fz + DFz), cytoplasmic *wg* pathway transducers (*dsh*) or transcriptional effectors (*dTCF*). These results can be explained by two alternative hypothesis (**Fig 1B**). The possibility remains that Wg directly induces the DRA fate in inner PRs at the dorsal rim, by using a different receptor / signal

transduction system (dashed line). For instance, the transmembrane protein Derailed (*drl*) has recently been shown to act as a Wnt receptor in the developing embryonic nervous system of *Drosophila* (Yoshikawa et al., 2003). Employment of different signal transduction cascades by Drl and Fz/DFz would therefore explain the lack of DRA-phenotypes in *dsh* (-/-) as well as LGMR > *tcf*[DN] mutant backgrounds. However, as all Wg effects on early eye development (repression of eye growth, establishment of ommatidial polarity) have been shown to be dependent on the Fz/DFz receptors, it remains unclear why DRA specification would act through a different system. Alternatively, the DRA-inducing effect of Wg can be explained by the deployment of a secondary signal. According to this hypothesis, expression of a second diffusible signal (X) would be induced by Wg in the head cuticle. Diffusion of this factor into the developing eye would therefore be responsible for DRA development downstream of *wg*. This model certainly appears more complicated and less likely due to the current lack of precedents. However, cell non-autonomous inductive effects downstream of both *wg* and *Arm* have now been reported to influence cell fate determination at the periphery of the fly retina, including the DRA (Tomlinson, 2003).

Two genes expressed in developing PRs were shown to play an important role in the specification of DRA ommatidia. Expression of both the *Iroquois* complex *IRO-C* and *optomotorblind* (*omb*) was shown to be restricted to either dorsal (*IRO-C*) or marginal (*omb*) PRs (Tomlinson, 2003; Wernet et al., 2003). Combination of the positional information provided by these two genes therefore seemed an adequate strategy for restricting the generation of DRA ommatidia to the dorsal rim of the eye. Although the *IRO-C* genes have been suggested to act exclusively in undifferentiated cells anterior to the MF (McNeill et al., 1997); (Heberlein et al., 1998), a later role during ommatidial rotation of developing PRs posterior to the MF has been suggested (Cavodeassi et al., 1999). The data presented revealed that *IRO-C* genes indeed act as selector genes to specify the dorsal compartment of the developing eye, by fulfilling at least two typical features proposed for such selector genes: persistence of expression and induction of transformations when mis-expressed in the ventral compartment. It
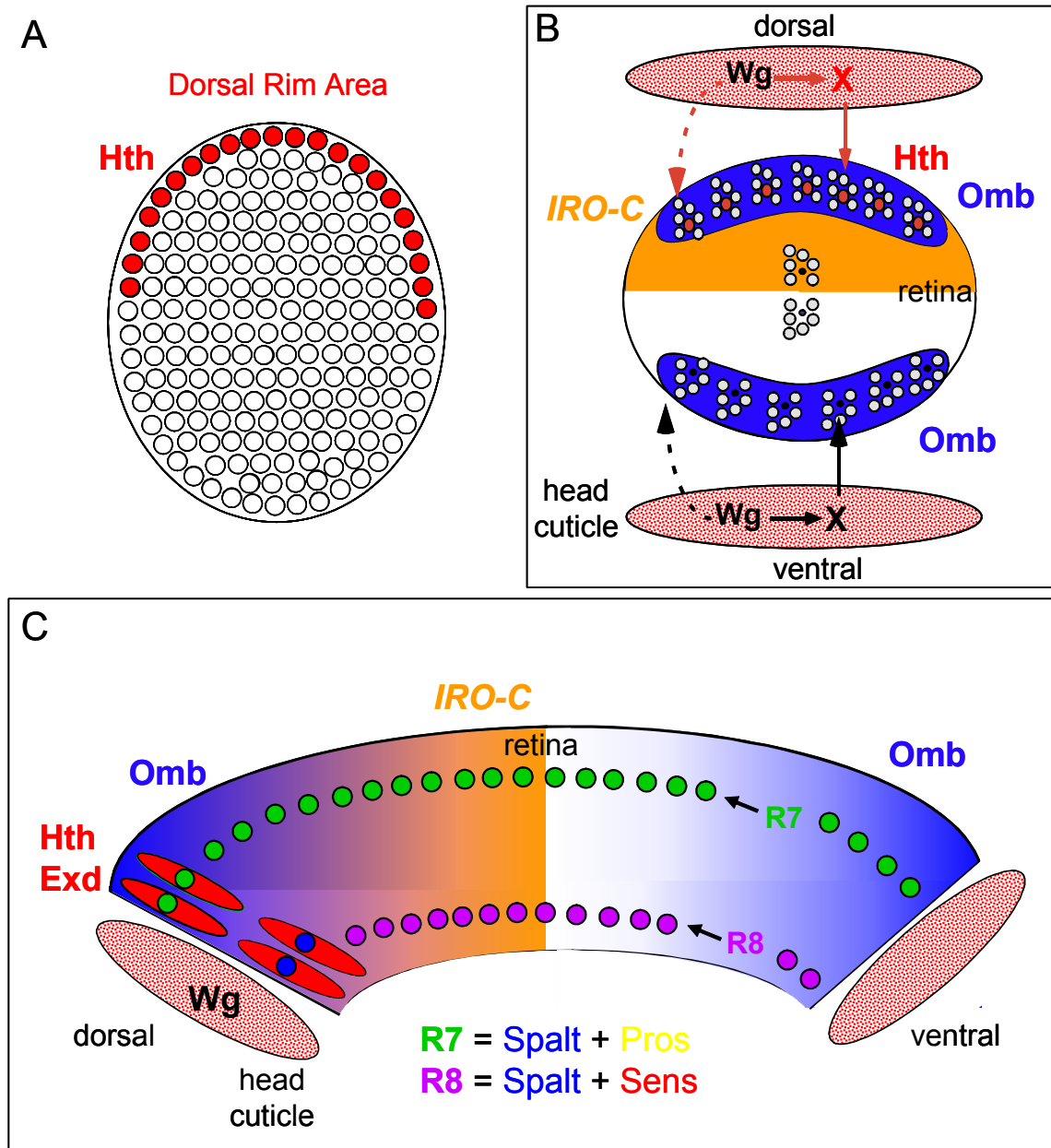
Fig IV.1: Overview over the specification of DRA ommatidia

(A) Schematic representation of a developing retina (dorsal is up). DRA ommatidia (red) are always found in one or two rows along the dorsal rim.

(B) The DRA develops in response to *wg* signaling and requires positional information. The diffusible morphogen Wingless (Wg) is expressed in the head cuticle, but not in the retina. It is not clear whether Wg directly (dashed arrow) induces DRA ommatidia (symbolized by a red inner PR with enlarged rhabdomere diameter) or whether a second diffusible Factor (X) gets activated downstream of *wg* (straight arrow). Ommatidia at the ventral rim do not choose the DRA fate (symbolized by blue inner PRs with a small inner PR rhabdomere diameter) as they lack expression of the dorsal selector gene complex *IRO-C* (orange). Additional positional information is provided by *omb* (blue) expressed in photoreceptors at the dorsal and ventral eye margins.

(C) Inner PR cell types in the DRA. Schematic representation showing a cross section through an adult retina (dorsal to the left). The iner PR marker Spalt (Sal) is specifically expressed in all R7 and R8. In R7 cells, Sal is co-expressed with Prospero (Pros) within and outside of the DRA (red cells). In R8 cells outside of the DRA, Sal co-localizes with Senseless (Sens). IN the DRA however, Sens is specifically excluded from the DRA, resulting in the unusual DRA R8 cells type (blue nuclei). Wingless (Wg) is still expressed both in the dorsal and ventral head cuticle. IRO-C expression is specific to the dorsal compartment in the adult, and omb expression is specific to the dorsal and ventral poles.

was shown that expression of the *IRO-C* reporter rF209 persists at very low levels during pupal stages before returning to high levels in adults. One possible explanation for such transient down-regulation could be that high levels of *IRO-C* genes are toxic for the developing PRs. Indeed, massive cell death was observed when either Araucan, Caupolican or Mirror were over-expressed under the control of strong GAL4 drivers. However, over-expression at weaker levels resulted in the formation of 'ventral rim areas'. The *IRO-C* complex therefore provides crucial positional information to the developing ommatidia. The exact role of the *omb* locus in this process remains more obscure. In the eye imaginal disc, as well as in the developing optic lobes, *omb* expression is induced upon activation of the *wg* pathway. Expansion of DRA ommatidia and Hth expression in the *omb* gain-of-function mutant QUADROON (see below) suggests a role of Omb in DRA development upstream of Hth. However, neither loss nor gain of *omb* resulted in DRA phenotypes. The interplay between *wg*, *IRO-C* and *omb* therefore remains to be described in more detail.

The role of Hth in DRA development represents a unique example illustrating how late PR differentiation events specify one of the three ommatidial subtypes. Furthermore, it provides evidence that establishment of ommatidial subtypes in *Drosophila* is achieved fairly late by shaping the different PR cell fates using consecutive determination steps. Different PR cell types can therefore be identified by the combination of transcription factors they express (**Fig 1C**). In a simple model, basic PR cell fate decisions (i.e. determination of the 8 types of PRs) occur early during third instar larval stage. The distinction between inner and outer PRs is controlled by the *spalt* (*sal*) complex (*salm* and *salr*) and is believed to occur shortly after, as Sal expression is already detectable in developing larval R7 and R8 of the eye imaginal disc (Domingos et al., 2004; Mollereau et al., 2001). Loss of both *salm* and *salr* results in transformation of adult inner into outer PRs: The inner PR rhodopsin genes (*rh3-rh6*) are replaced by the outer PR *rh1,* although most axons still maintain their projections to the medulla (Mollereau et al., 2001). Following this specification of inner PRs by Sal (shown in blue), R7 and R8 are then further distinguished from

each other by expression of Prospero (yellow) and Senseless (red), respectively. This segregation of inner cell fates occurs early during larval stages and Pros as well as Sens have been shown to be lost in Sal (-/-) mutant tissue, confirming their role downstream of Sal (Domingos et al., 2004). The specification of DRA ommatidia appears to be a specification event occurring significantly later. We found that the onset of Salm expression precedes Hth by several days: While Sal is expressed early in both R7 and R8 of all ommatidia, Hth expression in the DRA is only initiated during early pupation, and remains co-expressed with Sal until adulthood. It appears that in a first step during 3rd instar larval life, R7 and R8 cells commit to the inner PR fate by expressing Sal. Only these cells are then competent to face another cell fate decision at the beginning of pupation: the inner PRs of ommatidia close to the dorsal rim come under the influence of a DRA inducing signal that includes Wg and start expressing Hth. In all other ommatidia the inner PRs develop into two different pairs of color-sensitive PRs in a stochastic manner. Consistent with this model, the outer PRs, which do not express Sal, are not transformed by forced expression of Hth, and Hth expression is lost in Sal (-/-) mutant eyes.

Adult R7 cells located in the DRA express the combination of the three crucial transcription factors Sal, Pros and Hth. This situation can be viewed as a recapitulation of the cell fate decisions these cells have taken by choosing the inner PR fate (Sal), the R7 fate (Pros) and the DRA fate (Hth). It must be pointed out that both DRA inner PRs always express the **p**R7 opsin Rh3 and therefore manifest a closer molecular resemblance to R7 cells than to R8. Persistence of Pros expression in DRA R7 cells therefore suggests that these cells represent true R7 cells that have adopted the additional cell fate decision of becoming DRA inner PRs. The situation of R8 cells in the DRA is significantly different, as DRA R8 cells specifically exclude the R8 marker Sens and do not express Pros. Adult DRA R8 cells therefore express the unusual combination of the markers Sal (inner PRs) and Hth (DRA). Ectopic over-expression of Hth is sufficient to induce DRA ommatidia and leads to a complete repression of Sens in all R8 cells. It appears therefore that loss of Sens expression is essential for DRA R8 cells to

escape the typical color-sensitive **p** and **y** R8 cell fates and for switching to the DRA R8 fate with its R7-type *rh3* expression. This is in agreement with the strong gain-of-function phenotype observed for Sens, when ectopically over-expressed: As Sens very potently activates *rh6* expression and represses *rh3*, exclusion from the DRA by Hth appears to be an efficient way to push these cells away from the ordinary R8 cell fate. It seems likely that a transcriptional complex involving Hth and Exd directly represses Sens expression. Furthermore, based on the dissection of the *rh3* promoter, it has been proposed that different factors might be responsible for expression of Rh3 in **p**R7 and in the DRA. However, promoter deletion analysis has not yet proven this hypothesis. Nevertheless, the Hth/Exd transcription complex also seems an attractive candidate for the activation of *rh3* expression in DRA R8 cells.

Taken together, the inner PRs R7 and R8 get specified by Sal, Pros and Sens and serve as color sensors throughout the main part of the eye. However, a sub-population at the dorsal rim takes the crucial decision to form highly specialized detectors of e-vector polarization by gaining Hth expression. As Hth expression results from combining *wg* pathway activity with the positional information provided by *IRO-C* and *omb*, formation of DRA ommatidia therefore depends uniquely on their location within the retina.

DRA ommatidia as a model system for w*ingless* pathway activity

DRA ommatidia were the only ommatidial subtype discovered based on morphological criteria (Wada, 1974). Since their discovery in *Calliphora*, DRA ommatidia have also been described morphologically in a multitude of other insect species (Labhart and Meyer, 1999). Furthermore, the axon projection pattern of DRA inner PRs has been described and a detailed model has been built describing how polarization-sensitive PRs and higher order POL neurons integrate e-vector information in order to improve navigation of the animal (Hardie, 1984; Labhart, 1988; Labhart and Meyer, 2002). In *Drosophila*, the DRA forms a band of 1-2 ommatidial rows along the dorsal head cuticle, spanning the whole dorsal compartment from equator to equator (**Fig 2A**, top). Cloning of the

rhodopsin genes has allowed an even more detailed description of DRA ommatidia in *Drosophila*, like their unusual monochromatic rhodopsin expression in inner PRs (Fortini and Rubin, 1990; Fortini and Rubin, 1991). However, development of DRA ommatidia was not understood at all. Using *Drosophila* genetics, the discovery of Hth's role in DRA development has now allowed a detailed analysis of the development of DRA ommatidia, revealing the genes and signaling pathways involved in their specification (Tomlinson, 2003; Wernet et al., 2003).

The homeodomain transcription factor Hth is both necessary and sufficient for DRA development. Ectopic over-expression of Hth in all developing PRs lead to a transformation of the whole retina into DRA ommatidia (**Fig 2B**, top left). Ommatidia are completely transformed into polarizartion sensors in these LGMR > hth flies, both molecularly (Rh3 expression, Sens exclusion from DRA R8) as well as morphologically (inner PR rhabdonmere diameter, elevated nuclear position of DRA R8). This is particularly interesting, as axon projections of all inner PRs to the medulla remain unchanged. In the wildtype, inner PRs form DRA ommatdia always project to the dorsal-most part of the medulla, while the rest of the medulla receives information relevant for color discrimination from the remaining non-DRA ommatidia. It is therefore tempting to speculate how the information coming from ectopic DRA ommatidia gets computed in the brain of LGMR > hth flies. Due to the PR-specificity of the GMR driver used, mis-expression of Hth should not have any effect on brain development. It is therefore possible that e-vector information is interpreted as color by these flies. Behavioral paradigms have been set up for different dipterans to investigate behavioral responses to polarized light (von Philipsborn and Labhart, 1990; Wolf et al., 1980). Although color discrimination has been proven to be a rather difficult behavior to study, behavioral paradigms also exist and are currently being refined for *Drosophila*. It will therefore be extremely interesting to study the behavior of GMR > hth flies, under different light conditions.

An important new role for the dorsal selector genes of the *IRO-C* complex was revealed in developing PRs posterior to the morphogenetic furrow, by using

the DRA as a model system. Strong expression of *IRO-C* exists in all adult dorsal PRs and ectopic over-expression of any *IRO-C* member using weak GMR-GAL4 drivers gives rise to an unusual 'ventral rim area'. A circular band of DRA ommatidia was now observed in these sGMR > *ara* flies (top right). Therefore, during early pupal stages, low levels of the dorsally expressed *IRO-C* genes might be employed to restrict formation of DRA ommatidia to the dorsal half of the eye rim. These results further indicate that all other factors required for DRA induction are also present at the ventral rim and that positional information provided by *IRO-C* is the only component missing there. However, loss of all three *IRO-C* genes does not result in a loss of the DRA. One possible explanation is that there exists a fourth unknown factor which is functionally redundant with the *IRO-C* genes. Alternatively, the deficiency used to eliminate activity of the three *IRO-C* genes might bear some residual activity. Recent results published on late dorsoventral eye development support this second hypothesis (Tomlinson, 2003). The *IRO-C* system is a striking example of how genetic modules are combined to give rise to localized morphological structures. It is possible that the more restricted DRAs of different insect species were developed by slight changes in the *IRO-C* expression pattern.

Activation of the Wg pathway has a strong DRA inducing potential throughout the dorsal half of the eye. DRA ommatidia are dramatically expanded in flies ectopically activating the *wg* pathway in developing PRs (center left). Strikingly, formation of DRA ommatidia is limited to the *IRO-C* compartment in LGMR > ArmS10 flies. This result supports an important role of the *IRO-C* complex in transducing the effects of *wg* pathway activity onto ommatidial development. Interestingly, early larval expression of the *IRO-C* complex itself had been shown to be activated by the *wg* pathway. In developing PRs, however, *IRO-C* expression is not affected by *wg* pathway over-activation. The transient down-regulation observed for the *IRO-C* reporter rF209 at pupal stages therefore remains mysterious as the signaling mechanism driving re-expression of *IRO-C* remains unknown. It is possible, however, that dorsal-specific expression of *IRO-C* genes is epigenetically locked using modification of the local chromatin and
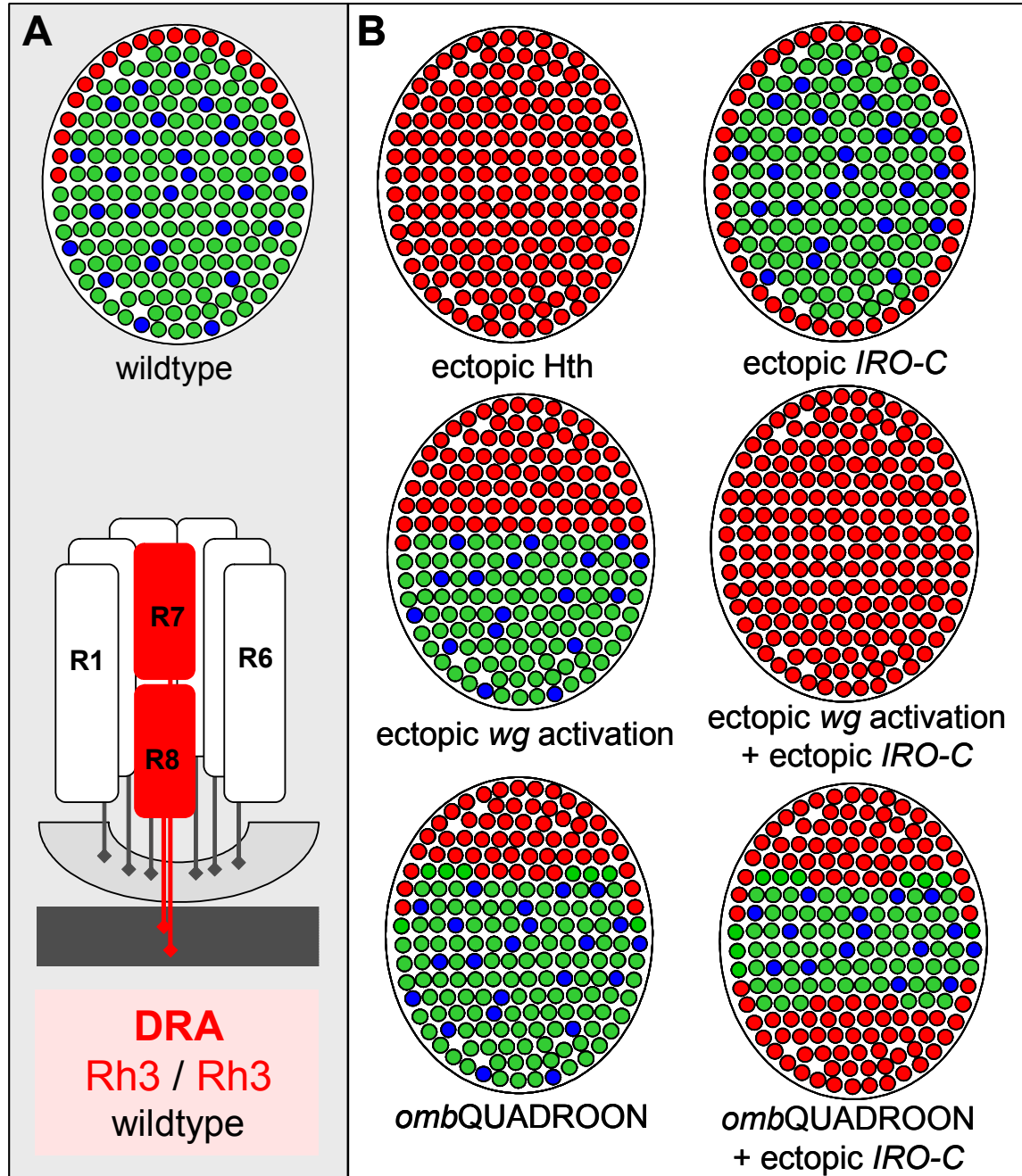
Fig IV.2. DRA ommatidia as a model system for w*ingless* pathway activity

(A) The wildtype DRA. Top: Schematic of the ommatidial pattern (dorsal is up). DRA ommatidia are found localized as a band along the dorsal head cuticle (red) while pale ommatidia (blue) and yellow ommatidia (green) are distributed stochastically , and un-evenly (30:70) throughout the rest of the retina. Bottom: Drawing of a wildtype DRA ommatidium. DRA ommatidia manifest a dramatically enlarged rhabdomere diameter as well as monochromatic Rh3/Rh3 expression in both inner PRs.

(B) Different mutant backgrounds affecting *wg* signaling lead to an expansion of DRA ommatidia. Top left: ectopic over-expressionj of Hth in all PRs leads to the expansion of DRA ommatidia throughout the whole eye. Top right: Ectopic *IRO-C l*eads to the induction of an atypical 'ventral rim area', suggesting all other factors required for DRA formation are prent at the ventral rim. Center left: Over-expression of activated Armadillo (ArmS10) activates the wg pathway in al PRs and leads to the expansion into the whole dorsal compartment, supporting the requirement of *IRO-C*. Center right: Co-over-expression of both ArmS10 and *IRO-C* leads to a phenotype identical to the Hth gain-of-function, suggesting that combination of high wg activity and *IRO-C* are sufficient to induce DRA development. Bottim left: DRA ommatdia are expanded in QUADROON gain-of-function alleles of the optomotorblind (*omb*) locus. During early eye development, *omb* expression had previously been shown to be be activated by *wg* signaling. Bottom right: Expansion of the 'ventral rim area' in *omb*QUADROON mutants ectopically over-expressing *IRO-C*.

that the expression strength gets merely modulated over time. Only ommatidia located within the *IRO-C* expression domain are competent to respond to the *wg* signal. Therefore, ectopically providing both *IRO-C* and *wg* pathway activation induce DRA ommatidia throughout the eye (center right). Over-expression of both ArmS10 and *ara* posterior to the morphogenetic furrow was sufficient to induce Hth expression in inner PRs throughout the retina. This phenotype is strikingly similar to the ectopic expression of Hth itself. Combination of the Wingless and *IRO-C* signals therefore appears to be sufficient to restrict specification of DRA ommatidia at the right place in the eye.

Another mutant affecting the specification of DRA ommatidia provides further insight into the regulatory network involving *wg* and *IRO-C* (Tomlinson, 2003). The *Quadroon* phenotype is due to a gain-of-function in the *optomotor-blind* (*omb*) locus (Kopp and Duncan, 1997). *omb* encodes a T-box transcription factor and plays an important role in the development of *Drosophila* appendages as well as in the establishment of planar polarity in the abdomen (Grimm, 1996; Lawrence, 2002). omb*Quadroon* flies show a dramatic expansion of DRA ommatidia which is very reminiscent of over-activation of the *wg* pathway, although the DRA does not quite extend through the entire dorsal eye (bottom left; Tomlinson 2003). *omb* might therefore play an important role in transducing the effect of *wg* onto the DRA ommatidia. In the wildtype, *omb* expression is limited to the dorsal and ventral poles of the eye. It appears therefore that Omb is used to limit the extent of the DRA to only few ommatidial rows. Expression of *omb* itself is induced by the *wg* pathway in developing PRs. However, *omb* expression is not affected in LGMR > ArmS10 flies, suggesting that *omb* expression has to be induced early during larval stages. Therefore, DRA expansion in LGMR > ArmS10 flies occurrs independently of *omb*, suggesting that boosting *wg* activity overcame the requirement of Omb. This points towards a model where *w*g-dependent expression of Omb in the most marginal PRs is used to raise responsiveness of these cells to the *wg* pathway activity. This effect of *omb* is particularly interesting from an evolutionary standpoint, as modulation of the *omb* activity domain (as seen in *omb*QUADROON mutants) provides yet

another possibility to achieve the wide variety of DRA morphologies observed in different insect species. However, only in the *IRO-C* compartment, this mechanism results in the specification of a limited number of DRA ommatidia. The requirement of *IRO-C* for the *omb*-mediated induction of DRA ommatidia was indirectly confirmed by ectopically providing *IRO-C* in an *omb*QUADROON mutant background. In these flies, both the DRA as well as the *IRO-C* induced 'ventral rim area' are dramatically expanded (top right). This clearly demonstrates that adding the positional information of *IRO-C* to the marginal information provided by Omb is sufficient to specify DRA ommatidia.

Taken together, the DRA ommatidia represent a powerful new model system for further study of the *wg/*wnt signal transduction pathway in greater detail.

The localized specification strategy of DRA ommatidia

DRA ommatidia form in one or two rows at the dorsal rim of the *Drosophila* eye (**Fig 3A**, left). The homeodomain transcription factor Hth was is a crucial key regulator both necessary and sufficient to induce DRA development in inner PRs. Through combination of positional information provided by the *IRO-C* complex and the *omb* locus, Hth expression is specifically induced in inner PRs of those dorsal ommatidia exposed to the highest levels of *wg* pathway activity (**Fig 3A**, right). Based on this model, any Spalt-positive inner PR located within close proximity to the dorsal head cuticle is expected to autonomously choose the Hth-expressing DRA fate. However, cell fate decisions of inner PRs from non-DRA ommatidia are tightly linked between R7 and R8 (Chou et al., 1999; Papatsenko et al., 1997). Analysis of different mutant background suggests that R7 cells instruct the underlying R8 cells to always choose the fate belonging to the same subtype (**p** or **y**). In order to build a complete mechanistic model for the localized specification strategy used for DRA ommatidia, the individual cell fate decisions of inner PRs can be analyzed in the DRA. Two simple mutant backgrounds that affect the initial cell fate specification of individual inner PRs were used to reveal the nature of the underlying instructive processes. For instance, in ommatidia
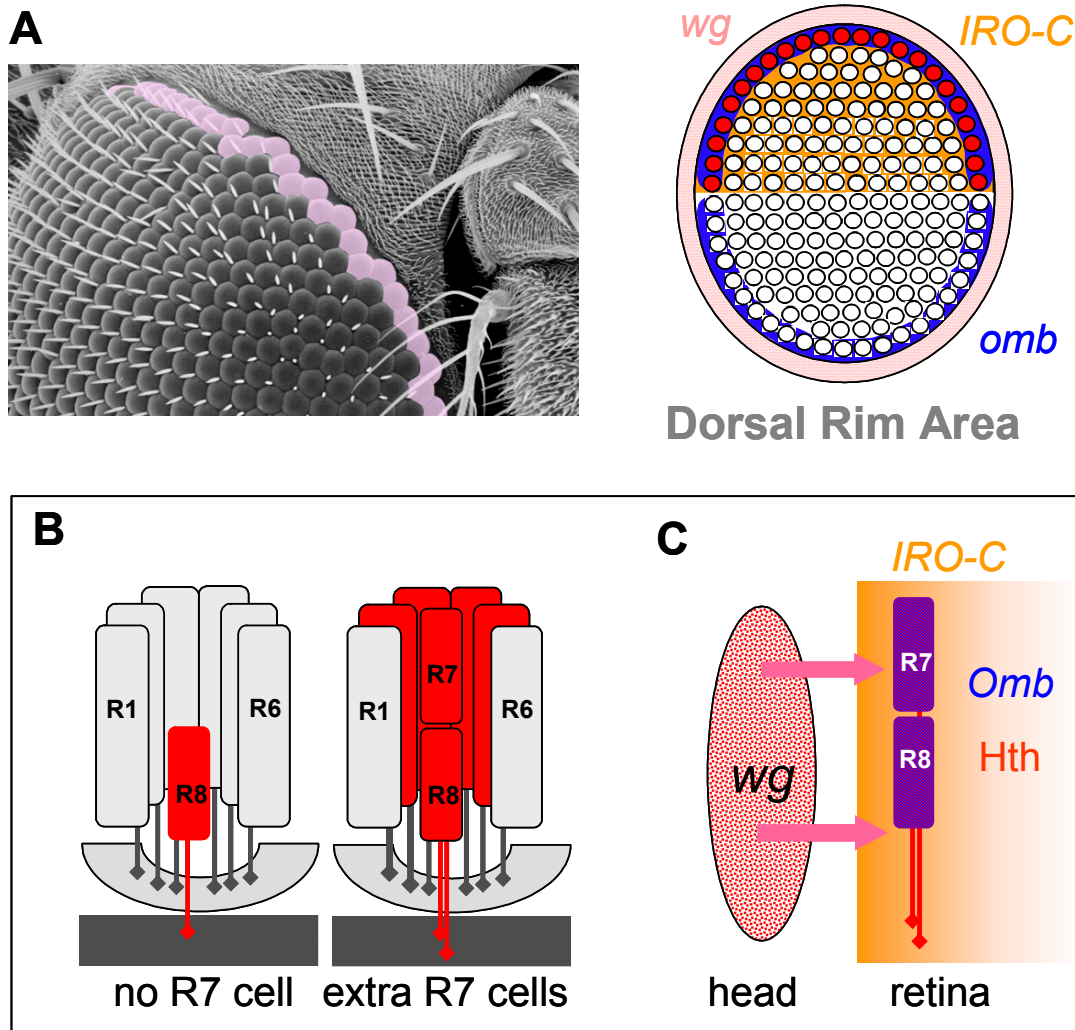
Fig IV.3: The localized specification strategy of DRA ommatidia

(A) Left: Scanning electron micrograph depicting the fronto-dorsal part of an adult Drosophila eye (kindly provided by T. Labhart). DRA ommatidia are arbitrarily highlightened in pink. Right: Schematic representation of a developing retina (dorsal is up). DRA ommatidia (shown in red) seem to form where expression of the dorsal selector gene complex IRO-C (orange) overlaps with the marginal expression domain of *omb* (blue).

(B) Cell fate decisions of individual inner PRs located in the DRA. The DRA develops normally in sevenless (sev) mutants lacking all R7cells, indicating that R8 does not require instruction by R7 cells in order to choose the Hth-expressing DRA fate (shown in red). Specification of extra R7 cells using different approaches (ectopic Ras pathway activation, loss of seven up) always results in super-numerary Hth-positive cells (shown in red) in the DRA, indicating that R7 cells also can autonomously choose the DRA fate when located close to the dorsal head cuticle.

(C) Model proposed for specification of DRA ommatidia. Ommatidia get recruited into the DRA fate simply based on their location close to the head cuticle. Only marginal ommatidia in the dorsal half receive both high wg signaling levels and the positional information of IRO-C. Wg-dependednt expression of Omb in few marginal ommatidia might be required to limit the extent of the DRA by specifically enhancing their responsiveness to Wg.

lacking R7 cells (*sevenless*), R8 always chose the DRA fate correctly, as long as they were located in close proximity to the dorsal head cuticle (**Fig 3B**, left). Reciprocally, extra inner PRs, induced by different genetic manipulation (mutation in *seven-up*, *rough* or by constitutively activating the Ras pathway*)* always acquire the DRA fate when induced at the dorsal rim (**Fig 3B**, right).

186

Therefore, It appears that both inner PRs can choose autonomously to acquire the DRA fate when located close to the dorsal head cuticle. These observations fit very well with a localized specification model involving a diffusible signal, like Wg, emanating from the developing dorsal head and reaching both R7 and R8 independently. (**Fig 3C**).

However, it must be noted that the DRA develops normally when both Wg receptors *Fz* and *DFz2*, the crucial intracellular signal transducer *dsh* or the transcriptional effector *TCF* are inactivated in PRs. It is possible that low levels of wild type protein could persist long enough for DRA development to proceed in homozygous *Fz/DFz2* or *dsh* clones generated with *ey*-flip or Wg could act through a different receptor pathway like the Derailed receptor (Yoshikawa et al., 2003). Alternatively, another diffusible factor could act in parallel with the Wg/Fz pathway to induce the DRA. Such a factor could even act downstream of Wg as a 'relay signal'. This certainly appears more complicated and less likely due to the current lack of precedents. However, cell non-autonomous inductive effects downstream of both *wg* and *Arm* have now been reported to influence cell fate determination at the periphery of the fly retina (Tomlinson, 2003). This data indeed suggests that Wg might not directly induce the DRA fate in R7 and R8, but rather require a second, diffusible downstream factor.

Taken together, specification of DRA ommatidia follows a strategy which is fundamentally different from that used for specification of **p** and **y** ommatidia. Inner PRs choose the DRA fate without communication between R7 and R8. Instead, they acquire expression of Hth solely based on their location within the *IRO-C / omb* territory. However, the exact nature of the diffusible signal inducing the DRA fate as well as the signal transduction machinery involved remain to be cleared up.

Loss of Homothorax and odd-coupled ommatidia

Inactivation of Hth function results in the transformation of the DRA into atypical color-sensitive ommatidia with unusual odd-coupled inner PR opsin expression. Over-expression of a dominant negative form of Hth (*hth^{HM}*) leads to

the mis-specification of DRA ommatidia, based on loss of the typically enlarged inner PR rhabdomere morphology as well as loss of Rh3 expression in R8 (**Fig 4A**). Interestingly, R8 cells in the DRA of LGMR > *hth*^{HM} flies always express Rh6, while R7 maintain expression of Rh3 (**Fig 4B**, left). Expression of Rh4 and Rh5 was never detected at the dorsal rims of flies over-expressing *hth*^{HM}. This suggests that loss of Hth function does not allow the full program of color PR specification to be activated at the dorsal rim. In the dorsal-most ommatidia of GMR>*hth*^{HM} flies, **p** and **y** subtypes are not distinguished stochastically as R7 cells always choose the **p**R7 fate, while R8 cells choose the opposite **y**R8 fate. Expression of Rh6 in R8 is particularly interesting, as R8 cells in *sev* mutants choose expression of the same 'ground state' opsin (Chou et al., 1999; Papatsenko et al., 1997). It appears therefore that in the absence of *hth* function, R8 cells at the dorsal rim do not get properly instructed by the **p**R7 cells and choose the 'naïve' expression of Rh6 instead. This is further explained by the fact that these cells gain expression of the non-DRA R8 marker Sens, which was shown to be sufficient to have a strong inductive effect on *rh6* expression when ectopically expressed. Maintenance of *rh3* expression in R7 cells at the dorsal rim of LGMR > *hth*^{HM} eyes, however, was unexpected. Since Rh6 was found to be the default state in R8 cells, *rh4* had previously been suggested by extrapolation to be the ground state in R7 (Chou et al., 1999). However, it is unclear why R7 cells at the dorsal rim should actively acquire the **p** fate in absence of *hth* function and then be unable to transmit this cell fate decision to the underlying R8 cell. Instead, these results suggest that Rh3 might in fact represent the ground state opsin expressed in R7 lacking the appropriate signals for terminal differentiation. This hypothesis is supported by the loss-of-function phenotype described for the gene *spineless (ss)*. Loss of *ss* results in the complete loss of *rh4* expression and the simultaneous expansion of *rh3* into all R7 cells (see below). As *ss* is expressed specifically in **y**R7 cells and is sufficient to induce the **y**R7 cell fate, it appears that the 'default state' of R7 cells is indeed *rh3*-expressing **p**R7.
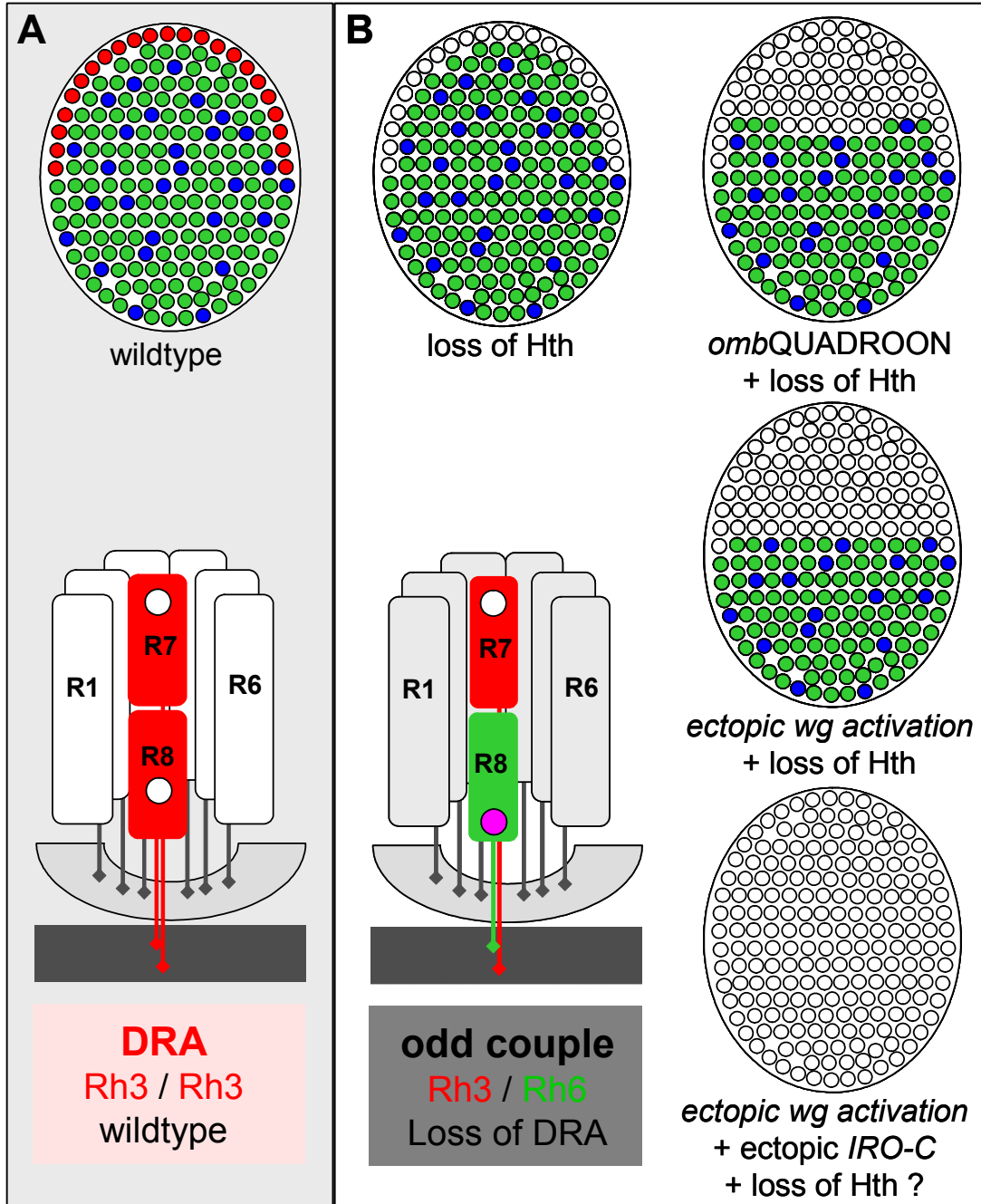
Fig IV. 4: Loss of Homothorax and odd-coupled ommatidia

(A) The wildtype DRA. Top: Schematic of the ommatidial pattern (dorsal is up). DRA ommatidia are found localized as a band along the dorsal head cuticle (red) while pale ommatidia (blue) and yellow ommatidia (green) are distributed stochastically , and un-evenly (30:70) throughout the rest of the retina. Bottom: Drawing of a wildtype DRA ommatidium. DRA ommatidia manifest a dramatically enlarged rhabdomere diameter as well as monochromatic Rh3/Rh3 expression in both inner PRs. The nucleus of DRA R8 cells is located significantly more distal as other R8 nuclei Sens exprerssion is specifically excluded (white circle).

(B) Loss of Hth leads to the formation of odd-coupled ommatidia. Top left and bottom left: Over-expression of dmominnant negative Hth (*hth*HM) leads to a complete loss of DRA morphology. Furthermore, expression of Rh3 is lost in R8. Instead, R6 expands into the DRA R8, resulting in coupled expression of Rh3 and Rh6 within the DRA ommatidia. Sens expression (pink circle) also expands into the nucleus of DRA R8, confirming the loss of DRA fate. Top right: Over-expression of *hth*HM in ombQUADROON mutants leads to the formation of many odd-coupled ommatidia in the dorsal compartment (data not shown). Center right: Co-over-expression of ArmS10 and hthHM leads to the transformation of the whole dorsal eye into odd coupled ommatidia. Bottom right: Triple over-expression of ArmS10, *IRO-C* and *hth*HM should therefore transform the whole eye into odd coupled omatidia.

189

The hypothesis about inner PR opsin ground states was further tested by transforming the whole dorsal half of the eye into odd coupled (Rh3/Rh6) ommatidia. Over-expression of both activated Armadillo and dominant negative Hth (GMR>ArmS10+hth^{HM}) has a dramatic effect on ommatidial specification. All dorsal R7 cells express Rh3 and their underlying R8 cells express Rh6 (right center). Rh4 and Rh5 are never detected in dorsal ommatidia, in these flies. This suggests that ectopic activation of the *wg* pathway directs dorsal ommatidia towards the DRA program, but without Hth function, the DRA program cannot be executed. Rh3 expression is therefore lost in all R8 cells, and odd-coupled ommatidia populate the whole dorsal eye. Based on these findings, it should be possible to create an adult fly eye composed exclusively of odd coupled ommatidia. Over-expression of both activated Armadillo and *IRO-C* is sufficient to induce DRA ommatidia throughout the entire eye. Intruduction of additional hth^{HM} transgenes into a LGMR > ArmS10 + *ara* background should abolish the DRA inducing program downstream of Hth, resulting in all R7 cells expressing Rh3 and Rh6 being the only opsin expressed in R8 (bottom right). Technically, this experiment has not been possible yet, due to the high toxicity of IRO-C genes when mis-expressed at high levels.

Taken together, it appears that the Rh3/Rh6 pair represents the combination of independent R7 and R8 'ground states' upon which PR subtype decisions are imposed: the stochastic choice made by R7 cells outside the DRA is usually linked to communication from these R7 to R8, resulting in coupling of *rh3*/*rh5* in **p** and *rh4*/*rh6* in **y** subtypes. This communication is suppressed in DRA inner PRs even when Hth function is lacking, suggesting that the high levels of wg pathway activity inducing Hth at the dorsal rim might also repress all the subtype decisions of color-sensitive ommatidia, including communication between R7 and R8. Interestingly, ss was found to be incapable of inducing *rh4* expression in DRA inner PRs, when ectopically expressed. Furthermore, ectopic expression of activated Armadillo neutralized *ss* function in the whole dorsal half of the eye (loss of *rh4*), confirming that, in the dorsal eye, high *wg* levels indeed suppress stochastic specification of **p** and **y** ommatidia.

Different default opsins in R7 and R8: Spalt gain-of-function

The *spalt* complex (*sal*) encodes two homologous zinc finger transcription factors (Spalt major and Spalt related) and loss of *sal* results in loss of inner PR identity: based on rhabdomere morphology as well as opsin expression, inner PRs become virtually identical to R1-R6 (Mollereau et al., 2001). Furthermore, inner PR-specific markers like the R7 marker Pros, the R8 marker Sens and the DRA marker Hth are lost in Sal (-/-) eye tissue. However, R7 and R8 still project to the medulla in sal (-/-) mutants, suggesting that inner PRs get initially specified correctly and project their axons to the right layer of the optic lobe, but then fail to mature correctly into adult R7 and R8. Sal also induces important inner PR-like features in R1-6 when ectopically over-expressed. Interestingly, Sal is sufficient to repress *rh1* and to activate *rh3* and *rh6* expression in outer PRs (see below). It appears therefore that mis-expression of Sal specifically induces the two inner PR 'default state' opsins in outer PRs. This observation confirms the hypothesis presented before, that naïve inner PRs expressing Sal, but lacking additional inner PR specification markers (Pros, Sens, Hth, Ss), always choose expression of these two default state opsins. To illustrate this argument, the Sal gain-of-function data will be briefly reviewed.

Expression of Salm becomes specific to R7 and R8 rather early during third instar larval stages. Several rows posterior to the morphogenetic furrow (MF), R8 cells already start co-expressing Sal and Sens (**Fig 5A**). The role of Sal in R8 cells is particularly interesting as the R8 marker Sens was found genetically to be placed both upstream and downstream of Sal: It appears that very early during inner PR specification, Sens plays an important role upstream of Sal in specifying the R8 cell. Loss of Sens results in the loss of inner PRs and therefore the loss of Sal expression. Later, however, Sens is indispensable for the correct maturation of R8 cells, as reflected by its strong ability to activate expression of the R8 default state opsin *rh6*. This late role of Sens has been shown to be dependent on Sal, as late Sens expression is lost in Sal clones. Onset of Sal expression therefore represents an important event during PR development, the transition between PR specification and PR maturation. As R7 cells are the last
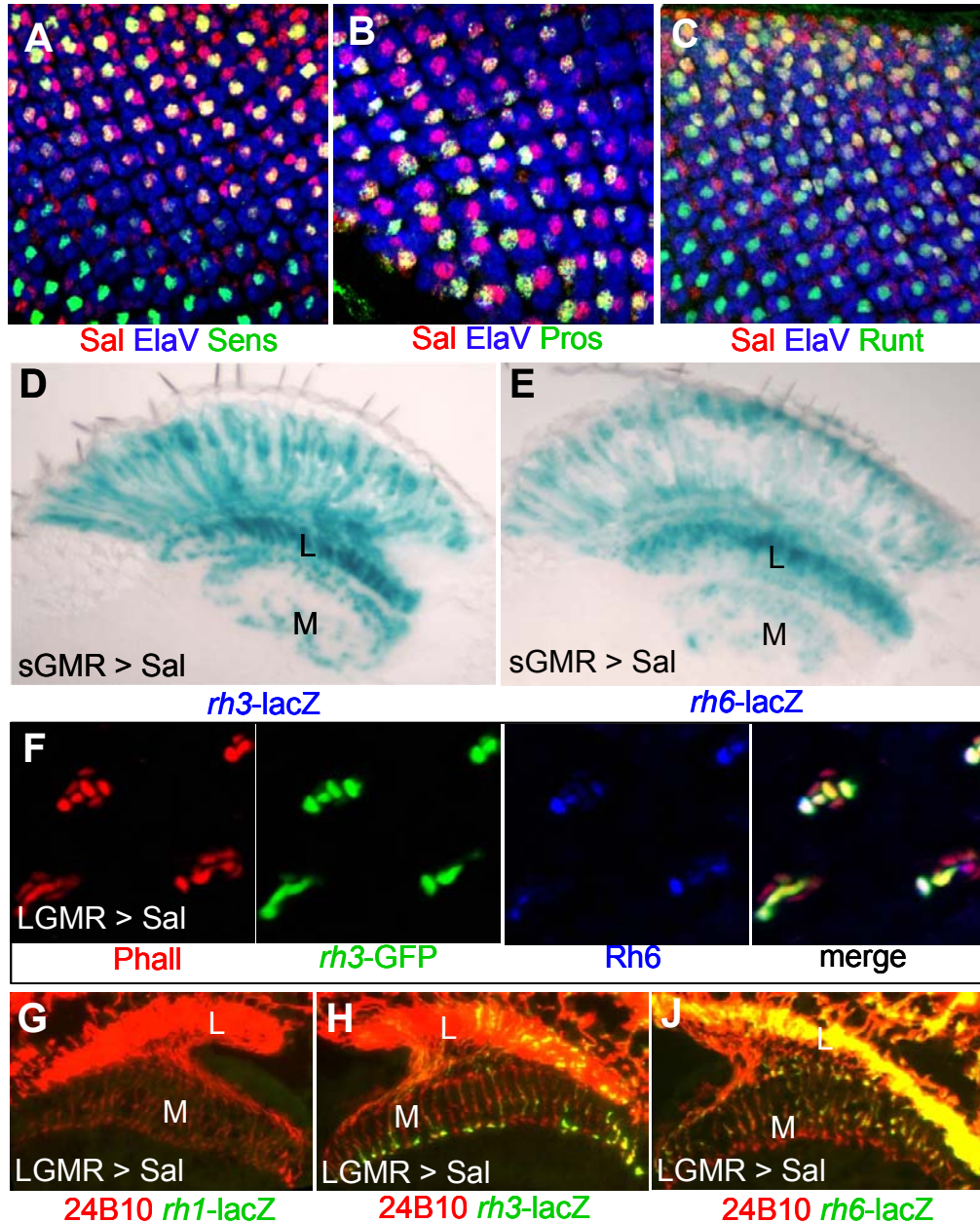
Fig IV.5: Different default opsins in R7 and R8: Spalt gain-of-function

(A)-(C) Summary of Spalt (Sal) expression in larval inner PRs. Eye imaginal disc dissected from wandering third instar larvae and triple stained with antibodies against Sal (red), the R8 marker Sens (green) and ElaV (blue). R8 begins to co-express Sal and the early marker Sens approx. 6 rows posterior to the morphogenetic furrow. (B) Eye imaginal disc triple stained with antibodies against Sal (red), the R7 marker Pros (green) and ElaV (blue). Developiong R7 cells co-express Sal and Pros from the very beginning. (C) Eye imaginal disc triple stained with antibodies against Sal (red), the early inner PR marker Runt (green) and ElaV (blue). Both R7 and R8 (marked by Run) start expressing Sal during larval stages.

(D)+(E) Ectopic Sal specifically expands *rh3* and *rh6* expression. Frozen section through an adult eye from flies ectopically over-expressing Sal in all developing PRs. Expression of the **p**R7 reporter *rh3*-lacZ, stained with X-Gal, is dramatically expanded into all PRs (sGMR > *sal*), with projections to both the lamina (L) and the medulla (M). (E) Expression of the **y**R8 reporter *rh6*-lacZ is also dramatically expanded into all PRs as seen on frozen sections through sGMR > *sal* eyes stained with X-Gal. Projections to both the lamina (L) and the medulla (M) are clearly stained.

(F) Expansion of rh3 and rh6 expression visualized in whole mounted adult sGMR > *sal* retinas. Co-expression of *rh3*-GFP (green), Rh6 (blue) and the rhabdomeric marker Phalloidin (red) is frequently observed.

(G)-(J) Expression of rh1 is completely lost in LGMR > *sal* flies, sup[porting the loss of in outer PR identity. Instead, expression of rh3 and rh6 is expanded into outer PRs as seen by labeling expression of lacZ reporter constructs on frozen sections with

192

cell to be recruited into the ommatidial cluster, these cells co-express Pros and Sal from the very beginning (**Fig 5B**). Recently, the gene *runt* (*run*) has also been reported to play an important role in inner PR development. Run encodes a transcription factor homologous to the Acute Myeloid Leukemia 1 protein (AML-1) and is required for correct segmentation of the early *Drosophila* embryo. Interestingly, early over-expression of Run in all developing PRs results in the mis-projection of outer PR axons into the medulla, suggesting that these cells have acquired an inner PR-like identity. Indeed, Run was found to be specifically expressed in larval inner PRs R7 and R8. However, the onset of Run expression in these cells precedes Sal, resulting in co-expression of Run and Sal only in larval inner PRs in the posterior part of the eye imaginal disc (**Fig 5C**). Based on both the Run gain-of-function phenotype and the expression pattern of Run and Sal, these two proteins could act sequentially in the same process of inner PR development. This hypothesis was tested by ectopically over-expressing Sal in developing PRs, under GMR-GAL4 control. Sal specifically activates expression of *rh3* and *rh6* in outer PRs, while *rh4* and *rh5* are not expanded (**Fig 5D**-**H**). This is particularly interesting as these are the two opsins expressed in inner PRs at the dorsal rim of flies over-expressing dominant negative Hth. Finally, expression of *rh1* was completely lost in LGMR > Sal flies, supporting the model, that the gaining Sal expression was sufficient to repress this terminal marker of outer PRs (**Fig 5J**). It should be noted that axon projection of outer PRs to the lamina was not affected in these LGMR > Sal flies. This suggests that mis-expression of Sal in outer PRs results in a partial re-programinng of their cell fate, away from the outer PR fate (loss of *rh1*) and towards a naïve inner PR fate (expression of inner PR default opsins). The Sal gain-of-function phenotype therefore confirms the hypothesis of the two inner PR 'default states' belonging to different ommatidial subtypes.

Taken together, the gain-of-function phenotype observed for Sal confirms the hypothesis that the *rh3*-expressing **p**R7 cell fate is indeed the default state of R7 cells. R7 and R8 default states therefore belong to different ommatidial subtypes, as R8 express the **y**R8 opsin *rh6* in *sev* mutants.

Spineless provides new insights into the formation of a retinal mosaic

Loss of the gene *spineless* (*ss*) results in a dramatic change in the ommatidial subtype pattern. In the wildtype, 30% of all ommatidia outside of the DRA express the **p** opsin Rh3 in R7 and Rh5 in R8, while the remaining 70% of **y** ommatidia show coupled expression of Rh4 in R7 and Rh6 in R8 (**Fig 6A**). Prior to this study, mutants affecting expression of *rh4* were not known. In *ss* (-/-) mutants eyes, expression of Rh4 is completely lost and Rh3 expression is expanded into all R7 cells (**Fig 6B**). The *ss* mutant phenotype is even more surprising, considering that it seems to clearly contradict the previous model of how co-ordinated opsin expression in **p** and **y** ommatidia its achieved. As described before, *rh4* was proposed to be the default opsin in R7 cells, from which **p**R7 cells have to are distinguished, by switching to the expression of *rh3* (Chou et al., 1999; Wernet et al., 2003). Although the question of which opsin gene represents a true 'default state' might indeed be argued, the *ss* phenotype strongly supports a model in which **y**R7 cells get distinguished from a *rh3* expressing default state by gaining *ss* expression. Using a ~1.6 kb of genomic DNA from the *ss* locus, expression of *ss* was visualized in developing PRs. Expression of this 'eye enhancer' is specific to a large subset of pupal R7 cells, highly reminiscent of the **y**R7 subtype (**Fig 6C**). However, no *ss* expression is detectable at later stages, when Rh4 protein begins to be expressed. It appears therefore, that a relatively short pulse of Ss might be used in **y**R7 cells to induce their final cell fate decision. This situation seems very different from the induction of specialized inner PR cell fates in DRA ommatidia by Hth. Hth expression becomes detectable early during pupation and remains in DRA inner PRs until the end of the animal's life, suggesting that Hth is also required for maintaining the DRA fate, possibly by regulating opsin expression directly. A short window of *ss* expression in **y**R7 supports a role of *ss* as a regulatory switch inducing the **y** fate and repressing the **p** fate. The expansion of Rh3 expression into all R7 cells observed in ss (-/-) mutant eyes supports such a model. Additional factors are therefore required downstream of *ss* to maintain the cell fate decisions in R7, for instance by regulating Rh4 expression throughout the
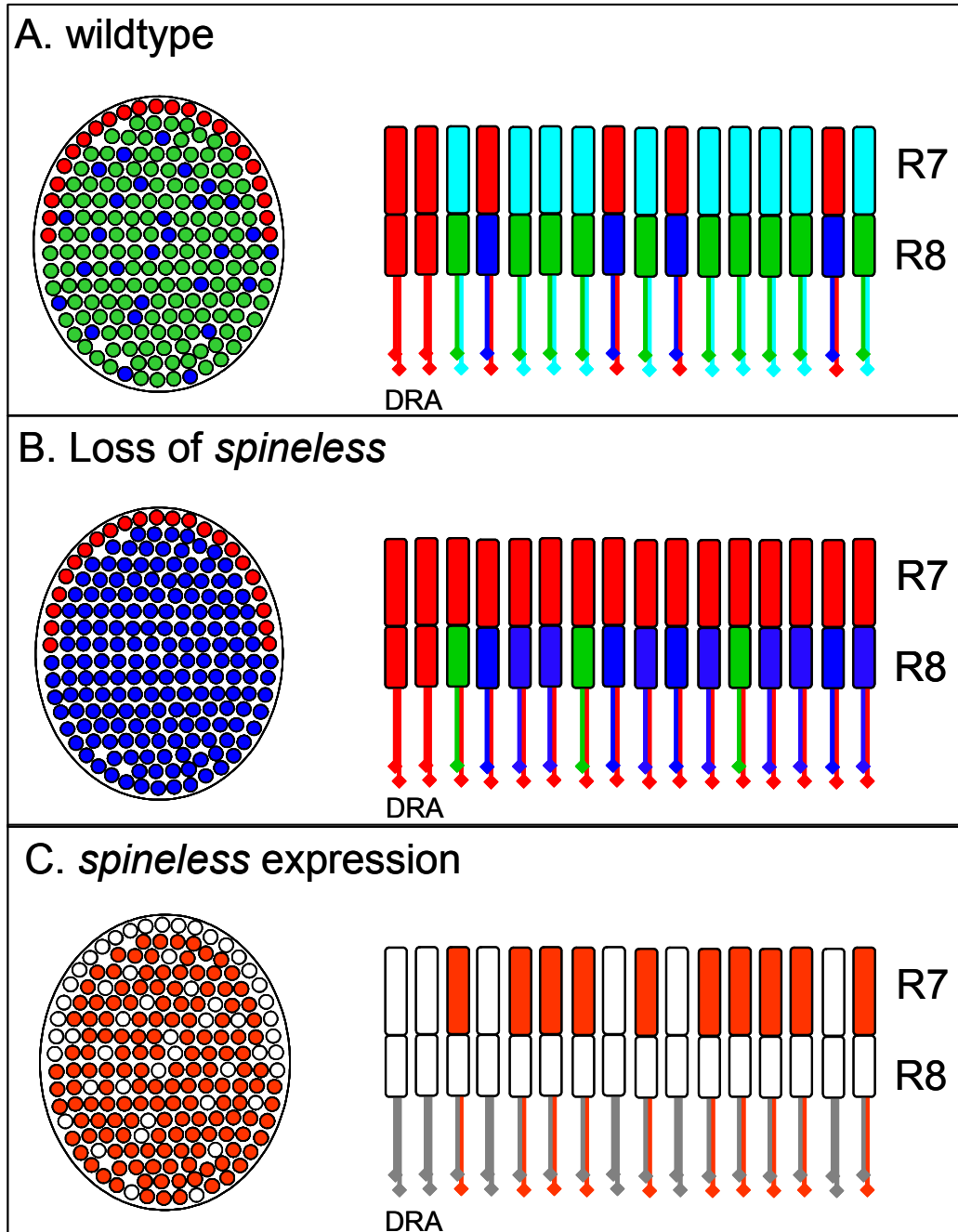
Fig IV.6: Spineless provides new insights into the formation of a retinal mosaic
(A) The retinal mosaic in wildtype *Drosophila*. Left: schematic representation of a developing wildtype retina (dorsal is up). DRA ommatidia are shown in red, pale and yellow ommatidia in blue and green, respectively. Right: Schematic representation of inner PR opsin expression in a wildtype retina. Coupled expression of Rh3 (red) in R7 and rh5 (blue) in R8 is seen in a small subset of ommatidia, whereas a larger subset expresses Rh4 (cyan) in R7 and Rh6 (green) in R8. Inthe DRA, both R7 and R8 express Rh3.
(B) Spineless loss-of-function phenotype. Left: The ommatial mosaic is severely altered in ss (-/-) retinas as y ommatidia are comepletely lost. Specification of DRA ommatidia (red), however, appears to be normal. Right: Expression of *rh4* is completely lost in ss mutant eyes and expression of *rh3* is expanded into all R7 cells instead. As a result, the ratio of **p** ommatidia is dramatically increased. In the R8 layer, however, a varying number cells retain expression of Rh6, resulting in ~5-50% of odd-coupled (Rh3/Rh6) ommatidia.
(C) Spineless expression pattern. Left: Using the ss_{eye}-GAL4 reporter construct, specific expression was detected in a large subset of ommatidia (red), strongly resembling the **y** subset of ommatida. Right: Expression of ss_{eye}-GAL4 was found to be specific to a large subset of R7 cells (shown in red), supporting the model that ss might specifically induce the **y**R7 fate in these cells.

adult life of the fly. Unfortunately, no antibodies against Ss are available to confirm the pulse of Ss protein expression in **y**R7 cells. Several attempts have been made to generate anti-Ss antibodies, but none of them has been successful yet. In situ hybridizations using antisense RNA probes against the ss cDNA have also been performed in the developing visual system, but no clear result has been obtained yet. For now, the ss$_{eye}$-GAL4 driver therefore represents the only way to investigate *ss* expression, with a significantly limited use. For instance, ss$_{eye}$-GAL4 expression remains to be analyzed in different mutant backgrounds like sal (-/-) tissue. Furthermore, *ss$_{eye}$*-GAL4 can be used in 'memory experiments', in which the flip/FRT system is used to sustain subset-specific *ss* expression in PRs until adulthood. Several FRT-constructs have already been tested (Act-FRT-CD2-FRT-lacZ:NLS, gift from Gary Struhl; Act-FRT-CD2-FRT-GAL4, from Jessica Treisman) in combination with ss$_{eye}$-GAL4 and UAS-flip. However, the efficiency of flip/FRT recombination appears to be extremely low during later stages of PR development, as even positive controls (*rh4*-GAL4, UAS-flip, Act-FRT-CD2-FRT-lacZ:NLS) resulted in negative results (no co-expression of βGal and Rh4 in the adult; data not shown). Taken together, it must be concluded that these experiments are quite difficult to perform, partly due to technical problems as well as the high number of transgenes that have to be introduced. Furthermore, expression of ss$_{eye}$-GAL4 cannot be visualized at all in mutant backgrounds involving GAL4 mis-expression, like LGMR > hth or LGMR > ArmS10, thereby clearly limiting the use of this reporter construct. Antibodies against Ss therefore represent a very high priority for the near future.

The retinal mosaic of *Drosophila* seems to be generated in mid-pupal PRs (~48 hrs APF), when ~70% of the R7 cells stochastically express *ss*. Expression of *ss* results in the induction of the **y**R7 fate, whereas the remaining R7 cells fall into the default fate **p**R7. It is unknown how stochastic expression of *ss* is regulated, but a relatively short piece of genomic DNA has been isolated which seems to faithfully reproduce the *ss* expression pattern. Further analysis of *ss* expression will hopefully allow a better understanding of how stochastic choices are regulated to create retinal mosaics.

Transcriptional control of R7 opsin expression in color ommatidia

Loss of the *Drosophila* aryhydrocarbon receptor Spineless results in a complete loss of *rh4* expression and currently represents the only mutation to specifically affect specification of the **y** subtype of R7 cells. Based on different lines of evidence, a new model for R7 'default state' opsins was proposed in which ~70% of R7 cells stochastically gain expression of *ss,* which then drives these cells into the **y** fate and away from the **p**R7 fate. Expansion of *rh3* expression into all R7 cells in *ss* mutants argues that Ss does not simply act on a transcriptional level, by directly or indirectly activating *rh4* transcription (**Fig 7A**). Instead, data seem to point toward a role for Ss as a key regulator placed upstream of the regulators of opsin transcription. This appears to be confimed by the pulse of **y**R7-like *ss* expression observed in pupal PRs. As no *ss* expression is detectable in adult PRs, it appears therefore that *ss* does not directly participate in the activation of *rh4* expression.

Recently, we have reported that mutations in the homeodomain transcription factor Orthodenticle (*otd*) result in a dramatic opsin phenotype which is characterized by the specific loss of **p** opsin expression (Tahayato et al., 2003). For instance, eyes lacking *otd* function completely lose *rh3* expression, whereas *rh4* seems to persist. However, in contrast to the phenotype observed in *ss* mutant eyes, *rh4* expression does not expand into all R7 cells (**Fig 7B**). As Rh4 expression is still specific to a subset of R7 cells in *otd* mutants, the specification of **p** and **y** ommatidia must occur correctly. Otd was shown to directly bind to the *rh3* promoter to acting as a direct opsin regulator downstream of the **p** / **y** decision, in which Ss plays a crucial role. It must be pointed out that the choice of **p** and **y** subtypes in R7 cells can therefore be dissociated from R7 opsin gene expression. In the olfactory system, expression of a given sensory receptor was shown to influence cell fate decisions by excluding expression of all other odorant receptors by allelic exclusion. Loss of Rh3, however, does not lead to the automatic gain of Rh4 expression in *otd* mutants. Conversely, late induction of Rh4 in the **p**R7 subtype using over-expression of Ss under *rh3*-GAL4

control resulted in co-expression of Rh3 and Rh4. These findings indicate that opsin proteins are not involved in **p** / **y** subtype decisions in *Drosophila*.

As Otd is expressed in all PRs (Vandendries et al., 1996), its activating effect on *rh3* expression has to be neutralized in cells that have adopted the **y**R7 fate in response to Ss. As transcriptional regulation of *otd* can be excluded, it seems most likely that additional factors are recruited by Ss to neutralize *otd* function in **y**R7 cells. However, these transcription factors remain to be identified. Interestingly, the vertebrate Estrogen receptor, a member of the superfamily of nuclear receptors, and the Arylhydrocarbon receptor have been shown to interact at the transcriptional level (Klinge et al., 2000). The *Drosophila* homologue of the nuclear receptor dimerization partner RXR, Ultraspiracle (Usp), has been shown to play a role in eye development (Oro et al., 1990) and might be required together with the Ecdysone receptor for the induction of Hth expression in the DRA. Specification of R7 cells was reported to be affected in *usp* mutants, as a loss of rh4-lacZ expression was reported (Oro et al., 1992). A possible role of Usp in concert or downstream of both Hth and Ss is currently being tested.

The generation of antibodies against Ss has very high priority. They will allow to rule out the possibility that Ss itself remains expressed in **y**R7 cells to antagonize Otd and activate *rh4* transcription. Mutational screens are currently being performed to identify the potential factors regulating *rh4* expression downstream of Ss. It is particularly interesting to speculate whether a phenotype similar to that of *otd* will be discovered, in which *rh4* expression is lost without *rh3* expanding into all R7 cells (**Fig 7C**). Such 'Factor Y' phenotype would indicate that activation of *rh4* transcription and neutralization of Otd downstream of Ss are dependent on different factors. However, it also possible that the putative *rh4* activator is the same factor that antagonizes Otd. In this case, mutants should resemble *ss* mutants in R7 cells. Both Ss and Otd play an important role in regionalizing the head tissue. It is therefore tempting to speculate that these two genes also genetically interact in different model systems and that antagonism between *ss* and *otd* are more widely used molecular mechanism to regulate specification of different cell fates. Identification of more mutants affecting opsin
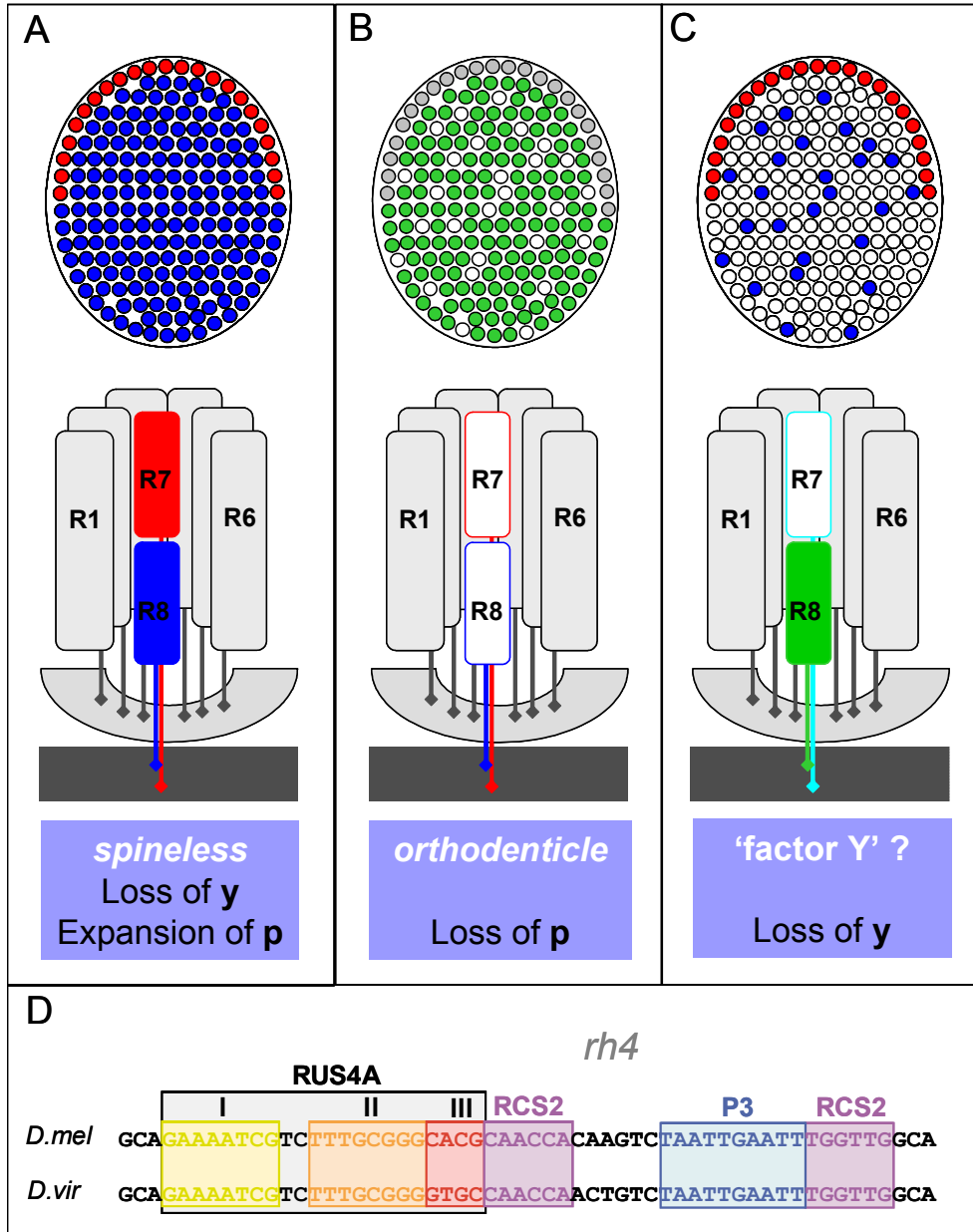
Fig IV.7: Transcriptional control of R7 opsin expression in color ommatidia

(A) Loss of *rh4* transcription in *ss* mutants. Top: schematic representation of a mutant retina lacking ss function (dorsal is up). Yellow ommatidia are completely lost due to the loss of rh4 expression. Instead, **p** omatidia are dramatically expanded. It should be noted that a varying number of odd coupled ommatidia (Rh3/Rh6) was also found replace the lost **y** ommatidia. Bottom: Depiction of a **p** ommatidium as found dramatically expanded in *ss* mutants.

(B) Loss of **p** opsin expression in *orthodenticle* (*otd*) mutants. Top: Schematic representation of a developing retina lacking otd (dorsal is up). Specification of **p** ommatidia (white circles) as well as the DRA (grey circles) is affected in otd mutants, due to the loss of *rh3* and *rh6* transcription. However, **y** ommatidia do not expand. Bottom: Transcription of both p opsins rh3 and rh5 is lost in otd mutants (white cells). It is unclear which opsins are expressed in **p** ommatidia in these mutants as rh4 expression does not expand. Instead, expansion of both *rh1* and *rh6* into R7 cells was observed.

(C) Predicted mutant 'Factor Y'. As Ss was shown to play a role in subtype choice rather than opsin gene transcription, mutant phenotypes are predicted which affect yR7 specification downstream of ss, for instance by regulation expression of *rh4* ('Factor Y'). Top: Mutant phenotype predicted for a 'Factor Y' mutant retina, I which specification of y ommatidia is specificaslly affected without p ommatidia expanding. Bottom: 'Factor Y' mutant ommatidium, with rh4 expression being los. R8, however is expected to express Rh6 as in sev mutants.

(D) Conserved sequences in the *rh4* promoter. Cloning and sequence comparison of *rh4* promoters from both *Drosophila melanogaster* (top) and *D. virilis* (bottom) has revealed several conserved boxes which are believed to be bound by opsin regulators. Using one-hybrid techniques, these sequences might reveal factors acting downstream of Ss ('Factor Y').

expression in **p**R7 and **y**R7 will therefore allow a refinement of the epistatic relationships within the transcriptional network regulating the specification of ommatidial subtypes.

Until recently, no mutations in inner PR opsin genes were identified. Using P-element excision mutagenesis, a null mutation in the *rh5* gene was recently generated (S. Yamaguchi, unpublished). Interestingly, **p**R8 PRs seem to be void of any opsin gene, indicating that neither Rh6 expression expands into all R8 cells, nor any other 'default opsin' (*rh1*) expands into these cells. These findings further confirm the independence of ommatidial subtype decisions from opsin gene expression. Furthermore, they allow the prediction that at least one mutant should exist with a phenotype similar to the above postulated 'Factor Y'. Mutants in the **y**R7 opsin *rh4* should not expand *rh3* expression due to all the findings described so far and attempts to mutate *rh4* are currently undertaken.

Cloning of the *rh4* promoters from different *Drosophila* species, as well as promoter dissection analysis have revealed several short, conserved stretches of promoter DNA absolutely required for *rh4* expression (**Fig 7D**; (Fortini and Rubin, 1990). No factors have yet been shown to bind to these sequences *in vitro* or *in vivo*, but it appears likely that factors required downstream of ss, like the putative 'Factor Y', should be acting through these sequences. It should be noted, that one of the previously identified boxes (RUS4A III) has a high resemblance to the consensus binding sites of AHR/Arnt arylhydrocarbon receptors (CACGT; for review: (Crews and Fan, 1999). Recently, RUS4A III has been mutated in a *rh4-*lacZ reporter transgene (T. Cook, unpublished). However, expression of is indistinguishable from wildtype *rh4*-lacZ. It appears therefore, that the RUS4A III sequence is not absolutely required for *rh4* expression. This result fits very well with previous observations that Ss is not expressed at times when *rh4* is activated. Furthermore, the *Drosophila* AHR dimerization partner Tango does not seem to be required for induction of the **y**R7 fate by Ss. It is therefore unclear to what consensus sequence Ss is binding to activate downstream genes. It is possible that Ss binds to DNA as a homodimer or in co-operation with other PAS HLH proteins. However, either of these scenarios has not yet been described in

any other model system. The yeast one-hybrid technique has recently been successfully used to identify the trans-activating factor (Pros) that binds to conserved sequences in the *rh5* and *rh6* promoters. The same technique is currently applied to the conserved sequences identified from the *rh4* promoter. The factors required in terminal differentiation of yR7 cells downstream of Ss might therefore soon be known.

Taken together, comparison of the *ss* and *otd* loss-of-function phenotypes place Ss as the regulator of **p** / **y** cell fate decisions in R7 upstream of opsin regulators like Otd and additional yet unknown factors.

Ommatidial subtype specification as a transcriptional model system

The genetic programs induced by Hth and Ss controlling the complex morphological changes in DRA inner PRs and **y**R7 remain largely unknown. However, both Hth and Ss have conserved counterparts in vertebrates which are the subjects of intense research (for review: (Sagerstrom, 2004); (Aoki, 2000). The advantages of modern *Drosophila* genetics therefore make ommatidial subtype specification an attractive new model system to study how both Hth/Meis and Ss/AHR proteins regulate transcription. The fact that Hth and Ss seem to antagonize each other to some extent in order to ensure clear distinction between DRA and color ommatidia makes this model system even more interesting, as it allows the study of more complex transcriptional networks.

A better understanding of Hth function *in vivo* is of great importance as mammalian homologues of Hth (Meis1a) cooperate with HOX factors to induce acute myeloid leukemia (AML; (Moskow et al., 1995); (Nakamura et al., 1996b); (Nakamura et al., 1996a). It has been proposed however, that direct association with HOX factors is not always necessary (Calvo et al., 2001). Since no HOX proteins have yet been implicated in *Drosophila* eye development, DRA development represents an attractive model system for identifying new factors interacting with Hth and Exd *in vivo*. In the *Drosophila* embryo as well as in developing appendages, Hth acts in concert with its crucial co-factor Exd and with HOX proteins by forming transcriptional complexes. One of the major roles

of Hth is to translocate Exd into the nucleus (Jaw et al., 2000); (Kurant et al., 2001). Consistent with this, Exd was found to be exclusively localized to the nuclei in inner PRs of the DRA, but not in color-sensitive ommatidia, suggesting that Hth and Exd function together as key regulators in DRA development.

From the GAL4 / GFP enhancer trap screen, we have recently identified new factors involved in cell fate regulation downstream, or together with, Hth/Exd. Loss of the two homologous Zn finger transcription factors encoded by the *elbow* / *no ocelli* complex (*elB*/*noc;* (Dorfman et al., 2002; Weihe et al., 2004) results in a molecular phenotype identical to the loss of Hth. Inner PRs in the DRA always express Rh3 in R7 and Rh6 in R8. Expression of Hth/Exd in the DRA persists in these mutants, indicating that these genes act downstream of Hth (M.F. Wernet and C. Desplan, in preparation). Loss of *elB* and *noc* also results in co-expression of the R8 marker Sens and Hth in DRA R8 cells. As presented before, repression of Sens by Hth represents another important example of how this transcriptional system specifies the individual cell types of the different ommatidial subtypes. Interestingly, conserved homologues for both Elb and Noc have been identified in worms, fish and humans (Andreazzoli et al., 2001). The role of the worm homologue TLP-1 is particularly interesting as it induces cell fate changes in the male tail tip in response to wnt signaling, a situation very similar to the role of *elB* / *noc* in the DRA of *Drosophila* (Zhao et al., 2002). Further experiments using the DRA as a model system will therefore reveal to what extent the role of these proteins is conserved.

The transcription factor Orthodenticle (Otd) represents another member of the transcriptional network regulating ommatidial subtype specification and its interaction with Hth and Ss was presented in detail. For instance, Otd was shown to be required as an activator of Rh3 in DRA inner PRs downstream of Hth. Ectopic expression of Hth does not induce Rh3 expression in an *otd^{uvi}* mutant background. Furthermore, Otd is indispensable for expression of the R7 'default state' opsin *rh3*, which is repressed by Ss very efficiently. The analysis of the transcriptional interaction between Hth/Exd, Otd and Ss will provide new insights into the molecular function of these genes.

The role of the Sal complex in specifying inner PRs has been introduced in some detail. All inner PR markers like Pros (R7), Sens (R8) and Hth (DRA) are under the control of Sal. Expression of these genes is lost in Sal (-/-) tissue and Hth is not able to induce DRA development in cells which have not been 'primed' by Sal. However, the competence to execute the **y**R7-inducing genetic program imposed by Ss is not limited to inner PRs and Ss is capable to induce *rh4* expression in *sal* mutants. It appears therefore that Hth and Ss act in a different transcriptional context. However, it seems likely that Ss still acts downstream of *sal*. Based on the data presented, Ss activity appears to be regulated by a tight control of its expression over both time and space: only very restricted expression of Ss in a large subset of R7 cells is observed during pupation. Furthermore, both loss of Rh4 in ss mutants as well as the strong *rh4*-inducing effect of Ss indicates that expression of Rh4 is completely dependent on *ss*. As *rh4* expression is lost in *sal* mutants, expression of *ss* should therefore also be lost in sal (-/-) tissue. This hypothesis has not yet been tested using ss_{eye}-GAL4. However, generation of Anti-Ss antibodies will allow to further test the epistatic relationship of the different factors involved in maturation of R7 cells: Sal, Pros and Ss.

Both Ss and its homologue, the vertebrate arylhydrocarbon receptor, play an important role in regulating transcription (for review: (Crews and Fan, 1999; Kewley et al., 2004). However, the mechanisms of transcriptional regulation by these proteins seem to be significantly different. In vertebrates, the AHR is stabilized in the cytoplasm by binding to hsp90 proteins as well as the 'arylhydrocarbon interacting protein' (AIP). Upon binding of the arylhydrocarbon ligand (Dioxin, for instance), AHR frees itself from its binding partners and translocates alone into the nucleus. In the nucleus, AHR associates to its binding partner, the 'aryl hydrocarbon receptor nuclear translocator' (Arnt, the homologue of *Drosophila* Tango) to activate transcription. In *Drosophila*, it is unknown whether Ss requires binding of an arylhydrocarbon-like ligand. Unlike in vertebrates, its mandatory co-factor Tango (Tgo, D-Arnt) is localized in the cytoplasm and transcription of Ss is absolutely required for translocating Tgo into

the nucleus. Within the nucleus, the Ss/Tgo complex activates transcription by sequence-specific binding to well-characterized response elements. The mechanism by which Ss/Tgo function as transcription factors in flies is therefore astonishingly similar to Hth and Exd. However, it was shown that *tgo* does not seem to be required to specify **y**R7 cells, indicating that the molecular mechanism of *ss* function might be different in developing PRs. In this context, the existence of a *Drosophila* homologue of the vertebrate AIP is particularly interesting. Further experiments will reveal how Ss (and possibly Tgo or *Drosophila* AIP) interact with the factors involved in the transcriptional network of ommatidial subtype specification.

Taken together, both Hth and Ss are part of a complex, steadily growing transcriptional network regulating retinal pattering in *Drosophila*. This model system will not only lead to a better understanding of their molecular function in the fly, but might also provide further insight into what roles their vertebrate counterparts play in carcinogenesis and drug resistance.

Instruction of opsin expression in R8 cells

Opsin expression in color sensitive ommatidia was shown to be tightly linked between R7 and R8 cells. Although inner PRs express 4 different opsins, only two large ommatidial subtypes are distinguishable: ~30 % the ommatidia form the **p** subtype and express Rh3 in R7 and Rh5 in R8, whereas the remaining ~70% of **y** ommatidia express Rh4 in R7 and Rh6 in R8 (**Fig 8A**). Analysis of *ss* expression pattern and loss-of-function phenotype has lead to a refined model of how **p** and **y** subtypes get specified in R7 cells. However, little is known about how R7 cells impose their subtype decision onto the underlying R8 cell. The ss loss-of-function phenotype observed in R8 cells as well as mis-expression of Ss in developing PRs has allowed some insight into this process.

In *ss* mutants, the **y** subtype is completely lost in R7 cells, as visualized by the complete loss of *rh4* expression and the expansion of *rh3* into all R7 cells. (**Fig 8B**). However, this phenotype is less penetrant in R8 cells, as a varying ratio of R8 cells retains expression of Rh6. Although the ratio of Rh5 vs Rh6 is

dramatically altered in favor of Rh5 (sometimes reaching over 95% of Rh5), almost equal distribution (50:50) of Rh5 and Rh6 was observed in some cases in *ss* mutant eyes. Interestingly, *ss* is only in R7 cells, which is in agreement with its observed expression pattern in a large subset of pupal R7 cells. Dramatic up-regulation of the **p**R8 subtype is therefore a consequence of the loss of *ss* in R7 cells. However, the *ss* phenotype in R8 cells also clearly illustrated that instruction of R8 cells is not 100% effective, resulting in a varying amount of odd-coupled Rh3/Rh6 ommatidia. Interestingly, a low amount (~7%) of odd coupled ommatidia occurs in the wildtype, suggesting that correct instruction of **p**R8 cells also frequently fails in wildtype ommatidia (Chou et al., 1999). Based on different lines of evidence, Rh6 has been shown to be the 'default state' opsin expressed in R8 cells. It appears therefore that odd coupled ommatidia in the wildtype as well as in *ss* mutants are the result of un-instructed R8 cells located below **p**R7 cells, getting stuck in their default state.

Early ectopic over-expression of Ss in all developing PRs, starting few ommatidial rows posterior to the morphogenetic furrow, results a dramatic phenotype. Expression of *rh4* expands into virtually all PRs (**Fig 8C**). Interestingly, inner PRs in the DRA do not gain expression of *rh4*, indicating that high *wg* pathway activity antagonizes *ss* function. In the main part of the retina, however, Ss is sufficient to induce the **y**R7 fate in every PR, as expression of Rh3 is completely lost. Consequently, no expression of *rh5* was detectable in LGMR > *ss* flies. Ss is therefore provided early enough to all R7 cells to avoid the formation of **p**R7 cells. As a consequence, instruction of underlying **p**R8 cells also does not occur. This was not unexpected, as the onset of GMR-GAL4 expression in developing PRs precedes expression of endogenous *ss* by several days. Interestingly, a significant number of **y**R8-like cells seemed to be specified, as *rh6* expression was detectable in R8 cells. Furthermore, these cells were found to co-express *rh4* and *rh6*. It is therefore unclear, which cell type these R8 represent. However, it was shown that the R8 marker Sens is not affected in LGMR > *ss* flies. Taking into account that Sens is sufficient to induce *rh6* expression when over-expressed, it appears that these cells are R8 cells lacking

A. wildtype

R7
R8
DRA
~30% pale

B. Loss of spineless

R7
R8
~30% odd coupled

C. Early ectopic Spineless

LGMR > *ss*
DRA
R7
R8
~100% atypical

D. Late spineless in all R7

[*rh3+rh4*] > *ss*
DRA
R7
R8
~30% odd coupled

E. 'Factor Y' ?

DRA
R7
R8
~70% *sev*-like?
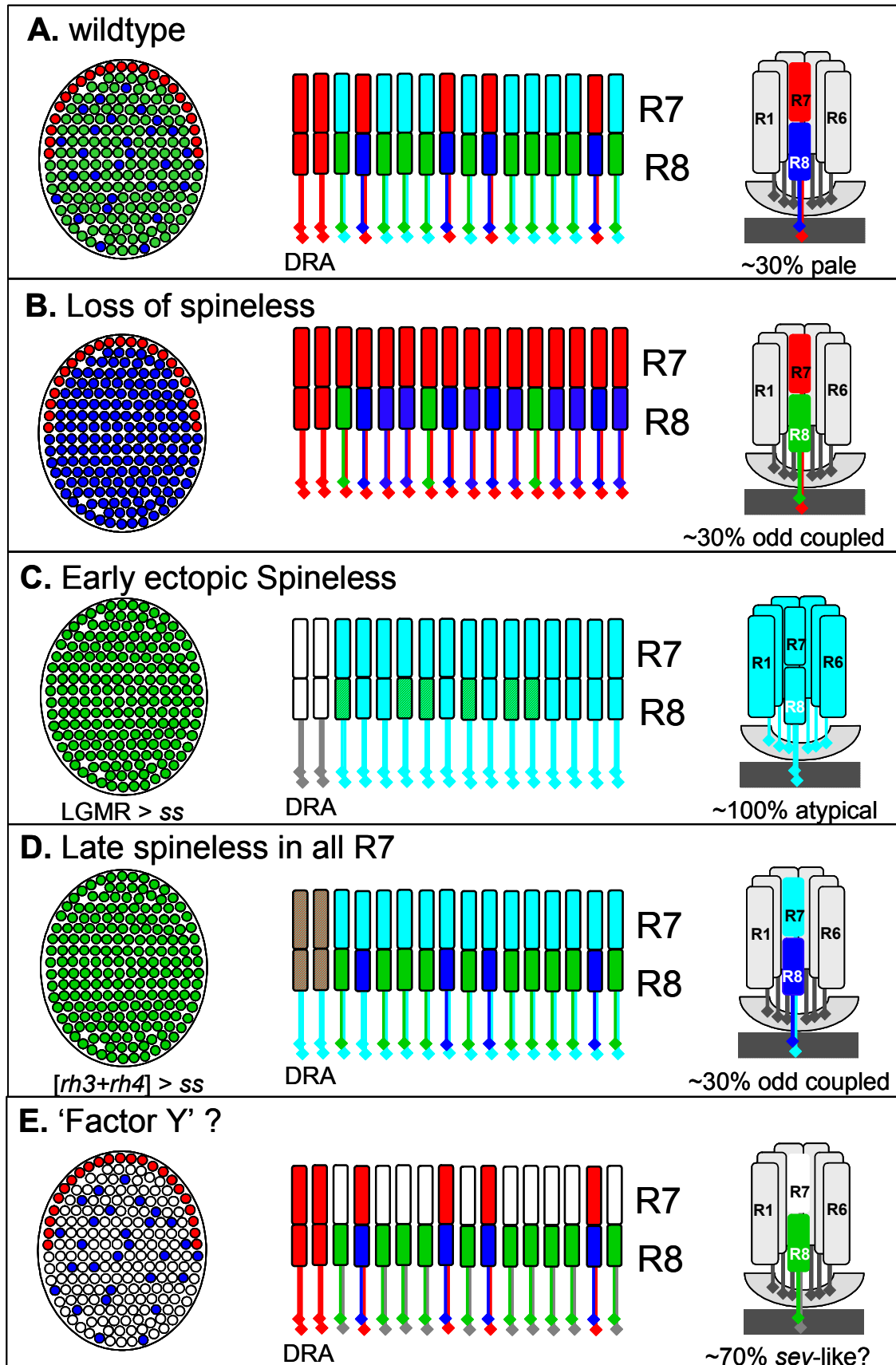
Fig IV.8: Instruction of opsin expression in R8 cells
(A) Ommatidial mosaic and opsin expression in the wildtype retina. Rh5 expression gets induced in ~30 of **p** ommatidia (right).
(B) Spineless loss-of-function. Expression if rh4 is completely lost. A varying number of ommatidia (average ~30%) have odd coupled expression of Rh3 in R7 and Rh5 in R8.
(C) Early ectopic expression of ss. Ectopic over-expression of Ss in all developing PRs using GMR-GAL4 drivers (LGMR > ss) results in a dramatic opsin phenotype. All PRs express rh4, including outer PRs. In the DRA, however, rh4 expression is specifically excluded from inner PRs (white cells). Expression of *rh3* is completely repressed by ss over-expression and *rh5* expression does not get induced due to the lack of instruction by **p**R7 cells. Interestingly, some R8 cells co-express rh4 and rh6 (striped cells), indicating that no molecular mechanism exists to exclude expression of these two opsins within the same cell. The cell afte of these cells is therefore ambiguous as they manifest both yR7 and R8 characteristica.
(D) Late mis-expression of ss in all R7 cells. Left: schematic representation of a developing retina mis-expressing Ss late under the control of the hybrid [*rh3+rh4*] ospin-GAL4 driver (dorsal is up). All ommatidia seem to have adopted the **y** fate as expression of *rh4* is expanded into all R7 cells and the inner PRs of the DRA (center). However, **p**R8 and **y**R8 fates are not affected in R8, suggesting that instruction of R8 cells has been successful in these flies. As a result, ~30% of the ommatidia manifest verey unusual odd coupled expression of Rh4 in R7 and Rh5 in R8 (right). Interestingly, rh3 and Rh4 were occasionally found co-expressed in DRA inner PRs (striped cells), confirming that the ability of Ss to induce *rh4* in the DRA is reduced.
(E) Phenotype predicted for 'Factor Y'. Mutants affecting opsin regulation in the yR7 subtype downstream of Ss will provide important tools to further study the instruction of R8 cells. For instance, R8 opsin expression should be indistinguishable from the wildtype, in mutants specifically lacking expression of Rh4 ('Factor Y').

any instructive signal, therefore choosing expression of their default opsin Rh6. However, *rh4* and *rh6* do not exclude each other in this case. While Ss prevents ambiguity between the **p**R7 and **y**R7 fates by excluding expression of *rh3*, no comparable molecular exclusion mechanism exists therefore for *rh4* and *rh6*.

Late over-expression of Ss in all R7 cells and the DRA using a GAL4 driver controlled by the hybrid [*rh3+rh4*] ('panR7') promoter resulted in a very different phenotype. In this case, *rh4* expression was expanded into all R7 cells, but not into R8 or outer PRs (**Fig 8D**). Rh3 expression was completely lost in R7 cells outside of the DRA, suggesting that all R7 cells had indeed chosen the **y**R7 fate. This result was also very different from the phenotype obtained by over-expressing Ss under the control of *rh3*-GAL4. In the latter case, expression of Rh4 was expanded without affecting Rh3, resulting in co-expression of Rh3 and Rh4 in **p**R7 and the DRA. The *rh4* portion of the panR7 promoter was therefore necessary in these late mis-expression experiments, for the R7 cells to choose the **y**R7 fate completely. This can be explained by the fact that cell fate changes induced by Ss were shown to ultimately repress *rh3* expression. Over-expression of Ss under *rh3* control should therefore have a negative feed-back effect on the GAL4 driver itself. As a result, relatively low expression of Rh4 was observed in **p**R7 cells of *rh3* > ss flies. However, by adding *rh4* promoter sequences to the GAL4 driver, R7 cells can be pushed completely towards the **y**R7 fate, as the *rh4* portion of the hybrid promoter becomes active in these newly transformed cells thereby confirming the transformation event. Interestingly, co-expression of Rh3

and Rh4 was occasionally observed the DRA. This finding again demonstrates the reduced ability of Ss to induce the **y**R7 fate in the DRA, when mis-expressed there. Surprisingly, the **p** / **y** ratio is normal in R8 cells of [*rh3+rh4*] > ss flies, although transformation of all R7 cells into **y**R7 is complete outside of the DRA. As a result, unusual pairing of Rh4 and Rh5 within the same ommatidium is observed in [*rh3+rh4*] > ss flies. This kind of odd coupled ommatidia is never observed in wildtype flies. The presence of *rh5* expressing **p**R8 cells of [*rh3+rh4*] > ss flies indicates that these cells have previously received an instructive signal, probably from overlying **p**R7 cells which were then later transformed into the **y**R7 fate due to late Ss mis-expression. It appears therefore that subtype choice in R7 cells and instruction of R8 cells are two separate events that can be dissociated using late mis-expression of Ss. Furthermore, the **p** / **y** cell fate decision in R7 appears to be a process which can be reverted within a certain window of time, clearly reaching through late pupation until the onset of opsin expression. Instruction of R8, however, does not seem to be reversible, due to the inability of **p**R8 cells to change the identity of the whole ommatidium back to a true **y** fate. This inability of R8 cells might be due to a molecular consolidation mechanism by which the R8 cell fate becomes frozen once a decision is taken. Indeed, two genes have recently been identified to be expressed specifically in **p**R8 and **y**R8, mutually antagonizing each other and thereby consolidating the subtype of R8 cells (T. Mikeladze-Dvali , MF Wernet and C Desplan, in preparation). Although such a system would seem surprisingly elaborate, it appears that a correct ratio between **p**R8 and **y**R8 subtypes is particularly important for the animal, as these cells contain the blue- and green-specific opsins required for color vision. According to this model, mutants lacking terminal differentiation of the **y** subtype downstream of Ss ('Factor Y') should have a subtype distribution in R8 cells that resembles the wildtype (**Fig 8E**).

Taken together, instruction of R8 cells by R7 is a non-reversible process occurring before the onset of opsin expression. This process can be dissociated from the original subtype choice in R7, which appears to be reversible and more

plastic. Establishment of a correct **p** / **y** ratio in R8 cells therefore seems to be essential for color vision.

The stochastic specification strategy for color ommatidia

A localized specification strategy was proposed for DRA ommatidia, in which inner PRs autonomously choose the Hth-expressing DRA fate when exposed to high levels of *wg* pathway activity in close proximity to the head cuticle (for review: (Wernet and Desplan, 2004). Specification of DRA ommatidia is highly dependent on positional cues, as their location within the *IRO-C / omb* territory is necessary for correct specification. In contrast to this specification strategy, recruitment of **p** and **y** ommatidia clearly does not follow such a localized approach. Instead, color ommatidia are found in a stochastic, but un-even distribution throughout the main part of the retina (**Fig 9A**). The results obtained by manipulating the gene *spineless* have revealed serious inconsistencies in the current model for specification of **p** and **y** ommatidia. A new model has therefore been drawn based on the results discussed so far.

The current model for specification of **p** and **y** ommatidia was divided into two steps. The identity of an ommatidium was proposed to be defined in a first step by the R7 cell choosing between the **p**R7 and **y**R7 fates. In a second step, only the **p**R7 cells were then proposed to actively instruct the underlying R8 to ensure expression of the **p**R8 opsin Rh5 within the same ommatidia. The remaining R8 cells, however, were believed to choose the expression of the 'default opsin' Rh6, as this opsin is the opsin of choice in R8 cells of *sev* mutants, clearly lacking any instructive signal. In this model, expression of the **y**R7 opsin Rh4 was considered the default state of R7 cells, from which **p**R7 had to be distinguished. This model seemed to harmonize well with the experimental data, as expression of both *rh3* and *rh5* were specifically lost in otd mutants. Furthermore, it seemed reasonable that both default states in R7 and R8 would belong to the same ommatidial subtype. However, several lines of evidence were presented here supporting the hypothesis that instead, *rh3*-expressing **p**R7 cells represent the true R7 default state. The expression pattern of *ss*, as well as the
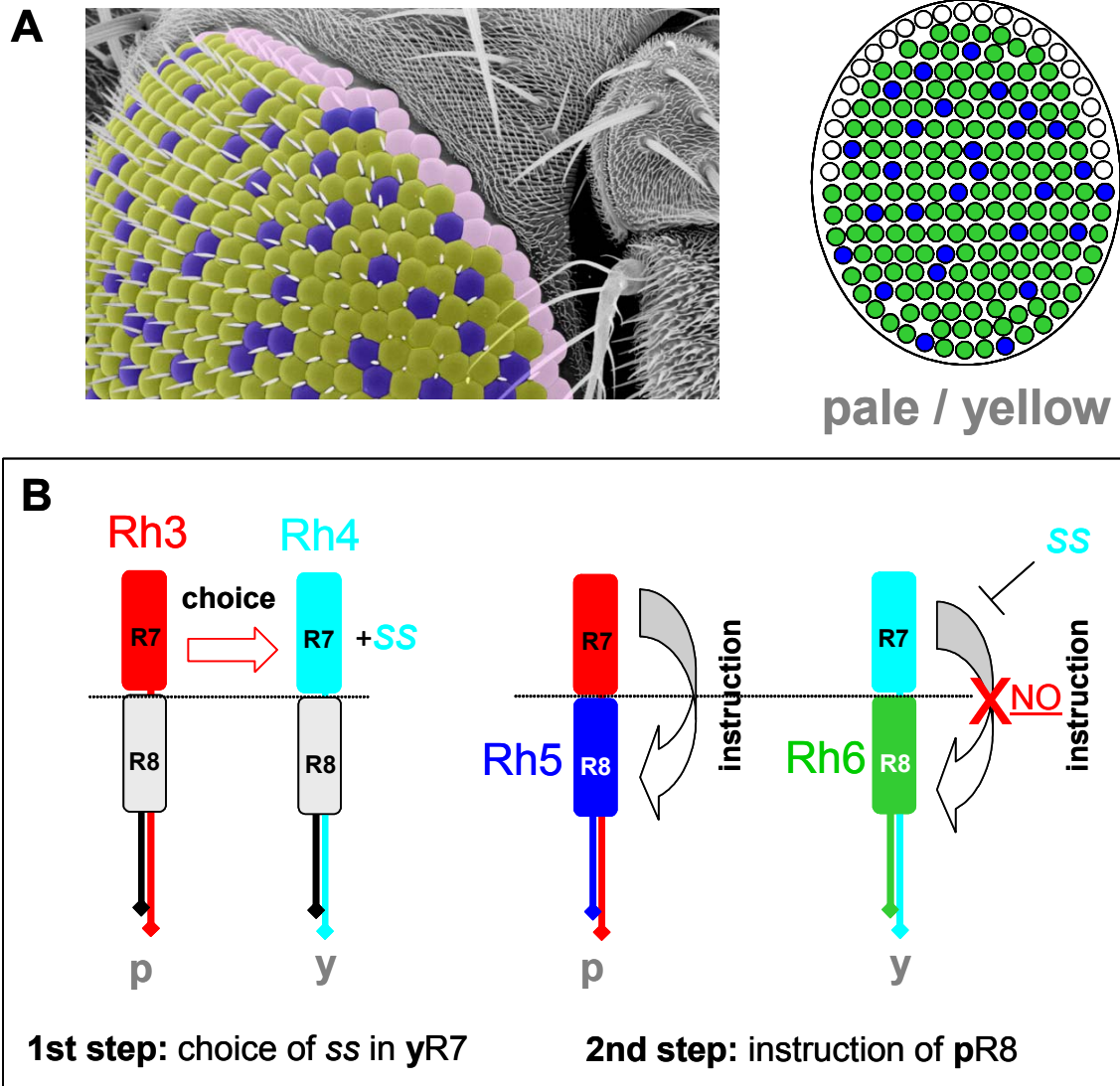
Fig IV.9: The stochastic specification strategy for color ommatidia
(A) Left: three ommatidial subtypes are distributed throughout the Drosophila retina. Scanning electron micrograph (kindly provided by T. Labhart) with the three ommatidial subtypes arbitrarily labeled. DRA ommatidia are shown in pink, pale and yellow subtypes are shown in blue and yellow, respectively. Right: Schematic representation of the stochastic distribution observed for **p** and **y** ommatidia in a developing retina (dorsal is up).
(B) The new specification model proposed for color ommatidia. Left: in contrast to previous models describing specification of **p** and **y** ommatidia, data obtained for ss indicates that **y**R7 cells get distinguished from the **p**R7 'default state', by specifically gaining expression of ss. According to this model, Rh3 (red) therefore represents the ground state opsin in R7 cells, and expression of Rh4 gets induced in the first step. Right: Only rh3-expressing pR7 cells are capable to instruct underlying R8 cells to express Rh5 (second step). Rh4 expressing **y**R7 cells that had been specified by Ss do not instruct R8, which therefore expresses its 'default opsin' Rh6. It appears therefore that gaining Ss expression makes the R7 cell incapable of instructing underlying R8 cells.

loss-of-function and gain-of-function phenotypes discussed for *ss* support a new model, in which **y**R7 gets distinguished from the default **p**R7, by gaining the expression of Ss (**Fig 9B**). Interestingly, the role of *rh6*-expressing **y**R8 as the default state in R8 was confirmed. Creation of naïve ommatidia (*sal* gain-of-

function / loss of *hth* / loss of *elB*&*noc*) always resulted in expression of rh6 in R8, suggesting that instruction of R8 (or R8-like cells) was defective in these ommatidia.

In the new model, different default states in R7 and R8 can simply be explained by Ss preventing the instruction of pR8 cells. Loss of Ss therefore results in all R7 remaining in the default state (*rh3*) capable of instructing R8 to express Rh5. In some cases (~7%) this instruction is not successful and odd coupled ommatidia are generated, even in the wildtype (Chou et al., 1999). This might be due to the relatively short time window available for this process, as well as to the consolidation mechanism making subtype choice in R8 an irreversible process. Interestingly, this model might have the logical advantage that the likelihood of errors can be reduced due to the fact that both active decisions (choice and instruction) are not performed by the same subtype. It seems more efficient to determine the number of **y**R7 cells with tightly regulated ss expression and then freeze these cells by abolishing their instructive potential. It must be noted that all consecutive cell fate decisions then occur automatically and can be performed by pleiotropic signaling components: signaling from **p**R7 to **p**R8 and the default determination of **y**R8.

Retinal patterning in *Drosophila*: combination of two strategies

In many species, the retinal mosaic is the result of a nearly perfect adaptation to the challenges that the environment imposes onto the animal. For instance, one necessity is the regional specification of certain parts of the retina: patches of retinal tissue which exhibit an optimal exposure to an important stimulus develop a heightened sensitivity to it. Examples for such localized specifications are the fovea in vertebrates, used when the subject fixes an object and the DRA ommatidia in *Drosophila*, which faces the sky which reflects polarized light. Specification of such parts of the retina requires the use of short-range patterning mechanisms like the diffusible morphogens, as well as patterning genes providing positional information within the retina. As the animal depends on many different visual stimuli and therefore has to 'multi-task' most of

the time, it is most effective to limit the expanse of such highly specialized retinal regions. For instance, this is very obvious in the very limited surface area of DRA's in most insects. Throughout the remaining retina, a second approach is used by both humans and *Drosophila* to stochastically distribute PRs with different spectral sensitivity, as only comparison between their inputs will allow effectively discrimination between colors. Interestingly, although the distribution is stochastic, there are biases in the proportion of the different subtypes: For instance there are fewer S cones in the human fovea and fewer **p** ommatidia in the fly mosaic, presumably to accommodate their function. Relatively few mutations in genes affecting retinal patterning have been described in the fly as well as in vertebrates. Furthermore, it is not understood on a molecular level, how regional and stochastic specification strategies are combined. However, the work presented here allows drawing some general conclusions about how morphogens, signaling molecules and transcription factors interact to pattern the developing retina.

The morphogen Wingless (Wg) was shown to have a strong inducing effect on the localized DRA ommatidia. Based on genetic experiments, a diffusible morphogen emanating from the developing head cuticle was predicted to induce localized spezification of DRA omatidia. Both Wg expression pattern as well as the DRA expansion phenotype observed after ectopic activation of *wg* signaling pathway confirmed the crucial role of Wg in this process. Furthermore, positional information provided by the *IRO-C* and *omb* genes is crucial for limiting DRA specification to the most marginal dorsal ommatidia exposed to the highest levels of *wg* pathway activity. It appears therefore that this relatively simple combination of factors allows the decoding of a gradient in *wg* activity existing at the eye margins. As a result, the key regulator Hth is specifically activated in inner PRs of the DRA to execute the molecular specification program (**Fig 10A**). Using this molecular mechanism, specification of DRA ommatidia is efficiently limited to the dorsal rim of the eye. However, to avoid ambiguity between ommatidial fates, it appears logical that the factors inducing DRA ommatidia would also have a repressive effect on the induction of **p** and **y** fates. Indeed, in
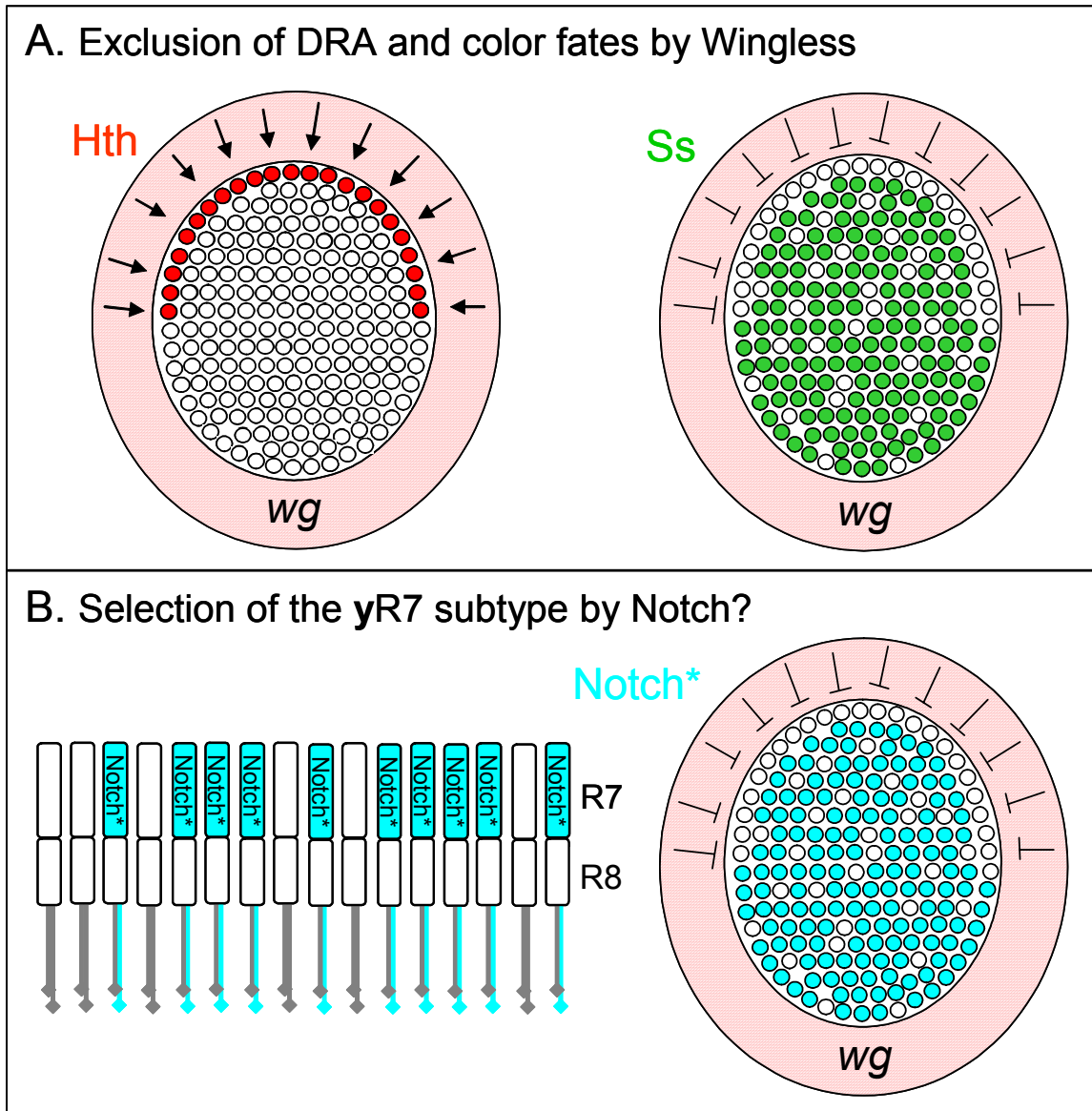
Fig IV.10: Retinal patterning in *Drosophila*: combination of two strategies
(A) Exclusion of DRA and color fates by Wingless (Wg). The morphogen Wg is expressed in the developing head cuticle around the retina (pink). Left: It was shown that Wg has a strong inducing effect of DRA ommatidia (red), which form along the dorsal head cuticle. Right: It was also shown that high *wg* signaling activity at the dorsal rim prevents formation of **p** and **y** ommatidia. This probably occurs by several different meachanisms, like repression of *ss* expression through Hth as well as independent of Hth. Furthermore, Wg can repress Ss function even when its expression is forced in the DRA.
(B) Possible selection of the **y**R7 subtype by Notch (N). Using ectopic over-expression of constitutively active forms of N and suppressor of Hairless / su(H), expression of rh4 was specifically induced in outer PRs. The N pathway therefore represents an attractive cabndidate pathway for the stochastic activation of ss expression in yR7 cells (left). However, activity of N signaling in these cells at the time of ommatidial subtype specification has not been shown yet. Furthermore, dominant negative forms of N were not able to disrupt retinal patterning. Right: In a preliminary model, ommatidial subtype specification in Drosophila might be regulated by the interplay of wg and N signaling pathways. Specification of DRA and color ommatidia was always found to exclude each other, which is represented by the strong antagonism of the two key regulators Hth and Ss, and possibly by the antagonism of wg and N signaling during pupal eye development.

the absence of Hth function, DRA ommatidia do not stochastically choose between the two color-sensitve fates. Instead, these ommatidia are immune to any instructive signals, with their inner PRs expressing 'default state' opsins. A

new specification model was proposed for **p** and **y** ommatidia, in which stochastic expression of the key regulator Spineless in ~70% induces the **y**R7 fate. Interestingly, *wg* signaling seems to have a strong antagonizing effect on Ss function. Expression of *ss* is never observed in DRA ommatidia, suggesting that high *wg* pathway activity represses its expression, either directly of via Hth. As Rh4 expression is completely lost when Hth is ectopically expressed, it seems likely that Hth itself can effectively repress *ss* expression. However, even in the absence of *hth* function, **y** Rh4 does not expand into the DRA (see above), suggesting that the *wg* pathway still excludes *ss* from the DRA. Furthermore, Ss was found to be incapable of inducing *rh4* expression in DRA inner PRs, even when ectopically mis-expressed, suggesting that cells exposed to high *wg* levels are made incompetent to execute the genetic grogram imposed by Ss. It appears therefore, that *wg* signaling can exclude specification of color ommatidia from the DRA, by using several different strategies. Considering the different perceptive tasks that these ommatidia are involved in, it appears that localized and stochastic specification strategies have to be seperated very effectively, in *Drosophila*. Interestingly, the combination of both strategies is used in humans to create the cone mosaic in the fovea. This further demonstrates the creative possibilities arising from different combination of these approaches.

Little is known about how stochastic cell fate decisions are taken in different model systems. Cell fate decisions of color sensitive PRs are even more obscure as their choice is biased, most of the times, resulting in PR subtype populations of different size. In *Drosophila*, distribution of **p** and **y** ommatidia was found to show important differences along the D/V axis of the eye. While **p** ommatidia are found at a higher ratio ventrally, **y** ommatdia prefer the dorsal compartment. It appears therefore that the same genes providing positional information to the DRA ommatidia (*IRO-C*, *omb*) might also influence the cell fate decision in color ommatidia. However, all statistical attempts to predict the formation of p and y ommatidia based on their location or based on the identity of neighboring ommatidia have failed so far. The Notch (N) pathway has a very specific inducing effect on *rh4* expression. Weak ectopic over-expression of both

constitutively active *su(H)*:VP16 as well as N^{intra} was sufficient to induce *rh4* expression in outer PRs. Raising N activity levels in ~70% of pupal R7 cells might therefore be responsible for the formation of **y**R7 cells (**Fig 10B**). The Notch pathway has been shown before to be required in all larval R7 cells in order for these cells to properly acquire their cell fate (Cooper and Bray, 2000; Tomlinson and Struhl, 2001). It is therefore possible that during later eye development this specification strategy is re-utilized in R7 cells to further sub-divide this cell type. However, an activating effect of the N pathway on *ss* expression has not yet been shown due to technical difficulties. Furthermore, the **y**R7-inducing potential of N remains obscure due to the fact that two different dominant negative approaches to abolish N signaling late during eye development had no effect on ommatidial specification. Clearly, more sophisticated genetic experiments have to be performed to investigate the role of N. Due to the important roles the N pathway plays during early eye development, ommatidial specification cannot be analyzed in N mutant eyes generated using the *ey*-FLIP/FRT system. However, temperature sensitive loss-of-function alleles have been described for N. Shifting these mutants to the restrictive temperature during early pupation should allow a detailed analysis of the role of N signaling. It is unclear how the N pathway would be stochastically activated in a subset of R7 cells as N signals have been shown to be exchanged amongst populations of cells, in most cases. During lateral inhibition, for instance, one cell out of a pool of cells mutually repressing each other's ability to change their fate, gets promoted randomly into a new cell fate. Furthermore, expression of the N ligand Delta (Dl) is believed to be rather pleiotropic. It can therefore not be excluded that constitutive activation of the N pathway mimics the **y**R7-inducing effect of another signaling pathway, maybe through the use of similar signaling components.

Taken together, the interplay of localized and stochastic specification strategies is used in the *Drosophila* eye to generate the retinal mosaic. Antagonism between the key regulators Hth and Ss is particularly interesting as these factors have been to positively different mode systems, like the developing antennae. Furthermore, the *wg* and *N* pathways, which might be responsible for

the induction of localized and stochistc cell fates, have been shown to both co-operate (planar cell polarity) as well as antagonize each other (early: growth) during eye development. Further experiments will hopefully clarify this emerging picture of how retinal patterning is regulated.

Similarities to retinal patterning in vertebrates

The retinal mosaic in *Drosophila*, like that of vertebrates, reflects a set of complex events that lead to the specification of different types of PRs within one adult ommatidium (inner *vs*. outer PRs, R7 *vs*. R8) as well as to 3 subtypes of ommatidia within the same retina (**p** *vs*. **y** *vs*. DRA). The data discussed here already point towards a model in which the fate of a given PR becomes increasingly restricted by a series of consecutive cell fate decisions, through the recruitment of transcription factors. Further genetic experiments, as well as the precise time course of expression of the genes involved in this process will allow a detailed description of their epistatic relationship. For instance, expression of Prospero or Homothorax is lost in *spalt* mutants, suggesting that the establishment of the inner PR fate by *spalt* is necessary for all further ommatidial specification steps to occur. The vertebrate retina similarly seems to use related strategies (for review: (Cepko, 1999; Harpavat and Cepko, 2003). Although the initial recruitment of retinal cells follows a different strategy with multipotent progenitor cells being restricted in their fate by both intrinsic and extrinsic events, it is clear that cascade of transcription factors are able to sequentially refine the fate of cells from the multipotent fate to a highly differentiated state. The example of rods cells best illustrates this: rod cells are distinguished from the 'ancestral' cone fate by the gene Nrl (Mears et al., 2001), whose function is similar to that of *spalt*, which, in *Drosophila,* distinguishes inner from outer PRs. In mammals, Crx plays a role similar to that of *otd* in controlling *rhodopsin* expression in a subset of PRs (Furukawa et al., 1997). Finally, the regionalization of the fly retina by *hth* can be compared to the function of the Thyroid hormone receptor TR2β which, in mice, affects the distribution of S and M cones along the dorso-ventral axis of the retina (Ng et al., 2001). It appears therefore that both similar strategies, as well

as similar factors are involved in retinal patterning in flies and vertebrates.

Many animals generate their retinal mosaic by combining localized and stochastic specification strategies as shown in some detail for *Drosophila*. Nevertheless, it should also be noted that some species form particularly stereotypical PR mosaics by purposely avoiding stochastic or localized mechanisms. The retina of most fishes for instance, is organized as a very regular lattice of the different types of cones. Furthermore, salmonid fish have the ability to considerably re-organize their retinal mosaic with developmental time. It has been shown that sexually mature salmonids regenerate their previously lost UV-sensitive cones and therefore their ability to detect polarized light (for review: (Hawryshyn, 2000). This represents a striking example for the metamorphosis of a retinal mosaic as the animal enters a new developmental phase: In order to reproduce, the animals have to leave the ocean and to migrate back to their place of birth, a task for which they have to re-gain an increased ability to navigate.

It appears that the instructive and permissive cell fate choices underlying the localized *vs*. biased-stochastic choice between DRA, **p** and **y** ommatidial fates in *Drosophila* represent rather fundamental neurobiological problems. A more complete understanding of the fly retinal mosaic might therefore allow us to get a clearer view on how our own retina helps us to enjoy our environment with all its shapes and colors.

V. MATERIAL AND METHODS

1. Genetic procedures

1.1. Drosophila strains and crosses

Flies were raised on standard corn-meal-molasses-agar medium and grown at room temperature (24 ± 1°C) unless otherwise noted. All genetic symbols not described in the text are in the Drosophila reference works [Lindsley, 1992 #2180].

Several previously established fly strains carrying mutations or reporter constructs were used. In table 1 these strains are listed and described.

Name of line	Description	Chromosome
1. lacZ reporters		
arm-lacZ	*Armadillo enhancer* driving E.Coli *lacZ-armadillo* fusion cDNA	1,2,3
hth-lacZ	PZ (lacZ) enhancer trap l(3)06762 in homothorax	3
IroC-lacZ	PZ (lacZ) enhancer trap rF209 in caupolican	3
pomb19-lacZ	*optomotorblind* eye enhancerdriving E.Coli *lacZ*	3
pros-lacZ	PZ (lacZ) enhancer trap in prospero	3
rh1-lacZ	*rh1* promoter (-926 to +32) driving E.Coli *lacZ*	2,3
rh3-lacZ	r*h3* promoter (-345 to +18) driving E.Coli *lacZ*	2,3
rh4-lacZ	r*h4* promoter (-359 to +85) driving E.Coli *lacZ*	2,3
rh5-lacZ	r*h5* promoter (-690 to +50) driving E.Coli *lacZ*	2,3
rh6-lacZ	*rh6* promoter (-555 to +121) driving E.Coli *lacZ*	2,3
stat92E-lacZ	PZ (lacZ) enhancer trap 06346 in caupolican	3
svp-lacZ	PZ (lacZ) enhancer trap in seven-up	3
2. GAL4 drivers		
hth-GAL4	pGawB (GAL4) enhancer trap in homothorax	3
panR7-GAL4	fusion of rh3 and rh4 promoters driving S.cerevisiae GAL4	2,3
Rh1-GAL4	r*h1* promoter (-926 to +32) driving S.cerevisiae GAL4	1,2,3
Rh3-GAL4	r*h3* promoter (-345 to +18) driving S.cerevisiae GAL4	2,3
Rh4-GAL4	r*h4* promoter (-359 to +85) driving S.cerevisiae GAL4	2,3
LGMR-GAL4	(5x) LONG glass 38 bp binding site driving S.cerevisiae GAL4	2,3
Mδ4-GAL4	E(spl) complex member *Mδ4* enhancer driving S.cerevisiae GAL4	
sGMR-GAL4	(5x) SHORT glass 29 bp binding site driving S.cerevisiae GAL4	2
ss[E1.6]-GAL4	Spineless eye enhancer (1.6 kb) driving S.cerevisiae GAL4	3
3. UAS-constructs		
UAS-ara	(5x)*GAL4 UAS* fused to an araucan cDNA	3
UAS-ArmS10	(5x)*GAL4 UAS* fused to a cDNA of activated Armadillo	2

UAS-caup	(5x)*GAL4 UAS* fused to a caupolican cDNA	2
UAS-lacZ	(5x)*GAL4 UAS* fused to E.Coli *lacZ*	2,3
UAS-lacZ::NLS	(5x)*GAL4 UAS* fused to E. Coli lacZ with a NLS	2,3
UAS-eGFP	(5x)*GAL4 UAS* fused to eGFP (Clonetech)	2,3
UAS-eGFP:hth	(5x)*GAL4 UAS* fused to an eGFP-*homothorax* fusion cDNA	3
UAS-exd	(5x)*GAL4 UAS* fused to an extradenticle cDNA	3
UAS-exd:NLS	(5x)*GAL4 UAS* fused to an *extradenticle* cDNA with NLS	3
UAS-hth51A	(5x)*GAL4 UAS* fused to an point-mutated ho*mothorax* cDNA	3
UAS-mirr	(5x)*GAL4 UAS* fused to a mirror cDNA	1,3
UAS-myc:hth	(5x)*GAL4 UAS* fused to an myc-*homothorax* fusion cDNA	2
UAS-N(DN)	(5x)*GAL4 UAS* fused to cDNA of dominant negative Notch	2
UAS-Nintra	(5x)*GAL4 UAS* fused to the cDNA of Notch intracellular domain	2
UAS-eGFP:hthHM	(5x)*GAL4 UAS* fused to an eGFP-*homothorax* (HM) fusion cDNA	3
UAS-sal	(5x)*GAL4 UAS* fused to a spalt cDNA	2
UAS-sens	(5x)*GAL4 UAS* fused to a *senseless* cDNA	1,2,3
UAS-ss	(5x)*GAL4 UAS* sites fused to the *spineless* cDNA	2,3
UAS-tcfΔN	(5x)*GAL4 UAS* fused to a cDNA of dominant negative dTCF	3
UAS-tgo	(5x)*GAL4 UAS* fused to a tango cDNA	3
UAS-tgo(DN)	(5x)*GAL4 UAS* fused to an dominant negative *tango* cDNA	3
UAS-VP16:exd	(5x)*GAL4 UAS* fused to an VP16-extradenticle fusion cDNA	3
UAS-VP16:su(H)	(5x)*GAL4 UAS* fused to an VP16-su(H) fusion cDNA	2

4. Other transgenes

CyOHoP$_2$	Carries transposase HoP2 on balancer chromoseome CyO	W. Gelbart
ey-Flip	ey promoter driving flip recombinase	B. Dickson
FRT19A	P[FRT; neo+] insertion at map position 19	FlyBase
FRT2A	P[FRT; neo+] insertion at map position 79	FlyBase
FRT80	P[FRT; neo+] insertion at map position 80	FlyBase
FRT82B	P[FRT; neo+] insertion at map position 82B	FlyBase
GMR-hid	(5x) glass 29 bp binding site driving *head involution defective*	1,2,3
GMR-Upd	(5x) glass 29 bp binding site driving Unpaired *(os)*	3
rh1-eGFP	*rh1* promoter (-926 to +32) driving eGFP	2,3
rh3-Rh:eGFP	*Rh3* promoter (-345 to +18) driving a Rh3-eGFP fusion cDNA	2,3
Rh4-GFP	*Rh3* promoter (-359 to +85) driving a Rh3-eGFP fusion cDNA	2,3
sev-RasVal12	Sevenless promoter driving activated Ras	2
ubi-eGFP:NLS	ubiquitin promoter driving eGFP cDNA with an NLS	1,2,3

5. Mutants

cn bw	Cinnabar brown double mutants	2
DFzC1	dFz (Fz2) null mutant	3
DMF3	Deficiency covering the *IRO-C* (*Iroquois*) locus	3
dshV26	dishevelled null mutant	1
exd1	extradenticle null mutant	1
fzH51	frizzled null mutant	3
hthB2	homothorax hypomorph (point mutant)	3
hthP2	homothorax null mutant (P-element insertion)	3
omb3198	Optomotorblind null mutant (point mutant)	3
ombQd[For]	Optomotorblind Quadroon gain-of-function mutant	1
os1A	Outstretched null mutant 1A	1
roX63	rough null mutant (X-ray mutant)	3
Sal[Def]	Deficiency covering the spalt locus	2

sev	sevenless null mutant	1
ssD105.7	spineless null mutant (point mutant)	3
stat06346	STAT92E hypomorph 06346	3
svpE22	seven-up null mutant	3
tgo1	strong tango hypomorph (point mutant)	3
tgo5	Close-to-null tango mutant (point mutant)	3
wr135	flies carrying balancer chromosomes CyO / Sp ; TM2 / MKRS	E. Wimmer
yw122; QB	flies carrying balancer chromosomes CyO / Sp ; TM2 / TM6B	A. Tomlinson

Table V.1 Fly strains used.

1.2. Generation of transgenic flies by germ line transformation

Transgenic lines were generated by injection of freshly purified plasmid DNA (see 2.3.6.) at a concentration of 0.3 $\mu g/\mu l$ into ~250 embryos of 0-10 minutes of age using standard procedures [Rubin, 1982 #279]. Single G_0 flies were separately crossed with the balancer stock wr135 and transgenic flies were selected in F1 according to their eye color. Insertions were mapped and balanced again using wr135 flies and following the standard balancer chromosome markers.

1.3. The pGawB / UAS-EGFP enhancer detection screen

New insertions were generated by remobilizing the previously described GAL4 enhancer trap element pGawB (gift from Brand and Perrimon, **Fig V.1**). A lethal insertion in the gene *apterous* was chosen as a jump start. The P-element was mobilized using a transposase source inserted on the *CyO* balancer chromosome on an immobile hobo element (*CyOHoP2*, gift from W. Gelbart Harvard University). These F0 flies were then crossed to UAS-GFP reporter flies. (see crossing scheme, **Fig V.2**).
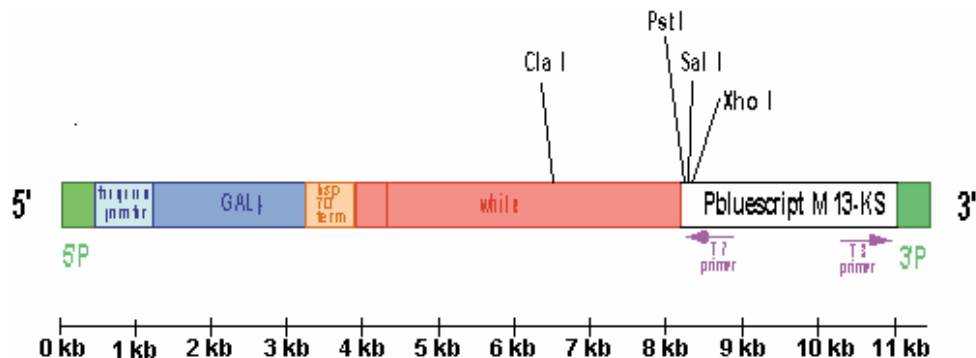
Fig V.1 Map of the P-Element pGawB built by Brand et al. (Brand et al., 1993). The GAL4 cDNA is represented as a blue box. The position of restriction enzyme recognition sites used for plasmid rescue of flanking genomic DNA are indicated.

Flies carrying new pGawB insertions were enriched by introducing a lethal point mutation in the gene *apterous* (ap^4) which does not complement lethality caused by *ap*-GAL4. After pre-schreening for straight-winged flies under the binocular, adult F1 flies were anesthetized using CO_2 and analyzed for GFP fluorescence under blue illumination using a standard dissecting microscope. Flies showing GFP signals in the "deep pseudopupil" coming from photoreceptors were collected, separated and amplified by crossing with the reporter flies (UAS-GFP).
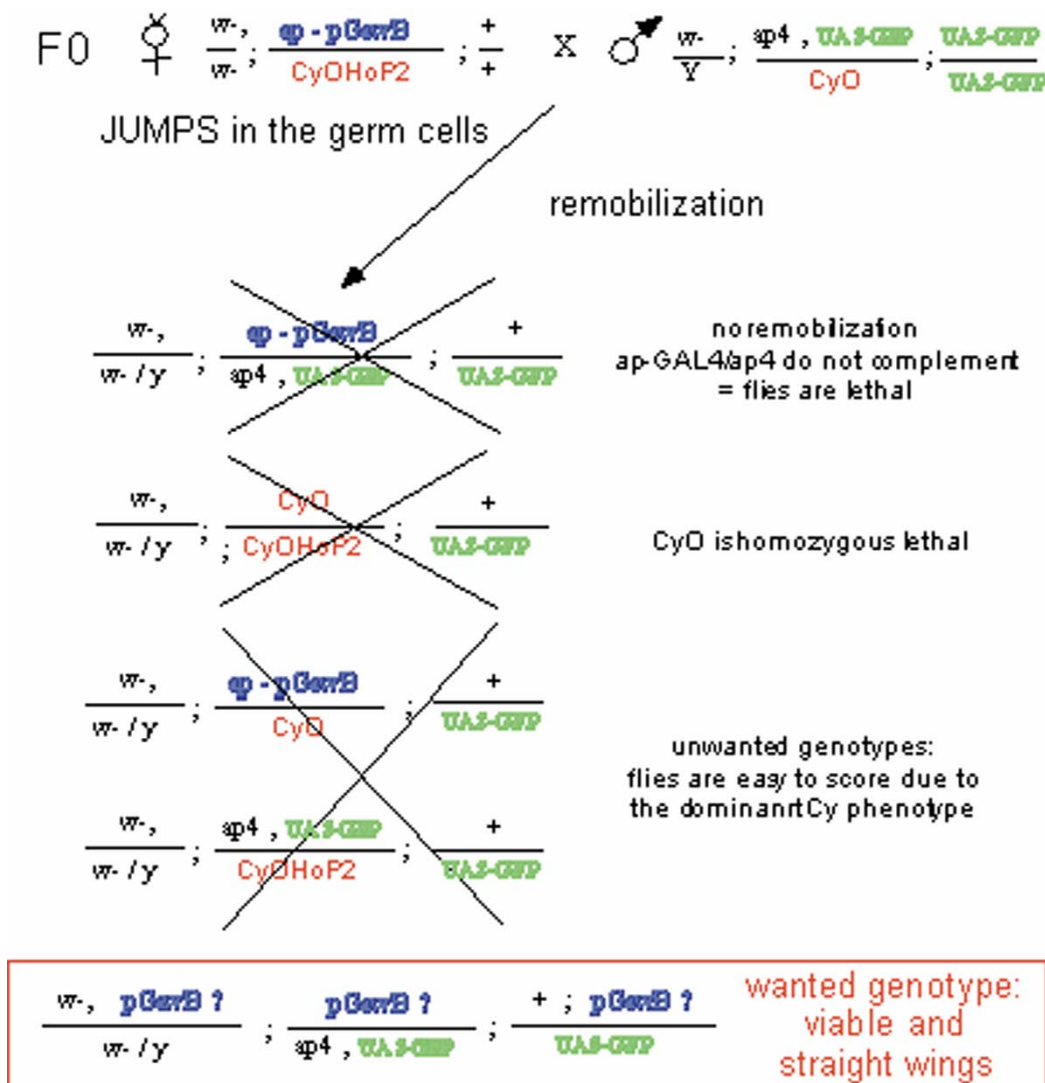
Fig V.2 The pGawB /UAS-GFP crossing scheme.
A high ratio of F1 survivers with straight wings carried new pGawB insertions at unknown genomic locations. Unwanted genotypes were eliminated based on lethality (ap-GAL4 / ap4 or CyO/CyO) or based on wing morphology (Cy).

Lines expressing GFP in photoreceptors were further analyzed by the "cornea neutralization" technique, to check for expression in subtypes of PRs. All insertions were mapped to their chromosome by following their phenotype using standard genetic methods. The flies used carried different combinations of balancers and UAS-GFP reporter constructs: w-/y ; UAS-GFP / CyO; UAS-GFP / MKRS and w- / w-; UAS-EGFP / CyO; UAS-EGFP / TM2, respectively. The GAL4 expression pattern of the obtained enhancer trap lines was characterized in more detail by introducing different reporter constructs like UAS-lacZ and UAS-lacZ:NLS.

2. Immuno Histochemistry and other staining techniques

2.1. Antibody stainings on eye imaginal discs

Cerebral complexes of *Drosophila* late third instar larvae were dissected in PBS (1x) and fixed in PBS + 4 % Formaldehyde for 20 min at RT. After four washes in PBT The first antibody was added overnight at 4°C. After four washes with PBT, the primary antibody was added overnight at 4°C. After four washes with PBT, the secondary antibody was then added for at least 2 hours at RT. After another four washes in PBT, each eye imaginal disc was separated from the head skeleton by using two Thungsten needles and then mounted in Aquamount (Lerner Laboratories).

2.2. Antibody stainings on mid-pupal retinas

Pupal cases were collected ~40 hrs after puparium formation and the head was dissected under ice cold PBS(1x). Several eye-brain complexes were extracted by gentle pipetting and collected in PBS (1x) on ice. After 20 min of fixation using PBS(1x) + 4% Formaldehyde, the samples were washed four times with PBT. The first antibody was added overnight at 4°C. After four washes with PBT, the secondary antibody was added for at least 2 hours at RT. After another

four washes in PBT, each retina was separated from the brain by using two Thungsten needles and then mounted in Aquamount (Lerner Laboratories).

2.3. Antibody stainings on frozen fly head sections

10 μm horizontal eye sections were performed using a cryostat (Zeiss) and deposited on superfrost Plus slides (Fisher). The slides were then fixed 15 minutes in PBS(1x) + 4% Formaldehyde. Fixation was slightly different for Anti-24B10 (chaoptin) stainings: Heads of anesthetized flies were cut, the proboscis was removed and the heads were fixed in PBS(1x) + 2% Formaldehyde for 90 minutes at 4°C. The heads were washed and incubated in PBS(1x) + 12% sucrose overnight. After four washes with PBT, the first antibody was added overnight at 4°C. After four washes with PBT, the secondary antibody was added for at least 2 hours at RT. After four washes with PBT, the slides were mounted in Aquamount (Lerner Laboratories).

Name	antigen	species	dilution
1. Primary antibodies			
24B10	chaoptin	Guinea pig	1:10
cappel	Beta Gal	rabbit	1:5000
ElaV1	ElaV	mouse	1:10
ElaV2	ElaV	rat	1:10
Exd	Extradenticle	rabbit	1:1000
GFP	GFP	rabbit	1:500
Hth	Homothorax	Guinea pig	1:500
Promega	beta Gal	mouse	1:500
Pros	Prospero	mouse	1:4
Rh1	Rhodopsin1	mouse	1:10
Rh3 a	Rhodopsin3	mouse	1:10
Rh3 b	Rhodopsin3	rabbit	1:10
Rh3 c	Rhodopsin3	chicken	1:10
Rh4	Rhodopsin4	rabbit	1:300
Rh5	Rhodopsin5	mouse	1:100
Rh6	Rhodopsin6	rabbit	1:5000
Sal	Spalt	rabbit	1:100
Sens	Senseless	guinea pig	1:10
Tgo	Tango	mouse	pure
2. Secondary antibodies			
Cy3	goat	rabbit	1:800

Cy3	donkey	mouse	1:200
Cy3	goat	chicken	1:200
Alexa555	goat	guinea pig	1:200
Alexa488	goat	rabbit	1:200
Alexa488	goat	mouse	1:200
Alexa488	goat	rat	1:200
Alexa488	goat	Guinea pig	1:200
Cy5	goat	mouse	1:200
Cy5	goat	rat	1:200

Table V.2 Antibodies used

2.4. X-Gal stainings on frozen sections of adult fly heads

10 μm horizontal eye sections were performed using a cryostat microtome (Zeiss) and deposited on superfrost Plus slides (Fisher). Slides were fixed 5-10 minutes in PBS 1X + 0.25% gluteraldehyde. They were then stained in a solution of 7.2mM Na_2HPO_4, 2.8mM NaH_2PO_4, 150mM NaCl, 1mM MgCl2, 3mM $K_3[Fe(CN)_6]$, 3mM $K_4[Fe(CN)_6]$, containing a 1/30 dilution of X-Gal (30 mg/ml 5-Bromo-4-chloro-3-indoyl β-D-galactoside in dimethyl formamide). After washing several times in PBS(1x), slides were mounted in aquamount (Lerner Laboratories, Fischer).

2.5. The "cornea neutralization" technique

Although not a real staining reaction, this technique was used as a complementary tool in addition to the stainings mentioned above to further analyze EGFP patterns emanating from photoreceptors. Photoreceptor signals can normally only be seen as a virtual, superimposed image in the "deep pseudopupil" due to the curvature of the cornea. This was neutralized by using water immersion so that EGFP signals coming from every individual ommatidium could be resolved [Franceschini, 1981 #283]. For immobilization, flies were anesthetized and poured into warm agarose (~50˚C). After solidification of the agarose, the flies were covered with a film of water. The eyes were analyzed under blue illumination using an immersion microscope with blue light source.

2.6. Plastic sections of adult fly heads

For the morphological examinations with transmission light and electron microscopy, the eyes were fixed with 2% glutaraldehyde (sometimes plus 1% OsO_4) in 0.05 M Na-cacodylate buffer (pH 7.2) for 2 h at 4°C. Following post-fixation with 2% OsO_4 in 0.05 M Na-cacodylate buffer (pH 7.2) for 2h at 4°C, the tissue was dehydrated with 2,2-dimethoxypropane and embedded in Epon 812. 1 µm sections for light microscopy were stained with methylene blue. Silver sections for electron microscopy were stained with uranyl acetate and lead citrate.

2.7. Scanning electron microscopy of adult fly heads

Fly heads were dehydrated by a series of ethanol washes (12-24 hours each): 25%, 50%, 75% and 100% (2x). Samples were then dried using a critical point drier. Samples were then mounted and analyzed using a standard scanning electron microscope.

3. Molecular Biology Techniques

3.1. Standard recombinant DNA techniques

A. Restriction: All generation of recombinant DNA was performed by creating the cloning fragments by cutting 1 to 10 µg of plasmid DNA with 10-20 units of the appropriate restriction endonuclease(s) in a final volume of 10 to 100 µl at 37°C for 2 hours using the appropriate restriction enzyme buffer (New England Biolabs). Purification of cloning fragments was performed by electrophoresis using 1% agarose gels and subsequent gel extraction using the "QIAQUICK gel extraction kit" (Qiagen).

B. Ligation: Vector DNA was treated with 20 units of alkaline phosphatase in a final volume of 20 µl for 20 minutes at 37°C. Every ligation reaction was performed using 100 ng to 1 µg of linearized insert and vector DNA as well as 400 units T4 DNA Ligase (New England Biolabs) at 16°C overnight.

C. Transformation: 10-50 ng of ligated DNA were transformed into competent DH5α bacteria using a standard CaCl$_2$ transformation protocol (20 minutes incubation on ice, 2 minutes heat-shock at 42˚C, 2 minutes on ice). Bacteria were plated on agar plates containing Ampicilline (50 μg / ml) after adding 250 μl LB medium and 60 minutes incubation at 37˚C.

3.2. Ligation of the ss$_{eye}$-GAL4 injection construct

The ss 'eye enhancer' / ss(E1.6) had previously been identified as a ~1.6 kb EcoR1 fragment (D. Duncan and I. Duncan, in preparation). This DNA fragment was ligated into the previously designed fly injection vector pCasper[hs43-GAL4-SV40]. Into this plasmid, promoterless enhancer sequences can be sub-cloned 5' to the GAL4 cDNA, which is flanked by an hs43 TATA box sequence (T. Cook, unpublished). Additionally, the GAL4 sequence is flanked by SV40 polyadenylation signal sequences at its 3' end (**Fig V.3**). pCasper[hs43-GAL4-SV40] was cut with EcoR1, and ligation of pCasper[*ss*(E1.6)-hs43-GAL4-SV40] was performed as described before.
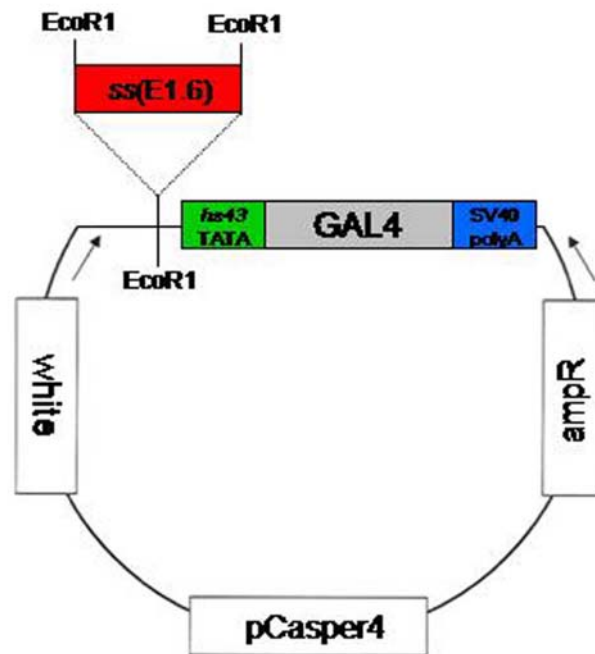
Fig V.3 Ligation of ss$_{eye}$-GAL4
The ~ 1.6 kb eye enhancer fragment from ss (E1.6) was ligated EcoR1/EcoR1 into the pCasper[*ss*(E1.6)-hs43-GAL4-SV40] injection vector. (white = minigine *w*, transformation marker; Casper4 = plasmid backbone; ampR = ampicilline resistence gene).

Injections into fly embryos were performed by following standard transformation protocols, with DNA concentrations being 0.3 µg/µl (injection construct) and 0.05 µg/µl (helper plasmid), respectively.

Transformands were identified based on eye color and the insertions were localized to their chromosome using combinations of dominant markers (yw ; CyO / Sp ; TM2 / TM6B).

Expression of ss$_{eye}$-GAL4 was analyzed by crossing different transgenic lines to reporter flies like UAS-GFP, UAS-lacZ or UAS-lacZ:NLS.

3.3. Plasmid Rescue of genomic DNA flanking P-Element insertions

Three flies were homogenized in an 1,5 ml eppendorf reaction tube containing 150 µl DNA homogenization buffer using a disposable pestle. After adding 150 µl Lysis buffer [Ashburner, 1989 #2187], the tubes were incubated for 15 minutes at 70°C. 45 µl of Potassium Acetate (8M) were added and the tubes were incubated on ice for 30 minutes. After Spinning down debris, the supernatant was extracted using phenol/chloroform (1:1), precipitated and the pellet of genomic DNA was resuspended in 20 µl of water. The genomic DNA was digested with the appropriate restriction endonucleases (Pst1, Sal1 or Cla1), ligated in a final volume of 600 µl and transformed into ultra competent bacteria (Epicurian Coli XL 10-Gold) following the Stratagene transformation protocol. Clones were analyzed by mini-preparation of plasmid DNA using the QIAPREP miniprep Kit (Qiagen) and digestion with restriction endonucleases. Plasmid DNA containing flanking genomic DNA were amplified by doing DNA maxi preparations using the QIAFILTER maxi prep Kit (Qiagen) and sequenced.

3.4. Rescue of genomic DNA flanking P-Elements by inverse PCR

A. Genomic DNA extraction, restriction and ligation: 15 flies were homogenized in an 1,5 ml eppendorf reaction tube containing 200 µl of homogenization buffer A using a disposable pestle. After 30 min incubation at 65°C, 400 µl of a mix (1:2.5) of Lithium Chloride (6M) and Potassium Acetate (5M) solutions was added and the tubes were incubated on ice for at least 10

minutes. After Spinning down debris for 15 min at RT, the supernatant was extracted using phenol/chloroform (1:1) and precipitated using 600 μl of Isopropanol. The pellet of genomic DNA was washed with 70% Ethanol, air dried and ultimately resuspended in 20 μl of distilled water. 5 μl of genomic DNA solution were then digested with 10 units of either one of the three appropriate restriction endonucleases (Sau3A1, Msp1 or Dra1) in a volume of 25 μl. After heat inactivation (20 min at 65°C), 10 μl of the restriction mix were ligated in a final volume of 400 μl, using 40 μl of T4 DNA ligase buffer (10x) and 2 μl of T4 DNA Ligase (NEB) at 16 degrees, overnight. The ligation mix was then precipitated by adding 40 μl Sodium Acetate (5M, pH 5.2) and 1 ml of pure Ethanol. The DNA pellet was washed with 70& ethanol, air dried and resuspended in 60 μl of distilled water.

B. Inverse PCR on circularized DNA: Genomic DNA sequences flanking the 3' end of the P-element were rescued (see figure). A first PCR was performed in a total volume of 50 μl using 10 μl of the ligated genomic DNA mix, 20 pmol of the two divergent primers located closest to each other (Pry5 and Pry6, see below), 5 nmol of dNTPs, as well as 5 μl of (10x) Boehringer taq buffer and 5 units of taq polymerase (boehringer). The PCR program used was: 94°C: 5' / (94°C for 1min / **53°C for** 2min / 72°C for 3min) * 40 / 72°C for 10 min. 2 μl of the PCR mix were then used as template for a second PCR, without further purification. Similar conditions were used, except that this time, the two outermost excentric primers (Pry2 and Rry7, see below) were used: 94°C: 5' / (94°C for 1min / 55°C for 1min / 72°C for 1min) * 35 / 72°C for 10 min. The result of both PCRs was run on a 1% Agarose Gel, PCR bands excised using a scalpel and DNA extracted using the 'DNA Extraction Kit' (Qiagen). ~20 ng of the obtained DNA solution were then sequenced using the PCR primer Pry1. Primers: Pry2: CCT TAG CAT GTC CGT GGG GTT TGA AT, Pry5: CTG AGT GAG ACA GCG ATA TGA TTG TT, Pry6: CAC TCG CAC TTA TTG CAA GCA TAC GT, Pry7: GAG TAC GCA AAG CTC TAG CTA GAG GAT.
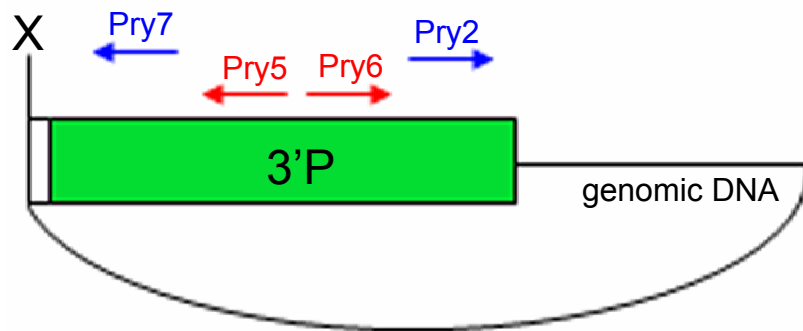
Figure V.4 Inverse PCR rescue of genomic DNA flanking a P-element. 2 PCRs were performed on previously circularized DNA consisting of known P-element sequences (green) and unknown genomic DNA (black). The product of the first PCR (red primers) served as a template for PCR #2 (blue primers).

VI. REFRENCES

Andreazzoli, M., Broccoli, V., and Dawid, I. B. (2001). Cloning and expression of noz1, a zebrafish zinc finger gene related to Drosophila nocA. Mech Dev *104*, 117-120.

Aoki, Y. (2000). [Effects of dioxins on protein kinases and disruption of signal transduction pathways]. Nippon Rinsho *58*, 2458-2463.

Arendt, D., and Wittbrodt, J. (2001). Reconstructing the eyes of Urbilateria. Philos Trans R Soc Lond B Biol Sci *356*, 1545-1563.

Bach, E. A., Vincent, S., Zeidler, M. P., and Perrimon, N. (2003). A sensitized genetic screen to identify novel regulators and components of the Drosophila janus kinase/signal transducer and activator of transcription pathway. Genetics *165*, 1149-1166.

Baker, N. E., Mlodzik, M., and Rubin, G. M. (1990). Spacing differentiation in the developing Drosophila eye: a fibrinogen-related lateral inhibitor encoded by scabrous. Science *250*, 1370-1377.

Banerjee, U., Renfranz, P. J., Pollock, J. A., and Benzer, S. (1987). Molecular characterization and expression of sevenless, a gene involved in neuronal pattern formation in the Drosophila eye. Cell *49*, 281-291.

Baonza, A., and Freeman, M. (2001). Notch signalling and the initiation of neural development in the Drosophila eye. Development *128*, 3889-3898.

essa, J., Gebelein, B., Pichaud, F., Casares, F., and Mann, R. S. (2002). Combinatorial control of Drosophila eye development by eyeless, homothorax, and teashirt. Genes Dev *16*, 2415-2427.

Bourgouin, C., Lundgren, S. E., and Thomas, J. B. (1992). Apterous is a Drosophila LIM domain gene required for the development of a subset of embryonic muscles. Neuron *9*, 549-561.

Brand, A. H., and Perrimon, N. (1993). Targeted gene expression as a means of altering cell fates and generating dominant phenotypes. Development *118*, 401-415.

Brennan, C. A., and Moses, K. (2000). Determination of Drosophila photoreceptors: timing is everything. Cell Mol Life Sci *57*, 195-214.

Brodsky, M. H., and Steller, H. (1996). Positional information along the dorsal-ventral axis of the Drosophila eye: graded expression of the four-jointed gene. Dev Biol *173*, 428-446.

Brown, S., Hu, N., and Hombria, J. C. (2001). Identification of the first invertebrate interleukin JAK/STAT receptor, the Drosophila gene domeless. Curr Biol *11*, 1700-1705.

Burgess, E. A., and Duncan, I. (1990). Direct control of antennal identity by the spineless-aristapedia gene of Drosophila. Mol Gen Genet *221*, 347-357.

Cagan, R. L., and Ready, D. F. (1989). Notch is required for successive cell decisions in the developing Drosophila retina. Genes Dev *3*, 1099-1112.

Calleja, M., Moreno, E., Pelaz, S., and Morata, G. (1996). Visualization of gene expression in living adult Drosophila. Science *274*, 252-255.

Calvo, K. R., Knoepfler, P. S., Sykes, D. B., Pasillas, M. P., and Kamps, M. P. (2001). Meis1a suppresses differentiation by G-CSF and promotes proliferation by SCF: potential mechanisms of cooperativity with Hoxa9 in myeloid leukemia. Proc Natl Acad Sci U S A *98*, 13120-13125.

Casares, F., and Mann, R. S. (1998). Control of antennal versus leg development in Drosophila. Nature *392*, 723-726.

Cavodeassi, F., Diez Del Corral, R., Campuzano, S., and Dominguez, M. (1999). Compartments and organising boundaries in the Drosophila eye: the role of the homeodomain Iroquois proteins. Development *126*, 4933-4942.

Cavodeassi, F., Modolell, J., and Campuzano, S. (2000). The Iroquois homeobox genes function as dorsal selectors in the Drosophila head. Development *127*, 1921-1929.

Cavodeassi, F., Modolell, J., and Gomez-Skarmeta, J. L. (2001). The Iroquois family of genes: from body building to neural patterning. Development *128*, 2847-2855.

Celniker, S. E., and Rubin, G. M. (2003). The Drosophila melanogaster genome. Annu Rev Genomics Hum Genet *4*, 89-117.

Cepko, C. L. (1999). The roles of intrinsic and extrinsic cues and bHLH genes in the determination of retinal cell fates. Curr Opin Neurobiol *9*, 37-46.

Chen, C. M., and Struhl, G. (1999). Wingless transduction by the Frizzled and Frizzled2 proteins of Drosophila. Development *126*, 5441-5452.

Cho, K. O., and Choi, K. W. (1998). Fringe is essential for mirror symmetry and morphogenesis in the Drosophila eye. Nature *396*, 272-276.

Chou, W. H., Hall, K. J., Wilson, D. B., Wideman, C. L., Townson, S. M., Chadwell, L. V., and Britt, S. G. (1996). Identification of a novel Drosophila opsin reveals specific patterning of the R7 and R8 photoreceptor cells. Neuron *17*, 1101-1115.

Chou, W. H., Huber, A., Bentrop, J., Schulz, S., Schwab, K., Chadwell, L. V., Paulsen, R., and Britt, S. G. (1999). Patterning of the R7 and R8 photoreceptor cells of Drosophila: evidence for induced and default cell-fate specification. Development *126*, 607-616.

Clandinin, T. R., and Zipursky, S. L. (2002). Making connections in the fly visual system. Neuron *35*, 827-841.

Cohen, B., McGuffin, M. E., Pfeifle, C., Segal, D., and Cohen, S. M. (1992). apterous, a gene required for imaginal disc development in Drosophila encodes a member of the LIM family of developmental regulatory proteins. Genes Dev *6*, 715-729.

Cook, T., and Desplan, C. (2001). Photoreceptor subtype specification: from flies to humans. Semin Cell Dev Biol *12*, 509-518.

Cook, T., Pichaud, F., Sonneville, R., Papatsenko, D., and Desplan, C. (2003). Distinction between Color Photoreceptor Cell Fates Is Controlled by Prospero in Drosophila. Dev Cell *4*, 853-864.

Cooper, M. T., and Bray, S. J. (1999). Frizzled regulation of Notch signalling polarizes cell fate in the Drosophila eye. Nature *397*, 526-530.

Cooper, M. T., and Bray, S. J. (2000). R7 photoreceptor specification requires Notch activity. Curr Biol *10*, 1507-1510.

Crews, S. T., and Fan, C. M. (1999). Remembrance of things PAS: regulation of development by bHLH-PAS proteins. Curr Opin Genet Dev *9*, 580-587.

Dacke, M., Doan, T. A., and O'Carroll, D. C. (2001). Polarized light detection in spiders. J Exp Biol *204*, 2481-2490.

Diez del Corral, R., Aroca, P., JL, G. m.-S., Cavodeassi, F., and Modolell, J. (1999). The Iroquois homeodomain proteins are required to specify body wall identity in Drosophila. Genes Dev *13*, 1754-1761.

Domingos, P. M., Brown, S., Barrio, R., Ratnakumar, K., Frankfort, B. J., Mardon, G., Steller, H., and Mollereau, B. (2004). Regulation of R7 and R8 differentiation by the spalt genes. Dev Biol *273*, 121-133.

Dominguez, M., and de Celis, J. F. (1998). A dorsal/ventral boundary established by Notch controls growth and polarity in the Drosophila eye. Nature *396*, 276-278.

Dorfman, R., Glazer, L., Weihe, U., Wernet, M. F., and Shilo, B. Z. (2002). Elbow and Noc define a family of zinc finger proteins controlling morphogenesis of specific tracheal branches. Development *129*, 3585-3596.

Duncan, D. M., Burgess, E. A., and Duncan, I. (1998). Control of distal antennal identity and tarsal development in Drosophila by spineless-aristapedia, a homolog of the mammalian dioxin receptor. Genes Dev *12*, 1290-1303.

Emmons, R. B., Duncan, D., Estes, P. A., Kiefel, P., Mosher, J. T., Sonnenfeld, M., Ward, M. P., Duncan, I., and Crews, S. T. (1999). The spineless-aristapedia and tango bHLH-PAS proteins interact to control antennal and tarsal development in Drosophila. Development *126*, 3937-3945.

Feiler, R., Bjornson, R., Kirschfeld, K., Mismer, D., Rubin, G. M., Smith, D. P., Socolich, M., and Zuker, C. S. (1992). Ectopic expression of ultraviolet-rhodopsins in the blue photoreceptor cells of Drosophila: visual physiology and photochemistry of transgenic animals. J Neurosci *12*, 3862-3868.

Finkelstein, R., Smouse, D., Capaci, T. M., Spradling, A. C., and Perrimon, N. (1990). The orthodenticle gene encodes a novel homeo domain protein involved in the development of the Drosophila nervous system and ocellar visual structures. Genes Dev *4*, 1516-1527.

Fortini, M. E., and Artavanis-Tsakonas, S. (1994). The suppressor of hairless protein participates in notch receptor signaling. Cell *79*, 273-282.

Fortini, M. E., and Rubin, G. M. (1990). Analysis of cis-acting requirements of the Rh3 and Rh4 genes reveals a bipartite organization to rhodopsin promoters in Drosophila melanogaster. Genes Dev *4*, 444-463.

Fortini, M. E., and Rubin, G. M. (1991). The optic lobe projection pattern of polarization-sensitive photoreceptor cells in Drosophila melanogaster. Cell Tissue Res *265*, 185-191.

Franceschini, N., and Kirschfeld, K. (1971a). [In vivo optical study of photoreceptor elements in the compound eye of Drosophila]. Kybernetik *8*, 1-13.

Franceschini, N., and Kirschfeld, K. (1971b). [Pseudopupil phenomena in the compound eye of drosophila]. Kybernetik *9*, 159-182.

Franceschini, N., Kirschfeld, K., and Minke, B. (1981). Fluorescence of photoreceptor cells observed in vivo. Science *213*, 1264-1267.

Frankfort, B. J., Nolo, R., Zhang, Z., Bellen, H., and Mardon, G. (2001). senseless repression of rough is required for R8 photoreceptor differentiation in the developing Drosophila eye. Neuron *32*, 403-414.

Freeman, M. (1996). Reiterative use of the EGF receptor triggers differentiation of all cell types in the Drosophila eye. Cell *87*, 651-660.

Fryxell, K. J., and Meyerowitz, E. M. (1987). An opsin gene that is expressed only in the R7 photoreceptor cell of Drosophila. Embo J *6*, 443-451.

Furriols, M., and Bray, S. (2000). Dissecting the mechanisms of suppressor of hairless function. Dev Biol *227*, 520-532.

Furukawa, T., Morrow, E. M., and Cepko, C. L. (1997). Crx, a novel otx-like homeobox gene, shows photoreceptor-specific expression and regulates photoreceptor differentiation. Cell *91*, 531-541.

Gaul, U., Mardon, G., and Rubin, G. M. (1992). A putative Ras GTPase activating protein acts as a negative regulator of signaling by the Sevenless receptor tyrosine kinase. Cell *68*, 1007-1019.

Gehring, W. J. (2002). The genetic control of eye development and its implications for the evolution of the various eye-types. Int J Dev Biol *46*, 65-73.

Giraldez, A. J., and Cohen, S. M. (2003). Wingless and Notch signaling provide cell survival cues and control cell proliferation during wing development. Development *130*, 6533-6543.

Golic, K. G. (1991). Site-specific recombination between homologous chromosomes in Drosophila. Science *252*, 958-961.

Gomez-Skarmeta, J. L., Diez del Corral, R., de la Calle-Mustienes, E., Ferre-Marco, D., and Modolell, J. (1996). Araucan and caupolican, two members of the novel iroquois complex, encode homeoproteins that control proneural and vein-forming genes. Cell *85*, 95-105.

Grether, M. E., Abrams, J. M., Agapite, J., White, K., and Steller, H. (1995). The head involution defective gene of Drosophila melanogaster functions in programmed cell death. Genes Dev *9*, 1694-1708.

Grimm, S., and Pflugfelder, G. O. (1996). Control of the gene optomotor-blind in Drosophila wing development by decapentaplegic and wingless. Science *271*, 1601-1604.

Hafen, E., Basler, K., Edstroem, J. E., and Rubin, G. M. (1987). Sevenless, a cell-specific homeotic gene of Drosophila, encodes a putative transmembrane receptor with a tyrosine kinase domain. Science *236*, 55-63.

Hardie, R. C. (1984). Properties of photoreceptors R7 ansd R8 in dorsal marginal ommatidia in the compound eyes of Musca and Calliphora. J Comp Physiol *154*, 157-165.

Hardie, R. C. (1985). Functional organization of the fly retina. In Sensory physiology 5, D. Ottoson, ed. (Berlin, Heidelberg, New York, Tokyo, Springer-Verlag), pp. 1-79.

Harpavat, S., and Cepko, C. L. (2003). Thyroid hormone and retinal development: an emerging field. Thyroid *13*, 1013-1019.

Harrison, D. A., McCoon, P. E., Binari, R., Gilman, M., and Perrimon, N. (1998). Drosophila unpaired encodes a secreted protein that activates the JAK signaling pathway. Genes Dev *12*, 3252-3263.

Hawryshyn, C. W. (2000). Ultraviolet polarization vision in fishes: possible mechanisms for coding e-vector. Philos Trans R Soc Lond B Biol Sci *355*, 1187-1190.

Heberlein, U., Borod, E. R., and Chanut, F. A. (1998). Dorsoventral patterning in the Drosophila retina by wingless. Development *125*, 567-577.

Hediger, M., Niessen, M., Wimmer, E. A., Dubendorfer, A., and Bopp, D. (2001). Genetic transformation of the housefly Musca domestica with the lepidopteran derived transposon piggyBac. Insect Mol Biol *10*, 113-119.

Hou, S. X., Zheng, Z., Chen, X., and Perrimon, N. (2002). The Jak/STAT pathway in model organisms: emerging roles in cell movement. Dev Cell *3*, 765-778.

Huber, A., Schulz, S., Bentrop, J., Groell, C., Wolfrum, U., and Paulsen, R. (1997). Molecular cloning of Drosophila Rh6 rhodopsin: the visual pigment of a subset of R8 photoreceptor cells. FEBS Lett *406*, 6-10.

235

Irvine, K. D. (1999). Fringe, Notch, and making developmental boundaries. Curr Opin Genet Dev *9*, 434-441.

Jaw, T. J., You, L. R., Knoepfler, P. S., Yao, L. C., Pai, C. Y., Tang, C. Y., Chang, L. P., Berthelsen, J., Blasi, F., Kamps, M. P., and Sun, Y. H. (2000). Direct interaction of two homeoproteins, homothorax and extradenticle, is essential for EXD nuclear localization and function. Mech Dev *91*, 279-291.

Kauffmann, R. C., Li, S., Gallagher, P. A., Zhang, J., and Carthew, R. W. (1996). Ras1 signaling and transcriptional competence in the R7 cell of Drosophila. Genes Dev *10*, 2167-2178.

Kehl, B. T., Cho, K. O., and Choi, K. W. (1998). mirror, a Drosophila homeobox gene in the Iroquois complex, is required for sensory organ and alula formation. Development *125*, 1217-1227.

Kewley, R. J., Whitelaw, M. L., and Chapman-Smith, A. (2004). The mammalian basic helix-loop-helix/PAS family of transcriptional regulators. Int J Biochem Cell Biol *36*, 189-204.

Kidd, S., Lieber, T., and Young, M. W. (1998). Ligand-induced cleavage and regulation of nuclear entry of Notch in Drosophila melanogaster embryos. Genes Dev *12*, 3728-3740.

Kirschfeld, K., and Franceschini, N. (1968). Optische Eigenschaften der Ommatidien im Komplexauge von Musca. Kybernetik, 47-52.

Klinge, C. M., Kaur, K., and Swanson, H. I. (2000). The aryl hydrocarbon receptor interacts with estrogen receptor alpha and orphan receptors COUP-TFI and ERRalpha1. Arch Biochem Biophys *373*, 163-174.

Klingensmith, J., Nusse, R., and Perrimon, N. (1994). The Drosophila segment polarity gene dishevelled encodes a novel protein required for response to the wingless signal. Genes Dev *8*, 118-130.

Koelle, M. R., Talbot, W. S., Segraves, W. A., Bender, M. T., Cherbas, P., and Hogness, D. S. (1991). The Drosophila EcR gene encodes an ecdysone receptor, a new member of the steroid receptor superfamily. Cell *67*, 59-77.

Kopczynski, C. C., Alton, A. K., Fechtel, K., Kooh, P. J., and Muskavitch, M. A. (1988). Delta, a Drosophila neurogenic gene, is transcriptionally complex and encodes a protein related to blood coagulation factors and epidermal growth factor of vertebrates. Genes Dev *2*, 1723-1735.

Kopp, A., and Duncan, I. (1997). Control of cell fate and polarity in the adult abdominal segments of Drosophila by optomotor-blind. Development *124*, 3715-3726.

Kuhnlein, R. P., Frommer, G., Friedrich, M., Gonzalez-Gaitan, M., Weber, A., Wagner-Bernholz, J. F., Gehring, W. J., Jackle, H., and Schuh, R. (1994). spalt encodes an evolutionarily conserved zinc finger protein of novel structure which provides homeotic gene function in the head and tail region of the Drosophila embryo. Embo J *13*, 168-179.

Kumar, J. P., and Moses, K. (2001). EGF receptor and Notch signaling act upstream of Eyeless/Pax6 to control eye specification. Cell *104*, 687-697.

Kurant, E., Eytan, D., and Salzberg, A. (2001). Mutational analysis of the Drosophila homothorax gene. Genetics *157*, 689-698.

Labhart, T. (1988). Polarization-opponent interneurons in the insect visual system. Nature, 435-437.

Labhart, T., and Meyer, E. P. (1999). Detectors for polarized skylight in insects: a survey of ommatidial specializations in the dorsal rim area of the compound eye. Microsc Res Tech *47*, 368-379.

Labhart, T., and Meyer, E. P. (2002). Neural mechanisms in insect navigation: polarization compass and odometer. Curr Opin Neurobiol *12*, 707-714.

Lai, E. C. (2004). Notch signaling: control of cell communication and cell fate. Development *131*, 965-973.

Lee, C. H., Herman, T., Clandinin, T. R., Lee, R., and Zipursky, S. L. (2001). N-cadherin regulates target specificity in the Drosophila visual system. Neuron *30*, 437-450.

Lee, J. D., and Treisman, J. E. (2001). The role of Wingless signaling in establishing the anteroposterior and dorsoventral axes of the eye disc. Development *128*, 1519-1529.

Lin, H. V., Rogulja, A., and Cadigan, K. M. (2004). Wingless eliminates ommatidia from the edge of the developing eye through activation of apoptosis. Development *131*, 2409-2418.

Llimargas, M. (1999). The Notch pathway helps to pattern the tips of the Drosophila tracheal branches by selecting cell fates. Development *126*, 2355-2364.

Maurel-Zaffran, C., and Treisman, J. E. (2000). pannier acts upstream of wingless to direct dorsal eye disc development in Drosophila. Development *127*, 1007-1016.

McNeill, H., Yang, C. H., Brodsky, M., Ungos, J., and Simon, M. A. (1997). mirror encodes a novel PBX-class homeoprotein that functions in the definition of the dorsal-ventral border in the Drosophila eye. Genes Dev *11*, 1073-1082.

Mears, A. J., Kondo, M., Swain, P. K., Takada, Y., Bush, R. A., Saunders, T. L., Sieving, P. A., and Swaroop, A. (2001). Nrl is required for rod photoreceptor development. Nat Genet *29*, 447-452.

Meinertzhagen, I. A., and Hanson, T. E. (1993). The development of the optic lobe. In The development of *Drosophila melanogaster*, M. Bate, and A. Martinez Arias, eds. (New York, Cold Spring Harbor Laboratory Press), pp. 1363-1491.

Mlodzik, M., Baker, N. E., and Rubin, G. M. (1990a). Isolation and expression of scabrous, a gene regulating neurogenesis in Drosophila. Genes Dev *4*, 1848-1861.

Mlodzik, M., Hiromi, Y., Weber, U., Goodman, C. S., and Rubin, G. M. (1990b). The Drosophila seven-up gene, a member of the steroid receptor gene superfamily, controls photoreceptor cell fates. Cell *60*, 211-224.

Mollereau, B., Dominguez, M., Webel, R., Colley, N. J., Keung, B., de Celis, J. F., and Desplan, C. (2001). Two-step process for photoreceptor formation in Drosophila. Nature *412*, 911-913.

Mollereau, B., Wernet, M. F., Beaufils, P., Killian, D., Pichaud, F., Kuhnlein, R., and Desplan, C. (2000). A green fluorescent protein enhancer trap screen in Drosophila photoreceptor cells. Mech Dev *93*, 151-160.

Montell, C., Jones, K., Zuker, C., and Rubin, G. (1987). A second opsin gene expressed in the ultraviolet-sensitive R7 photoreceptor cells of Drosophila melanogaster. J Neurosci *7*, 1558-1566.

Montell, C., and Rubin, G. M. (1988). The Drosophila ninaC locus encodes two photoreceptor cell specific proteins with domains homologous to protein kinases and the myosin heavy chain head. Cell *52*, 757-772.

Morante, J., and Desplan, C. (2004). Building a projection map for photoreceptor neurons in the Drosophila optic lobes. Semin Cell Dev Biol *15*, 137-143.

Moses, K., and Rubin, G. M. (1991). Glass encodes a site-specific DNA-binding protein that is regulated in response to positional signals in the developing Drosophila eye. Genes Dev *5*, 583-593.

Moskow, J. J., Bullrich, F., Huebner, K., Daar, I. O., and Buchberg, A. M. (1995). Meis1, a PBX1-related homeobox gene involved in myeloid leukemia in BXH-2 mice. Mol Cell Biol *15*, 5434-5443.

Nakamura, T., Largaespada, D. A., Lee, M. P., Johnson, L. A., Ohyashiki, K., Toyama, K., Chen, S. J., Willman, C. L., Chen, I. M., Feinberg, A. P.*, et al.* (1996a). Fusion of the nucleoporin gene NUP98 to HOXA9 by the chromosome translocation t(7;11)(p15;p15) in human myeloid leukaemia. Nat Genet *12*, 154-158.

Nakamura, T., Largaespada, D. A., Shaughnessy, J. D., Jr., Jenkins, N. A., and Copeland, N. G. (1996b). Cooperative activation of Hoxa and Pbx1-related genes in murine myeloid leukaemias. Nat Genet *12*, 149-153.

Nathans, J. (1999). The evolution and physiology of human color vision: insights from molecular genetic studies of visual pigments. Neuron *24*, 299-312.

Ng, L., Hurley, J. B., Dierks, B., Srinivas, M., Salto, C., Vennstrom, B., Reh, T. A., and Forrest, D. (2001). A thyroid hormone receptor that is required for the development of green cone photoreceptors. Nat Genet *27*, 94-98.

Nolo, R., Abbott, L. A., and Bellen, H. J. (2000). Senseless, a Zn finger transcription factor, is necessary and sufficient for sensory organ development in Drosophila. Cell *102*, 349-362.

Noordermeer, J., Klingensmith, J., Perrimon, N., and Nusse, R. (1994). dishevelled and armadillo act in the wingless signalling pathway in Drosophila. Nature *367*, 80-83.

Ohshiro, T., and Saigo, K. (1997). Transcriptional regulation of breathless FGF receptor gene by binding of TRACHEALESS/dARNT heterodimers to three central midline elements in Drosophila developing trachea. Development *124*, 3975-3986.

O'Kane, C. J., and Gehring, W. J. (1987). Detection in situ of genomic regulatory elements in Drosophila. Proc Natl Acad Sci U S A *84*, 9123-9127.

Oro, A. E., McKeown, M., and Evans, R. M. (1990). Relationship between the product of the Drosophila ultraspiracle locus and the vertebrate retinoid X receptor. Nature *347*, 298-301.

Oro, A. E., McKeown, M., and Evans, R. M. (1992). The Drosophila retinoid X receptor homolog ultraspiracle functions in both female reproduction and eye morphogenesis. Development *115*, 449-462.

Pai, C. Y., Kuo, T. S., Jaw, T. J., Kurant, E., Chen, C. T., Bessarab, D. A., Salzberg, A., and Sun, Y. H. (1998). The Homothorax homeoprotein activates the nuclear localization of another homeoprotein, extradenticle, and suppresses eye development in Drosophila. Genes Dev *12*, 435-446.

Papatsenko, D., Nazina, A., and Desplan, C. (2001). A conserved regulatory element present in all Drosophila rhodopsin genes mediates Pax6 functions and participates in the fine-tuning of cell-specific expression. Mech Dev *101*, 143-153.

Papatsenko, D., Sheng, G., and Desplan, C. (1997). A new rhodopsin in R8 photoreceptors of Drosophila: evidence for coordinate expression with Rh3 in R7 cells. Development *124*, 1665-1673.

Pflugfelder, G. O., Roth, H., Poeck, B., Kerscher, S., Schwarz, H., Jonschker, B., and Heisenberg, M. (1992). The lethal(1)optomotor-blind gene of Drosophila melanogaster is a major organizer of optic lobe development: isolation and characterization of the gene. Proc Natl Acad Sci U S A *89*, 1199-1203.

Pichaud, F., and Casares, F. (2000). homothorax and iroquois-C genes are required for the establishment of territories within the developing eye disc. Mech Dev *96*, 15-25.

Pichaud, F., and Desplan, C. (2001). A new visualization approach for identifying mutations that affect differentiation and organization of the Drosophila ommatidia. Development *128*, 815-826.

Porter, J. A., Hicks, J. L., Williams, D. S., and Montell, C. (1992). Differential localizations of and requirements for the two Drosophila ninaC kinase/myosins in photoreceptor cells. J Cell Biol *116*, 683-693.

Presente, A., Shaw, S., Nye, J. S., and Andres, A. J. (2002). Transgene-mediated RNA interference defines a novel role for notch in chemosensory startle behavior. Genesis *34*, 165-169.

Quandt, K., Frech, K., Karas, H., Wingender, E., and Werner, T. (1995). MatInd and MatInspector: new fast and versatile tools for detection of consensus matches in nucleotide sequence data. Nucleic Acids Res *23*, 4878-4884.

Reinke, R., and Zipursky, S. L. (1988). Cell-cell interaction in the Drosophila retina: the bride of sevenless gene is required in photoreceptor cell R8 for R7 cell development. Cell *55*, 321-330.

Rieckhof, G. E., Casares, F., Ryoo, H. D., Abu-Shaar, M., and Mann, R. S. (1997). Nuclear translocation of extradenticle requires homothorax, which encodes an extradenticle-related homeodomain protein. Cell *91*, 171-183.

Rossel, S., and Wehner, R. (1986). Polarization vision in bees. Nature, 128-131.

Ryoo, H. D., Marty, T., Casares, F., Affolter, M., and Mann, R. S. (1999). Regulation of Hox target genes by a DNA bound Homothorax/Hox/Extradenticle complex. Development *126*, 5137-5148.

Sagerstrom, C. G. (2004). PbX marks the spot. Dev Cell *6*, 737-738.

Schweisguth, F., and Posakony, J. W. (1992). Suppressor of Hairless, the Drosophila homolog of the mouse recombination signal-binding protein gene, controls sensory organ cell fates. Cell *69*, 1199-1212.

Sheng, G., Thouvenot, E., Schmucker, D., Wilson, D. S., and Desplan, C. (1997). Direct regulation of rhodopsin 1 by Pax-6/eyeless in Drosophila: evidence for a conserved function in photoreceptors. Genes Dev *11*, 1122-1131.

Sivasankaran, R., Vigano, M. A., Muller, B., Affolter, M., and Basler, K. (2000). Direct transcriptional control of the Dpp target omb by the DNA binding protein Brinker. Embo J *19*, 6162-6172.

Sonnenfeld, M., Ward, M., Nystrom, G., Mosher, J., Stahl, S., and Crews, S. (1997). The Drosophila tango gene encodes a bHLH-PAS protein that is orthologous to mammalian Arnt and controls CNS midline and tracheal development. Development *124*, 4571-4582.

Stowers, R. S., and Schwarz, T. L. (1999). A genetic method for generating Drosophila eyes composed exclusively of mitotic clones of a single genotype. Genetics *152*, 1631-1639.

Struhl, G., and Adachi, A. (1998). Nuclear access and action of notch in vivo. Cell *93*, 649-660.

Struhl, G., and Greenwald, I. (2001). Presenilin-mediated transmembrane cleavage is required for Notch signal transduction in Drosophila. Proc Natl Acad Sci U S A *98*, 229-234.

Strutt, H., and Strutt, D. (2003). EGF signaling and ommatidial rotation in the Drosophila eye. Curr Biol *13*, 1451-1457.

Tahayato, A., Sonneville, R., Pichaud, F., Wernet, M. F., Papatsenko, D., Beaufils, P., Cook, T., and Desplan, C. (2003). Otd/Crx, a dual regulator for the specification of ommatidia subtypes in the Drosophila retina. Dev Cell *5*, 391-402.

Thummel, C. S. (1996). Files on steroids--Drosophila metamorphosis and the mechanisms of steroid hormone action. Trends Genet *12*, 306-310.

Tomlinson, A. (2003). Patterning the peripheral retina of the fly: decoding a gradient. Dev Cell *5*, 799-809.

Tomlinson, A., Bowtell, D. D., Hafen, E., and Rubin, G. M. (1987). Localization of the sevenless protein, a putative receptor for positional information, in the eye imaginal disc of Drosophila. Cell *51*, 143-150.

Tomlinson, A., Kimmel, B. E., and Rubin, G. M. (1988). rough, a Drosophila homeobox gene required in photoreceptors R2 and R5 for inductive interactions in the developing eye. Cell *55*, 771-784.

Tomlinson, A., and Struhl, G. (1999). Decoding vectorial information from a gradient: sequential roles of the receptors Frizzled and Notch in establishing planar polarity in the Drosophila eye. Development *126*, 5725-5738.

Tomlinson, A., and Struhl, G. (2001). Delta/Notch and Boss/Sevenless signals act combinatorially to specify the Drosophila R7 photoreceptor. Mol Cell *7*, 487-495.

Tree, D. R., Ma, D., and Axelrod, J. D. (2002). A three-tiered mechanism for regulation of planar cell polarity. Semin Cell Dev Biol *13*, 217-224.

Treisman, J. E., and Rubin, G. M. (1995). wingless inhibits morphogenetic furrow movement in the Drosophila eye disc. Development *121*, 3519-3527.

Tsai, S. F., Jang, C. C., Prikhod'ko, G. G., Bessarab, D. A., Tang, C. Y., Pflugfelder, G. O., and Sun, Y. H. (1997). Gypsy retrotransposon as a tool for the in vivo analysis of the regulatory region of the optomotor-blind gene in Drosophila. Proc Natl Acad Sci U S A *94*, 3837-3841.

van de Wetering, M., Cavallo, R., Dooijes, D., van Beest, M., van Es, J., Loureiro, J., Ypma, A., Hursh, D., Jones, T., Bejsovec, A*., et al.* (1997). Armadillo coactivates transcription driven by the product of the Drosophila segment polarity gene dTCF. Cell *88*, 789-799.

Van Vactor, D., Jr., Krantz, D. E., Reinke, R., and Zipursky, S. L. (1988). Analysis of mutants in chaoptin, a photoreceptor cell-specific glycoprotein in Drosophila, reveals its role in cellular morphogenesis. Cell *52*, 281-290.

Vandendries, E. R., Johnson, D., and Reinke, R. (1996). orthodenticle is required for photoreceptor cell development in the Drosophila eye. Dev Biol *173*, 243-255.

Veeman, M. T., Axelrod, J. D., and Moon, R. T. (2003). A second canon. Functions and mechanisms of beta-catenin-independent Wnt signaling. Dev Cell *5*, 367-377.

von Philipsborn, A., and Labhart, T. (1990). A behavioral study of polarization vision in the fly, Musca domestica. J Comp Physiol, 737-743.

Wada, S. (1971). Ein spezieller Rhabdomerentyp im Fliegenauge. Experimentia, 1237-1238.

Wada, S. (1974). Spezielle randzonale Ommatidien der Fliegen (Diptera: Brachycera): Architektur und Verteilung in den Komplexaugen. Z Morphol Tiere, 87-125.

Ward, M. P., Mosher, J. T., and Crews, S. T. (1998). Regulation of bHLH-PAS protein subcellular localization during Drosophila embryogenesis. Development *125*, 1599-1608.

Weihe, U., Dorfman, R., Wernet, M. F., Cohen, S. M., and Milan, M. (2004). Proximodistal subdivision of Drosophila legs and wings: the elbow-no ocelli gene complex. Development *131*, 767-774.

Wernet, M. F., and Desplan, C. (2004). Building a retinal mosaic: cell-fate decision in the fly eye. Trends Cell Biol *14*, 576-584.

Wernet, M. F., Labhart, T., Baumann, F., Mazzoni, E. O., Pichaud, F., and Desplan, C. (2003). Homothorax switches function of Drosophila photoreceptors from color to polarized light sensors. Cell *115*, 267-279.

Wolf, R., Gebhardt, B., Gademann, R., and Heisenberg, M. (1980). Polarization sensitivity of course control In Drosophila melanogaster. J Comp Physiol *139*, 177-191.

Wolff, T. a. R., D.F. (1993). Pattern formation in the Drosophila Retina. In The Development of Drosophila melanogaster, M. M.-A. Bate, A, ed. (Cold Spring Harbor, Cold Spring Harbor Laboratory Press), pp. 1277-1325.

Xu, T., and Rubin, G. M. (1993). Analysis of genetic mosaics in developing and adult Drosophila tissues. Development *117*, 1223-1237.

Yan, R., Small, S., Desplan, C., Dearolf, C. R., and Darnell, J. E., Jr. (1996). Identification of a Stat gene that functions in Drosophila development. Cell *84*, 421-430.

Yoshikawa, S., McKinnon, R. D., Kokel, M., and Thomas, J. B. (2003). Wnt-mediated axon guidance via the Drosophila Derailed receptor. Nature *422*, 583-588.

Zecca, M., Basler, K., and Struhl, G. (1996). Direct and long-range action of a wingless morphogen gradient. Cell *87*, 833-844.

Zeidler, M. P., Perrimon, N., and Strutt, D. I. (1999). Polarity determination in the Drosophila eye: a novel role for unpaired and JAK/STAT signaling. Genes Dev *13*, 1342-1353.

Zhao, X., Yang, Y., Fitch, D. H., and Herman, M. A. (2002). TLP-1 is an asymmetric cell fate determinant that responds to Wnt signals and controls male tail tip morphogenesis in C. elegans. Development *129*, 1497-1508.

Zipursky, S. L., Venkatesh, T. R., Teplow, D. B., and Benzer, S. (1984). Neuronal development in the Drosophila retina: monoclonal antibodies as molecular probes. Cell *36*, 15-26.

Zuker, C. S., Cowman, A. F., and Rubin, G. M. (1985). Isolation and structure of a rhodopsin gene from D. melanogaster. Cell *40*, 851-858.

VII. ACKNOWLEDGEMENTS

VIII. APPENDIX

Molecularly localized

GAL4 enhancer traps

line #002: insertion of pGawB in gene *CG14408*

SH3 domain binding protein

whole fly

002 > lacZ

water immersion

002 expression is inner PR specific
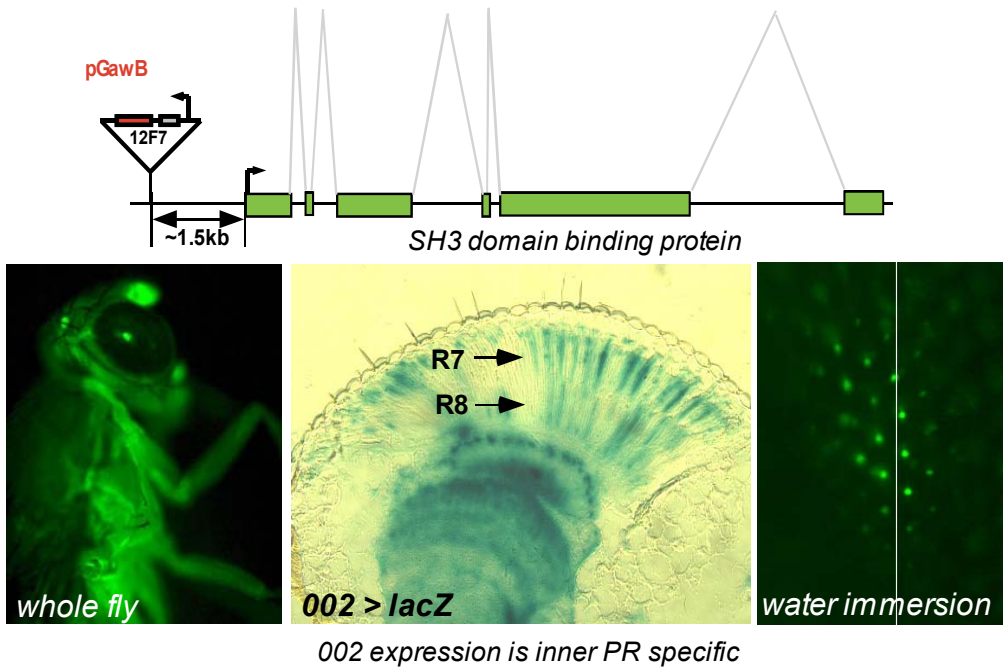
gene #008: inserted in X-chromosome heterochromatin

gene product/enhancer unknown

whole fly

008 > lacZ

water immersion

008 expression is outer PR specific
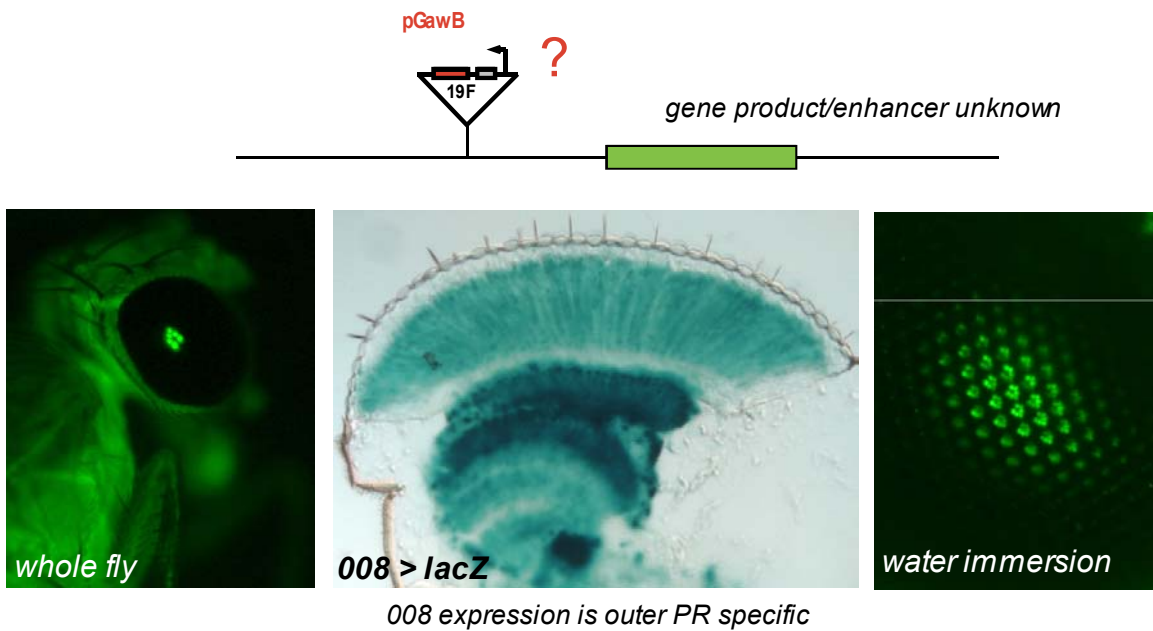
line #010: Insertion of pGawB in the gene *elbow*

transcription factor (Zn-finger)

whole fly

010 > lacZ

water immersion

subsets of inner PRs: DRA and R8

line #012: insertion of pGawB in gene α-Man-IIb

whole fly

012> lacZ

water immersion

all PRs
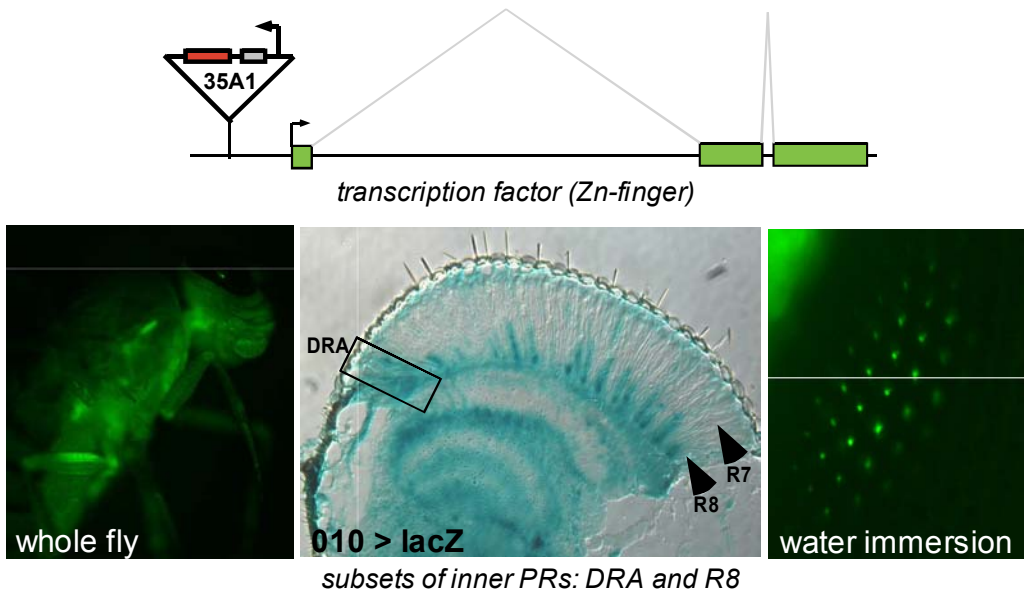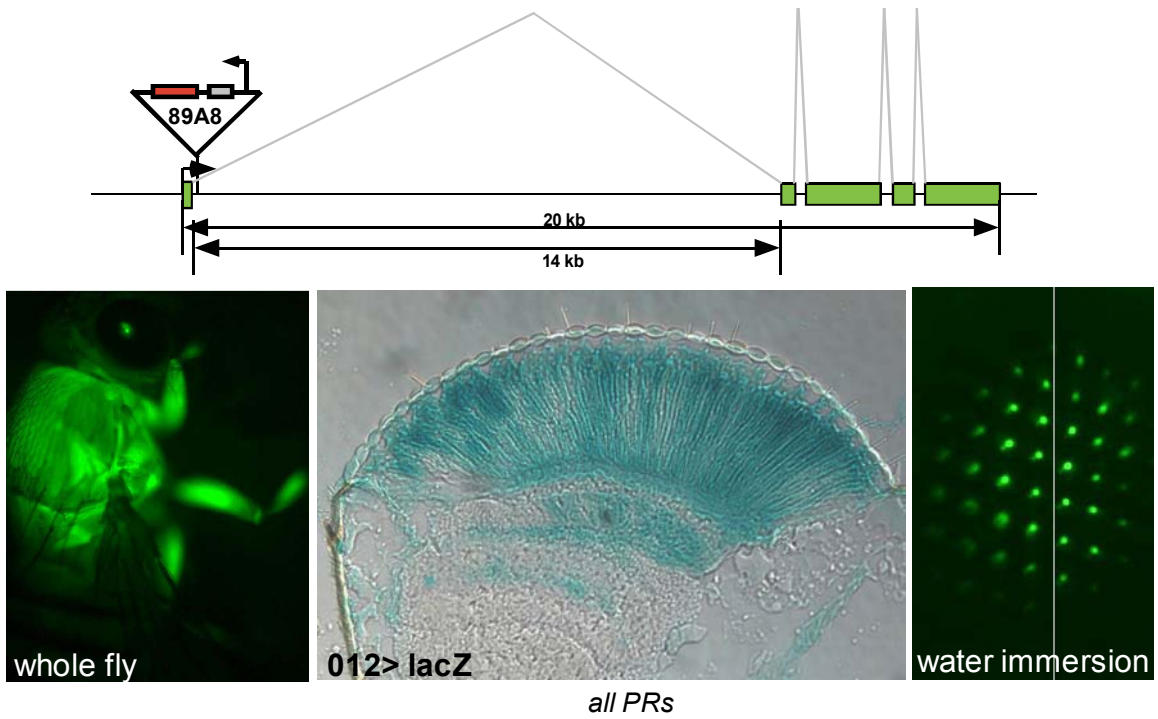
gene #013: insertion of pGawB in gene *CG9602*

ubiquitin conjugating enzyme

87F

~1kb

~1.2kb

whole fly

LL

OL

013 > lacZ

closeup
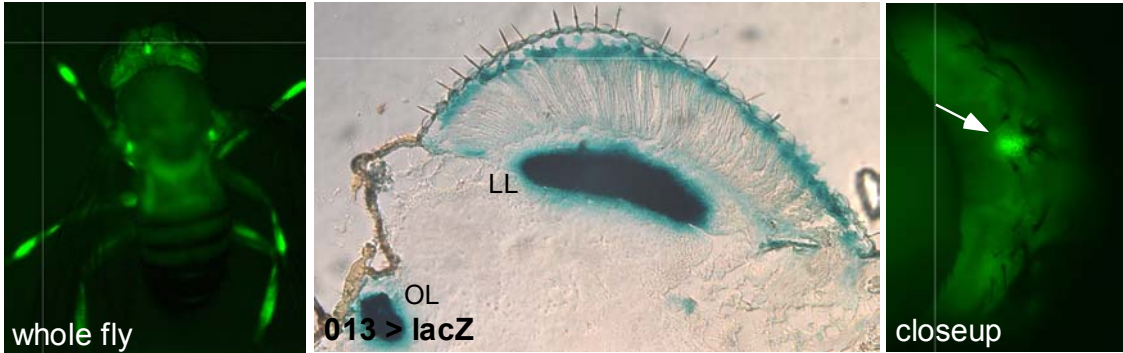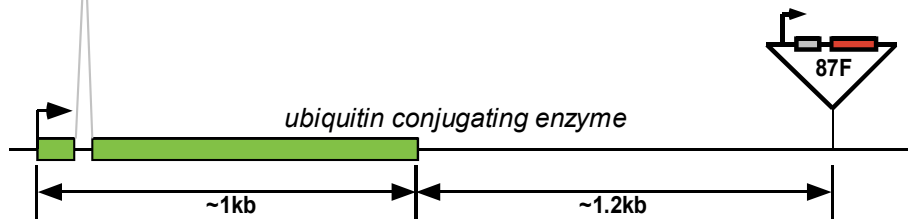
expression in: lamina (LL) and ocellar (OL) lobes

line #015: insertion of pGawB in gene CG2991

23B

EGF-domain containing protein

11 kb

whole fly

015 > lacZ

water immersion
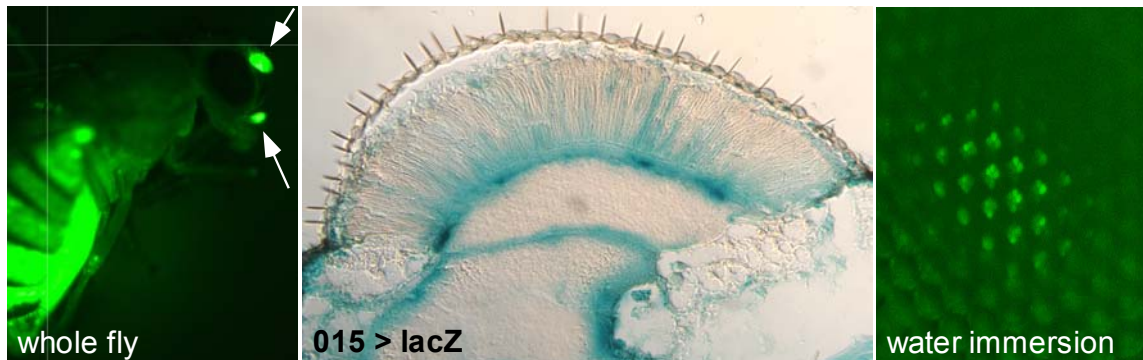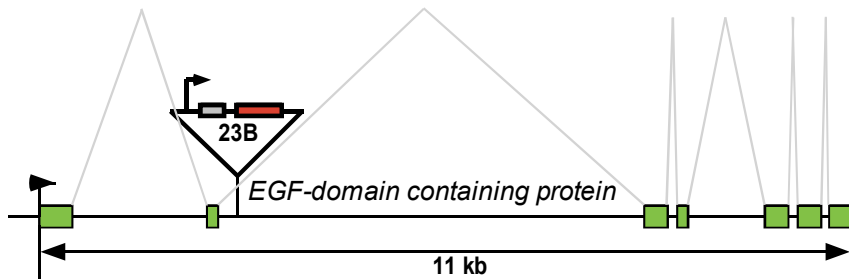
very weak PRs, antennae, maxillary palps

gene #016: insertion of pGawB in *rhodopsin1/ninaE*

outer PR opsin

whole fly

water immersion

expressed in: outer PRs + ocelli
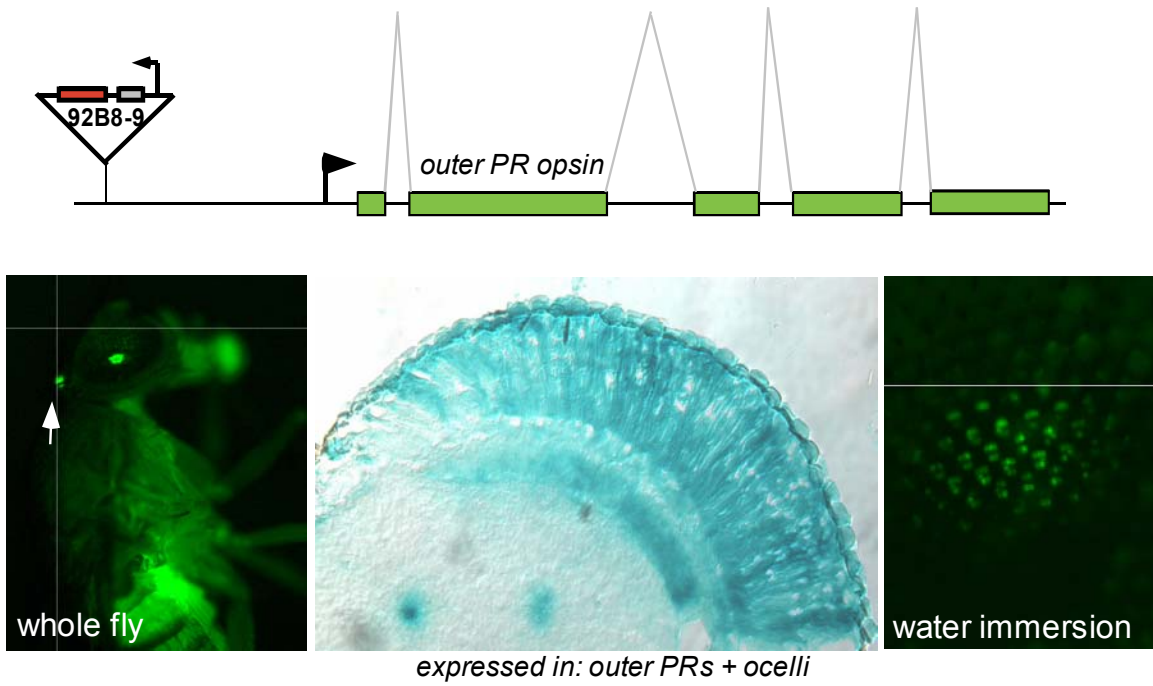
gene #021: insertion of pGawB in gene *kekkon-1*

TM molecule, negative regulator of DER signaling

0 kb   1 kb   5 kb

whole fly

water immersion

all PRs, variegated
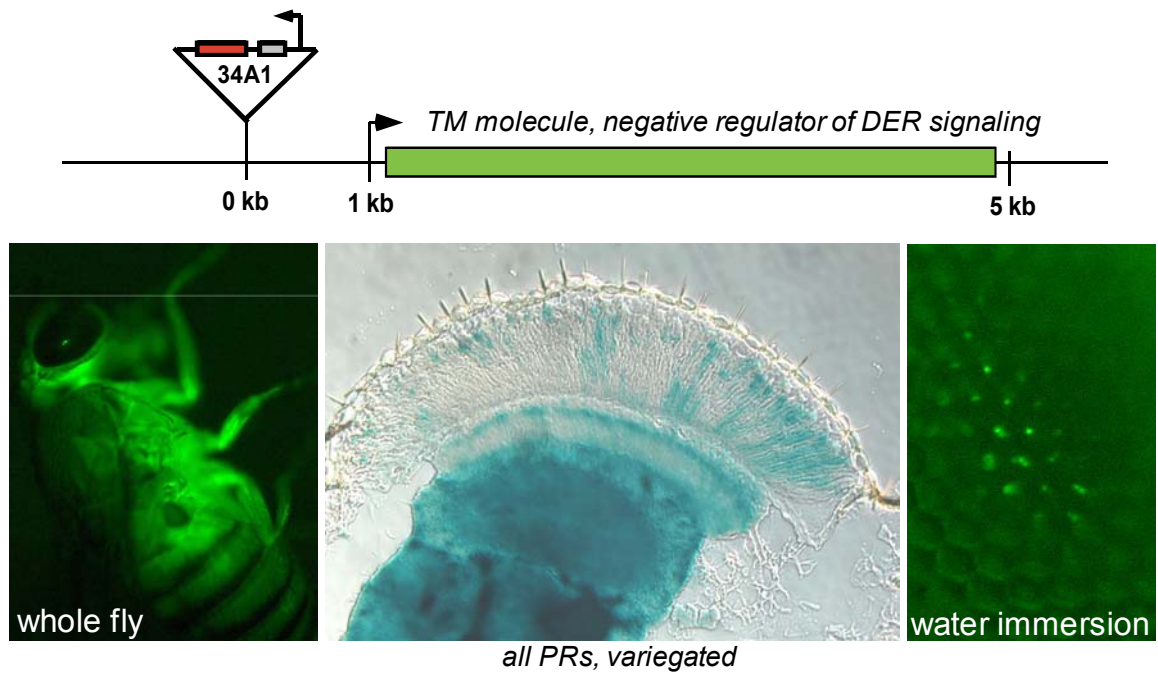
gene #022: insertion of pGawB in gene *slamdance*

97D

~ 3 kb

~1.8 kb

'alanyl (membrane) aminopeptidase

whole fly

022 > lacZ

water immersion
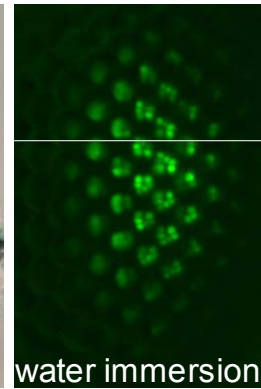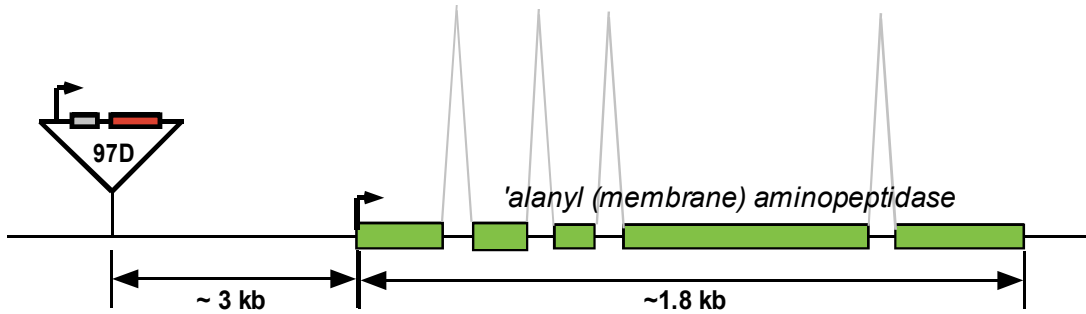
expressed in:outer PRs

gene #030: insertion in the gene *lats (warts)*

100A6

Ser-/Thr-kinase involved in cell-cycle regulation

whole fly

030 > lacZ

R7

DRA

water immersion
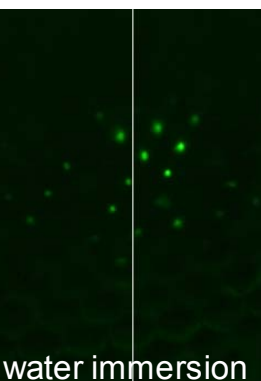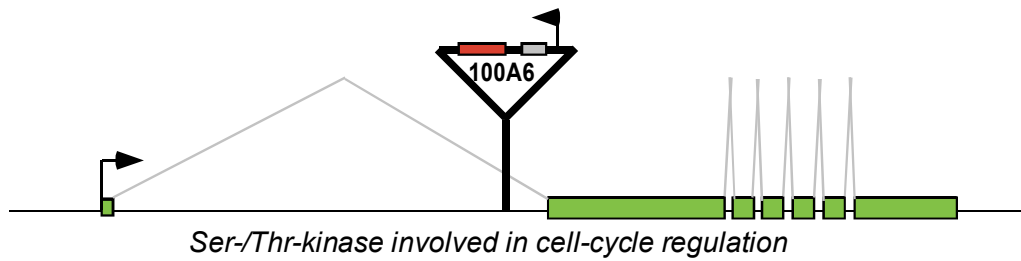
subsets of PRs: DRA, R8, R7 and outer PRs (ventrally)

line#033: insertion of pGawB in the gene *no ocelli*

pGawB

35A4

transcription factor (Zn-finger)

whole fly

033 > lacZ

R7

R8

water immersion
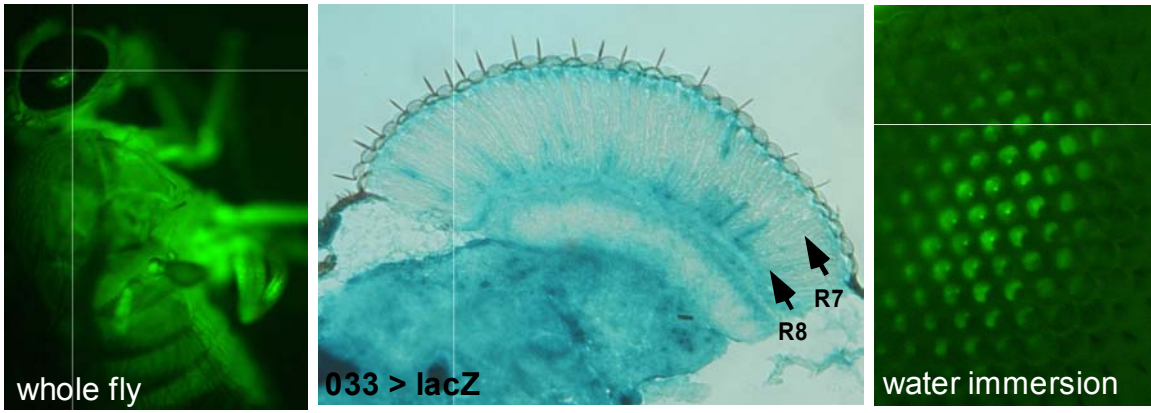
expressed in: subsets of inner PRs (R7, R8)

line#40: insertion of pGawB in *dachsous*

pGawB

21C7

Cadherin-family TM cell-adhesion molecule

whole fly

040 > lacZ

blowup
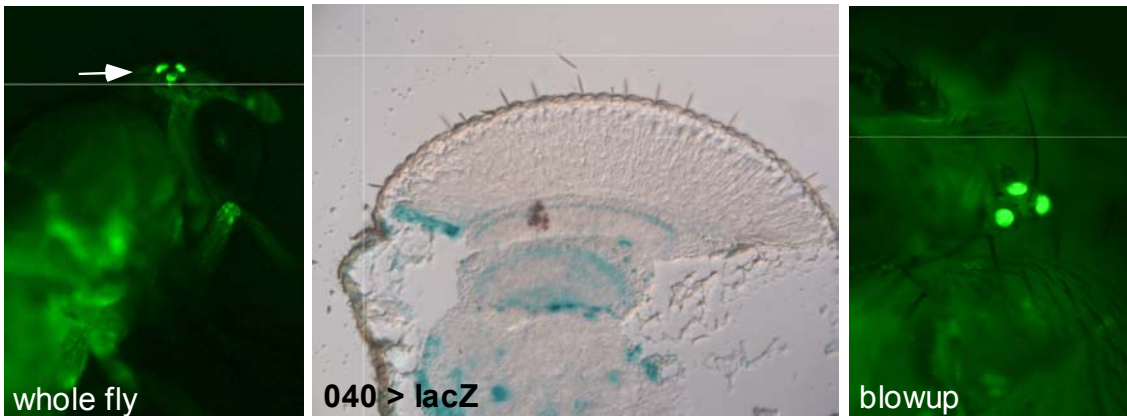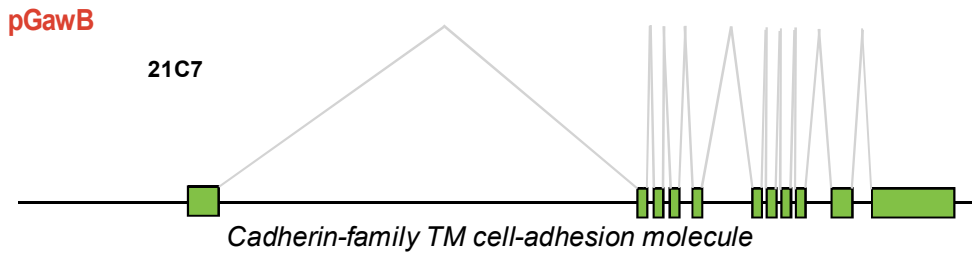
expressed in:ocelli

253

line #041: insertion of pGawB in gene *retinal degeneration B*

Ca-transporting ATPase

13 kb

whole fly

041 > lacZ

water immersion
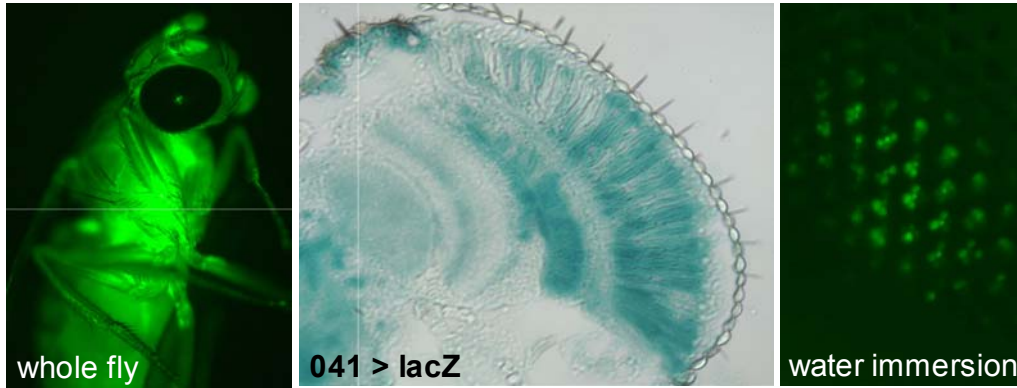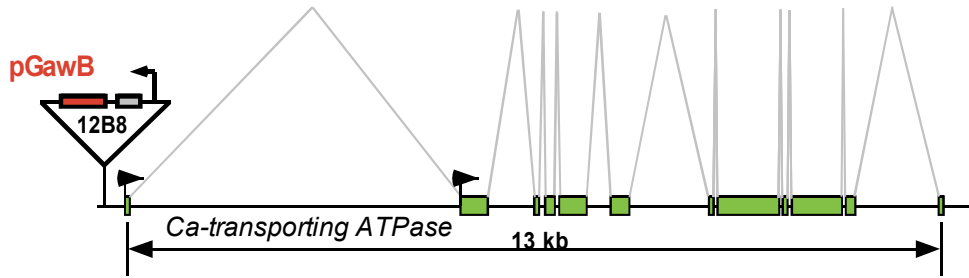
expressed in: all PRs

line #043: insertion of pGawB in gene *CG3364*

gene product shows no homologies

~1.8 kb

whole fly

043 > lacZ

water immersion
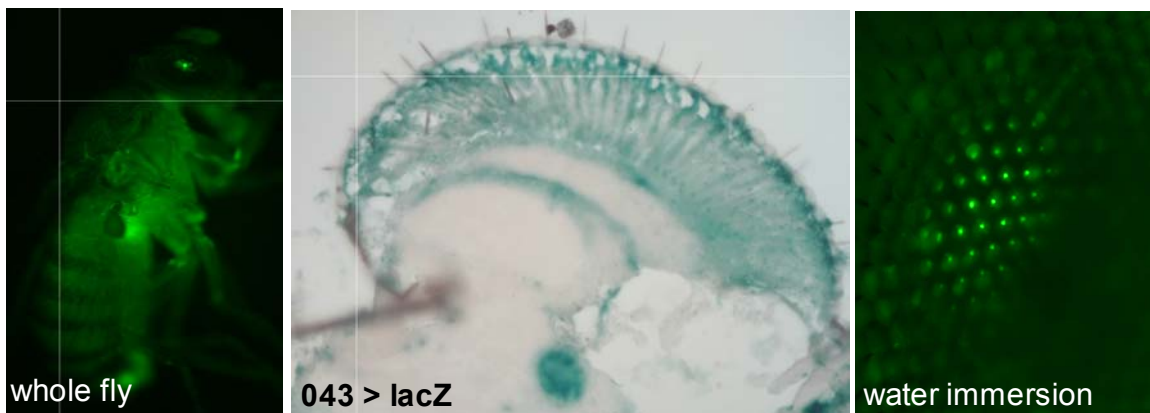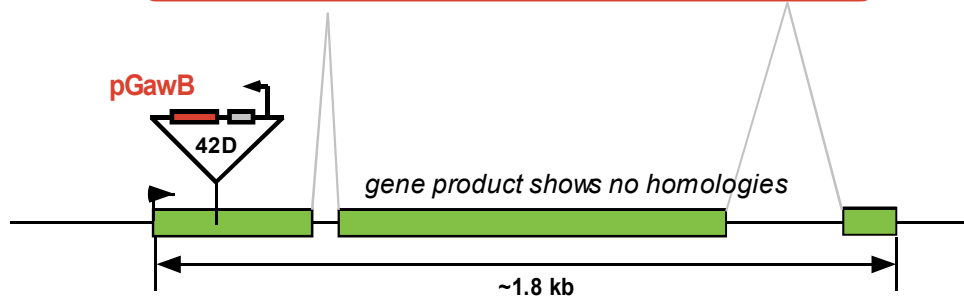
inner PRs and cone cells

line #046: insertion of pGawB in gene CG4449

pGawB

94E9

Ubiquitin-like

2 kb

whole fly

046 > lacZ

very few inner PRs R7 and R8

water immersion
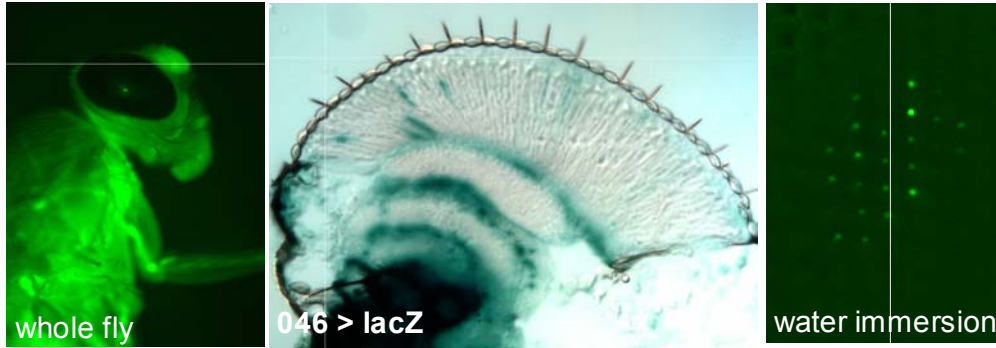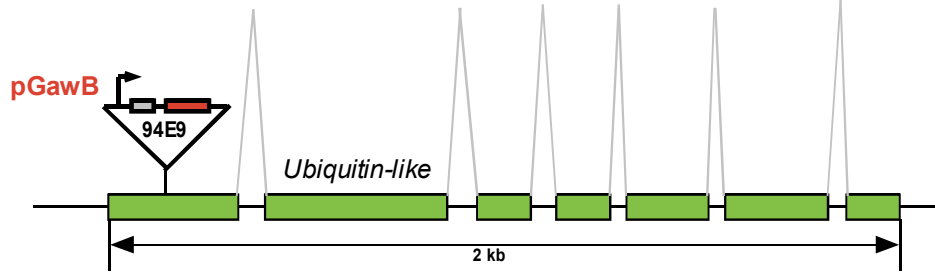
line#53: insertion of pGawB in the gene *homothorax*

pGawB

86B1-C1

homeodomain transcription factor

~8kb

pseudopupil

046 > lacZ

R7 R8

DRA inner PRs

water immersion
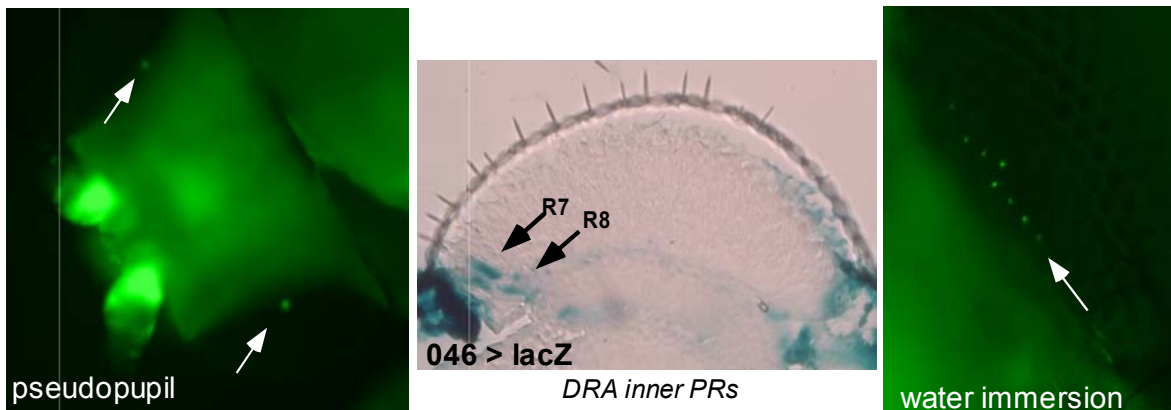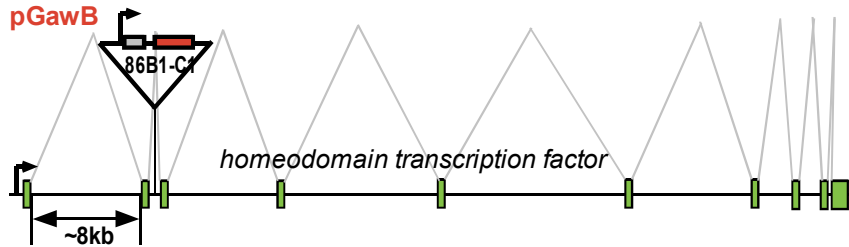
gene #056: insertion of pGawB in CG32767

pGawB

4D5

transcription factor (7 predicted Zn fingers)

whole fly

056 > lacZ

water immersion
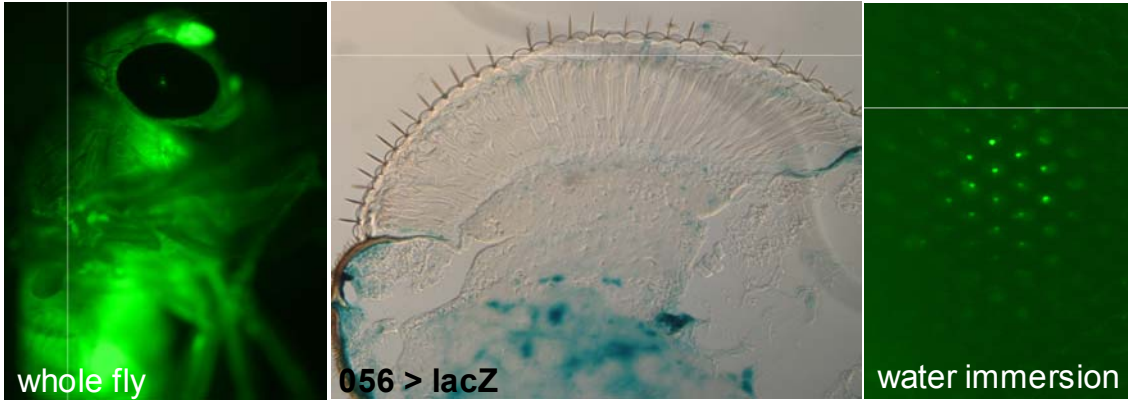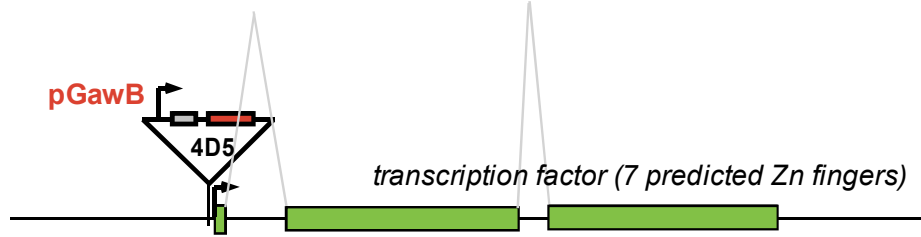
expressed extremely weak in inner PRs (R7, R8

gene #058: insertion of pGawB in gene CG2055

pGawB

45C1-3

PKC family kinase

whole fly

058 > lacZ

water immersion
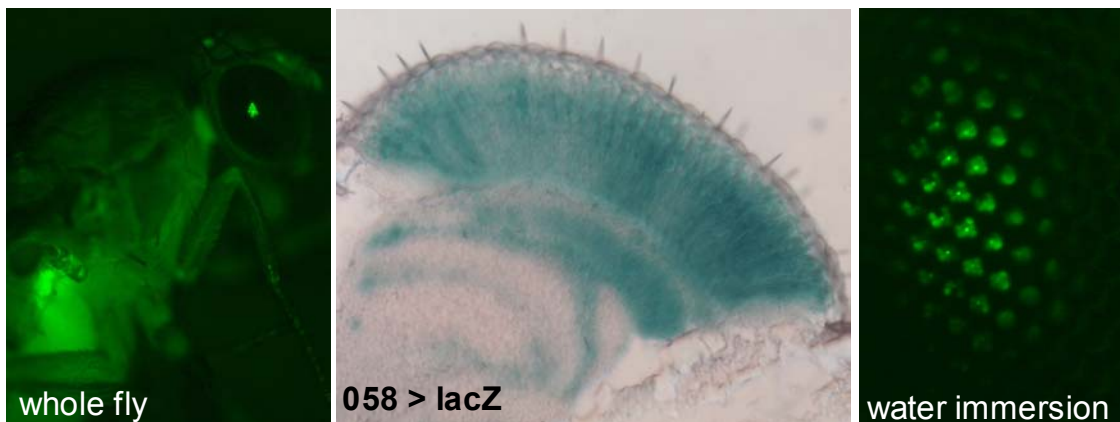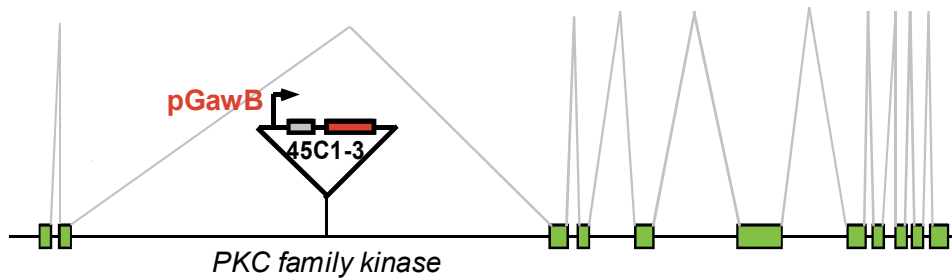
very specific, all PRs

gene #062: insertion of pGawB in gene *Tsp42Ec*

pGawB

42E1

cell-surface molecule of the tetraspan family

~5 kb

whole fly

062 > lacZ

water immersion
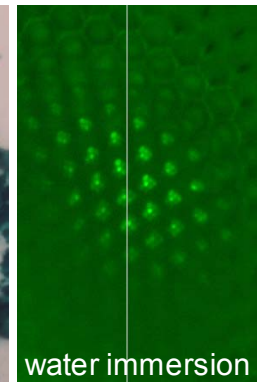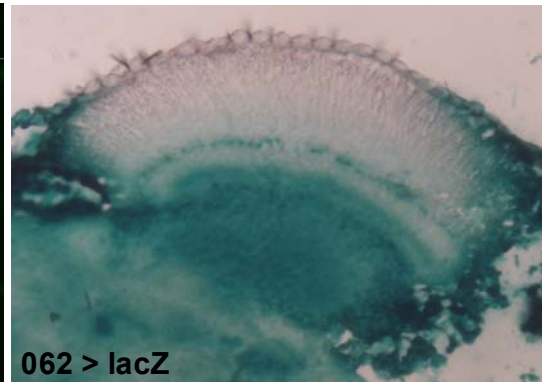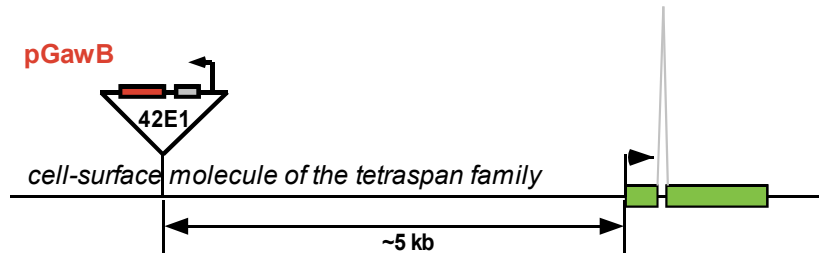
expressed very weak all PRs

gene #063: insertion of pGawB in gene *CG10600*

pGawB

37B3

predicted nuclear protein

whole fly

063 > lacZ

water immersion

outer PR specific

257
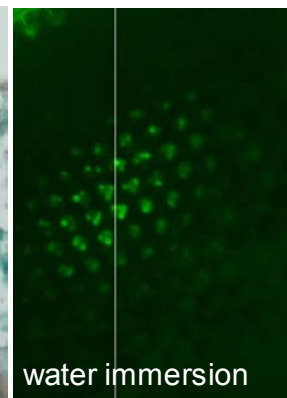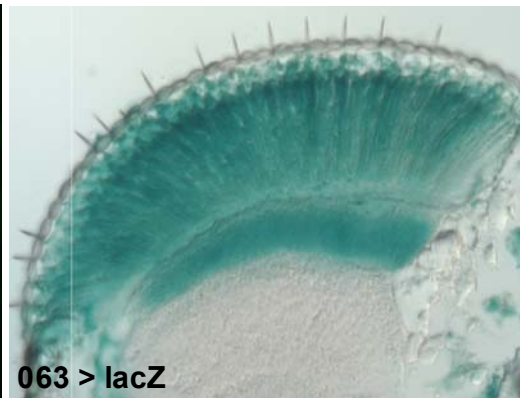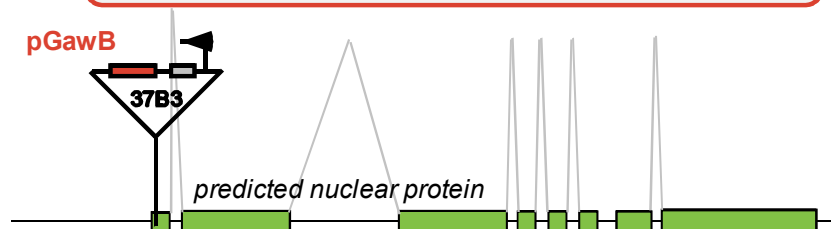
gene #069: insertion of pGawB in gene *bunched*

pGawB

33E

transcription factor, TSC22-homologue

80 kb

whole fly

069 > lacZ

blowup
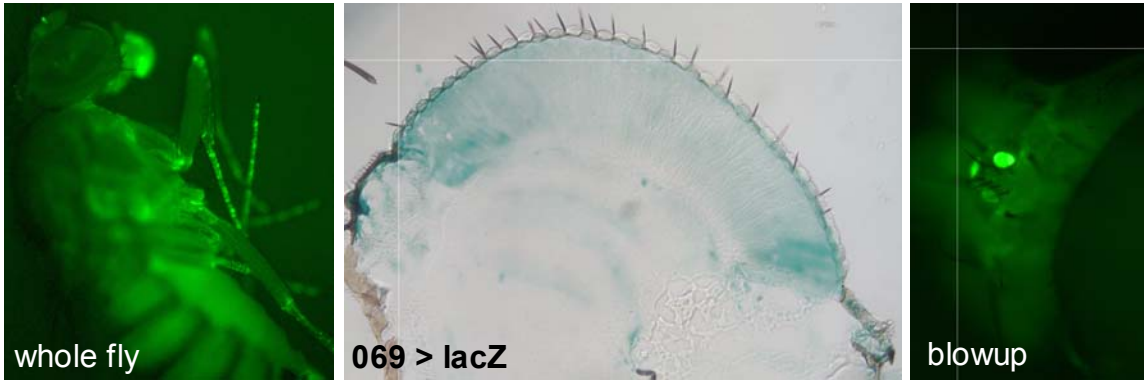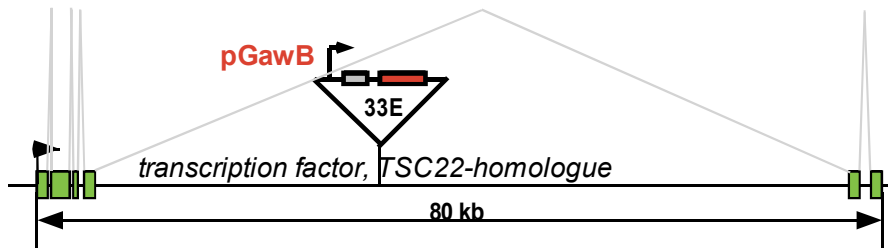
weak PRs, stronger in the periphery

gene #072: insertion of pGawB in the gene *slit*

pGawB

52D9

~30kb

Robo ligand

whole fly

072 > lacZ

water immersion
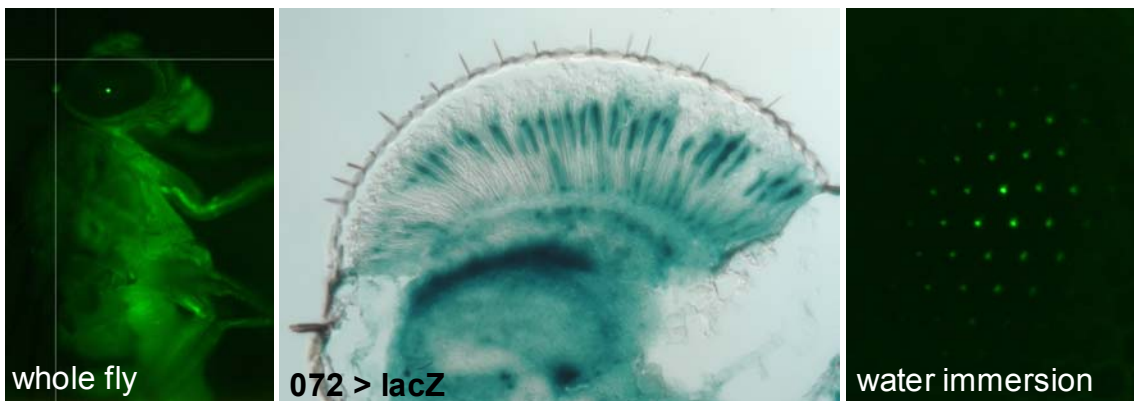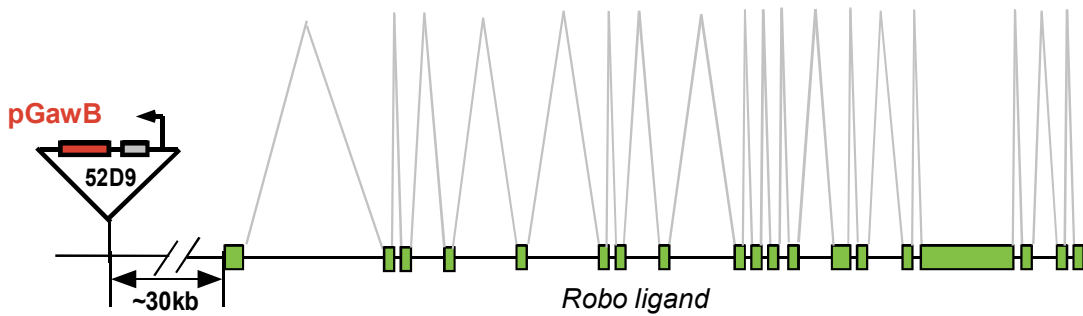
specific to inner PRs R7 and R8

gene #73: insertion of pGawB in gene *combgap*

transcription factor with 10 Zn fingers

pGawB

50E4

1 kb

4.3 kb

whole fly

water immersion

expressed in all PRs
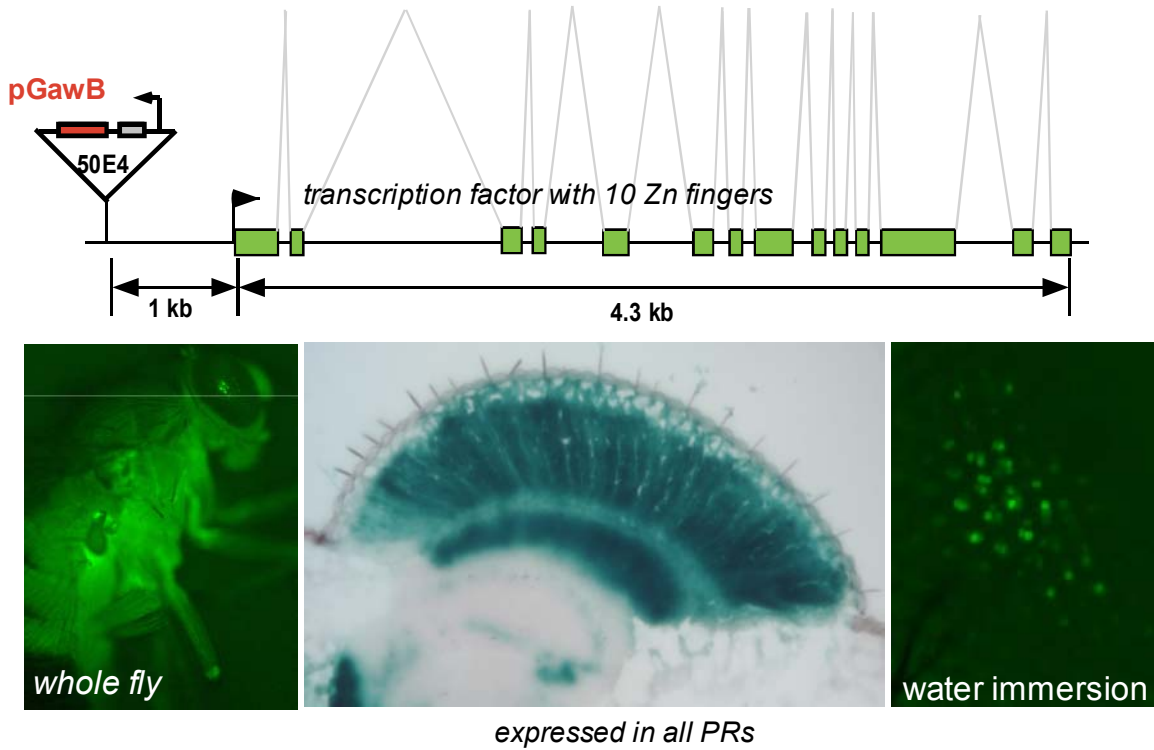
gene #75: insertion of pGawB near the gene *hybrid male rescue*

transcription factor

CG1619

pGawB

9D2

3 kb

6 kb

whole fly

antennae

maxillary palps

subset of olfactory & taste cells
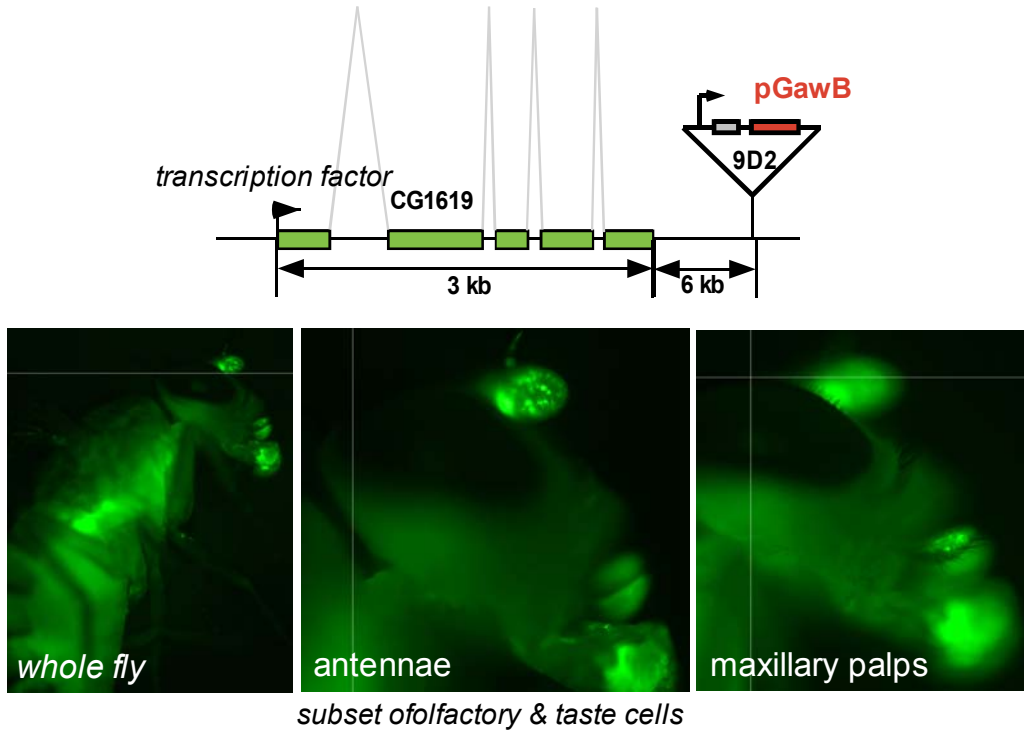
line #077: insertion of pGawB in gene CG6424

pGawB

54E3

nuclear; homologue of human KIAA0914

~0.4kb

~ 12 kb

whole fly

077 > lacZ

water immersion

expressed very weak in all PRs
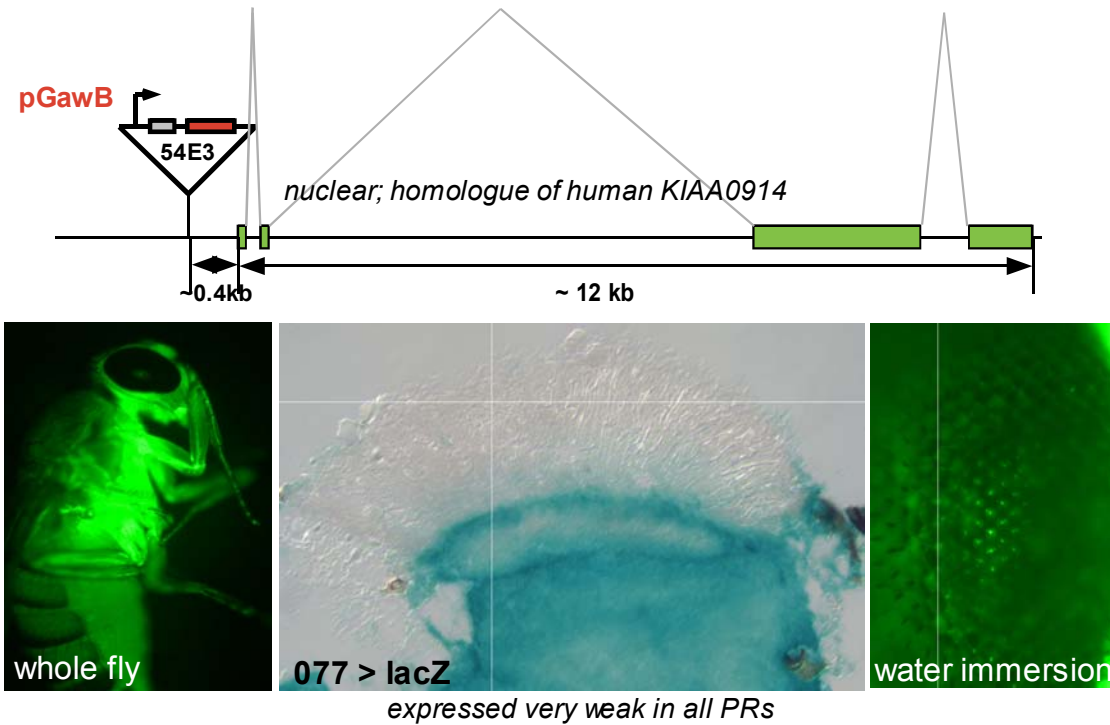
line #078: insertion of pGawB near gene CG30428

protein with no known homologies

pGawB

60F3

4 kb

whole fly

078 > lacZ

water immersion

very weak inner PR expression
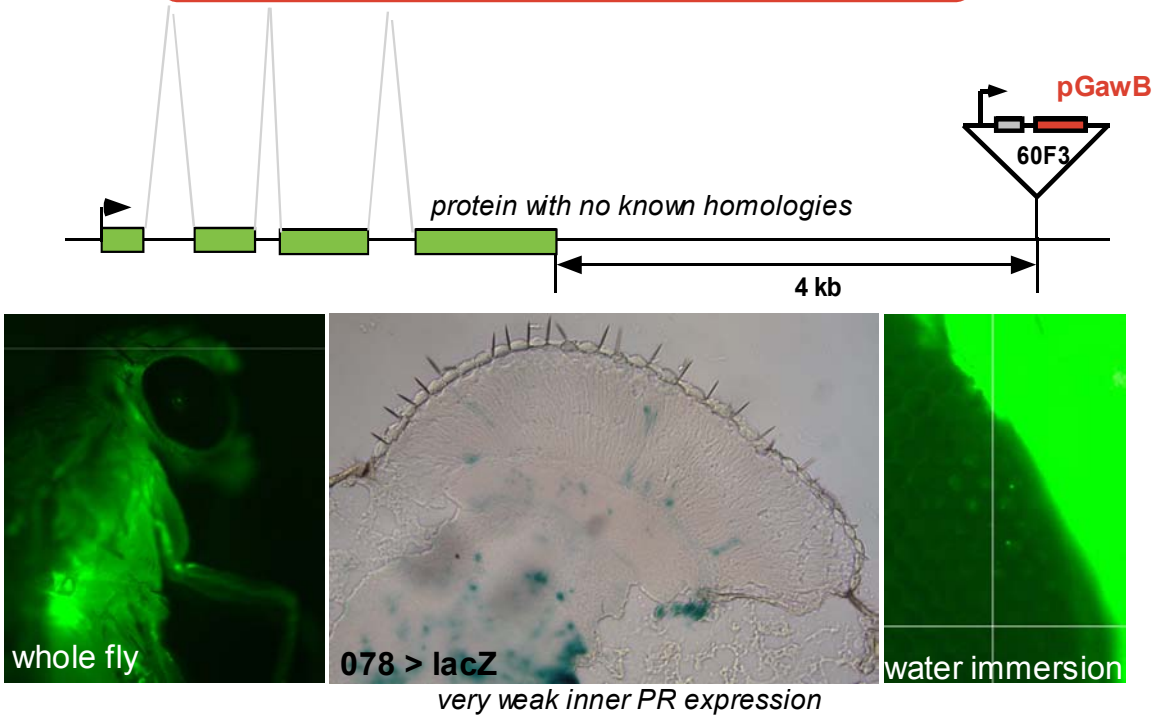
line #092: insertion of pGawB in gene CG6241

Metalloendopeptidase

2.1 kb   3.3 kb

whole fly   092 > lacZ   blowup

lamina and ocellar lobes
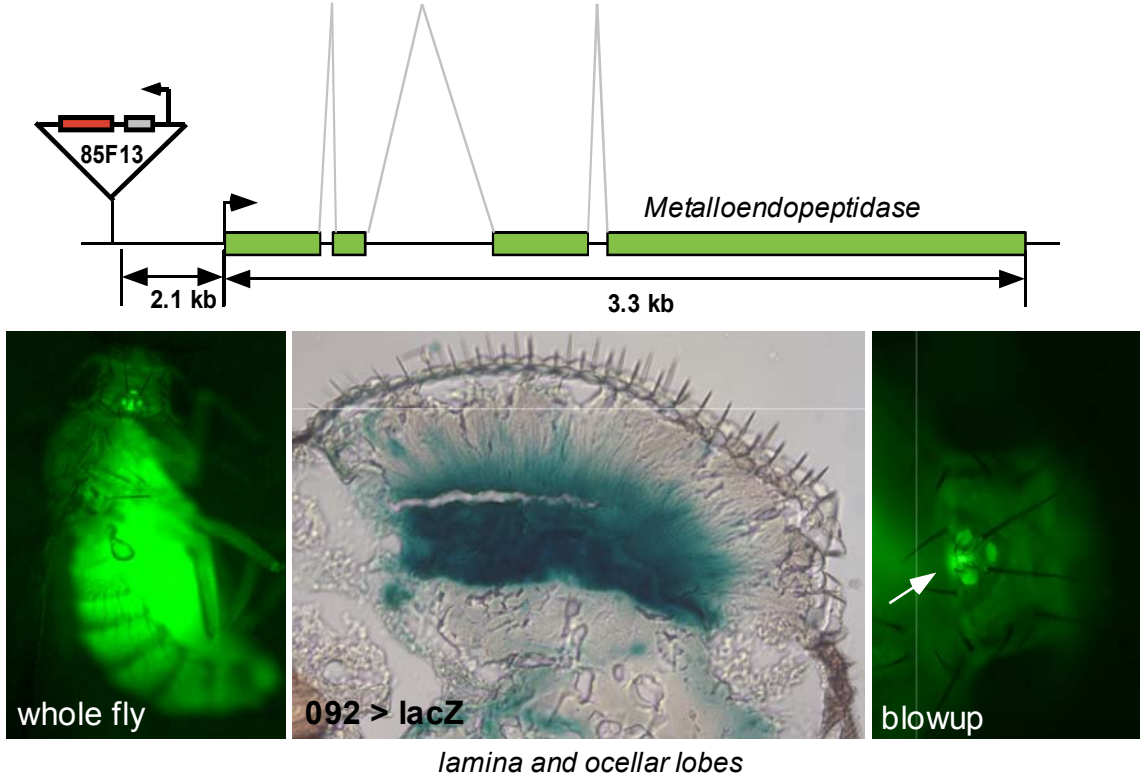
line #098: insertion of pGawB in gene CG6499

predicted (methyl) ammonium transporter

whole fly   blowup   blowup

subset of antennal cells
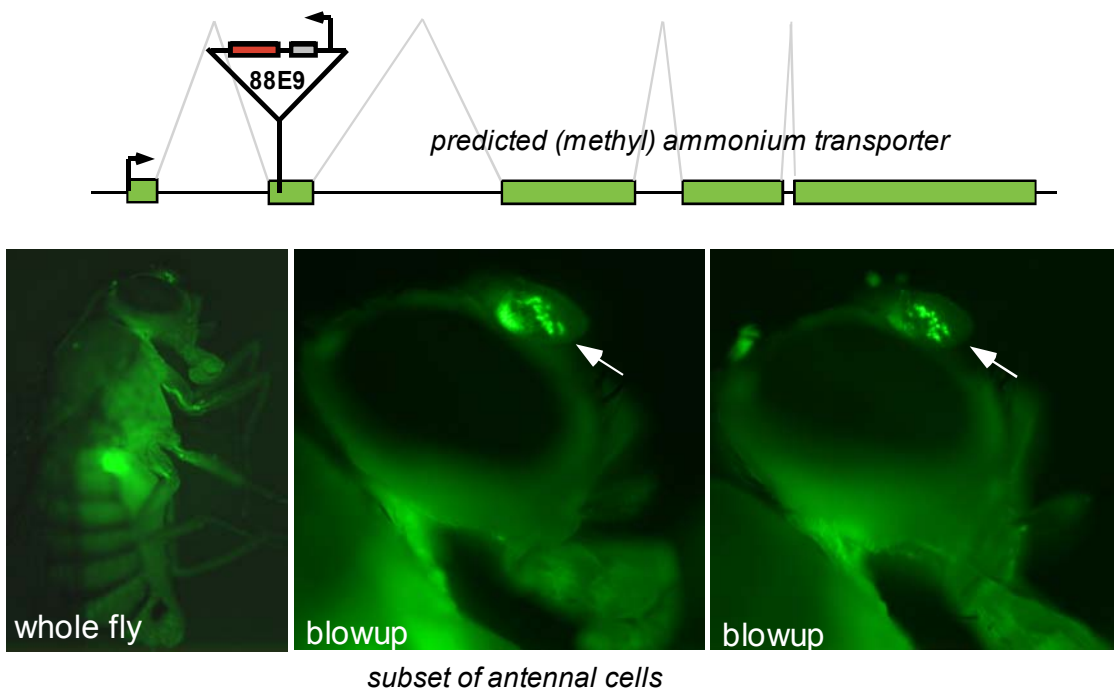
gene #100: insertion of pGawB at 88C5

no gene ~GAL4 promoter, but lethal P I(3)06951

~30 kb

whole fly | antennae | legs

second antennal segment
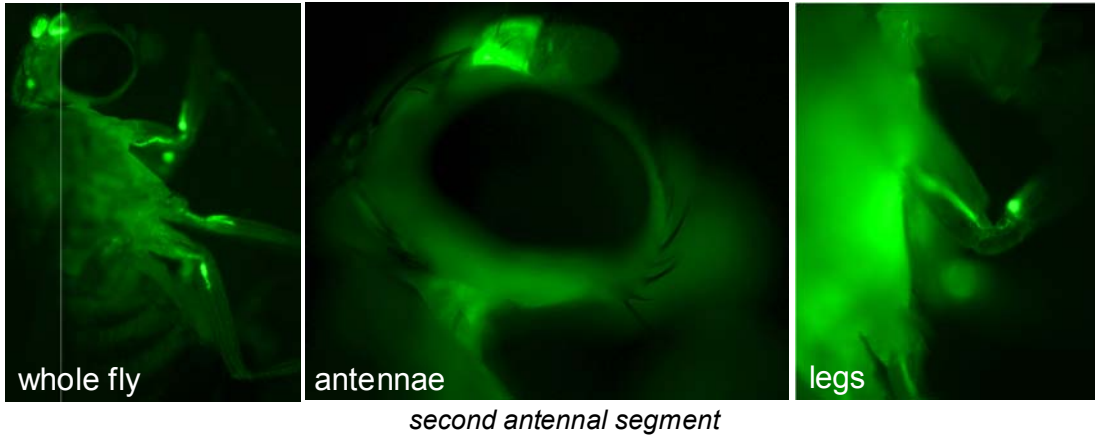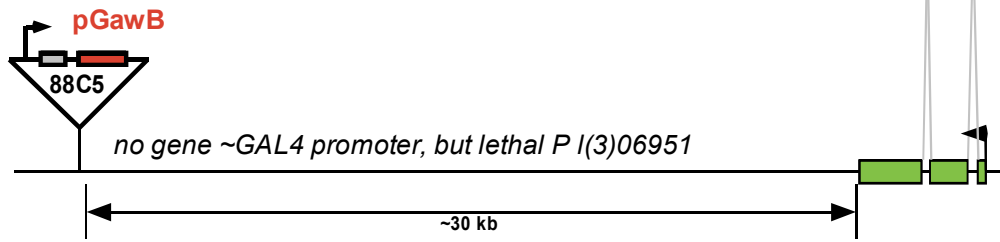
gene #103: insertion of pGawB in gene CG5735

RRM domain RNA binding protein

alt1   alt2   alt3

12 kb

whole fly | 103 > lacZ | water immersion
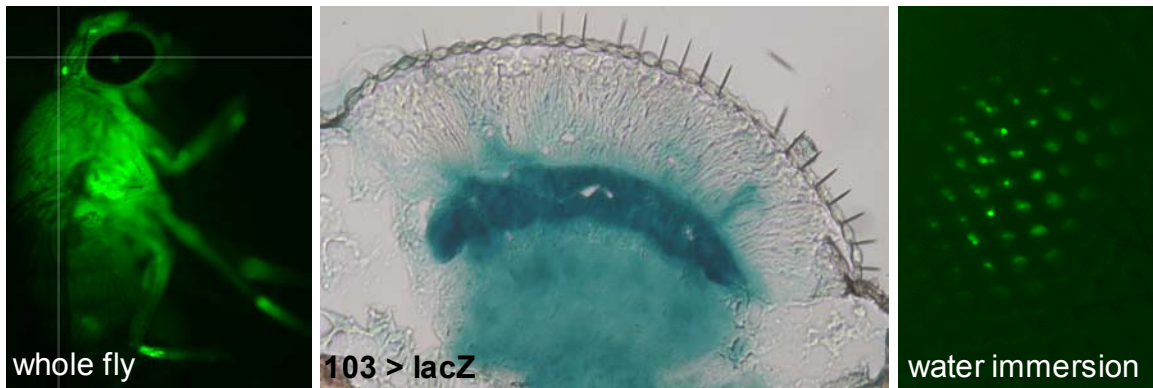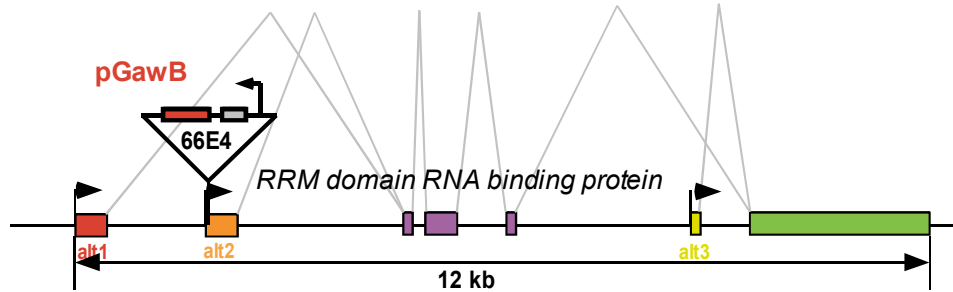
gene #112: insertion of pGawB in gene *CG14045*

Cdc42 RhoGEF, PDZ domain, C2 domain

whole Fly

112 > lacZ

water immersion

very strong in R7 cells
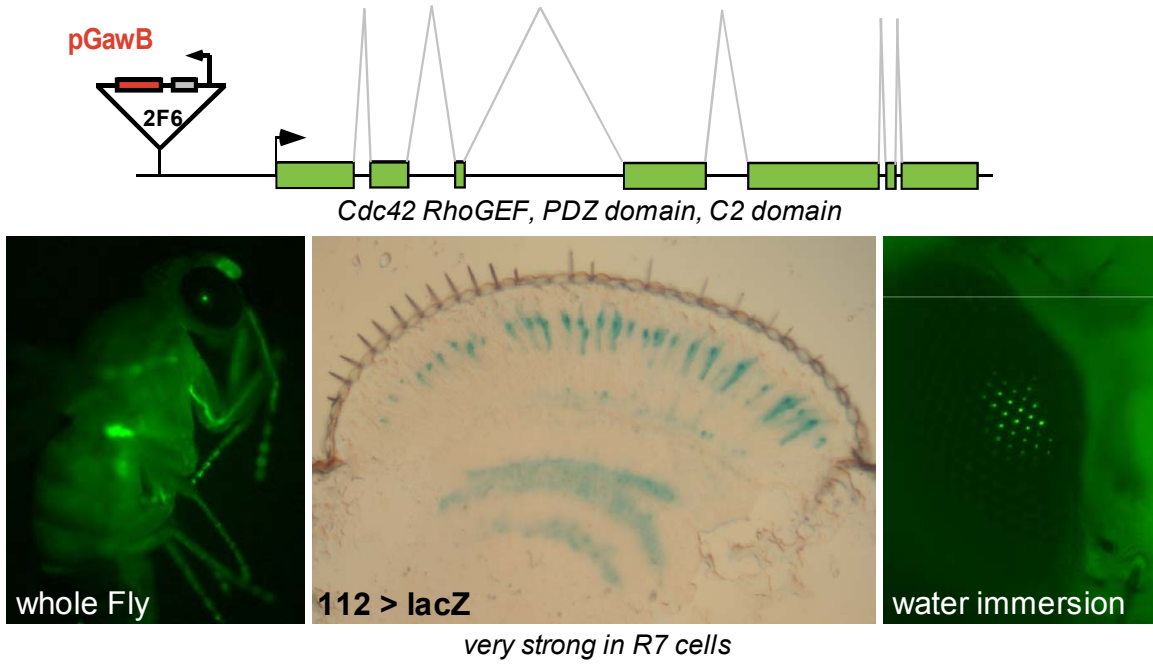
gene #114: insertion of pGawB in gene *CG14185*

no known homologies

~2.3kb

whole Fly

114 > lacZ

water immersion

all PRs,inners very strong
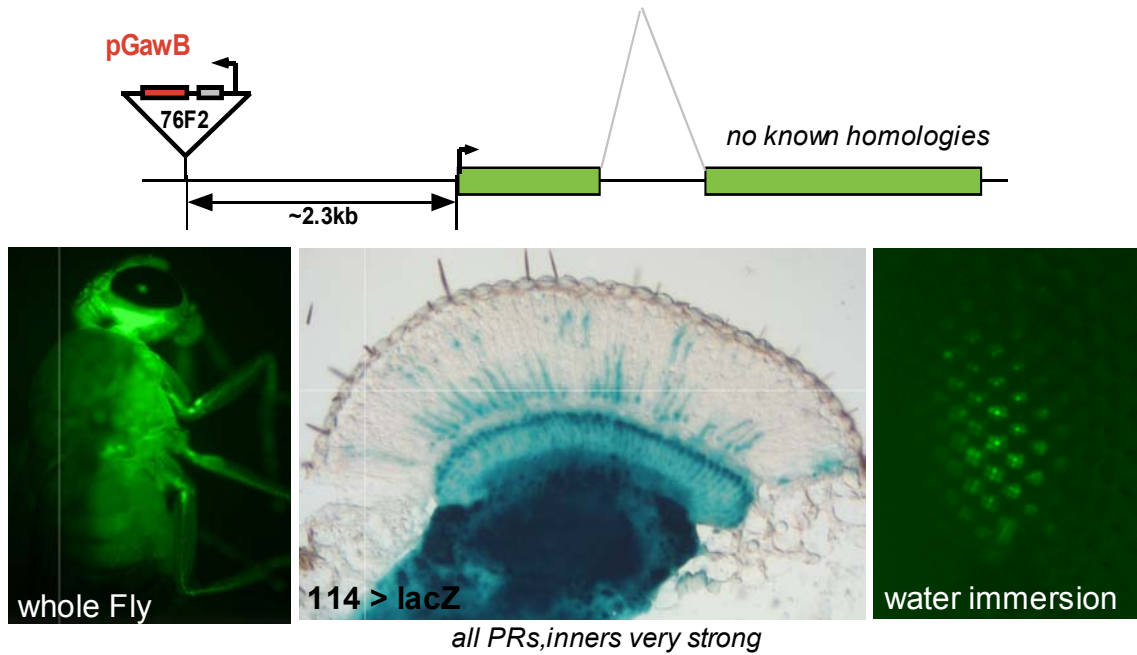
line #116: insertion of pGawB in gene *lamina ancestor*

expressed in the ocelli and optic lobes
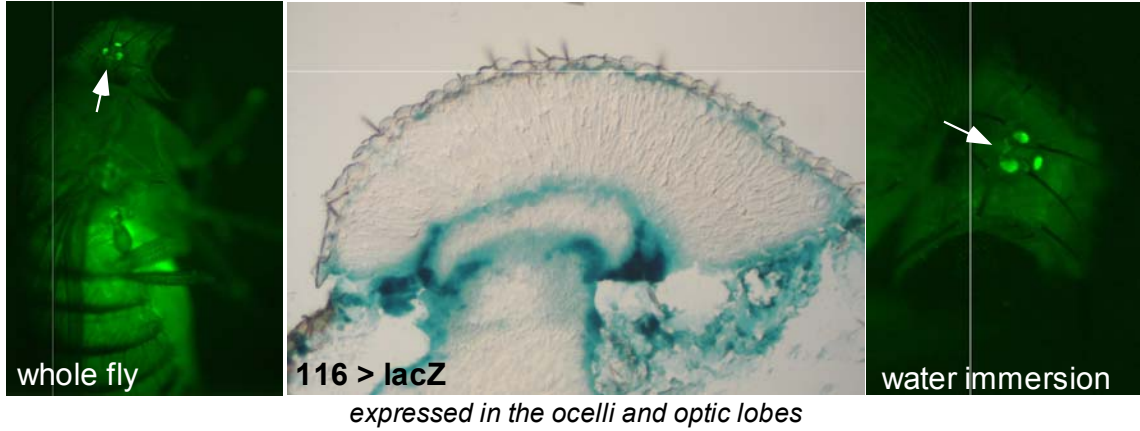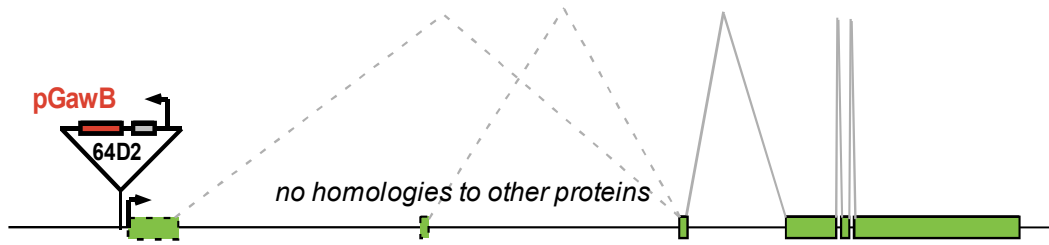
line #123: insertion of pGawB in gene *no ocelli*

subsets of inner PRs: DRA and R8
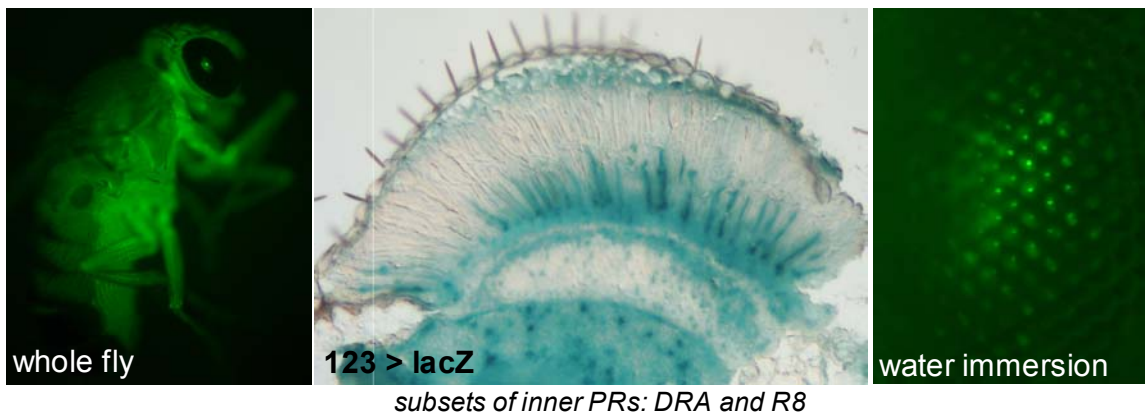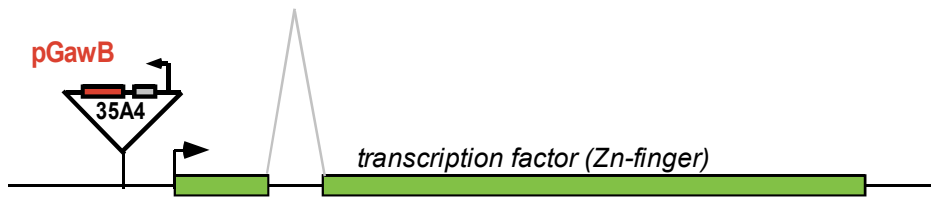
line #128: insertion of pGawB in the genes *CG11731* and *CG11732*

CG11732
odorant binding protein

CG11731
Immunglobulin protein

whole fly

128 > lacZ

water immersion

expressed in inner PRs and cone cells
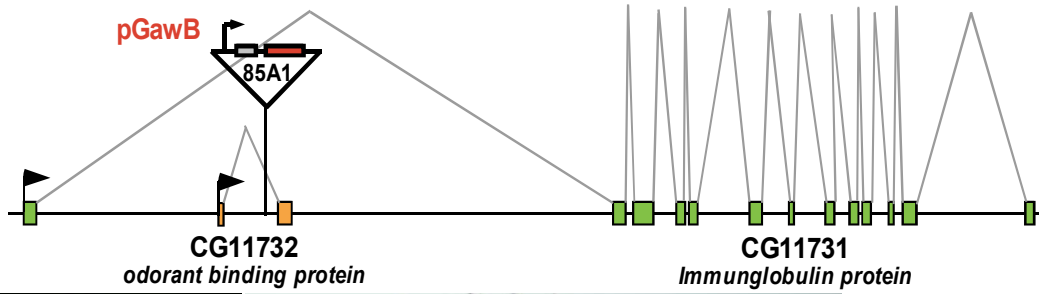
line #129: insertion of pGawB in repetitive sequences

gene product/enhancer unknown

whole fly

129 > lacZ

water immersion
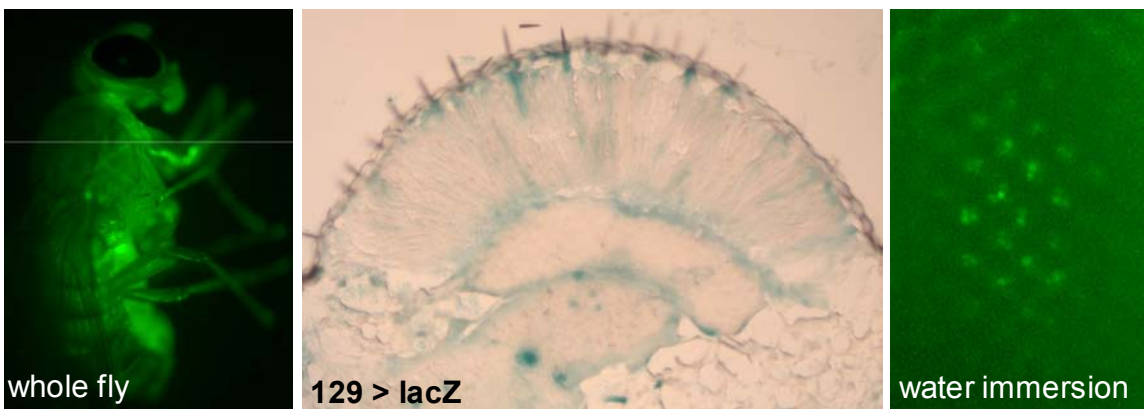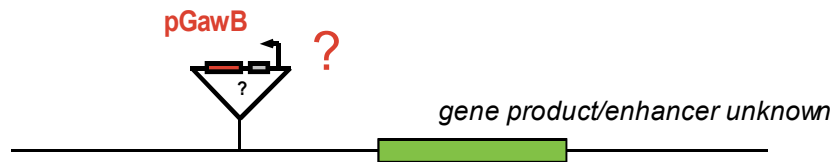
gene #134: insertion of pGawB in gene *CG7145*

pGawB

79A5

→ *d-1-Pyrrolidine-5-Carboxylate Dehydrogenase*

whole fly

134 > lacZ

water immersion

weak expression in all PRs
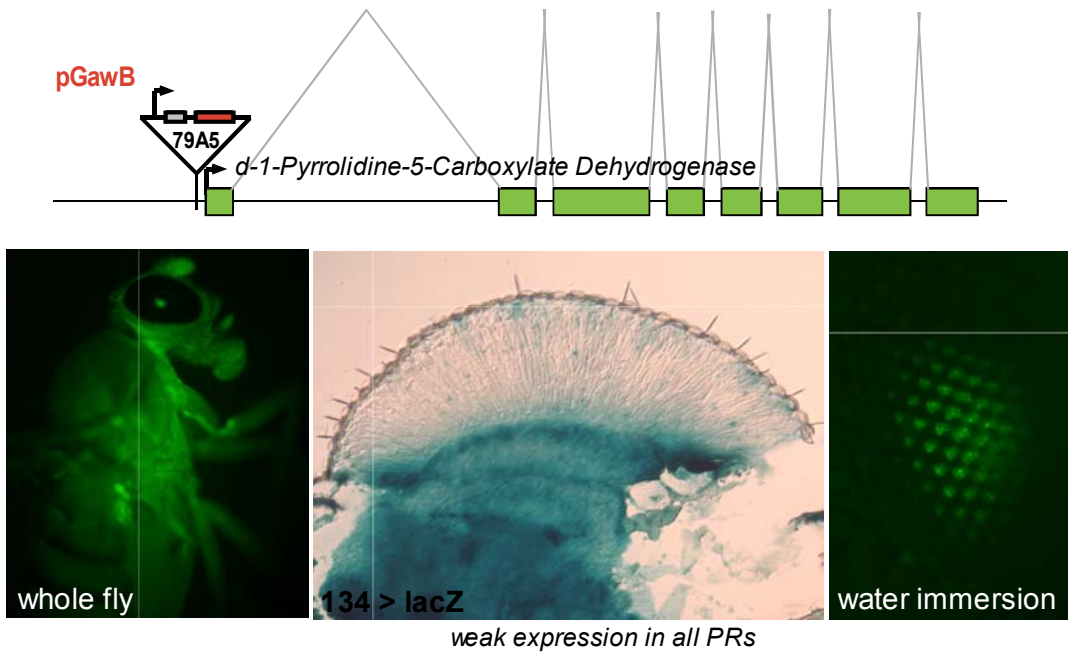
gene #137: insertion of pGawB in gene CG2264

pGawB

46D8

EF-hand cell adhesion molecule

whole fly

137 > lacZ

water immersion

expressed in the ocelli
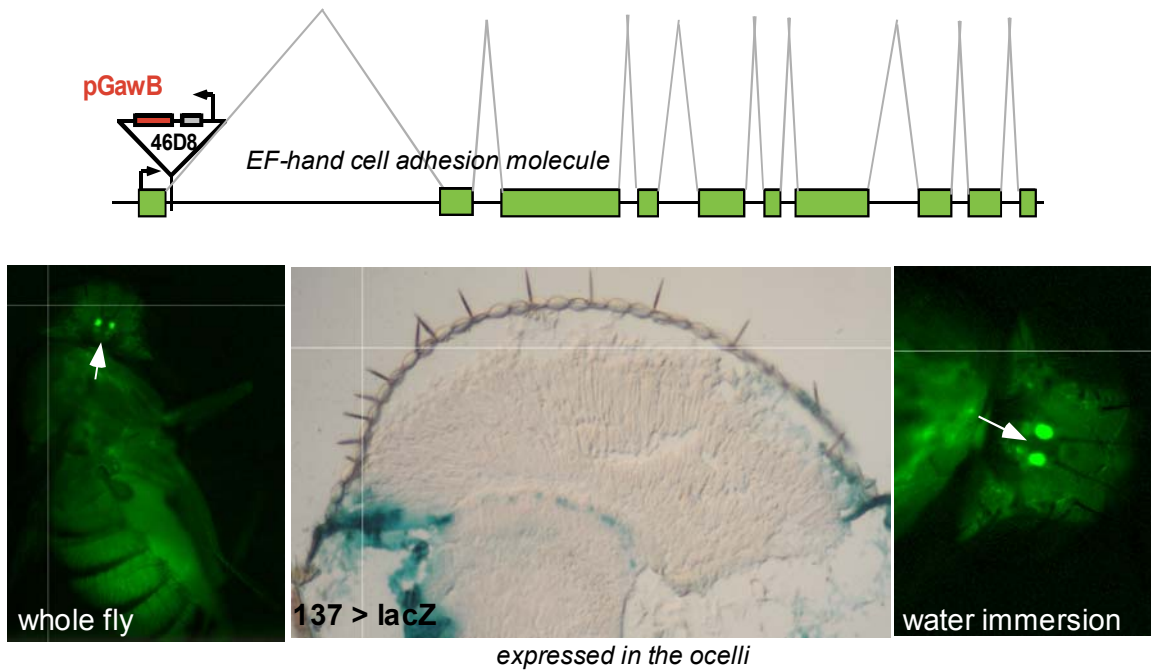
line #139: insertion of pGawB in gene *CG15512*

pGawB

99C7

Immunoglobulin protein

| whole fly | 139 > lacZ | water immersion |

rxpressed in all PRs
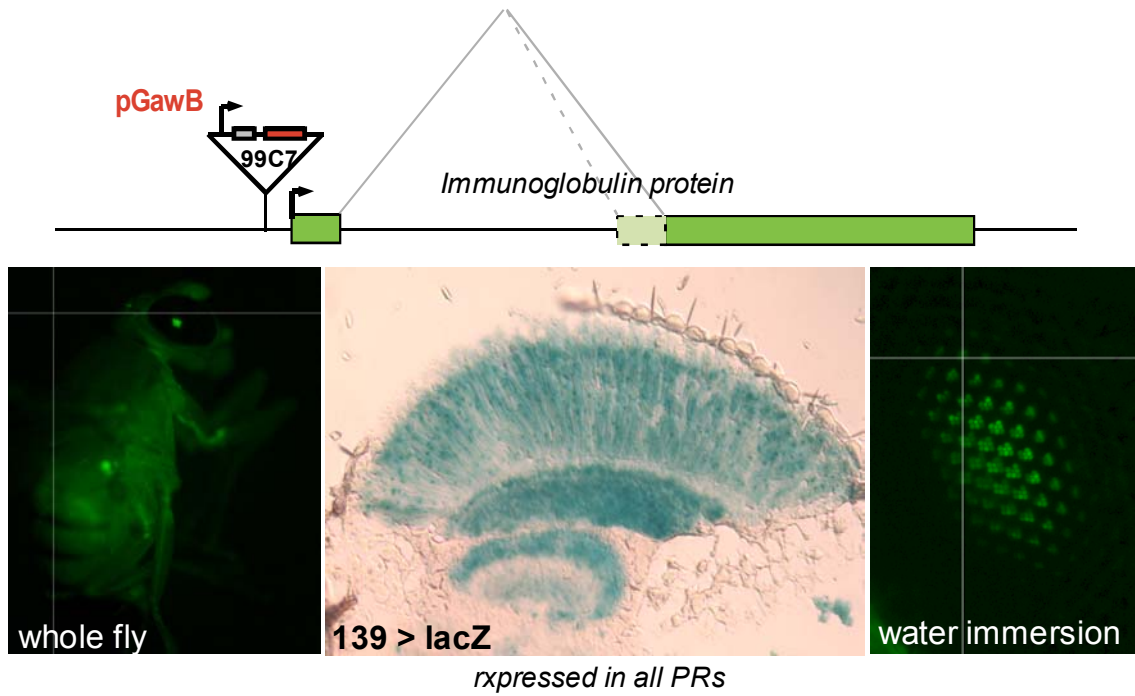
line #141: insertion of pGawB near *methuselah-like 8*

pGawB

61A1

G-protein coupled receptor

| whole fly | 141 > lacZ | water immersion |

rxpressed in all PRs
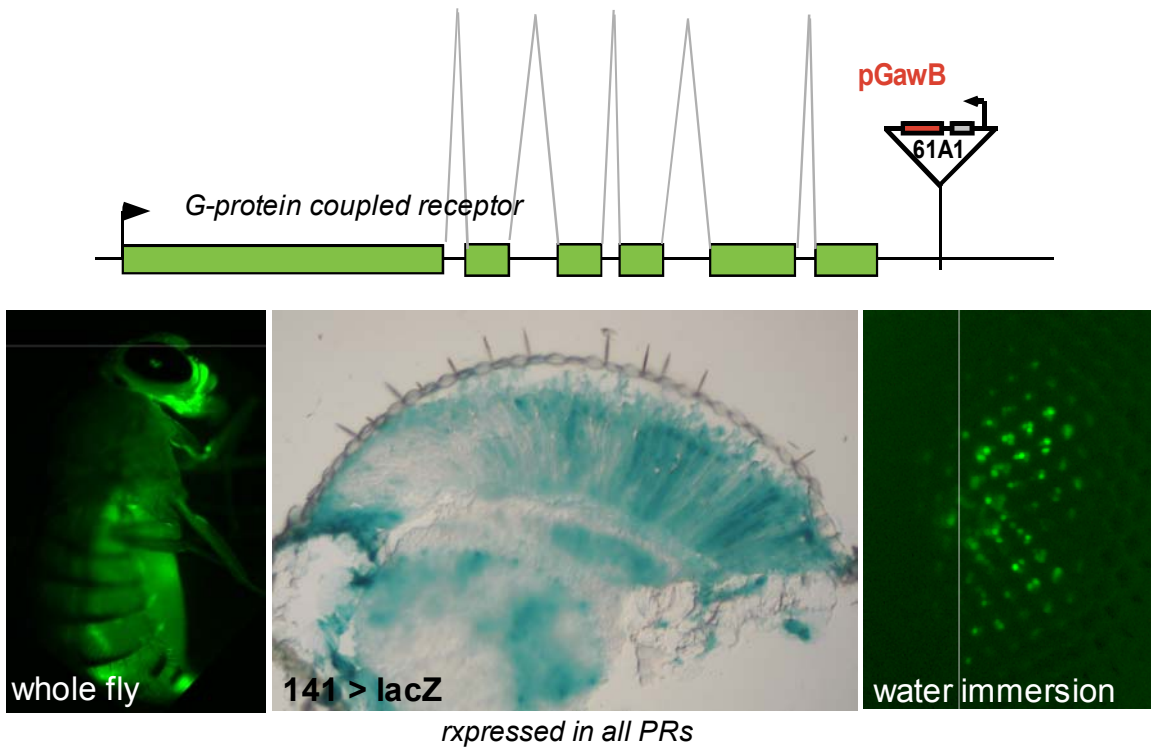
line #142: insertion of pGawB in gene *no ocelli*

transcription factor (Zn-finger)

whole fly

142 > lacZ

water immersion
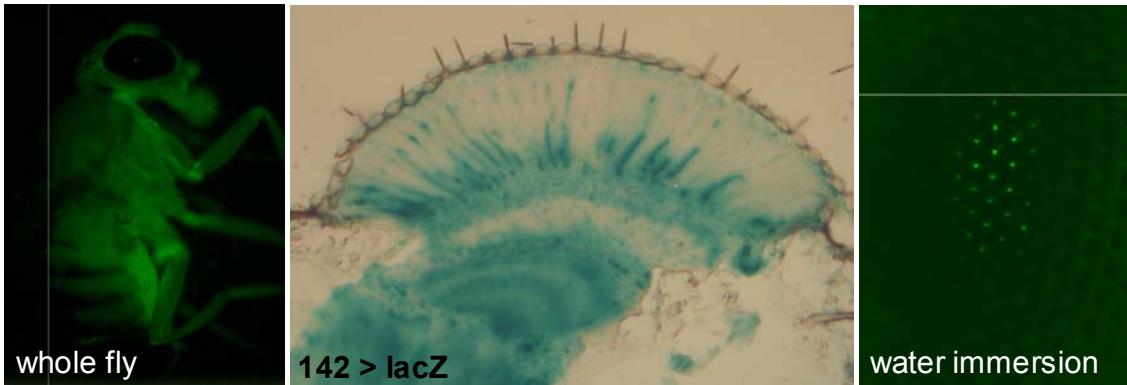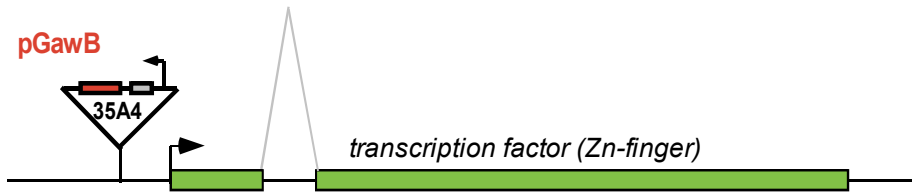
subsets of inner PRs: DRA, R7 and R8

line #145: insertion of pGawB in gene *coronin*

actin binding protein

~0.5kb

whole fly

145 > lacZ

water immersion
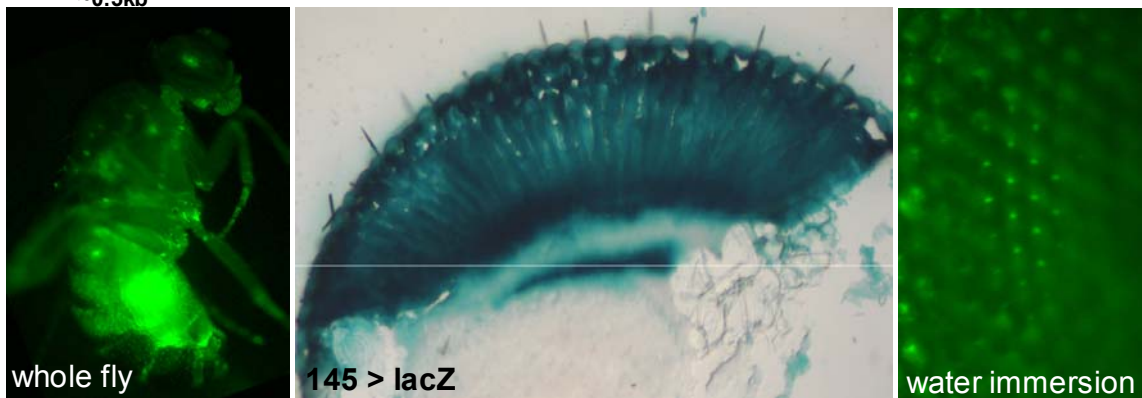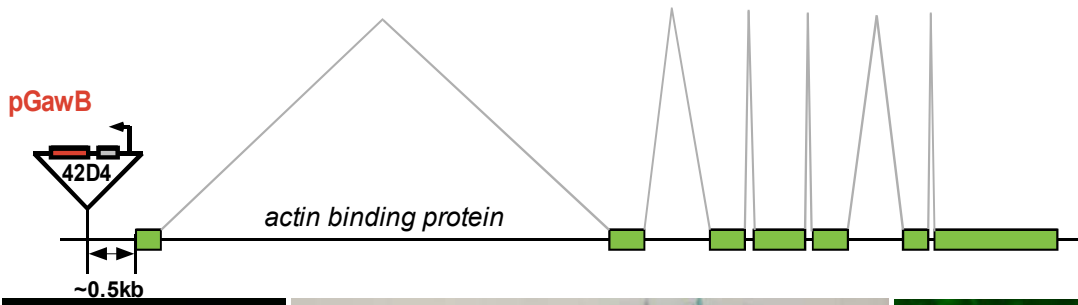
expressed in Inner PRs and pigment cells

line #147: insertion of pGawB in gene longitudinals lacking

weak expression in all PRs
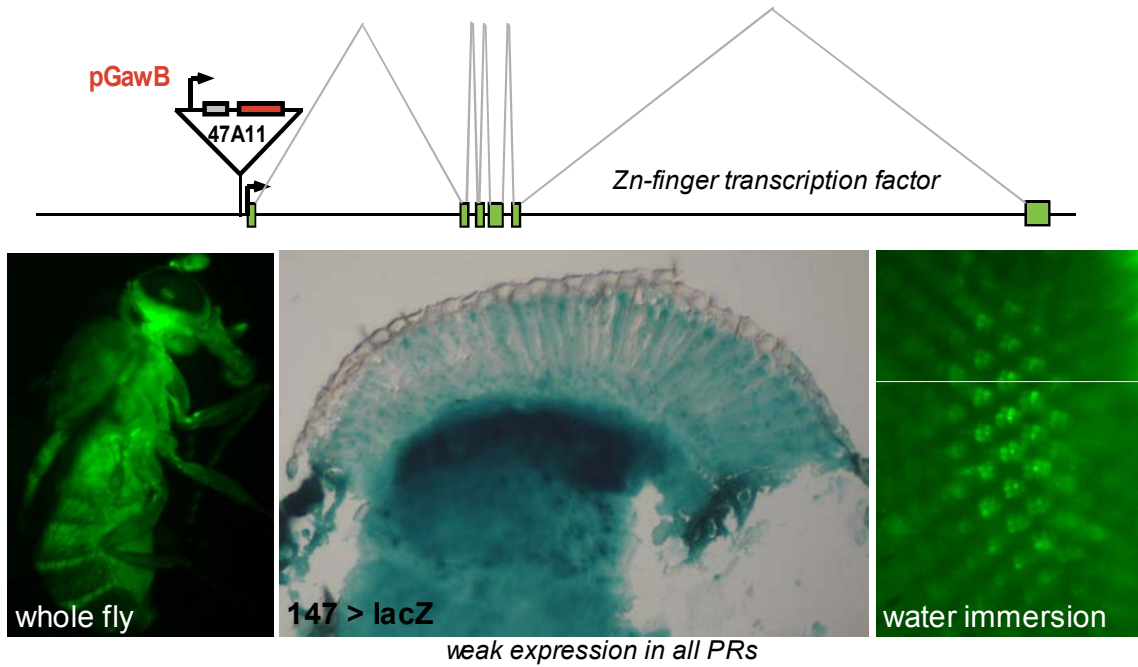
line #148: insertion of pGawB in gene *polyhomeotic distal*

weak expression in all PRs
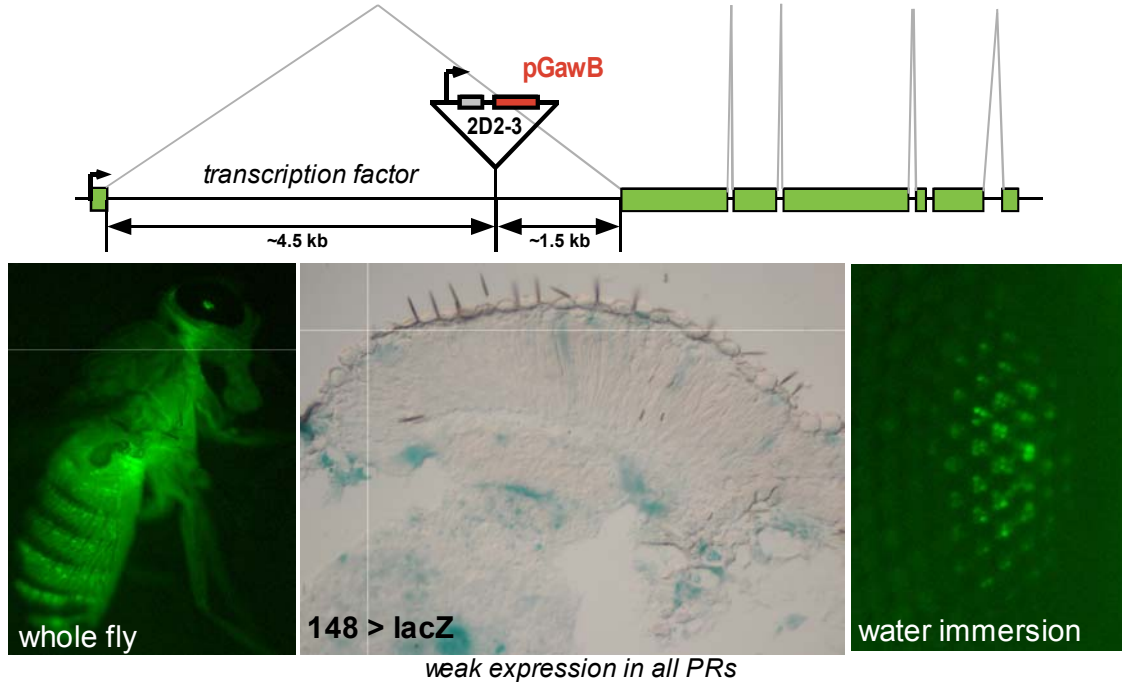
line #149: insertion of pGawB in repetitive sequences

pGawB

?

gene product/enhancer unknown

whole fly

149 > lacZ

water immersion
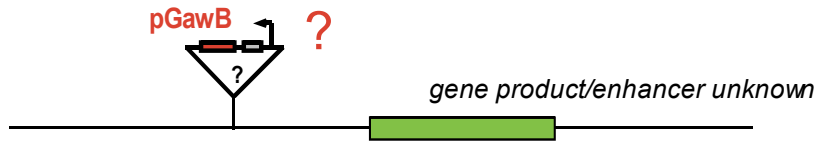
line #154: insertion of pGawB in gene *CG6024*

pGawB

68D1

CG7303
gustatory
receptor 68D.1

whole fly

154 > lacZ

water immersion
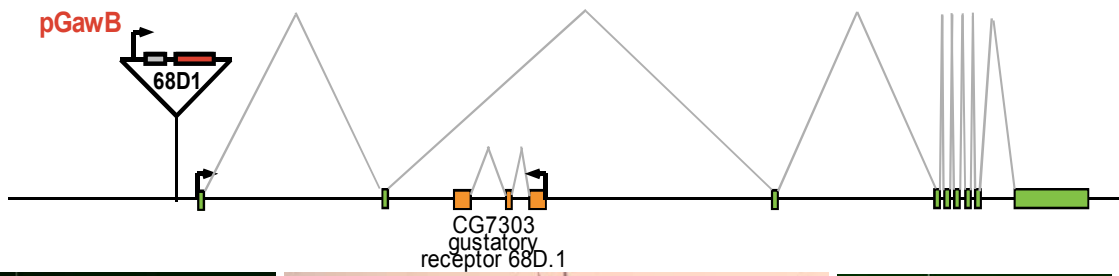
line #155: insertion of pGawB in gene *gilgamesh*

drosophila casein kinase I

whole fly

155 > lacZ

water immersion
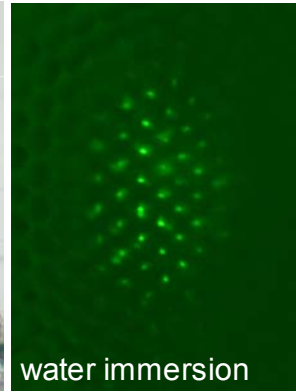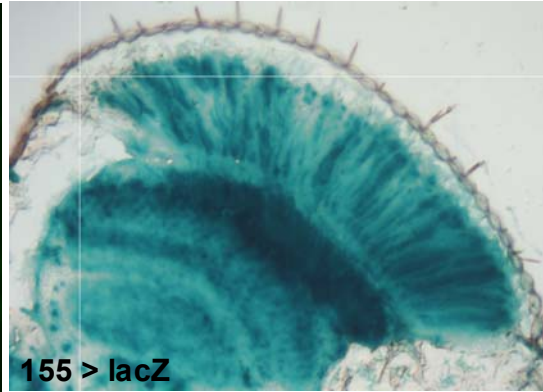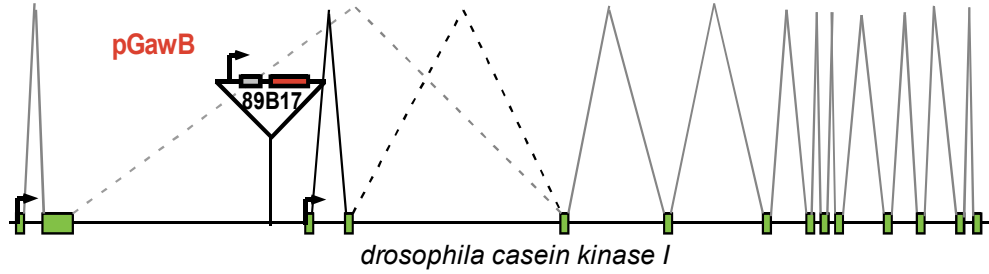
expressed in all PRs

gene #156: insertion of pGawB in gene *RhoGAP18b*

small GTPase activating protein

CG7502

~20kb

whole fly

156 > lacZ

water immersion
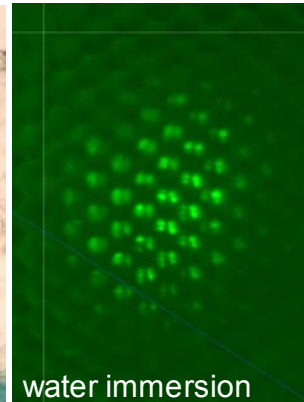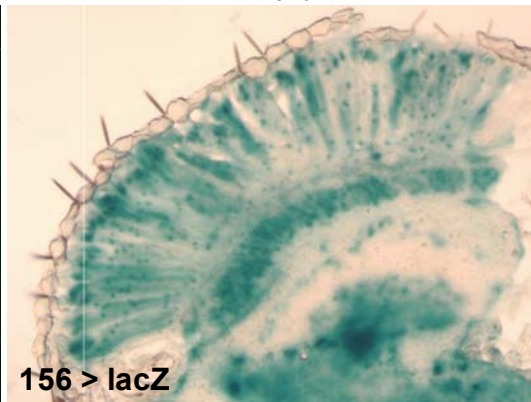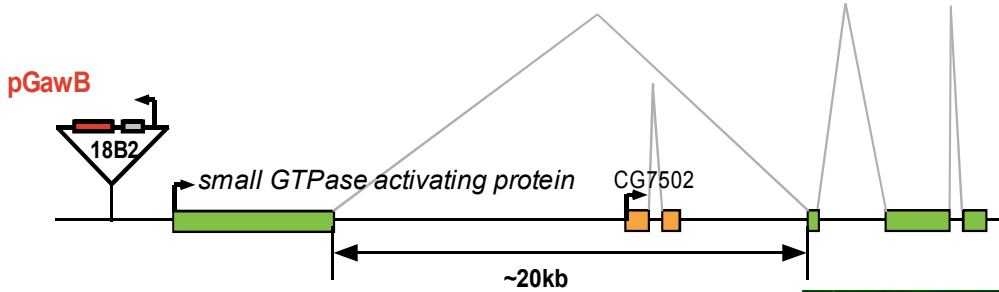
expressed in outer PRs

line #158: insertion of pGawB in gene *CG18742*

Tetraspan family transmembrane protein

whole fly

158 > lacZ

water immersion

weak expression in inner PRs and other cells
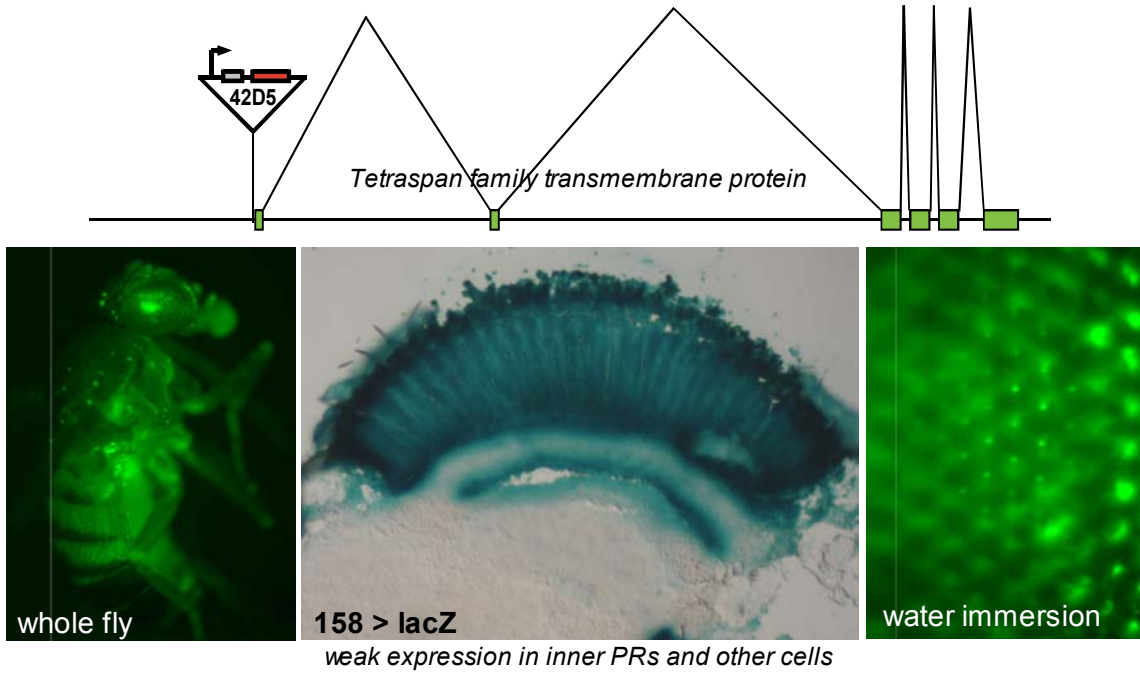
line #163: insertion of pGawB near gene *CG8005*

Deoxyhyposine synthase

CG7357 *CG8005* *CG7366*

whole fly

163 > lacZ

water immersion

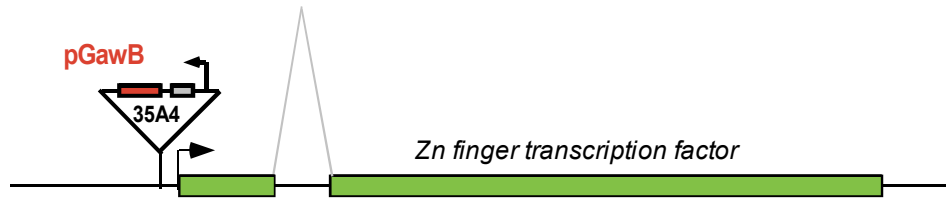*weak expression in all PRs*
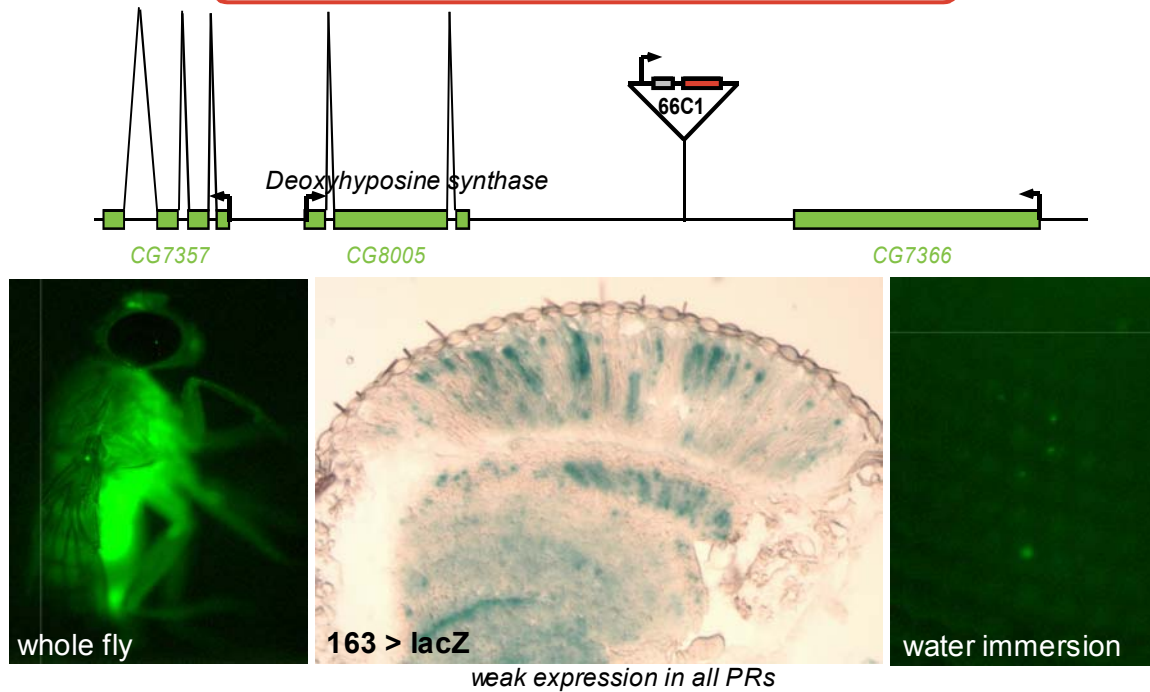
line #173: insertion of pGawB in *darkener of apricot*

| whole fly | 173 > lacZ | water immersion |
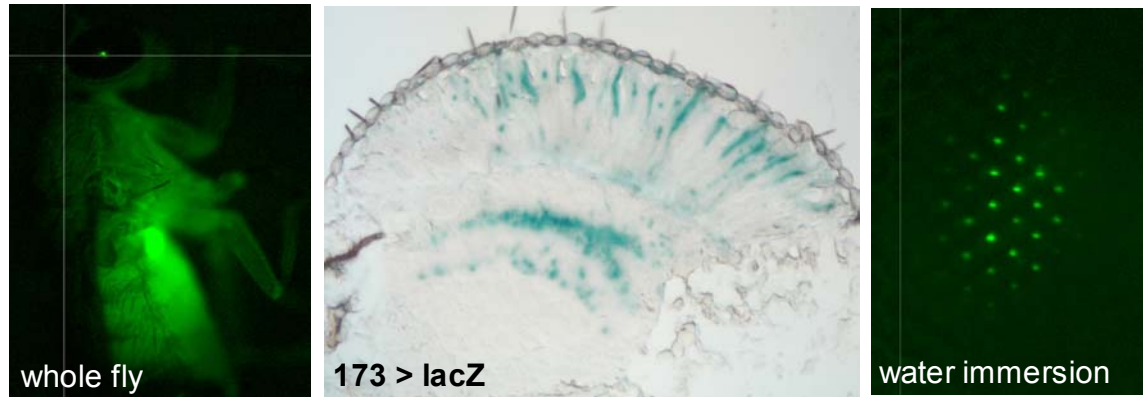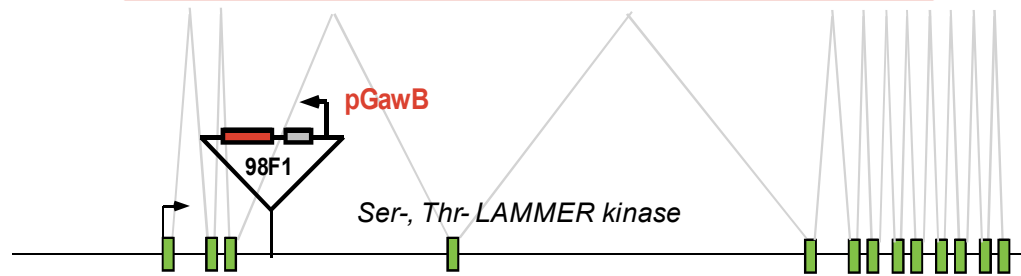
expressed in R7 cells

line #175: insertion of pGawB in gene *CG14408*

| whole fly | 175 > lacZ | water immersion |
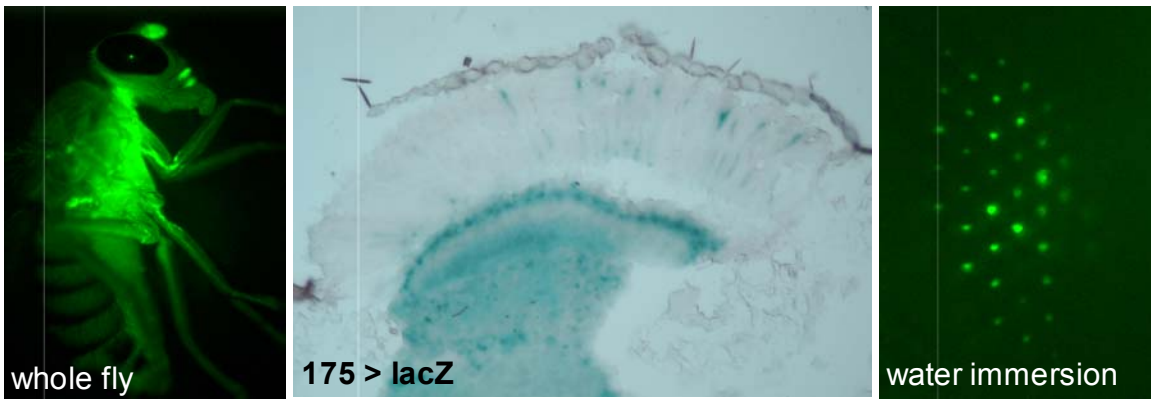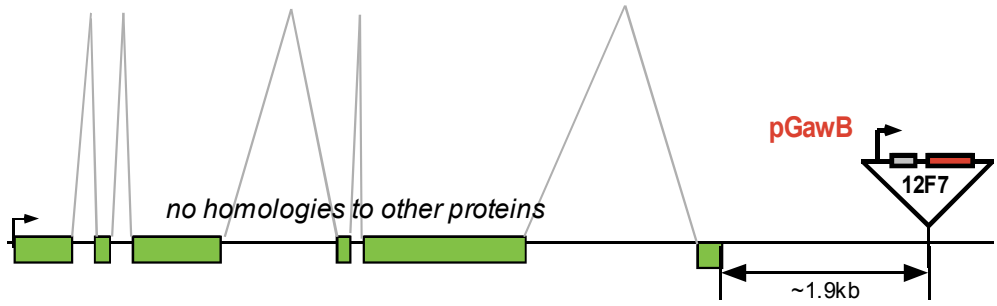
expressed in inner PRs

line #181: insertion of pGawB in gene *no ocelli*

pGawB

35A4

Zn finger transcription factor

whole fly | 181 > lacZ | water immersion
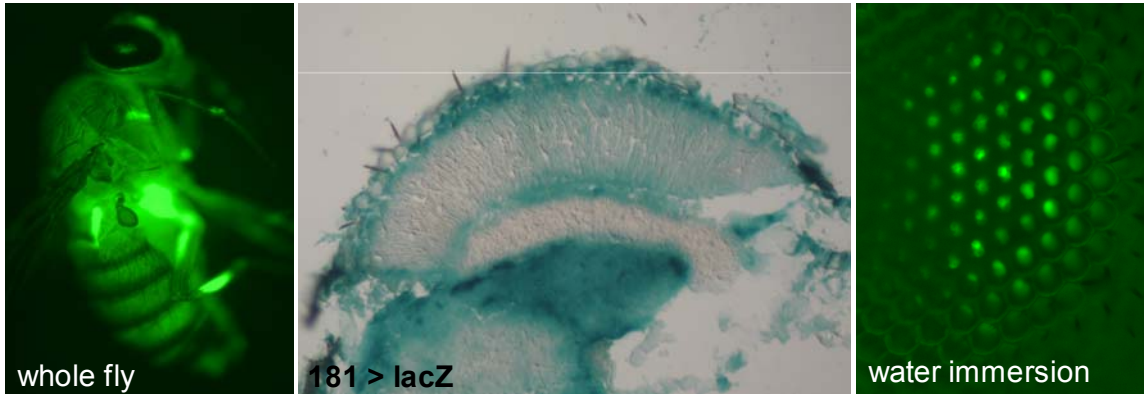
expressed in inner PRs

line #184: insertion of pGawB *mindmelt*

pGawB

54B9

nuclear Cys3His-type zinc-finger protein

whole fly | 184 > lacZ | water immersion
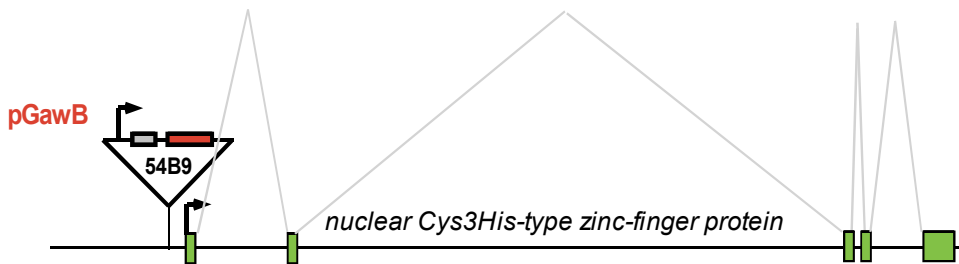
expressed in inner PRs and cone cells

line #185: insertion of pGawB in gene *CG3927*

RNA-bindingprotein / p62 tumor suppr. homologue

~1.6kb

whole fly

185 > lacZ

water immersion

expressed in all PRs
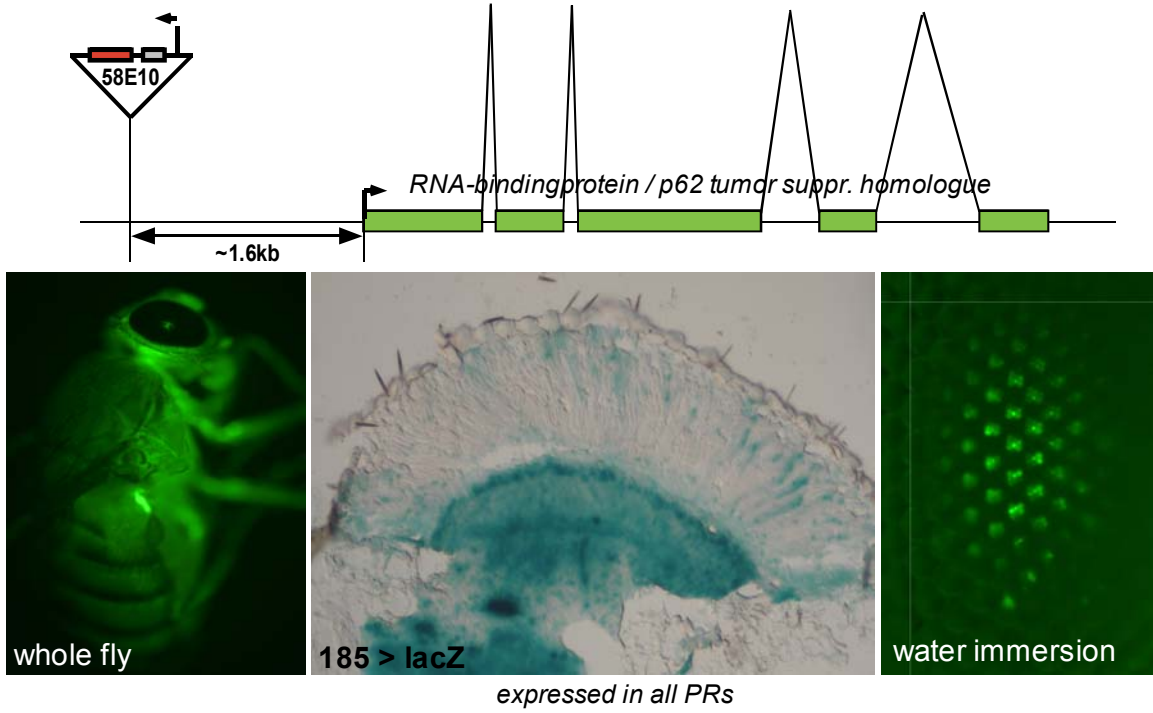
line #186: insertion of pGawB in gene *sticky ch1*

pGawB

86B1

RNA polymerase II transcription factor

whole fly

186 > lacZ

water immersion

expressed in inner PRs and cone cells
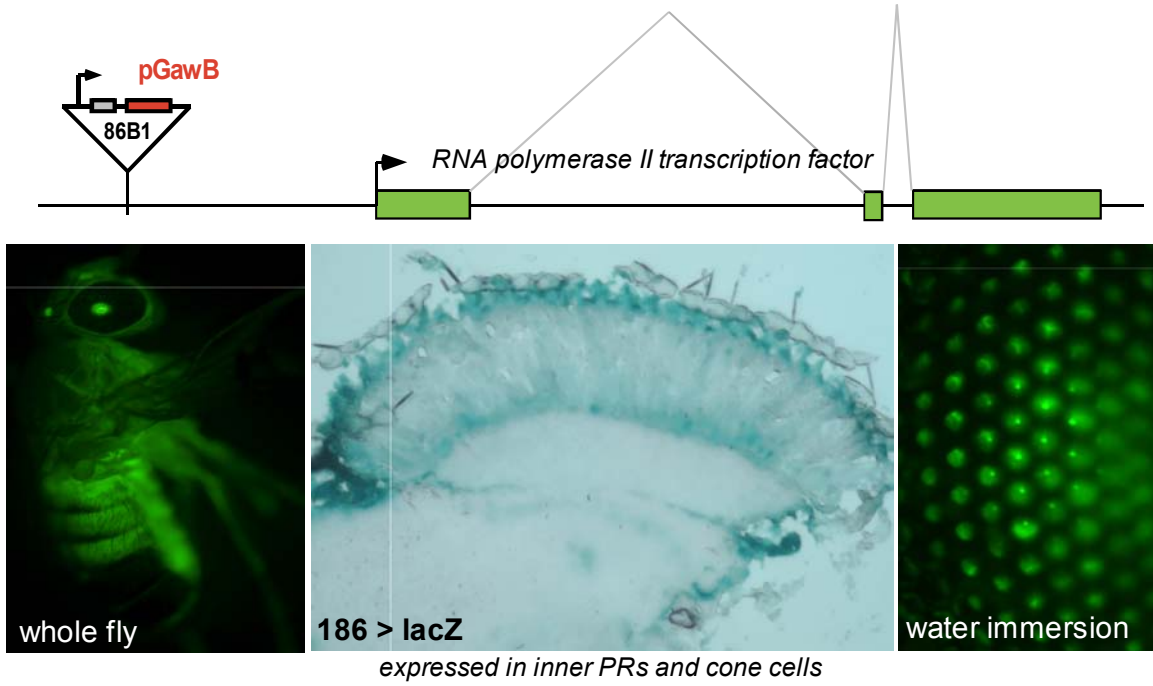
line #190: insertion of pGawB in gene *syndecan*

pGawB

57D12

Cytoskeletal anchor protein

~5k

~66 kb

whole fly

190 > lacZ

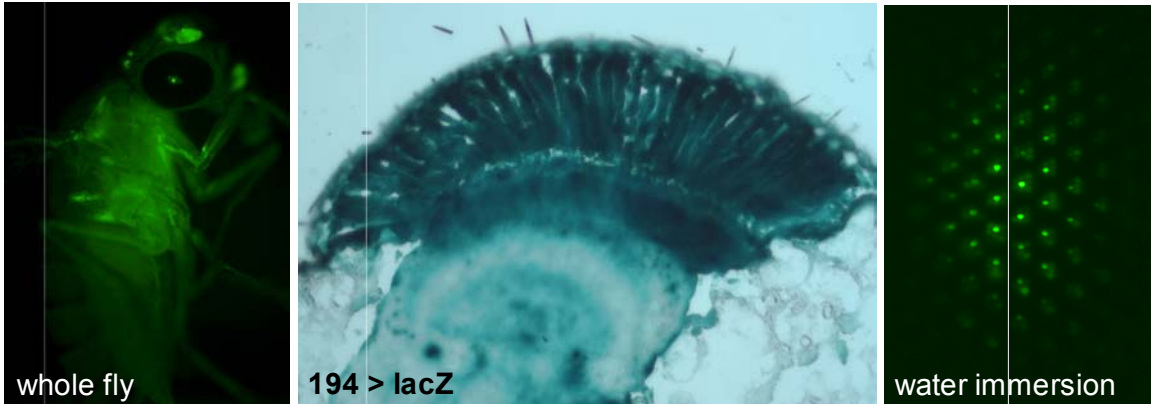water immersion
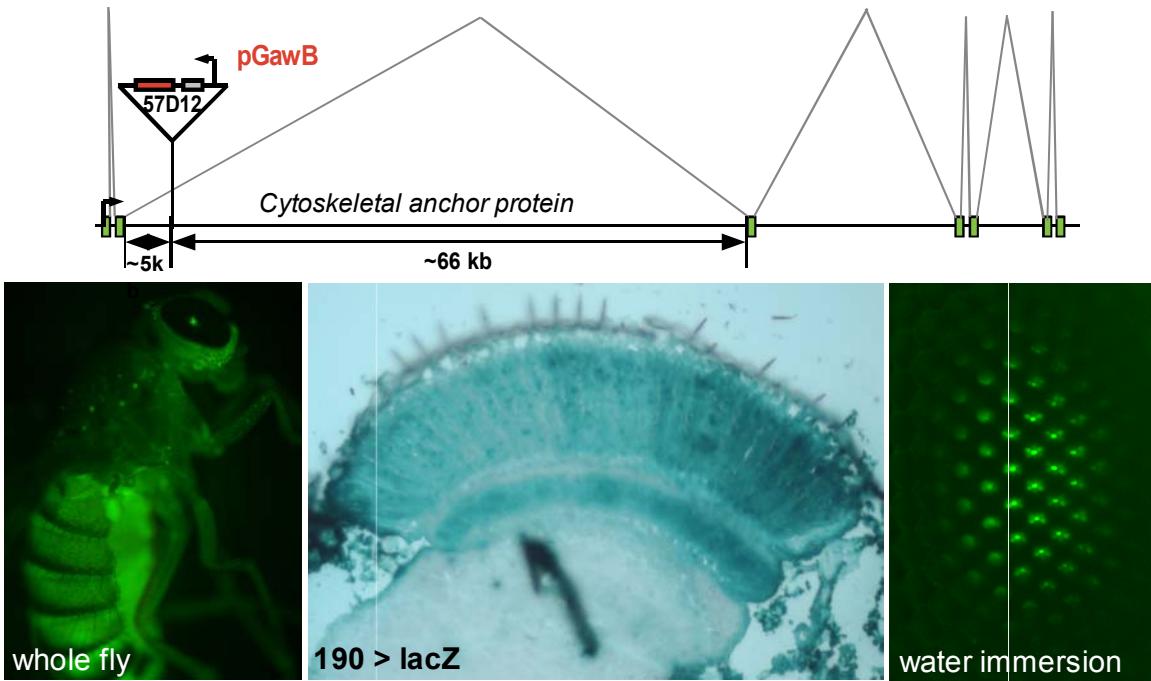
expressed in all PRs

line #193: insertion of pGawB in gene *CG31038*

pGawB

99C7

no homologies to other proteins

whole fly

193 > lacZ

water immersion
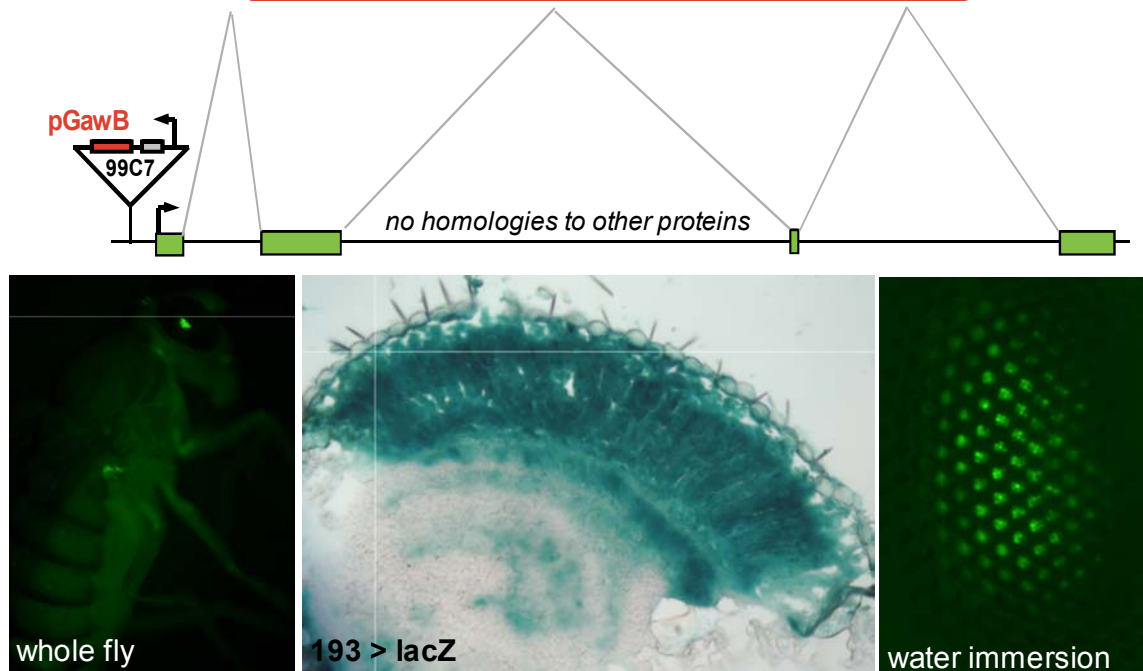
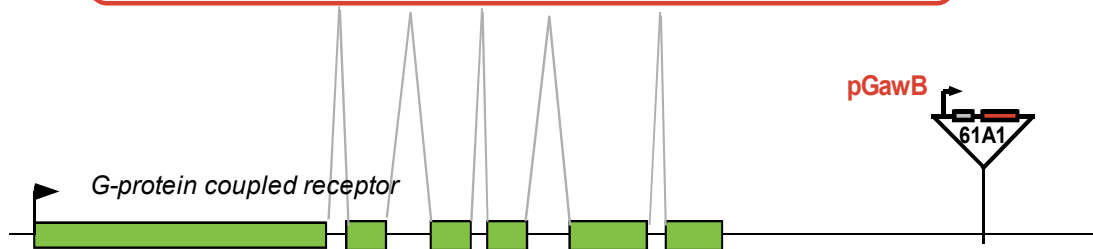*strong expression in all PRs*

line #194: insertion of pGawB in gene RhoGAP18b

whole fly

194 > lacZ

water immersion
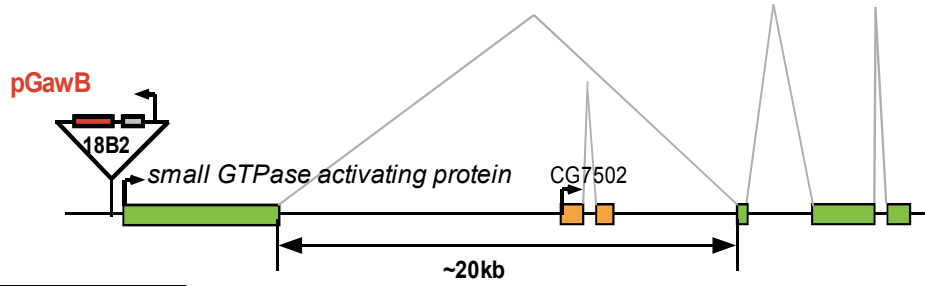
weak expression in all PRs

line #196: insertion of pGawB near gene methuselah-like 8

whole fly

196 > lacZ

water immersion

expressed in inner PRs

line #197: insertion of pGawB in gene mindmelt

pGawB

54B9

nuclear Cys3His-type zinc-finger protein

whole fly

197 > lacZ

water immersion
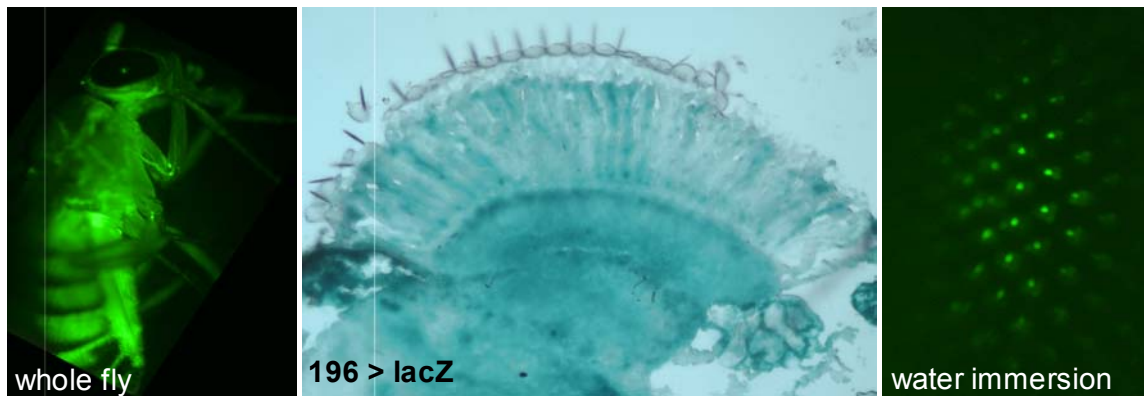
expressed in all PRs
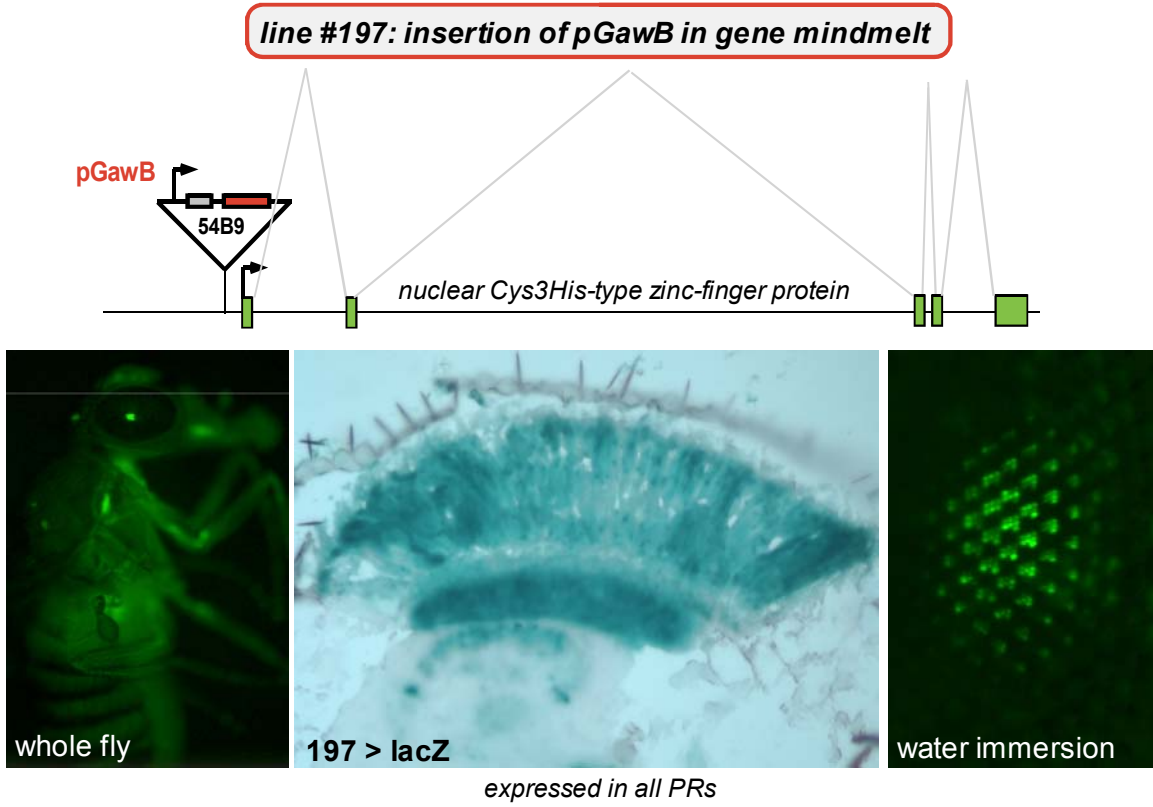
ERKLÄRUNG

Ich versichere, dass uch die von mir vorgelegte Dissertation selbständig angefertigt, die benutzten Quellen und Hilfsmittel vollständig angegeben und die Stellen in der Arbeit – einschliesslich Tabellen, Karten und Abbildungen -, die anderen Werken im Wortlaut oder dem Sinn nach entnommen sind, in jedem Einzelfall als Entlehnung kenntlich gemacht habe; dass diese Dissertation noch keiner anderen Fakultät oder Universität zur Prüfung vorgelegen hat; dass sie – abgesehen von den unten angegebenen Teilpublikationen – noch nicht veröffentlicht woeden ist, sowie dass ich eine solche Veröffentlichung vor Abschluss des Promotionsverfahrens nicht vornehmen werde. Die Bestimmungen dieser Promotionsordnung sind mir bekannt. Die von mir vorgelegte Dissertation ist von Prof. Dr. D. Tautz betreut worden.

New York, den 17.10.2004

LEBENSLAUF

Name: Mathias François Wernet

Geburtsdatum/-ort: 24.02.1974 in Strasbourg, Frankreich

Staatsangehörigkeit: deutsch, französisch

Schulbildung:

1980-1984 Gerhart-Hauptmann Grundschule, Freiburg im Breisgau

1984-1993 Deutsch-Französisches Gymnasium, Freiburg im Breisgau

1993 deutsch-französisches Abitur

Zivildienst:

1993-1994 Mobiler Sozialer Hilfsdienst, Paritätischer Wohlfahrtsverband, Freiburg.

Studium:

1994-1999 Studium der Biochemie/Molekularbiologie an der Universität Hamburg

1998-1999 Diplomarbeit im Labor von Prof. Claude Desplan an der Rockefeller University, New York. Titel: "An enhancer trap screen in *Drosophila* photoreceptor cells using the green fluorescent protein".

1999 Diplom, Biochemie/Molekularbiologie, Universität Hamburg.

Promotion:

1999-2004 Anfertigung der einzureichenden Arbeit im Labor von Prof. Claude Desplan an der New York University, New York. Betreuung durch Prof. Dr. Diethard Tautz, Institut für Genetik der Universität zu Köln. Titel: "Patterning the retina of *Drosophila melanogaster* for color and polarized light vision".

Stipendien:

1996-1999 Studienstifung des deutschen Volkes.

1999-2002 Promotions-Stipendium des Boehringer-Ingelheim Fonds (BIF).

Publikationen: siehe Anlage.

New York, den 7.10.2004